Genotypic adaptation of Indian groundnut cultivation to climate change: an ensemble approach

Julian Armando Ramirez Villegas

Submitted in accordance with the requirements for the degree of
Doctor of Philosophy

The University of Leeds
School of Earth and Environment
February 2014

Declaration of Authorship

The candidate confirms that the work submitted is his own, except where work which has formed part of jointly-authored publications has been included. The contribution of the candidate and the other authors to this work has been explicitly indicated below. The candidate confirms that appropriate credit has been given within the thesis where reference has been made to the work of others.

The following published material, first authored by the author of this thesis, has been used herein:

- Chapter 4 is based on the analyses published in Ramirez-Villegas and Challinor (2012) and Ramirez-Villegas et al. (2013a), which comprise all the analyses presented in the chapter.
- Chapter 7 is partly based on the methodology and model described in Jarvis et al. (2012) and Ramirez-Villegas et al. (2013b). Ramirez-Villegas et al. (2013b) described the EcoCrop model and the methodology for model calibration used within the chapter.

During the preparation of this thesis, the author has also contributed to other studies, from which ideas and/or methods have been extracted. The author's contributions to Vermeulen et al. (2013), Glenn et al. (2013), and Berry et al. (2013), and the recently published article Ramirez-Villegas and Khoury (2013) have all ocurred during the course of this PhD.

Acknowledgements

Completing this PhD has taken more of my life and energy than I would ever had expected, and I know I couldn't have even started without the help, support and contributions of many people. Difficult it is, therefore, to thank people that in some way have contributed to the completion of this PhD, because it means going back to how many people have in any way shaped my life –of course including my short research career. From these, only a handful remain in the posterity of my memory. These are the ones that I want to thank.

My parents, of course, as the only people that have supported me for as long as I have memories. My mother for making me read lots of literature before presenting my school homework, and thus inculcating in me an almost obsessive interest in research. My father, for his advice –only when it was strictly necessary. I thank my family, but foremost my brother Juan Felipe, who I think has influenced me as much as I have influenced him. We must both pursue excellence at all times. I thank my friend Juan José, for his unforgettable words *"¿vos crees que tus papás pagan para eso?"* during the high school. To my undergraduate lecturers –the good ones, although they should open their universe of possibilities and try to make the *Universidad Nacional* much more academically-oriented and international. The support of my wife, Sandra, in this long-standing battle has also been critical –thanks for not allowing me to work more than I should.

But this acknowledgments section wouldn't be complete without acknowledging Andy and Andy. One more in the past, one more recently. Mentors, advisors and great researchers. Thanks for your ideas, support and encouragement. Thanks for always sparing a bit of your busy agendas for discussing my work. Both: thanks for making the funding happen, and for the help provided throughout my career, and for the help and ideas to come.

I also thank friends and colleagues who have taken part in the writing of this thesis by proof-reading one or more of its chapters: A. K. Köhler, B. J. Parkes, L. Parker, and C. K. Khoury. A final word of thanks to Peter Knippertz for his insightful suggestions during the course of this PhD.

Abstract

Climate change has been projected to significantly affect agricultural productivity and hence food availability during the 21^{st} century, with particularly negative effects across the global tropics. However, the uncertainty associated with projecting climate change impacts is a barrier to agricultural adaptation. The work reported in this thesis is a contribution to the understanding of genotypic adaptation to near-term (i.e. 2030s) climate change and many of the associated uncertainties, using model ensembles. This work focuses on Indian groundnut and uses the General Large Area Model for annual crops (GLAM) and the EcoCrop niche model to investigate the response of groundnut under future climate scenarios, and to develop a genotypic adaptation strategy.

Under the future representative concentrations pathway (RCP) 4.5, robust positive climate change impacts on crop productivity were found in 3 (western, northern and south-eastern) out of 5 groundnut growing regions. From the remainder of regions, one presented robust negative impacts and in the other uncertainties precluded a robust statement being made about productivity changes. Yield gains were associated with seasonal precipitation increases, a lower frequency of occurrence of terminal drought and its effect on cropping season length. Yield loss in central India was associated with less radiation interception and reductions in crop duration, whereas in the south there was large uncertainty due to temperature biases in GCMs triggering (or not) heat stress during anthesis. The latter result suggests that decisions of whether to correct or not GCM biases and the method of correction may be at least as important as the choice of climate scenario, or the choice of crop model parameters.

Adaptation simulations indicated that the most critical traits for groundnut adaptation under future scenarios are increases in maximum photosynthetic rates, greater partitioning to seeds and, where enough soil moisture is available, also increases in the maximum transpiration rate. Changes to crop duration were beneficial if durations did not exceed those of the baseline, and hence allowed for enough water uptake at the end of the cropping season. Yield gains in adaptation scenarios were particularly large in eastern and northern India, and more moderate across the rest of the country.

Contents

List of Figures

List of Tables

Symbols

Symbol	Name	Units
AUC_I	Area under the ROC curve	
C_{d1}, C_{d2}, C_{d3}	Empirical constants for drainage calculation	
C_{YG}	Yield gap parameter	
D	Drainage rate	cm day^{-1}
e_{sat}	Saturation vapour pressure	kPa
E_T	Transpiration efficiency	Pa
$E_{TN,max}$	Normalised transpiration efficiency	g kg^{-1}
F_{sw}	Sensitivity of the crop to terminal drought	
H_I	Integrated harvest index	fraction
H_I^{min}	Minimum value of harvest index for terminal drought	
l_v	Root length density by volume	
k	Light extinction coefficient	
k_{sat}	Saturated soil hydraulic conductivity	cm day^{-1}
K_{ks}	Empirical constant for calculating k_{sat}	cm day^{-1}
L_{cr}	Critical value of LAI below which transpiration is reduced	
$P(i)$	Percentage of pods for day i	%
P_{tot}	Total percentage of pods	%
P_{cr}	Critical value of percentage of pods for reduction in H_I	%
R	Pearson correlation coefficient	
$RMSD$	Root mean square difference	of measured quantity

$RMSE$	Root mean square error	of measured quantity
$RMSE_V$	RMSE variation, for a parameter	%
$RMSE_M$	RMSE normalised by mean	%
$RMSE_{SD}$	RMSE normalised by standard deviation	%
R_N	Net all-wave radiation	W m^{-2}
R_{SUIT}	Crop suitability as determined by precipitation	%
R_{MIN}	Minimum seasonal precipitation at which the crop can thrive	mm
R_{OPMIN}	Minimum optimum seasonal precipitation for the crop	mm
R_{OPMAX}	Maximum optimum seasonal precipitation for the crop	mm
R_{MAX}	Maximum absolute seasonal precipitation for the crop to be suitable	mm
S	Soil water stress factor	
S_{cr}	Water stress factor for damage to leaves	
S_{rad}	Solar radiation	W m^{-2}
$SUIT$	Crop suitability	%
t_{TT}	Thermal time	°C day^{-1}
$\bar{T}$	Mean daily temperature	°C
T_{max}	Maximum daily temperature	°C
T_{min}	Minimum daily temperature	°C
T_{AM}	Mean temperature between 8:00 and 14:00 hours	°C
T_{cr}	Critical temperature for damage to flowers	°C
T_{cr}^{min}	Minimum critical temperature for damage to flowers	°C
T_{lim}	Limit temperature for damage to flowers	°C
T_{lim}^{min}	Minimum limit temperature for damage to flowers	°C
T_{eff}	Effective temperature	°C
T_b	Base temperature for development	°C
T_o	Optimum temperature for development	°C
T_m	Maximum temperature for development	°C

T_{ter1}	Temperature at which photosynthesis starts to be affected by temperature	°C
T_{ter2}	Temperature at which photosynthesis = 0 due to temperature	°C
T_T	Rate of transpiration	cm day^{-1}
T_{Tmax}	Maximum rate of transpiration	cm day^{-1}
T_{Tpot}	Rate of potential transpiration	cm day^{-1}
T_{SUIT}	Crop suitability as determined by temperature	%
T_{KILL-C}	Crop killing temperature	°C
T_{MIN-C}	Crop minimum absolute temperature	°C
$T_{OPMIN-C}$	Crop optimum minimum temperature	°C
$T_{OPMAX-C}$	Crop optimum maximum temperature	°C
T_{MAX-C}	Crop maximum absolute temperature	°C
T_V	Total uncertainty (typically of crop yield)	kg ha^{-1}
V	Vapour pressure deficit (VPD)	kPa
V_{EF}	Velocity of extraction front	
V_I	Variability index	
V_{ref}	VPD reference value	
W	Crop biomass	kg ha^{-1}
$\bar{X}$	Average of variable X	of measured quantity
Y	Crop yield	kg ha^{-1}
z	Depth of soil profile	cm
z_{max}	Maximum depth of soil profile	cm
α_0	Priestley-Taylor pre-correction value	
$(\partial L/\partial t)_{max}$	LAI growth rate	day^{-1}
$\partial W/\partial t$	Rate of biomass accumulation	kg day^{-1}
δ	Latent heat of vaporisation of water	kJ kg^{-1}
γ	Ratio of the specific heat of air at constant pressure to the latent heat of vaporisation of water	
σ_x	Standard deviation of variable x	of measured quantity
θ	Soil moisture content	fraction

θ_{ll}	Soil moisture content at permanent wilting point	fraction
θ_{dul}	Soil moisture content at field capacity	fraction
θ_{sat}	Soil moisture content at field capacity	fraction
θ_{pe}	Potentially extractable soil water	fraction

Abbreviations

Acronym	Meaning
AEZ	Agro-Ecological Zoning
AgMIP	Agricultural Model Inter-comparison Project
APSIM	Agricultural Production Systems Simulator
BMM	Basic mechanistic model
CCAFS	CGIAR Research Program on Climate Change, Agriculture and Food Security
CER	Carbon exchange rate
CMIP	Coupled Model Inter-comparison Project
CO2	Carbon dioxide
DEL	Delta method (for bias correction)
DSSAT	Decision Support System for Agrotechnology Transfer
ECMWF	European Centre for Medium-Range Weather Forecasts
ENM	Ecological Niche Model
EPIC	Erosion-Productivity Impact Calculator
ERA-40	40+ year ECMWF Reanalysis
FAO	Food and Agriculture Organization of the United Nations
FACE	Free-Air CO_2 Enrichment
GCM	Global Climate Model
GDP	Gross Domestic Product
GHG	Greenhouse gas
GIEWS	Global Information and Early Warning System
GLAM	General Large Area Model for annual crops
HTS	High temperature stress
HWSD	Harmonized World Soil Database

ICAS	Institute for Climatic and Atmospheric Science
ICRISAT	International Crops Research Institute for the Semi-Arid Tropics
IIASA	International Institute for Applied Systems Analysis
IMD	Indian Meteorological Department
IPCC	Intergovernmental Panel on Climate Change
ISI-MIP	Inter-Sectoral Impact Model Intercomparison Project
ISRIC	International Soil Reference and Information Center
ISS-CAS	Institute of Soil Science Chinese Academy of Sciences
JRC	Joint Research Centre of the European Commission
LAI	Leaf area index
LOCI	Local Intensity Scaling
MCWLA	Model to capture the Crop–Weather relationship over a Large Area
MLR	Multiple Linear Regressions
MMM	Multi-model mean
NCC	National Climate Centre
PDF	Probability density function
PRYSBI	Process-based Regional-scale Rice Yield Simulator with Bayesian Inference
RCM	Regional Climate Model
ROC	Receiver Operating Characteristic Curve
RSCM	Regional-scale Crop Model
RuBisCO	Ribulose-1,5-bisphosphate carboxylase oxygenase, the enzyme of photosynthesis
RUE	Radiation-use efficiency
SH	'Nudging' to means (for bias correction)
SIMRIW	Simulation Model for Rice-Weather relations
SLA	Specific leaf area
SLPF	Soil Fertility Factor
STICS	Simulateur mulTIdisciplinaire pour les Cultures Standard
TDS	Terminal drought stress
UNESCO	United Nations Educational, Scientific and Cultural Organization
VPD	Vapour pressure deficit
WISE	World Inventory of Soil Emission potentials

WOFOST	World Food Studies
WUE	Water-use efficiency

Chapter 1

Introduction

"The student now guesses the state of the case, but is impelled, as I have before explained, by the human thirst for self-torture, and in part by superstition"

E. A. Poe

1.1 Summary

This chapter brings up the work presented in this thesis into context by first stating the motivation of the work. The global importance of agriculture (Sect. 1.3), the projected changes in global and regional climates (Sect. 1.4), and their consequences for food systems (Sect. 1.5) are then briefly reviewed. The chapter then presents the objectives (Sect. 1.6) underlying the work presented. Section 1.7 finally describes the overall research strategy and the structure of this thesis.

1.2 Motivation

There is no doubt that agriculture is one of the sectors that influences the most the development of local, national and global economies whilst at the same time influencing people's livelihoods. Agriculture constitutes the sole means to feed a globally growing

population of roughly 7 billion people, and contributes significantly the national Gross Domestic Product (GDP) of all countries around the world. Numerous studies have shown that climate change can be a significant threat to food availability and stability by reducing crop productivity and/or increasing interannual variations in commodity prices (Easterling et al., 2007; Lobell et al., 2008; Wheeler and von Braun, 2013). This all is expected to exacerbate vulnerability in many already-poverty-prone areas across the global tropics.

Model-based projections of climate change impacts on crop productivity and/or suitability are critical for understanding cropping system responses under climate change scenarios so as to plan adaptation (Howden et al., 2007; Moser and Ekstrom, 2010). However, such projections are subjected to numerous uncertainties which in cases can hinder adaptation planning (Koehler et al., 2013; Vermeulen et al., 2013). Major knowledge gaps relating to the understanding of the relevance of certain mechanisms and uncertainties associated to crop responses in future scenarios remain (Challinor et al., 2013; Lobell et al., 2013). A better understanding of impacts and their associated uncertainties will allow focusing on reducing the important sources of uncertainty so as to develop more robust projections of climate change impacts and hence enable adaptation.

This work aims at improving the existing methodological base for projecting climate change impacts on crop productivity and quantifying their associated uncertainties in order to develop genotypic-level adaptation options. The methodology is applied to groundnut in India and used to comprehensively report and understand both uncertainties inherent to crop-climate simulation as well as the processes behind a robust crop yield projection.

1.3 Global importance of agriculture for food security and development

Agriculture contributes to between 20-46 % of the national Gross Domestic Product (GDP) of all countries around the world (Figure 1.1(a)), and is the sole source of income of a considerable proportion of national population (Figure 1.1(b)) (World-Bank, 2012). Agriculture is also the main means to reduce poverty and the 850 million undernourished people across the developing world (Wheeler and von Braun, 2013). Thus, there is no doubt that agriculture is one of the sectors that exerts the greatest influence on people's livelihoods

(FAO, 2009; World-Bank, 2012) and the environment, ecosystems and ecosystem services (Tilman et al., 2002).

Currently, however, agricultural production faces numerous challenges, including the need of feeding a rising global population coupled with an steady degradation of the natural resource base (Benayas et al., 2009; Licker et al., 2010), the limited space available for sustainable crop and pasture land expansion (Ellis et al., 2010; Klink and Machado, 2005; Ramankutty et al., 2008), the limited access to technologies for rural poor (Chapman, 2002; Reynolds et al., 2011), pests and diseases (Harper and Zilberman, 1989; Patil and Fauquet, 2009; Stephens et al., 2009), and the difficulty in managing climate risks (Dixit et al., 2011; Licker et al., 2010; Wilby et al., 2009).

If global agriculture is to produce enough food supplies to feed a projected population 50 % larger than now (IPCC, 2000; UN, 2010; World-Bank, 2012), two increasingly important development goals need to be pursued: (1) the reduction of crop yield gaps (i.e. the difference between potential yield at a given location and actual observed farmers' yields at the same location) through better management, technology targeting and input optimisation (Foley et al., 2011; Tilman et al., 2002); and (2) the increase of potential crop yields (defined as the yield obtained with all inputs being optimal –i.e. weather, nutrients, soil fertility) through genetic improvement of existing crop varieties (Reynolds et al., 2011).

Yield gaps limit food supply, exacerbating poverty and hunger, and exist in most regions throughout the developing world for virtually all crops (Gollin et al., 2007; Licker et al., 2010; Lobell et al., 2009). Estimations of yield gaps for a number of crops have been attempted (see Licker et al. 2010). Additionally, potential climate-adjusted as well as farmers' yields of the world's major grains seem to have stagnated in the last 15-20 years (Bakker et al., 2005; Mall and Aggarwal, 2002; Tilman et al., 2002). The causes of these trends might include: price stagnation or decline, a trend for using more environmentally friendly technologies without necessarily increasing yields, the reaching of genetic potentials, and climate change (Subash and Ram Mohan, 2012).

Transformations are necessary in the agricultural sector and these may include: (1) stopping agricultural expansion, (2) bringing technological improvements (including integrated pest management, better crop rotations, and new varieties) to close yield gaps, (3) increasing water- and nutrient-use efficiency, (4) increase food delivery by shifting diets (including

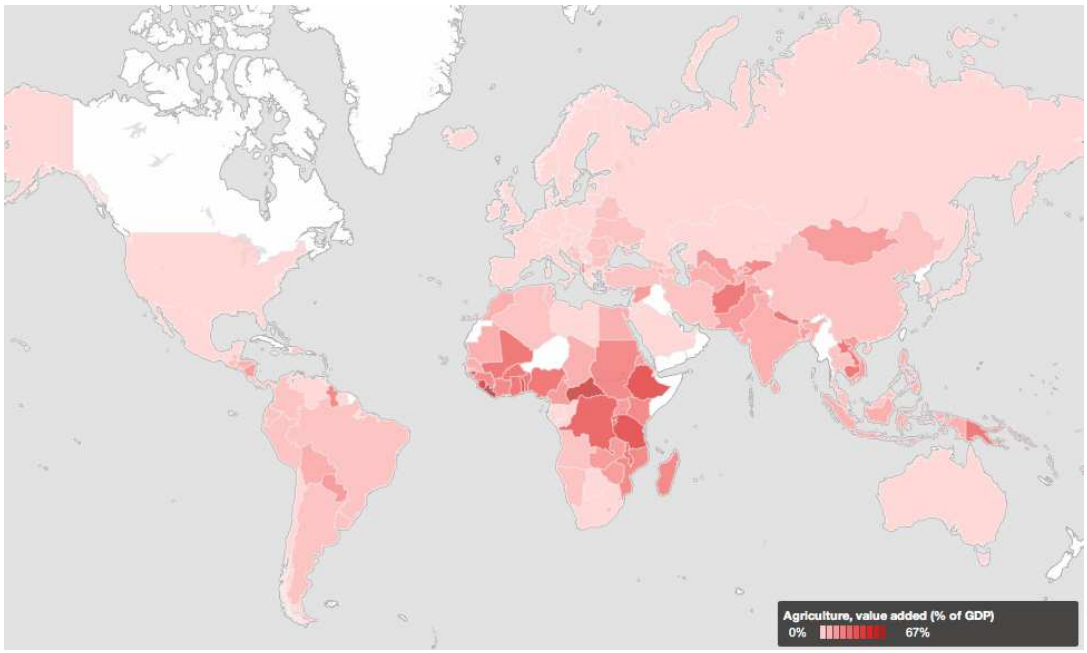

(a) Percent contribution of agriculture to national GDP across the world

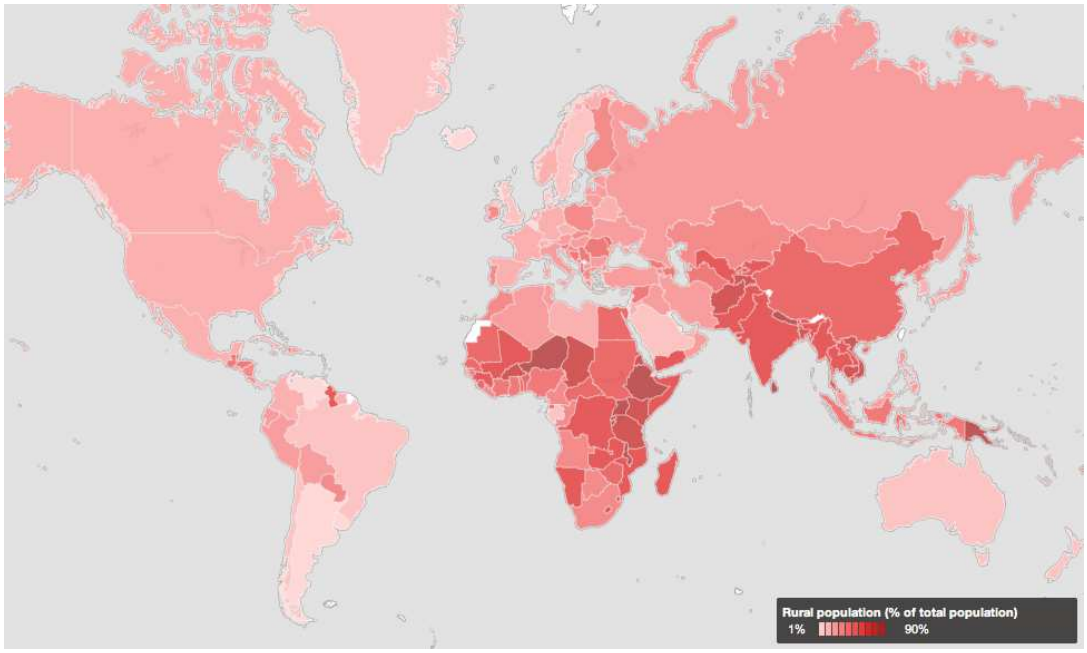

(b) Percent of total population considered as "rural"

FIGURE 1.1: Global agriculture importance indicators. Data and maps taken from the World Development Indicators database (World-Bank, 2012). White areas indicate where no data was available. Data correspond to the period 2007–2011.

producing food in areas where livestock, biofuel and other non-food land uses exist), and (5) improve sustainability of livestock production, including better management of confined production or even the shift to pastoral systems (Foley et al., 2011; Tilman et al., 2002). Another dimension that can be added is the sustainable use, exchange and conservation of plant genetic resources that are key to crop improvement (Burke et al., 2009; Dusen et al., 2007; Guarino and Lobell, 2011).

Implementing solutions is not a trivial issue and might require large national and international investment in addition to research- and subsidy-paradigm changes (Foley et al., 2011; Tilman et al., 2002). Important agreements at the global level have been reached and these are expected to be strengthened in the coming decades (Carney and Shackley, 2009; Viglizzo et al., 2011; Webster et al., 2012), which might indicate better prospects towards the future for agriculture (UNFCCC, 2012).

Future agricultural systems will also need to adapt in order to respond to changes in the climate system (see Sect. 1.4 and 1.5 below) that are driven by increased GHG emissions from anthropogenic activities (Howden et al., 2007). These changes will require responding to key scientific questions (Park et al., 2012; Pretty et al., 2010) and help in shifting past research and policy paradigms for the (a) incorporation of novel traits to existing crop varieties (Hajjar and Hodgkin, 2007), (b) conservation, sharing and use of plant genetic resources (Guarino and Lobell, 2011; Pandey et al., 2008), and (c) incorporation of farmers needs and traditional knowledge into adaptation strategies (Kristjanson et al., 2012; Rufino et al., 2012). Policy makers are now aware about the environmental risks of unsustainable food and livestock production, but there is a need to ground research results in the field and find ways to best adapt agricultural systems to an uncertain future (Muller, 2011; Smith et al., 2011; White et al., 2011b).

1.4 Projected changes in climates

The last of the IPCC reports concluded that (1) the earth's surface has been warming during at least the last two centuries (Gleckler et al., 2012; IPCC, 2001; Meehl et al., 2005; Rohde et al., 2013), (2) the most intense period of warming has occurred in the period 1950-2010 (Gleckler et al., 2012; IPCC, 2007), and (3) the most sensible cause of

such increases is the intensification the greenhouse effect due to the increase in greenhouse-gas (GHG) concentrations in the atmosphere caused by anthropogenic activities (Gleckler et al., 2012; Rohde et al., 2013).

The climate system responds to anthropogenic forcing, hence recent warming trends are attributed to the increases in GHG concentrations in the atmosphere (Hansen et al., 1981, 1997). Large numbers of simulation experiments in conjunction with field, cloud, ice-core and atmospheric measurements have been carried out (Skinner, 2012). Global and regional increases in mean land surface temperature have been measured by a number of different research groups (Foster and Rahmstorf, 2011; Hansen et al., 2007; Rohde et al., 2013; Solomon et al., 2007), thus increasing the scientific confidence on the fact that climate change is caused by anthropogenic activities (Figure 1.2). Climate change science is now focused on enhancing the understanding of the climate system and human responses, the attribution of recent warming to increases in concentrations of GHGs (Skinner, 2012), and the development of future climate scenarios (Nakicenovic et al., 2000; Taylor et al., 2012) that can be used by other researchers for assessing impacts and adaptation (Parry et al., 2007).

Projections must be made about how the climate system responds to a given set of constraints (Moss et al., 2010; Nakicenovic et al., 2000). Global Climate Models (also referred to as General Circulation Models or simply GCMs) constitute the most appropriate and robust means to predict the climate system response under any future socio-economic scenario (Moss et al., 2010; Nakicenovic et al., 2000). A GCM simulates mass, energy and momentum fluxes that occur within the atmosphere, by applying Navier-Stokes fluid dynamics equations within three-dimensional analysis units (often referred to as a "cells"). Solving these equations requires computer programs executed in high performance computing units.

Average global warming (with respect to year 2000 temperature) under the SRES (RCP) scenarios has been projected to be in the order 1-2.5 °C (0.5-2.5 °C) by 2050s and in the order 1.5-4 °C (0.5-8.5 °C) by 2100 (Figure 1.2). A trend to higher degrees of warming is expected near the north pole and the tropics, and a high likelihood for these areas to reach a +2 °C warming earlier than other areas (e.g. Europe, Central Asia, and southern South America) (Figure 1.3). Along the tropics, temperature is projected to rise at the highest rates in Sub-Saharan Africa, particularly across the Sahel and in northern East Africa

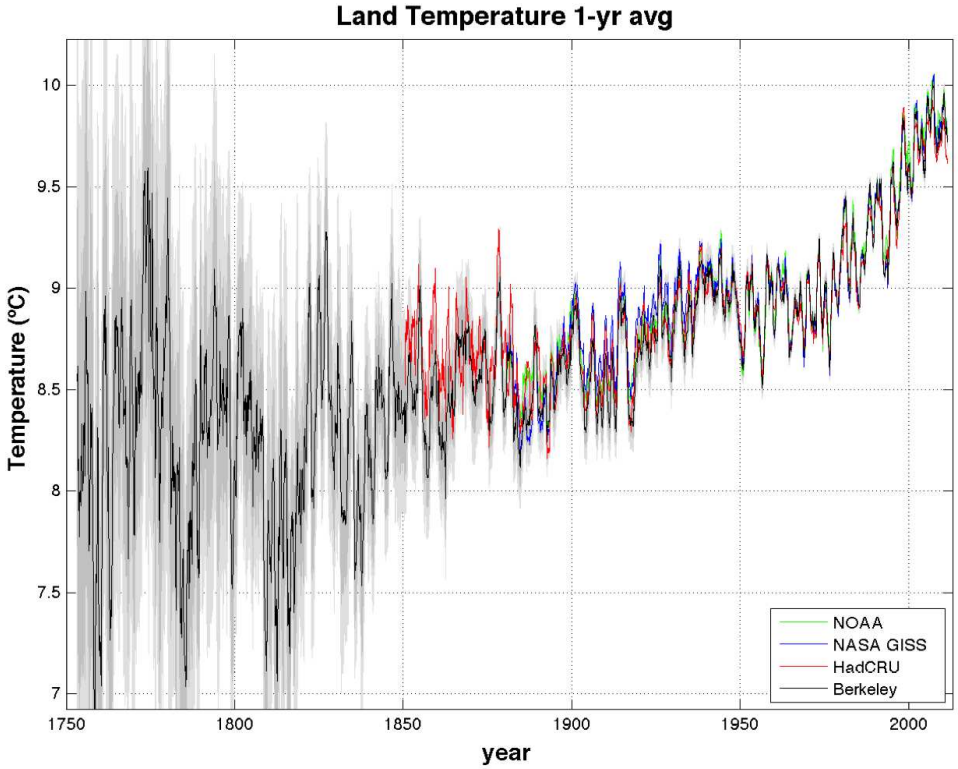

FIGURE 1.2: Comparison of land warming estimates (1-year running averages) of four independent research groups using different datasets (NOAA: National Oceanic and Atmospheric Administration; GISS: NASA's Goddard Institute for Space Studies; HadCRU: Hadley Centre and Climatic Research Unit UK; Berkeley: University of Berkeley). Shading indicates standard spread of the estimates of each dataset. Taken from Rohde et al. (2013).

(Joshi et al., 2011). Under SRES-A1B, Asia is predicted to warm slightly less quickly, and Latin America's warming occurs at the lowest rates, with +2 °C warming being reached exactly during 2050s for most tropical Latin America (except Mexico, where the +2 °C warming is reached during 2060s).

Precipitation changes are regionally varied, but with a global average of 1-2 % increase (depending on the emissions scenario used, Figure 1.4). Precipitation projections are generally much more uncertain than temperature ones (Joshi et al., 2011; Nakicenovic et al., 2000). Figure 1.4 depicts the precipitation changes simulated by the CMIP3 ensemble as average of all GCMs and the period 2080-2099 for the SRES-A1B emissions scenario. IPCC estimates indicate that drier climates are expected along Central America, southern and northern Africa, the Sahel (low certainty), and most of Brazil. By contrast, wetting trends are projected along the Pacific coasts of South America, over the Andes (low certainty), eastern Africa, and most of Asia. Nevertheless, as shown by the black dots of Figure 1.4,

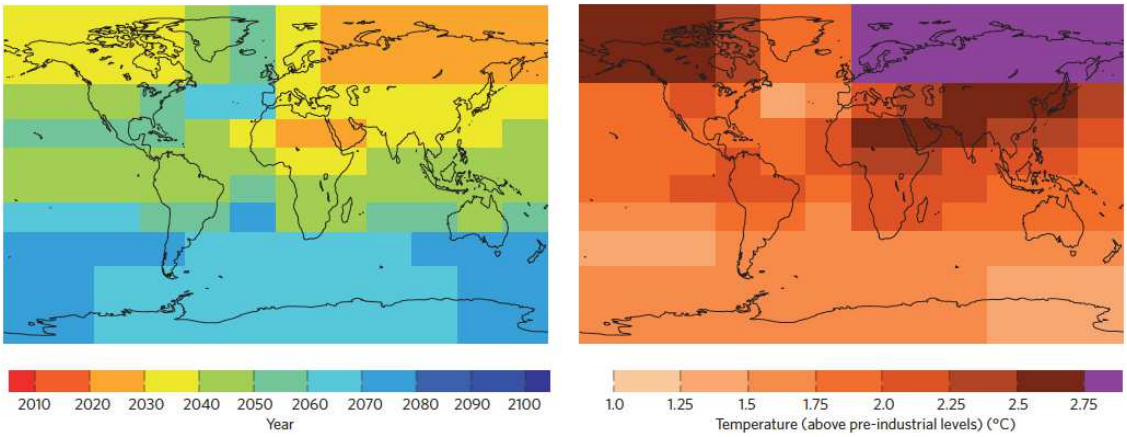

FIGURE 1.3: Projections of temperature increases using IPCC 4AR models (CMIP3) for the IPCC SRES A1B emissions scenario. Median (across GCMs) year of crossing a 2 °C threshold per gridcell (left); and predicted temperature change when global average temperature reaches +2 °C. Taken from Joshi et al. (2011).

precipitation changes need to be treated more carefully than temperature changes due to the inherent uncertainties and lack of skill in existing climate models (Gleckler et al., 2008; Liu et al., 2012; Pierce et al., 2009). Uncertainties and errors in climate models are further discussed in Chapter 4.

1.5 Climate change impacts on agriculture

Agriculture plays an important role in the context of climate change. On one hand, it is a major cause of global warming and as such is part of the solution (i.e. potential to mitigate greenhouse gases emissions) (Hutchinson et al., 2007; Reay et al., 2012). Currently, agriculture contributes to about 20 % of total CO_2 emissions (Hutchinson et al., 2007), 50 % of methane and 70 % of nitrous oxide (Hutchinson et al., 2007; Reay et al., 2012; Thornton and Herrero, 2010) at the global level. In addition, land clearing due to agricultural expansion contributes to 12 % of CO_2 global emissions (Foley et al., 2011; Friedlingstein et al., 2010; West et al., 2010). In order to fully exploit agriculture's potential to mitigate climate change, better waste management, changes in consumer behaviour, policies on land clearing, and improved management practices that allow carbon sequestration will be required. For instance, the use of improved pastures in livestock systems could reduce global agriculture emissions (methane and carbon dioxide) by 12 % (Thornton and Herrero, 2010).

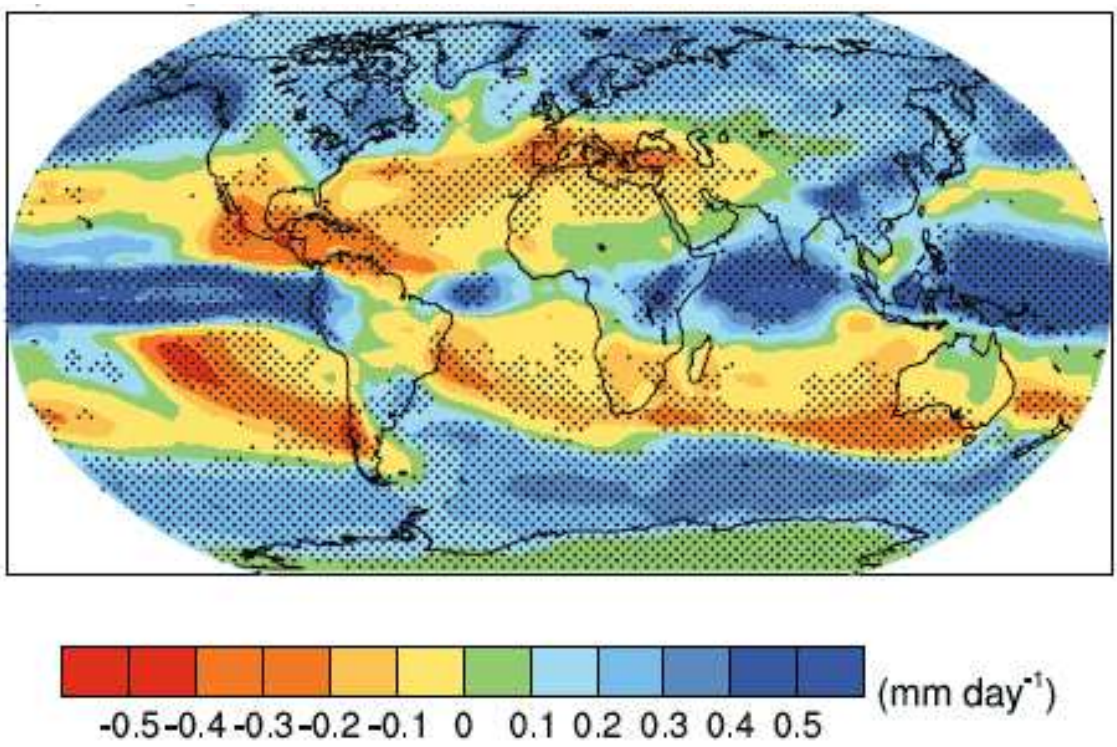

FIGURE 1.4: Multi-model (CMIP3) mean changes in precipitation (mm day[1]) for the period 2080-2099 relative to 1980-1999 for the emissions scenario SRES-A1B. Areas with black dots indicate areas where 80 % or more of the models agree in the sign of change. Taken from Meehl et al. (2007a).

On the other hand, agriculture is one of the most vulnerable sectors to changes in climates, due to its reliance on adequate environmental conditions for achieving high productivity (Huntingford et al., 2005; IPCC, 2007; Lobell et al., 2008). Crops are affected by shortages of water or high temperatures during key periods of their growing cycle (Huntingford et al., 2005; Rattalino Edreira et al., 2011; van der Velde et al., 2012). Effects from adverse environmental conditions have been largely studied and reported by several authors, using combinations of models and data (Allen et al., 2005; Boote et al., 2005; Fuhrer, 2003) and are reviewed in Chapter 2. These can be used to provide initial insights on what could happen under future climate scenarios (Jarvis et al., 2010, 2011a).

Although figures are varied, some of the projected trends in the expected changes are consistent across studies in tropical and temperate regions (Figure 1.5). Most recent literature indicates that negative impacts are expected to affect the basic food basket (i.e. wheat, rice, maize and grain legumes), and the cash crops (i.e. sugarcane, coffee, cocoa) (Krishna Kumar et al., 2004; Laderach et al., 2011; Lobell et al., 2008; Roudier et al., 2011).

The impacts of climate change on agriculture are expected to be widespread across the globe, but it is the developing world where the most severe impacts are likely to be observed (Knox et al., 2012; Lobell et al., 2008; Schlenker and Lobell, 2010) (Figure 1.5), given the larger rates of warming (Figure 1.3), and the lack of adaptive capacity (Park et al., 2012; Tompkins et al., 2010). Decreases in cereal yields of up to 30 % have been projected across Sub-Saharan African, Middle East and Central American countries under unmitigated future scenarios (Lobell et al., 2008; Parry et al., 2004). Even by 2030s decreases of 3-5 % (in the most optimistic scenarios) are expected for legumes (i.e. soybean, dry bean, cowpea), cereals (i.e. rice, maize, sorghum, wheat, barley, millet) in sub-Saharan Africa, western, eastern and southern Asia, and Latin America (Lobell et al., 2008). By contrast, relatively positive impacts have been reported for most root crops due to their hardiness (Jarvis et al., 2012; Schlenker and Lobell, 2010).

Considerable work has been done regarding agriculture and food security under the context of climate change (see e.g. Cooper et al. 2012; Howden et al. 2007; Jarvis et al. 2011a). Adaptation strategies have been suggested for food systems and these include varietal and crop substitution, water and soil conservation practices, better timed fertiliser and agro-chemicals applications, among others. However, a substantial research opportunity arises from the jointure of the agricultural and climate modelling communities. Local and detailed impact assessments and adaptation strategies are still lacking a more comprehensive treatment, analysis and communication of uncertainties, a better depiction of underlying processes governing crop yield responses under future climate scenarios, and a better matching of modelling results with local stakeholder capacities. These evaluations should allow at the same time the identification of knowledge gaps, the identification and testing of appropriate adaptation strategies, and the development of policies at the national and international level (Ranger et al., 2010; Ziervogel and Ericksen, 2010).

1.6 Objectives of the study

This thesis aims at developing a framework for climate change impact and uncertainty assessment for groundnut cultivation in India. Ensemble approaches are used for producing a robust assessment of climate change impacts on crop productivity and suitability as well as to assess associated uncertainties. A process-based ensemble is then used to

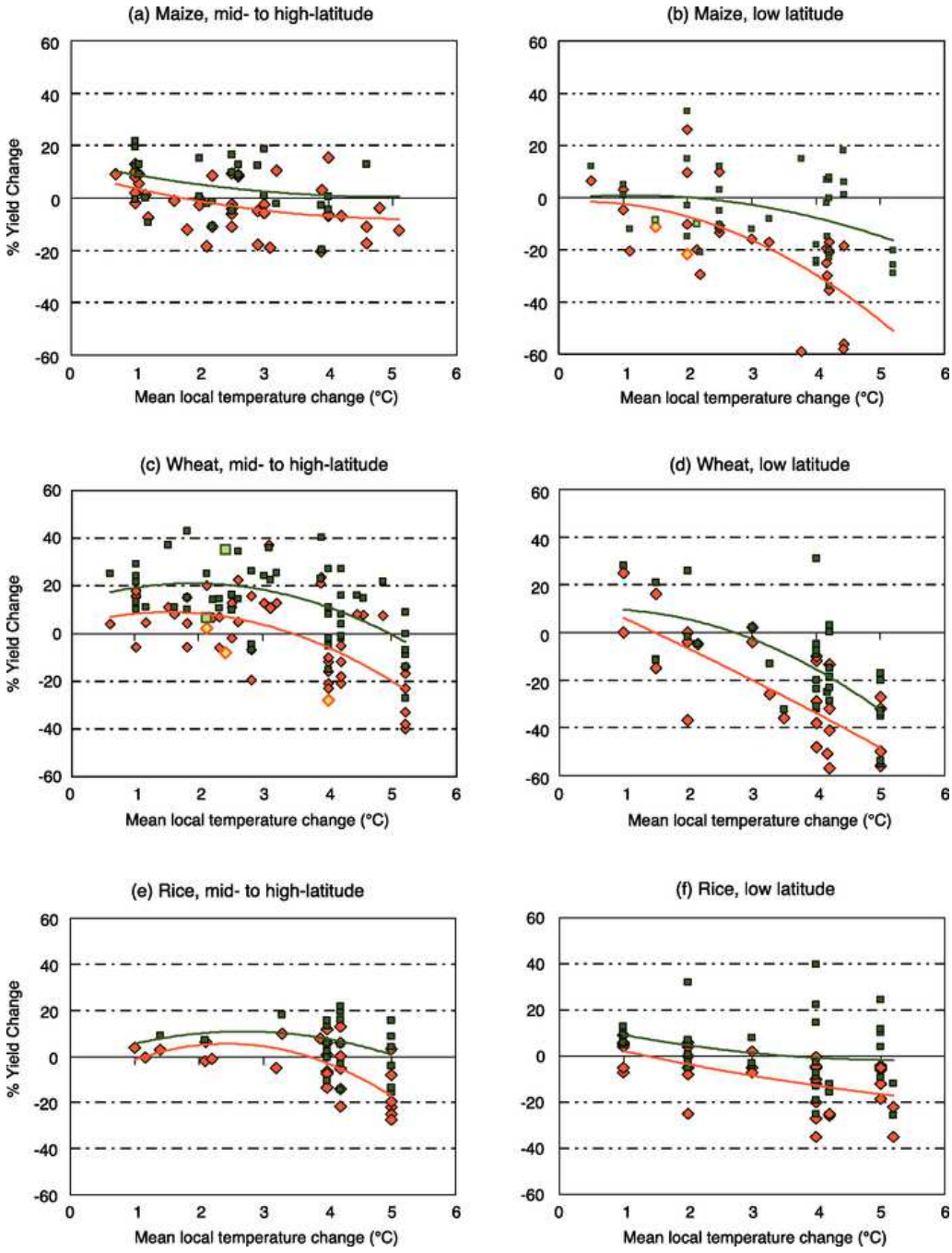

FIGURE 1.5: Sensitivity of cereal yield to climate change for maize, wheat and rice, as derived from the results of 69 published studies at multiple simulation sites, against mean local temperature change used as a proxy to indicate magnitude of climate change in each study. Responses include cases without adaptation (red dots) and with adaptation (dark green dots). Adaptations+ represented in these studies include changes in planting, changes in cultivar, and shifts from rain-fed to irrigated conditions. Lines are best-fit polynomials and are used here as a way to summarise results across studies rather than as a predictive tool. The studies span a range of precipitation changes and CO_2 concentrations, and vary in how they represent future changes in climate variability. Taken from Easterling et al. (2007).

then derive genotypic-level adaptation strategies based upon established concepts of crop ideotypes (i.e. varieties with "ideal" genetic characteristics), to report which processes are most important and which types of varieties would be better adapted to future projected conditions. The main thesis objectives are as follows:

O1 To assess the skill and robustness of observed and simulated available climate data for their use in agricultural studies in Sub-Saharan Africa and South Asia

- O1-A Understand the use of climate data in agricultural impact studies
- O1-B Determine how useful and robust is existing climate information, as predicted based on existing coverage of weather stations
- O1-C Assess how well GCMs reproduce regional mean climates and interannual climate variability

O2 Develop a GLAM perturbed parameter ensemble and quantify the sensitivity of Indian historical (1966-1993) groundnut-simulated yield, harvest index, leaf area index, and biomass to parameter perturbations.

O3 Assess the skill of CMIP5-based crop yield hincasts

O4 Assess the impacts of climate change on Indian groundnut cultivation using ensembles based on GLAM and EcoCrop

- O4-A Project the changes in yields and quantify the uncertainties that arise from climate model structure and initial conditions, bias-correction methods, crop model parameters, crop sowing date, and CO_2 response.
- O4-B Project changes in crop suitability using an EcoCrop-based model ensemble and produce a joint assessment of crop suitability and crop productivity.

O5 Develop a genotypic adaptation strategy for Indian groundnut, using the GLAM ensemble, to reduce negative and capitalise on positive impacts of climate change in Indian groundnut cultivation.

1.7 Research strategy

As stated above, the ultimate goal of this work is the development of adaptation strategies for groundnut cultivation in India. The Indian groundnut cropping system has been selected since (1) India is the second largest producer of groundnut worldwide, (2) groundnut is within the ten most important crops of India in terms of area harvested, (3) production of oil from groundnuts is a key contribution to agricultural GDP (Talawar, 2004), and (4) currently the system is exposed to intense drought in major growing areas (Challinor et al., 2003; Talawar, 2004). The framework of the work presented here is expected to comprehensively account for uncertainties in climate and crop modelling and report on the best-bet and most appropriate genotypic-level adaptation strategies.

The bulk of the work was carried out in five major phases as follows:

- The first phase (Chapter 2) provides, in the form of an extensive literature review, a summary of earlier work (not already reported in this chapter), and summarises the available crop modelling approaches and the ways they have been used for impact assessment. This phase also describes all the data and models used to perform the work presented (Chapter 3).

- The second phase (Chapter 4), based on two published journal articles Ramirez-Villegas and Challinor (2012) and Ramirez-Villegas et al. (2013a) reviews existing and used observed and climate model data, provides an overview of the most-frequently used climate datasets in impacts literature and provides an analysis of errors and uncertainties in present-day interpolated and climate model data (CMIP3 and CMIP5 model ensembles). The chapter concludes by providing recommendations to the use of the CMIP model ensembles and depicting strategies for impact assessment given known errors in input datasets and sensitivities in crop models. The conclusions and recommendations of this chapter are further cited by subsequent chapters.

- The third phase (Chapter 5) parameterises and calibrates GLAM. An optimisation procedure that accounts for the uncertainty in crop model parameters is developed and used to develop a set of equally-plausible parameter sets that can be further

used to assess impacts and adaptation options as well as to assess the robustness of the simulated crop yields.

- Chapters 6 and 7 (fourth phase) perform the climate change impact assessment on indian groundnut using CMIP5 runs for the period 2010-2039 ("2030s") under the RCP4.5 scenario. This phase starts by simulating groundnut yields under baseline and future climates with GLAM (Chapter 6) and then parameterises EcoCrop for assessing climate change impacts on crop suitability (Chapter 7). The two crop models are also combined in Chapter 7. The chapters conclude by showing future vulnerabilities of groundnut production systems in India, and showing the uncertainties arising from the joint assessment of two different measures (suitability and productivity).

- Finally, Chapter 8, based on the projections of Chapter 6 as well as on identified genotypic ranges for crop improvement scenarios uses GLAM to inform about which genotypic adaptation strategies are possible. Impacts of improved varieties are studied using GLAM. The chapter concludes by stating which traits are expected to be the most effective in abating any negative or capitalising on positive impacts of climate change.

As such, the work described here has not been reported in previous literature and is expected to provide a basis for the use of crop models in conjunction with global climate models for the development of regional-level adaptation strategies. The framework developed in this work can be applied to other crops and regions, with the most likely region (where data and/or calibrated GLAM versions exist) being West Africa (sorghum and groundnuts), and the most likely crops (in India) being sorghum and rice.

Chapter 2

Literature review

"Dormir es distraerse del mundo"

J. L. Borges

2.1 Summary

Agriculture relies on appropriate environmental conditions to be successful. In the context of global climate change, it is necessary to understand how plants are likely to respond and what are the necessary adjustments that cropping systems need to make to be able to withstand any stresses associated with or to capitalise upon those opportunities arising from climate change. In this chapter, a literature review is presented that covers the main aspects of climate change impacts and adaptation. The chapter starts by reviewing knowledge on crop responses to elevated temperatures, drought, increased CO_2 concentrations and ozone, and their interactions at the plant level (Sect. 2.2). Plants respond to water, CO_2 and solar radiation because these are used directly in photosynthesis. However, there are a variety of other environmental factors that affect crop growth, amongst which temperature, air humidity and soil fertility are probably the most influential. Four types of crop modelling approaches were reviewed given of the need to represent biophysical processes of crop growth for impact assessment (Sect. 2.3.2). These approaches are varied in input requirements, their outcomes and the scales at which they are normally used, with field-scale process-based models being the most data intensive and complex, and all other types of models having intermediate and somewhat flexible degrees of complexity. The

chapter then describes how crop models are used in a typical projection-based (i.e. predict-then-act) framework (Sect. 2.3). Choices in climate and crop models and in the ways the outcomes of these models are treated in such a framework are expected to produce large uncertainties. Hence, the use of crop-climate ensembles is suggested as a way to quantify such uncertainties. Adaptation of agriculture to climate change is finally discussed, with a particular focus on genotypic adaptation, which in the light of existing literature and to the best of the author's knowledge, can represent a great potential for anticipating and adapting to the negative effects of climate change (Sect. 2.4).

2.2 Crop responses to environmental variations

Agriculture relies on appropriate environmental conditions to be successful. Many crop plants are sensitive to even small variations of temperature, soil moisture, and cloud cover (solar radiation). Production of carbohydrates through photosynthesis depends on appropriate availability of water across the soil profile, CO_2, and light. While increased CO_2 concentrations (such as those expected with climate change) can enhance crop productivity through the production of more biomass (all other factors kept constant) (Leakey et al., 2009; Rosenthal et al., 2012), shortages of water, high temperatures, lack of nutrients and shading can considerably reduce or inhibit photosynthesis (Hew et al., 1969; Rosati and Dejong, 2003). Too low or too high temperatures can decrease photosynthetic rates (Hew et al., 1969; Thuzar et al., 2010), detrimentally accelerate maturation (Lobell et al., 2012; Saman et al., 2010), or damage reproductive organs (Challinor et al., 2005b; Vara Prasad et al., 2002). Likewise, decreases in air humidity (through increases in vapour pressure deficit -VPD) decrease photosynthetic rates, transpiration and biomass production (El-Sharkawy et al., 1985). These and additional stresses are discussed in more detail in subsequent subsections.

2.2.1 Water availability

Either wetter or drier than normal conditions affect crop yields through effects on roots and water uptake, including hypoxia, increased soil impedance, and lodging (Whitmore and Whalley, 2009). Hastened maturity due to terminal drought can cause yield losses in

the range 50-70 % in dry beans (Frahm et al., 2004), 15-80 % in groundnut (Boontang et al., 2010; Rao et al., 1989), 30-40 % in wheat (Dalirie et al., 2010), 12-60 % in chickpea (Saman et al., 2010), and 40-60 % in soybean (Dornbos et al., 1989). The combined effects of intermittent and terminal drought can be catastrophic: 60-80 % reduction in maize yields (Earl and Davis, 2003), 8-10 % per 100 mm rainfall decrease in bananas (van Asten et al., 2011), and 40-100 % yield reduction in groundnut (Rao et al., 1989). Very few crops are reported to respond well (i.e. little or no yield loss) to drought. One exception may be cassava, which keeps the energetic reserves until the stress has been released. Even this hardy crop will decline in productivity if water is not available for more than 2-3 months (El-Sharkawy, 2012; El-Sharkawy and Cock, 1987).

Drought in the first layers of the soil profile can stimulate root deepening (Adiku et al., 1996; Sponchiado et al., 1989) and reduce the amount of available carbohydrate for growth of other plant organs (Chapman et al., 1993; Whitmore and Whalley, 2009). Prolonged stress can cause crop failures if the number of available days with sufficient soil moisture is not enough for a crop to mature appropriately (Jones and Thornton, 2009).

2.2.2 Temperature and light

Photosynthetic efficiency varies with temperature in all crop species because it affects stomatal conductance, intercellular CO2 concentration, and the RuBisCO (Ribulose 1,5 biphosphate carboxylase oxygenase) activity (Bunce, 1992; El-Sharkawy, 2012; Hew et al., 1969). Optimal temperatures for photosynthesis vary by species. Maximum photosynthetic rates have been reported to occur at 30 °C for cassava (El-Sharkawy et al., 1984); 25 °C for arabica coffee (Kumar and Tieszen, 1980); 35 °C for sorghum (Vara Prasad et al., 2006); 28 °C for sweet potato (Sage and Kubien, 2007); 32 °C in cotton (Crafts-Brandner and Salvucci, 2000); and roughly 25 °C for the C3 crops wheat, tomato, and sugarbeet (Kemanian et al., 2004) (Figure 2.1(a)). Above or below these values, net photosynthetic rates can decrease, thus producing less assimilate and leading to reduced productivity.

Apart from decreases in photosynthetic rates, high temperatures can affect reproduction and accelerate senescence. Lobell et al. (2012) report yield losses of ∼50 % for every 2 °C increase in temperature over northern India (the largest producer of wheat globally) due to increased senescence under high (>34 °C) temperatures. Similarly, Lobell et al. (2011a)

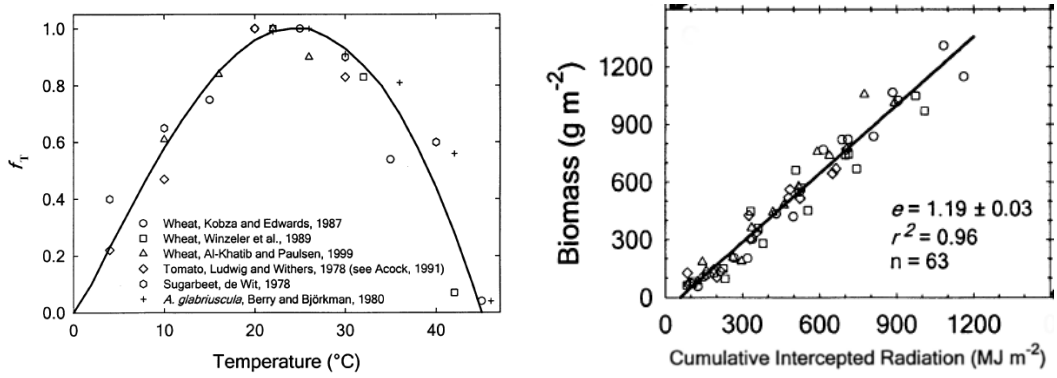

(a) Temperature (b) Solar radiation

FIGURE 2.1: Temperature and radiation responses. **a**: Temperature dependence of photosynthesis for wheat, tomato, sugarbeet and *Atriplex glabriuscula* E. The f_T factor (y-axis) represents a temperature factor that describes the sensitivity of photosynthesis to temperature. **b**: Cumulative biomass (g m^{-2}) as a function of intercepted solar radiation (MJ m^{-2}) in two cultivars of barley. In both cases, details and graph references are provided in Kemanian et al. (2004), from which these figures were taken.

report a reduction between 10-30 % in maize crop yields per +1 °C increase in growing season temperature across most Sub-Saharan African maize growing areas. Effects on other crops might differ in numbers but not in trend. Day temperatures of 36 °C (40 °C) during the flowering stage reduce yield of sorghum by 20 % (100 %) (Vara Prasad et al., 2006) (Figure 2.2(a)). Temperatures of 34 °C (40 °C) during the flowering stage of dry beans can reduce yields by 30 % (100 %) (Vara Prasad et al., 2002) (Figure 2.2(b)). Challinor et al. (2005c), based on data from Kakani (2001), Vara Prasad et al. (1999) and Nigam et al. (1994), reported yield decreases in the range 40-100 % in moderately tolerant genotypes due to prolonged exposure to high temperatures during flowering in groundnut (Figure 2.2(c)). Yields of rice and soybean can be reduced by 54 % and 10 %, respectively, due to high temperatures affecting pollen viability or flower fertility (Allen et al., 2005).

The amount of solar radiation available and intercepted by the crop canopy is also a critical determinant of biomass and yield (Deckmyn and Impens, 1995; El-Sharkawy et al., 1992; Kemanian et al., 2004). Intercepted radiation is generally directly related to biomass and yield (Figure 2.1(b)). At any temperature, net photosynthesis reduces almost linearly with decreases in light intensity and hence shading should be avoided (Long et al., 1983), unless there is a trade-off with excessively high canopy temperatures –such as in coffee (e.g. Schroth et al. 2009).

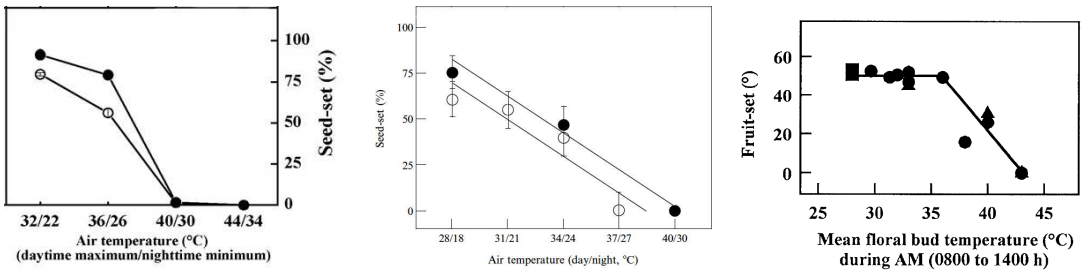

(a) Sorghum (b) Dry bean (c) Groundnut

FIGURE 2.2: Effects of high temperature on seed-set for three globally important crops. (a) Sorghum; (b) common beans; and (c) groundnut. The x-axis in (a) indicates the day/night temperature treatments. In each case, the percent of viable seeds is shown (seed-set percentage). Figures taken from Vara Prasad et al. (2006) for (a), from Vara Prasad et al. (2002) for (b), and from Vara Prasad et al. (2000) for (c). Different circle fillings in (a) and (b) indicate two different CO_2 concentration treatments: 350 ppm (full circles) and 700 ppm (hollow circles).

2.2.3 CO_2 concentrations

Increased CO_2 concentrations are thought to increase dry matter and thus yield (Leakey et al., 2009). CO_2 stimulation experiments have only been carried out in a limited number of places or for a limited number of crops. Comprehensive reviews exist that document the effects of elevated CO_2 on crop production (e.g. Fuhrer 2003, Kimball et al. 2002, Boote et al. 2005, and Leakey et al. 2009). These and other studies point out to the following figures: 12 % increase in biomass of C3 grasses, 10-15 % yield increase in rice and wheat (Amthor, 2001; Kimball et al., 2002), 28 % increase in potato yield (Fuhrer, 2003; Kimball et al., 2002), 20 % higher yields in sweet potatoes (Bhattacharya et al., 1985), 100 % increase in cassava root yield (Rosenthal et al., 2012); 45 % yield increase in soybean (Baker et al., 1989); 25 % yield increase in sorghum (Vara Prasad et al., 2006); and 16 % increase in groundnut yields (Vara Prasad et al., 2003). Led by the consensus of previous studies, Leakey et al. (2009) drew six important inferences about CO_2 enrichment:

1. Carbon uptake is enhanced by elevated CO_2 concentrations
2. Photosynthetic nitrogen use efficiency increases at elevated CO_2 concentrations
3. Water use both at leaf and canopy scales declines at elevated CO_2 concentrations
4. Dark respiration is significantly stimulated in soybean leaves grown under elevated CO_2 concentrations

5. Stimulation of carbon uptake from elevated CO_2 concentrations in C4 plants is indirect and occurs only in situations of drought

6. The CO_2 'fertilisation' effect in FACE (Free-Air CO_2 Enrichment) studies on crop plants is less than expected.

The effects of increased CO_2 are beneficial for almost any food crop. However, knowledge on crop responses to elevated CO_2 concentrations is in need of further development, and this has been a priority for research on crop-climate impacts for the last 15 years (Ainsworth and Long, 2005; Leakey et al., 2009) and will likely remain to be critical for future climate impacts research. Particular attention must be placed on understanding the interactions between CO_2 and other environmental controls (particularly drought and high temperatures), as these remain only partially understood (White et al., 2011b), and also because high CO_2 concentrations could (in some cases) worsen the effects of other stressors such as high temperatures or drought (Vara Prasad et al., 2006).

2.2.4 Other factors

A large number of other factors exert control on plant growth and, particularly, on photosynthesis, biomass accumulation and yield. Leaf nitrogen (N) content is strongly and positively associated with carbon exchange rates (CER), radiation use efficiency (RUE) and total plant biomass (Sinclair and Horie, 1989). Maize and rice are amongst the most sensitive crop species to N deficiencies, whereas the grain legumes (i.e. soybean, dry bean, peanut) have less sensitive responses. In maize, even relatively small ($\sim$15 %) decreases in leaf N content can severely decrease CER and RUE ($>$ 50 % decreases) (Sinclair and Horie, 1989). Similarly, low phosphorous (P) and potassium (K) contents can also lead to limited CER and biomass production (Fredeen et al., 1990; Longstreth and Nobel, 1980). Effects of other nutrients (e.g. calcium, magnesium, sulphur, zinc, and iron, among others) are evident but research on their effects on plant processes is sparse. Limited availability of one or more of these nutrients can limit plant growth and reduce the nutritional quality of the harvested product (Fredeen et al., 1990; Gaidashova et al., 2010). Responses to ozone (O_3) are expected to be detrimental, but limited research has been carried out regarding its effects on most food crops (Ewert and Porter, 2000; Fuhrer, 2003; Hollaway et al., 2011).

2.2.5 Interactions between factors

Plant responses to environmental factors and their interactions are largely non-linear (Asseng et al., 2004; Boote et al., 2013). Factors operate against plant growth and also against each other in ways that are often difficult to understand. For an example: under optimal temperatures and water availability, photosynthesis and transpiration from leaves occur at normal rates; however, under high temperatures plants open their stomata to avoid heat stress, which increases CO_2 concentrations and thus biomass accumulation (exception being made under high VPD conditions –dry air, as in such a case stomata would remain closed to avoid excessive transpiration). If the available soil water is limited, this induces desiccation and stomata are then closed. Drought causes desiccation and stomatal closure, but at the same time water is a direct input of photosynthesis and so the effects on carbon fixation are more direct than those of temperature. In addition, stomatal closure causes within-leaf CO_2 concentrations to decrease, thus decreasing inputs to photosynthesis, in some cases also increasing photorespiration (Kobza and Edwards, 1987). This causes lower biomass production and limits growth (Hew et al., 1969; Huntingford et al., 2005). Low light incidence (i.e. solar radiation) also reduces photosynthesis, whereas winds increase transpiration. Salinity in soils increases osmotic pressure and reduces the available water to the plant thus causing drought stress. Many limiting conditions can occur simultaneously in a given site, thus making any prediction a challenging task (Challinor et al., 2009b).

Interactions between the abovementioned factors add further complexity to understanding plant responses, while also impacting crop productivity. Mueller et al. (2012) report that most of the yield gaps in the developing world are caused by a combination of lack of nutrients and water. In recent analyses using multi-site trial data, Lobell et al. (2011b) report that the sensitivity of maize genotypes to temperature increases more than twofold under drought. Gourdji et al. (2013) have shown that low values of VPD (i.e. dry air conditions) increase the sensitivity of wheat genotypes to higher temperatures by roughly 50 %, particularly during grain filling (Figure 2.3).

Under high temperatures CO_2 effects might be offset or even detrimental. In sorghum and dry bean, for instance, increased CO_2 concentrations under high temperatures have been found to enhance the negative effects of high temperatures (Vara Prasad et al., 2002, 2006)

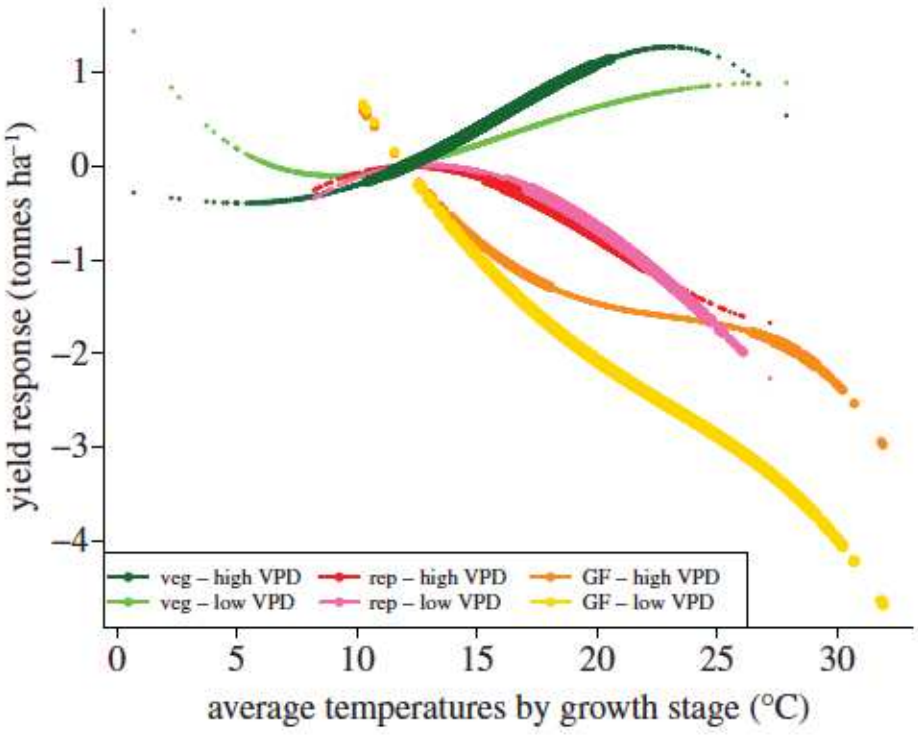

FIGURE 2.3: Inferred temperature response curves by growth stage for wheat. Taken from Gourdji et al. (2013).

(Figure 2.2(a), 2.2(b)). Some of these responses, however, might vary spatially and temporally due to changes in VPD, water availability and soil characteristics (Whitmore and Whalley, 2009). Moreover, experiments that quantify the genotype-by-environment (GxE) interaction of these responses are generally lacking, which results in increased uncertainty in model predictions (Challinor and Wheeler, 2008b).

2.3 Assessing impacts and quantifying uncertainty

In order to adapt agriculture to future climates, policies regarding investments on adaptation need to be set (Howden et al., 2007). Policy makers and other researchers need to have information on the characteristics of impacts (i.e. which systems, when, to what extent, and where) and because anything that can be said regarding the future is merely a projection, also on the uncertainties associated to such impacts. A variety of methods have been developed that use information of different types and scales to develop projections of how agricultural systems might look like in the future, and from these, propose adaptation

options to respond to these changes. These methods are summarised in the sub-sections below.

2.3.1 Approaches for climate change impact assessment

According to Challinor et al. (2013), methods to assess impacts can be classified in projection-based approaches and utility-based approaches. Utility-based approaches (also known as decision-based approaches) focus on making decisions that are robust against the known uncertainties. This is usually done by exploring the outcomes of decisions under a number of plausible scenarios and then choosing those decisions whose outcomes are not affected by the underlying uncertainties (Dessai et al., 2009; Mearns, 2010). Projection-based approaches (also known as predict-then-act approaches) are based on the use of models and data to produce projections of a given system's future state that can be used by decision makers (Challinor et al., 2013). Projection-based approaches therefore focus in reducing uncertainties in order to provide decision-makers with information that can be directly used to make a decision (Challinor et al., 2013; Mearns, 2010). The work presented in this thesis can be classified as a predict-then-act approach. Therefore, a summary of related methods is provided. For further discussion on decision-based approaches the reader is referred to Dessai et al. (2009).

Figure 2.4 shows the process of agricultural impact assessment in a typical projection-based framework. Global climate model projections are produced on the basis of a given set of forcing scenarios (see e.g. Moss et al. 2010) and then scaled and/or bias-corrected to produce climate scenarios with which crop models are forced to produce a range of projections that are then used to conceptualise and develop adaptation strategies that are then implemented at different scales (from global to the field). Within this process, information can be produced at different scales and using different methods, to reach the final goal of developing a robust adaptation measure.

Ramirez-Villegas and Challinor (2012) conducted a meta-analysis of circa 250 peer-reviewed publications published between 1981 and 2011. Publications that use climate information of any sort for any type of agricultural modelling were used to determine general trends in the use of both models and data (see Chapter 4 and Ramirez-Villegas and Challinor 2012 for methodology, and Appendix A for list of publications). The analysis revealed that most

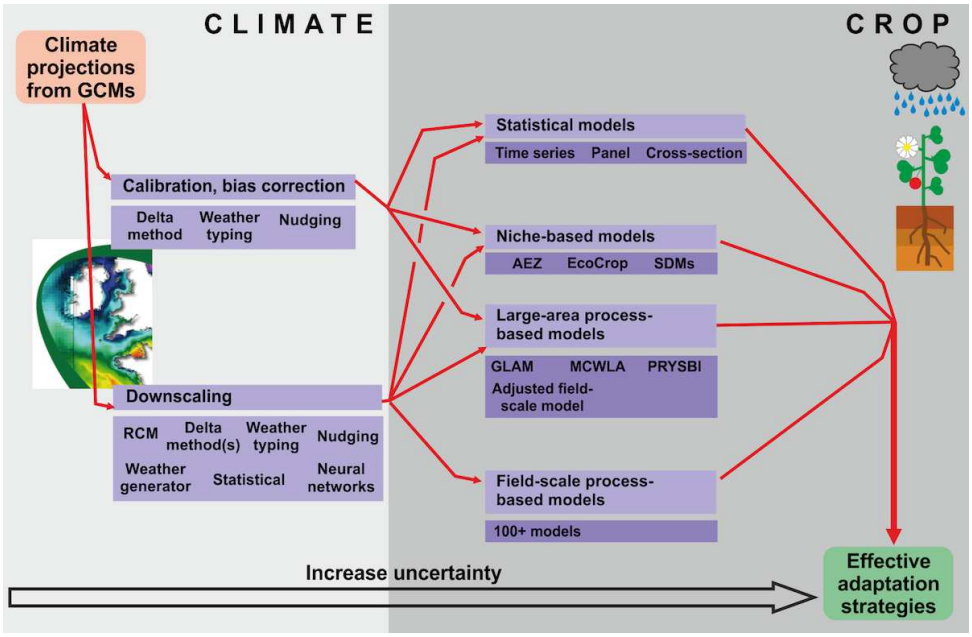

FIGURE 2.4: Ways in which impact assessment has been done in projection-based frameworks. Red arrows indicate flow of information. The black hollow arrow in the bottom shows that as long as more information is derived from climate projections, uncertainties are likely to increase, as a result of what is known as "cascade of uncertainties" (every step in the process of impact assessment has its own associated uncertainties).

of the studies focused on a site-specific scale (Figure 2.5) and used process-based models (Figure 2.6). From the studies using process-based models, field-scale models constituted the vast majority. Hence field-scale crop models have played and will probably continue playing a critical role for agricultural modelling, both for present-day and future simulations of crop yield. The more frequent use of these models is because they often include a wider range of complex processes related to photosynthesis and respiration (Challinor et al., 2009b; El-Sharkawy, 2005; Whisler et al., 1986) and thus give a sense of precision. As a trade-off, field-scale models are highly data intensive (Craufurd et al., 2013).

The choice of both crop models and climate model projection types for climate change impact assessment varies across modelling studies (White et al., 2011b). Such choice is contingent on the methods that can be used to match the scales between GCMs and the crop models, and on the associated uncertainties (Challinor et al., 2009b). To some extent, however, it is also a subjective choice made by the researcher. Agricultural, and more specifically, crop models, require climate information as an input to develop predictions of crop yields. For developing impacts projections, ideally, the outputs of a high resolution GCM should be plugged directly into the field-scale crop models. However, due to the

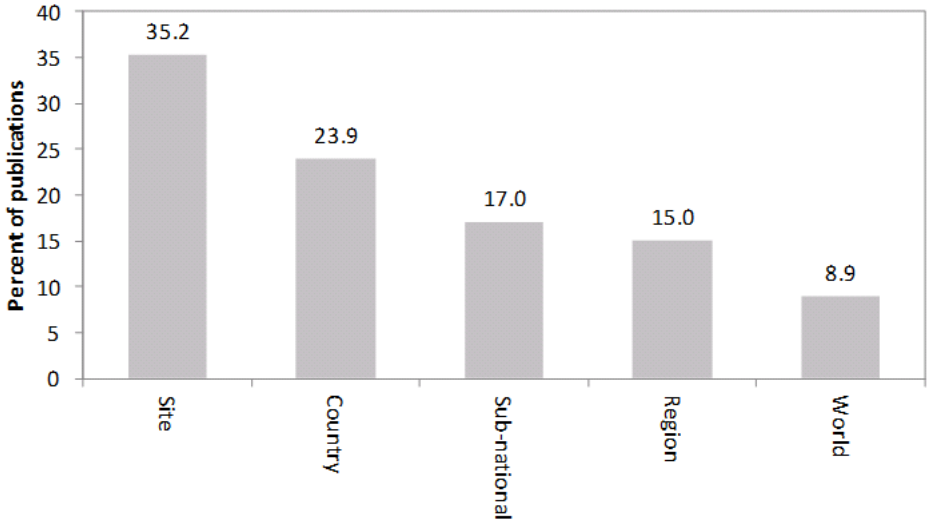

FIGURE 2.5: Scale at which agricultural modelling studies have focused.

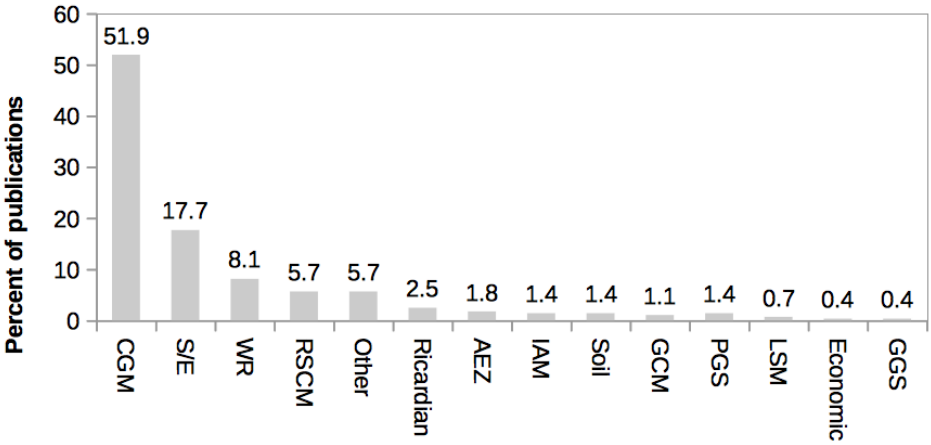

FIGURE 2.6: Types of models typically used in agricultural modelling studies. CGM: field-scale process-based model, S/E: Statistical and/or empirical, WR: water resources and/or hydrology model, RSCM: regional-scale crop model, AEZ: Agro-Ecological Zoning, IAM: Integrated assessment model, GCM: global climate model, PGS: pest and/or disease simulation model, LSM: livestock simulation model, GGS: grassland simulation model.

inherent errors and uncertainties in climate models and to lack of computational capacity, the issue of scale-matching is not a trivial one (Challinor et al., 2009b; Gleckler et al., 2008; Weaver et al., 2013). Matching scales between crop and climate models requires either upscaling the crop model output to the climate model grid (e.g. Jagtap and Jones 2002), downscaling the climate model output to the crop model scale (Giorgi et al., 2009; Themessl et al., 2012), or upscaling the model parameters and/or processes to the climate grid (Challinor et al., 2004; Iizumi et al., 2011).

For producing impacts projections without downscaling, GCM information can be bias-corrected in various ways so as to feed crop models or can also be used in its raw form. Bias correction consists of calculating the GCM bias (or another type of error) using the "true" values (i.e. observations) of a given climate field and then using it to correct the GCM output. There are various types of bias correction methods, including a simple 'nudging' to the means, or a correction to the means and the variability (Hawkins et al., 2013b), but also more complex methods based on mapping of probability distributions (see Ehret et al. 2012). Coarse resolution GCM output can also be treated via weather typing (Jones and Thornton, 2013). That is, matching current observed with future predicted monthly weather patterns and then associating daily weather to these characterised monthly patterns. Bias corrected GCM simulations at coarse scales can be used as inputs into statistical, niche-based models, and into regional-scale process-based models.

Downscaling can be exercised in various ways so as to produce high resolution impacts projections. RCMs are the most climatologically robust means to downscale GCM information (Giorgi, 1990; Wilby et al., 2009), but as RCMs are climate models themselves they are subjected to similar uncertainties and errors as GCMs, and may require further bias correction (Baigorria et al., 2008). Other methods include the use of weather generators (Jones and Thornton, 2013), the use of statistical regressions (Zhang et al., 2012), quantile mapping (Iizumi et al., 2012a), artificial neural networks, and the delta method (Tabor and Williams, 2010). Each method has its own pros and cons. Wilby et al. (2009) provide a more comprehensive overview of existing downscaling methods than is attempted in this thesis. The choice of downscaling or bias correction technique can add significant uncertainty to an assessment (Hawkins et al., 2013b; Iizumi et al., 2012a; Khan et al., 2006). To the best of the author's knowledge, the skill of these methods and how well they compare with statistical and large-area models is yet to be seen, as no study has focused on comparing uncertainties due to this process with uncertainties in other processes in impact assessment (e.g. parameter uncertainty, crop-model uncertainty, climate model uncertainties, uncertainty in initial conditions).

The various ways in which GCM outputs can be post-processed, in combination with the large number of crop models that exist (Sect. 2.3.2) have given rise to a rather large number of paths for impact assessment (Figure 2.4). These include the use of models of different natures together with or without downscaled data, and with or without bias corrected

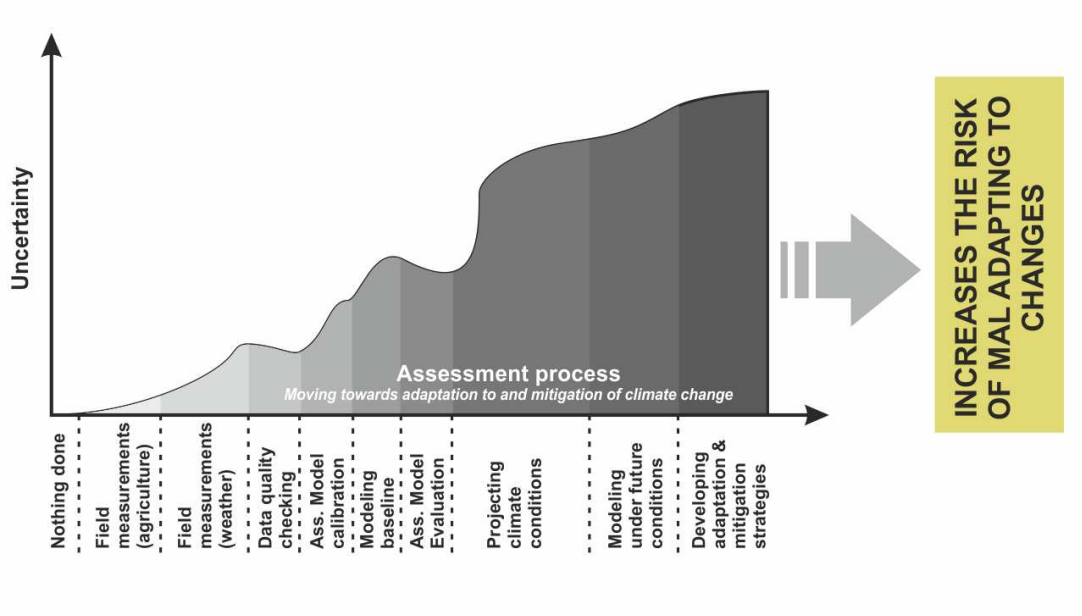

FIGURE 2.7: Uncertainties involved in climate change impact assessment. The more processes involved, the larger the uncertainty, and the larger the likelihood of choosing an inappropriate pathway for adaptation. Slopes and sizes of columns are not meant to indicate real relationships between relative uncertainty contributions.

data. Steps in the projection-based framework shown in Figure 2.4 are thus varied and can produce differing responses, thus causing uncertainty (Figure 2.7). It is expected for almost all steps in the impact assessment process that uncertainty is increased, although it can be reduced via model calibration and evaluation. The reviews of Knox et al. (2012) for South Asia and Africa, of Roudier et al. (2011) for Africa and the IPCC Fourth Assessment Report (Easterling et al., 2007) are particularly useful in identifying the large uncertainties to which impact projections are subjected.

It is due to this uncertainty that choices of GCMs, emissions pathways, crop models and the methods used for treating GCM outputs need to be done judiciously (Challinor et al., 2013, 2014). Cropping systems need to be simulated with an appropriate degree of complexity, although assessing such a degree may require an stepwise add-and-remove modelling approach, which may imply longer lead times in the research process (Affholder et al., 2012). Enough complexity needs to be put in models so as to capture well enough the spatio-temporal variations in cropping systems responses. Likewise model over-parameterisation needs to be avoided (Challinor et al., 2009b). This will reduce the risk of having models that are incapable of simulating the processes implied in a given response, or model parameters that cannot be adequately constrained with the available observational data

(Challinor et al., 2013). The use of multiple approaches to assess a single response (e.g. Rosenzweig et al. 2013, Tubiello and Ewert 2002), or novel approaches that sample uncertainties (Iizumi et al., 2011) to create multi-model ensembles is a way in which the robustness of the results can be assessed (Challinor et al., 2013). This would also allow the exploration of new ways to report impacts, processes underlying such impacts and any associated uncertainties. The further study of the relative importance of the different sources of uncertainty is also a topic of suggested future focus (Hawkins and Sutton, 2009).

2.3.2 Crop modelling

Based upon knowledge on plant responses, models that simulate one or more aspects of crop production have been created. These are also referred to as crop simulation models or simply crop models. Crop models have been created in an attempt to develop tools that are helpful for research, farming and policy making (Boote et al., 1996; Challinor et al., 2009c). Models are useful to make inferences of crop plant responses under novel conditions, including those that can arise from climate change. This process has the advantage of avoiding carrying out extensive agronomic trials (Craufurd et al., 2013; Reynolds et al., 2011), but requires extensive knowledge and data to be incorporated into the crop model in order to avoid mis-prediction (Challinor et al., 2009c). It also requires a careful assessment of the modelling outputs.

Rivington and Koo (2011) report the existence of 122 crop models, from which roughly a half are process-based. Three quarters of the 122 models operate at field. With the increasing importance of climate change impacts and adaptation, the development of new crop models and/or the improvement of existing ones have become critical tasks (Rosenzweig et al., 2013). In the below sub-sections, models of different nature are described, including a discussion of their relative benefits and limitations. These are followed by a review of crop model ensembles.

2.3.2.1 Statistical modelling

In statistical models, linear or non-linear regressions are fitted using weather variables (i.e. precipitation, temperature) as predictors of an independent variable (e.g. yield, production). Statistical models are being increasingly used for climate change studies, often

at relatively large spatial scales and in areas where yield-climate relationships are strong (e.g. Schlenker and Lobell 2010), such as in rainfed systems where seasonal precipitation is the main driver of crop yields (Lobell et al., 2008). Under these conditions robust regression fits can be achieved with measures of weather during the growing season (Lobell and Burke, 2010).

Statistical models can be constructed using different types of spatio-temporal data. Time series models are constructed for individual points or regions using a time series of both yield and weather. Panel models develop regressions using both temporal and spatial data. Cross-section methods are used only with spatial data (Lobell and Burke, 2010; Mueller et al., 2012). Time series models are often preferred due to their better performance, and because they are able to capture the site- or region-specific crop yield responses (Lobell and Burke, 2010; Schlenker and Lobell, 2010). However, cross-section and panel methods have been used to explore crop responses using multi-site agronomic trial data (Lobell et al., 2011b).

There are many advantages in the use of statistical models to describe crop responses to environmental factors. First, parameterising the models is a relatively simple process in which observations of both agricultural yields and weather are used in a multiple linear or non-linear regression. Second, parameter uncertainties can be quantified (e.g. by using cross-validation) and explicitly accounted for in any predictions and projections (see e.g. Lobell et al. 2008; Schlenker and Roberts 2009). Third, even simple measures of weather (e.g. mean growing season temperature, seasonal total precipitation) can be used to produce robust regression fits, thus making the approach less data intensive in relation to process-based models, which require daily data (Lobell and Burke, 2010). Fourth, the nature of the model and of its constituting elements (i.e. regression terms) allows the researcher to assess the importance and effect of the variables included in the model (e.g. by comparing the parameter estimates in the regression). Fifth, it is easy to include non-climatic factors that affect crop yields in the model (i.e. pests or diseases, management practices) or more detailed measurements of weather, provided the data are available. Finally, the models are easy to implement within a system (e.g. a seasonal forecasting system) and are computationally inexpensive.

The use of the simple and convenient statistical models has, however, a number of caveats. First, there is a higher likelihood of failing to capture the response of the crop. A crop

model that fails to reproduce observations may indicate the lack of certain processes, including pests and diseases, management, and competition with weeds. Secondly, transferability of the models may be limited and thus predictions in ranges under which the model has not been developed must be exercised with caution. Third, variable co-linearity can be detrimental and/or mis-leading (Lobell and Burke, 2010; White, 2009). Lastly, given that the models are purely data-driven, it is difficult, if at all possible, to account for the interactions between processes at the plant level (White, 2009). For instance, accounting for the effects of increased CO_2 on canopy temperature (Long et al., 2006), or accounting for the interactions between high temperatures, drought and high CO_2 concentrations (Challinor et al., 2009c).

2.3.2.2 Niche-based modelling

A general principle in niche-based modelling is that its outcome is (generally) not agricultural yield. Predictions made by means of these techniques are subject to the development of intermediate, yet useful measures of crop potential suitability (Lane and Jarvis, 2007; Schroth et al., 2009). These measures can be used to plan agronomic trials, transfer technologies, expand existing croplands, and project the impact of climate change (Laderach et al., 2011). Suitability is here referred to as the degree at which a crop species can successfully grow at a given location or under a specific combination of biotic and abiotic factors, and is commonly measured in a scale that ranges from 0 (not suited) to 1 (perfectly suited). Measures of crop suitability are also often expressed as percentages (Lane and Jarvis, 2007).

Niche-based modelling can itself be divided into two main categories. The first and probably most widespread technique is **ecological niche modelling (ENM)**. ENM is based on the development of empirical relationships between a set of environmental predictors and the probability of presence of a species (Jimenez-Valverde et al., 2008; Soberon and Nakamura, 2009). ENM techniques aim at identifying the potential niche of a species, which is the potential "*subset of environmental conditions in which a species can have positive growth rates*" (Jackson and Overpeck, 2000; Soberon and Nakamura, 2009). ENMs predict relative occurrence rates, or, under certain assumptions also the probability of occurrence (Merow et al., 2013). A number of ENM models (ENMs) of varied mathematical principles exist to date. Amongst the most frequently used there are the maximum entropy algorithm

(Phillips et al., 2006), boosted regression trees (Elith et al., 2008), simple climate-envelope models (Busby, 1991), support vector machines (Drake et al., 2006), general linear models (Austin, 2002), and generalised linear models (Guisan et al., 2002). These models have been used to estimate potential crop production niches and to subsequently estimate the impact of changing climate conditions on such niches (e.g. Schroth et al. 2009).

A second category of niche-based modelling techniques is that of **agro-ecological zoning (AEZ)** (Fischer et al., 2002, 2005), also referred to as **basic mechanistic models (BMM)** (Hijmans and Graham, 2006; Ramirez-Villegas et al., 2013b). In these models, crop-specific limitations of prevailing climate, soil, and terrain resources are identified and used to estimate crop suitability. In some cases, crop suitability is then scaled to determine maximum potential and agronomically attainable crop yields for land units, under varied crop management assumptions (Fischer et al., 2002, 2005). In other cases (e.g. EcoCrop, Ramirez-Villegas et al. 2013b), crop suitability indices from AEZ/BMM models are used as indicators of the probability of occurrence or success of plant populations -as in ENMs (see above). AEZ/BMM approaches sit in between process-based models and the more general niche-based models in the sense that they take into account some of the mechanistic detail in the crop-climate interactions, whilst at the same time generalising the results to broad agro-ecological areas in which crop suitability and production potentials are at maximum levels. AEZ/BMM methodologies have been used to predict the impact of climate change on agriculture and trade at the global level (Teixeira et al., 2013). These models are capable of reproducing, realistically, regional and global trends in crop production and suitability (Fischer et al., 2005; Ramirez-Villegas et al., 2013b; Teixeira et al., 2013).

A number of advantages exist when using niche-based models for predicting crop responses and these can be generalised for the two aforementioned approaches. First, similar to statistical regressions, niche-based models have the advantage of being relatively easy to parameterise and implement in computational systems. Parameterisation in ENMs is similar to developing regression fits (Elith et al., 2006), and in AEZ/BMM models is based on defining a relatively low number of model parameters (Fischer et al., 2002; Ramirez-Villegas et al., 2013b). A second advantage of niche modelling is that the models can be generalised to spatial domains (e.g. country, continent, or the globe) (Merow et al., 2013; Soberon and Nakamura, 2009). Third, AEZ/BMM also allow mapping some of the

interactions between environmental factors in a relatively mechanistic fashion, which allows a better analysis of climate-related constraints to agriculture (Jarvis et al., 2012; Schroth et al., 2009). Fourth, as a result of the easiness in parameterising the models, a larger number of crops can be analysed using niche-based models. For example, Lane and Jarvis (2007) used EcoCrop to assess 43 food crop species under climate change. This provides the opportunity of performing more comprehensive analyses of food security. Finally, the models are generally flexible in terms of incorporating new drivers of production and often do not require a high level of temporal detail in the input data (Jarvis et al., 2012; Soberon and Nakamura, 2009).

Many of the limitations to niche-based models have been discussed elsewhere: Soberon and Nakamura 2009 and Terribile et al. 2010 for ENMs, Ramirez-Villegas et al. (2013b) and Chapter 7 for EcoCrop, and Fischer et al. (2005) for AEZ. Here, the limitations are thus listed only in general terms. First of all, the models lack the necessary varietal detail to develop more precise predictions at the farm level, or to develop adaptation strategies. In principle, however, sufficient varietal-level data or characterisation should allow making predictions of individual varieties. Secondly, ENMs are generally not transferable into areas or conditions for which they were not developed. Sample bias and spatial autocorrelation has a significant impact the accuracy of ENM predictions (Hijmans, 2012), and can lead to predicting unrealistic niche shrinkage in future climate scenarios (Loiselle et al., 2008; Peterson et al., 2007). Suitability or even yield potentials are also difficult to relate to actual farmers yields and have limited applicability in managed systems where fertilisation and/or irrigation are prevalent (see Chapter 7). Finally, testing varietal-level adaptation strategies (i.e. breeding scenarios) is not possible. This may be attributed to the simplicity of the approaches. None of these models can appropriately account for responses to CO_2 fertilisation.

2.3.2.3 Field-scale process-based modelling

Field-scale crop models are tools aimed to simulate growth processes in plants so that technological changes and environmental effects at the farm level can be assessed (El-Sharkawy, 2005; Hoogenboom et al., 1994). Initially, crop models were conceived with the objective of being perfect and comprehensive, and able to reproduce all plant functions (Affholder et al., 2012; Sinclair and Seligman, 1996). However, researchers rapidly realised

that developing approaches that were theoretically coherent, yet different in their implementation and purpose was more efficient and probably more informative. Crop modelling science has thus evolved, and this evolution has led to the development of a large number of crop models (Rivington and Koo, 2011).

Field-scale models attempt to capture as many as possible key processes that occur in the plant with the greatest level of detail possible. The choice of which processes to represent in detail, and the level of detail achieved for a given process is mostly limited by the understanding of crop physiology and by available data (Boote et al., 2001; Craufurd et al., 2013). In some cases, this choice may be driven by the purpose of the model (Affholder et al., 2012; Challinor et al., 2009c). For example, developing a crop model for hydrological and soil-related applications would require the water balance component of the model to be very well developed and calibrated (Williams et al., 1989). By contrast, developing a model to predict phenology and frost damage does not even require a water balance to be calculated (Eccel et al., 2009). Developing a model that can accurately predict agricultural yields and harvest timings at the field scale would require both processes (and many others) to be correctly parameterised (Boote et al., 1996).

Field-scale models all hold different assumptions and hence show varied predictive skill. Jamieson et al. (1998) demonstrated that high predictive skill in yield prediction in various crop models does not imply agreement in the underlying processes (e.g. LAI evolution, biomass assimilation) both across the models and between each model and the observations (Figure 2.8). Similarly, Bachelet and Gay (1993) found that impacts of high temperatures on grain yield varied significantly (12-62 %) among four rice simulation models, but showed that more detailed models were also the most skilled ones (CERES-Rice and MACROS). The same study showed that these two crop models held significant differences in the ways they simulated the interaction between high temperature and high CO_2 concentrations (Figure 2.9) (Bachelet and Gay, 1993). In principle, however, models can be parameterised to match observations or to match other models by varying the so-called "genetic coefficients", a concept that has been widely practiced by crop modellers (Baenziger et al., 2004; Boote et al., 2003).

Probably the main advantage of a field-scale model is the fact that the models can be used to make decisions that can have a direct effect on farmers. Many crop modelling studies rely on the use of a field-scale model, primarily because the prediction of the model (if

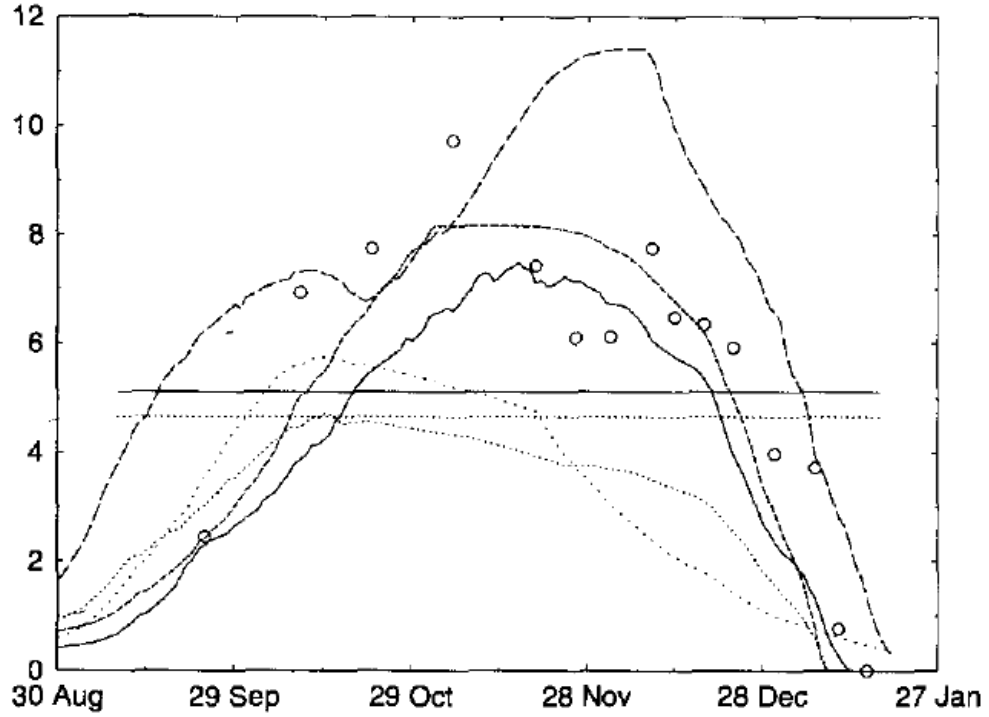

FIGURE 2.8: Comparison of model predictions of the time course of LAI with observations for a number of models. Hollow dots are observations. AFRCWHEAT2 (___), CERES-Wheat (.....), Sirius (_ _ _ _ _), SUCROS2 (. . . . . .) and SWHEAT (– – – – – –). The horizontal lines represent a radiation interceptance of 90 %. (____) for AFRCWHEAT2 and Sirius, (.....) CERES-Wheat, SWHEAT and SUCROS2. Taken from Jamieson et al. (1998).

the model is well parameterised and if all associated data –soils, initial conditions and weather– correctly reflect the field's conditions) would closely reflect the response of the plants in the field (Boote et al., 1996; Easterling et al., 2003; Meinke et al., 1997). This allows the researcher making decisions at the scale that is relevant for the farmer, and allows impacting agricultural production more directly (Jones et al., 2003). Second, by modelling more processes and in more detail, the models can be used to identify a wider variety of processes that are influential to crop yields under future scenarios. Third, by being modular, most of these crop models allow some flexibility in how certain processes are modelled. For instance, some of the Decision Support System for Agrotechnology Transfer (DSSAT) models allow the use of three biomass accumulation equations (including Farquhar's photosynthesis, Alagarswamy et al. 2006) and two evapotranspiration equations (Jones et al., 2003). Fourth, carbon balances in the plant are often modelled, thus allowing a more profound analysis of source-sinks in the plant. Fifth, the detailed incorporation of "genetic coefficients" allows the further link with actual genetic data into crop model

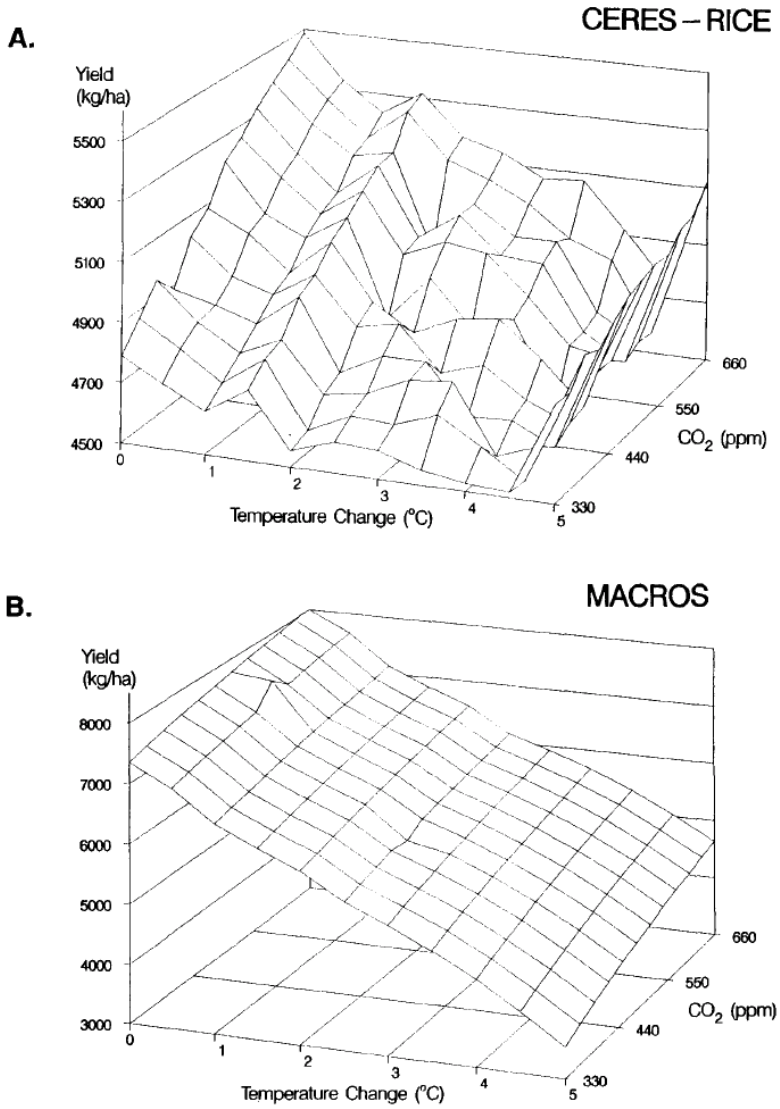

FIGURE 2.9: Differences in the parameterised response of two rice crop models to changes in temperature and CO_2. (A) CERES-Rice, and (B) MACROS. Taken from Bachelet and Gay (1993).

predictions (Hoogenboom and White, 2003). Although predictive skill may not improve, it bridges the gap between crop breeders, physiologists and modellers (Boote et al., 2003; Hoogenboom and White, 2003; White et al., 1996). Finally, as more data becomes available from targeted agronomic trials (Craufurd et al., 2013), it is more logical to pursue the inter-comparison and improvement of field-scale models as tools that are already well advanced for predicting plant responses to varying environment and management conditions at scales in which decisions can be made regarding changes in cropping systems.

One of the most critical caveats of field-scale models is the difficulty of using them at larger

spatial scales, a topic of high interest in the context of climate change. Despite various successful attempts to using these models at larger scales (Baron et al., 2005; Challinor and Wheeler, 2008b; Jagtap and Jones, 2002), it remains unclear as to what extent, for example, using a field-scale model at a larger scale is comparable or better than using a large-area model directly (see Sect. 2.3.2.4). Field-scale models also have a very large number of model parameters, which increases the likelihood of over-parameterisation. For example, many of the crop models in DSSAT have around 150 or more coefficients to which a given simulation is sensitive. With such large number of parameters there is an increasing likelihood of predicting accurate yield responses for the wrong reasons (Jamieson et al., 1998). Another potential caveat in field-scale models is related to the concept of "genetic coefficient", which has prevented crop modellers from quantifying parametric uncertainty, a subject widely recognised and investigated by other crop modellers (Challinor et al., 2005d; Lobell and Burke, 2010; Tao et al., 2009), and also in climate science (Murphy et al., 2007; Stainforth et al., 2005). The belief that genetic coefficients are unique combinations of parameters that represent a given cultivar has prevented crop modellers from quantifying parameter uncertainty in field-scale crop models. This is particularly relevant given that not all model parameters are sufficiently constrained by observed data (Beven, 2006; Challinor et al., 2009b).

For a basic operational mode, field-scale crop models require daily data for maximum, minimum temperatures, precipitation and solar radiation. However, if more complex water balance and photosynthesis equations are used, more detailed meteorological data are required (e.g. relative humidity, dew point temperature). Thus, field-scale models tend to be much more data-intensive than empirical models. Similarly, parameterising or evaluating the outputs of a field-scale model requires a significant amount of field measurements, including leaf area index, biomass, crop transpiration, stomatal conductance, amongst others (Boote et al., 2013; Craufurd et al., 2013). When available measurements are limited to yields and phenology, uncertainties in parameterising the models can be rather large (Adam et al., 2011; Challinor and Wheeler, 2008b; Ruane et al., 2013). Field-scale models are also sensitive to a wider range of inputs to which other models are normally not sensitive (Challinor et al., 2009b; Lobell and Burke, 2010). These include initial soil nutrient (nitrogen, phosphorous, potassium), residue and organic carbon contents, soil fertility and salinity, fertiliser input, type of crop rotations, tillage, residue incorporation during the growing season, and sowing density. In many cases, due to lack of data, researchers

must make assumptions of management and initial conditions, thus constraining the skill of the model's predictions (Pathak et al., 2003; Ruane et al., 2013), and potentially being a source of uncertainty in impacts projections. Sampling of these uncertainties is possible and should be a topic for future research in crop modelling, particularly under future scenarios, when initial conditions cannot be ascertained.

2.3.2.4 Regional-scale process-based modelling

The difference in spatial scales at which climate and field-scale process-based crop models operate has led to the development of the so-called large-area models (hereafter also referred to as regional-scale crop models) (Challinor et al., 2004; Tao et al., 2009). Regional-scale models can include enough mechanistic detail in plant growth processes as to be used with reasonable confidence under future climate scenarios, including increased CO_2 concentrations, and higher rates of extreme temperature and drought events (Challinor et al., 2003, 2007; Tao et al., 2009). At the same time, large-area crop models are less complex than field-scale models and can thus be optimised using a more limited set of input data, and at scales typical of global or regional climate models (Challinor et al., 2004, 2009c). The final goal of a regional-scale crop model is to capitalise on the large-scale relationships between seasonal and sub-seasonal weather and agricultural productivity, thus being able to predict agricultural yields, yet being capable of interpreting climate model outputs directly (i.e. without any subsequent downscaling). Other approaches to regional-scale modelling include the use of correction factors into field-scale models to account for non-modelled processes at the large scale (Jagtap and Jones, 2002) and the direct use of field-scale models at large scales (Baron et al., 2005; Xiong et al., 2008), both of which remain to be compared with regional-scale models.

As such, regional-scale models have various advantages. Firstly, regional-scale models are capable of accounting for effects of sub-seasonal stresses such as terminal drought (Challinor et al., 2009a), drought and high temperature during flowering (Challinor et al., 2005b, 2009a), increased CO_2 (Challinor and Wheeler, 2008a) and its effects on stomatal conductance (Tao et al., 2009), and decreased photosynthetic activity under high temperatures (Challinor et al., 2009a). Thereby, the models can be reliably used to analyse the effects of changing climate conditions. In addition, due to the simple parameterisation of a number

of processes, it is relatively easy to account for uncertainty in model parameters. Parametric uncertainty has been quantified in these models using simple parameter perturbation (Challinor et al., 2005d) and Monte Carlo simulations (Tao et al., 2009). Regional-scale models also present the advantage of allowing coarse-resolution climate model outputs to be used directly into the crop model, thus avoiding any issues related with downscaling (Hawkins et al., 2013b; Wilby et al., 2009) and weather generation (Jones and Thornton, 2013). The simplicity of these models also allows them to be coupled directly with climate models (Osborne et al., 2007). Finally, the models are easier to understand, parameterise and modify, thus reducing the likelihood of the model becoming a "*black box*", the likelihood of over-parameterisation, and the likelihood of accurately reproducing crop yields for wrong reasons (see e.g. Figure 2.8). This fosters a more appropriate use amongst their users.

Caveats arise when attempting to model at large areas. These are due to the lack of detail in certain processes, or the disconnection between processes in the crop model. First, inconsistencies can arise when processes are modelled independently. For example, Challinor and Wheeler (2008a) report that under certain conditions, GLAM simulates an unrealistic SLA response, thus requiring an empirical adjustment to be made in the first few days of the simulation in order for the model to be able to simulate a realistic crop. Second, the models fail to simulate critical aspects of assimilate distribution in the plant (given their primary focus is on yield) and thus fail at incorporating processes such as assimilate re-distribution (i.e. once a given organ has senesced) that may be critical under drought stress conditions, or for crops with large storage capacity such as cassava or potato (Matthews and Hunt, 1994; Wolf and Van Oijen, 2003). Third, leaf area dynamics in these models can lead to over-estimating canopy extent and accumulated biomass. Fourth, the use of model correction factors (such as the yield gap parameter - C_{YG}) can lead to underestimating internal errors in the crop model, and thus over-stating the predictive skill of the model (Tao et al., 2009). This may, however, be solved by constraining the model using the outputs of other models or using a more complete set of observations. Fifth, individual organs are not simulated in these models, thus the possibility of incorporating processes such as nutrient balance is rather limited. Doing this would require a substantial modification not only in the structure but also in the rationale of the model. Thus, certain management strategies such as changes in fertiliser input, tillage, and soil conservation cannot be tested with these models. Finally, the models

work best when there is a significant climate signal on the yield response, particularly from rainfall and are thus unlikely to work when the yield response is governed by management or biotic factors (Challinor et al., 2003).

2.3.2.5 Differences between models

Crop models can be classified by scale into field-scale and regional-scale (Challinor et al., 2013) and by nature into process-based and empirical (Challinor et al., 2009c). Empirical models can be further classified into statistical models and niche-based models (Challinor et al., 2009c). Models can be also classified by the nature of their outcome into probabilistic and deterministic. In comparing the work of Lobell et al. (2008) with the work of Parry et al. (1999), of Lane and Jarvis (2007), and of Tao et al. (2009) and Challinor et al. (2004) differences become evident and can be summarised as follows:

1. The scale at which the models are used is different. Statistical models and niche-based models are used at continental or sub-continental scales. Process-based models are used at higher spatial scales, with the highest scale being for field-scale models.

2. The amount of information that can be extracted is different. Yield predictions can be extracted from any models except those niche-based. Information on sub-seasonal stresses can only be extracted from process-based models, and sometimes also from statistical models (e.g. Lobell et al. 2012).

3. The number of parameterised processes is significantly higher in process-based models as compared to all other models, thus requiring larger amounts of input data to constrain the model during the calibration process and increasing the risk of modelling the target quantity using unrealistic parameters or parameter values.

4. The sensitivity of models to errors within input data and with regard to initial conditions is varied, with statistical and niche-based models being generally less sensitive (e.g. Vermeulen et al. 2013).

2.3.3 The use of ensembles in crop modelling

The concept of model ensemble has been largely used in climate science and is becoming increasingly used in crop modelling science. The term model ensemble, as used here, refers to a set of representations of a system that are considered all at once, with all such representations being equally plausible and in accordance with the macroscopic behaviour of the system being represented (Stainforth et al., 2005). Ensembles in crop modelling can be created by using various crop models, by using various climate models with a single crop model, by using various crop model parameter sets, or by a combination of all the above. In some situations (particularly those related to future climate scenarios) crop model ensembles can also be created from sampling initial field conditions. Among these, the most common is the use of several climate models with a single crop model, followed by the use of various crop models (under present-day conditions) and then by the sampling of model parameters (also see Chapter 4). To the knowledge of the author, ensembles of initial conditions havent been practiced in crop modelling.

2.3.3.1 Ensembles of models

Various examples exist of the use of multi-crop model simulations, although little has been done towards the conceptualisation and/or application of a more complete model ensemble approach (but see Challinor et al. 2013 and Rosenzweig et al. 2013). Bachelet and Gay (1993) used four rice models and found agreement in direction of yield changes to increasing temperatures, but substantial disagreement in the way the models treated the effects of increased CO_2 concentrations and its interactions with temperature (Figure 2.9), and large variability in the predicted yield responses. Jamieson et al. (1998) compared five wheat models and found agreement between simulated yields but substantial variation in leaf area evolution, biomass, transpiration and soil water extraction patterns. Errors within each model are likely to cancel out as an effect of local calibration procedures. Tubiello and Ewert (2002) reported substantial differences between the calibrated absolute CO_2 responses in both water stressed and well-watered conditions for five wheat crop models, but agreement in the direction of the response both within models and between models and observations (i.e. there was a larger relative benefit from CO_2 in water-stressed than in well-watered environments).

Challinor and Wheeler (2008a) found more than 50 % variation in modelled yields in response to CO_2 fertilisation for three groundnut crop models. Challinor et al. (2009a) reported significant differences between three groundnut models in the direction and extent of changes in simulated yield due to combinations of high temperatures and higher CO_2 concentrations. Adam et al. (2011) reported that the multi-model mean of simulated yields when using different methods to model leaf area dynamics significantly agreed with observations. However the variance in simulated yields across the different methods can be larger than that caused by environmental differences across Europe. Vermeulen et al. (2013) used three groundnut crop models in the state of Gujarat in India, representing crop yields accurately (Figure 2.10), primarily due to the strong signal of seasonal precipitation on crop yields (Challinor et al., 2003). These simulations show differences in the skill of crop models to simulate certain aspects of the interannual variability in crop yields, with statistical models being less capable of simulating failed seasons. More recent studies, including those of Asseng et al. (2013), Rötter et al. (2012), and Palosuo et al. (2011) have shown that crop model uncertainty can be rather large, particularly if the models are not sufficiently 'tuned' to specific cultivars and sites.

2.3.3.2 Parameter ensembles

As opposed to those using multi-crop models, studies that investigate parametric uncertainty have focused on the implications for climate change impact projections (Challinor et al., 2005d; Iizumi et al., 2011; Tao et al., 2009). This particular topic is discussed in detail in Chapter 5. The creation of model parameter ensembles (also referred to as perturbed parameter ensembles) consists of taking advantage of the trade-offs in the model parameterisation process to develop a number of parameter sets that can realistically simulate observed yields. Simulations of crop yields with each parameter set have varied skill, but represent the challenge of parameterising processes for which there are not enough observations. Iizumi et al. (2011) modelled rice using a Bayesian approach to sample parameter values in order to represent the fine-scale spatial variability in varieties and management. Tao et al. (2009) used a similar approach to quantify the uncertainties in parameter estimates of a rice crop model optimised using yield observations. In both cases, the predicted responses by each of the ensemble members provided a realistic representation of the historical crop yields, while allowing the assessment of parametric uncertainty

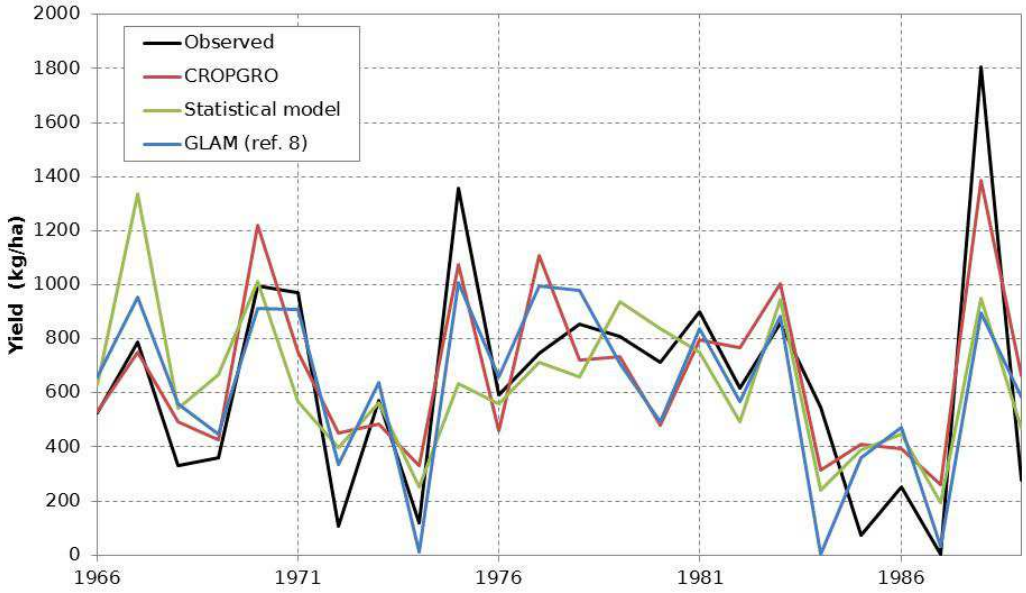

FIGURE 2.10: Comparison between observations and simulations of groundnut yields using three crop models for the state of Gujarat (India) between the years 1966-1989. Observations have been detrended to 1966 levels (see Challinor et al. 2004). Note the differences between the crop models and the skill of each model to reproduce certain aspects of the yield time series (e.g. process-based models more capable of reproducing extremes). Figure taken from Vermeulen et al. (2013).

and its variation in time (Figure 2.11(a) and 2.11(b)). Challinor et al. (2005d) compared the differences in simulated groundnut yield as impacted by parametric uncertainty in a climate model and in the crop model. Their results imply that: (1) uncertain climate and crop parameters can impact yields in different directions, (2) impacts of uncertain parameters in simulated crop yield are location-specific, and (3) climate model parameter uncertainty is generally the dominant source of uncertainty (see Figure 2.12).

2.3.3.3 A way forward

The differing responses of crop models when environmental conditions are changed, and particularly those under which the models have not been extensively tested (such as when CO_2 concentrations are increased), and the fact that little is known about the feedbacks and conditions that can arise under future climate scenarios suggests that there is a substantial opportunity to increase confidence in future crop yield projections by a more

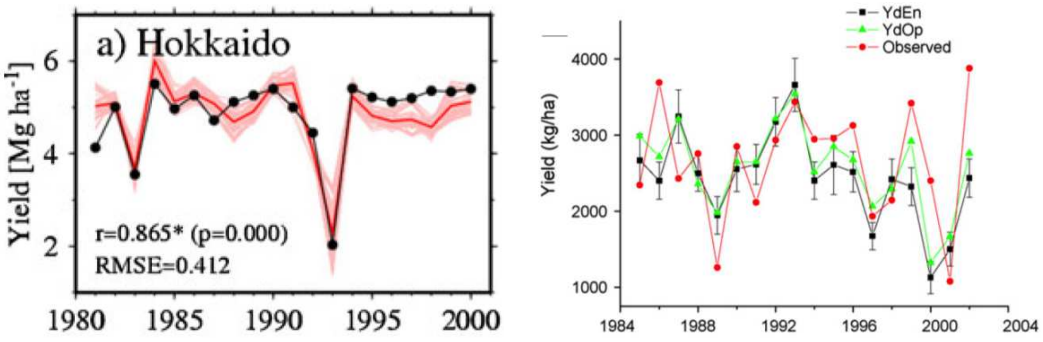

(a) rice (Japan) (b) maize (China)

FIGURE 2.11: Two parameter ensembles from previous studies: (a) Time series of the observed yield and 50 ensemble members of the simulated yield for the Hokkaido district in Japan. The black line and dots are observations, the thick red line is the ensemble mean, and the narrow pink lines are each of the 50 ensemble members. Taken from Iizumi et al. (2011); (b) Time series in the modelled and observed yield at the crop model grid scale for spring maize at Harbin, China. YdEn is the crop model perturbed parameter ensemble, YdOp is a deterministic prediction using the same model. Taken from Tao et al. (2009).

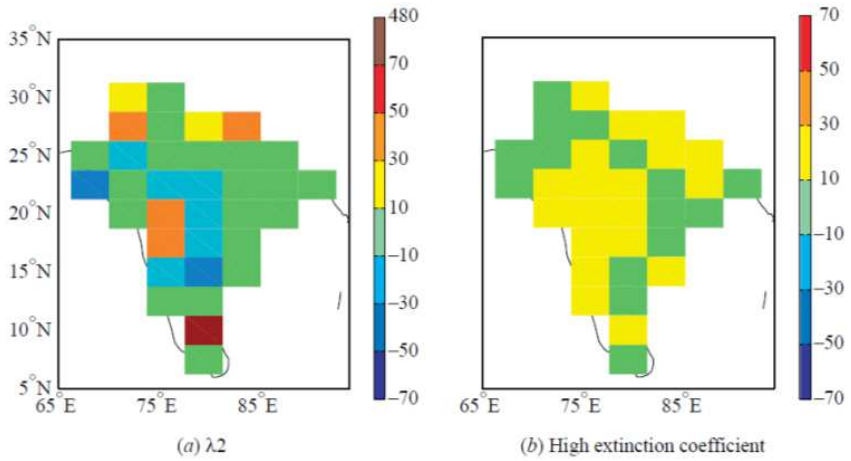

FIGURE 2.12: Percentage difference in mean groundnut yield between the control simulation and two perturbed simulations; $\lambda 2$ is a parameter in the driving GCM (ice fall speed) and extinction coefficient (k) is part of the parameters used in the light interception equations in GLAM. Taken from Challinor et al. (2005d).

appropriate sampling of uncertainties. Achieving a multi crop model ensemble is not trivial, partly because of the limited knowledge in crop modelling regarding uncertainties. In addition, with knowledge and methodologies developed in climate change science, a whole new range of possibilities and limitations arise. Crop modelling science needs to adjust in order to provide policy makers and other stakeholders with the necessary information for adaptation.

Provided the uncertainties in climate modelling, crop modelling science itself has to adapt and to some extent transform some of its governing principles to better respond to the scientific challenges arising from climate change impact assessment. Climate science principles regarding uncertainties can, to some extent, be used to improve crop modelling science. Nevertheless, this may require a paradigm shift, due to the way in which crop models have been designed. The advent of global programs on crop-climate modelling (Jarvis et al., 2011a; Rosenzweig et al., 2013) is leading to improved impacts prediction and to the use of multiple crop models to make predictions and may facilitate this process (e.g. Asseng et al. 2013). Work will, however, have to be extended towards the use of parameter and initial conditions ensembles to at least inform the research community on the extent to which these uncertainties are comparable to those arising from multiple climate or crop models.

2.4 Adaptation of agricultural systems to climate change

2.4.1 General concepts in climate change adaptation

Adaptation to climate change is the final target of any impact projection (Challinor et al., 2013; Moser and Ekstrom, 2010). Adaptation can be seen as an iterative process that starts from the development of knowledge about a system and its problems (i.e. quantifying impacts). This knowledge is then used to develop and select options, which are finally implemented and evaluated (Figure 2.13). Such an iterative process can happen at a variety of scales, ranging from seasonal to multi-decadal (Howden et al., 2007; Moser and Ekstrom, 2010; Park et al., 2012).

Figure 2.14 illustrates the different types of adaptive responses in agriculture as the degree of climate change increases. In agricultural systems, farmers constantly change their management practices in response to climate and climate-related stresses (e.g. pests and diseases). These adjustments can be considered as short-term coping strategies, are typically incremental and happen in a non-planned (disorganised) manner (Moser and Ekstrom, 2010). Such adjustments may include changes in the amount and timing of fertiliser, irrigation and fungicide applications, changes in sowing dates, and changes in varieties. For example, most farmers in the wheat growing areas of the Indo-Gangetic Plains would

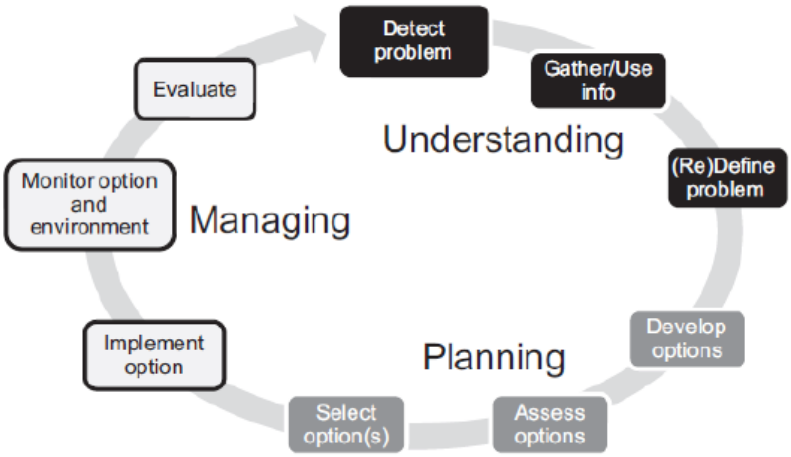

FIGURE 2.13: Steps in the adaptation process. Taken from Moser and Ekstrom (2010).

rapidly adopt newly released cultivars (Aggarwal, 2008; Aggarwal et al., 2004). Sowing dates in rainfed systems change on yearly basis according to the onset of seasonal rains (Sacks et al., 2010; Velde et al., 2012).

Under longer time periods, the degree of climate change is expected to be higher (Joshi et al., 2011). Adaptation planning at these time scales needs to consider further and more substantial changes to the system (Moser and Ekstrom, 2010; Park et al., 2012). The approach of relying solely on incremental short-term adjustments may not be successful with more intense or extended climate change pressures. This is because there is a degree of change in climate beyond which the available short-term options for a farmer may not work or because the negative impacts of climate change may arise at rates and in a multi-dimensional fashion that would make it difficult for farmers to respond. For example, genetic variation within a given crop's genepool as well as the speed at which climate-adaptation beneficial genes can be incorporated in existing varieties both have limits (Reynolds et al., 2011).

Systems adaptation (Figure 2.14) involves changes in the whole cropping system such as changing the crops in the rotation, diversifying the system to include a wider range of species with diverse uses (e.g. agro-forestry), or optimising production at the maximum extent possible through precision agriculture where such an apoproach approach is not used (Rickards and Howden, 2012).

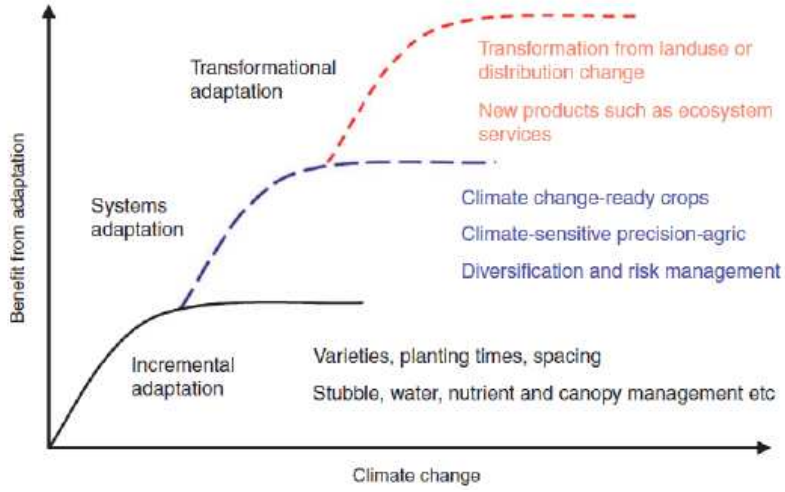

FIGURE 2.14: Levels of adaptation in relation to benefits from adaptation actions and degree of climate change, with illustrative examples. Taken from Howden et al. (2010).

The last type of adaptation would be needed when a given farming system becomes completely economically or environmentally unsustainable. Transformational adaptation planning is required when the degree of climate change is expected to cause an irreversible loss to the system object of analysis (Moser and Ekstrom, 2010; Rickards and Howden, 2012). In that sense, it is designed to avoid severe impacts of climate change and/or capitalise on increasingly positive effects that can arise from a system shift (Park et al., 2012). Transformational changes in a cropping system can occur in different dimensions and often overlap with system-level adjustments (Figure 2.14). Transformational adaptation may include livelihood changes such as changes from cropping to livestock systems (Jones and Thornton, 2009), community migration, or a complete change in the focus of the system (e.g. from an agricultural system to a national park) (Rickards and Howden, 2012).

The time at which each type of change is required in a given farming system largely depends upon the type of system. Perennial systems are expected to substantially benefit from longer-term transformational planning, given the high costs associated with establishing these cropping systems. Annual rotations are somewhat more flexible, because crops can be changed in a yearly basis. Socio-economic and market-related barriers would however be expected in both cases (Moser and Ekstrom, 2010). For more comprehensive reviews on adaptation the reader is referred to Howden et al. (2007), Moser and Ekstrom (2010), and Park et al. (2012). Of particular relevance to transformational adaptation is the review of Rickards and Howden (2012).

2.4.2 Genotypic adaptation

Genetic variation within the genepool of a crop can to a large extent allow the adaptation of agricultural systems. On one hand, promising but already existing varieties can be used to replace currently growing ones. On the other hand, specific traits and/or genes can be incorporated into existing varieties by means of conventional breeding or genetic engineering (Hajjar and Hodgkin, 2007). Genes to tolerate drought, excessive heat, and to resist pests and diseases can be found both in existing landraces (Beaver et al., 2003; Reynolds et al., 2011), and in wild relatives of crops (Guarino and Lobell, 2011; Hajjar and Hodgkin, 2007; Jansky et al., 2009). Crop improvement networks have historically focused on incorporating stress-tolerance and/or disease-resistance genes into high-yielding cultivars (Reynolds et al., 2011; Stamp and Visser, 2012) as a way to decrease production costs and close yield gaps (Reynolds et al., 2011).

There is increased evidence that climate change stresses can, to a large extent, be managed or completely offset through the incorporation of beneficial traits into existing crop varieties (Ortiz et al., 2008). Thus, genotypic adaptation is relevant in the context of both short-term adjustments and systems adaptation (Jarvis et al., 2011b). Genotypic adaptation involves both the replacement of currently used cultivars (i.e. varietal shifts) and also the development of new cultivars through the incorporation of traits that may become beneficial under certain degrees of climate change (i.e. developing climate-ready crops). Breeding programmes are currently challenged with having to set priorities based on climate change impacts projections. Decisions of which traits to breed and by when would varieties need to hold such traits are expected to be largely influenced by the type (e.g. increase in mean, increase in extreme events), direction (e.g. drier and warmer, wetter and warmer), and extent (how warmer, how drier) of the predicted climatic changes in a given area (Stamp and Visser, 2012).

Modelling studies have attempted to quantify the benefits of genotypic adaptation. Challinor et al. (2007) show substantially reduced impacts from climate change if adaptation to mean temperatures is increased in Indian groundnut varieties. Similarly, Challinor et al. (2009a) showed that increased accumulated thermal time in Indian groundnut can completely offset the negative effects of climate change. Challinor et al. (2010) found that adapting Chinese wheat varieties to high temperature stress thresholds during anthesis,

and to water stress can reduce the percent of failed seasons under future scenarios by 30 % and 50 %, respectively. Water-stress adaptation alone, in particular, can account for all negative effects of climate change. Jarvis et al. (2012) report that in addition to cassava's tolerance to climate change stresses, capitalising benefits from further improving its drought and cold tolerance may bring substantial benefits under future climate scenarios.

2.4.3 Crop ideotypes

Breeding climate-ready crops would allow farmers to adapt to climate change at a relatively low cost (Habash et al., 2009; Jarvis et al., 2011a). However, this would require a substantial scientific and coordinating effort in the determination of those traits that are both needed and feasibly incorporable into existing crop varieties, as well as breeding them in time and distributing them (Habash et al., 2009; White, 1998). To this aim, the design of future crop varieties arises as a need in the context of climate change. Such need is further catalysed by the possibility of speeding the breeding process through through molecular tools such as genomic selection, or in addition through genetic engineering (Habash et al., 2009). With time, cis- or transgenic transformations of food or cash crops are expected to become more frequent (Habash et al., 2009; Ortiz et al., 2008).

The concept of crop ideotypes thus reflects the need and possibility of designing crop varieties that are apt for certain environmental conditions. Although the concept is not new (Donald, 1968), crop ideotypes are idealised plants (i.e. plant models) that have the greatest effectiveness in producing dry matter and yield under given environmental conditions. Breeding programs typically pursue crop ideotypes. The erect, dwarf and photoperiod insensitive wheat cultivars are clear examples of ideotype designs (White, 1998). Defining a crop ideotype thus involves a definition of the physical (e.g. height, maximum leaf size, leaf thickness) and physiological (e.g. stomatal conductance, photosynthetic efficiency) characteristics of a given crop plant, that would allow such a plant to respond well under certain conditions (e.g. in a drought-prone environment).

In the context of climate change, the final aim of a crop ideotype is to produce a climate-smart variety (Habash et al., 2009; Jarvis et al., 2011a). Ideotypes can be designed using crop models, given an appropriate degree of complexity in the model and an appropriate link between the crop model parameters and the real traits in cultivars (White, 1998). Of

particular concern would therefore be the extent to which barriers in breeding (i.e. the ability of existing techniques to incorporate certain genes), limits in the available genetic diversity of crops (i.e. the range of traits available) and required breeding time constrain the unlimited set of virtual possibilities.

Examples in the literature exist that illustrate the potential of crop models to design crop ideotypes (see the review of White 1998), but few modelling studies have attempted to do so using future climate scenarios (Challinor et al., 2007; Jarvis et al., 2012). The responses of virtual crops can be tested using crop models in conjunction with climate models in order to assess the robustness of choosing a particular mode of action in breeding (e.g. breeding for heat tolerance or breeding for drought tolerance). There is, however, a limitation to the extent to which genetic improvement strategies can be tested with models, as this is largely constrained by the complexity of the model and the uncertainties associated with its use.

Chapter 3

Data and models

"Y la juego, o la cambio por el más infantil espejismo,
la dono en usufructo, o la regalo..."
L. de Greiff

3.1 Introduction

Models have become an increasingly important tool for assessing the impacts of and adaptation to climate change (Challinor et al., 2013; Vermeulen et al., 2013). In the work presented in this thesis, two crop models were used: EcoCrop and GLAM. EcoCrop is a niche-based model that simulates suitability of a crop to the environment using monthly temperatures and total seasonal precipitation. The suitability index predicted by EcoCrop is a measure of how similar an environment is to the set of optimal conditions in which the crop can successfully thrive, or, in other words, an indication of whether an species is suited to the climate conditions of a given site –as measured by seasonal and monthly means (Hijmans et al., 2001; Ramirez-Villegas et al., 2013b). GLAM, by contrast, is a regional-scale process-based model. As other process-based models, but with less complexity, GLAM simulates crop growth and development on a daily basis (Challinor et al., 2004, 2009c). In this thesis, the two models are used in conjunction with observed and climate model simulations of the CMIP3 (Meehl et al., 2007a) and CMIP5 (Taylor et al., 2012) ensembles to project climate change impacts and, in the case of GLAM, also to

inform adaptation. The reader will thus find the constant use of various datasets, models and concepts throughout this work.

In this chapter, a description of the key concepts, modelling tools, and input data is done. The chapter starts by describing concepts that are key for understanding the work presented (Sect. 3.2), then describes the study areas (Sect. 3.3) and the different datasets used for the variety of analyses presented in subsequent chapters (Sect. 3.4). The data section is divided into climate data (Sect. 3.4.1), crop data (Sect. 3.4.2) and soil data (Sect. 3.4.3). Section 3.5 provides a detailed description of GLAM (Sect. 3.5.1) and EcoCrop (Sect. 3.5.2) including their constituting equations and structure. The chapter concludes by presenting in full the methods used to assess the skill of crop and/or climate simulations (Sect. 3.6) and to understand the uncertainties in crop yield and suitability projections (Sect. 3.7).

3.2 Concepts and definitions

During the writing up of this thesis, one of the most daunting challenges was the repeated use of certain terms that, when used under different contexts, may have different interpretations or different definitions. Based on existing literature and on the author's knowledge, an attempt to define these terms has been done. This may improve the readability of the work while reducing (at least to some extent) the uncertainties involved with conceptualising the problem of research. Substantial effort has been put in trying to make these definitions consistent both throughout the document and between the document and the existing literature.

3.2.1 Abundance and crop yield

Abundance is a measure of the amount (of individuals, biomass, or produce) normalised per unit area. Abundance can be seen as a measure of frequency of a species or a characteristic of the species in a given site, or also a measure of habitat utilisation (Pearce and Ferrier, 2001; VanDerWal et al., 2009a). In agriculture, crop yield is the preferred measure of abundance (Estes et al., 2013a).

Yield is a measure of agricultural productivity. Yield is expressed as the amount of harvest product by weight (in kilograms, tonnes, or any weight unit) by unit area (typically

hectares). In this work, yield and productivity are used interchangeably. In all reported figures, yield was measured in kg ha^{-1}.

3.2.2 Suitability

Suitability of a species is referred to as the degree to which the physiological and ecological requirements of a species are met at a site. In other words, suitability is a measure of whether a species can thrive at a given site. Suitability can also be interpreted as the probability of occurrence (Soberon and Nakamura, 2009; Wiens et al., 2009). Climatic suitability is thus used to refer to the solely climate component of suitability –since there may be soil and ecosystem components to it.

3.2.3 Adaptation

Two definitions of adaptation were adopted. Both of them are described and fully discussed in Chapter 2 (Sect. 2.4). The first one is the IPCC definition, which reads:

> "*Adjustment in natural or human systems in response to actual or expected climatic stimuli or their effects, which moderates harm or exploits beneficial opportunities. Various types of adaptation can be distinguished, including anticipatory and reactive adaptation, private and public adaptation, and autonomous and planned adaptation*" (IPCC, 2001)

A second, more general definition of adaptation was also adopted. This was done in order to keep consistency with state-of-the art social and biophysical sciences. The second definition reads:

> "*Adaptation involves changes in social-ecological systems in response to actual and expected impacts of climate change in the context of interacting nonclimatic changes. Adaptation strategies and actions can range from short-term coping to longer-term, deeper transformations, aims to meet more than climate change goals alone, and may or may not succeed in moderating harm or exploiting beneficial opportunities*" (Moser and Ekstrom, 2010)

3.2.4 Predictability

Is the degree to which a prediction of the state of a system can be made. As it is impossible to achieve perfect determinism when modelling a systems state (Walker et al., 2003), a system can never be fully predictable. Predictability is a function of the complexity of a system, the knowledge or information available on the system, and the available computational power. Although predictability is difficult to measure, it is related to prediction error and model skill (below). High model skill (low error) is an indicator of a high degree of predictability. However, low model skill may not indicate a low degree of predictability, as low model skill can also be the product of an incorrect model formulation, errors in input data, initial conditions, or be a product of all three in combination.

3.2.5 Prediction error

Another way of referring to prediction error is by referring to accuracy, because the existence of prediction error means there is a lack of accuracy in a simulated quantity. In short, accuracy is the degree of veracity in a simulation. Such degree is measured as the difference between a simulation and the accepted truth (i.e. reality, or in this case the existing observations). This difference is what is termed here prediction error. Because models are all imperfect approximations to the real world, there will always be prediction error and thus a certain lack of accuracy inherent to the model's structure, its implementation, or the inputs used to drive it. Accuracy and prediction error are tightly related to model skill.

3.2.6 Model skill

Model skill, either of a climate or a crop model, refers to the ability of the model to reproduce certain aspect of reality. Model skill is measured by determining how well a model reproduces observations of a given variable at a given location or set of locations. Lack of skill in a model produces what is here termed prediction error (see above). Climate model skill is explored in detail in Chapter 4 and is assessed for two characteristics: mean climate and interannual variability. For each of these cases, metrics to compare model results with observations are used. Mean climate is typically assessed using the model bias

(see below), the root mean squared error ($RMSE$), the $RMSE$ normalised by the observed mean ($RMSE_M$) or standard deviation ($RMSE_{SD}$), and the correlation coefficient (R), whereas interannual variability is assessed using an interannual variability index (V_I). Crop model skill is in this work treated in Chapter 5, 6, and 7. GLAM (Chapter 5) is typically assessed using the $RMSE$, R, or the perfect-correlation MSE. EcoCrop (Chapter 7) is assessed using presence-absence related measures such as rates of false negatives, true positives, and the area under the receiving operating characteristic (ROC) curve (AUC).

3.2.7 Model bias

The term bias throughout this thesis is used under the strict international definition ascribed by the World Meteorological Organization (WMO), which states that bias "*is the correspondence between a mean forecast and mean observation averaged over a certain domain and time*" (WWRP, 2009). Bias is therefore used to refer to the differences between observations and predictions for a mean state of a system. Ehret et al. (2012) present a more loose definition of bias by stating that it refers to "*any deviation of interest (e.g. with respect to the mean, variance, covariance, length of dry spells, etc.) of the model from the corresponding true value*". However, the international definition of bias has been kept in order to avoid confusion and keep consistency with any previous work (Gleckler et al., 2008; Pierce et al., 2009; Taylor, 2001). In the context of the present thesis, therefore, bias is measured for climate models for a given field (i.e. variable, x) as the difference between the climate model (M) output and the observations (O) (Eq. 3.1).

$$bias = x_M - x_O \tag{3.1}$$

Model bias can be calculated on a gridcell basis for the mean climate of a year or of a season. Bias is expressed in the scale of the variable being assessed.

3.2.8 Uncertainty

Uncertainty is probably amongst the most frequently used terms in this thesis. The concept of uncertainty deserves particular attention. Uncertainty may have even deserved an individual single chapter in this thesis. The author restrained from doing this for

two reasons. First, definitions of the term have been attempted extensively in existing literature (see e.g. Challinor et al. 2013, 2009c; Kennedy and O'Hagan 2001; Walker et al. 2003). Secondly, a full treatment or quantification of uncertainty is impossible, so it may be more reasonable to account for uncertainty whenever a prediction or a projection is done. Thereby, a definition is attempted, and uncertainty is treated as a cross-cutting topic across this whole research piece.

In short, uncertainty is referred to as the spread of any set of predictions. It is also referred to as precision. Put simple, uncertainty is typically reflected as range bars in a given plot, except where bars are used to indicate spatial or temporal spread. In that sense, uncertainty can be measured using statistical dispersion measures such as the range, variance, standard deviation and the coefficient of variation. However, additional measures of uncertainty are possible. For instance, the IPCC reports the agreement in direction of model predictions as a measure of future precipitation uncertainty (IPCC, 2007). Substantial agreement can be found in the direction of precipitation changes in a number of areas, although the variation in actual precipitation estimates across the models can be very high (see Figure 1.4, IPCC 2007).

Uncertainties result from the impossibility of modelling either the climate or cropping system with complete determinism (Walker et al., 2003). These uncertainties arise from model structure, model parameters, algorithms and computational systems, interpolation, and experimental data (Kennedy and O'Hagan, 2001; Walker et al., 2003). In climate modelling, uncertainties arise from the uncertain pathways of greenhouse gas (GHG) emissions and concentrations (Moss et al., 2010), the response of the system to a given radiative forcing (caused in turn by GHG concentrations), the initial conditions and parameterised physical processes (Challinor et al., 2009c; Ehret et al., 2012; Stainforth et al., 2005). Most of the work in crop modelling has focused in assessing model structure (Palosuo et al., 2011; Rötter et al., 2012) and parameter uncertainty (Challinor et al., 2005d; Iizumi et al., 2009b), albeit typically in an independent manner.

Limits to ensemble size exist given the limitations in computational capacity (Challinor et al., 2009c; Stainforth et al., 2005) and therefore uncertainties can be only partly quantified. Uncertainties through the writing of this work have been explored for both the climate system and the groundnut cropping system. The measures of uncertainty employed here are defined below (Sect. 3.7) and, where not, in each individual chapter and

attempt to provide an overview as well as a comparison of the importance of different sources of uncertainty for the cropping system being modelled.

3.2.9 Calibration and optimisation

In Chapter 5, the words calibration and optimisation are both used for the first time. In some contexts these two words can be used interchangeably (e.g. Hoogenboom et al. 1992; Ruane et al. 2013), but in this thesis, and in general in GLAM studies, a difference is made. Such difference arises from the way optimal values for the model parameters are determined and how parameters are allowed to vary across space. In GLAM, all model parameters other than the C_{YG} are constant in space, but the C_{YG} is allowed to vary on a location basis. The term **optimisation** refers to finding a value that is reduces the model error for any model parameter, except the C_{YG}. The term **calibration** refers to finding a value for the C_{YG} that reduces the model error. Optimisation is therefore often done for a group of grid cells ("globally") whereas calibration is always done for a single grid cell ("locally"). In both cases simulated and observed yield time series are used to calculate the model error.

3.3 Study areas

Two different areas were studied in this work. The first area included Africa and South Asia, where several studies have identified that significant vulnerabilities exist (see Chapter 1, and Chapter 2) (Knox et al., 2012; Lobell et al., 2008; Thornton et al., 2011). This area was studied in Chapter 4, which comprehensively assesses the quality of climate data for climate change impact studies. In particular, the analyses of Chapter 4 focus on: West Africa (Senegal, Mali, Burkina Faso, Ghana and Niger), East Africa (Ethiopia, Tanzania, Uganda and Kenya), Southern Africa (South Africa, Namibia, Botswana, Zimbabwe and Mozambique) and South Asia countries (India, Nepal, and Bangladesh), hereafter referred to as WAF, EAF, SAF and SAS, respectively (Figure 3.1).

The second study area was India, in which the analyses of Chapter 5 to 8 focused. Following Talawar (2004) and Mehrotra (2011), the study region was divided in five groundnut growing zones (Figure 3.2), which reflect the variation in the germplasm grown in India.

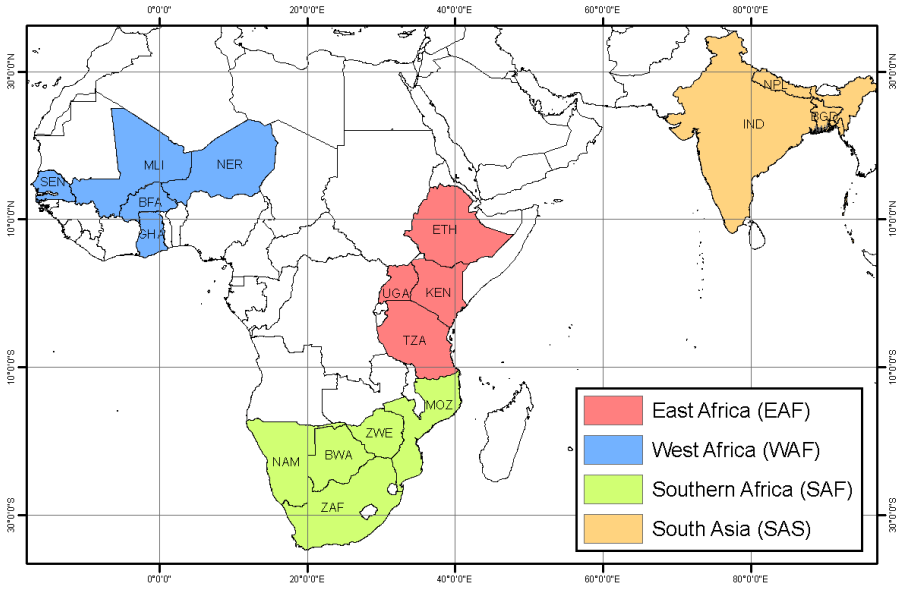

FIGURE 3.1: First study area, analysed in Chapter 4. For visualization purposes, country names were reduced to their 3-letter standardised unique identifier (ISO), and are noted as follows: East Africa: ETH (Ethiopia), UGA (Uganda), KEN (Kenya), TZA (Tanzania); West Africa: SEN (Senegal), MLI (Mali), NER (Niger), BFA (Burkina Faso), GHA (Ghana); Southern Africa: MOZ (Mozambique), ZWE (Zimbabwe), BWA (Botswana), NAM (Namibia), ZAF (South Africa); South Asia: IND (India), NPL (Nepal), BGD (Bangladesh).

These regions receive different amounts of rainfall during the monsoon season (June to September, Figure 3.3) and have different soil profiles.

3.4 Data

Many different types and sources of data were used in the development of this thesis. These were grouped by type in climate data (Sect. 3.4.1) and crop data (Sect. 3.4.2). Climate data includes observed, reanalysis and GCM data –including different forms of bias correction. Crop data include crop yields, crop locations, irrigation rates, planting dates, and soils.

3.4.1 Climate data

Four sources of climate data were used: long-term interpolated time series (Sect. 3.4.1.1), mean climate data (Sect. 3.4.1.2), reanalysis data (Sect. 3.4.1.3), and CMIP climate model

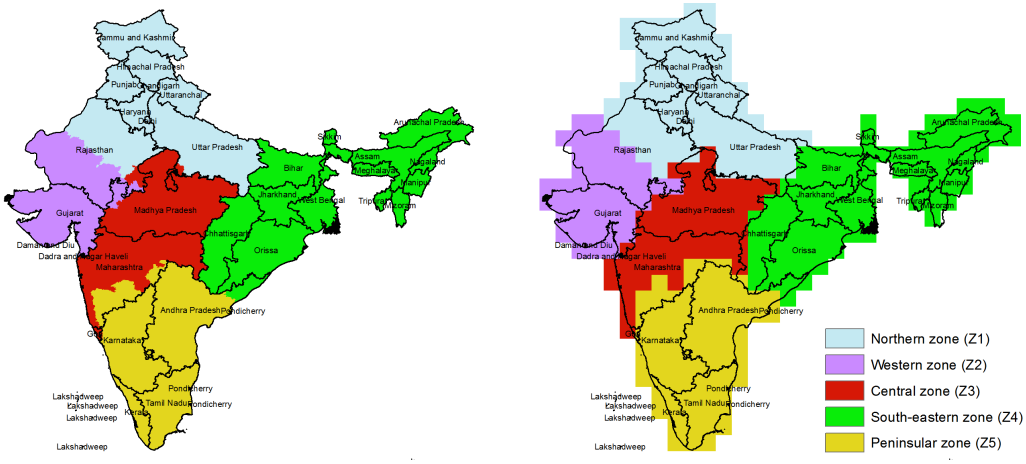

(a) high (b) low (1x1 degree)

FIGURE 3.2: Groundnut growing regions of India, as per the study of Talawar (2004) at the original district-level divisions resolution (high), and at the IMD grid resolution (1x1 degree, low, see Figure 3.3).

TABLE 3.1: Summary of all climate datasets used throughout this work.

Dataset	Source / Description	Described in	Used in
TS_WS-QA	Monthly time series from weather stations (1960–2000)	Sect. 3.4.1.1	Chapter 4
TS_CRU-QA	Monthly time series from interpolation (1960–2000)	Sect. 3.4.1.1	Chapter 4
TS_CRU-GM	Daily linearly interpolated temperature data (1966–2000)	Sect. 3.4.1.1	Chapter 5, 6
TS_IMD-GM	Daily precipitation from IITM (1966–1993)	Sect. 3.4.1.1	Chapter 5, 6
TS_E40-QA	Monthly time series from ERA-40 (1960–2000)	Sect. 3.4.1.3	Chapter 4
TS_E40-GM	Daily solar radiation from ERA-40 (1966–1993)	Sect. 3.4.1.3	Chapter 5, 6
TS_C3-QA	Monthly time series from CMIP3 (1960–2000)	Sect. 3.4.1.4	Chapter 4
TS_C5-QA	Monthly time series from CMIP5 (1960–2000)	Sect. 3.4.1.5	Chapter 4
TS_C5-GM	Uncorrected daily meteorology from CMIP5 (1966–1993)	Sect. 3.4.1.5	Chapter 5, 6, 8
CL_WS-QA	Mean monthly climatology from weather stations (1960–2000)	Sect. 3.4.1.2	Chapter 4
CL_WC-QA	Mean monthly climatology from interpolation (1960–2000)	Sect. 3.4.1.2	Chapter 4, 7
CL_CRU-QA	Mean monthly climatology from interpolation (1960–2000)	Sect. 3.4.1.2	Chapter 4
CL_CRU-EC	Mean monthly climatological temperatures from CRU (1966–1993)	Sect. 3.4.1.2	Chapter 7
CL_E40-QA	Mean monthly climatology from ERA-40 (1960–2000)	Sect. 3.4.1.3	Chapter 4
CL_C3-QA	Mean monthly climatology from CMIP3 (1960–2000)	Sect. 3.4.1.4	Chapter 4
CL_C5-QA	Mean monthly climatology from CMIP5 (1960–2000)	Sect. 3.4.1.5	Chapter 4
CL_C5-EC	Uncorrected mean climatology from CMIP5 (1966–1993)	Sect. 3.4.1.5	Chapter 7
CL_IMD-EC	Mean monthly climatological precipitation from IITM (1966–1993)	Sect. 3.4.1.2	Chapter 7
C5-SH	Bias corrected ('nudged') GCM output (1966–1993)	Sect. 3.4.1.6	Chapter 6–8
C5-DEL	Delta method bias corrected GCM output (1966–1993)	Sect. 3.4.1.6	Chapter 6–8
C5-LOCI	Local intensity scaling corrected GCM output (1966–1993)	Sect. 3.4.1.6	Chapter 6–8

data (Sect. 3.4.1.4 and 3.4.1.5). A summary of which chapters use the different datasets is provided in Table 3.1. Datasets are given a suffix so as to easily identify the main purpose of each dataset. 'GM' for those used only for GLAM (Chapters 5, 6 and 8), 'QA' for those only used for quality assessment (Chapter 4) –except QA-WCL that was also used to calibrate EcoCrop, and 'EC' for those only used for EcoCrop modelling (Chapter 7).

3.4.1.1 Long-term observed climate time series

As opposed to climatological means (Sect. 3.4.1.2) that describe the state of a climate field as the time-average over a period of time (in this study the 40 years between 1961 and 2000), the climate time series used here are historical observations for each month and year in the period 1961–2000. These data were used to assess the simulated climate variability from the GCMs (Randall et al., 2007) and to perform GLAM simulations. The following observed climate time series datasets were gathered:

1. The CRU time series (CRU-TS3.0 at `http://www.cru.uea.ac.uk/cru/data/hrg`) of monthly precipitation, mean temperature, diurnal temperature range and the number of rain days for the period 1961-2000 were downloaded at the resolution of 0.5 degree. These data were used at two different temporal scales:

   (a) At daily scale for GLAM, by linearly interpolating monthly data in the period 1966-1993. Only maximum and minimum temperature data were subjected to this process (**TS_CRU-GM**). These data were used for GLAM simulations in Chapters 5, and 6; and

   (b) at monthly scale for all climate data quality analyses presented in Chapter 4 (**TS_CRU-QA**).

2. Monthly time series of precipitation, mean, maximum and minimum temperature were downloaded from the GHCN version 2 (Peterson and Vose, 1997) dataset and were then combined with daily precipitation series (accordingly aggregated to the monthly level) that were previously assembled by researchers at CIAT, also used in the study of Jones and Thornton (1999). The CIAT weather station database contained data only for precipitation, and so this was the only variable for which the two sources (i.e. GHCN and CIAT) accounted data (i.e. temperature data consisted only of GHCN stations). Monthly total rainfall was calculated for each month, year and weather station in the CIAT database only if all days in the month were reported with data. The number of wet days was not computed because the data were spatially too sparse (also see New et al. 2000). Precipitation data were subsequently merged with the GHCN precipitation dataset. Finally, duplicates were carefully removed, diurnal temperature range was calculated from maximum and minimum

temperature data, and data for years 1961–2000 were selected for all further analyses. The final dataset (hereafter termed **TS_WS-QA**), at the global level, comprised 29,736 rainfall locations (CIAT and GHCN), 7,198 mean temperature locations (only GHCN), and 4,959 diurnal temperature locations (only GHCN); although not all locations had data for all months and years and many had data for less than 10 years.

3. Observed daily precipitation data were gathered from the Centre for Climate Change Research (CCCR) of the Indian Institute for Tropical Meteorology (IITM) for the purposes of modelling with GLAM (Chapters 5, 6 and 8). Data were downloaded from the CCCR portal (`http://cccr.tropmet.res.in/cccr/home/index.jsp`) in NetCDF format at the native 1x1 degree resolution and for the period 1961 –2008. Data were available only for India. This dataset (referred to as **TS_IMD-GM**), was developed by the Indian Meteorological Department (IMD) of the National Climate Centre (NCC). These data are an update of the daily 1x1 degree resolution daily rainfall dataset of Rajeevan et al. (2006) that originally covered the period 1951–2003. The dataset is based on the interpolation of daily rainfall data from 1,803 rain gauges across India, most of which are concentrated towards the west and northwest of the country. Weather stations used to develop this dataset all have a minimum of 90 % data availability during the interpolated period (1951–2008). In developing the dataset, Rajeevan et al. (2006) used the interpolation method proposed by Shepard (1968), where each interpolated value is the result of the distance-weighted average of an n number of neighbouring points. Shepard's method has also been used in other climatological datasets (e.g. Huffman et al. 2009; Willmott et al. 1985).

   Figure 3.3 shows the monthly climatology derived from the TS_IMD-GM dataset. The dataset successfully reproduces the spatial and temporal consistency of rainfall (Rajeevan et al., 2006). For more details on the potential uses and caveats of the TS_IMD-GM dataset, the reader is referred to Rajeevan et al. (2005, 2006), and more recently to Rajeevan and Bhate (2008). The TS_IMD-GM dataset was hereby used because (1) it includes a large number of rainfall stations for the GLAM baseline simulation period (1966 – 1993, see Chapters 5 and 6) and the analysis domain (India, Figure 3.2); (2) it is the only gridded dataset that covers the entire analysis period at a daily time step needed for GLAM; (3) as reported by Rajeevan

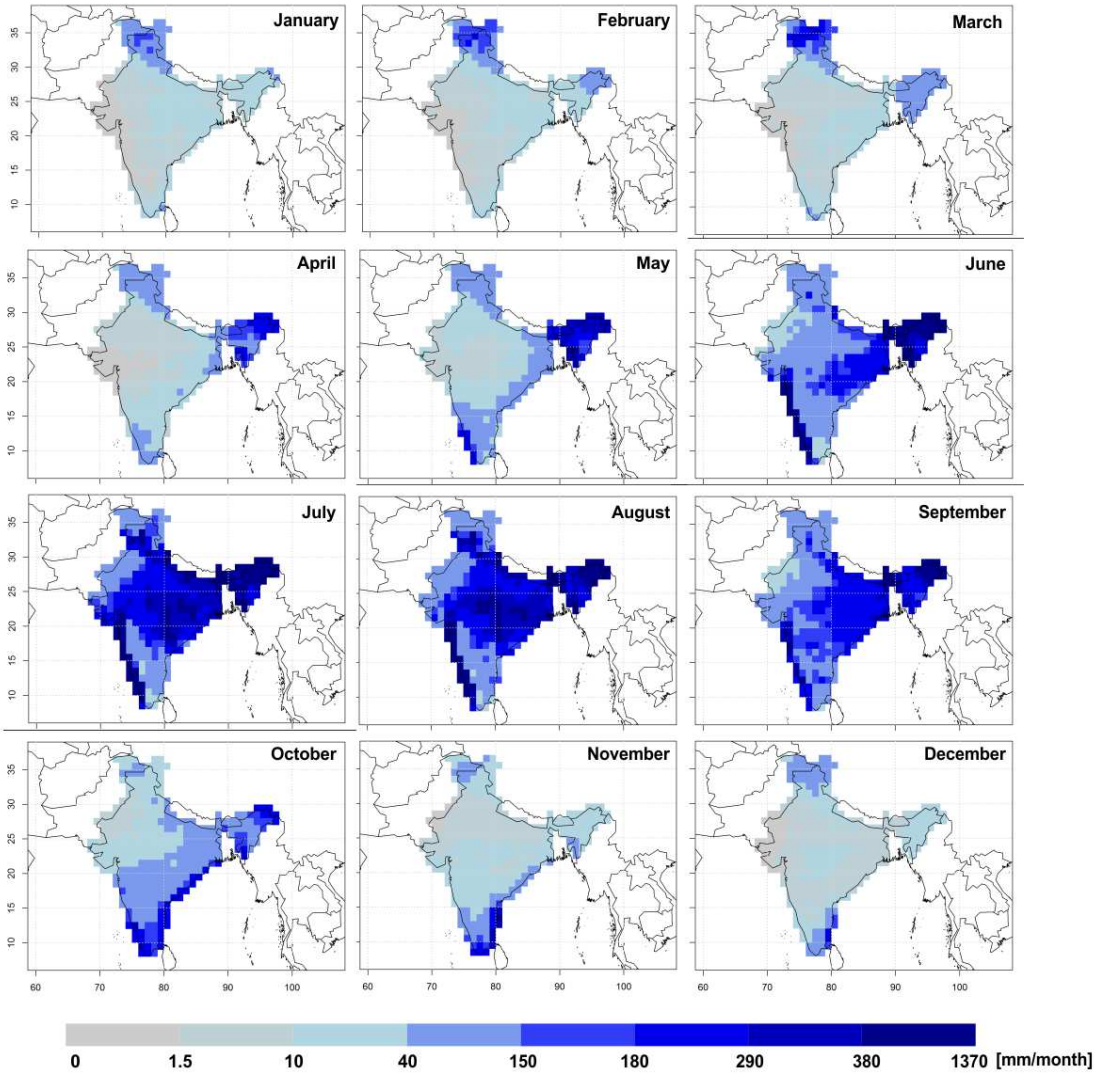

FIGURE 3.3: Average monthly climatology in the IMD dataset.

et al. (2005, 2006), there is substantial agreement between the TS_IMD-GM dataset and the Global Precipitation Climatology Project (GPCC) (Huffman et al., 2009), and the Variability Analysis of Surface Climate Observations (VASClimo, `ftp://ftp-anon.dwd.de/pub/data/gpcc/html/vasclimo_download.htm`); and (4) it has a spatial resolution at which GLAM can be operated (Challinor et al., 2004, 2005a).

3.4.1.2 Long-term observed mean climatology from interpolated surfaces

Four different datasets representing long-term mean climatology were gathered as follows:

TABLE 3.2: Number of locations per data source in CL_WS-QA (global).

Source	Precipitation stations	Mean temperature stations	Min., Max. temperature stations	Period
GHCN v2	20,590	7,280	4,966	1950-2000
WMO CLINO	4,261	3,084	2,504	1961-1990
FAOCLIM 2.0	27,372	20,825	11,543	1960-1990
CIAT	18,895	13,842	5,321	1950-2000

Notes: Sources are as follows: GHCN v2: Global Historical Climatology Network version 2 (Peterson and Vose, 1997); WMO CLINO: World Meteorological Organization Climatology Normals; FAOCLIM 2.0: Food and Agriculture Organization of the United Nations Agro-Climatic database (FAO, 2001); CIAT: Database assembled by Peter J. Jones at the International Center for Tropical Agriculture (CIAT).

1. Long term climatological means of monthly precipitation and mean, maximum and minimum temperatures from weather stations were assembled following Hijmans et al. (2005). Data were gathered from the Global Historical Climatology Network (Peterson and Vose, 1997) (GHCN, available at `http://www.ncdc.noaa.gov/pub/data/ghcn/v2`), the World Meteorological Organization Climatology Normals (WMO CLINO), FAOCLIM 2.0 (Food and Agriculture Organization of the United Nations Agro-Climatic database) (FAO, 2001), and a number of other minor (i.e. country-specific) sources previously compiled by researchers at the International Center for Tropical Agriculture (CIAT, also see Jones and Thornton 1999) (Table 3.2). Additional sources such as R-Hydronet (available at `http://www.r-hydronet.sr.unh.edu/english/`) and the Oldeman (1988) database for Madagascar were also included. Any weather station with less than 10 years of data was discarded. Data were carefully checked for errors in locations and in data, and duplicates were removed or merged (Hijmans et al., 2005).

   The final dataset (after quality control and duplicates removal, see Hijmans et al. 2005 for more details) comprised 13,141 (35,608) locations with monthly precipitation data, 3,744 (16,875) locations with monthly mean temperature, and 2,684 (12,458) locations with diurnal temperature range for the study region (the globe). Data for the number of wet days was not available and thus could not be included in this dataset. This dataset is hereafter referred to as **CL_WS-QA**.

2. The high resolution climate surfaces in WorldClim (Hijmans et al., 2005), available at `http://www.worldclim.org`. WorldClim is a 30 arc-seconds (∼1 km at the

equator) global dataset produced from the interpolation of long-term climatology as measured in weather stations (for precipitation, and mean, minimum and maximum temperatures). As opposed to CL_CRU-QA (see below), WorldClim does not contain data for the number of wet days. Global gridded data were downloaded at the 30 arc-second resolution, then masked to the analysis domain, and aggregated to 10 arc-minute using bilinear interpolation in order to reduce computational and storage needs. Monthly maximum and minimum temperatures were used to compute diurnal temperature range. The final dataset (referred to as **CL_WC-QA** hereafter) comprised monthly climatological means of precipitation, mean temperature and diurnal temperature range for the 12 months of the year).

3. The University of East Anglia Climatic Research Unit (CRU) dataset (New et al., 2002), available through `http://www.cru.uea.ac.uk/cru/data/hrg/` (CRU-CL-2.0). This dataset holds significant similarities to WorldClim in terms of input data, methods and resulting predictions (Hijmans et al., 2005), but is acknowledged to be more robust by climatologists, as input data quality checking is reported to be much more rigorous (Mitchell and Jones, 2005; New et al., 2002). Global data for monthly total precipitation, and monthly mean temperature, diurnal temperature range, and the number of wet days (i.e. days with precipitation greater than 0.1 mm, New et al. 1999) were downloaded at the only available resolution (10 arc-min). These data are herein termed **CL_CRU-QA**. These data, along with CL_WC-QA were used only for the climate data quality assessment presented in Chapter 4.

4. A dataset of climatological monthly means for the period 1966–1993, named **CL_CRU-EC**, was calculated using the TS_CRU-QA data. These were used in the EcoCrop simulations of Chapter 7.

5. The TS_IMD-GM dataset was also aggregated to the monthly climatological scale by first calculating monthly precipitation totals and then averaging each month for the period 1966–1993 (**CL_IMD-EC** hereafter). These aggregated data were used to run EcoCrop (Chapter 7).

3.4.1.3 Reanalysis data

The open-access version (i.e. 2.5 x 2.5 degree) of the European Centre for Medium-Range Weather Forecasts (ECMWF) 40+ Reanalysis (ERA-40) (Uppala et al., 2005) was used as it is a fair intermediate between observations and coupled climate model outputs (Challinor et al., 2005c; Ma et al., 2009). In the ERA-40 reanalysis, temperature observations are assimilated directly into the reanalysis system, which makes temperature predictions consistent and reliable, and hence useful for assessing the skill of climate models (Ma et al., 2009; Weedon et al., 2011); however, there is no analysis of precipitation in ERA-40, meaning that the model output is directly generated in the numerical weather prediction model (i.e. via parameterized microphysical processes in clouds) (Ma et al., 2009; Uppala et al., 2005). This leads to similar precipitation biases as those found in climate models. Despite that, ERA-40 precipitation data was also used in order to provide a comparison with the CMIP climate models.

Six-hourly temperatures, total precipitation and total downwards shortwave solar radiation were retrieved from the ECMWF archive (at `http://data-portal.ecmwf.int/data/d/era40_daily/`) for the period 1961-2000. Three processes were then performed:

1. ERA-40 solar radiation data were scaled onto the TS_IMD-GM dataset grid (1x1 degree) using nearest-neighbour interpolation (**TS_E40-GM**). These daily data were used for GLAM's baseline simulations (Chapters 5 and 6). ERA-40 was preferred instead of the interpolated total solar radiation from CRU used by previous GLAM studies (Challinor et al., 2004) as it provided a realistic representation of daily solar radiation (Ma et al., 2009; Uppala et al., 2005; Weedon et al., 2011).

2. Diurnal temperature range was calculated from maximum and minimum daily temperatures and the number of wet days (i.e. those where precipitation > 0.1 mm day^{-1}) was computed from total daily precipitation. The daily mean temperature, diurnal temperature range, total precipitation and wet-day frequency were finally aggregated to the monthly scale. This produced monthly gridded (2.5 x 2.5 degree) datasets of total precipitation, mean temperature, diurnal temperature range and the number of wet days for every year between 1961 and 2000 (**TS_E40-QA**, hereafter).

3. TS_E40-QA were used to compute 1961–2000 monthly climatological means of the mean temperature, diurnal temperature range, total precipitation and wet-day frequency. These data are termed **TS_E40-QA**.

3.4.1.4 CMIP3 climate model data

CMIP3 GCM simulations comprised the sole state-of-the-art public and official source of climate data for use in impact studies after the public release of the IPCC Fourth Assessment Report (AR4) in 2007 (IPCC, 2007), and before projections of the IPCC Fifth Assessment Report (AR5) were publicly available (Taylor et al., 2012).

Present day (1961–2000) simulations of global climate at original GCM resolution (∼100 km) were downloaded from the CMIP3 (Coupled Model Intercomparison Project phase 3) web data portal at `https://esg.llnl.gov:8443/index.jsp` (PCMDI, 2007). Monthly time series of mean, maximum, minimum temperature and precipitation flux in NetCDF format were downloaded for 24 coupled GCMs (Table 3.3). Separately for each GCM, diurnal temperature range was calculated for each month and year as the difference between maximum and minimum temperatures. Similarly, total monthly precipitation was calculated as the product between the precipitation rate, the water density at sea level pressure and the number of seconds in the month. The number of wet days was not analysed for CMIP3 since daily data were not available for the whole period of analysis in the CMIP3 data portal. The multi-model-mean (MMM) was calculated for all variables for every month and year using all GCMs. Each climate model monthly time series was used in further analyses (**TS_C3-QA** hereafter).

In addition, the mean 1961–2000 climatology was calculated by averaging, for each variable (mean temperature, diurnal temperature range and total precipitation) and every month, the values of the whole 1961–2000 period (**CL_C3-QA** hereafter). Thus, the final datasets (i.e. TS_C3-QA and CL_C3-QA, respectively) consisted of three variables (mean temperature, diurnal temperature range and total monthly precipitation) for 24 different GCMs and the MMM.

Table 3.3: Available CMIP3 GCMs, resolutions, and main references.

Model	Country	Atmosphere	Ocean	Reference
BCCR-BCM2.0	Norway	T63, L31	1.5x0.5, L35	Furevik et al. (2003)
CCCMA-CGCM3.1-T47	Canada	T47, L31	1.85x1.85, L29	Scinocca et al. (2008)
CCCMA-CGCM3.1-T63	Canada	T63, L31	1.4x0.94, L29	Scinocca et al. (2008)
CNRM-CM3	France	T63, L45	1.875x(0.5-2), L31	Salas-Mlia et al. (2005)
CSIRO-Mk3.0	Australia	T63, L18	1.875x0.84, L31	Gordon et al. (2002)
CSIRO-Mk3.5	Australia	T63, L18	1.875x0.84, L31	Gordon et al. (2002)
GFDL-CM2.0	USA	2.5x2.0, L24	1.0x(1/3-1), L50	Delworth et al. (2006)
GFDL-CM2.1	USA	2.5x2.0, L24	1.0x(1/3-1), L50	Delworth et al. (2006)
GISS-AOM	USA	4x3, L12	4x3, L16	Russell et al. (1995)
GISS-MODEL-EH	USA	5x4, L20	5x4, L13	Schmidt et al. (2006)
GISS-MODEL-ER	USA	5x4, L20	5x4, L13	Schmidt et al. (2006)
IAP-FGOALS1.0-G	China	2.8x2.8, L26	1x1, L16	Yongqiang et al. (2004)
INGV-ECHAM4	Italy	T42, L19	2x(0.5-2), L31	Gualdi et al. (2008)
INM-CM3.0	Russia	5x4, L21	2.5x2, L33	Diansky and Zalensky (2002)
IPSL-CM4	France	2.5x3.75, L19	2x(1-2), L30	Marti et al. (2005)
MIROC3.2-HIRES	Japan	T106, L56	0.28x0.19, L47	Hasumi and Emori (2004)
MIROC3.2-MEDRES	Japan	T42, L20	1.4x(0.5-1.4), L43	Hasumi and Emori (2004)
MIUB-ECHO-G	Germany	T30, L19	T42, L20	Groetzner et al. (1996)
MPI-ECHAM5	Germany	T63, L32	1x1, L41	Jungclaus et al. (2006)
MRI-CGCM2.3.2A	Japan	T42, L30	2.5x(0.5-2.0)	Yukimoto et al. (2001)
NCAR-CCSM3.0	USA	T85L26, 1.4x1.4	1x(0.27-1), L40	Collins et al. (2006)
NCAR-PCM1	USA	T42, L18	1x(0.27-1), L40	Washington et al. (2000)
UKMO-HADCM3	UK	3.75x2.5, L19	1.25x1.25, L20	Gordon et al. (2000)
UKMO-HADGEM1	UK	1.875x1.25, L38	1.25x1.25, L20	Johns et al. (2006)

3.4.1.5 CMIP5 climate model data

Daily CMIP5 outputs of the historical and RCP4.5 transient simulations were downloaded from the CMIP5 archive, freely available at `http://pcmdi9.llnl.gov/esgf-web-fe/` (Taylor et al., 2012). A total of 26 GCMs presented data for the historical simulation at the time queried (February 2012, Table 3.4). Available simulations (a total of 70, Table 3.4) at the daily scale for five variables were downloaded: mean, maximum, minimum temperature, precipitation flux, and shortwave downwards radiative flux. Data for the years 1961–2000 (historical) and 2020-2049 (RCP4.5) were downloaded to produce the following four sets of data:

1. Historical data of maximum and minimum temperatures were used to compute diurnal temperature range, whereas daily precipitation was used to calculate the wet-day frequency. All daily historical data were aggregated to monthly. This produced time series of total monthly precipitation, number of wet days, and means for mean temperature and diurnal temperature range for the period 1961–2000, which was termed **TS_C5-QA**. The MMM was calculated using all available climate models.

2. Using TS_C5-QA, climatological means of monthly precipitation, number of wet days, and means for mean temperature and diurnal temperature range were produced (**CL_C5-QA** hereafter). As with TS_C5-QA, the MMM was calculated for the four variables.

3. Daily-scale data for India were extracted for the periods 1966-1993 (baseline) and 2020-2049 (RCP4.5). These were termed **TS_C5-GM** and were used for GLAM simulations. Owing to lack of consistency in the availability of the needed variables (i.e. precipitation flux, minimum and maximum surface temperatures and downwards radiative flux) across GCMs and periods, only outputs from 15 out of the 26 GCMs were used in the analyses (marked with § in Table 3.4). Initial conditions ensemble members for some GCMs were available, and thus the total of GCM simulations used as inputs for GLAM was 32. These daily data were used for the GLAM simulations of Chapter 6 and 8. Data were available in most cases for the years 1950-2005; however, since these data were used for baseline GLAM simulations, the period was limited to that of the yield time series (1966-1993, Sect. 3.4.2.1). To keep consistency with the length of the baseline (28 years), the future period was chosen to be 2022-2049.

4. Using TS_C5-GCM, the monthly means and totals were first calculated for mean, minimum and maximum temperatures and for daily precipitation. These data, named **CL_C5-EC**, were then averaged over the whole 1966-1993 (2020-2049) period so as to be used as baseline (future) data for EcoCrop (see Chapter 7).

3.4.1.6 Bias corrected CMIP5 output

Previous studies where GLAM was used have employed raw climate model output directly into the crop model, with only a limited account for climate model bias through the calibration of C_{YG} (Challinor et al., 2007, 2009a, 2010), or have reported little benefit from bias correction (Challinor et al., 2005a). Nevertheless, climate model bias has been acknowledged as a critical barrier for crop model simulation (Berg et al. 2010; Iizumi et al. 2009a; Ines et al. 2011, also see Chapter 4 of this thesis and Ramirez-Villegas et al. 2013a). Particularly for threshold-dependent model processes, there is a risk that climate model bias could trigger or prevent threshold exceedance, and in turn significantly under-

Table 3.4: CMIP5 GCMs used in the study and their main characteristics.

Model name	Ensemble members	NC	HRx	NR[1]	HRy	Calendar
BCC-CSM1.1 §	r1i1p1	128	2.8125	64	2.8125	365
BNU-ESM §	r1i1p1	128	2.8125	44	4.0909	365
CCCMA-CanCM4	r[1-10]i1p1	128	2.8125	64	2.8125	365
CCCMA-CanESM2 §	r[1-5]i1p1	128	2.8125	64	2.8125	365
CNRM-CM5 §	r1i1p1	256	1.4063	128	1.4063	366
CSIRO-ACCESS1.0 §	r1i1p1	192	1.875	145	1.2414	366
CSIRO-Mk3.6.0 §	r[1-10]i1p1	192	1.875	96	1.875	365
ICHEC-EC-EARTH	r[6,8]i1p1	320	1.125	160	1.125	366
INM-CM4 §	r1i1p1	180	2.0	120	1.5	365
IPSL-CM5a-LR §	r[1-4]i1p1	96	3.75	96	1.875	365
IPSL-CM5a-MR	r1i1p1	144	2.5	143	1.2587	365
IPSL-CM5b-LR §	r1i1p1	96	3.75	96	1.875	365
MIROC-ESM	r1i1p1	128	2.8125	64	2.8125	366
MIROC-ESM-CHEM	r1i1p1	128	2.8125	64	2.8125	366
MIROC-MIROC4h	r[1-3]i1p1	640	0.5625	320	0.5625	366
MIROC-MIROC5	r1i1p1	256	1.4063	128	1.4063	365
MOHC-HadCM3	r[1-10]i1p1	96	3.75	73	2.4658	360
MOHC-HadGEM2-CC §	r1i1p1	192	1.875	145	1.2414	360
MOHC-HadGEM2-ES §	r1i1p1	192	1.875	145	1.2414	360
MPI-ESM-LR §	r[1-3]i1p1	192	1.875	96	1.875	366
MPI-ESM-MR §	r1i1p1	192	1.875	96	1.875	366
MRI-CGCM3 §	r[1,5]i1p[1,2]	320	1.125	160	1.125	366
NCAR-CCSM4 §	r[1,2]i1p1	288	1.25	192	0.9375	365
NCC-NORESM1-M	r1i1p1	144	2.5	96	1.875	365
GFDL-ESM2G	r1i1p1	144	2.5	90	2.0	365
GFDL-ESM2M	r1i1p1	144	2.5	90	2.0	365

Notes: Ensemble member names as specified in Taylor et al. (2012), with r referring to the realization (i.e. equally realistic runs but initialized with different initial conditions), i referring to the initialization method (not relevant for historical runs), and p referring to any perturbed physics ensemble. NC and NR Number of columns (NC) and rows (NR) in the climate grid. HRx and HRy refer to horizontal resolution in the x-axis (longitude, HRx) and the y-axis (latitude, HRy), in decimal degree. Calendar type refers to that used in the climate model run: 365 is a calendar without leap years, 366 is the standard Gregorian calendar (with leap year), and 360 refers to the calendar in which all months have 30 days only used by the UK MetOffice climate models. The symbol § indicates that the GCM output was also used for GLAM and EcoCrop simulations

or over-estimate the effects of future projected climate change (Hawkins et al., 2013a,b; Ramirez-Villegas et al., 2013a). In addition, climate model bias could have a significant impact on threshold-dependent processes of GLAM or on suitability responses to climate in EcoCrop.

For these reasons, both raw and bias corrected simulated GCM outputs were used as inputs into GLAM and EcoCrop in this work. Bias corrected GCM output is here defined as any treatment of the raw GCM output in an attempt to make it more realistic (Hawkins et al., 2013b; Ines and Hansen, 2006). Here, the definition of bias correction includes the delta method (DEL, see below and Ver Hoef 2012). Three different methods were used. The first two are based on the methodology of Hawkins et al. (2013b), who described two climate model output bias correction methods: simple bias correction (or nudging, SH) and change factor (or delta method, DEL), both of which can be applied onto means or

onto both means and variability. Here, the two methods were used only to correct for bias in the mean, without accounting for variability. This was done because the observed temperature data used here were scaled from monthly means, and thus no account of variability could be done.

The SH method used the difference between the observed and simulated climatological means in the baseline to correct the mean of the raw daily data of the GCM. The SH method, thus, produces a time series where the daily variability is that simulated by the GCM. For temperature, the arithmetic difference was used (Eq. 3.2), whereas for precipitation and solar radiation the relative differences were used (Eq. 3.3).

$$M_{SH}(t) = M_{RAW}(t) + \left(\overline{O_B} - \overline{M_B}\right) \tag{3.2}$$

$$M_{SH}(t) = M_{RAW}(t) * \left(1 + \frac{\overline{O_B} - \overline{M_B}}{\overline{M_B}}\right) \tag{3.3}$$

where M refers to the model data and O to the observations. Time averages (i.e. climatological means of the period 1966-1993) are indicated by a bar above the symbol. The corrected values (subscript SH) for each day t were calculated by adding the mean bias of the model with respect to the observations in the baseline period (subscript B) to the raw climate model output (subscript RAW), where raw is either the historical or future GCM output. Daily SH method outputs are hereafter referred to as **C5-SH** and were produced both for the baseline (1966-1993) and the future climate scenario (2022-2049, RCP4.5).

The DEL method is most commonly referred to in the impacts and statistics literature as the 'delta approach' or 'delta method' (Ruane et al., 2013; Ver Hoef, 2012). It has been widely used to downscale climate change model simulations for input into impact studies (Ruane et al., 2013; Singh et al., 2012; Tabor and Williams, 2010). As implemented here, the method consisted of adding the GCM projected change in each variable to the observations. As for SH, DEL temperatures were calculated using the arithmetic difference (Eq. 3.4), but for precipitation and solar radiation the relative difference was used instead (Eq. 3.5).

$$M_{DEL}(t) = O_B(t) + \left(\overline{M_P} - \overline{M_B}\right) \tag{3.4}$$

$$M_{DEL}(t) = O_B(t) * \left(1 + \frac{\overline{M_P} - \overline{M_B}}{\overline{M_B}}\right) \tag{3.5}$$

where the subscript P refers to the future projection (2022-2049 in this study) and the climatological means are indicated with a bar above respective letters. DEL corrected data are hereafter referred to as **C5-DEL**.

Both SH and DEL methods were independently applied for each grid cell and GCM simulation (i.e. correction factors varied spatially). Correction factors were in both cases derived for each month and then applied to daily values. For a more complete description and analysis of these two methods and a review of other methods the reader is referred to Hawkins et al. 2013a,b.

The last method used here is called local-intensity scaling (LOCI) and is classified as an 'empirical-statistical downscaling and error correction method' (Schmidli et al., 2006; Themessl et al., 2011). The technique consists in correcting both wet-day intensity and frequency. In other words, it corrects biases in the number of rainy days and in the total precipitation falling in such days. The underlying assumption in LOCI is that climate model precipitation integrates all relevant predictors. Therefore, to apply LOCI to a given model simulation, other climate fields are irrelevant (Themessl et al., 2011). This means that solar radiation and temperatures are not corrected. Although this assumption may not hold valid under a number of conditions (Ehret et al., 2012; Piani and Haerter, 2012; Themessl et al., 2012), LOCI has been found to be amongst the best performing bias correction techniques (Ehret et al., 2012; Themessl et al., 2011). Since LOCI corrects using parameters that are valid over a sufficiently long period of time (e.g. 30-year climatology), it is capable of correcting both numerical weather predictions and transient climate change simulations (Schmidli et al., 2006; Themessl et al., 2011).

On a monthly basis, two parameters were estimated: the model wet-day threshold (WT^{mod}) and the scaling factor (S). First, WT^{mod} was estimated as the threshold above which the number of wet days predicted by the model equalled the number of wet days in the observations. The number of wet days in the observations is hereby defined following Schmidli

et al. (2006) as the number of days above a threshold WT^{obs} of 1 mm day^{-1} (also see New et al. 2000). Next, S was estimated using Eq. 3.6.

$$S_{t,i} = \frac{\overline{PWD_{t,i}^{obs}} - WT_{t,i}^{obs}}{\overline{PWD_{t,i}^{mod}} - WT_{t,i}^{mod}} \tag{3.6}$$

where $\overline{PWD}$ is the climatological mean of wet days for observations (*obs*) and GCM (*mod*). $\overline{PWD}$ is calculated for days above the respective WT threshold. The scaling factor is calculated for each location (i) and for each month in the year (t), and is a single value representing the whole baseline period. The monthly correction factor and the WT^{mod} threshold are then used to correct the intensity and frequency of each month in both the baseline and the future GCM simulations. As with the SH method, there is an assumption that the model bias stays constant or has negligible variation through time. Given that the analyses presented here focus on the 2030s, this assumption is unlikely to bias the results presented (see e.g. Hawkins et al. 2013a). LOCI-corrected data are termed **C5-LOCI**.

All methods were applied at the resolution of the TS_IMD-GM dataset (1x1 degree) and thus there was some degree of downscaling involved in the application of the three techniques (Hawkins et al., 2013b). The resulting datasets were all at daily scale for the periods 1966-1993 and 2022-2049.

Bias corrected data were also used for EcoCrop suitability simulations. Since EcoCrop uses monthly climatological means, daily precipitation and mean, maximum and minimum surface temperature were totalised or averaged over each month and then averaged over the entire baseline (1966–1993) and future scenario (2022–2049) periods in order to obtain bias-corrected GCM climatological means for C5-SH, -DEL and -LOCI (see Table 3.1). Because the climatological means of the DEL and BC methods are mathematically equivalent (see Hawkins et al. 2013b), this reduced EcoCrop bias corrected inputs to 2 (DEL and LOCI) as opposed to the 3 used for GLAM (SH, DEL, LOCI). Since EcoCrop did not make use of solar radiation data, no further processing was done for that variable.

3.4.2 Crop data

3.4.2.1 Crop yield and irrigated areas

Time series of groundnut crop yields and irrigated area for the period 1966–1993 were obtained from a previous GLAM study (Challinor et al., 2004). Using the district-level harvested area and total production, yearly crop yields were calculated. These crop yields were first linearly de-trended to remove any monotonic trend (due to improvement of technologies, higher fertilizer use, and new varieties) to the technology levels of 1966, and then scaled onto the IMD grid by assuming that the crop is evenly distributed within each district. Irrigated area data at the district level were also scaled onto the IMD grid. Whenever a grid cell was composed by fractions of various districts, the detrended yield or irrigated fraction of the grid cell was calculated as the weighted-area average of all districts. Districts and years with missing data were not used in calculating grid cell values for those specific years, but they were used for those years for which data were available. The resulting spatially observed gridded yield data are shown in Figure 3.4.

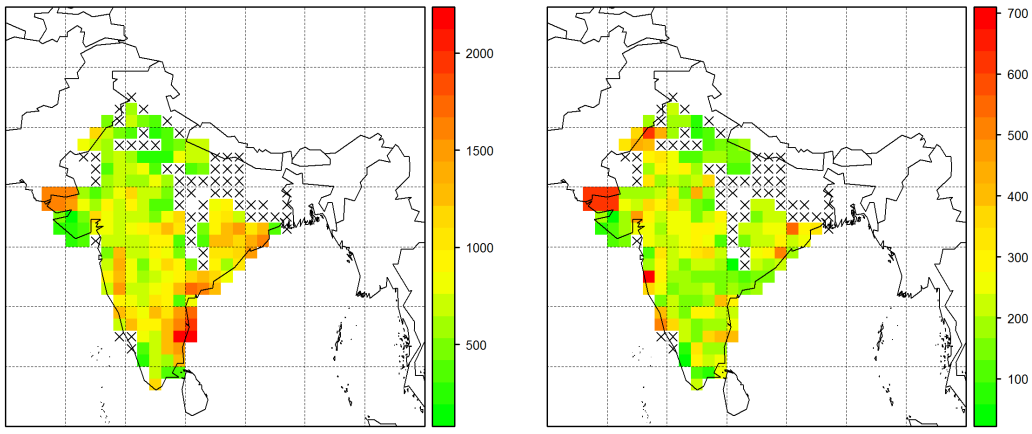

(a) $\bar{Y}$ (b) σ_Y

FIGURE 3.4: Observed mean ($\bar{Y}$) and standard deviation (σ_Y) of groundnut yields. Grid cells marked with an "X" indicate locations where area harvested is less than 0.2 % of the total grid cell area.

The highest mean yield areas are located in northern Gujarat, and along the east coast of India (states of Andhra Pradesh, Tamil Nadu and Orissa). The largest yield variability was found in northern Gujarat as well as in central India. Marginal yields (i.e. green areas of Figure 3.4) were generally observed in areas where irrigation rates were also very low

(Figure 3.5) (e.g. Rajasthan, Uttar Pradesh, and southern Gujarat). In these areas, there is generally a low use of inputs, thus leading to large yield gaps (Bhatia et al., 2009). A more complete description of these data has been done by Challinor et al. (2003, 2004).

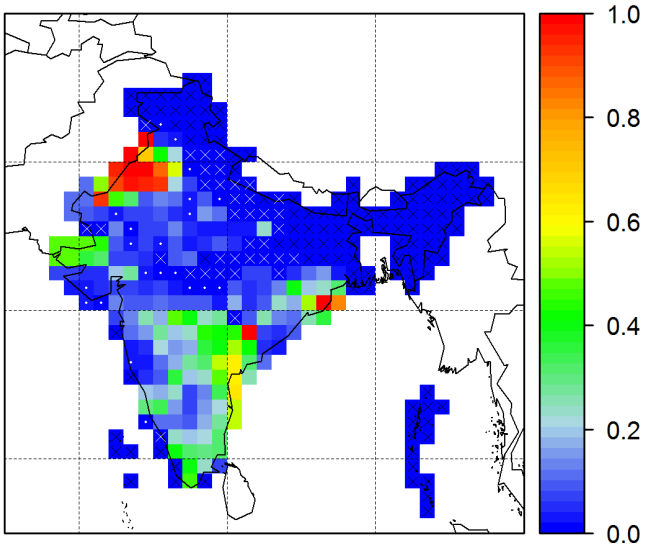

FIGURE 3.5: Observed mean irrigated fraction scaled to the IMD grid. Grid cells with a black "X" indicate places where mean irrigated fraction equals zero, white "X" are in places where irrigated area is between 0 and 1 %, and white dots indicate places where irrigated area is between 1 and 3 %.

3.4.2.2 Crop presence and absence data

Two different presence-absence datasets were used. The first one was used for calibrating EcoCrop, while the second was used for evaluating the model.

For the first dataset, occurrences (i.e. presence observations) of groundnut were gathered from the Global Biodiversity Information Facility (GBIF, `http://data.gbif.org`), and the study of (Bhatia et al., 2006). The data consisted of geographic coordinates of 1,716 locations of groundnut (*Arachis hypogaea* L.) representing areas where the crop is grown within India. The data were carefully verified for the consistency of its geographic coordinates (latitude, longitude) and corrected or removed as needed. Only unique locations in a 30 arc-second spatial resolution grid were used for all further steps (1,464 locations, "EcoCrop calibration dataset" hereafter, Figure 3.6). Crop locations were used since the alternative approach of using crop distribution gridded data (Monfreda et al., 2008; You

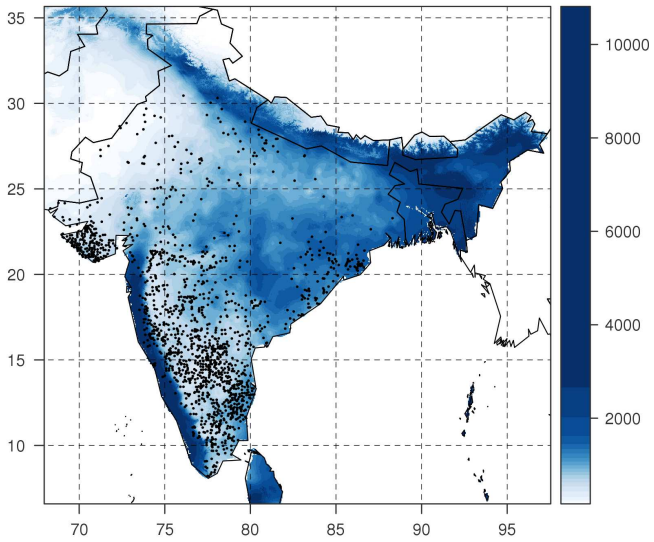

FIGURE 3.6: Crop locations used for EcoCrop's calibration overlaid with total annual rainfall. Total annual rainfall as in the CL_WCL-QA dataset.

et al., 2009) can lead to inaccuracies due to the known spatial scale differences in those datasets (Licker et al., 2010). The crop presence points dataset was used to calibrate EcoCrop.

For the second dataset, the district-level harvested area described above (Sect. 3.4.2.1) were used to produce a presence-absence evaluation dataset, whereby any districts where there was no harvested area reported between 1966–1992 were considered absences. This dataset was gridded at two resolutions: 2.5 arc-minutes (roughly 5 km), and 1x1 degree (roughly 100x100 km) (Figure 3.7) in order to evaluate the baseline suitability predictions at those two resolutions (see EcoCrop's evaluation procedure in Sect. 7.3.2).

3.4.2.3 Crop calendar data

Two crop calendar datasets were used. The first dataset was used in GLAM simulations. This source consisted in the planting windows from the global study of Sacks et al. (2010). Sacks et al. (2010) assembled a global dataset of planting and harvest dates for 19 major crops using six different sources: FAOs Global Information and Early Warning System (GIEWS) (FAO, 2007), USDA (2006), USDA-FAS (2008), USDA-NASS (1997), USDA-FAS (2003), and IMD-AGRIMET (2008). The dataset of Sacks et al. (2010) is the first

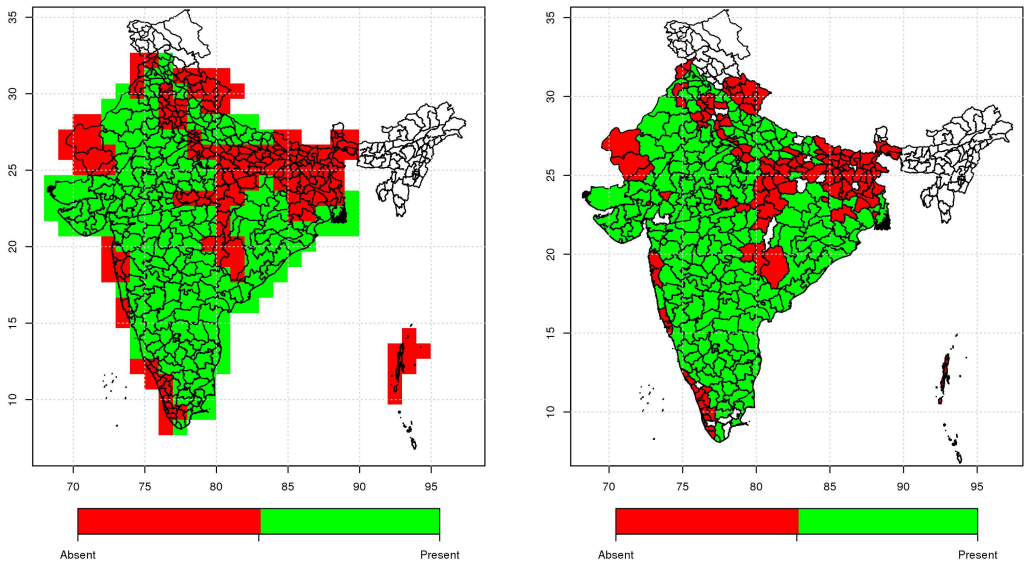

(a) 2.5 arc-minute (b) 1x1 degree

FIGURE 3.7: Gridded district-level crop presence evaluation data at 2.5 arc-minute and 1x1 degree spatial resolutions. Absence areas are those where no harvested area was reported between 1966 and 1993.

global dataset with georeferenced crop planting and harvesting information. The filled dataset for groundnut was used because (1) it is trustable for India, and (2) it provides spatially continuous values of planting windows for the region of analysis. The data were aggregated onto the TS_IDM-GM precipitation grid using area-weighted averages and carefully checked for inconsistencies. Sacks et al. (2010) crop calendar data are hereafter referred to as GLAM-SPD dataset

The second source was the growing season data of Ericksen et al. (2011), who determined the start and length of the growing season across the global tropics and sub-tropics using a simple water balance module (fully described by Jones 1987) and spatially-explicit time series of weather generated using the MarkSim weather generator (see Jones and Thornton 2000) at a resolution of 5 arc-minutes. In this dataset (further referred to as E-LGP dataset), the growing season starts after 5 consecutive growing days and ends after 12 consecutive non-growing days, with a growing day defined as that with ratio of actual to potential evapotranspiration (E_a/E_p) greater than 0.35 and minimum daily temperature greater than 6 °C (Ericksen et al., 2011; Jones et al., 2009). These estimations of growing season duration were used instead of the growing season data of Sacks et al. (2010) (described above) since these were available at a sufficiently high resolution for EcoCrop

calibration and captured the spatial variation in the rainfall-driven growing season start and duration (Mehrotra, 2011). The E-LGP dataset was used directly to drive the EcoCrop model (see Chapter 7). In turn, these estimates were not used for GLAM simulations since it was preferred that GLAM planted the crop according to its own water balance model using an automatic planting routine (see Chapter 5, Sect. 5.3.2).

3.4.3 Soil data

GLAM requires soil hydrological parameters to be defined. In previous GLAM studies, a number of soil classes were defined, with each class having a prescribed value for the three soil moisture limits, namely, the volumetric moisture contents at permanent wilting point (θ_{ll}), field capacity (θ_{dul}) and saturation (θ_{sat}). In the present study, spatially variable soil hydrological parameters were derived from the Harmonized World Soil Database (HWSD) (Batjes, 2009). The HWSD contains over 16,000 different soil mapping units. This database combines regional and national soil studies with the information contained within the 1:5,000,000 scale FAO-UNESCO Soil Map of the World (FAO/UNESCO, 1974). The spatially explicit properties in the soil classes occurring within the analysis domain were calculated as the area-weighted-average of each soil profile in each 1x1 grid cell of the IMD grid. This resulted in three (one for each soil moisture limit) spatially explicit continuous 1x1 degree datasets that covered the analysis domain. In each grid cell, a GLAM simulation was always associated with its three respective soil moisture content values.

3.5 Models

3.5.1 The GLAM crop model

The crop model used in this study falls in the category of regional-scale process-based crop models (see Chapter 2, Sect. 2.3.2). The General Large Area Model for annual crops (GLAM) is a model designed to capitalise on the large-scale relationships between climate and crop yields (Challinor et al., 2004). Here, release version 2 of the groundnut GLAM model was used (GLAM-R2). For simplicity, the name GLAM is used to refer to the latest release of GLAM hereinafter. GLAM is a process based model in which some varietal-level detail is skipped but enough detail is retained to ensure that the weather-yield relationships

are captured. GLAM explicitly models the controls of soil water availability, temperature and solar radiation on crop growth, but accounts for nutrition, management practices, pests and diseases through a yield gap parameter (C_{YG}). To some extent, GLAM's C_{YG} can also account for biases in input data (Challinor et al., 2005c; Watson and Challinor, 2013).

GLAM integrates the benefits of process-based approaches (i.e. transferability across space and time) and the benefits from empirical approaches (i.e. low data intensity, validity over large areas), thus constituting an approach for assessing the impacts of climate variability and change (Challinor et al., 2004). The model is mathematically one-dimensional and simulations can thus be performed at any resolution, provided that crop-climate relationships exist. GLAM has been used at scales between tens to hundreds of kilometres, which is consistent to that of regional and global climate models. GLAM can be used with pre-processed or raw climate model output at a variety of spatial scales (Challinor and Wheeler, 2008b).

GLAM is less complex than field-scale models, but more complex than statistical and niche based models. GLAM, therefore, allows to reduce the risk of over-parameterisation, while at the same time providing a model that can be used under a variety of spatio-temporal domains without involving the risk of extrapolation (Challinor and Wheeler, 2008b; Challinor et al., 2009b). However, these advantages may present a number of drawbacks, including the difficulty in modelling non-climatic processes that influence crop yields (Challinor and Wheeler, 2008b), or the risk of aggregation error (Hansen and Jones, 2000).

GLAM has been used extensively to simulate groundnut crop yields in India. Challinor et al. (2004) optimised the model over 2.5-by-2.5 grid cells and found the model to be in broad agreement with reported crop yield and other observations. Challinor et al. (2005b) further developed the model and tested its predictive skill under high temperature stress conditions. Challinor et al. (2005c) used raw and bias-corrected reanalysis data as input into GLAM, while Osborne et al. (2007) incorporated it within the land surface component of a GCM, thus permitting fully coupled crop-climate simulation. More recently, Challinor et al. (2010) used GLAM to estimate the future risk of wheat crop failures, develop genotypic adaptation options and associate the model output with socio-economic data.

3.5.1.1 Model structure

Figure 3.8 shows GLAM-R2 structure as a whole. In GLAM, total crop biomass is estimated on a daily basis using the product of the total plant transpiration and the transpiration efficiency (T_E), whereas grain yield is estimated using the total biomass and the time-integrated rate of change in the harvest index ($\partial H_I/\partial t$). To estimate transpiration, a daily water balance is computed based on the Priestley-Taylor evapotranspiration equation (Priestley and Taylor, 1972) and the potential water uptake (Passioura, 1983). Leaf area growth, which in GLAM is simulated using a prescribed constant leaf area index growth rate ($\partial L/\partial t$) is a key input to water balance as it defines the total potential energy-limited transpiration. Total evapotranspiration is thus affected by leaf size, soil structure, and soil water availability.

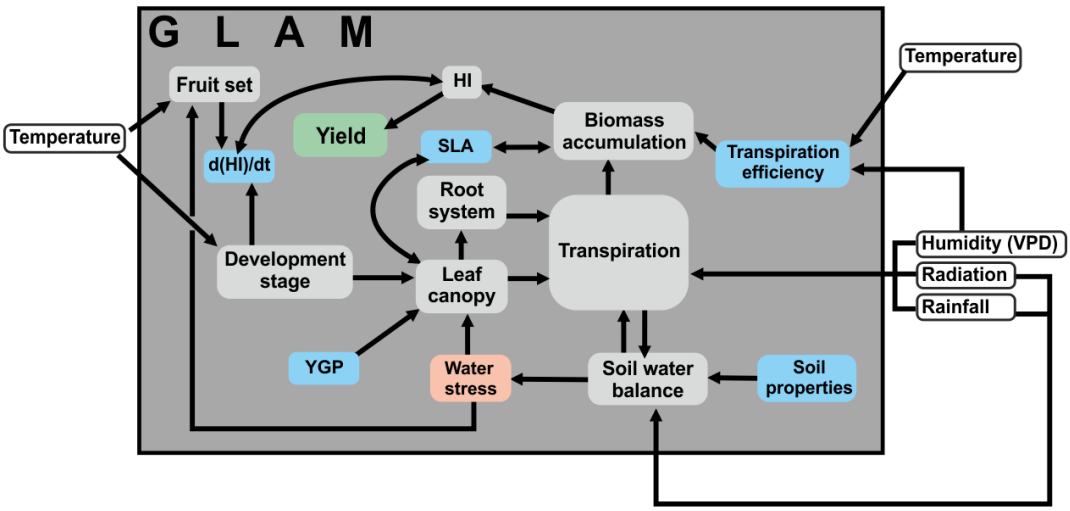

FIGURE 3.8: Structure of the model GLAM. SLA is specific leaf area, H_I is harvest index, $\partial H_I/\partial t$ is the rate of change in the harvest index, and YGP is the yield gap parameter (C_{YG}). Blue boxes indicate model constants, grey boxes are model prognostic variables (except yield, which is shown in green), and light orange box indicates intermediate variables. Weather inputs are in hollow rectangles outside the model box. Arrows show flow of information. Adapted from Challinor and Wheeler (2008a).

Crop development phases in GLAM are calculated using a thermal time accumulation equation with three cardinal temperatures. As mentioned above, the yield gap parameter C_{YG} is a model constant introduced to account for non-modelled processes that reduce crop yields (such as sub-optimal management and pests and diseases). Model internal consistency is kept using a prescribed value of SLA (specific leaf area, Challinor and

Wheeler 2008a). Additional processes are parameterised in GLAM, such as the effect of high temperatures during flowering (Challinor et al., 2005b) and on photosynthesis (Challinor et al., 2009b), the effect of water stress on flowering (Challinor et al., 2006), and the effect of elevated CO_2 concentrations (Challinor and Wheeler, 2008a). Further details on GLAM are provided in subsequent sections.

3.5.1.2 Crop development

Sowing occurs either on a given day (specified in as model input) or on the first day that soil moisture exceeds C_{sow} (a fraction of maximum available soil water). If C_{sow} is not reached after 30 days, the crop is planted regardless of soil moisture. Crop growth and development then starts after a number of days have passed (emergence time, t_{em}, in days), when the leaf area index (LAI) becomes non-zero, and thermal time (t_{TT}) starts to be calculated (Eq. 3.7).

$$t_{TT} = \int_{t_i}^{T} (T_{eff} - T_b)\,\mathrm{d}t \tag{3.7}$$

where,

t is the time (in days)

T_b is the base temperature below which development ceases

i is the development phase, and

T_{eff} is the effective temperature, defined by Eq. 3.8

and

$$T_{eff} = \begin{cases} \bar{T} & T_b \leq \bar{T} \leq T_o \\ T_o - (T_o - T_b)\left(\frac{\bar{T}-T_o}{T_m-T_o}\right) & T_o \leq \bar{T} \leq T_m \\ T_b & \bar{T} < T_b \text{ or } \bar{T} > T_m \end{cases} \tag{3.8}$$

where,

T_o is the optimal temperature for crop development,

T_m is the maximum temperature for crop development, and

$\bar{T}$ is the observed mean air temperature of the day, calculated as the average of maximum (T_{max}) and minimum (T_{min}) daily observed temperatures.

Groundnut is modelled using four development phases. These are in agreement with those proposed by Hammer et al. (1995), whilst being a simplification of the 13 stages considered by the field-scale peanut model PNUTGRO (Hoogenboom et al., 1992). The value of i varies from 0 to 3, with 0 when the crop is between sowing and flowering, 1 when the crop is between flowering and start of pod-filling, 2 when the crop is between start of pod-filling and maximum leaf area (maximum LAI) and 3 when the crop is between maximum LAI and harvest maturity. Each stage starts at a given time (t_i) and is completed when a stage-specific thermal requirement is met. Harvest occurs at maturity, unless there is terminal drought stress (see Sect. 3.5.1.11) or a harvest date is specified.

3.5.1.3 Leaf area dynamics

Leaf area growth is determined via Eq. 3.9, as follows:

$$\frac{\partial L}{\partial t} = \begin{cases} \left(\frac{\partial L}{\partial t}\right)_{max} * C_{YG} * min\left(\frac{S}{S_{cr}}, 1\right) & i < 3 \\ 0 & i = 3 \end{cases} \tag{3.9}$$

where,

L is the effective LAI,

$\left(\frac{\partial L}{\partial t}\right)_{max}$ is the parameterised maximum rate of growth of the leaf area index,

C_{YG} is the yield gap parameter,

S_{cr} is a critical value of S below which leaf area growth is affected by water stress, and

S is the soil water stress factor (Eq. 3.10)

$$S = \frac{T_T}{T_{Tpot}} \tag{3.10}$$

where,

T_T is the rate of transpiration, and

T_{Tpot} is the rate of potential transpiration

3.5.1.4 Root growth

Root growth is parameterised using the following equations:

$$\frac{\partial l_v(z=0)}{\partial L} = \text{prescribed constant} \tag{3.11}$$

$$V_{EF} = \text{prescribed constant} \tag{3.12}$$

$$l_v(z=z_{ef}) = \text{prescribed constant} \tag{3.13}$$

where,

l_v is the root length density by volume,

z is the depth across the soil profile,

z_{ef} is the depth of the root extraction front, and

V_{EF} is the extraction front velocity

3.5.1.5 Biomass and yield

Biomass is determined using the transpiration efficiency (E_T), the maximum normalised transpiration efficiency ($E_{TN,max}$), the vapour pressure deficit (V), and the actual crop transpiration (T_T) (Eq. 3.14)

$$\frac{\partial W}{\partial t} = T_T * min\left(\frac{E_T}{V}, E_{TN,max}\right) \tag{3.14}$$

The vapour pressure deficit (V) is estimated using the maximum and minimum saturated vapour pressure (e_{sat}) (Eq. 3.15)

$$V = C_V \left[e_{sat} \left(T_{max} \right) - e_{sat} \left(T_{min} \right) \right] \tag{3.15}$$

where,

C_V is a constant (Tanner and Sinclair, 1983), and

e_{sat} is parameterised as a function of temperature (T) after Bolton (1980) (Eq. 3.16)

$$e_{sat}(T) = 6.112 * e^{\frac{17.67*T}{T+243.5}} \tag{3.16}$$

Yield is determined using the total crop biomass (W) and the harvest index (H_I) in any day after the start of pod-filling ($i \geq 2$) (Eq. 3.17).

$$Y = H_I * W \tag{3.17}$$

where the rate of change in the harvest index ($^{\partial H_I}/_{\partial t}$) is parameterised as a constant.

3.5.1.6 Soil water balance

The soil is assumed to be divided in N_{SL} layers, all with the same values of field capacity (θ_{dul}), wilting point (θ_{ll}), and saturation (θ_{sat}). The depth of the profile is z_{max} and each soil layer has a depth z, and an associated value of $l_v(z)$, which is in turn determined by Eq. 3.13. A value of volumetric water content (θ) is calculated for each day by first calculating runoff using the US Soil Conservation Service method (USDA-SCS, 1964) (Eq. 3.18)

$$R = \frac{P^2}{P + S} \tag{3.18}$$

where R is the runoff, P is the precipitation and S is the amount of water that can soak into the soil. The value of S is assumed to be equal to the saturated hydraulic conductivity of the soil k_{sat}. Drainage is then calculated according to (Suleiman, 1999) (Eq. 3.19 – 3.22).

$$\frac{\partial \theta}{\partial t} = -FD\left(\theta_s - \theta_{dul}\right) \tag{3.19}$$

$$D = C_{d1}\theta_{dul}^2 + C_{d2}\theta_{dul} + C_{d3} \tag{3.20}$$

$$F = 1 - \frac{\ln(Q_i + 1)}{\ln(k_{sat} + 1)} \tag{3.21}$$

$$k_{sat} = K_{ks}\left(\frac{\theta_{sat} - \theta_{dul}}{\theta_{dul}}\right)^2 \tag{3.22}$$

where,

D is the drainage rate,

F is a fraction of the drainage rate that accounts for simultaneous inflow from the layer above,

θ_s is the initial value of θ,

Q_i is the incoming water flux from the layer above ($P - R$ in the case of the uppermost layer),

C_{d1}, C_{d2}, C_{d3} and K_{ks} are all empirical constants derived from statistical fits to observed data by Suleiman (1999); Suleiman and Ritchie (2003) and Ritchie et al. (2009). Values adopted were $C_{d1} = 2.96$, $C_{d2} = -2.62$, $C_{d3} = 0.85$, and $K_{ks} = 37$ cm day^{-1}

Water is finally extracted from a parameterised depth (z_{ed}) by evaporation and from the root zone by roots, in agreement with transpiration. A value of N_{SL} of 25 has been adopted in all studies using GLAM (Challinor et al., 2004).

3.5.1.7 Evaporation and transpiration

Transpiration (T_T) and evaporation (E) rates are in GLAM limited by plant-soil structure, energy and water availability. Physiologically-limited transpiration is computed following Azam-Ali (1984) (Eq. 3.23)

$$T^p_{Tpot} = \begin{cases} T_{Tmax}\left(1 - \frac{L_{cr}-L}{L_{cr}}\right) & L < L_{cr} \\ T_{Tmax} & L \geq L_{cr} \end{cases} \tag{3.23}$$

where,

L_{cr} is the critical value of LAI below which transpiration is affected by leaf size, and

T_{Tmax} is the maximum potential transpiration rate

The Priestley-Taylor equation (Priestley and Taylor, 1972) is then used to calculate the energy-limited evaporation (E^e) and transpiration (T^e_T) rates (Eq. 3.24).

$$E^T_{pot} = E^e + T^e_T = \frac{\alpha}{\delta}\frac{\Delta(R_N - G)}{\Delta + \gamma} \tag{3.24}$$

where,

R_N is the net all-wave radiation,

G is the soil heat flux,

δ is the latent heat of vaporisation of water,

γ is the ratio of the specific heat of air at constant pressure to the latent heat of vaporisation of water

α is defined following Jury and Tanner (1975) (Eq. 3.25)

$$\alpha = 1 + (\alpha_0 - 1)\frac{V}{V_{ref}} \tag{3.25}$$

where,

$\alpha_0 = 1.26$ is a pre-correction value (Priestley and Taylor, 1972), and

V_{ref} is a reference value for VPD (vapour pressure deficit) (Steiner et al., 1991)

Net radiation is parameterised using the crop albedo (A) and the incoming short-wave solar radiation (from observations), under the assumption that net-long wave radiation is zero (Eq. 3.26)

$$R_N = (1 - A)S_{rad} \tag{3.26}$$

Light interception by the canopy is modelled following Challinor et al. (2009a) (Eq. 3.27 and 3.28)

$$E^e = E^e_{pot} e^{-kL} \tag{3.27}$$

$$T^e_T = E^e_{pot}(1 - e^{-kL}) \tag{3.28}$$

where k is the light extinction coefficient. Potential energy and soil-structure limited evaporation is modelled following Cooper et al. (1983) (Eq. 3.29)

$$E^s_{pot} = \frac{E^e}{t_R} \tag{3.29}$$

where t_R is the number of days since the daily total rainfall was greater than $P_{cr} = 1$ mm. The potential energy and physiology limited transpiration is then calculated as the minimum value between the potential energy- and the potential physiologically-limited transpiration rates (Eq. 3.30)

$$T_{Tpot} = min(T^p_{Tpot}, T^e_T) \tag{3.30}$$

Finally, water availability constraints to transpiration are accounted for by partitioning the available water according to demand (Eq. 3.31).

$$\begin{aligned} T_T &= T_{Tpot} \text{ and } E = E_{pot} \text{ for } \theta_{pe} \geq E^T_{pot} \\ T_T &= \theta_{pe} \frac{T^e_T}{T^e_T + E^e} \text{ and } E = \theta_{pe} \frac{E^e}{T^e_T + E^e} \text{ for } \theta_{pe} < E^T_{pot} \end{aligned} \tag{3.31}$$

where the potentially extractable soil water (θ_{pe}) is calculated following Passioura (1983) (Eq. 3.32),

$$\theta_{pe} = \int_0^{z_{max}} (\theta(z) - \theta_{rll})(1 - e^{-k_{DIF} l_v(z)}) \mathrm{d}z \tag{3.32}$$

where k_{DIF} is the uptake diffusion coefficient.

3.5.1.8 Heat stress during flowering

High temperatures during the flowering stage have been reported to cause crop failures (Vara Prasad et al., 2000, 1999). Challinor et al. (2005b) simulated the effect of high temperature on the flowering distribution, pod-set, in the harvest index, and yields. Their parameterisation consists of 5 different equations. The first two equations (Eq. 3.33 and 3.34) are used to determine the critical and limit temperature (T_{cr} and T_{lim}) before anthesis (from $t = 6$ to $t = 0$, relative to anthesis) and after anthesis (from $t = 1$ to $t = 12$, relative to anthesis) of flowers that open on each day of the flowering stage. Before anthesis, the temperatures vary as a function of:

$$\left.\begin{aligned} T_{cr}(t) &= min\left[T_{cr}^{min}, 36 + S_c(t-6)\right] \\ T_{lim}(t) &= 60 + S_l(t-6) \end{aligned}\right\}, -6 \leq t \leq 0 \tag{3.33}$$

where

T_{cr} is the temperature above which pod-set starts to be decreased,

T_{lim} is the temperature at which pod-set is zero,

T_{cr}^{min} is the minimum possible value of T_{cr}, and

S_c and S_l are regression slopes developed from empirical data for three different types of cultivars (Table 3.5).

Moderately tolerant cultivars do not exhibit variation in T_{cr} with time, whereas tolerant and sensitive cultivars increase the value linearly from 36 to 34 °C within the flowering period. Table 3.5 shows the heat stress parameters from the study of Challinor et al. (2005b). After anthesis, the critical and limit temperatures are parameterised as follows (Eq. 3.34):

$$\left.\begin{aligned} T_{cr}(t) &= min\left[T_{cr}^{min}, 37.8 + 1.8t - 3d\right] \\ T_{lim}(t) &= T_{ia} + 0.75t - 1.5d \end{aligned}\right\}, 0 < t \leq 12 \tag{3.34}$$

TABLE 3.5: Parameter values for heat-tolerant, moderately-sensitive and sensitive groundnut cultivars, as reported by Challinor et al. (2005b).

Parameter	TOL	MOD	SEN
T_{cr}^{min}	37.0	34.0	36.0
S_c	0.3	0.0	0.3
S_l	2.0	2.5	3.0
T_{ia}	53.0	51.0	48.8
P_{cr}	0.60	0.60	0.95
T_{lim}^{min}	40.0	40.0	40.0

Notes: T_{lim}^{min} was introduced by Challinor et al. (2007).

In Eq. 3.34 the temperature sensitivity values also depend on duration (d). In these equations, the values of T_{cr} and T_{lim} will increase with time (i.e. the further from anthesis the less sensitive the plant is) and will decrease with duration (i.e. the longer the duration the lower temperature is required to have an effect). A maximum duration of 6 days is defined for groundnut so that events of day $i-6$ can affect flowers opening on day i (Challinor et al., 2005b). A new parameter (T_{lim}^{min}) was introduced in the original heat stress formulation by Challinor et al. (2007) as unrealistically low values of T_{lim} can be found in some simulations.

After the determination of the two temperature thresholds, the percentage of pods setting is determined using a simple linear reduction (Eq. 3.35):

$$P(i) = 1 - \frac{T_{AM}(t) - T_{cr}}{T_{lim} - T_{cr}}, T_{AM} > T_{cr} \tag{3.35}$$

where i is the time in days relative to the start of the pod-filling period, and T_{AM} is the temperature between 8:00 and 14:00 during the day. According to this, flowers opening on day $i = 1$ set pods on the first day of pod-filling, and so on. The total reduction in pod-set of each high temperature stress (HTS) episode is then computed (Eq. 3.36):

$$P_{tot} = \sum_{i=1}^{i=N_f} P(i)F_f(i) \tag{3.36}$$

where $F_f(i)$ is the fraction of flowers opening on day i, derived from the flowering distribution (standard cumulative normal distribution). The values of width and offset of the

distribution (parameters) can be used to produce plausible time series, with $width = 6$ and $offset = 0.3$ being typical values for groundnut (Challinor et al., 2005b). The minimum percentage of pods on each day between the pre- and post-anthesis values is taken for each day. After the total pod-set is calculated, the impact on the harvest index ($\partial H_I / \partial t$) is calculated (Eq. 3.37):

$$\frac{\partial H_I}{\partial t} = \left(\frac{\partial H_I}{\partial t}\right)_0 \left(1 - \frac{P_{cr} - P_{tot}}{P_{cr}}\right), P_{tot} < P_{cr} \tag{3.37}$$

The rate of change in the harvest index is linearly reduced from its optimal value (subscript 0) when the total cumulated percentage of pods goes below a critical value P_{cr}. In tolerant genotypes the value of P_{cr} would be low because these genotypes could cope with a low number of pods by increasing seed number per pod, for example.

3.5.1.9 Drought stress during flowering

Drought can severely constrain the formation of flower buds (Rao and Nigam, 2003). Challinor et al. (2006) parameterised the effect of low water availability during the reproductive phase of the groundnut crop, by modifying Eq. 3.38 so that:

$$P_{tot} = \sum_{i=1}^{i=N_f} P(i) F_f(i) \left(\frac{S_i}{S_{cr}}, 1\right) \tag{3.38}$$

where S_i is the water stress factor (ratio of available water to transpirative demand) and S_{cr} is a threshold value below which pod-set is affected by water stress. Challinor et al. (2006) used $S_{cr} = 0.2$.

3.5.1.10 Decreased photosynthetic rates under high temperatures

In order to reflect the effect of reduced photosynthetic rates under high temperatures (Nigam et al., 1994), Challinor et al. (2009a) introduced a parameterisation to reduce transpiration efficiency under high temperatures. Under high temperatures, transpiration efficiency is linearly reduced from its non-stressed value (E_{T0}) (Eq. 3.39)

$$E_T = E_{T0}\left(1 - \frac{T - T_{ter1}}{T_{ter2} - T_{ter1}}\right) \tag{3.39}$$

where T is the daily mean temperature, T_{ter1} is the temperature at which transpiration efficiency starts to be affected, and T_{ter2} is the temperature at which transpiration efficiency is zero. Challinor et al. (2009b), based on data from Ferreyra et al. (2000) and Vara Prasad et al. (2003), used $T_{ter1} = 35$ °C and $T_{ter2} = 47$ °C.

3.5.1.11 Terminal drought stress

Challinor et al. (2009b) introduced a parameterisation to simulate terminal drought stress using a minimum value of the harvest index (H_I^{min}) that needs to be reached to allow harvest due to terminal drought and a critical value of soil extractable water (θ_{crit}) below which terminal drought is triggered. The latter is calculated (Eq. 3.40) using the potentially extractable soil water (the difference between field capacity and wilting point), and a parameter that controls the sensitivity of the crop to terminal drought (F_{sw}, varying from 0 [insensitive] to 1 [highly sensitive]).

$$\theta_{crit} = \theta_{ll} + (\theta_{dul} - \theta_{ll})F_{sw} \tag{3.40}$$

In the study of Challinor et al. (2009b) two different configurations of $\left[H_I^{min}, F_{sw}\right]$ were tested: (a) [0.1, 0.1], and (b) [0.25, 0.01]. Both of these were considered equally realistic, with the former reflecting a more sensitive crop.

3.5.1.12 Further clarifications, bug-fixes and changes to GLAM-R2

During the development of this work, a conceptual difference between GLAM and other crop models and between GLAM and existing literature arose. This difference lies in the treatment of SLA. SLA is used in GLAM to ensure the simulation is internally consistent. SLA acts as a control over biomass during the first N_D days of simulation and over the leaf area growth during the remainder of days (Challinor and Wheeler, 2008a). This control was introduced because unrealistically high values of the relationship between biomass and LAI occurred in the first days of most simulations, particularly when there was drought

stress (Challinor and Wheeler, 2008a). In GLAM, SLA is calculated as the ratio of LAI and the aboveground biomass. Physiologically, SLA is defined as the ratio of leaf area to leaf dry weight (Banterng et al., 2003; Rao and Wright, 1994). This trait can take maximum growing season values between 280 and 300 cm^2 g^{-1} (Banterng et al., 2003). The ratio of leaf area to aboveground biomass (what in GLAM is termed SLA) is more commonly termed LAR (leaf area ratio) (Anyia and Herzog, 2004; Medek et al., 2007). LAR and SLA share the same units (area by mass), with values of LAR being generally lower than those of SLA. Nevertheless, a maximum value of 300 cm^2 g^{-1} remains a realistic assumption for GLAM (Quilambo, 2000; Venkatarao, 2005). For convenience and consistency with all previous studies using GLAM, the acronym SLA and the maximum value of 300 cm^2 g^{-1} were both kept.

In addition to the above conceptual difference a bug in GLAM's FORTRAN code was found (hereafter referred to as LAI-BMASS-order-bug). Biomass and water balance outputs of day i were being calculated using the LAI of day i-1. The bug was corrected, which resulted in a more internally consistent simulation: the values of SLA were generally lower although the SLA control was still deemed necessary in the model. Using GLAM's benchmark configuration (i.e. that of the Gujarat grid cell, fully described by Challinor et al. 2004), a slight decrease in the correlation coefficient (from 0.75 to 0.70) and an increase in the $RMSE$ (from 303.3 to 321.3 kg ha^{-1}) if the SLA control is turned off were found.

The last change introduced was the correction of the observed range of the uptake diffusion coefficient (k_{DIF}, used in Eq. 3.32). The range 0.2 – 0.3 cm^2 day^{-1} was considered to be more realistic according to Dardanelli et al. (1997).

3.5.1.13 Response to increased CO_2 concentrations

Groundnut is a grain legume featuring a C3 photosynthesis pathway (Seeni and Gnanam, 1982). Physiologically, therefore, the effects of increase in atmospheric CO_2 concentrations have a direct impact on the production of assimilate (Chen and Sung, 1990; Leakey et al., 2009). Under climate change scenarios of increased CO_2 concentrations (Moss et al., 2010), C3 crops are expected to increase their rate of photosynthesis (Chen and Sung, 1990; Leakey et al., 2009; Long et al., 2006). The additional production of assimilate

is expected to increase water use efficiency, leaf area index, biomass, specific leaf area, radiation use efficiency (RUE) and the harvest index (Tubiello and Ewert, 2002). As a result, crop yields in C3 crops are expected to increase with increased CO_2 concentrations (Challinor and Wheeler, 2008a; Vara Prasad et al., 2003). The parameterisation of CO_2 response in GLAM is thus important for assessing crop growth CO_2 stimulation (Tubiello and Ewert, 2002) as well as the combined effects of CO_2 stimulation and high temperature (e.g. Vara Prasad et al. 2003) or drought (e.g. Clifford et al. 2000) stress on reproductive plant processes (i.e. flowering and grain filling).

The CO_2 response of the crop was parameterised following Challinor and Wheeler (2008a). The methodology developed by Challinor and Wheeler (2008a) consisted of two major steps: (1) establishing a relationship between the optimal value of the maximum normalised transpiration efficiency ($E_{TN,max}$) and its doubled-CO_2 value (Eq. 3.41), and (2) perturbing certain crop model parameters to enhance biomass production, except $E_{TN,max}$, which is calculated following Eq. 3.41.

$$E_{TN,max} = (1 - T_{fac})E^{opt}_{TN,max} + T_{fac}E_T\frac{E^{opt}_{TN,max}}{E^{opt}_T} \tag{3.41}$$

where the use of superscript *opt* refers to the optimal values (i.e. baseline values), T_{fac} is a scaling factor that controls the response of the normalised transpiration efficiency (E_{TN}) to varying humidity levels (also see Challinor and Wheeler 2008a). The mechanism for this to occur in GLAM is achieved through Eq. 3.14. For $T_{fac} = 0$, $E_{TN,max}$ under increased CO_2 equals the baseline value. This means that at low VPD (V) conditions the value of $E_{TN} = E_{TN,max}$ (see Eq. 3.42, below), thus reflecting no stimulation at low VPD. For T_{fac} =1, $E_{TN,max}$ increases in the same proportion as E_T. This means that at low V conditions the value of $E_{TN} = {}^{E_T}/_V$, reflecting stimulation at low VPD. In both cases, E_{TN} increases at high humidity levels (see Fig. 1 in Challinor and Wheeler 2008a). The simulated value of E_{TN} is then used in GLAM to compute biomass (see Eq. 3.14), which is in turn used to compute yield via the harvest index (see Eq. 3.17).

$$E_{TN} = min\left(\frac{E_T}{V}, E_{TN,max}\right) \tag{3.42}$$

Once the relationship that allows for a consistent simulation across historical and enhanced CO_2 concentration scenarios was established, Challinor and Wheeler (2008a) used an 18-member ensemble to quantify the uncertainty in the response of groundnut to doubled CO_2. Specifically, they introduced changes to the baseline values of the maximum rate of transpiration (TT_{max}), transpiration efficiency (E_T) and specific leaf area (SLA_{max}) in order to account for the increased production of assimilate at higher-than-normal CO_2 concentrations (Chen and Sung, 1990; Stanciel et al., 2000; Vara Prasad et al., 2003).

In the study of Challinor and Wheeler (2008a), first, the baseline value of TT_{max} was reduced by 17 % owing to the expected reduction in transpiration (Stanciel et al., 2000). To reflect increased biomass production they increased the value of E_T (increases of either 24 % or 40 % were used). They also used two values of T_{fac} (0 and 0.4) to quantify uncertainty in the differential response to high and low VPD conditions. Finally, they reduced the baseline value of SLA_{max} by 10 %. Similar approaches to CO_2 stimulation are used in other crop models, where either the radiation use efficiency (Jones et al., 2003) or the transpiration efficiency (Keating et al., 2003) are increased to reflect increases in net photosynthesis.

In this study, the same four GLAM parameters were changed, but the factors differed. This was because the factors employed by Challinor and Wheeler (2008a) were defined for doubled CO_2 conditions. Scaling was thus needed for 2030s climate as used here. Future projected CO_2 concentrations under the Representative Concentrations Pathways (RCP) scenario RCP4.5 were derived from Meinshausen et al. (2011). A value of 450 ppm was adopted for the period of study (RCP4.5 by 2030s). All crop model parameters were linearly scaled using the baseline (at 330 ppm) and doubled CO_2 values (also see Challinor et al. 2010). A summary of the CO_2 parameterisations is shown in Table 3.6.

In all cases, the value of $E_{TN,max}$ was calculated following Eq. 3.41.

3.5.2 The EcoCrop model

The EcoCrop model implemented here uses environmental ranges as inputs to determine the main niche of a crop and then produces a suitability index as output. The model was originally developed by Hijmans et al. (2001) and named EcoCrop since it was based on the FAO-EcoCrop database (FAO, 2000).

TABLE 3.6: Parameterisations of CO_2 response used and changes to relevant GLAM model parameters.

ID	Description	T_{fac}	T_E	TT_{max}	SLA_{max}
C1	No stimulation at low VPD Moderate increase in T_E	0.0	+8.8 %	-6.23 %	-3.67 %
C2	No stimulation at low VPD Large increase in T_E	0.0	+14.7 %	-6.23 %	-3.67 %
C3	Moderate stimulation at low VPD Moderate increase in T_E	0.4	+8.8 %	-6.23 %	-3.67 %
C4	Moderate stimulation at low VPD Large increase in T_E	0.4	+14.7 %	-6.23 %	-3.67 %

Notes: In all cases a reduction in maximum transpiration (i.e. higher water use) and a reduction in maximum SLA were considered.

In the model, there are two ecological ranges for a given crop, each one defined by a pair of parameters for each variable (i.e. temperature and precipitation). First, the absolute range, defined by T_{MIN-C} and T_{MAX-C} (minimum and maximum absolute temperatures at which the crop can grow, respectively), and by R_{MIN-C} and R_{MAX-C} (minimum and maximum absolute rainfall at which the crop grows, respectively). Second, the optimum range, defined by $T_{OPMIN-C}$ and $T_{OPMAX-C}$ (minimum optimum and maximum optimum temperatures, respectively), and $R_{OPMIN-C}$ and $R_{OPMAX-C}$ (minimum optimum and maximum optimum rainfall, respectively). An additional temperature parameter is used (T_{KILL-C}) to illustrate the effect of the minimum temperature in a month (explained below).

When the conditions over the growing season (i.e. temperature, rainfall) at a particular place are beyond the absolute thresholds there are no suitable conditions for the crop (white area, Figure 3.9); when they are between absolute and optimum thresholds (dark grey area, Figure 3.9) there are a range of suitability conditions (from 1 to 99), and whenever they are within the optimum conditions (light grey area, Figure 3.9) there are highly suitable conditions and the suitability score is 100 %. The model performs two different calculations separately, one for precipitation and the other for temperatures and then calculates the interaction by multiplying them (Figure 3.9).

The first parameters that need to be defined are the start and end of the growing season (G_S and G_E, respectively), which in this version of the model are prescribed by the E-LGP dataset. For a given site (P), for each month (i) of the growing season, the temperature

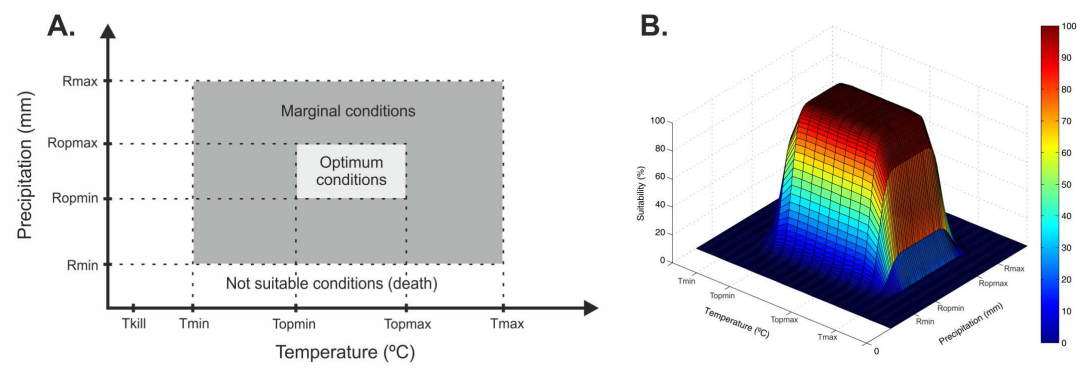

FIGURE 3.9: Two- (A) and three-dimensional (B) diagrams of EcoCrop.

suitability (T_{SUIT}) is calculated by comparing crop parameters with the climate data at that site (Eqn. 3.43).

$$T_{SUITi} = \begin{cases} 0 & T_{MIN-Pi} < T_{KILL-C} \\ 0 & T_{MEAN-Pi} < T_{MIN-C} \\ a_{T1} + m_{T1} * T_{MEAN-Pi} & T_{MIN-C} \leq T_{MEAN-Pi} < T_{OPMIN-C} \\ 100 & T_{OPMIN-C} \leq T_{MEAN-Pi} < T_{OPMAX-C} \\ a_{T2} + m_{T2} * T_{MEAN-Pi} & T_{OPMAX-C} \leq T_{MEAN-Pi} < T_{MAX-C} \\ 0 & T_{MEAN-Pi} > T_{MAX-C} \end{cases} \quad (3.43)$$

Where T_{SUITi} is the temperature suitability index for the month i, T_{MIN-C}, $T_{OPMIN-C}$, $T_{OPMAX-C}$ and T_{MAX-C} are defined on a crop basis (Sect. 7.3.1), a_{T1} and m_{T1} are the intercept and slope (respectively) of the regression curve between $[T_{MIN-C}, 0]$ and $[T_{OPMIN-C}, 100]$, a_{T2} and m_{T2} are the intercept and slope (respectively) of the regression curve between $[T_{OPMAX-C}, 100]$ and $[T_{MAX-C}, 0]$. T_{MIN-Pi} is the minimum temperature of the month i at the site P, $T_{MEAN-Pi}$ is the mean temperature of the month i at site P, T_{KILL-C} is the crops killing temperature plus 4 °C (Hijmans et al., 2001). The model assumes that if the minimum temperature of the month in a particular place is below $[T_{KILL} + 4\,°C]$, then the minimum absolute killing temperature will be reached in at least one day of the month, and the crop will freeze and fail. This assumption is a compromise between the temporal scale of the input data for EcoCrop (i.e. monthly), and the need to include sub-monthly temperature variability (Hijmans et al., 2001; Ramirez-Villegas

et al., 2013b). The final temperature suitability (T_{SUIT}) is the minimum value of all months within the growing season.

For precipitation, the calculation is done only once, using the crop's growing season total precipitation (sum of precipitation in all the growing season's months), and using both the minimum, and maximum absolute and optimum crop growing parameters (Eqn. 3.44).

$$R_{SUITi} = \begin{cases} 0 & R_{TOTAL-P} < R_{MIN-C} \\ a_{R1} + m_{R1} * R_{TOTAL-P} & R_{MIN-C} \leq R_{TOTAL-P} < R_{OPMIN-C} \\ 100 & R_{OPMIN-C} \leq R_{TOTAL-P} < R_{OPMAX-C} \\ a_{R2} + m_{R2} * R_{TOTAL-P} & R_{OPMAX-C} \leq R_{TOTAL-P} < R_{MAX-C} \\ 0 & T_{MEAN-Pi} > T_{MAX-C} \end{cases} \tag{3.44}$$

Where $R_{TOTAL-P}$ is the total precipitation of the crop's growing season at site P, R_{SUIT} is the rainfall suitability score, the crop parameters (R_{MIN-C}, $R_{OPMIN-C}$, $R_{OPMAX-C}$ and R_{MAX-C}) are defined on a crop basis. The parameters a_{R1} and m_{R1} are the intercept and the slope of the regression curve between [R_{MIN-C}, 0] and [$R_{OPMIN-C}$, 100], and a_{R2}. m_{R2} are the intercept and the slope of the regression curve between [$R_{OPMAX-C}$, 100] and [R_{MAX-C}, 0]. Finally, R_{SUIT} and T_{SUIT} are each divided by 100 and the total suitability score is the product (multiplication) of the temperature and precipitation suitability scores calculated separately times 100 (Eqn. 3.45).

$$SUIT = T_{SUIT} * R_{SUIT} * 100 \tag{3.45}$$

All the model parameters (i.e. T_{KILL-C}, T_{MIN-C}, $T_{OPMIN-C}$, $T_{OPMAX-C}$, T_{MAX-C}, R_{MIN-C}, $R_{OPMIN-C}$, $R_{OPMAX-C}$, and R_{MAX-C}) are referred to as "EcoCrop parameters" hereafter.

3.6 Methods for assessment of skill

In this thesis, the skill of various types of models was assessed. Foremost, the very next chapter (Chapter 4) presents an assessment of climate data, including GCM outputs. The

skill of GLAM to reproduce mean and interannual variability of crop yields and the skill of EcoCrop to predict the presence of groundnut were both also assessed. Such assessments required the repeated use of skill metrics. This section summarises all of them.

3.6.1 Pearson product-moment correlation cefficient (r)

The correlation coefficient was used as a measure of the strength of the direction of the linear relationship between observed and predicted quantities. r is calculated as the covariance of the two measures divided by the product of their standard deviations.

3.6.2 Root mean square error ($RMSE$)

Probably the most important and robust metric for assessing model skill, and hence the most frequently one used here is the root mean square error ($RMSE$, Eq. 3.46).

$$RMSE = \sqrt{\frac{\sum_{i=1}^{n} (O_i - P_i)^2}{n}} \tag{3.46}$$

where O and P refer to observed and predicted quantities of a series of n elements. The $RMSE$ is a measure of how close a prediction is to its corresponding observed value. Hence, it provides a complete measure of the model errors (Taylor, 2001).

3.6.3 RMSE normalised by mean or standard deviation

In some cases, it was convenient to express the $RMSE$ as a fraction (or per cent) of the mean or the standard deviation of the corresponding observations. This often provides an idea of how significant is the model error with respect to the quantities being measured. The $RMSE$ normalised by the observed mean ($RMSE_M$) is shown in Eq. 3.47.

$$RMSE_M = \frac{RMSE}{\bar{O}} = \frac{RMSE}{\frac{\sum_{i=1}^{n} O_i}{n}} \tag{3.47}$$

The $RMSE$ normalised by the observed standard deviation ($RMSE_{SD}$) is shown in Eq. 3.48.

$$RMSE_{SD} = \frac{RMSE}{\sigma_O} = \frac{RMSE}{\sqrt{\frac{\sum_{i=1}^{n}(O_i - \bar{O})^2}{n}}} \tag{3.48}$$

3.6.4 Perfect correlation mean square error ($PMSE$)

In this work, GLAM simulations were performed both with observed meteorology and with simulated outputs of transient GCM simulations. In the case of observations, individual year GLAM predictions can be directly compared with observed ones. The same cannot be done when GLAM simulations are conducted using transient GCM output because these are initialised arbitrarily on the basis of a pseudo-equilibrium control run (Challinor et al., 2007; Gleckler et al., 2008; Scherrer, 2011). It is, however, expected that the statistical characteristics (i.e. mean and σ) of the observed and simulated time series match each other.

Thus, in order to measure the skill of GLAM simulations driven by transient GCM output, the 'perfect-correlation mean square error ($PMSE$)' was used (Challinor et al., 2007). The $PMSE$ is defined as follows:

Taylor's (Taylor, 2001) definition of Root Mean Square (RMS) difference (E) is based on a decomposition of the total RMS difference into two components: mean bias ($\bar{E}$) and centred RMS error (E') (Eq. 3.49).

$$E = \bar{E}^2 + E'^2 \tag{3.49}$$

The centred RMS error (E') is related to the correlation coefficient through the law of cosines (Eq. 3.50, also see Taylor 2001).

$$E = (\bar{f} - \bar{r})^2 + (\sigma_f^2 + \sigma_r^2 - 2\sigma_f\sigma_r r) \tag{3.50}$$

where f and r are the model and observations, respectively. Means are indicated with a bar above the letter, and the symbol σ represents the standard deviations (with subscripts f and r to indicate model and observations, respectively). r is the correlation coefficient. Through simple manipulation of Eq. 3.50, E can be expressed as the square difference of

the means, the standard deviations, and the double product of the standard deviations times the additive inverse of the correlation coefficient (Eq. 3.51– 3.53, also see Challinor et al. 2007).

$$E = (\bar{f} - \bar{r})^2 + \sigma_f^2 + \sigma_r^2 - 2\sigma_f\sigma_r r + 2\sigma_f\sigma_r - 2\sigma_f\sigma_r \tag{3.51}$$

$$E = (\bar{f} - \bar{r})^2 + (\sigma_f^2 - 2\sigma_f\sigma_r + \sigma_r^2) + (2\sigma_f\sigma_r - 2\sigma_f\sigma_r r) \tag{3.52}$$

$$E = (\bar{f} - \bar{r})^2 + (\sigma_f - \sigma_r)^2 + 2\sigma_f\sigma_r(1 - r) \tag{3.53}$$

This transformation (Eq. 3.53) allows the $RMSE$ to be expressed as the total sum of the difference between the means (first term), the difference in standard deviations (second term), and a third term involving the correlation coefficient. However, since as stated earlier transient simulations do not permit individual simulated years to be compared with observed ones, the correlation was assumed to be 'perfect' (i.e. $r = 1$). This allowed the calculation of the RMS difference on the basis of the squared difference of the simulated and observed means and standard deviations (Eq. 3.54).

$$E = (\bar{f} - \bar{r})^2 + (\sigma_f - \sigma_r)^2 \tag{3.54}$$

The $PMSE$ was used as a measure of error for finding optimal grid cell-specific values of the C_{YG}. Although this could lead to underestimating the actual $RMSE$ (Challinor et al., 2007), this method was preferred instead of the alternative method of comparing ordered time series (see e.g. Iizumi et al. 2009a) that could have led to inappropriate sorting under circumstances where errors in GCM simulations affect threshold-dependent processes such as high temperature stress and terminal drought. Despite inherent limitations owing to the $r = 1$ assumption, thus, the $PMSE$ is unlikely to result in bias in the resulting values of C_{YG} (Challinor et al., 2007), and has yielded realistic modelling results when used to calibrate C_{YG} in previous studies (Challinor and Wheeler, 2008b; Challinor et al., 2005b, 2010).

3.6.5 The Taylor diagram

A Taylor diagram summarises how well a model simulation matches observations in terms of correlation, $RMSE$ and ratio of variances. In the Taylor diagram, a single point in a two-dimensional plot is used to indicate these three measures, which are related through the law of cosines (Eq. 3.50).

Figure 3.10 shows an example Taylor diagram. The point referred to as 'reference' indicates the position of the observations, whereas the 'test' indicates the position of the prediction to be assessed. The plot is constituted by three axes. The x-axis is proportional to the standard deviation. The arcs concentric to the reference measure the centred $RMSE$ (in the same units as the standard deviation). The azimuthal position of the 'test' indicates the correlation.

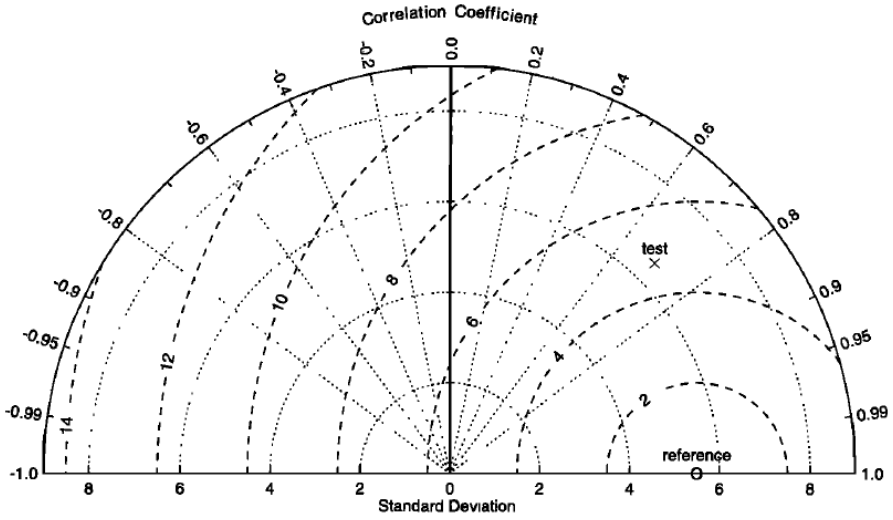

FIGURE 3.10: Example of a Taylor diagram for visualising model skill statistics. The points 'reference' and 'test' indicate the observed and predicted values, respectively. Taken from Taylor (2001).

The diagram can also be presented by normalising the standard deviations and the centred $RMSE$ by the observed standard deviation. In such case, the position of the 'reference' point along the x-axis is 1.

3.6.6 Interannual variability index (V_I)

Interannual variability in climate models was assessed following Gleckler et al. (2008) and Scherrer (2011), in which an interannual variability index (V_I) is calculated for each climate model run as the differences between the ratios of model (M) and observed (O) standard deviations (Eq. 3.55).

$$V_I = \left(\frac{\sigma^i_{Mv}}{\sigma^i_{Ov}} - \frac{\sigma^i_{Ov}}{\sigma^i_{Mv}} \right)^2 \tag{3.55}$$

where σ is the standard deviation of the time series (1961-2000) of a variable (v) for a given grid point (i). The index is always positive and has no upper limit. Previous work with the CMIP3 model ensemble has suggested that values of $V_I < 0.5$ are indicative of high model skill (Scherrer, 2011) (Table 3.7). Thus, values of V_I below 0.5 at a given grid cell for a given model run were considered as accurate predictions in the present study because these will ensure errors are never beyond 25 % (Table 3.7; also see Scherrer 2011).

TABLE 3.7: Values of (V_I, Eq. 3.55) and the corresponding ratio of variances (s/s_{ref}), expressed in both fraction and percentage. Taken from Scherrer (2011).

V_I	s/s_{ref}	
	Fraction range	Percentage range
0	1	0
< 0.2	[0.801; 1.25]	[-19.9; +24.8]
< 0.5	[0.707; 1.41]	[-24.3; +41.4]
< 1.0	[0.618; 1.62]	[-38.2; +61.8]
< 2.0	[0.518; 1.93]	[-48.2; +93.2]
< 5.0	[0.382; 2.62]	[-61.8; +162]
< 10.0	[0.290; 3.45]	[-71.0; +245]

Scherrer (2011) note: "*Depending on the acceptance range of s/s_{ref}, V_I values larger than the corresponding value can be defined as a limit for 'bad' representation of variability. For example, if $V_I = 0.5$ is the chosen limit, the $0.707 < s/s_{ref} < 1.414$, or in other words s is between 29.3 % below to 41.4 % above s_{ref}.*

3.7 Uncertainty decomposition methods

In modelling the impact of climate change on crop productivity, limitations in the models and/or data employed can lead to uncertainties and lack of predictability (Koehler et al.,

2013). Identifying the sources these uncertainties is key in order to improve modelling frameworks and make more informed decisions (Vermeulen et al., 2013). Here, the total uncertainty in mean yield was decomposed into its different sources. The method of Hawkins and Sutton (2009), whereby each source of uncertainty is assumed to be independent of all other sources was followed (also see Koehler et al. 2013). In this methodology, the total uncertainty (T_V) is first calculated as the sum of the uncertainties (V, measured using the standard deviation) of each source (i), from a total of n sources (Eq. 3.56).

$$T_V = \sum_{i=1}^{n} V_i \tag{3.56}$$

In this thesis, n varies depending upon how many differnet uncertainty sources are investigated, which varies according to the configuration of the simulations and the period analysed (baseline vs. future climate).

For each source, the fractional uncertainty (F_U) can be calculated as the ratio of uncertainty of a given source to the total uncertainty. For instance, measuring fractional uncertainty of the CO_2 response parameterisations requires averaging all simulations for each parameterisation and then calculating the fractional uncertainty of CO_2 response (Eq. 3.57).

$$F_{U-CO_2} = \frac{V_{CO_2}}{\sum_{i=1}^{n} V_i} \tag{3.57}$$

Uncertainty decomposition was done for the baseline and future crop yield and suitability simulations of Chapters 6 and 7, respectively. This method allows, in a simple way, to compare the importance crop and climate uncertainties for crop yield and suitability simulations. As such, this information allows drawing strategies on which uncertainties should be reduced through more research.

Chapter 4

Assessing the quality of climate data

"...y hay días en que somos tan sórdidos, tan sórdidos,
como la entraña oscura de oscuro pedernal"
Porfirio Barba Jacob

4.1 Summary

The skill and robustness of observed and simulated available climate data for their use in agricultural studies in Sub-Saharan Africa and South Asia was analysed (Objective 1, Sect. 1.6). First, using meta-data from the scientific literature trends in the use of climate and weather data in agricultural research were examined. The findings indicate that despite agricultural researchers' preference for field-scale weather data (50.4 % of cases in the assembled literature), large-scale datasets coupled with weather generators are frequently used as a surrogate of observations. Using well-known interpolation techniques, the sensitivities of the weather station network to the lack of data were then assessed. High sensitivities to data loss were found mainly over mountainous areas in Nepal and Ethiopia (random removal of data impacted precipitation estimates by ± 1,300 mm year^{-1} and temperature estimates by ± 3 °C). Finally, a numerical analysis was performed that assessed 24 Coupled Model Intercomparison Project phase 3 (CMIP3) and 70 CMIP5 climate

model simulations with regards of mean climates and interannual variability. Errors in precipitation climatological means were large (root mean square error normalized to mean, $RMSE_M$ above 40 %) in 70 - 100 % of areas and seasons for both ensembles. Errors in wet-day frequency were assessed only for CMIP5 but were even larger than those of precipitation, and frequently reached half of a year (roughly 150 days). Errors in climatological mean temperatures and daily temperature extremes were lower, with generally less than 30 % of areas and seasons showing large errors ($RMSE_M > 40$ %). Interannual variability in GCMs warrants particular attention given that no single model matched observations in more than 30 % of the areas for monthly precipitation, 70 % for mean temperatures, and 90 % for diurnal range and wet-day frequency. Improvements were observed from CMIP3 to CMIP5 in the simulated climatological means of temperatures and, importantly, also of total precipitation. Improvements in physical plausibility and resolution are a significant step forward in CMIP5 with respect to its predecessor; however, climate model errors remain large with respect to the known sensitivities of crop models to biased weather inputs. A number of recommendations for the use of CMIP5 (and other model ensembles data) in agricultural impacts studies are given. These include the quantification of climate and crop model uncertainty, the use of bias correction techniques, and the matching of scales between climate and crop models.

4.2 Introduction

Agricultural and climate data are crucial for assessing both agricultural sensitivity to climate and future climate change impacts, and hence are crucial for adaptation. Nevertheless, these data are scarce in their basic forms (data from agricultural research and weather stations, respectively) or not very well managed or maintained in certain parts of the world (Figure 4.1), although with some notable exceptions (e.g. Keatinge et al. 2012). Most importantly, climate databases and their derived products are sometimes inaccurate, or else lack the documentation necessary to facilitate their use within the agricultural research community. In some instances, this may be indicative of the gap between the agricultural and climate research communities (Pielke et al., 2007; Thornton et al., 2011). Even when the two do collaborate, agricultural researchers face critical constraints when accessing basic sources of meteorological data (i.e. weather stations) due to a number

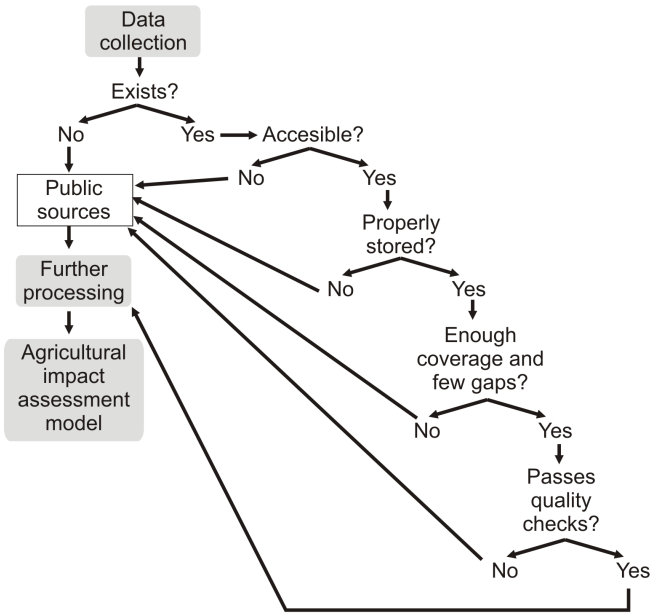

FIGURE 4.1: Cascade of constraints to climate data, as normally observed in agricultural research. Originally published in Ramirez-Villegas et al. (2013b)

of factors, from access to data, to weather maintenance and data quality checks, to the weather itself (DeGaetano, 2006).

In the last 10 years, various datasets have been developed by different institutions, usually based on either a combination of weather station data, satellite data, and numerical weather prediction models in addition to interpolation methods, or on the sole application of climate models with some degree of bias correction (Sheffield et al., 2006; Weedon et al., 2011). Assessments of these data (particularly climate models) have been done with a focus on processes or variables that are not directly relevant to agriculture (Gleckler et al., 2008; Pierce et al., 2009), for a limited number of variables (Jun et al., 2008; Reifen and Toumi, 2009), or for a reduced realm (Jourdain et al., 2013; Walsh et al., 2008). Climate model simulations, in particular, play a critical role with regards to climate change impacts. The Coupled Model Intercomparison Project phase 3 (CMIP3) has been the base of a large number of agricultural impact studies (White et al., 2011a), and it is likely that the new CMIP5 model ensemble will form the basis of many future impact prediction studies (Taylor et al., 2012). If impact studies that use CMIP5 are to be designed and interpreted judiciously, agricultural researchers need to develop appropriate understanding on the main features of CMIP5's experimental design, its predictive skill regarding

impacts-relevant variables and the associated uncertainties at different scales. Agricultural researchers thus have to engage fully in the climate-model discussion to understand the implications of this new climate model ensemble for impact assessment and where necessary, make adjustments to previously issued claims and estimates of climate change impacts (Knutti and Sedlacek, 2012).

This chapter addresses Objective 1 (see Sect. 1.6). Towards that aim, a three-step thorough analysis on fundamental aspects related to agricultural modelling was performed. The aim of the analyses was to enhance the understanding on the available climate data for agricultural research. Based on the review of Chapter 2 the following analyses were performed:

1. A meta-analysis on the usage of climate and weather data for agricultural modelling purposes, summarising the desirable characteristics sought when modelling crop productivity.

2. An analysis of the robustness of the existing weather station network was performed by assessing both the ability of these data to correctly fill information gaps via interpolation methods, and the networks sensitivities to information loss.

3. An analysis of skill of impacts-relevant climate model outputs from the CMIP3 (Meehl et al., 2007b) and CMIP5 (Taylor et al., 2012) GCM ensembles. Outputs of total precipitation, mean temperature, diurnal temperature range and where possible, the number of wet days from GCM simulations were assessed against different observational datasets. Metrics and methods used were similar to those used in the climate-science literature (Gleckler et al., 2008; Pierce et al., 2009; Scherrer, 2011), yet the metrics used were kept relatively simple, as the analyses are focused on agricultural impacts research.

The main implications of the findings on agricultural impact assessment were analysed and discussed.

4.3 Methodology

4.3.1 Analysis of trends in the usage of climate data in agricultural studies

4.3.1.1 Meta-data from agricultural studies

Data from a number of publications on any topic that made use of climate data for any sort of agricultural modelling were gathered. Searches using various search engines were conducted between December 2010 and June 2011, resulting in the identification and download of peer-reviewed publications related to agricultural modelling. All publications that in any way used climate data for agricultural modelling purposes were analysed. As the selection of the impact assessment model(s) is the first decision that any researcher needs to make before embarking in a modelling study, the focus here was on the driving factors of this decision. Different variables from the studies were recorded as follows:

1. Problem and/or topic in question: classified in categories such as impact assessment, seasonal yield forecasting, sole crop modelling, climate attribution, crop adaptation, pests and diseases. Each study was classified into only one category by taking into account only the main issue addressed by the paper;

2. Spatial scale of the assessment: includes site, sub-national, country, regional (i.e. group of countries), and global;

3. Use of weather generators: whether the study did or did not use a weather generator was recorded for both present and future;

4. Climate dataset (current): GCM and/or RCM used, weather station, satellite, and observational datasets (e.g. CRU, WorldClim, GPCP);

5. Climate dataset (future): the nature of used future projections was recorded here including the downscaling method, if applicable. Classifications were: GCM "as is" when studies used raw GCM outputs as inputs, pattern scaled GCMs (Mitchell et al., 2004), RCMs, systematic changes to current climate data (sometimes also referred to as sensitivity analysis), statistical downscaling (Wilby et al., 2009), and weather generator downscaled GCM (Jones et al., 2009).

For further details on the above categories the reader is referred Table 4.1. A total of 205 peer-reviewed publications were reviewed, all published between the years 1983 and 2011 (see Appendix A for a complete list). Most of the studies were published immediately before or after the IPCC AR4 was released in 2007 (IPCC, 2007). When a certain study made use of two different sources of present-day climate data, it was considered twice (totalling 247 cases).

4.3.1.2 Analysing the usage of climate data in agricultural studies

Relevant trends in modellers' preferences were assessed using the meta-data of Sect. 4.3.1.1. The analysis involved determining the most studied topics (i.e. nature of the problem being assessed) and the scale at which being studied. The most frequently used weather input types (both for current and future climate analyses) and the processes involved in preparing weather inputs (e.g. use of weather generators, downscaling, bias-correction) were also determined. Finally, these choices were related to the most frequently used model types (e.g. field-scale process-based, regional-scale process-based models, statistical). By doing this, it was ensured that all the main factors related to an agricultural researchers decision to select a particular approach for a given problem were covered.

4.3.2 Analysis of robustness and utility of the weather station network

Many methods exist that allow the researcher or user to determine the value of a parameter (e.g., monthly rainfall) in a given condition (i.e. in a given site, at a given time, or both), where it has never been measured before. Some of these methods are already popular with researchers using climate data (Hijmans et al., 2005; Hutchinson, 1995; Jones and Thornton, 1999; New et al., 2002) either on a regional or on a global basis. For climate-variable interpolations, the utility (i.e. ability of existing records to yield accurate interpolation results) and robustness (i.e. sensitivity to information loss) of the observational record is critical for an accurate result.

The weather station network (CL_WS-QA, see Sect. 3.4.1.2) was analysed by testing both its utility as well as its robustness. Monthly precipitation and temperature data were used to fit a thin plate spline interpolation algorithm (Hutchinson, 1995) for Sub-Saharan Africa and South Asia (Figure 3.1). The effect of weather station availability was investigated by

using 100 cross validated folds for four variables (monthly maximum, minimum and mean temperatures and total precipitation). Similar methods as in Hijmans et al. (2005) and New et al. (2002) were used for each fold. Longitude, latitude and elevation were used as independent variables. In each fold, 85 % data points were randomly selected for fitting the splines, whilst the remaining 15 % were used for evaluating the result for each variable and month. For the evaluation, the determination coefficient (r^2) and the Root Mean Square Error ($RMSE$, Eq. 3.46) were computed and used to produce boxplots of the 100-fold-by-12-month interpolations for each of the four variables. As the number of stations considerably exceeded the amount of available memory for processing, the whole region of study was divided in 5 tiles, each with an equivalent number of locations. The fitted splines were then projected onto 30-arc-second gridded datasets of latitude, longitude and altitude (Jarvis et al., 2008), thus producing a total of 4,800 interpolated surfaces (12 months times 4 variables times 100 folds). Finally, the spatial variability of standard deviations and the performance of the interpolation technique were analysed as proxies for sufficient distribution and geographic density of weather stations.

4.3.3 Are climate models useful tools for climate change impact assessment?: An analysis of the CMIP3 and CMIP5 Global Climate Model ensembles

4.3.3.1 Ability to represent mean climates

Climate models outputs and the MMM of the **CL_C3-QA** and **CL_C5-QA** datasets (see Table 3.1 were assessed for their ability to represent mean climates for each of the variables. Performance was assessed for the regions of Figure 3.1. Comparisons were performed on a country basis in order to produce country-specific results. Analyses were done for annual totals and also for totals of four seasons: December-January-February (DJF), March-April-May (MAM), June-July-August (JJA) and September-October-November (SON). For each region and season the climate model predictions and the observed (or reanalysis) were compared data using all pixels in that particular geographic domain. That is, comparisons were done spatially using all pixels within a country. Four metrics were used:

1. The Pearson product-moment correlation coefficient (r, Sect. 3.6.1);

2. the root mean squared error ($RMSE$, Eq. 3.46, Sect. 3.6.2);

3. the $RMSE$ normalised by the mean ($RMSE_M$, Eq. 3.47, Sect. 3.6.3); and

4. the $RMSE$ normalised by the standard deviation ($RMSE_{SD}$, Eq. 3.48, Sect. 3.6.3).

$RMSE_M$ and $RMSE_{SD}$ were used since it is useful to compare model errors with the actual variability or the mean climate of the areas being analysed. For interpretation of results, mostly the $RMSE_M$ and $RMSE_{SD}$ are used to indicate whether skill is high or low in the climate models. This was because normalised skill metrics allowed better comparisons across climate models, regions and seasons than the absolute $RMSE$ alone (Taylor, 2001; Willmott, 1982). Temporal means and standard deviations were not used for normalisation as these were unavailable in the data sources used here.

Finally, in order to summarise the large amount of information produced in the analyses performed, skill measures for individual GCMs, seasons and countries were divided into classes. Thresholds for r, $RMSE_M$, and $RMSE_{SD}$ were defined and results were classified in two categories for each skill metric. For r, the threshold chosen was 0.5, as this is in the middle of its positive range. For $RMSE_M$ and $RMSE_{SD}$ two values were chosen: 40 % and 90 %. Although somewhat arbitrary, these thresholds were chosen because they facilitate the interpretation of the numerical results. In addition, the 40 % threshold is consistent with the threshold chosen for the V_I (described below, see Table 3.7), and is representative of boundaries beyond which impact models, and particularly GLAM, would be severely constrained (Watson and Challinor, 2013). The 90 % threshold was chosen as an extreme. Cases where a model simulated output showed values of R below 0.5 were classified as poorly skilled, and similarly for cases where $RMSE_M$ and $RMSE_{SD}$ were above 40 %. Cases where $RMSE_M$ and $RMSE_{SD}$ were above 90 % are likely to be extremely poorly skilled simulations. These cases were counted and the corresponding percentage of total was then computed (total being 17 countries times 4 seasons = 68).

4.3.3.2 Ability to represent climate variability

Interannual variability in climate models was assessed via the V_I (Sect. 3.6.6). The models (term M in Eq. 3.55) were TS_C3-QA and TS_C5-QA, and the observations (term O in Eq. 3.55) were TS_WS-QA, TS_CRU-QA and TS_E40-QA (see Table 3.1). As opposed

to all mean climate calculations, V_I calculations were performed individually for each grid cell using all years in the period 1961-2000. Results of these analyses were then mapped. Similar to the mean climate assessment (Sect. 4.3.3.1), proportions of locations with $V_I > 0.5$ were counted for summarizing the skill of the two GCM ensembles.

4.3.4 Comparison between CMIP3 and CMIP5

Results from the two model ensembles were compared in a visual manner in order to test whether or not the models in CMIP5 had increased their skill in relation to CMIP3. This comparison was performed in three ways:

1. A Taylor diagram (Sect. 3.6.5). Due to the large number of regions and GCMs analysed, this was done only for India's mean climate. Skill of simulated seasonal outputs of the 24 (26) CMIP3 (CMIP5) GCMs and their multi model mean were then summarised in the diagram. Discrimination was done for individual seasons, the four variables (precipitation, wet days, mean temperature, and diurnal temperature range) and the two ensembles.

2. Probability density functions (PDF) of each GCM were drawn for each variable and skill metric (r, $RMSE_M$, $RMSE_{SD}$, and the V_I) were drawn using al countries and observed datasets only for the annual totals (of precipitation and wet-day frequency) and means (of temperature and diurnal temperature range).

3. Using the summaries of skill metrics, the total percentage of country-season combinations classified as poorly skilled for the correlation coefficient (i.e. $r < 0.5$), the $RMSE_M$ ($RMSE_M < 40$ %), and the V_I ($V_I > 0.5$) were plotted in scattergrams for each variable.

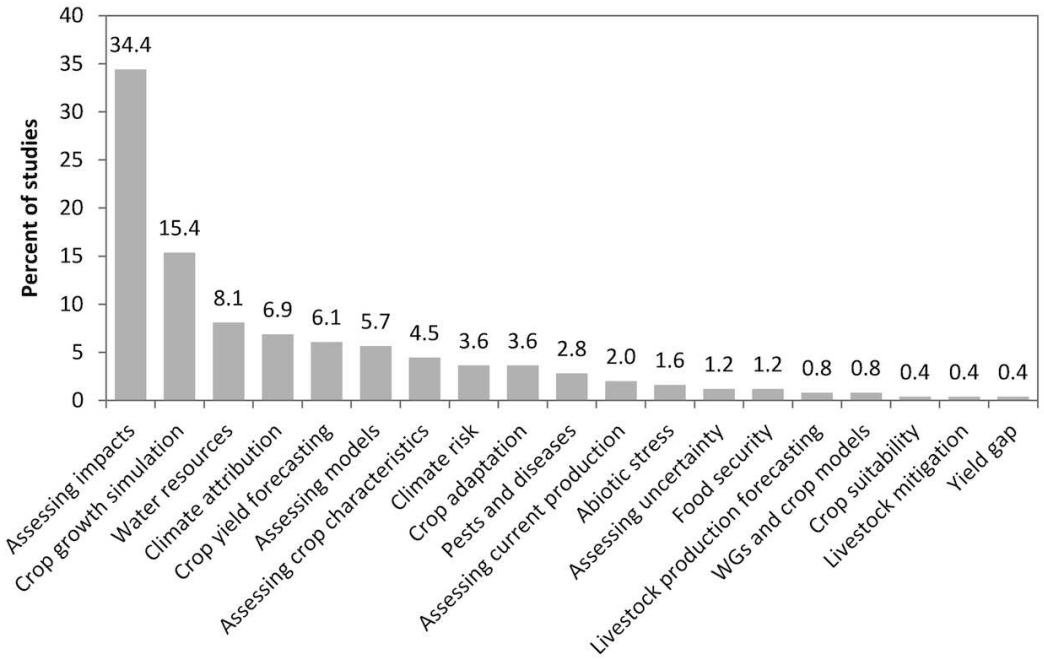

FIGURE 4.2: Topics treated in the analysed agricultural studies.

4.4 Results

4.4.1 Usage of climate data in agricultural studies

4.4.1.1 Topics of study

The most addressed topic (41.4 % of the studies) in the literature review was climate change impact assessment (Figure 4.2), followed by crop growth simulation (18.5 %). Water resources-impact studies was the third top topic studied (8.1 %), followed by climate attribution (6.9 %), crop yield forecasting (6.1 %), and model assessment (5.7 %). Importantly, formal studies addressing adaptation were rather scarce (3.6 %). Pests and diseases, soils, abiotic stresses and climate risks appeared to be a lot less addressed than impact assessment and crop growth simulation studies, which together accounted for more than 50 % of the total publications. Despite that, the absolute numbers of studies whose focus is on pest and disease (Garrett et al., 2013; Gouache et al., 2013; Kroschel et al., 2013) or adaptation (Boateng, 2012; Jarvis et al., 2012; Rickards and Howden, 2012) have been steadily increasing in recent years.

TABLE 4.1: Full list of categories found in reviewed studies per variable analysed across the 247 considered cases.

Variable	Category	Percent of studies (%)
Problem and/or topic	Assessing impacts	34.4
	Crop growth simulation	15.4
	Water resources	8.1
	Climate attribution	6.9
	Crop yield forecasting	6.1
	Assessing models	5.7
	Assessing crop characteristics	4.5
	Climate risk	3.6
	Crop adaptation	3.6
	Pests and diseases	2.8
	Assessing current production	2.0
	Abiotic stress	1.6
	Assessing uncertainty	1.2
	Food security	1.2
	Livestock production forecasting	0.8
	Weather generators and crop models	0.8
	Crop suitability	0.4
	Livestock mitigation	0.4
	Yield gap	0.4
Current climate data	Weather station	50.4
	Climatic Research Unit time series	10.9
	Global Climate Model	10.5
	Other	7.7
	Regional Climate Model	4.0
	Satellite	3.6
	WorldClim	2.8
	Climatic Research Unit climatology	2.8
	MARS European project	1.6
	Global Summary of the Day (GSOD)	1.2
	ARTES (Africa rainfall and temperature evaluation system)	1.2
	VEMAP (United States comprehensive dataset)	0.8
	ATEAM (Advanced Terrestrial Ecosystem Analysis and Modelling)	0.8
	PRISM (United States dataset)	0.4
	Global Precipitation Climatology Project (GPCP)	0.4
	Global Precipitation Climatology Centre (GPCC)	0.4
	Global Historical Climatology Network (GHCN)	0.4
Future climate data	Global Climate Model as is (GCM-AI)	42.9
	Regional Climate Model (RCM)	19.0
	Statistically Downscaled GCM (SD GCM)	17.5
	Pattern Scaled GCM (PS GCM)	8.7
	Weather Generator with GCM (WG GCM)	5.6
	Systematic Changes to variables (SC Variables)	4.8
	Unclear	0.8
	The ARPEGE Atmospheric GCM	0.8
Scale	Site	35.2
	Sub-national	23.9
	Country	17.0
	Regional (group of countries)	15.0
	Global	8.9
Use of weather gen.	Used	5.6
	Not used	94.4

4.4.1.2 Scale of studies and types of models

Most of the studies performed their models at a scale less than the size of a country: site-specific or sub-national level together comprised 55 % of the studies. Very few (7 %) of the studies were performed at the global level. This can be attributed to the fact that field-scale mechanistic crop growth models were the most utilised overall (51.9 %); followed by statistical and/or empirical approaches (17.7 %), hydrological models (8.1 %), and finally by regional-scale process-based models (5.7 %). The frequent use of field-based crop growth models suggests that the time step requirement for input data is rather high (El-Sharkawy, 2005), also confirmed by the usage of weather generators (8.5 and 11.2 % for present and future climates, respectively).

4.4.1.3 Climate data sources

The sources of present climate data varied substantially, with a total of 32 different sources being used for present climate data (Figure 4.3(a)). On average, a different present-day-climate dataset was used for every 7 agricultural studies. The most commonly used data source was local (non-public) weather stations (50.4 % of the cases), followed by University of East Anglia Climatic Research Unit (CRU) gridded datasets with 13.7 % (10.9 % for CRU-TS [monthly time series], and 2.8 % for CRU-CL [monthly climatology]). Climate model outputs were used in 14.5 % of the cases: within this group, 10.5 % used GCM data and 4 % RCM (Regional Climate Model) data. Some 9.4 % of studies did not make use of any observational data, thus basing their estimates on historical GCM or RCM simulations. Satellite imagery was used in 3.6 % cases, followed by the 2.8 % of WorldClim. A number of other less frequent sources accounted for the remaining 7.2 %. The Global Precipitation Climatology Project (GPCP) (Adler et al., 2003; Huffman et al., 2009), the Global Precipitation Climatology Centre (GPCC) (Schneider et al., 2010) and the Global Historical Climatology Network (GHCN) (Peterson and Vose, 1997) were rarely reported overall (0.4 % each).

The future climate data used was found to be less variable overall, with only 7 different types of data employed in the 125 cases stating to have used future climate data (Figure 4.3(b)). Importantly, out of these 125, only one study did not clearly state which type of climate data was used. The vast majority of cases (42. 9 %) used GCM data “as is” (AI

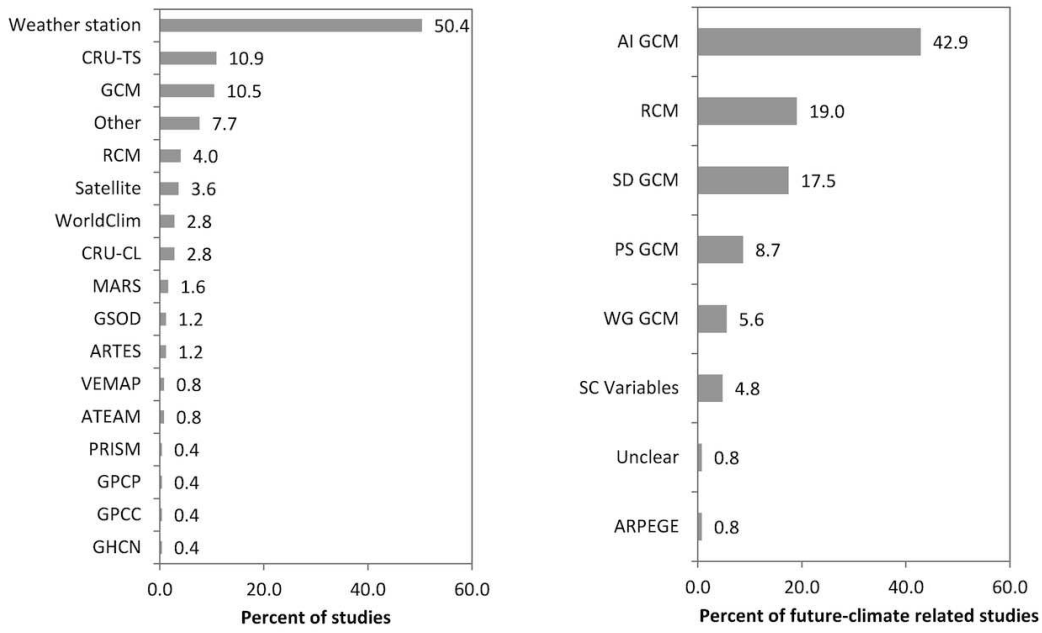

(a) Present (b) Future

FIGURE 4.3: Frequency of use of the different data sources in agricultural studies. 4.3(a) Present-day climates. 4.3(b) Future climates. Datasets acronyms are as follows: CRU-TS: Climatic Research Unit monthly time series product at 0.5 degree, GCM: global climate model output, RCM: regional climate model, CRU-CL: CRU monthly climatology product at 10 arc-minute, MARS: Data from the MARS European project, GSOD: Global summary of the day, ARTES: Africa rainfall and temperature evaluation system, VEMAP: United States comprehensive dataset, ATEAM: Advanced Terrestrial Ecosystem Analysis and Modelling, PRISM: United States dataset, GPCP: Global Precipitation Climatology Project, GPCC: Global Precipitation Climatology Centre, GHCN: Global Historical Climatology Network, AI GCM: GCM data as is, SD GCM: statistically downscaled GCM, PS GCM: pattern scaled GCM, WG GCM: GCM data through a weather generator, SC Variables: systematic changes in target key variables, Unclear: not specified clearly in study, ARPEGE: the ARPEGE Atmospheric GCM (Deque et al., 1994).

GCM), meaning that predictions on agricultural yields were based on predicted changes at coarse resolution (∼100 km). All other studies involved some type of downscaling, except those that employed the systematic changes approach (SC variables), which can be assumed to be sensitivity analyses rather than impact studies. RCMs were the most common way of downscaling GCMs, cited in 19 % of the studies, followed by statistical downscaling with 17.5 % (SD GCM) (Tabor and Williams, 2010), and pattern scaling with 8.7 % (PS GCM) (Mitchell et al., 2004) (Figure 4.3(b)).

Uncertainty was quantified in only 36.5 % of the studies (i.e. those studies where more than one single future scenario was used). Additionally, the average number of scenarios per study (rounded to the closest integer) was 3, indicating that climate uncertainties

are studied in agricultural science only to a limited extent. Few (< 5) studies used more than one crop model and no studies used a combination both parameter and crop model ensembles. This highlights a knowledge gap in agricultural research, an issue previously raised and discussed by other authors (Challinor and Wheeler, 2008b; Challinor et al., 2009c), although some studies addressing this aspect are underway (Rosenzweig et al., 2013).

4.4.2 Utility and robustness of existing weather station networks

The sensitivities of the weather station network to information loss were found overall low. Nevertheless, certain areas, variables and months were found highly sensitive. Agricultural lands (Ramankutty et al., 2008), as visually inspected, are in general less sensitive to data loss than non-agricultural lands, partly owing to a better weather monitoring by agro-climatological stations (Keatinge et al., 2012). Interpolations performance varied depending upon the variable, month and parameter used to evaluate them (i.e. r^2 and $RMSE$), but were consistent, statistically significant ($p < 0.0001$) and with variability (of r^2 and $RMSE$) between 10 - 15 % in the worst cases, this highlighting the utility of the network (see Sect. 4.3.2). Precipitation presented the lowest r^2 values (Figure4.4), particularly in the months of April to August, during which there was a higher variability in the r^2 value and the values reached the absolute minima (0.8). Although it is possible that a high number of weather stations per unit area can improve accuracy, it does not seem to happen in all variables, areas and/or months.

Maximum $RMSE$ for temperatures was 1.7 °C, whilst for precipitation it was 100 mm year^{-1}, as seen in the evaluation data. The effect of geography and the difficulty of fitting unique and complex landscape features cause errors, leading to high standard deviations in some areas (Figure 4.5). In the highlands of Eastern Africa, particularly in the states of Benshangul-Gumaz, Addis Ababa and Southern Nations in Ethiopia, the central areas of the Eastern and Coast States in Kenya, and the very centre of Tanzania (i.e. regions of Morogoro, Dodoma and Manyara) between-fold variability was found to be high (above 150 mm year^{-1}). Generally, the lowest variance was found across Southern Africa.

Over South Asia, the largest variability was found in the coastal areas of Maharashtra, Karnataka and Kerala in India, where precipitation deviation was up to 600 mm year^{-1},

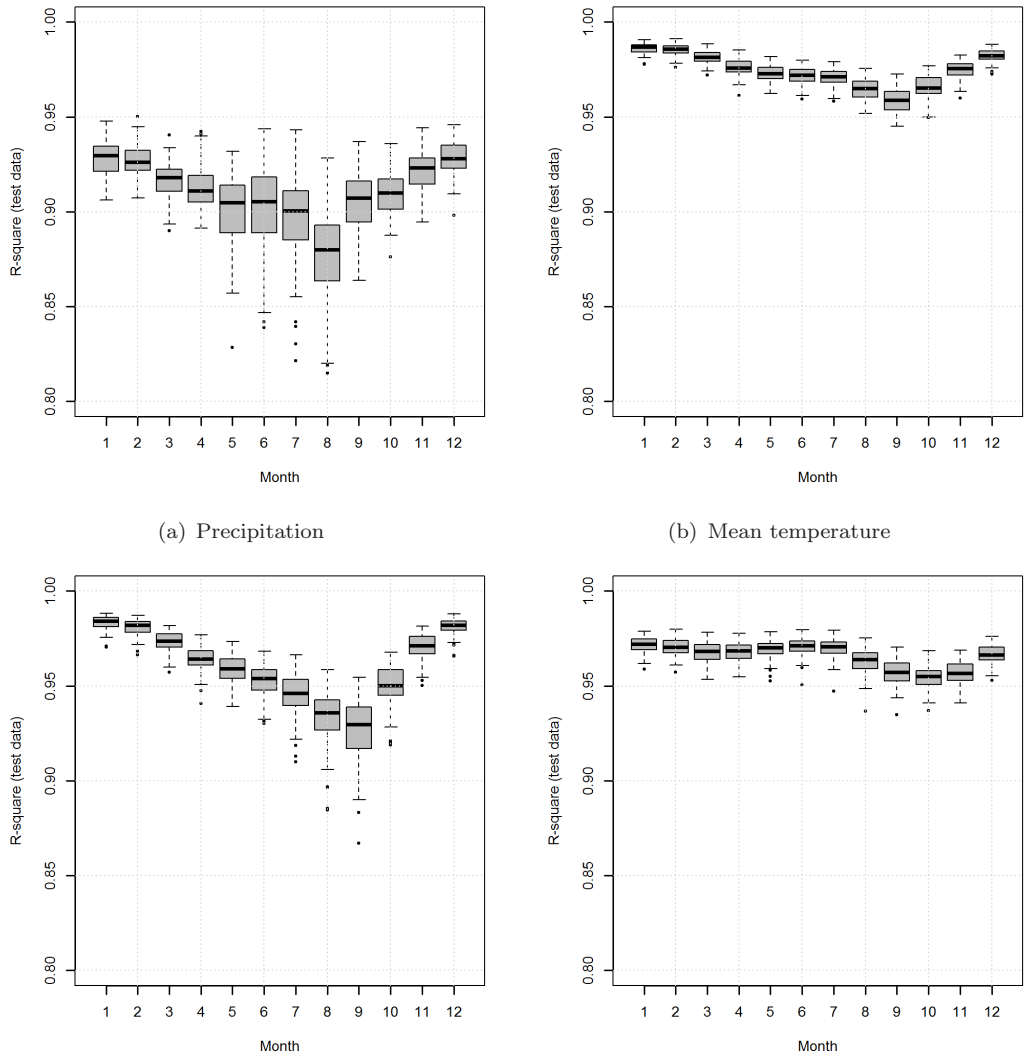

(a) Precipitation

(b) Mean temperature

(c) Max. temperature

(d) Min. temperature

FIGURE 4.4: Performance of the interpolations over South Asia and Africa for all variables and months as measured by the r^2 value. Values of r^2 were calculated using interpolated and observed values at randomly removed *testing* data points for 100 cross-validated folds.

and in Nepal (districts of Gorka, Dhawalagiri, and Lumbini), where precipitation variability can go up to 1,000 mm year^{-1}, and temperature uncertainties up to 3 °C, probably due to the combined effect of a more complex climate in the Himalayas and low weather station density.

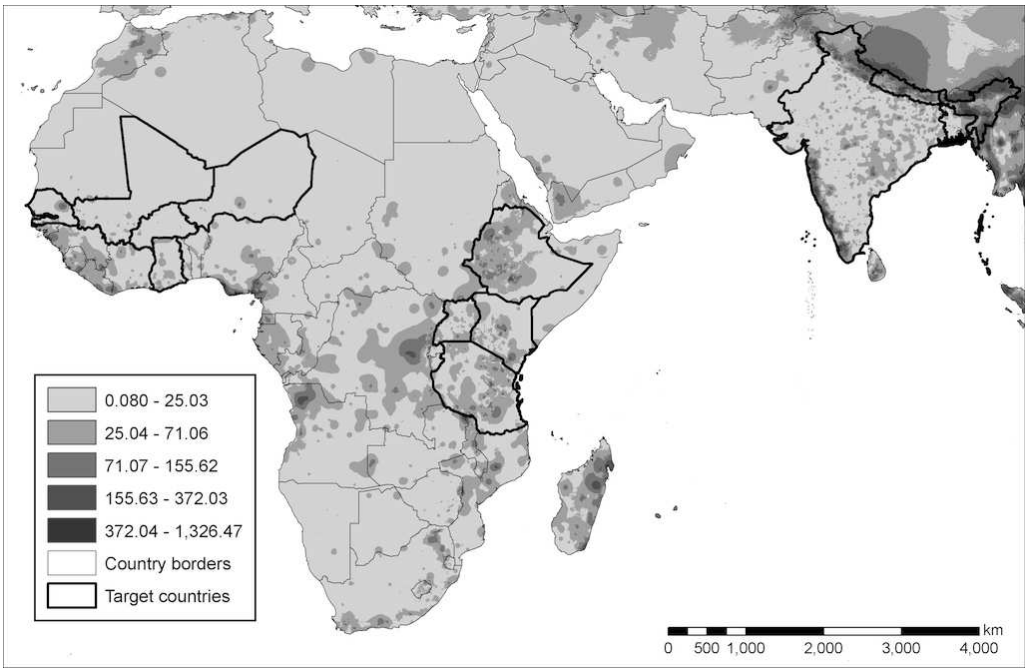

(a) Precipitation

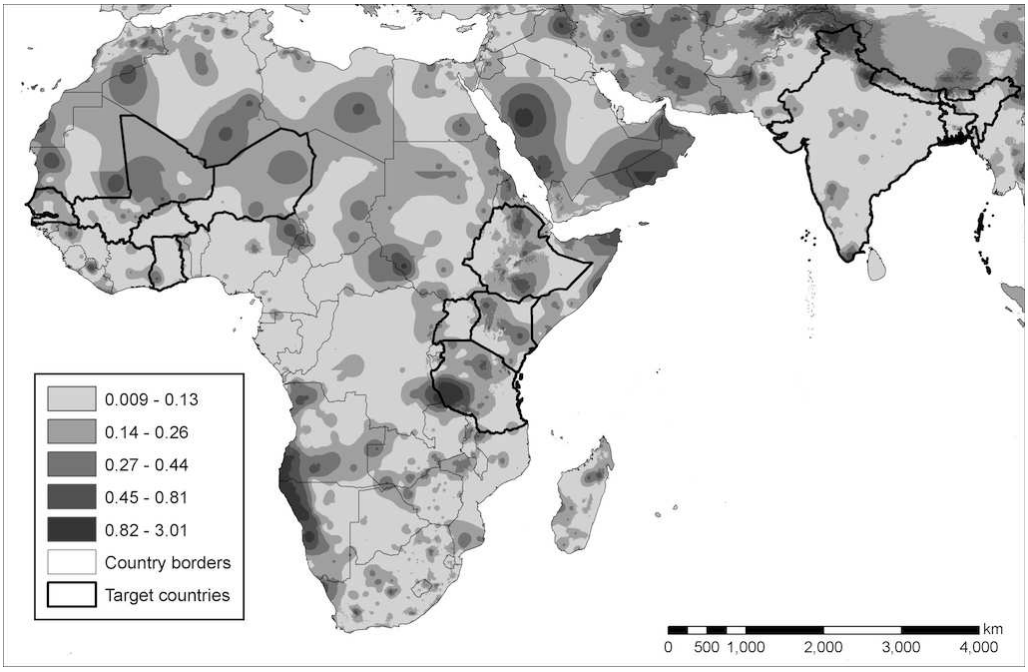

(b) Mean temperature

FIGURE 4.5: Uncertainties in WorldClim expressed as standard deviations from the mean of the 100 cross-validated folds total annual rainfall (in mm year^{-1}), annual mean temperature (in °C).

4.4.3 Ability of GCMs to represent mean climates

4.4.3.1 CMIP3 model ensemble

As expected, the climate models' skill varied on a variable, country and region basis (Figure 4.6 – 4.7). The ability of CMIP3 GCMs to represent mean climate patterns over a year was neither uniform nor consistent (Figures 4.6 – 4.7), with the lowest performance being observed for precipitation in the DJF period. Conversely, seasonal mean temperature showed the highest correlations and overall lowest $RMSE_M$ and $RMSE_{SD}$ values. These results agree with those of other studies (Gleckler et al., 2008; Masson and Knutti, 2011; Pincus et al., 2008). For mean temperatures, only 11.25 % of the GCM-region-season combinations showed $r < 0.5$, while only 6.5 % combinations showed $RMSE_M > 40$ % (Figure 4.6). These model errors, however, were generally larger than regional observed spatial variability, a result that was consistent across ensembles, variables, countries and seasons.

Absolute $RMSE$ values were in the range 1 - 5 °C for EAF, 0.5 - 10 °C for WAF, 1.5 - 7.5 °C for SAF, and 1 - 16 °C for SAS (specifically Nepal). $RMSE_M$ ($RSME_{SD}$) values were between 12 - 281 % (39 - 252 %), because there were large relative errors in the DJF season, particularly for the models CSIRO-Mk3.0, the GISS- models, IAP-FGOALS1.0-G, and INM-CM3.0. In WAF, the monsoon period showed relatively strong and strong correlations (r between 0.36 and 0.92) in combination with low (3.2 - 18 %) values of $RMSE_M$. Conversely, the dry period showed lower correlations (r between 0.2 and 0.8) and higher $RMSE_M$ (3.5 - 37 %). In EAF and SAF, correlations were generally lower and $RMSE_M$ values were higher, but there was significant variation across models (Figure 4.6).

Skill of simulated seasonal diurnal temperature range was more limited than that of mean temperatures, with roughly 50 % of the model-season combinations showing $r < 0.5$. This indicated that the representation of extreme daily temperatures is more limited in the climate models. In EAF, diurnal temperature range was found to be very poorly fitted, whereas the monsoon period in WAF was generally well simulated by the models ($RMSE_M$ of 20 - 30 % in most cases). By contrast, the skill to reproduce regional climates in EAF and SAS was much more limited (minimum $RMSE_M$ was roughly 40 %).

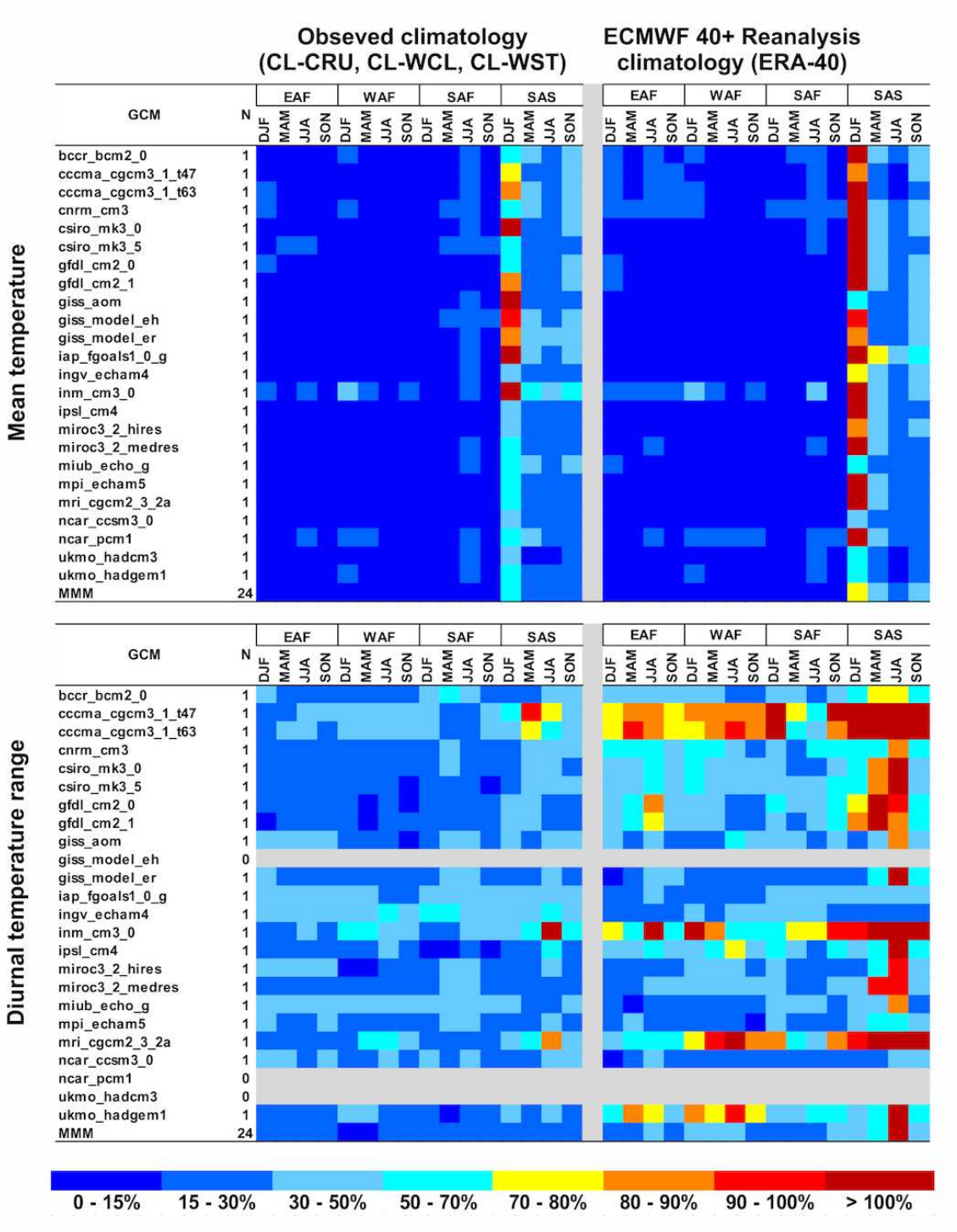

FIGURE 4.6: Variation in the $RMSE_M$ for 24 CMIP3 GCMs (and the multi-model-mean) and observed (left) and reanalysis (right) data for climatological mean temperatures (top heat map) and diurnal temperature range (bottom heat map). Values of correlation are shown across the analysis regions and seasons as averages of all countries and three observed datasets (CL_WS-QA, CL_WC-QA, and CL_CRU-QA). Grey areas indicate unavailability of input GCM data. See Figure 3.1 for region definitions.

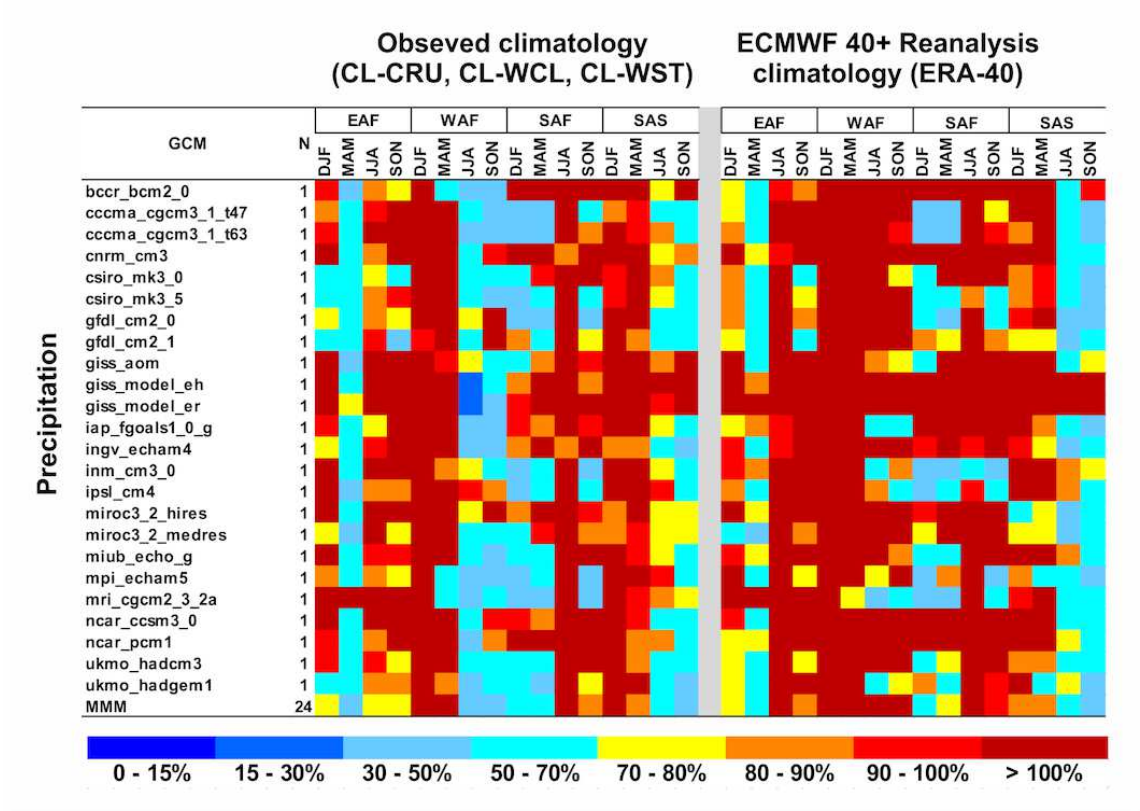

FIGURE 4.7: Variation in the $RMSE_M$ between 24 CMIP3 GCMs (and the multi-model-mean) and observed (left) and reanalysis (right) data for climatological total precipitation. Additional details as in Figure 4.6.

For annual precipitation, about 95 % of GCM-season-region combinations showed $RMSE_M$ > 40 %. In Mali, Niger, India and Bangladesh, model skill in representing precipitation, was consistently low, an issue also reported in other studies (Douglass et al., 2008; Gleckler et al., 2008; Reichler and Kim, 2008). The Bergen Climate Model (BCCR-BCM2.0) and the INM-CM3.0 model showed very poor performance ($r < 0.5$, $RMSE_M > 40$ %) in more than 25 % of the countries, while the climate model GISS-ModelE (Hansen et al., 2007) presented the poorest performance in all countries and seasons, except in the monsoon period of WAF (Figure 4.7).

4.4.3.2 CMIP5 model ensemble

Similar to CMIP3, CMIP5 model skill for climatological means varied significantly on a model basis (Figure 4.8 - 4.9). The UK MetOffice (UKMO) models tended to consistently perform better than all others. Absolute skill in climatological mean temperature and

diurnal temperature range was generally higher than for other variables ($RMSE_M < 40$ % in the majority of cases; Figure 4.8).

The largest errors ($RMSE_M > 40$ %) in the four climate fields were found in South Asia, which is consistent with previous studies and is related to the difficulties in representing mountain climates at low resolution (Gleckler et al., 2008). Values of correlation were negative in 0 %, 0.23 %, 0.5 %, and 2.25 % of region-season combinations for mean temperature, diurnal temperature range, precipitation, and the number of wet days, respectively. Generally, the monsoon season (in WAF and SAS) showed less skill than the dry season, and this was consistent with the poor skill of the models in predicting the number of wet days (Figure 4.9).

Absolute $RMSE$ for mean temperatures and diurnal temperature range was in the range 1 - 8 °C in all regions except in SAS (particularly in Nepal), where it was found to be as high as 17 °C. The $RMSE_M$ indicated mean temperatures were much more predictable. Individual GCMs showed $RMSE_M$ values above 40 % in only 1.1 - 6.8 % combinations for temperature. Cases with $RMSE_M > 40$ % were in the range 1.1 - 40 % for diurnal temperature range.

Seasonal precipitation $RMSE$ was observed to be as high as 2,000 mm season^{-1} (for the monsoon season in South Asia), while yearly $RMSE$ values were in the order of 200-3,000 mm year^{-1}. The average $RMSE$ was 190 mm season^{-1}, with 65 % of the country-season combinations having $RMSE$ below this value. Values of $RMSE_M$ for seasonal precipitation were higher, and ranged between 24.7-522 %. EAF showed significantly better model skill than all other regions (Figure 4.9).

The number of rain days was vastly different between the model and the observations, with $RMSE$ values often above 150 days year^{-1} (about half of the year). For precipitation, 81-100 % cases showed $RMSE_M > 40$ %. The number of wet days was observed to be less predictable, with cases with $RMSE_M > 40$ % in the order 95 - 100 %. The number of wet days was in all cases the least predictable variable, with $RMSE_M$ values of 50 - 3,500 % (Figure 4.9).

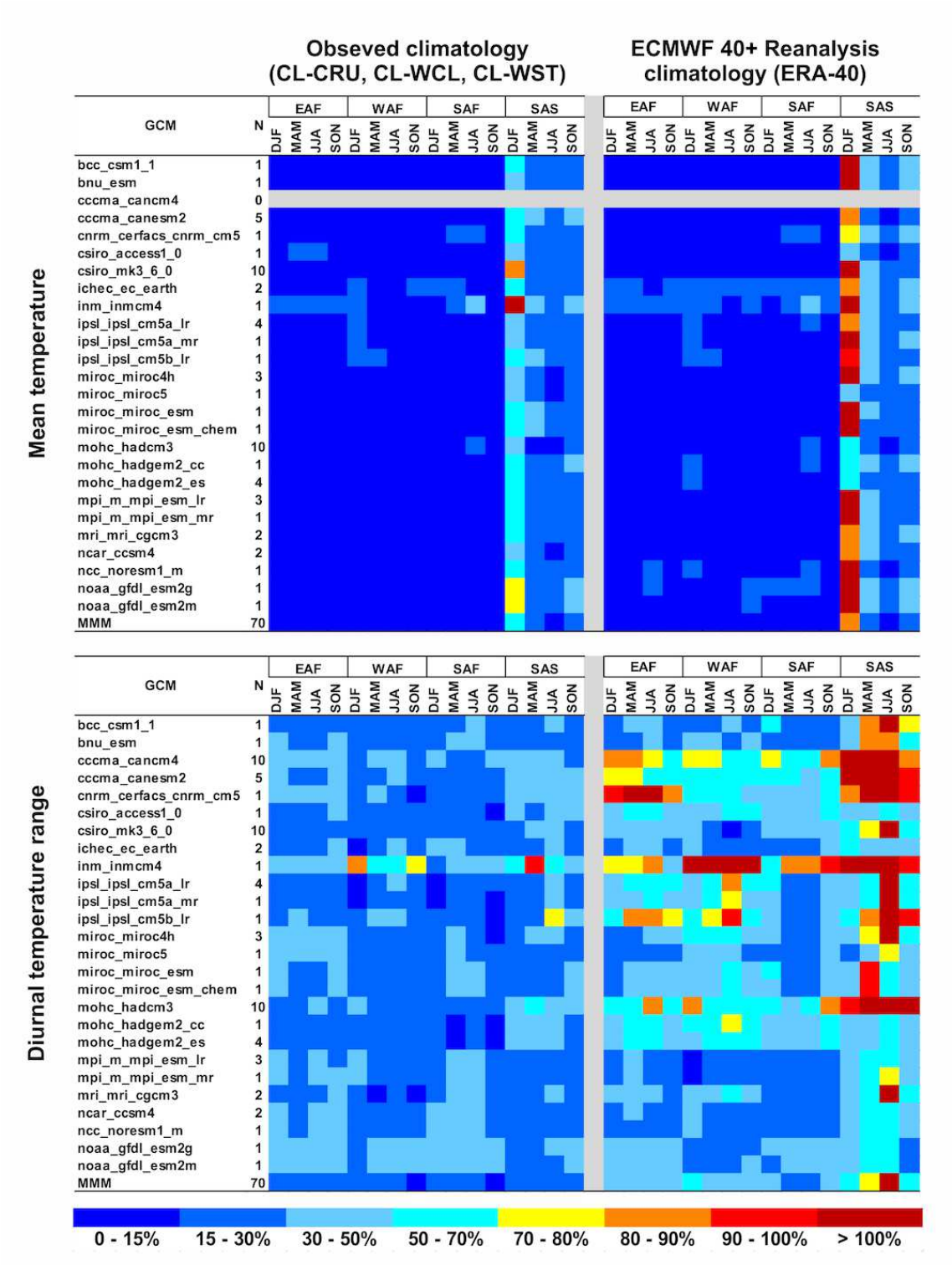

FIGURE 4.8: Variation in the $RMSE_M$ for 26 CMIP5 GCMs (and the multi-model-mean) and observed (left) and reanalysis (right) data for climatological mean temperatures and diurnal temperature range. Additional details as in Figure 4.6.

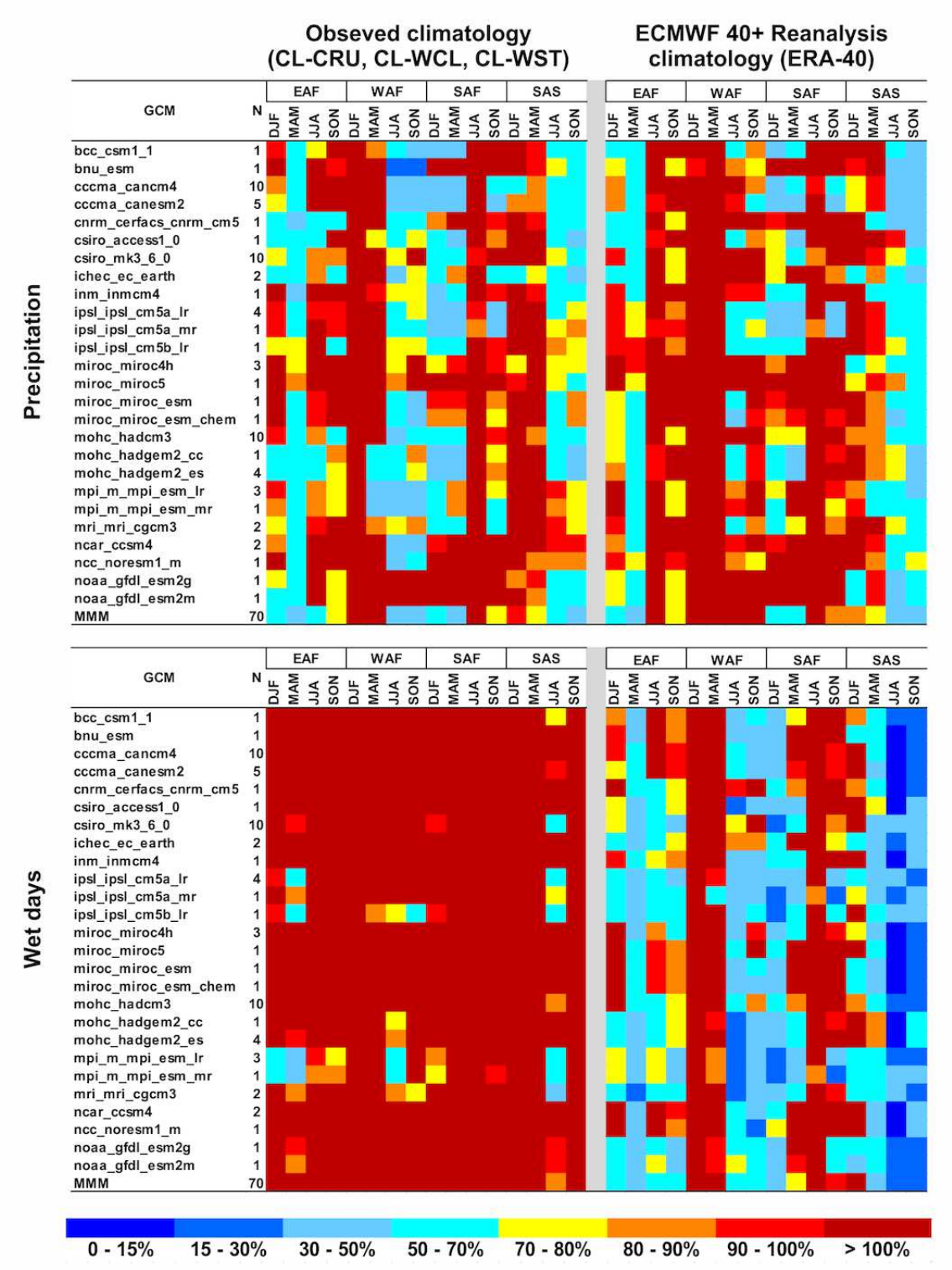

FIGURE 4.9: Variation in the $RMSE_M$ for 26 CMIP5 GCMs (and the multi-model-mean) and observed (left) and reanalysis (right) data for climatological total precipitation. Additional details as in Figure 4.6.

4.4.4 Ability to represent interannual variability

4.4.4.1 CMIP3 ensemble

Figure 4.10 shows the average of the V_I across all GCMs for annual total precipitation, mean temperature and diurnal temperature range. Excluded from this average is the MMM (multi-model mean), which presented very poor performance. In general, interannual variability was poorly captured by the models, although individual models showed strengths in some of the regions. At all grid cells, there was always at least one GCM with $V_I < 0.5$, but in all cases the maximum values were above this threshold. This indicated that errors in models' representations of interannual variability are generally not geographically consistent.

Interannual variability of mean temperatures in CMIP3 was better represented across WAF and SAF, where values of VI were in the order 0 - 0.5, with only few grid cells (< 15 %) exceeding this range. High skill ($V_I < 0.5$) was observed in 30 - 60 % country-season combinations. There was also significant spatial variation in the V_I, with central EAF (Kenya and Uganda) and northern SAS (particularly towards Nepal) showing the largest values.

Diurnal temperature range and total precipitation showed very few locations (i.e. less than 10 %) where V_I was below 0.5 (Figure 4.10). There was also little geographic consistency in skill between these two variables. This was evidenced since the areas where V_I values were very high for one variable, were lower for the other and vice versa. High values of V_I ($V_I > 0.5$) were found in 50.5 % (MIROC3.2-HIRES) to 100 % (NCAR-PCM1) of the areas. Such high values (indicating poor skill) for diurnal temperature range were found across SAF and SAS, while the lowest values were found in WAF and EAF (particularly in Ethiopia and Tanzania). For precipitation, V_I showed values above 0.5 in at least 72 % of the areas for all models. The poorest skill was found across the Sahel and in northern SAS, (Figure 4.10).

4.4.4.2 CMIP5 ensemble

CMIP5 interannual variability was also significantly misrepresented, particularly in areas with complex landscape features such as the Himalayas (Figure 4.11). No single climate

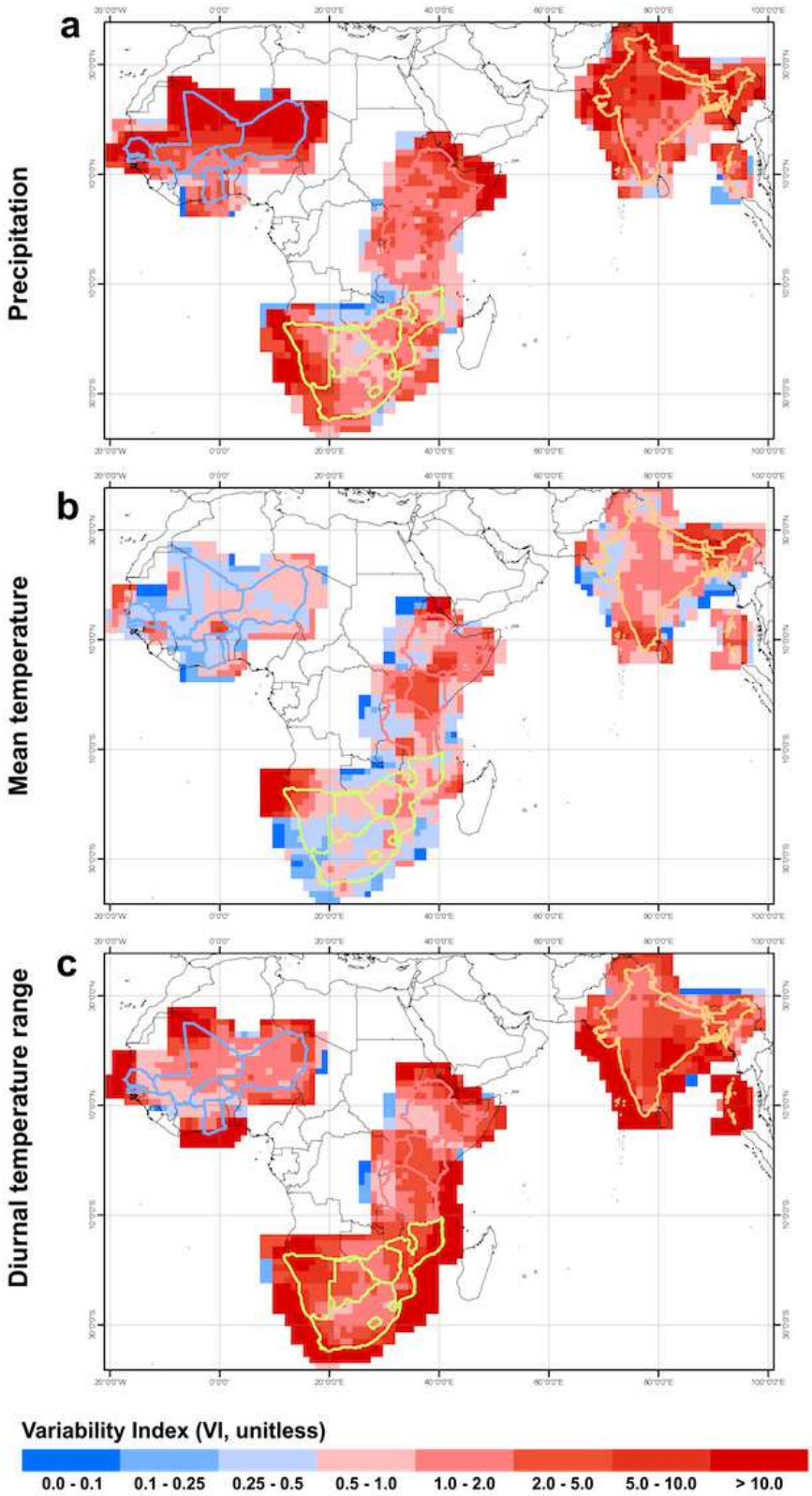

FIGURE 4.10: Average CMIP3 climate model skill in reproducing interannual variability as measured by the variability index (V_I, Eq. 3.55) for (a) annual total precipitation (mm/year), (b) annual mean temperature (°C), and (c) diurnal temperature range (°C). Blue areas (where $V_I < 0.5$) indicate high model skill. Values shown are means of all 23 climate model simulations (see Table 3.3) per grid cell.

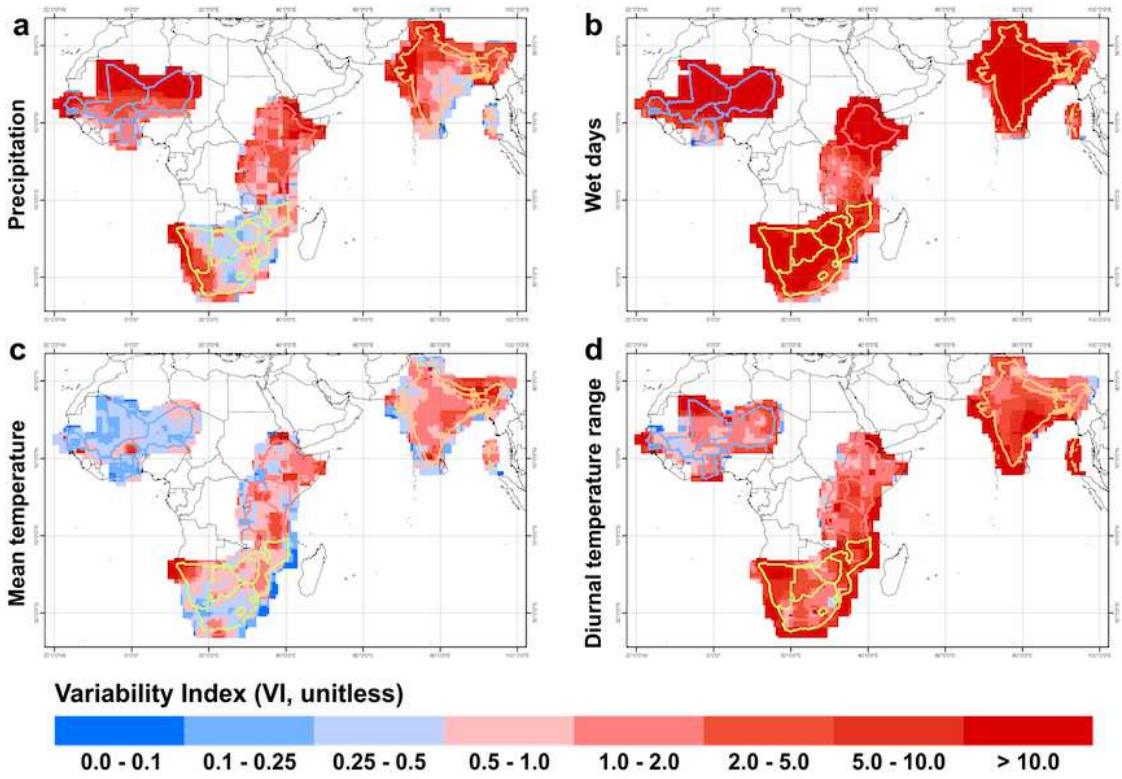

FIGURE 4.11: Average CMIP5 climate model skill in reproducing interannual variability as measured by the variability index (V_I, Eq. 3.55) for (a) annual total precipitation, (b) number of wet days, (c) annual mean temperature, and (d) diurnal temperature range. Blue areas (where $V_I < 0.5$) indicate high model skill. Values shown are means of all 26 climate model simulations (see Table 3.4) per grid cell.

model showed good agreement ($V_I < 0.5$) in more than 30 % of the areas for precipitation and 15 % for the wet-day frequency. However, the corresponding fractional area is 50 % for temperature range and to 70 % for mean temperatures. Although interannual variability was not adequately captured by most climate models in most areas for precipitation (with most models showing 70 - 80 % areas with low skill, $V_I > 0.5$), areas with high interannual variability skill (i.e. $V_I < 0.5$) ranged between 27.5 % (MIROC-4h) to 68 % (GFDL-ESM2-M) for mean temperature, and between 49.8 % (MIROC-4h) to 90.1 % (INM-CM4) for diurnal temperature range.

4.4.5 Comparison between CMIP3 and CMIP5

Here, the actual improvements in climate model skill were assessed using Taylor diagrams (Figure 4.12), and the probability density functions of both ensembles (Figure 4.13 - 4.14). Set CMIP3 as a reference, climate models in the CMIP5 ensemble (with no clear difference

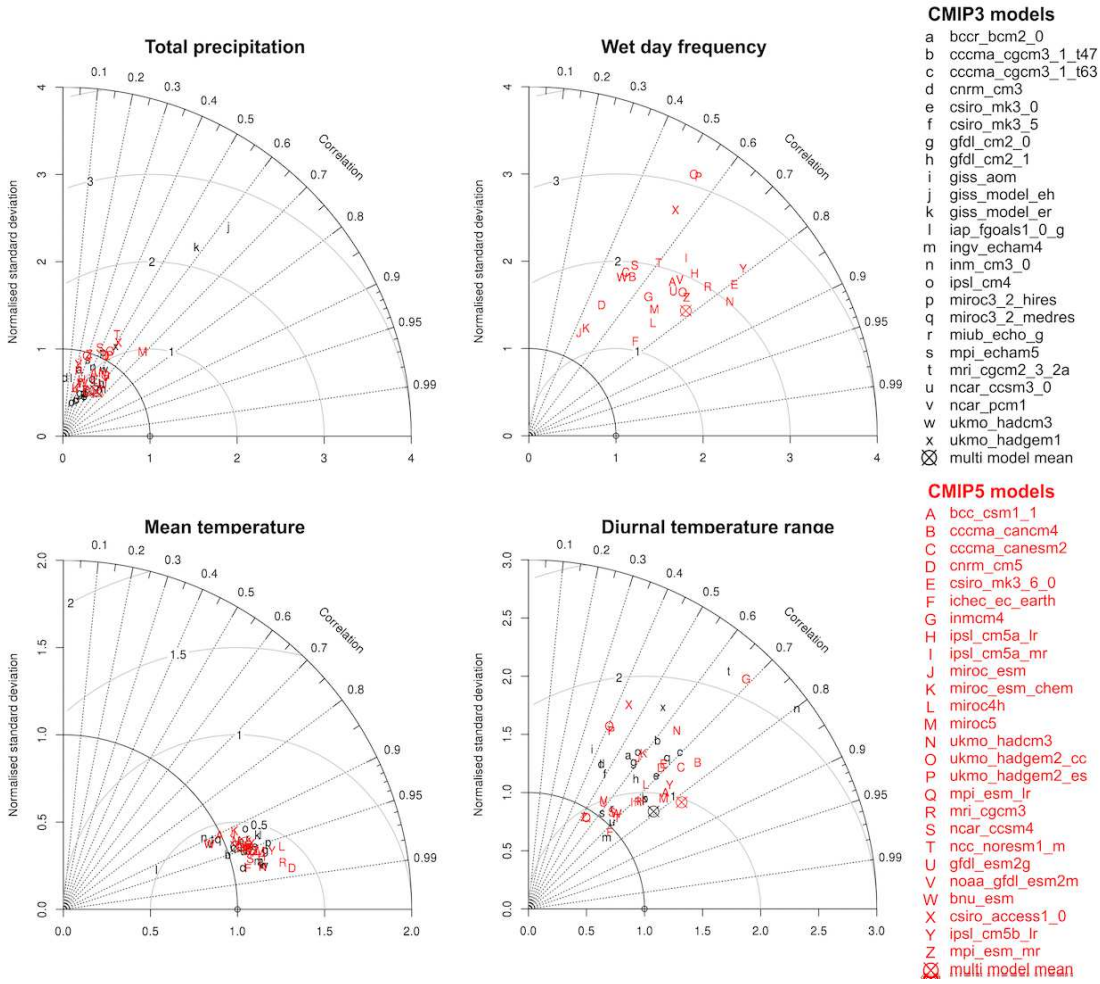

FIGURE 4.12: Taylor diagrams for 23 CMIP3 (black lower case letters) and 26 CMIP5 (red upper case letters). Multi model means are indicated by crossed circles in the respective colour. Only climatological means of simulated annual totals (precipitation and wet-day frequency) and means (mean temperature and diurnal temperature range) for India are shown. In all cases only comparisons with CL-CRU are shown. Due to the overlap between different ensemble members in the CMIP5 ensemble only one ensemble member is shown to improve clarity in the diagram. Note that in the wet day frequency, only CMIP5 output is shown owing to data availability in the CMIP3 archive.

in skill between Earth System Models ESMs, and Coupled Global Climate Models GCMs) have improved primarily in terms of mean climatology, particularly for mean temperature. The Taylor diagram for annual totals and means over India (Figure 4.12) shows less spread in CMIP5 models, and a more accurate representation of standard deviations (i.e. models are closer to the 1:1 arc). This is particularly true for total precipitation and mean temperature. Similar trends were observed for all other countries analysed. Despite a general improvement in model skill, however, errors remain large for some variables, particularly for daily temperatures extremes and the wet-day frequency.

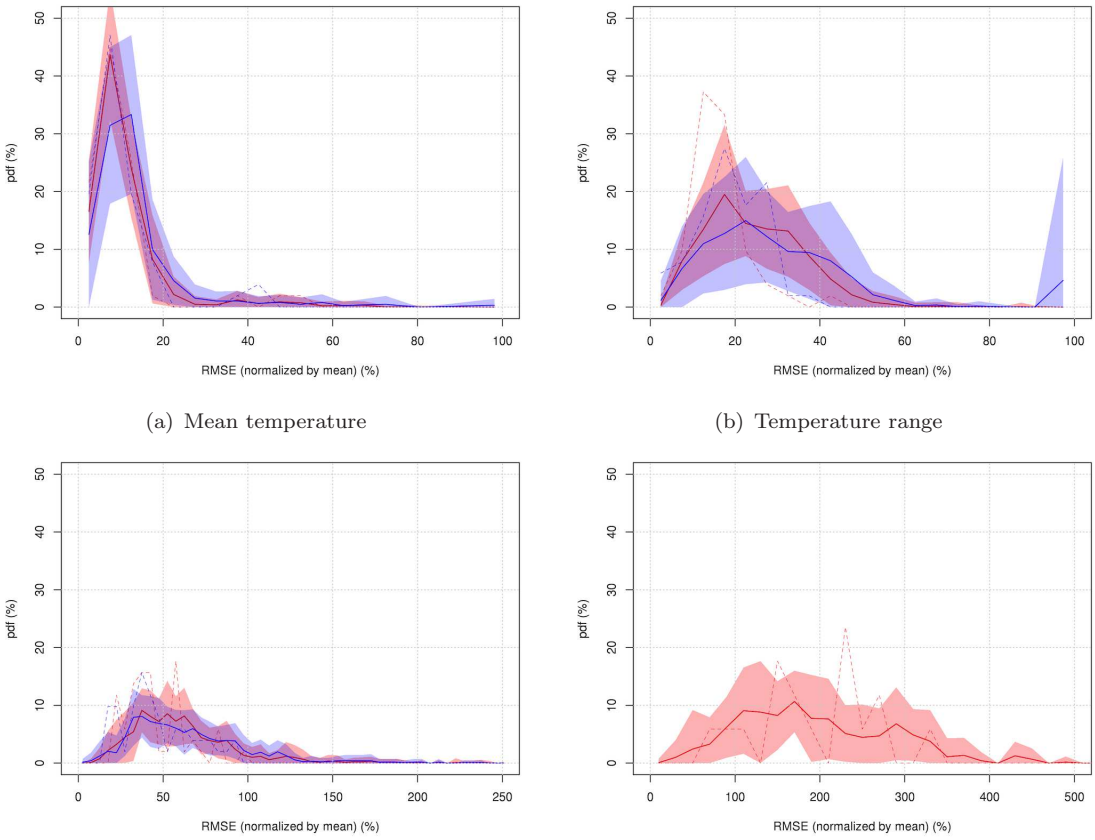

(a) Mean temperature

(b) Temperature range

(c) Total precipitation

(d) Wet-day frequency

FIGURE 4.13: Probability density functions of the $RMSE_M$ for the CMIP3 (blue) and CMIP5 (red) model ensembles and annual totals or means of precipitation, number of wet days, mean temperature, and diurnal temperature range. Shading indicates ± one standard deviation across the mean PDF (continuous lines). Dashed lines show the multi-model-mean. Note the differences in the x-axis scale across variables.

In agreement with the above, a more general analysis of the PDFs of the four skill metrics used here (three for mean climates and one for interannual variability) shows a displacement of the PDFs of the CMIP5 ensemble (Figure 4.13- 4.14). Such displacement is most evident for simulated climatological mean temperatures and total precipitation. Diurnal temperature range showed no clear trend, and the wet-day frequency could not be analysed. Skill in representing interannual variability showed no improvement at all. The PDFs of skill metrics also indicated that model spread (in the skill metrics) was the largest for diurnal range and wet-day frequency, and the smallest for mean temperatures. Importantly, in all the three variables that could be compared (precipitation, temperature and diurnal temperature range), CMIP5s MMM showed better skill than that of CMIP3.

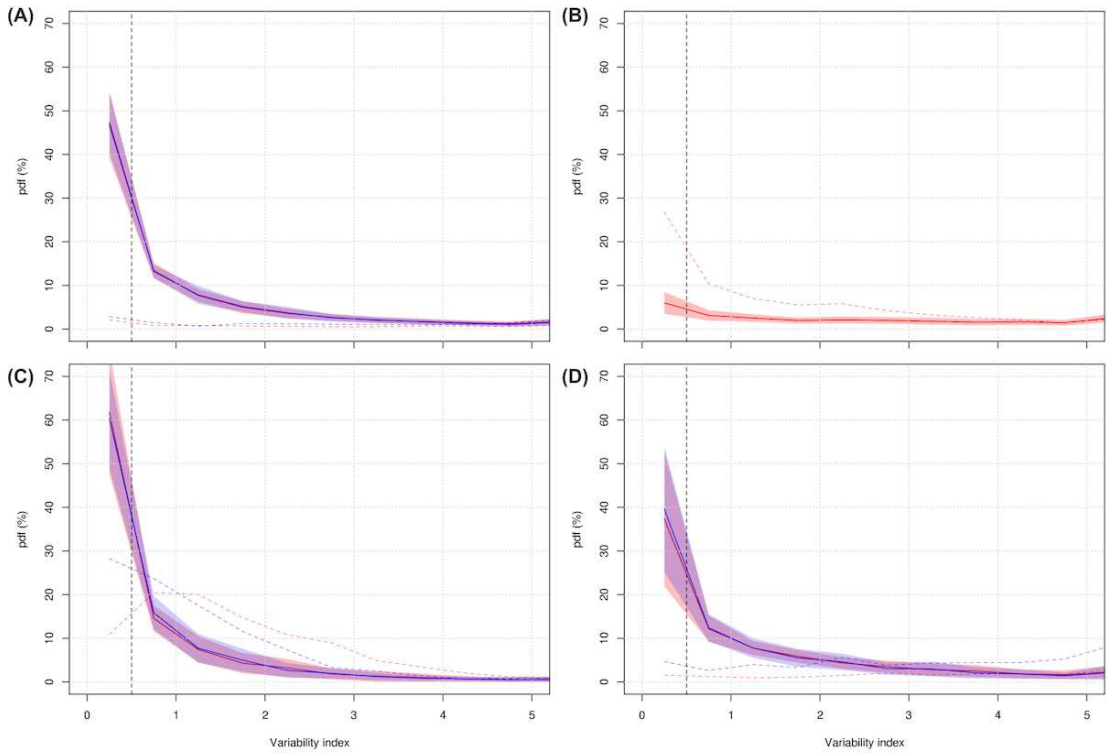

FIGURE 4.14: Probability density functions of the interannual variability index (V_I) for the CMIP3 (blue) and CMIP5 (red) model ensembles for annual totals or means of (a) precipitation, (b) number of wet days, (c) mean temperature, and (d) diurnal temperature range. Shading indicates one standard deviation around the mean PDF (continuous lines). Dashed lines show the multi-model-mean.

4.5 Discussion

4.5.1 Climate data and agricultural research

Although climate model data ("as is") are often preferred for impact studies (see Figure 4.3(b), Sect. 4.4.1.3), crop modellers and agricultural scientists should be cautious when developing future adaptation strategies based on crop models applied using future predictions of different (and sometimes unknown) nature (Jarvis et al., 2011a)), given the large uncertainties regarding the agricultural system and plant responses, the underlying uncertainty related to parameterised processes, and the differences in scales, all of which are reported in the impact-assessment literature (e.g. Challinor and Wheeler 2008b). This, however, does not necessarily imply that climate model data cannot or should not be used, but rather means that an adequate treatment of biases needs to be done before climate

and crop models can be properly used together (Challinor et al., 2010; Ehret et al., 2012; Osborne et al., 2007).

As showed in Sect. 4.4.1, products such as WorldClim (Jones and Thornton, 2003; Thornton et al., 2009) and CRU (Challinor et al., 2004) coupled with weather generation routines appear to be recurrently used in regional assessments (Hewitson and Crane, 2006; Jones and Thornton, 2003). Climate model data can also be used with appropriate bias treatment (Hawkins et al., 2013a; Iizumi et al., 2012a; Themessl et al., 2012). However, if studies are to be carried out on a site-specific scale (Parry et al., 2005), weather station data is the best means by which to calibrate the modelling approaches (see Figure 4.3(a)). While partnerships are constantly being built and this allows researchers to share data, currently global weather station data such as GSOD and GHCN seem to be good options in cases when no other data is available. The coupling of these sources with satellite data or other (country specific) historical weather records also appears as an appropriate strategy (Alvarez-Villa et al., 2010).

A further issue of importance, however, is related to how to use local-scale information together with global climate projections of uncertain and coarse-resolution nature. Agricultural research requires high quality and high resolution climatological data to yield accurate results (White et al., 2011b). To date, however, this has been impossible to achieve at detailed scales and with sufficient coverage. This is in part due to the difficulty in compiling and revising field data and partly due to the limited climatology knowledge of agricultural researchers (with some exceptions). Large-scale datasets can be matched to certain crop models, mostly when these models can be applied at large scales (e.g. Challinor et al. 2010) or do not rely on a detailed calibration of varietal-level crop parameters (e.g. Lobell et al. 2008, 2011a). However, matching different modelling scales is not a trivial matter (Baron et al., 2005; Challinor et al., 2009b).

Climate data can be aggregated up to any scale to match any intended use (Masson and Knutti, 2011), but agricultural impacts need to be informed at an scale such that information can be used for decision making and adaptation (Smith and Stern, 2011; Wilby et al., 2009). Hence, governments and international agencies should support common platforms through which data can be shared without restrictions between members of the research community. Best-bet methods can then be applied over such data to produce

useable datasets that can be further shared, used and assessed in multidisciplinary and transdisciplinary approaches (see e.g. Iizumi et al. 2012b; Semenov et al. 2010).

4.5.2 Robustness of the existing weather station network

It is acknowledged that the use of interpolated surfaces can lead to errors and biases when these data are used for impact assessment (Hijmans et al., 2005; Mitchell and Jones, 2005). However, it was demonstrated here that uncertainty (and its effect) is actually rather low in most of the cases, with very few exceptions (highlands of Ethiopia, the Himalayas, and some parts of the Sahara and Southern Africa, see Figure 4.5 and Sect. 4.4.2).

The results of Sect. 4.4.2 suggest that, despite weather station density being important, it may not be the only determining factor for a good ability to fill information gaps (Hijmans et al., 2005). In increasing the robustness and utility of the weather station network (i.e. increasing the weather station density), both the complexity of the landscape and the predictability of the variable being measured should be considered. This is because robustness and utility are largely dependent on landscape topographic complexity and predictability (see Figures 4.4 - 4.5). Improving weather station distribution and status, as well as improving the cross-checking, correction and evaluation of data collected at the different sites and access to such data, is fundamental for improving climate data for agricultural impact assessment.

4.5.3 Global climate model skill

4.5.3.1 CMIP3 model skill

GCM performance is highly reliant on the type of comparisons performed, on the GCM formulation and on the nature of climate conditions in the analysed areas (Gleckler et al., 2008; Masson and Knutti, 2011). Underlying factors driving GCM performance are indeed difficult to track, given the complexity of the models. CMIP3 models showed varied performance, and tended to show rather limited skill in simulating climatological precipitation, wet-day frequency and, to a lesser extent, daily temperature extremes both in terms of mean climate and interannual variability. These responses reportedly have their origin in different factors:

- First, some CMIP3 GCMs have weak forcing on sea surface temperatures (SSTs), whereas climate in Africa and Asia is strongly coupled with the Atlantic and Indian Ocean and with inland water bodies (Gallee et al., 2004; Lebel et al., 2000);
- second, models do not properly account for the relation between inter-annual variability, ENSO and the monsoonal winds (Gallee et al., 2004; Hulme et al., 2001);
- third, the resolution of the models prevents acknowledgement of local-scale land use, orographic patterns and small water bodies (Hudson and Jones, 2002);
- fourth, cloud thickness and latent heat and moisture flux between clouds is not properly resolved in the models (Gallee et al., 2004);
- fifth, moist convection parameterisations produce an early onset of the seasonal rains and over-prediction of wet days and high-rainfall events (Gallee et al., 2004; Gleckler et al., 2008); and
- finally, none of the CMIP3 models incorporated aerosol effects (Booth et al., 2012).

Similar results are reported by other authors that have assessed this or similar model ensembles (Jun et al., 2008; Pierce et al., 2009). Lack of detail in land use and land use changes (Eltahir and Gong, 1996), monsoon winds (Eltahir and Gong, 1996; Gallee et al., 2004), and sea surface temperature anomalies (SSTs) of the Atlantic and the Indian Oceans (Lebel et al., 2000; Sun et al., 1999) also cause the scales at which climate model information is robust to be varied (Masson and Knutti, 2011), and prevents regional-scale seasonal weather patterns from being modelled consistently (Douglass et al., 2008; Hansen et al., 2007).

4.5.3.2 CMIP5: how much improvement?

In relation to CMIP3, its immediate predecessor, CMIP5 has a wider range of numerical experiments (Taylor et al., 2012), and data for a larger number of models and model ensembles. CMIP3 historical ('20C3M') simulations included 24 CGCMs, whereas CMIP5's included more than 35 CGCMs (of which 26 were assessed here) (Taylor et al., 2012). In addition, CMIP5's experimental design includes individual perturbed physics and initial conditions ensemble members for a number of models, thus permitting the comparison

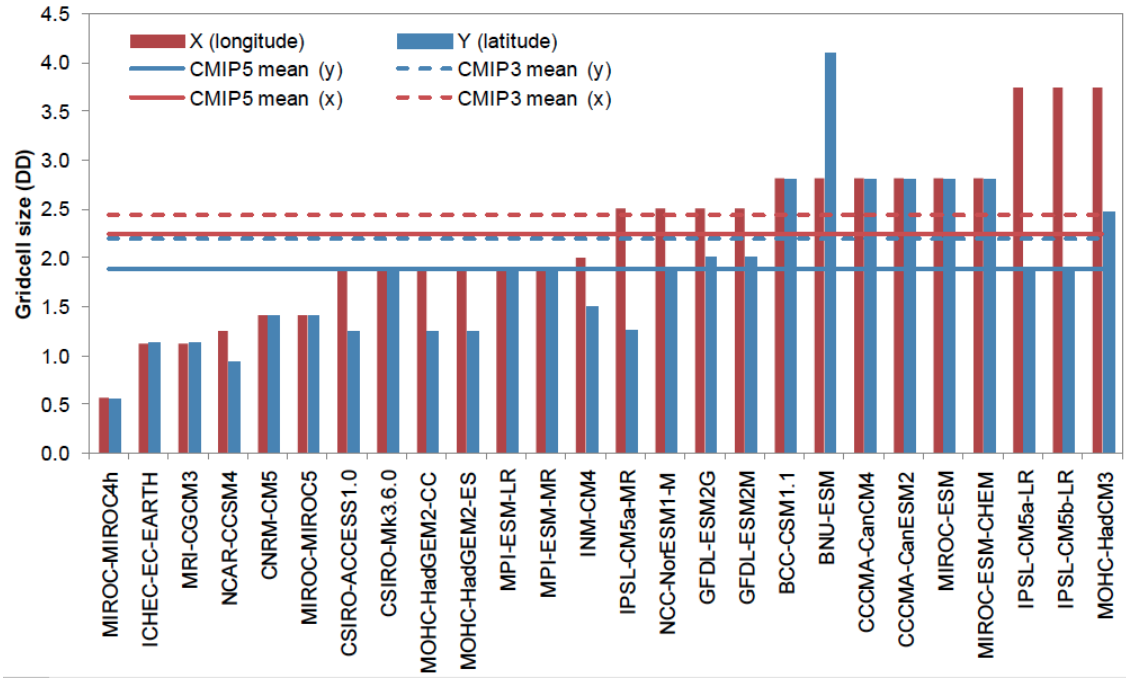

FIGURE 4.15: Overview of the CMIP5 climate model ensemble horizontal resolution in relation with CMIP3. Values correspond to sizes (latitude, longitude) of grid cells in decimal degrees (DD). Horizontal lines show means of all models for each CMIP ensemble (CMIP3 is the average of 24 GCMs of Table 3.3, and CMIP5 is the average of 26 GCMs of Table 3.4).

of climate uncertainties (see e.g. Knutti and Sedlacek 2012). Model resolution has also increased (Figure 4.15), and models have increased their complexity by including atmospheric chemistry, aerosols (Booth et al., 2012), the carbon cycle (Taylor et al., 2012), and decadal predictions (Meehl et al., 2009). Improvements in CMIP5 are in large part tied with increases in computational capacity: about one-third of the increase in computing power is estimated to be used solely in increasing model complexity (Knutti and Sedlacek, 2012).

Owing to its improved experimental design and the increased physical plausibility of its models, the CMIP5 climate model ensemble constitutes a considerable step forward in climate prediction (Taylor et al., 2012). CMIP5 has the conceptual advantage of having been carefully designed to match the needs of various communities (i.e. climate, impacts, policy). Furthermore, a recently published analysis of robustness and uncertainties further indicates that both ensembles are consistent in their predictions, highlighting the importance of CMIP5 in increasing confidence in global warming projections (Knutti and Sedlacek, 2012).

The analyses of skill presented here indicated that improvements occurred particularly in terms of representing regional climatological mean temperature (Sect. 4.3.4). Skill in representing daily temperature extremes has not increased noticeably, but it remains higher than that of precipitation yet worse than that of mean temperatures. A comparison of wet-day frequency was not possible, but given that model skill in precipitation has increased, it is likely that errors have also decreased for this quantity. The number of wet days was by far the least predictable quantity, yet one of the most critical ones for impact assessment (Baigorria et al., 2010; Berg et al., 2010). Similarly, simulated interannual variability showed some improvement for mean temperatures (Figure 4.14) (also see Scherrer 2011), but CMIP5 predictions of precipitation interannual variability do not show a significantly better picture to that of CMIP3. Various other researchers have previously analysed the CMIP3 model ensemble (e.g. Gleckler et al. 2008; Pierce et al. 2009; Scherrer 2011), and their results strengthen the validity of the conclusions presented here.

In spite of improvements, climate model outputs are probably not yet of enough quality for them to be used reliably in crop modelling (Hansen et al., 2009; Ines et al., 2011). Although a more definite conclusion regarding this statement is reached in a subsequent chapter (see Chapter 5), the fact that CMIP5 showed the same or more skill with more GCMs suggests that skill in the new generation of models has overall increased. Considering that model complexity has also increased, this means that while new components in the models have increased the physical plausibility of the models, skill has either maintained or increased. This is likely to be an important step forward, but still only one of many needed for impact assessment. This all shows the enhancements that can arise from research investments in last decades of climate research (Knutti and Sedlacek, 2012; Meehl et al., 2009; Taylor et al., 2012).

4.5.3.3 Plugging climate model data into agricultural research

GCMs do not provide realistic representations of climate conditions in a particular site, but rather provide estimated conditions for a large area. Results presented here, in agreement with those from the agricultural community (Baron et al., 2005; Challinor et al., 2003) and the climate community (Jun et al., 2008; Masson and Knutti, 2011), indicate that climate model outputs cannot be input directly into plot-scale (agricultural) models, but support the idea that higher resolution and added model complexity (e.g. aerosols, the carbon

cycle) contribute towards reducing model error. Either the CMIP3 or the CMIP5 climate model ensembles can be adequately used in agricultural modelling if: (1) the scales between the models are matched (see Sect. 4.4.1), (2) skill of models is assessed and ways to create robust model ensembles are defined (Tebaldi and Lobell, 2008), (3) uncertainty and model spread are quantified (Knutti and Sedlacek, 2012), and (4) decision making in the context of uncertainty viewed as a concerted process between model-based impacts estimates and farmer- or sector-based perceived sensitivities (Vermeulen et al., 2013). These four points are all treated in subsequent chapters of this thesis.

Limitations to skill in predicting impacts may limit the planning of adaptation strategies (Challinor et al., 2009b). Uncertainty in climate response and internal variability is known to be critical when planning short- and mid-term adaptation options (Hawkins and Sutton, 2009; Howden et al., 2007); it may well exceed scenario uncertainty over the next 2-4 decades (Hawkins and Sutton, 2009). Planning at these time scales has been identified elsewhere as being critical for some of the regions analysed here (e.g. South Asia, West and East Africa Howden et al. 2007; Lobell et al. 2008; Roudier et al. 2011). Therefore, improvement in GCMs, particularly in precipitation predictions and interannual variability, and more informed use of climate model predictions, is important for agricultural adaptation. Improved climate simulation would likely improve estimates of future crop failures, impacts of ENSO and other large-scale phenomena and underpin efforts to avoid inappropriate adaptation (Howden et al., 2007; Lobell et al., 2008; Roudier et al., 2011).

In a similar way CMIP3 has been of paramount importance in the last 5 years for impacts research, CMIP5 is likely to play a central role in climate impacts assessments over the coming years. As a way to guide the future use of these climate simulations, the following recommendations are provided:

- Quantify agricultural model uncertainty by using a wider assortment of crop models. Currently, research is being undertaken to address the need of both quantifying agricultural model uncertainty and improve model parameterizations (Asseng et al., 2013; Rosenzweig et al., 2013). These programs should allow developing robust probabilistic projections of climate change impacts, by taking appropriate account of climate and crop model uncertainties both at the structural and parameter level.

- Assess the sensitivities of agricultural models to errors in input weather datasets at different time scales for the region of analysis. Understanding the modes of climate variability that are important for skilful prediction, in combination with an assessment of GCM skill, enables more robust inference based on model results (Watson and Challinor, 2013).

- The present analyses demonstrate that, whilst CMIP5 is an improvement on CMIP3, significant biases remain. These biases have implications for impacts assessments. Bias correction techniques will therefore remain central to future impacts assessments. There are a number of techniques available and the choice of technique is known to be a significant source of uncertainty (Hawkins et al., 2013b; Iizumi et al., 2012a). Impact modellers make choices for their studies mostly on the basis of their previous experience and previous published studies (White et al., 2011b), but the robustness of one or other choice is rarely assessed (see e.g. Hawkins et al. 2013b; Iizumi et al. 2012a for notable exceptions). In future assessments, as done in this thesis (see Chapter 6- 8), multiple techniques should be used.

- Even though it is clear that climate and agricultural model scales need to be matched, it is not clear whether this has to be done through downscaling of GCM outputs (Ehret et al., 2012; Themessl et al., 2012), or through upscaling crop model processes and/or parameters (Challinor et al., 2004; Iizumi et al., 2009b; Tao et al., 2009). Research is being undertaken in the search of synergy between these two methodologies for some regions of the globe (van Bussel et al., 2011; van Wart et al., 2013). A more generalised exploration of synergies between upscaling model processes and downscaling GCM output is warranted towards the future.

- Increase the robustness of impact studies also using other climate modelling frameworks. These may include those that study model uncertainty (climateprediction.net Stainforth et al. 2005), parameter uncertainty (QUMP Murphy et al. 2007), and downscaling (CORDEX, Giorgi et al. 2009; Nikulin et al. 2012). This would allow better treatment of uncertainty (Roudier et al., 2011), the study of probabilistic projections, the assessment of the benefits of dynamical downscaling, and the tackling of additional research questions, such as those involving plausible geoengineering scenarios (Pongratz et al., 2012; Stainforth et al., 2005).

- Lastly, inform both the climate and agricultural research communities about those decisions that can lead to reducing uncertainties for prioritizing future model improvements.

As such, CMIP3 and CMIP5 GCMs can be used with a certain degree of confidence to represent large-area climate conditions for some areas and periods. Changes in CMIP5 with respect to CMIP3 are substantial in terms of experimental design and modelling capabilities (i.e. model complexity), but significant biases remain. It is critical to understand the implications of all this to agriculture. Crops are sensitive to shortages in water and heat stresses during key periods during their development (i.e. flowering, fruit filling). Therefore, lack of skill in representing seasonal and inter-annual variability is expected to produce a significant obstacle to agricultural impact assessment of climate change. Several examples in the literature exist that illustrate this (Baigorria et al., 2007, 2008). The importance of this factor depends on the strength of the climate signal on yields and the variables that drive this signal (Challinor et al., 2009c). In areas where predictions lack enough skill for agricultural modelling, models can be bias-corrected using different methods (see Challinor et al. 2009b; Hawkins et al. 2013b; Reifen and Toumi 2009). Whilst model skill is expected to improve with time (while more research on developing climate models is done and better processing power is achieved), climate model ensembles as well as different methods for calibrating (i.e. pre-processing for input into crop models) climate model data both need to be used, as uncertainties go beyond those derived from emissions scenarios (Hawkins et al., 2013b).

Chapter 5

Parametric uncertainty in GLAM

"De esos laberintos circulares lo salva
una curiosa comprobación, una comprobación
que luego lo abisma en otros laberintos más
inextricables y heterogéneos"
J. L. Borges

5.1 Summary

The General Large-Area Model for annual crops (GLAM) was used to develop a perturbed parameter ensemble and quantify the sensitivity in Indian historical (1966-1993) groundnut simulated yield, harvest index, leaf area index, and biomass to parameter perturbations (Objective 2, Sect. 1.6). GLAM reproduced observed historical crop yields, with location-specific Root Mean Square Error ($RMSE$) values below 30 % of mean yields and 50 % of standard deviations across the majority of India. The spatial correlation coefficient of mean yields was above 0.8 in all simulations (maximum r =0.98, p <0.001). Standard deviation was much less accurately simulated, with all ensemble members showing a spatial correlation coefficient below 0.5 (maximum r =0.45, p <0.001). An analysis of uncertainties in processes, simulated quantities and parameters showed that: (1) the uncertainties in simulated yields (i.e. variation in simulated yields across parameter sets) varied spatio-temporally, (2) water stress dominated across the region, (3) biomass accumulation and biomass-partitioning parameters were the most important parameters for

yield uncertainty, and (4) by contrast, soil parameters were the least influential on crop yields, yet are important for uncertainties in soil water dynamics. Measured by the coefficient of variation (CV), overall, mean simulated yields ($CV < 15$ %) and mean total crop biomass (CV between 15 – 30 %) were well constrained (i.e. low uncertainty). Their inter-annual variability, however, depicted a more uncertain outcome (CV between 5 and 30 % for yields and between 25 and 50 % for biomass). Significantly larger variation was found across simulations for other model prognostic variables such as leaf area index, radiation use efficiency and the harvest index. Two main aspects ought to be improved in order to reduce uncertainties in GLAM yield simulations: (1) more detailed local information on key model parameters (i.e. transpiration efficiency, harvest index and leaf area growth rate) so as to better constrain regional-scale model parameters; and (2) the improvement of key crop model parameterisations such as leaf area dynamics (currently very basic in GLAM). These two aspects could significantly reduce aggregation error and uncertainties by allowing the constraining of inputs and/or outputs, hence providing means by which parameter, inputs, and accounted processes can be appropriately tied with the scale of analysis.

5.2 Introduction

Model structure and model parameters arise as two of the main sources of uncertainty in crop simulation (Asseng et al., 2013; Challinor and Wheeler, 2008b). Parametric uncertainty arises from the unavailability of information so to assess the needed model outputs that allow the constraining of model parameters. Ideally, exhaustive and multi-location field measurements are required for a thorough calibration of crop model parameters. However, such measurements are often not available to crop modellers, thus resulting in crop model parameterisations that are incomplete and whose errors are uncertain (Angulo et al., 2013a; Challinor et al., 2009b). For example, soil moisture, root dynamics, photosynthesis and respiration are not always measured in crop experiments. Specifically for regional-scale models (the focus of this work), observations on other variables than crop yields are rarely (if at all) reported. This means that the crop model has to be calibrated using a single prognostic variable, which can lead to multiple sets of parameters that produce equally-realistic simulations. Parametric uncertainty has been mostly investigated

using regional-scale models, whose parameters are not treated as true and unique genetic coefficients, but are acknowledged to be a representation of the varieties grown over a large area with their associated uncertainty (Iizumi et al., 2009b). Work on parametric uncertainty has shown that such uncertainty could be larger than climate model uncertainty under some situations (Challinor et al., 2005d). Nevertheless, systematic exploration of parametric uncertainty has been studied only for few crop model parameters (Challinor et al., 2005d; Challinor, 2008), or under the assumption that parameter values follow a certain probability distribution (Iizumi et al., 2009b; Tao et al., 2009).

This chapter addresses Objective 2 (see Sect. 1.6) by quantifying crop model parameter uncertainty, as a result of using incomplete observations to constrain the model output. Using GLAM (Sect. 3.5.1) driven by observed data (TS_IMD-GM, TS_CRU-GM and TS_E40-GM, Table 3.1), a number of potential parameter sets were developed (Sect. 5.3.2) and then a subset chosen on the basis of their ability to reproduce observed crop yields (Sect. 5.3.3). Finally, the resulting parameter sets were used to assess the uncertainties in crop model predictions (Sect. 5.4.4). The information provided here contributes to improving crop model uncertainty quantification and allows a further comparison of this uncertainty with that arising from climate models and their outputs (Chapter 4, and Chapter 6), and from the uncertainty in parameterising CO_2 fertilisation effects (Chapter 6).

5.3 Methodology

5.3.1 Assessment of yield-climate relationships

Since in GLAM all non-climatic processes are accounted for using C_{YG}, a very first step before using the model is analysing the weather-yield relationships at the scale at which the model is intended to be used (Challinor et al., 2003; Li et al., 2010). In this study, all model runs were done at 1x1 degree resolution (TS_IMD-GM dataset, Table 3.1). At this resolution, an analysis of crop-climate relationships was performed in order to test the feasibility of using GLAM to capture the short- and long-term response of crop yields to climate.

Using a combination of empirical calculations, agro-climatic indices, weather data and the gridded detrended yield data, the crop-climate relationships were explored for the analysis

TABLE 5.1: Agro-climate indices used to assess the crop-climate relationship.

Parameter	Name	Units
D_{TB}	Number of days where $T > 10°C$ during the growing season	day
D_{TO}	Number of days where $T > 28°C$	day
D_{TX}	Number of days where $T > 50°C$	day
D_{TCRIT}	Number of days where $T_{max} > 34°C$	day
D_{TLIM}	Number of days where $T_{max} > 40°C$	day
CDD_{max}	Maximum number of consecutive dry days during the growing season	day
GDD	Total growing season degree days as calculated using Eq. 3.7 and 3.8, with $T_b = 10°C$, $T_o = 28°C$ and $T_m = 50°C$	°C day
$SRAD_{GS}$	Total sum of solar radiation during the growing season	W m^{-2}
$TMEN_{GS}$	Mean growing season temperature	° C
$RAIN_{GS}$	Total rainfall during the growing season	mm
RD_{GS}	Total number of days with rain during the growing season	day
$SRAD_{S2}$	Total sum of solar radiation during S2 [second semester of the year (Jul-Dec)]	W m^{-2}
$TMEN_{S2}$	Mean temperature during S2	°C
$RAIN_{S2}$	Total rainfall during S2	mm
RD_{S2}	Total number of days with rain during S2	day
$SRAD_{Q3}$	Total sum of solar radiation during Q3 [third quarter of the year (Jul-Sep)]	W m^{-2}
$TMEN_{Q3}$	Mean temperature during Q3	°C
$RAIN_{Q3}$	Total rainfall during Q3	mm
RD_{Q3}	Total number of days with rain during Q3	day
$SRAD_{Q4}$	Total sum of solar radiation during Q4 [fourth quarter of the year (Oct-Dec)]	W m^{-2}
$TMEN_{Q4}$	Mean temperature during Q4	°C
$RAIN_{Q4}$	Total rainfall during Q4	mm
RD_{Q4}	Total number of days with rain during Q4	day

region in all grid cells where both weather and yield data were available. A total of 23 agro-climatic indices were used (Table 5.1) (see e.g. Challinor et al. 2003; Trnka et al. 2011). For each 1x1 grid cell, these indices were calculated for each year when yield data were available (1966–1993). Finally, for each grid cell, the time series of detrended yield was correlated with the time series of each of the indices to produce spatially explicit correlation maps.

5.3.2 Crop model optimisation

In GLAM, crop model parameters are commonly derived by optimising the output of the model (Challinor et al., 2004). Various parameter sets were developed to quantify the uncertainties arising from uncertain parameter values.

Optimisation was carried out separately for each of the groundnut growing zones of Figure 3.2. Grid cells with missing data or with average 1966-1993 area harvested below

0.2 % were discarded, as this ensured that interannual variability in crop yields was less prone to errors in data collection, conversion and transcription. It is worth noting here that the terms *optimisation* and *calibration* are used in a different way (see Sect. 3.2.9 for definitions). Both procedures were here done by minimising the $RMSE$ (Eq. 3.46).

Various optimisation set-ups were tested as described in detail in Appendix B. These led to the conclusion that using a single grid cell per growing zone for optimisation was the most suitable option for the present study, and that a constant C_{YG} value of 1 had to be kept during the optimisation process. Based on the simulations of Appendix B, 19 model parameters out of the 23 tested in Appendix B were chosen to be optimised (see Table B.2). For the remainder of parameters, the values reported by previous GLAM studies were adopted, except for the uptake diffusion coefficient (k_{DIF}), for which the optimal value across all zones was adopted (see Appendix B, Table B.2). A total of 50 independent parameter sets were then developed by randomising the order in which the parameters (Table 5.2) were optimised.

As in the simulations of Appendix B, daily meteorological inputs were TS_CRU-GM for maximum and minimum temperatures, TS_E40-GM for solar radiation, and TS_IMD-GM for daily precipitation. Observed crop yields and irrigated areas were as described in Sect. 3.4.2.1, and soil data were as in Sect. 3.4.3. The Rabi (irrigated winter) season was simulated separately for each gridcell where irrigated area was reported by planting the crop between the 15th of November and 15th of January, defined per growing zone according to Talawar (2004). The optimisation procedure was then carried out as follows:

1. The 19 target model parameters (excluding C_{YG}, Table 5.2) were optimised sequentially following a pre-defined order. Optimisation was done by iteratively testing different values of each parameter within the ranges of values reported in Table 5.2.

2. The procedure in (1) above was repeated 15 times. This ensured that the optimum values of the parameters were stable; that is, the local minimum $RMSE$ was reached.

3. Once the 19 model parameters were optimised, the planting date was determined for each grid cell. For each grid cell, the start of a planting window was varied across reported ranges in the Sacks et al. (2010) dataset (Chapter 3, Sect. 3.4.2.3) so that the $RMSE$ (Eq. 3.46) was minimised for that grid cell. This procedure ensured that

the choice of the planting date did not affect model skill, while ensuring the planting windows were in agreement with observations.

4. C_{YG} values were determined for each grid cell by iteratively running the model with C_{YG} set between 0.01 and 1.0 (in steps of 0.01). The value that minimised the $RMSE$ was chosen as the optimal value.

Steps 1 to 4 were repeated 50 times with different prescribed order of parameters to optimise. This optimisation procedure was expected to give rise to parameter sets that internally compensate values of certain parameters, but that are equally realistic. These parameter sets were further analysed for skill and sub-selected for all final analyses.

5.3.3 Selection of parameter sets and model evaluation

The aim of selecting parameter sets was to both assess the skill of the 50 potential parameter sets (Sect. 5.3.2) and thus be able to select those parameter sets that most ably reproduced observed crop yields across time and space.

A combination of model skill measures was used to select the best parameter sets. For each zone and parameter set, the following 10 skill metrics were calculated:

- The number of negative correlations
- The mean, median and mode of
  - Pearson product-moment correlation coefficient (r, Sect. 3.6.1)
  - $RMSE$
  - $RMSE$ normalised by mean yield ($RMSE_M$)

Despite some degree of redundancy among these 10 skill metrics, their use ensured the most complete coverage of model errors (also see Sect. 3.6.5). The following selection steps were then followed:

1. Parameter sets were ranked (from 1 to 50) according to each of these metrics and the totals for each potential parameter set were calculated. This total rank value had a

TABLE 5.2: GLAM-R2 parameters and values adopted for the simulations of this chapter.

Parameter	Symbol	Range	C2004 value	Value adopted	Units	Reference
Growth and development						
FSWSOW	C_{sow}	0.1-0.9	0.5	0.5		Challinor et al. (2004)
DLDTMX	$(\partial L)/\partial t)_{max}$	0.01-0.1	0.1	OP	day^{-1}	Challinor et al. (2004)
SWF_THRESH	S_{cr}	0.5-1.0	0.7	OP		Challinor et al. (2004)
DLDLAI	$\partial l_v(z=0)/\partial L$	0.5-5.0	1	OP	km cm^{-1} m^{-2}	Challinor et al. (2004)
EFV	V_{EF}	1-2	1	OP	cm day^{-1}	Simmonds and Azam-Ali (1989)
RLVEF	$l_v(z=zef)$	0.18-0.42	0.3	OP	km cm^{-1} m^2	Matthews et al. (1988)
						Wright and Nageswara Rao (1994)
TE	E_T	1.3-4.5	1.4	OP	Pa	Simmonds and Azam-Ali (1989)
TEN_MAX	$E_{TN,max}$	1.5-5	3	OP	g kg^{-1}	Hammer et al. (1995)
						Chapman et al. (1993)
DHDT	$\partial H_I/\partial t$	0.0042-0.0098	0.007	OP	day^{-1}	Challinor et al. (2004)
IEMDAY	t_{em}	3-13	8	8	day	Challinor et al. (2004)
TB	T_b	8-12	10	OP	°C	Challinor et al. (2004)
TO	T_o	28-37	28	OP	°C	Ong (1986), Mohamed (1984)
TM	T_m	40-50	50	OP	°C	Ong (1986), Mohamed (1984)
GCPLFL	t_{TT0}	350-400	375	OP	°C day	Ong (1986), Mohamed (1984)
GCFLPF	t_{TT1}	310-400	320	OP	°C day	Challinor et al. (2004)
GCPFLM	t_{TT2}	200-300	250	OP	°C day	Challinor et al. (2004)
GCLMHA	t_{TT3}	500-750	620	OP	°C day	Challinor et al. (2004)
Evaporation and transpiration						
CRIT_LAI_T	L_{cr}	0.6-1.2	0.7	OP		Challinor et al. (2004)
P_TRANS_MAX	TT_{max}	0.15-0.4	0.3	OP	cm day^{-1}	Azam-Ali (1984)
PT_CONST	α_0	NA	1.26	1.26		Azam-Ali (1984)

Table 5.2: (Continued).

Parameter	Symbol	Range	C2004 value	Value adopted	Units	Reference
VPD_REF	V_{ref}	0.6-1.4	1	OP	kPa	Priestley and Taylor (1972)
ALBEDO	A	0.12-0.28	0.2	OP		Steiner et al. (1991)
SHF_CTE	C_G	0.22-0.51	0.4	OP		Monteith and Unsworth (1990)
EXTC	k	0.2-0.8	0.5	OP		Choudhury et al. (1987)
R_THRESH	P_{cr}	0-1	0.1	0.1	cm	Choudhury et al. (1987)
						Hammer et al. (1995)
UPDIFC	k_{DIF}	0.19-0.3	0.06	OP	$cm^2\ day^{-1}$	Dardanelli et al. (1997)
UPCTE	C_θ	0.3-0.7	0.5	0.5		Dardanelli et al. (1997)
Soil sub-model and miscellaneous						
ZSMAX	z_{max}	NA	210	210	cm	Allen et al. (1998)
NSL	N_{SL}	NA	25	25		Challinor et al. (2004)
D1	C_{d1}	NA	2.96	2.96	day^{-1}	Challinor et al. (2004)
D2	C_{d2}	NA	-2.62	-2.62	day^{-1}	Suleiman (1999)
D3	C_{d3}	0.75-0.95	0.85	0.85	day^{-1}	Suleiman (1999)
RKCTE	K_{ks}	19-74	37	37	$cm\ day^{-1}$	Suleiman and Ritchie (2001)
						Suleiman (1999)
ASWS	θ_s	0-1	θ_{ll}	θ_{ll}		Challinor et al. (2004)
E_DEPTH	z_{ed}	8.4-84	16.8	16.8	cm	Challinor et al. (2004)
VPD_CTE	C_V	0.42-0.98	0.7	OP	kPa	Challinor et al. (2004)
YGP	C_{YG}	0.1-1.0	0.1-1.0	OP		Tanner and Sinclair (1983)
RLL	θ_{ll}	0-1	data	data		Sect. 3.4.3
DLL	θ_{dul}	0-1	data	data		Sect. 3.4.3
SAT	θ_{sat}	0-1	data	data		Sect. 3.4.3

Table 5.2: (Continued).

Parameter	Symbol	Range	C2004 value	Value adopted	Units	Reference
High temperature stress						
TCSLOPE	S_c	0.0-0.3	NA	0.0	°C day^{-1}	Challinor et al. (2005b)
TLSLOPE	S_l	2.0-3.0	NA	2.5	°C day^{-1}	Challinor et al. (2005b)
TCRITMIN	T_{cr}^{min}	34-37	NA	34	°C	Challinor et al. (2005b)
TLINT	T_{ia}	48.8-53.0	NA	53	°C	Challinor et al. (2005b)
PPCRIT	P_{cr}	0.0-1.0	NA	0.6		Challinor et al. (2005b)
FDOFFSET	$offset$	-0.2-0.5	NA	0.3		Challinor et al. (2005b)
FDWIDTH	$width$	3.0-10.0	NA	6.0		Challinor et al. (2005b)
IDURMAX	–	NA	NA	6	day	Challinor et al. (2005b)
IBAMAX	–	NA	NA	6	day	Challinor et al. (2005b)
IAAMAX	–	NA	NA	12	day	Challinor et al. (2005b)
Other stresses						
RSPARE2	F_{SW}	0-1	NA	0.1		Challinor et al. (2009a)
RSPARE1	H_I^{min}	0-0.1	NA	0.1		Challinor et al. (2009a)
TETR1	T_{ter1}	NA	NA	35	°C	Challinor et al. (2009a)
TETR2	T_{ter2}	NA	NA	47	°C	Challinor et al. (2009a)
SWFF_THR	S_{cr}	0.2-0.4	NA	0.2		Challinor et al. (2006)
CO_2 response and SLA-control						
TENFAC	T_{fact}	0-1	NA	NA		Challinor and Wheeler (2008a)
B_TEN_MAX	$E_{TNc,max}$	1.5-5.0	NA	NA	g kg^{-1}	Challinor and Wheeler (2008a)
B_TE	E_{Tc}	1.3-4.5	NA	NA	Pa	Challinor and Wheeler (2008a)
NDSLA	N_D	1-10	NA	1	day	Challinor and Wheeler (2008a)
SLA_INI	SLA_{max}	250-300	NA	300	g cm^{-2}	Banterng et al. (2003)

Notes: **bold** letters indicate parameters that were optimised in the first test run of Appendix B (a total of 24, including the C_{YG}).
C2004 = Challinor et al. (2004).

minimum possible value of 10 when a parameter set was the best for all metrics, and a maximum value of 500 (50 parameter sets * 10 metrics) when a parameter set was the worst for all metrics. The single best parameter set (i.e. that having the lowest total) was then selected as a reference. Although the use of a single parameter set may increase the risk of over-tuning the model, this was considered to have little or no effect, given that the objective of this procedure is to identify parameter with varied, yet sufficiently high skill.

2. Using the reference parameter set, a Kolmogorov-Smirnov non-parametric test was performed in order to test whether the distributions of the 10 skill metrics of all parameter sets and the reference one were part of the same distribution. Any parameter set that was not part of the same distribution as the reference one at a level of significance of $p \leq 0.05$ in at least 50 % of the metrics was first discarded.

3. For each zone, then, any parameter set for which the grid cell-wise correlation coefficients of mean or standard deviations of yields were negative was discarded.

4. As a final step, all optimisation runs whose parameter sets were selected in at least 4 out of the 5 groundnut growing zones (80 %) were considered and used for all further analysis.

Using the final selection of parameter sets, probability density functions (PDFs) were calculated for each of the 19 optimised parameters to illustrate the uncertainty in each parameter. The following calculations were performed in order to show the skill of the selected parameter sets:

1. A Taylor diagram (Sect. 3.6.5). The skill of the 50 parameter sets can be summarised in different ways, and potentially, Taylor diagrams could be produced for each grid cell, meaning a total of 195 individual figures would be produced, or a single figure with a very large cloud of points (195 grid cells * 50 parameter sets = 9,750). Because this could complicate interpretation of results, diagrams were produced for two spatial characteristics of crop yields: mean and standard deviation. To do that, the mean and standard deviations of simulated and observed crop yields were calculated on a grid cell basis. Taylor diagram parameters were calculated using these.

2. The correlation coefficient (r) and the $RMSE$ were calculated for each grid cell and parameter set to produce maps of these two metrics across the geographic and parameter space.

Finally, for each model parameter and zone, the variation in the $RMSE$ ($RMSE_V$) was then calculated to measure the effect of the parameter on the model output (Eq. 5.1)

$$RMSE_V = \frac{RMSE_{max} - RMSE_{min}}{RMSE_{min}} * 100 \tag{5.1}$$

5.3.4 Stability of the yield gap parameter (C_{YG})

Testing the temporal stability of C_{YG} is important since such stability supports the use of a temporally-constant C_{YG} in future climate simulations (Chapter 6 and Chapter 8). For each grid cell, the time series of crop yield was split in two halves (1966-1979 and 1980-1993). The C_{YG} was calibrated using one series and then tested in the other. Variations in the C_{YG} values for each grid cell were assessed as a measure of temporal consistency.

5.3.5 Biophysical constraints to crop yields

Using the selected ensemble members, the sensitivity of the crop model simulation to various processes was tested in order to identify those processes more likely to constrain the crop yields. A total of 9 processes were tested: 4 related to drought, 4 related to temperature and the total radiation intercepted. The sensitivity of the crop to seasonal rainfall was tested by performing a fully irrigated run. The sensitivity of the crop to terminal drought stress was tested by switching off the parameterisation described in Sect. 3.5.1.11. The sensitivity to drought stress during flowering was assessed by switching off the parameterisation of Sect. 3.5.1.9. Sensitivity to mean temperature was tested in two ways: first, by allowing T_{eff} in Eq. 3.7 to have a maximum value for each day (Eq. 5.2, a modification temporarily introduced to GLAM's code), and secondly, by modifying the values of T_{max} and T_{min} in the input weather file so that $\bar{T} = T_o$ every day of the simulation (Eq. 5.3). Two tests were performed for mean temperature sensitivity since their effects may differ in cases. Specifically, modifying T_{eff} has a direct impact on thermal time accummulation, whereas changing $\bar{T}$ also has en effect on VPD (see Eq. 3.15).

$$T_{eff} = T_o - T_b \tag{5.2}$$

$$\begin{aligned} T_{max} &= T_o + 0.5 \\ T_{min} &= T_o - 0.5 \\ \bar{T} &= \frac{T_{max}+T_{min}}{2} \end{aligned} \tag{5.3}$$

Sensitivity of photosynthesis to high temperatures was tested by switching off the parameterisation of Sect. 3.5.1.10. Sensitivity to high temperature stress during flowering was tested by switching off the parameterisation of Sect. 3.5.1.8. Finally, the sensitivity of the crop to net absorbed radiation was tested by allowing the crop to intercept 100 % of the downwards net shortwave solar radiation ($A = 0$ in Eq. 3.26).

Some of these changes, however, may not imply an increase in simulated crop yields. For example, more radiation in a drought-prone environment implies more water demand for evapotranspiration and more water stress. Similarly, a shorter growing cycle would result from the modifications introduced by Eq. 5.2 and 5.3, and this would reduce crop yields. In addition, other seasonal stresses could further lower crop yields if certain phases (particularly flowering and pod-filling) change their timing. The importance of all these processes in simulated crop yield and the differences in the importance of the processes across parameter sets is examined using these model runs.

5.4 Results

5.4.1 Observed relationship between climate and crop yield

The relationship between crop yields and prevailing climate conditions is shown in Figure 5.1 for those indices specific to the growing season indicated by the crop calendar of Sect. 3.4.2.3 and in Figure 5.2 for those indices that are based on fixed periods (i.e. quarters or semesters of the year). The strength, significance, location and direction of the correlations between crop yields and climate were all largely dependent on the variable and the region. In general, the strongest signals were found in the western zone (Z2), central

zone (Z3) and the western part of the peninsular zone (Z5). Correlations were generally positive and strong for precipitation (maximum $r = 0.69$, $p \leq 0.001$).

A negative relationship between crop yields and most temperature-related indicators was observed in most parts where the rainfall signal was positive and strong. Particularly strong and negative was also the relationship between crop yield and total growing season solar radiation ($r = -0.65$, $p \leq 0.001$). Extreme temperatures and crop thermal duration were also negatively correlated with crop yields. The majority of areas where most of the groundnut crop is grown seemed to be largely limited by rainfall. A strong signal in solar radiation and temperature was observed across the same areas, indicating that high solar radiation could increase water stress. In other areas, where irrigation was prevalent and the signal of total rainfall on crop yields was weak or absent, the signal of seasonal (June-December) and growing season temperature as well as of the number of days above the critical temperature threshold (T_{crit}) was strong.

5.4.2 Crop model skill

5.4.2.1 Internal model consistency

GLAMs internal consistency has been examined previously (Challinor et al., 2004); however, it was herein revisited given that a number of model parameters (Table 5.2) are different, a bug-fix was done (Sect. 3.5.1.12), and that the SLA-control did not exist until more recently (Challinor and Wheeler, 2008a). End-of-season values for critical model prognostic variables were all within realistic ranges (Figure 5.3). The harvest index (H_I) varied between 0.15 and 0.8 in the rainfed simulations, and between 0.4 and 0.85 in the irrigated simulations (i.e. Rabi season). The most frequent values were between 0.35-0.5 for the rainfed simulations, mostly in agreement with observed values (Rao and Nigam, 2003). In water-stressed simulations, the harvest index was 30-50 % lower than in well-watered ones, which is in agreement with reported values (Ratnakumar et al., 2009; Songsri et al., 2009). Values of H_I were the largest in the southern and central zones, and the lowest in the west and north of India. The harvest index was particularly low in the north of Gujarat, where LAI was low. This agrees with previous studies (Rao and Nigam, 2003).

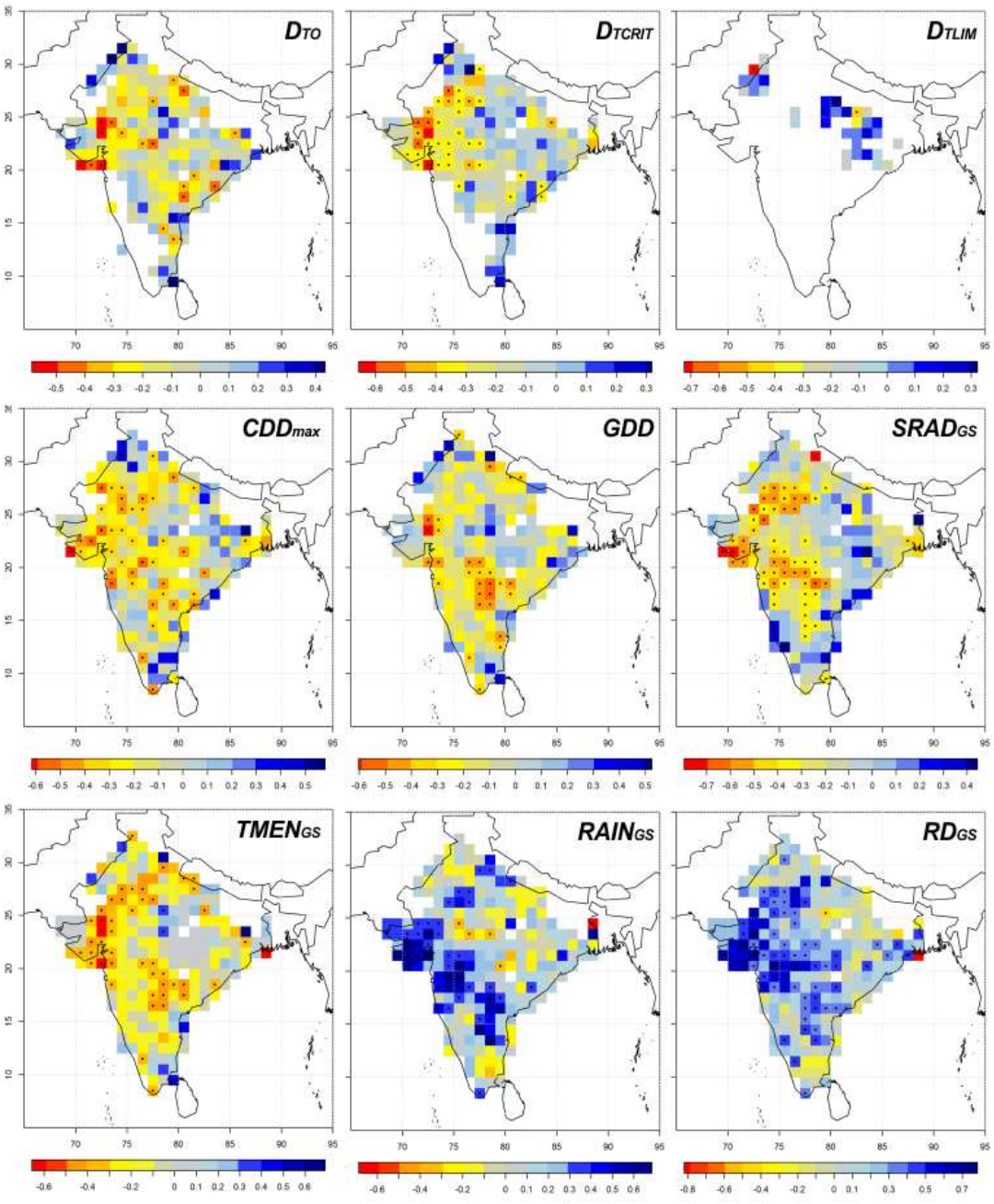

FIGURE 5.1: Correlations between groundnut crop yields and growing season indices of Table 5.1. Black dots indicate statistically significant correlations at $p \leq 0.1$.

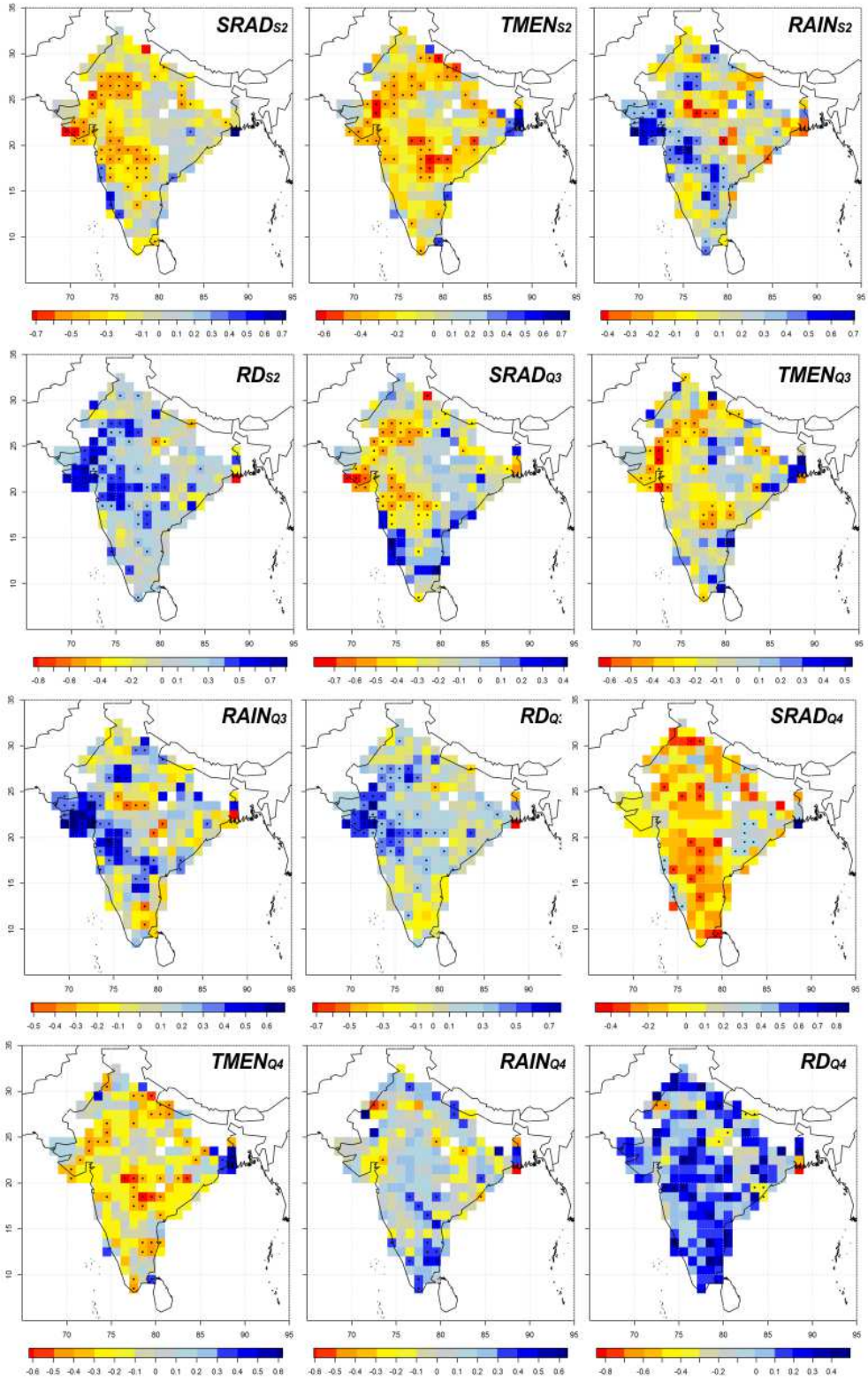

FIGURE 5.2: Correlations between groundnut crop yields and the static season indices of Table 5.1. Black dots indicate statistically significant correlations at $p \leq 0.1$.

Values of LAI were also within realistic ranges (0.1-0.55 for rainfed runs and 0.1-2.5 for irrigated runs), although unrealistically high values (i.e. LAI>10, Hammer et al. 1995) occurred in some simulations (i.e. irrigated simulations with $C_{YG} = 1$) of parameter sets with optimal values of near to the upper bound of the range (see Table 5.2). SLA values in non- C_{YG} limited simulations were between 25 and 75 g cm^{-2} for most simulations, and were considered realistic values in relation to observations (Quilambo, 2000; Venkatarao, 2005). Radiation use efficiency (RUE) showed a maximum value of RUE=2.5 g MJ^{-1} in some of the ensemble members, and the majority of values between 0.5 and 1.5 g MJ^{-1}. All values were in agreement with field measurement for peanut across a number of environments (Kiniry et al., 2005) as well as with reported values for other C3 grain legumes (Tesfaye et al., 2006). Irrigated simulations had lower RUE values given the lower radiation available during the Rabi season, and the limitation to LAI growth imposed by the use of SLA_{max} (Challinor and Wheeler, 2008a). The absence of water stress led to higher values of RUE in all model runs (Figure 5.3).

5.4.2.2 Model skill across parameter sets

The performance of the 50 parameter sets is shown in the form of two Taylor diagrams (Figure 5.4) for both the spatial consistency of the mean yields and of the interannual yield variability (i.e. standard deviation). Each dot in Figure 5.4 represents a single parameter set where all the three metrics have been calculated pair-wise using the time-mean (top diagram in Figure 5.4) and the time-standard deviation (bottom diagram in Figure 5.4) of all grid cells. Blue coloured dots show the 19 parameter sets that were considered to represent crop yields reliably (see Sect. 5.3.3). GLAM represented mean yields with a higher degree of accuracy as compared to interannual variations (Figure 5.4). The spatial correlation coefficient of mean yields was in all parameter sets above 0.8 (maximum $r = 0.98$, $p \leq 0.001$). The representation of standard deviations was much more limited in the model, with all parameter sets showing an spatial correlation coefficient below 0.5 (maximum $r = 0.45$, $p \leq 0.001$). The statistical characteristics of the crop yields were, however, well captured by the crop model, particularly in the selected parameter sets (blue dots that are close to the black continuous standard deviation arc in Figure 5.4).

Figure 5.5 shows some model skill metrics for a high and low performance parameter set (indicated with large filled dots in Figure 5.4). The low performance parameter set showed

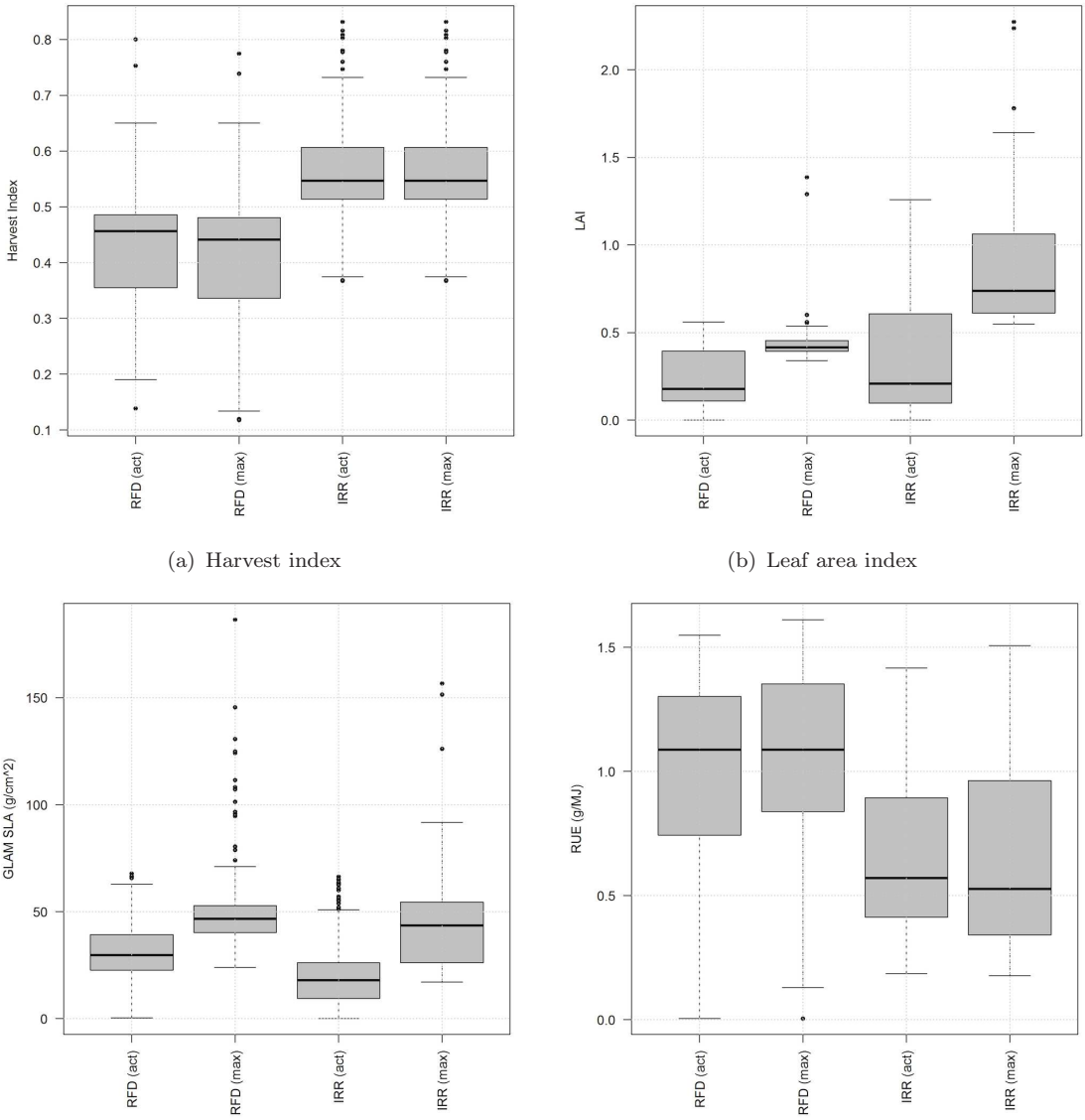

(a) Harvest index

(b) Leaf area index

(c) Specific leaf area

(d) Radiation-use efficiency

FIGURE 5.3: Spatial variation of model prognostic variables. (a) Harvest index, (b) leaf area index, (c) specific leaf area (SLA, as in GLAM), and (d) radiation use efficiency (calculated as the slope of the regression line between biomass and total absorbed radiation). Thick horizontal lines show the median, boxes extend the inter-quartile range and whiskers extend 5 % and 95 % of the distributions. Simulated data correspond to the experiment shown in Figure 5.4 (large blue dot).

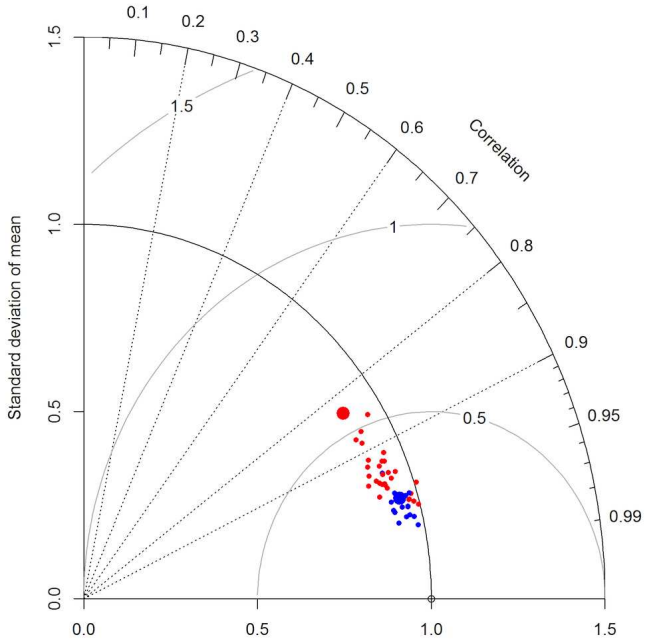

(a) $\bar{Y}$

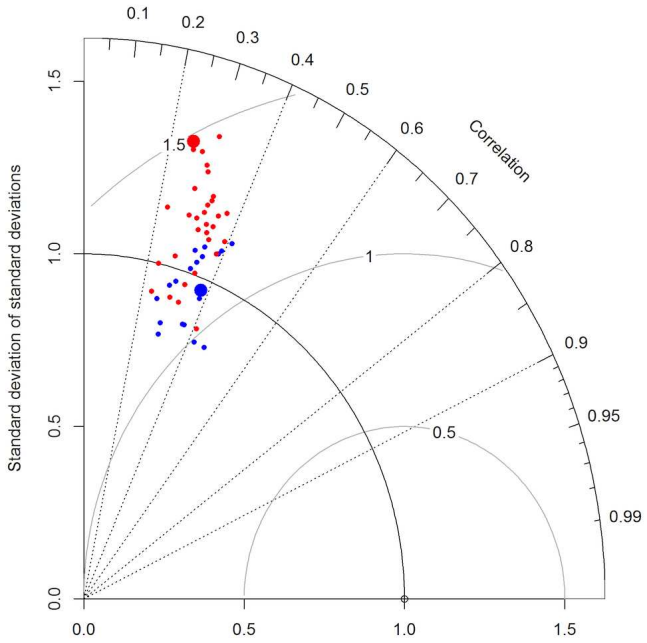

(b) σ_Y

FIGURE 5.4: Taylor diagram (Taylor, 2001) showing the performance of the 50 parameter sets in relation to the spatial variation in mean (a) and standard deviation (b) of yields. Spatial standard deviations are normalised to observed (hence the "perfect" standard deviation is the continuous black arc at 1.0 concentric to the origin). Gray arcs concentric to 1.0 in the x-axis represent the $RMSE$ normalised by the standard deviation of the observations. Blue and red colours indicate selected and not-selected parameter sets (Sect. 5.3.3), respectively. Large filled dots indicate parameter sets shown in detail in Figure 5.5.

one of the lowest correlations ($r = 0.25$ and $r = 0.83$ for standard deviation and mean yields, respectively), a significantly higher spatial standard deviation of the yield variability (about 1.3 times higher), and the largest centred $RMSE$ for both yield mean and variability (1.5 and 0.5, respectively). By contrast, the high performance parameter set showed a near-perfect representation of the standard deviations, a near-perfect correlation for mean yields ($r = 0.97$, $p \leq 0.0001$) and a relatively strong correlation for yield variability ($r = 0.38$, $p \leq 0.0001$). As expected, most of the statistically significant correlations were found across western, northern and central-north India, where the strongest climate signals on crop yields were observed (see Sect. 5.4.1). In particular, the best skill in the crop model was found in the western area of India, as measured by all indicators, in both the high and low-skill parameter sets.

Model skill in the low-skill parameter set was consistently low across southern and eastern India, with $RMSE$ values between 600 and 1000 kg ha^{-1} (between 150-200 % of the mean predicted yield and up to 400 % of the yield standard deviation), low or negative correlations and a trend to overestimate both the yield mean and variability. By contrast, in the high-skill parameter set the $RMSE$ values across the same areas were in the range 200-400 kg ha^{-1} (10-40 % of the mean, up to 100 % of the standard deviation -middle row maps of Figure 5.5), with only very few weak or negative correlations, a near-perfect representation of mean yields and a less strong trend to overestimate the yield variability. The representation of interannual variability was mostly in agreement with observations across western and central India (predicted σ is between 0.8-1.2 with respect to observations), but interannual variation was over-estimated in the southern zone and the east, and under-estimated in the northern India (predicted σ up to 1.5-2 times larger than observed).

Crop model errors were largely consistent across parameter sets (Figures 5.6- 5.7). Most of the parameter sets showed mean yield prediction between +20 and -20 % of observed yields in nearly 80 % of the analysed areas, regardless of the parameter set used. In the remainder of areas, a trend to under-estimate mean crop yields beyond -20 % (nearly up to -50 %) was observed (Figure 5.6).

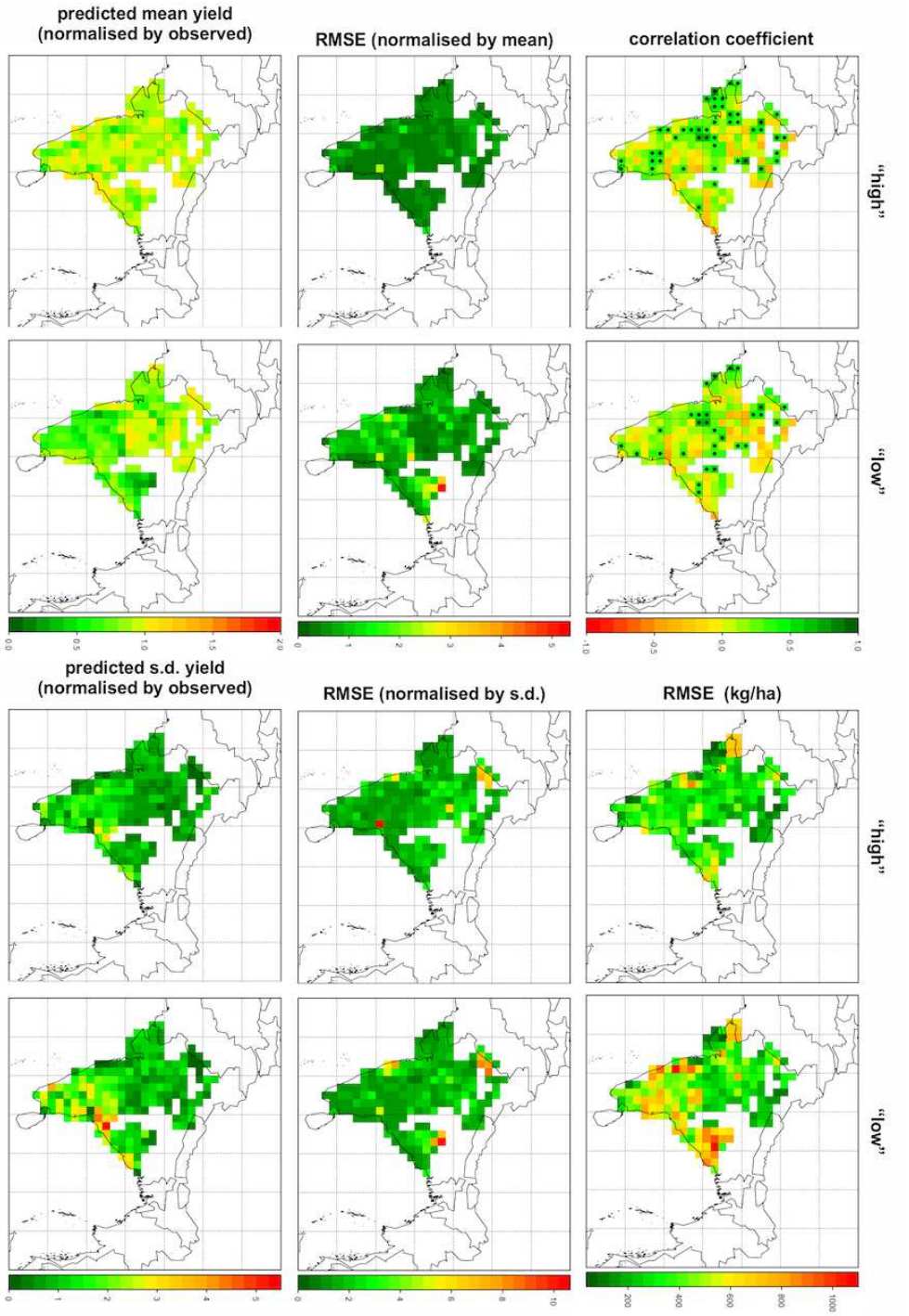

FIGURE 5.5: Spatial distribution of six crop model skill metrics for two selected parameter sets (marked with large filled circles in Figure 5.4). The captions "high" and "low" indicate that the parameter sets are high- and low-skill, respectively (differentiated by blue and red colours in Figure 5.4). Filled dots in the correlation coefficient maps indicate statistically significant correlations ($p \leq 0.1$).

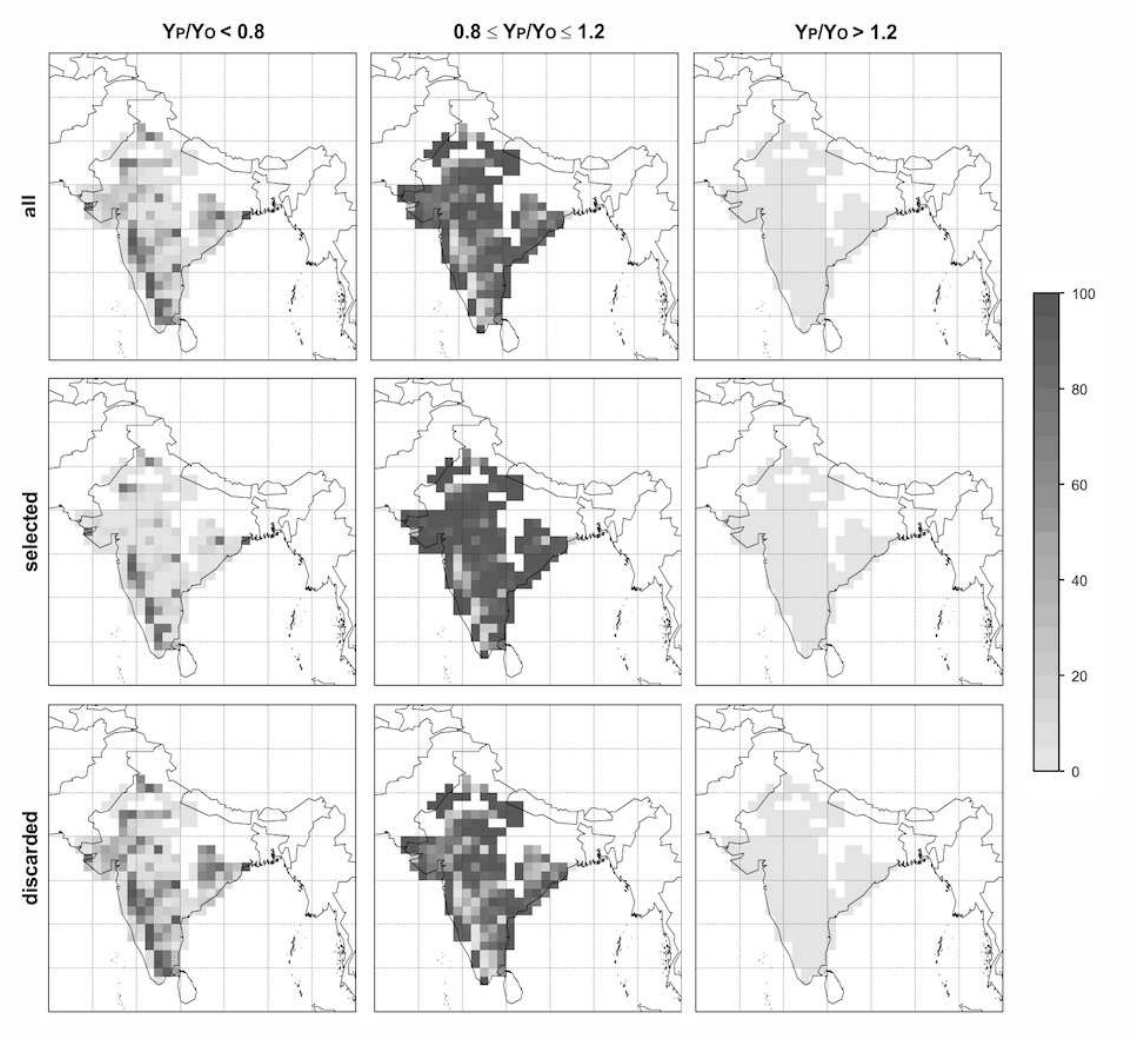

FIGURE 5.6: Percent of parameter sets for which the normalised-by-observed predicted mean yields falls in each of three categories: underestimating ($Y_P/Y_O < 0.8$), normal (Y_P/Y_O between 0.8 and 1.2), and overestimating ($Y_P/Y_O > 1.2$). Parameter sets are classified in three categories: all 50 parameter sets, selected 19 parameter sets and 31 discarded parameter sets (these can be seen in Figure 5.4).

5.4.2.3 Temporal stability of the yield gap parameter

The values of the yield gap parameter varied only slightly from one period to the other, particularly for the most skilful parameter sets. The areas where the most significant changes in C_{YG} occurred are located towards the very north of India. In these areas, C_{YG} increased by 30-40 % between the two periods.

A PDF of the spearman rank correlation (ρ) between the two time periods showed that the relationship is strong and statistically significant (Figure 5.8). In particular, for the

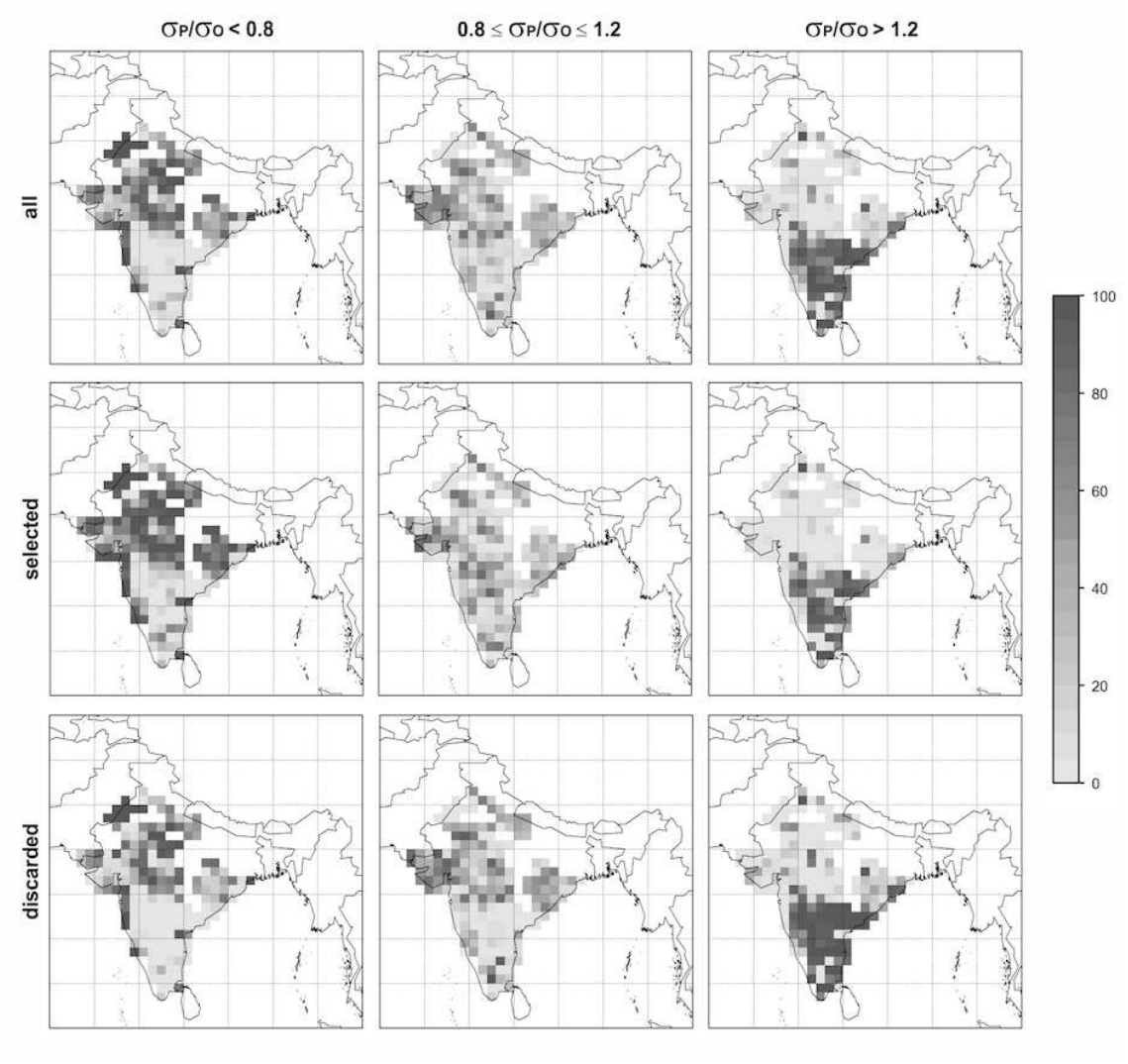

FIGURE 5.7: Percent of parameter sets for which the normalised-by-observed predicted yield standard deviations (σ) falls in each of three categories: underestimating ($\sigma_P/\sigma_O < 0.8$), normal (σ_P/σ_O between 0.8 and 1.2), and overestimating ($\sigma_P/\sigma_O > 1.2$). Parameter sets are classified in three categories: all 50 parameter sets, selected 19 parameter sets and 31 discarded parameter sets (these can be seen in Figure 5.4).

selected parameter sets (blue line in Figure 5.8), the values of ρ were high (0.75-0.9). Differences in the values of the C_{YG} through time can be attributed to changes in the main drivers of crop production through time (i.e. from water- to radiation-limited), noise in the yield time series, the assumption that the technology trend is linear (whereas it could in some cases be non-linear, see e.g. Baigorria et al. 2010), the fact that this area is largely irrigated (Figure 3.5), or to structural errors in the crop model.

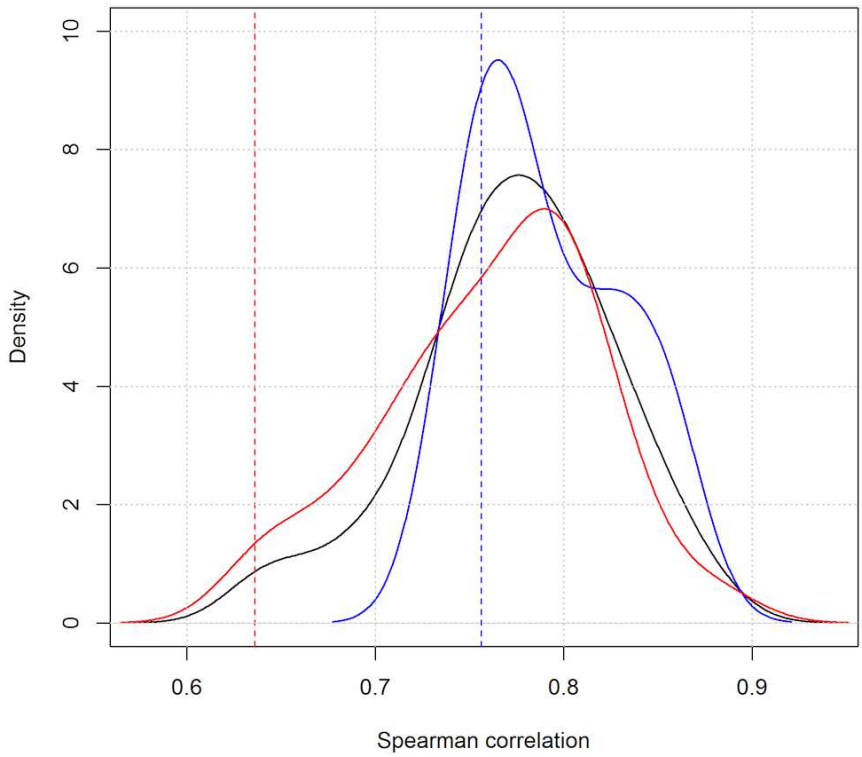

FIGURE 5.8: Probability density function of the Spearman rank correlation between the two C_{YG} values (C_{YG1}: 1966-1979 and C_{YG2}: 1980-1993) for all parameter sets ($n = 50$, black line), selected parameter sets ($n = 19$, blue line) and discarded parameter sets ($n = 31$, red line). Each PDF curve is calculated using the n parameter sets of each category. For each parameter set a single value of the Spearman correlation (rho, ρ) was computed using 195 pairs of [C_{YG1}, C_{YG2}] values, each corresponding to a grid cell of the analysis domain. Dashed vertical lines show the low (red) and high (blue) parameter sets indicated as large dots in Figure 5.4).

5.4.3 Variation in crop model parameters

Selected parameter sets (i.e. specific combinations of optimal parameters) were in most cases different across regions for a given optimisation run. Similarities existed across the different regions for some parameters, whereas notable differences were found for others. The optimal cardinal temperature (T_o) was constant across the geographic space (28 °C). This parameter adopted the same value ($T_o = 28$°C) in more than 95 % of the parameter sets and zones (Figure 5.9). The base temperature (T_b) had greater variability across regions, with the most frequent optimal value in all zones being 12 °C. The most frequent value for maximum cardinal temperature (T_m) was 40 °C. Similarly to cardinal temperatures, thermal time requirements were relatively stable across space. Thermal time requirements were found to be the lowest in the south-eastern zone (Z4) and the

largest in the northern (Z1) and the peninsular (Z5) zones, which agrees with reports of germplasm used across India (Table 5.3).

Model parameters where the largest variations occurred across growing zones were the extraction front velocity (V_{EF}), the root length density per unit leaf area ($\partial l_v/\partial L$), the transpiration efficiency (E_T), and the maximum normalised transpiration efficiency ($E_{TN,max}$) (Figure 5.10). E_T and $E_{TN,max}$ adopt values that span the whole range of possible values, with each zone showing different values. The V_{EF} showed a variety of different values, with the range 1-1.2 cm day^{-1} being the most frequent (occurring 45 %). The C_V (i.e. constant used to calculate VPD in Eq. 3.15) had a large number of different values, with low values (0.4-0.5) being preferred (i.e. in >40 % of the parameter sets) in all growing zones except in central India (Z3), in which the most frequent values were between 0.7 and 0.8.

The thermal time between flowering and pod-filling showed values in the mid- and upper-part of the range (320-330 °C day^{-1}) and the thermal time between planting and flowering showed values in the upper part of the range (385-400 °C day^{-1}). The crop albedo depicted values usually above 0.2, but were low ($A = 0.1$) in nearly 20 % of the cases; and the V_{ref} adopted either high (0.6 kPa) or low (1.4 kPa) values at similar rates. The rate of change in the harvest index adopted in nearly 80 % of the cases values that were either 0.0042 or 0.0098 (with 0.0042 occurring three times more often). The rate of change in LAI showed a very similar behaviour, with adopted values being either 0.01 or 0.1 in more than 90 % of parameter sets and zones, but this time the upper bound being more frequent than the lower bound.

5.4.4 Key processes and uncertainties

5.4.4.1 Uncertainty in model optimal parameter values

Uncertainty in the outcomes of certain processes is undoubtedly rooted in the uncertainty in crop model parameters. Uncertain parameters are those that cannot be sufficiently constrained by the data or the model structure, and hence adopt many different values depending upon the optimisation strategy, the model configuration, and/or the data used. This section focuses on analysing these variations and elucidating their causes. Parameters

TABLE 5.3: Groundnut varieties recommended and grown in India. Taken from Talawar (2004).

Zone	Varieties	Yield (kg ha^{-1})	Main features
I	ICGS-1	2,300	Spanish bunch type suitable for both monsoon and spring seasons
	CSMG 84-1	2,704	Virginia runner, tolerant to thrips, leafminers, pod borer and foliar diseases
	DRG 17	2,095	High yielding Virginia bunch type suitable for rainfed monsoon season
	ICGS 5	2,704	Virginia bunch type, tolerant to drought
	MA 10	1,500	High yielding Virginia runner with variegated kernel
	G 201, Kaushal	1,700	High yielding Spanish bunch type, early maturing
II	Somnath	1,926	Virginia runner, early maturing (120 days)
	GG 20	2,167	Virginia bunch, suited for rainfed monsoon
III	TAG 24	2,000	Short statured Spanish bunch with high harvest index and tolerant to BND
	J(E) 3	1,900	Early variety for rainfed monsoon season
IV	BAU 13	2,556	Bold seeded for export purpose
	BG 3	2,500	Virginia bunch variety with early maturity
	GG 2	3,100	High yielding Spanish bunch type suitable for acid upland soils
V	ICGS 76	1,300	A Virginia bunch variety with tolerance to foliar diseases
	ICGV 86325	3,000	High yielding Virginia bunch type, tolerant to BND, suitable for rainfed conditions
	K 134	1,919	Suitable for rainfed monsoon cultivation with wider adaptability
	VRI 2	1,500	High yielding, early maturing Spanish bunch type
	VRI 3	1,688	Early Spanish bunch type suitable for rainfed
	ICGV 86590	1,785	Multiple disease and pest resistant coupled with high yield
	Tirupathi -2	2,100	Spanish bunch, high peg strength and tolerant to Kalahasti malady (nematode)

were here classified into crop growth (Figure 5.10) and crop development (Figure 5.9). There was a clear trend in both soil and crop development parameters to be far less influential in the simulated yield as compared to the rest of the optimised parameters (Table 5.2), as well as a trend in highly-influential parameters to have fewer possible values (Figure 5.10- 5.9). In general, root dynamics and development parameters tended to have 4 to 5 different values, whereas leaf dynamics, biomass, yield and transpiration parameters have 2-3 different possible values. The only development parameter that had a relatively large effect in all optimisation zones was the optimum development temperature (T_o).

There were substantial similarities between the results across regions (Figure 5.10- 5.9),

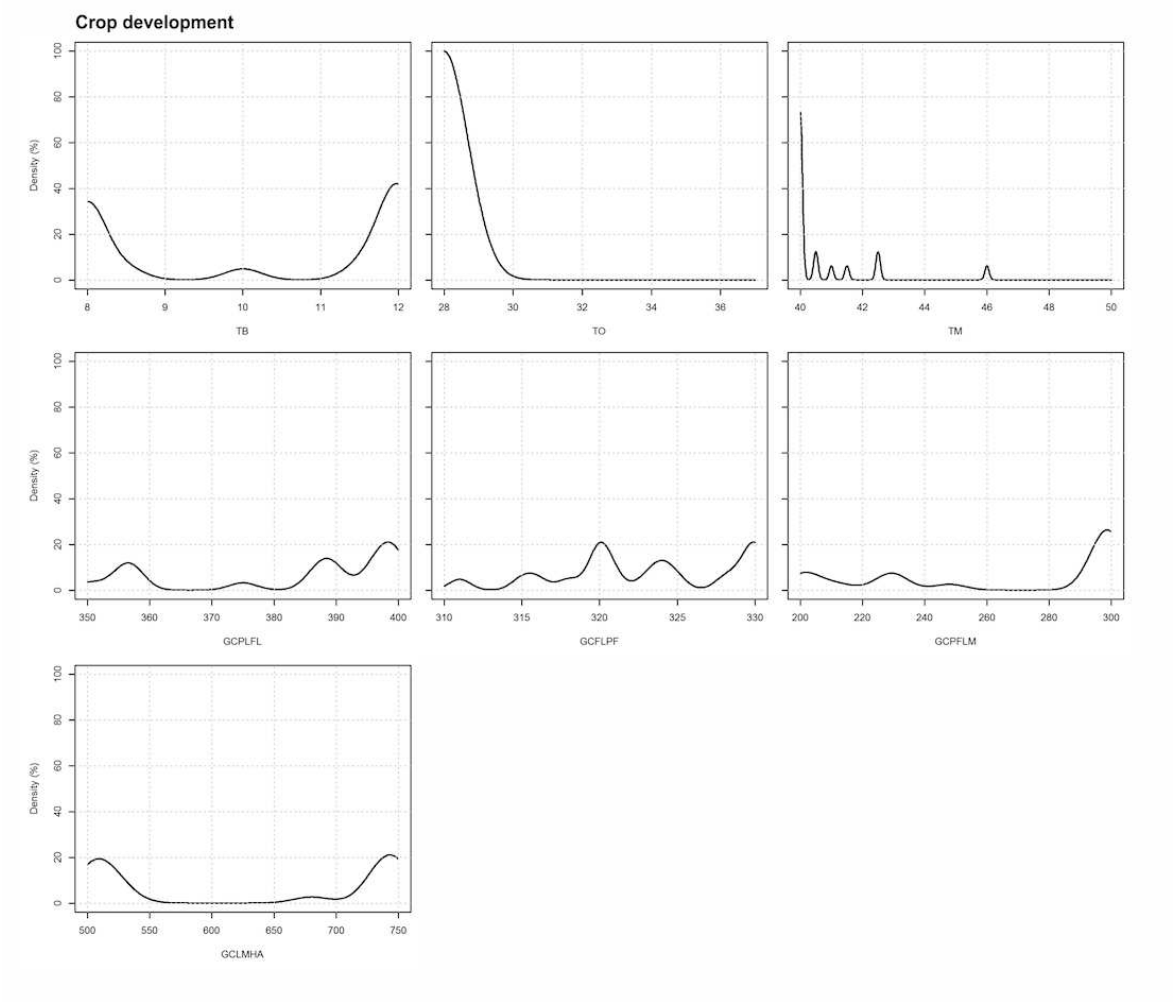

FIGURE 5.9: Probability density functions (PDF) of crop development parameters for zone 2 (western India). Names of parameters as in Table 5.2.

thus the results presented focus mainly on the western zone (Z2) as it is the zone where the model shows the best performance (Figure 5.5). A number of parameters showed significant variations across parameter sets (i.e. those of Table 5.2). These parameters were generally related to root dynamics (V_{EF}, $^{\partial l_v}/_{\partial L}$, C_G) and crop development (T_m, t_{TT0}, t_{TT1}), although similar variation was observed in the reference VPD (V_{ref}) and the crop albedo (A). Such variation in soil-related parameters may be caused by the very limited effect that these parameters had on simulated yield ($RMSE_V < 10$ %, Figure 5.11). Data on soil water dynamics could allow the constraining of these model parameters.

The duration of initial stages (i.e. t_{TT0}, t_{TT1}) is in GLAM important to define the initial total LAI development that is in turn used to calculate LAI-limited transpiration,

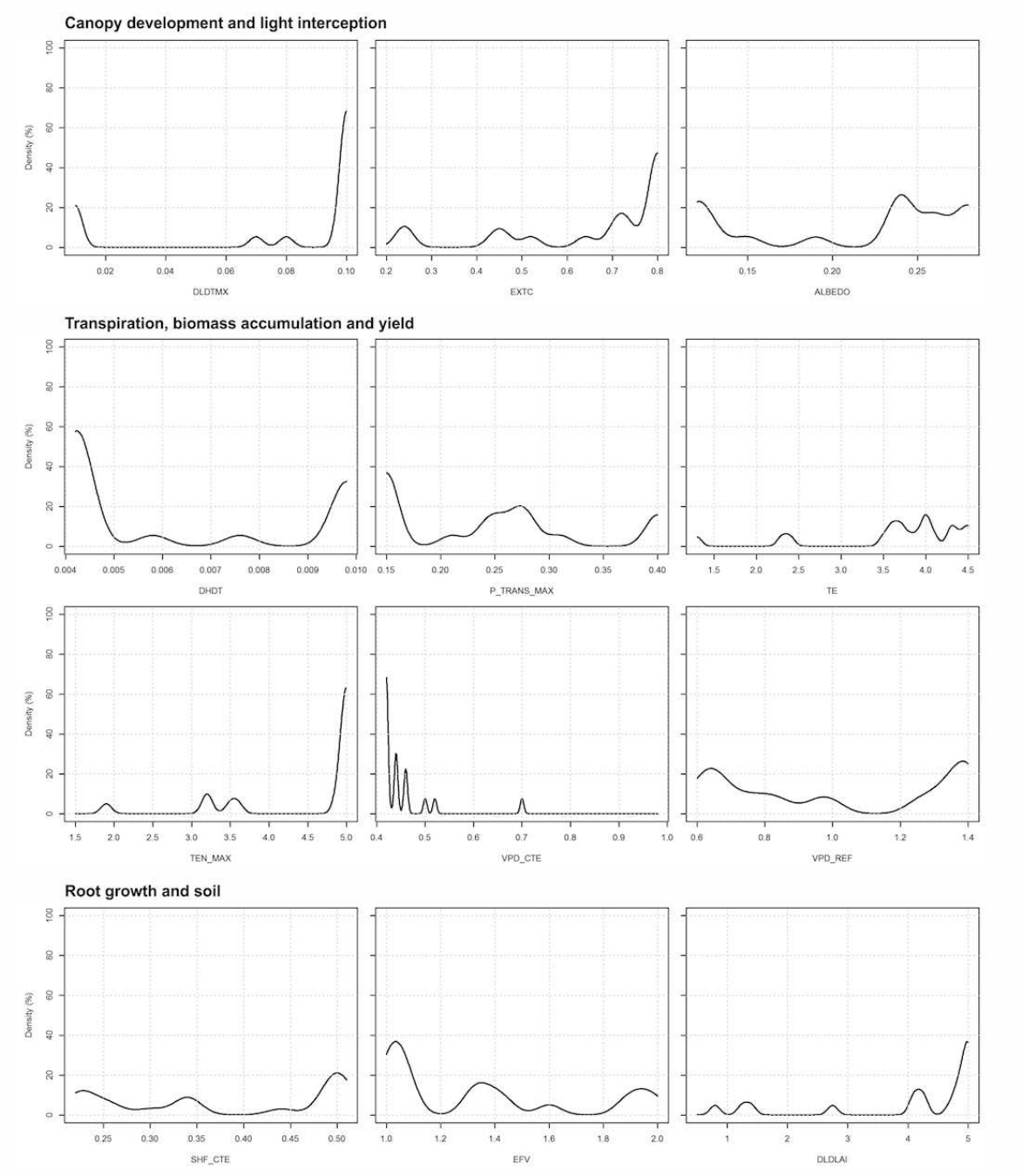

FIGURE 5.10: Probability density functions (PDF) of crop growth parameters for zone 2 (western India). Names of parameters as in Table 5.2.

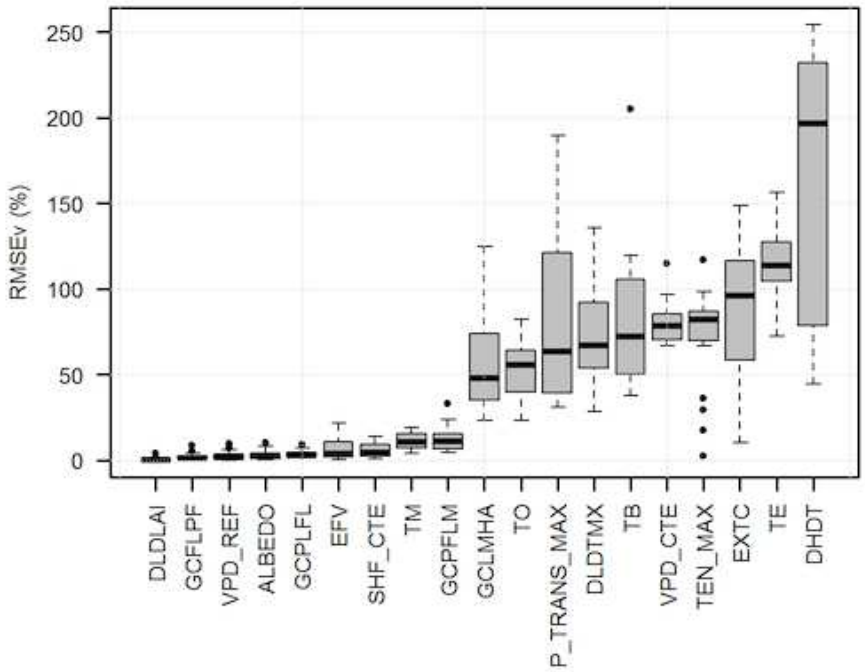

FIGURE 5.11: Variation in the root mean square error due to each of the calibrated parameters. Only zone 2 (western) is shown owing to similarity with others. The spread $RMSE_V$ (Eq. 5.1) values shown represents the values of all 19 selected parameter sets (blue dots in Figure 5.4). Thick horizontal lines show the median, boxes extend the inter-quartile range and whiskers extend 5 % and 95 % of the distributions. Names of parameters as in Table 5.2.

biomass and yield (see Sect. 3.5.1.7). These values were much less constrained in the simulation. However, both parameters seemed to have a rather limited effect on simulated yield ($RMSE_V < 15$ %). Thus, uncertainty in the values of these parameters did not greatly increase uncertainties in yield simulation (Figure 5.11).

Across the 19 selected parameter sets, often 2-3 different values of $^{\partial H_I}/_{\partial t}$, maximum LAI growth rate ($^{\partial L}/_{\partial t}$), and extinction coefficient (k) were found. By contrast, E_T and $E_{TN,max}$ tended to show large variations in their optimal values (Figure 5.10). In all simulations, these five parameters produced significant changes in the $RMSE_V$ (median $RMSE_V$ between 50-60 % Figure 5.11), indicating that uncertainties in their optimal values can significantly increase yield simulation uncertainties. These parameters were probably to be the most significant sources of parametric uncertainty in GLAM (Sect. 5.5.2.1).

5.4.4.2 Uncertainty in crop model outputs

Uncertainty in crop model predicted quantities was measured through the standard deviation normalised by the mean predicted value (i.e. the coefficient of variation, in per cent, CV). Variation in predicted mean yields across parameter sets was in most cases below 10 % (Figure 5.12), except in the Western Ghats, where mean yield variation was between 10 and 20 %. The uncertainty in yield variability was higher, but rarely exceeded 30 % (top-right of Figure 5.12), with the largest variations occurring in the high-variability landscapes of south-western India (CV between 40-50 %), and near the Himalayas (CV between 40-60 %). In contrast, the model's time-mean biomass calculation had a CV >40 % in 90 % of the areas, whereas the time-variance CV values were around 50 % in 60 % of the areas (second row of Figure 5.12). The southern and central zones showed the largest variations, with values of CV sometimes exceeding 80 %.

Model outputs such as RUE, LAI and H_I were highly uncertain as compared to biomass and yield across the parameter sets in most areas (Figure 5.12), with the southern and eastern region presenting the smallest variations (CV between 30-50 %), and the central and northern zone zones showing the largest variations (CV >90 %). Of these three predicted variables, the harvest index was the most uncertain, as it showed a larger number of grid cells with CV values near 100 %. Uncertainty in LAI was also high (third row of Figure 5.12, only Khariff runs are shown), with CV values between 90-100 % in almost the whole central and northern India. Values of RUE were more constrained, but large variations (CV >90 %) were found in north-eastern India in the Khariff runs, and a similar variation was found in the southern peninsula for the Rabi runs (bottom row of Figure 5.12). Variations in RUE, although large, were generally lower than those of LAI.

5.4.4.3 Key drivers of simulated crop yields

Figure 5.13 shows the probability distribution of simulated crop yields for constrained (i.e. "control" simulation, in red) and unconstrained (i.e. modified model simulation, in blue) model simulations (Sect. 5.3.5). Individual year simulations (28 years) of each ensemble member for each grid cell (195 grid cells) were used together (5,460 yield values) to construct individual PDFs. These PDFs were then used to compute a mean PDF (continuous line) and its corresponding standard deviation (shading). The responses were

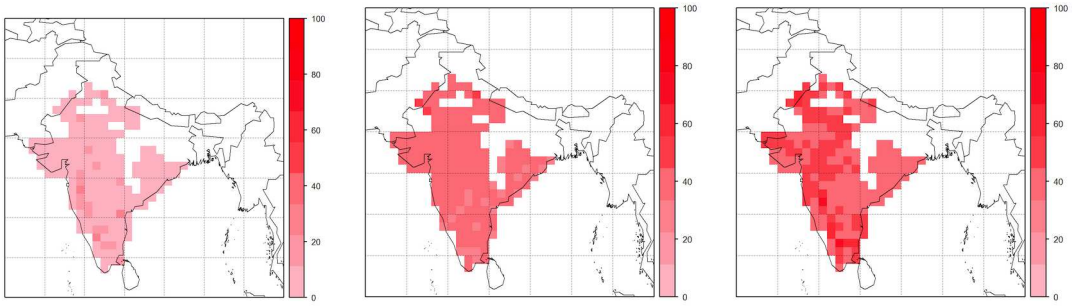

(a) Yield (kg ha^{-1}) (b) Biomass (kg ha^{-1}) (c) Harvest index

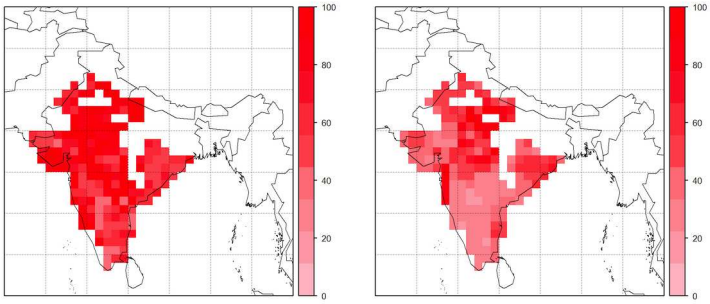

(d) LAI (e) RUE (g MJ^{-1})

FIGURE 5.12: Coefficient of variation (i.e. uncertainty) across parameter sets for four key model prognostic variables (yield, biomass, harvest index and LAI) and the radiation-use-efficiency (RUE, in g MJ^{-1}). Shown in the figure are the values corresponding to the *CV* associated with the 28-year means of each quantity.

generally consistent across ensemble members, except for those related to crop duration (Eq. 5.2 and 5.3). The most important sensitivity was water-stress the growing season, which removal increased crop yields by roughly 60 % in most grid cells (depicted by the shift in the PDF in the top-left panel of Figure 5.13). In a relatively large (about 20 %) number of years and grid cells, drought was a major constraint to crop yields. In particular, terminal drought was major limiting factor: the removal of terminal drought increased yields in almost all years and grid cells being constrained by this factor. The uncertainty in this response is rather low (i.e. a narrow shading), depicting uniformity in the response of the crop to terminal drought across ensemble members. Daily radiation absorbed increases non-water limited crop yields and as expected has no significant impact on water-limited years and locations (transpiration was water-limited rather than energy-limited).

Extreme temperatures and mid-season drought were found to have little effect on simulated crop yields. The lack of effect of extreme temperatures can be attributed to the

likely underestimation of extreme temperatures caused by the use of linearly-interpolated monthly values, and also to the relatively high values that need to be reached in order to produce significant reductions in crop yields. Effects of drought during flowering were negligible because flowering occurs in the middle of the Khariff season, when soil water availability is optimal (Figure 3.3) (Chapman et al., 1993; Kakani, 2001).

Responses to thermal time accumulation and mean temperature limitations were negative for some ensemble members and positive for others. Changes in thermal time accumulation and optimum temperatures had a direct impact on the crop duration, but changes in crop duration also affected the timing of certain cropping season events in some simulations. This caused the difference in the responses across parameter sets. Shorter durations improved drought escape, thus increasing yields, but significantly decreased crop yields in non-water limited environments, due to a reduction in the absolute time for grain filling.

5.5 Discussion

5.5.1 Predictability of Indian groundnut yields

GLAM has been designed with the purpose of simulating the effects of climate alone on crop yields (Challinor et al., 2004), in part because of the difficulty in modelling non-climatic processes at regional scales (Challinor and Wheeler, 2008b; Hansen and Jones, 2000). This means that the degree of predictability of crop yields depends on whether GLAM can ably reproduce crop yields using a weather time series as input, provided that observed relationships between crop yield and climate exist. In such case, therefore, limits to predictability can occur due to problems in the input data, lack of information regarding initial conditions, and lack of skill in the model due to structural problems (i.e. missing processes). Crop-climate relationships and model skill as fundamental aspects of predictability are discussed in detail below.

5.5.1.1 Crop-climate relationships

The strong and positive correlations of crop yields with total seasonal rainfall as well as with the number of rainy days indicated that successful cropping seasons across the

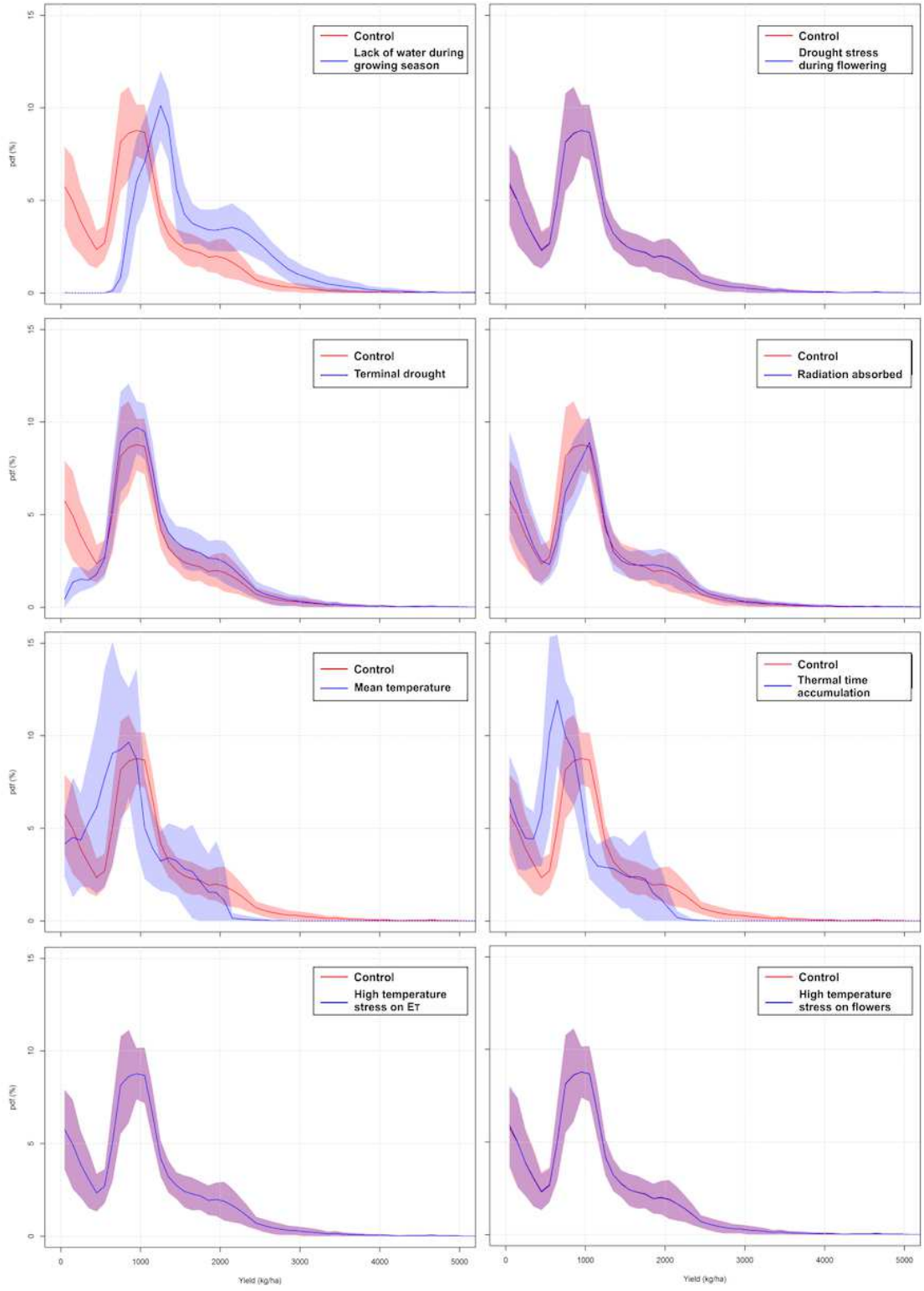

FIGURE 5.13: Changes in the PDF of predicted crop yields as a product of changes to certain constraints in GLAM. Curves are formed for each individual ensemble member using all years and grid cells (195*28 = 5,460 data points) and then used to compute the mean PDF (continuous line) and its corresponding standard deviation (shading). A purple-shaded curve is the product of an overlap of the two distributions, caused because that particular process was not constraining crop yields.

largest producing areas of western and central India largely depend upon both the amount and the distribution of rainfall throughout the growing season. This is also confirmed by the strong and negative correlations between crop yields and the maximum number of consecutive dry days, and by the fact that 83 % of the harvested groundnut in India is grown under rainfed conditions (Singh et al., 2012). Previous studies of groundnut yield and its variability have shown that rainfall amount is critical for groundnut production both at the site-specific (Bhatia et al., 2006, 2009; Singh et al., 2012) and the national and sub-national scale (Challinor et al., 2003, 2004).

Temperature and radiation were found important throughout the whole region, but the strongest relationships between these two variables and crop yields were found in drought-prone environments with little or no irrigation (Figure 3.5). Higher temperatures and higher solar radiation increase transpirative demand and thus water stress, and this, in turn, lowers crop yields. By contrast, in the states of Andhra Pradesh and Orissa, where irrigation is used (Figure 3.5), the relationship between crop yields and solar radiation tends to be positive and stronger than that of rainfall; this suggests that these environments can be potentially more limited by radiation availability (as opposed to water) and that if irrigation is available, increases in solar radiation are beneficial (through increased photosynthetic rates).

Two temperature-related processes were also observed relevant: heat stress and thermal time availability. High temperature stress (i.e. $T_{crit} > 34$ °C), as previously studied in experimental conditions, can cause damage to reproductive organs (Craufurd et al., 2000; Kakani, 2001; Vara Prasad et al., 2003) or affect partitioning to grain (Craufurd et al., 2002; Singh et al., 2012), was also here found to have a negative effect on crop yields, though it was limited to the north-west of India (Figure 5.1- 5.2). Increases in thermal time availability decreased crop yields since temperatures close to the optimal (i.e. more total GDD available per day) lower the crop yields through shorter duration. Longer duration crops, however, tend to be more sensitive to reduced amounts rainfall during the growing season (Figure 3.3), and to the occurrence of terminal drought (Boontang et al., 2010; Challinor et al., 2009a). All these findings support the argument that GLAM can provide reliable results at the IMD grid resolution (1x1 degree), for the cropping system and region under analysis.

5.5.1.2 Ability of GLAM to simulate crop yields

GLAM is a particularly strong model when attempting to represent mean crop yields (Challinor and Wheeler, 2008b). The optimisation method implemented here produced values of parameters and prognostic variables that were in agreement with previous studies on genotypic variation, crop modelling and with national reports on cultivated germplasm (Singh et al., 2008). Among a set of experiments revised in the literature, in a combination of well-watered and water-limited environments and trials, it was observed that the normalised transpiration efficiency varied from 0.6 to about 6.14 g kg^{-1}, with the most frequent values being around 1.5-4 g kg^{-1} (Jyostna Devi et al., 2009, 2010; Krishnamurthy et al., 2007; Puangbut et al., 2009; Sheshshayee et al., 2006; Songsri et al., 2009) (Figure 5.10). In particular, the northern (Z1) and peninsular (Z5) zones show lower values of the transpiration efficiency in a larger number of parameter sets than the other zones, whereas most of the growing zones show values of harvest index in the lower bound of the range (i.e. near 0.0042). This all agrees well with reported genotypic information (Ratnakumar and Vadez, 2011; Singh et al., 2008).

GLAM's simulation of groundnut yields was generally accurate. Not only it reproduced mean yields and (to a lesser extent) interannual yield variability, but it also allowed the identification of total annual rainfall as the main driver of variability (Figure 5.13). As stated above (Sect. 5.4.1), this relationship was also remarkably strong for observed crop yields. Water has also been reported as a critical driver in studies of yield gaps in groundnut across India (Bhatia et al., 2009). Furthermore, the model allowed crop duration (through thermal time) to be identified as an important (yet uncertain) driver of variability (Singh et al., 2012). In a number of cases, as in the observations (Figure 5.2), absorbed radiation was found an important driver either through enhanced water stress in drought-prone environments or through increase in radiation-limited transpiration, biomass and yield in well-watered areas.

Model skill was, however, limited by various factors. GLAM has been previously reported to have some limitations in representing interannual variability in some areas (Challinor et al., 2004, 2005d). Model error in the standard deviation was high (Figure 5.7, also see Sect. 5.4.2.2) and the C_{YG} varied in time for areas across the north of India. In addition, unrealistically high values (>10) of end-of-season LAI were observed in some simulations,

even though the SLA-control was always used (see Sect. 3.5.1.12). This suggests that in these areas the model may not represent fully the processes that in reality cause interannual variability. More specifically, missing processes related to soil nutrient availability (Bhatia et al., 2009; Quilambo, 2000) and the rather simplistic way in which leaf area dynamics and light interception are modelled in GLAM (Sect. 3.5.1.7) could have led to simulation errors in the radiation-limited environments of southern and south-eastern India. In addition, inherent errors in input data (Watson and Challinor, 2013) –particularly in ERA-40 solar radiation, and the underlying assumptions when scaling crop yield data to the model grid (Hansen and Jones, 2000) may have further reduced the simulation skill (Challinor et al., 2005d). These factors have also been shown in previous studies potentially large sources of uncertainty in crop modelling (Adam et al., 2011; Baron et al., 2005; Watson and Challinor, 2013).

Even though it must be noted that no model is capable of producing perfect simulations and that models are tools to produce and extract information (Challinor et al., 2013), improvement of simulation skill is possible within GLAM. For example, Affholder et al. (2003) significantly enhanced the simulation skill of the model STICS (Brisson et al., 2003) by adding two non-climatic processes: Aluminium toxicity and weed competition. Field-scale information on pests can also be used to improve crop yield simulation (Willocquet et al., 2008). Including these and other non-climatic processes in regional-scale simulations remains a topic meriting more research. In this regard, however, data has posed major constraints.

An important parameter for the high skill of GLAM to simulate historical mean yields is the yield gap parameter (C_{YG}). While C_{YG} is intended to be a parameter that accounts for non simulated processes (see Sect. 3.2.9 and 5.3.1), it can to some extent also correct for errors in input data (see e.g. Challinor et al. 2004, 2007), and probably also in model formulation, e.g. as in the inconsistency between LAI growth and biomass accumulation reported by Challinor and Wheeler (2008a). Importantly, because C_{YG} improves model skill, there is a risk that genotypically (i.e. physically) implausible parameter sets can produce skilful simulations of crop yield. In other words, that C_{YG} allows for unrealistic values of a parameter that cannot be linked to the genotypic characteristic of the crop. While the strategy employed in this work to develop a parameter ensemble attempted at minimising the effect of C_{YG} on the optimal values of all other optimised parameters

(see Appendix B for details), a potential caveat of the current study, and perhaps of other studies using GLAM, is the realism of C_{YG}. To this respect, evaluating and, where necessary, improving the physical plausibility of C_{YG} values could be the focus of crop model improvement efforts. To that aim, previous estimations of yield gap (e.g. Bhatia et al. 2009; Licker et al. 2010) could be used to constrain the range of C_{YG} for each grid cell, or as independent sources of data for evaluating calibrated C_{YG} values. Additionally, secondary field data on the prevalence of pests and diseases and the nutritional condition of the crops could also be used to compare their spatial structure with that of C_{YG}, or be integrated into GLAM to develop simple, yet robust, parameterisations on aspects that are currently not considered in the model. More broadly, data on non modelled-processes can be of use for other models where similar quantities are used to scale down potential yields to farmers yields, e.g. the Jones et al. (2003) model uses a parameter called the Soil Fertility Factor (SLPF).

Additional improvements could be sought in GLAM. Possible avenues for such improvements could involve a more appropriate parameterisation of SLA (i.e. response of SLA to temperature, drought), in addition to a better parameterisation of biomass partitioning (e.g. accounting for partitioning to leaves, stems, roots and grains), and the use of end-of-day adjustments to LAI growth in order to reduce over-estimation of LAI and accumulated biomass (Banterng et al., 2003; Hunt and Pararajasingham, 1995; Steduto et al., 2009). These possible improvements will likely lead to improved predictability at the regional scale using GLAM, in a similar way as have done previous improvements to climatic-related processes (Challinor and Wheeler, 2008b; Challinor et al., 2005b, 2006, 2009a).

5.5.2 Uncertainties in regional-scale simulations

5.5.2.1 Optimal parameter values

The different combinations of optimal parameters that produced the final set of 19 selected parameter sets were all considered equally-plausible. The values of the parameters depended partly on the optimisation procedure, the values of other model parameters, and GLAM structure (Sect. 3.5.1.1). Parameters influenced the GLAM's simulated yield

in a way that was largely dependent upon the use of the parameter in the model simulation. For instance, soil sub-model and development parameters tended to have little effect on yield, and the contrary happened with partitioning, biomass and leaf-area parameters (Figure 5.11).

GLAM's yield simulation was found highly sensitive to the choices of: maximum ($E_{TN,max}$) and normalised transpiration efficiency (E_T), the harvest index ($\partial H_I/\partial t$), the rate of growth of leaf area ($\partial L/\partial t$), and the light extinction coefficient (k). These are the parameters whose variations can substantially increase the yield uncertainties (Challinor et al., 2005d). However, some of these parameters were constrained by the model structure. There were certain combinations between parameters that were not observed in any region or parameter set. The physiological links between these traits thus appeared naturally as the model was optimised to reproduce observations, as a product of the model structure.

The clearest of these was the link between leaf production, water use and partitioning: a high rate of leaf area production was linked with either low E_T or $\partial H_I/\partial t$, but never both at the same time. Transpiration efficiency is negatively correlated with the specific leaf area (SLA, ratio of leaf weight to leaf area, in g cm^{-2}); hence, if the rate of leaf growth is high, in order to maintain a given SLA, the biomass accumulation (either via water-use-efficiency or the harvest index) has to remain low (Basu and Nautiyal, 2004; Lal et al., 2006; Rao and Nigam, 2003). By contrast, with low values of leaf area formation, high values of $\partial H_I/\partial t$ or E_T occurred simultaneously in some parameter sets. From the data of Rao and Wright (1994), further presented by Rao and Nigam (2003) it seems that there is no strong evidence to think that the E_T and $\partial H_I/\partial t$ are physiologically linked or mutually exclusive. Combinations of extremes of both traits are less likely to exist among genotypes, with the most frequent combination of traits being a low E_T and high $\partial H_I/\partial t$, or a high E_T with low $\partial H_I/\partial t$ (Basu and Nautiyal, 2004; Boote, 2004; Krishnamurthy et al., 2007; Lal et al., 2006; Nigam et al., 2001).

In spite of GLAM being capable of reproducing all key physiological mechanisms of the crop, the probability distributions presented in Figures 5.10 and 5.9 did not show a physically plausible behaviour. Previous studies where parametric uncertainty has been investigated have demonstrated that crop model parameters can be constrained by clear, single peaked posterior distributions (e.g. Gouache et al. 2013; Iizumi et al. 2009b). The PDFs of this work were, however, not well constrained. Such behaviour could be attributed to

three major factors. Firstly, structural errors in the crop model can lead to physically implausible simulations. While complete physical plausibility in a crop model can only be achieved if both energy and carbon balances are fully considered and closed, such level of detail is difficult, if at all possible, to achieve given inherent limitations to understanding of plant processes and available data (Challinor et al., 2004; Lizaso et al., 2011). There is no evidence, to the knowledge of the author, that GLAM crop simulations are internally inconsistent or unrealistic (see e.g. Challinor et al. 2004; Li 2008; Nicklin 2013). Another potential factor that could have lead to the unexpected parameter behaviour is poorly defined parameter ranges. In this study, the majority of GLAM parameters have been defined on the basis of experimental studies and/or data, exception being made for the rate of leaf area growth ($\partial L/\partial t_{max}$) and to some extent also the harvest index ($\partial H_I/\partial t$). Poorly defined ranges could have led to failure in capturing the true highest likelihood regions for these parameters. Finally, perhaps the main factor contributing to the behaviour in the PDFs is the correlation between parameters. Previous studies have suggested that reducing the parameter space to the maximum extent possible is necessary if the aim is to determine the probability distributions of the model parameters (Beven and Binley, 1992; Freer et al., 1996; Iizumi et al., 2009b). Because of the undesirable effects observed herein, in future studies, it is suggested that the parameter space be reduced by first analysing the correlations between pairs of parameters. Similarly, parameters with broad ranges for which literature is scarce such as the harvest index and the leaf area growth rate could be further constrained during optimisation using simple rules such as the use of observed parameter ranges (Challinor et al., 2004). These ranges could be based on available field sampling for varietal characteristics to determine the most frequent traits in farmers' fields.

5.5.2.2 Simulated outputs

Uncertainty in simulated yield is the direct product of uncertain parameter values (Figure 5.12 and Figure 5.14). The range of optimal values for the model parameters of interest (Table 5.2) produced crop yield simulations that were realistic, yet involved a degree of uncertainty (Figure 5.12). Such uncertainty also reflected on the varied responses of the simulated crop to different biophysical constraints (Sect. 5.4.4.3).

In general, crop yield was the least uncertain quantity of all model outputs (Figure 5.12). The method and results presented in the present study have shown that achieving a parameter ensemble is possible in regional-scale simulations. The perturbed parameter simulations of Challinor et al. (2005d), and the probabilistic hindcasts of Iizumi et al. (2009b) and Tao et al. (2009) further support these findings, and illustrate common ranges of uncertainty as caused by uncertain parameters. Although these studies do not show other model outputs than yield, it is highly likely that, as shown in this study, end-of-season values of biomass, LAI, RUE, among others, have larger uncertainties than the crop yield. This is often the case in present-day simulations because simulated yields are constrained so that they reproduce observed quantities. Interannual variability and individual individual-year predictions depicted a more uncertain outcome than time-mean yields (Figure 5.12). The strongest responses of the simulated crop yields were those related to water availability during the growth cycle (particularly during grain filling) and mean temperatures. Therefore, it is expected that transpiration, LAI and grain filling duration parameters would play the most important role in the extent to which simulated yields vary due to uncertain parameter values.

As uncertainties in yield are primarily rooted in biomass production and partitioning parameters, uncertainties in other model outputs may be primarily affected by other parameters. Uncertainties in predicted LAI and H_I can be attributed to the different possible values that the $\partial H_I/\partial t$ and the $(\partial L/\partial t)_{max}$ can adopt (Sect. 5.4.4.1), as well as directly to the value of SLA_{max}. End-of-season values of LAI are also influenced by two model parameters: the $(\partial L/\partial t)_{max}$ and the C_{YG}. However, LAI growth is also affected by water stress (see Eq. 3.9), meaning that transpiration-related parameters and soil hydrologic properties also play a role in accurate LAI prediction. This particular result regarding LAI is in agreement with Jamieson et al. (1998) who found that different calibrated crop models could produce realistic crop yield simulations with significantly different behaviours in leaf area dynamics. This was also related to the fact that the region is predominantly water-limited (Sect. 5.4.4.3) and so the SLA-control played an important role in defining the optimal values of LAI growth rate, transpiration efficiencies and the harvest index; thus increasing the uncertainty in the simulated crops response. RUE was less uncertain (Figure 5.12), partly due to the more limited variations in radiation absorbed caused by the crop being more limited by water than by available radiation, and to the lower uncertainty in crop albedo as compared to other growth parameters.

5.5.2.3 The importance of parametric uncertainty

Parameter uncertainty in regional-scale crop simulations, similar to regional and/or global climate model simulations, was found an important aspect of crop yield prediction, and is a relevant topic for climate change impact assessment (also see Challinor et al. 2009b). While climate simulations remain only available at coarse resolution (Taylor et al., 2012), parameter uncertainty and scaling issues will remain a topic of central debate for impact assessment. In this study, the construction of a parameter ensemble allowed to better capture variability, mainly through the ensemble mean and its variance (Figure 5.14). Moreover, the parameter sets developed here (Figure 5.14) produced comparable results to those of Iizumi et al. (2009b, 2011), and of Tao et al. (2009) (see Sect. 2.3.3), who also explored parameter uncertainties. These uncertainties led to a better quantification of uncertainty in the simulated outputs of the crop model and in the responses to climate variations, which constituted an advance over previous work (see e.g. Challinor et al. 2005d).

The parameter values and probability distributions found in this study (Figure 5.10- 5.9) showed that probability distributions of optimal values are not necessarily normal (Angulo et al., 2013a) and that sampling of parametric uncertainties for regional-scale models may require more than simple parameter perturbations (Challinor et al., 2005d). In varying parameter values in an attempt to quantify uncertainties, it is important to produce parameter perturbations that are consistent both with the model structure and the genotypic characteristics of the species (e.g. Challinor et al. 2009a and Ruane et al. 2013). This ensures that the perturbed values used are part of the real probability distribution of the parameter being perturbed, and can be as realistic as those originally used in the model. Uncertainty in parameter values was also a reflection of the available information used to define the ranges over which the parameters were varied (Table 5.2). More restricted (broader) parameter ranges may have resulted in lower (larger) crop yield uncertainties.

Parameter uncertainty arises as a topic to be considered for crop simulation studies and particularly for those involving future climate scenarios (i.e. under which processes dominating crop responses may change). More field information on the geographic variation of transpiration efficiency, leaf area growth rate and the harvest index as well as a better crop model parameterisation of leaf area dynamics (Challinor and Wheeler, 2008b) could

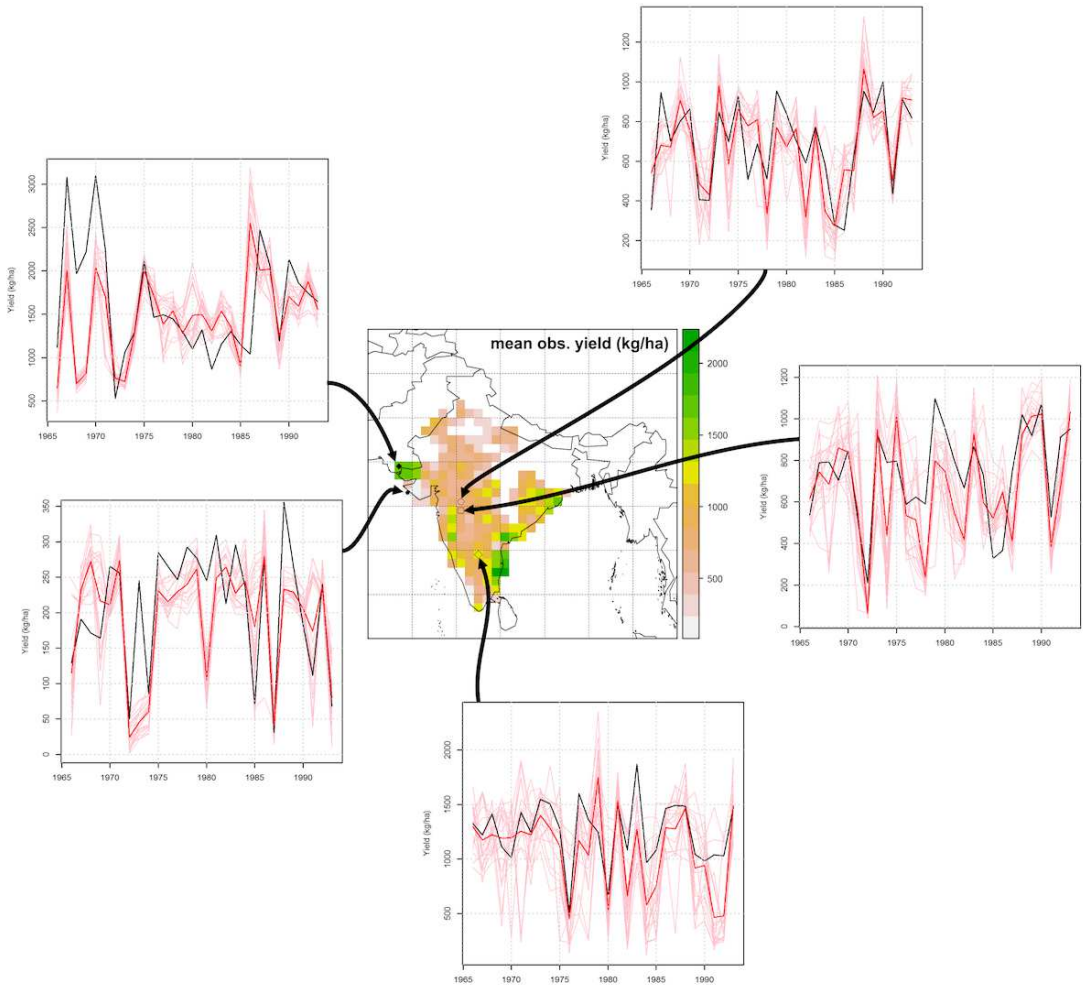

FIGURE 5.14: Historical 1966-1993 ensemble model predictions for selected grid cells across the analysis domain. The thick black line is the observed time series, thick red line is the ensemble mean and light red lines are individual ensemble members. Shown in the middle map are the mean 1966-1993 crop yields.

improve the model optimisation. This would allow uncertain parameters to be better constrained, hence resulting in a reduction of the uncertainties reported in this study and of the total uncertainty of future projections. As discussed previously in this study and by other authors (Ruane et al., 2013; White et al., 2011b), this information is critical for a better understanding of climate impacts on food crops, as is the comparison of different sources of uncertainty. Subsequent chapters will compare parametric uncertainty with that of climate model simulations and from parameterising CO_2 response (Chapter 6).

Chapter 6

Using GLAM to project crop yields

"Il matto lo riconosci subito.
E' uno stupido che non conosce trucchi
Tutto per lui dimostra tutto.
Umberto Eco

6.1 Summary

A large ensemble of GLAM model simulations was used to (1) assess the skill of CMIP5-based crop yield hincasts (Objective 3, Sect. 1.6), and to (2) project the changes in yields and quantify the associated uncertainties (Objective 4-A). Under the future climate scenarios explored here, robust positive climate change impacts were found in 3 out of 5 groundnut growing regions. From the remainder of regions, one presented robust negative impacts and in the other uncertainties precluded a robust statement being made about climate change impacts. Robust positive effects in two regions (west and north-west, states of Rajasthan, Punjab and Gujarat) were observed due to a substantial increase in seasonal rainfall, a lower frequency of occurrence of terminal drought and its indirect effect on cropping season length. Despite greater uncertainties, yield gains were also robust in the south-eastern region (states of Orissa and north of Andhra Pradesh) where water stress was also observed to decrease. In central India (Madhya Pradesh and Maharashtra)

robust yield loss projections (up to 70 % likely) primarily driven by decreased crop duration and reductions in solar radiation were found. Finally, high uncertainty arose from weather input types that produced increased heat stress in the south (Andhra Pradesh and Tamil Nadu). GCM structure and choice of GCM bias correction method were the most significant sources of uncertainty in the simulations presented, whereas CO_2 response and sowing date the least significant uncertainty sources. The analyses presented imply that drought tolerance will remain a significant abiotic constraint for Indian groundnut. Evidence from previous studies, however, suggests that it is likely that heat stress will play a more important role toward the end of the 21^{st} century, and hence heat tolerance could be a key trait to target in a second or latter breeding cycle (Challinor et al., 2007; Singh et al., 2012). A more thorough assessment of potential adaptation gains from the use of improved germplasm, however, is needed in order to disentangle the need for genotypic adaptation and the physiological traits whose improvement is more effective in abating negative or capitalising positive effects of climate change.

6.2 Introduction

Groundnut is a tropical grain legume widely grown across India, generally by smallholders under marginal conditions. Groundnut is produced mainly as a cash crop, with roughly 82 % of groundnut production used for edible oil, 12 % as seed, and 6 % as feed (Mehrotra, 2011). India is the second largest producer (∼6.4 billion tonnes in 2010) after China, and has the largest harvested area (∼6 billion hectares in 2010) (FAO, 2012). Despite that, Indian groundnut crop yields remain low (17 % below average in 2010) (FAO, 2012; Mehrotra, 2011). Low yields are the consequence of a cropping system that is heavily reliant on monsoon precipitation and hence highly sensitive to interannual climate variability (Challinor et al., 2003; Singh et al., 2012). Under climate change scenarios of increased temperatures and changing patterns of precipitation (Joshi et al., 2011; Sillmann et al., 2013), Singh et al. (2012) projected decreases in groundnut crop yields from 6 to 44 % across different regions of India by 2050, and Challinor et al. (2007) projected yield decreases of up to 70 % for rainfed groundnut areas by 2100. In spite of existing impacts estimates and the reported sensitivity of groundnut to climatic variations, a systematic

exploration of the impacts of climate change on groundnut productivity and associated uncertainties has not been carried out to date.

This chapter addresses Objective 3 and 4-A (see Sect. 1.6) by performing the following analyses:

1. An assessment of the effect of using biased and bias-corrected input weather data as inputs to GLAM. Both the skill of the model to simulate baseline crop yields and the uncertainty in projections of climate change impacts were analysed (Sect. 6.4.1).
2. The impacts of projected near-term climate change (i.e. 2030s, RCP4.5) and the driving processes at sub-national- and national-level groundnut productivity were assessed using a large ensemble of crop-climate model simulations (Sect. 6.4.2).
3. The large ensemble of simulations was used to quantify the relative importance of crop and climate uncertainties (Sect. 6.4.4)

Crop simulations were explicitly designed to quantify uncertainties arising from (1) crop model parameters, (2) the parameterised crop's response to increased CO_2 concentrations, (3) uncertainty in climate simulations (both structural and from initial conditions), (4) variability in GLAM-selected planting dates, and (5) the use of different GCM output bias correction (BC) methods. The analyses performed herein contribute to improve understanding of the processes driving crop responses under future scenarios, to quantify the relative importance of crop and climate model uncertainties in regional impacts estimates, and to assess the need for adaptation.

6.3 Methodology

6.3.1 Crop model simulations

The crop model simulations carried out were specifically designed to investigate two different aspects:

1. the skill of the model in the baseline period when driven with raw and bias-corrected GCM output, and

2. the future changes in yields and associated uncertainties.

As in Chapter 5, India was divided into five groundnut growing regions, with parameter sets being independent across regions. In all simulations, the full 19-member parameter ensemble developed in Chapter 5 was used. The simulations of Chapter 5 are hereafter referred to as 'control' simulations. All crop model inputs except the meteorology (see below) were kept the same as in Chapter 5. That is, soil data as in Sect. 3.4.3, planting dates as in the SPD dataset of Sect. 3.4.2.3.

6.3.1.1 Baseline simulations

Baseline yield simulations were done to reproduce historical yields using both raw CMIP5 climate simulations (TS_C5-GM, Sect. 3.4.1.5) and their 3 bias corrected versions (C5-SH, C5-DEL, C5-LOCI, Sect. 3.4.1.6). These simulations were conducted with two objectives: (1) to determine the extent to which the CMIP5 GCM simulations (marked with § in Table 3.4) could be directly used into GLAM as a critical step to improve understanding on the suitability of CMIP5 climate simulations for impacts research (also see Ramirez-Villegas et al. 2013a); and (2) to provide a set of baseline simulations with which future simulations could be compared. A first set of baseline simulations was carried out using the full raw GCM output; the second set used the LOCI-corrected GCM output; and the third set used the full SH-corrected GCM output. Given that the DEL method uses projected changes in monthly climatological means, the baseline runs for DEL-corrected simulations were the control simulations (i.e. driven by observed weather, presented in detail in Chapter 5). Each set of simulations consisted of 195 grid cells, 19 parameter ensemble members and 32 GCMs for the full 28-year baseline period 1966-1993.

For each grid cell, GCM simulation, bias correction method, and parameter set, C_{YG} was calibrated against observed crop yields (Sect. 3.4.2.1) using the perfect correlation MSE ($PMSE$, fully described in Sect. 3.6.4) through the simulation of both Khariff and Rabi seasons. Results of both seasons were combined using a constant irrigation rate that corresponded to the temporal mean of reported irrigation rates (see Sect. 3.4.2.1, Chapter 3). The skill of baseline simulations was assessed using the methods of Sect. 6.3.2.1 and compared with the control simulations of Chapter 5. Table 6.1 shows a summary of the simulations carried out.

TABLE 6.1: Model simulations carried out in this chapter.

ID	Type	Description
B-RAW	Baseline	Un-calibrated GCM output
B-LOCI	Baseline	GCM output with Local Intensity Scaling on precipitation
B-SH	Baseline	GCM output with bias correction to the means
B-DEL	Baseline	Observed weather (also referred to as CONTROL)
P-RAW	Projection	Uncorrected RCP4.5 GCM output
P-LOCI	Projection	GCM output with Local Intensity Scaling on precipitation
P-SH	Projection	GCM output with bias correction to the means
P-DEL	Projection	GCM output with delta method applied to the means

Notes: Projection simulations are those of RCP4.5 for the period 2022-2049. All projection simulations were carried out independently for each of the four CO_2 response parameterisations (shown in Table 3.6), and were simulated for 15 equally-plausible planting dates.

6.3.1.2 Future scenario simulations

Four sets of future yield simulations were carried out in this study, each consisting of 32 GCMs, 19 parameter ensemble members, the 4 CO_2 parameterisations (Table 3.6, Sect. 3.5.1.13), a span of 15 potential planting dates, and 195 grid cells (i.e. a total of 36,480 simulations per grid cell). Future scenario simulations used RCP4.5 (2022-2049) GCM output in both raw and bias corrected form. Simulations were conducted using raw GCM, LOCI-corrected, SH-corrected, and DEL-corrected GCM output (Table 6.1). C_{YG} values for each grid cell were taken from the respective baseline simulation and in the case of DEL-calibrated crop simulations from the control simulations. The monsoon and the winter season were simulated independently in the future scenario runs. In each of the 15 potential planting dates for the monsoon season, automatic planting was used, with the start of window defined by the chosen planting date and a window size of 30 days (see Sect. 3.4.2.3). Planting in the Rabi season (fully irrigated) simulations occurred on prescribed dates. Future scenario crop simulations were used to assess the impact of future climates on groundnut yields as well as the uncertainties arising from CO_2 response, unconstrained crop model parameters, uncertain planting dates, GCM bias correction (both decision and method), and climate model structure and initial conditions.

6.3.2 Data analysis

6.3.2.1 Evaluation of crop model skill

Evaluation of GLAM simulations focused on the evaluation of simulated against observed crop yields in the baseline simulations so as to determine the extent to which different input types than observations, including raw GCM output, can introduce errors in crop yield simulations. Two analyses were conducted:

1. A Taylor diagram see Sect. 3.6.5 to compare simulated standard deviations and mean yields over the analysis domain. The method used follows that described in Sect. 5.3.3.

2. Empirical probability density functions (PDF) of GLAM simulations were drawn using all years and grid cells. These were compared with the control simulations, and with the observations.

6.3.2.2 Quantifying future climate change impacts

The analyses herein presented focused on the impact of future climate on the means and variability of two key crop characteristics: crop yield and duration. In both cases, changes were computed using the relative differences between the future and the baseline (Eq. 6.1)

$$\Delta X = \frac{X_B - X_F}{X_B} * 100 \tag{6.1}$$

where X represents either the mean or the standard deviation of the crop yield or duration time series (i.e. over multiple simulated years), and the symbol Δ is used to indicate a change. The change is expressed as a percentage of the difference between the future (X_F) and the baseline (X_B), with respect to X_B. These calculations were done per grid cell, for each of the GCMs, GCM bias correction methods, parameter ensemble member, CO_2 response parameterisation, and potential sowing date.

In addition, probabilistic changes in crop yields and duration were calculated. In Sect. 6.3.1.2, a total of 145,920 future scenario simulations were performed for each grid cell; these arise

from the combination of 19 parameter sets (Chapter 5), 32 GCM simulations (Table 3.4), 4 CO_2 response parameterisations (Table 3.6), 4 different weather inputs (i.e. DEL, SH, LOCI calibrated and raw GCM output), and 15 potential planting dates. In the baseline, the total number of simulations per grid cell was 2,432 because planting dates and CO_2 response were constrained. Baseline and future scenario simulations were used to calculate the probabilities that crop yields and durations (and their temporal variability) were above and below the respective baseline values by 5 %, 10 % and 20 %. For each grid cell, the probability was calculated as the number of simulations above or below each threshold divided by the total number of simulations.

6.3.2.3 Identification of key processes under future scenarios

Identifying the relevant processes driving crop yield responses under future scenarios is critical for designing appropriate adaptation options (Challinor et al., 2010; Lobell et al., 2013). Thus, processes driving the response of the crop under future scenarios were identified by comparing changes in crop yield and specific model prognostic variables. To achieve this, three-dimensional scatter plots were drawn to illustrate the main drivers of crop yield response. Plots of mean yield change and mean seasonal temperature and total seasonal precipitation change were first drawn, and then colours were used to show a third variable. The third variable was one of the following GLAM's prognostic variables: crop duration (DUR), total absorbed radiation (TRADABS), potential water uptake (PUPTK), frequency of occurrence of terminal drought stress (TDS), extent of heat stress during flowering (HIT), and extent of water stress during flowering (WAT). These plots allowed identifying those variables whose changes were most related with changes in crop yields, and thus helped to disentangle the combined effects of climatic changes on crop productivity.

6.3.2.4 Uncertainty quantification

In modelling the impact of climate change on crop productivity, limitations in the models and/or data employed can lead to uncertainties and lack of predictability (Koehler et al., 2013). Identifying the sources these uncertainties is key in order to improve modelling frameworks and make more informed decisions (Vermeulen et al., 2013). Here, the total

uncertainty in mean yield was decomposed into its different sources using the methods described in Sect. 3.7. In this particular case, the number of sources (n) was $n = 3$: parameter sets, GCMs, and bias correction method, for the baseline; and $n = 5$: the same three as for the baseline, plus CO_2 response and sowing dates, for the future scenarios.

6.4 Results

The crop model simulations of this chapter assessed the effect of future projected climate change on groundnut production over India. Crop model runs were performed for both the Khariff and the Rabi seasons, although 83 % of production is done in the Khariff season (Mehrotra, 2011; Singh et al., 2012). For this reason, in this and the following sub-sections of the chapter, the major focus is on the Khariff season (owing to the large amount of numerical results produced), unless otherwise stated. Results for the Rabi season are also described, although with less detail.

6.4.1 Effects of biased and bias-corrected weather on crop simulations

6.4.1.1 Effect on crop model skill

Taylor diagrams for the spatial consistency of simulated mean and standard deviations for two of the 32 GCM simulations are shown in Figure 6.1 and 6.2, respectively. The skill of the model with biased baseline input weather varied primarily depending on the GCM, bias correction method and, to a lesser extent, also on the parameter set used. Spatial correlation coefficients for mean yields were around 0.95-0.99 for the control, but decreased to 0.8-0.9 when RAW input was used. Standard deviation tended to be overestimated with some of the RAW GCM input. The spatial consistency of yield standard deviation (Figure 6.2) was significantly more affected by GCM bias than that of mean yields, but this largely depended on how accurate was the GCM simulation of historical climate (also see Chapter 4, Figure 4.12). Bias correction methods improved baseline simulation skill. Correlations for LOCI and SH input types were consistently high, with values between 0.9-0.97 in most cases. As most of the interannual yield variability in India is driven by moisture availability, the rainfall error correction implemented by LOCI also represented a significant improvement over the B-RAW simulation skill for all GCMs.

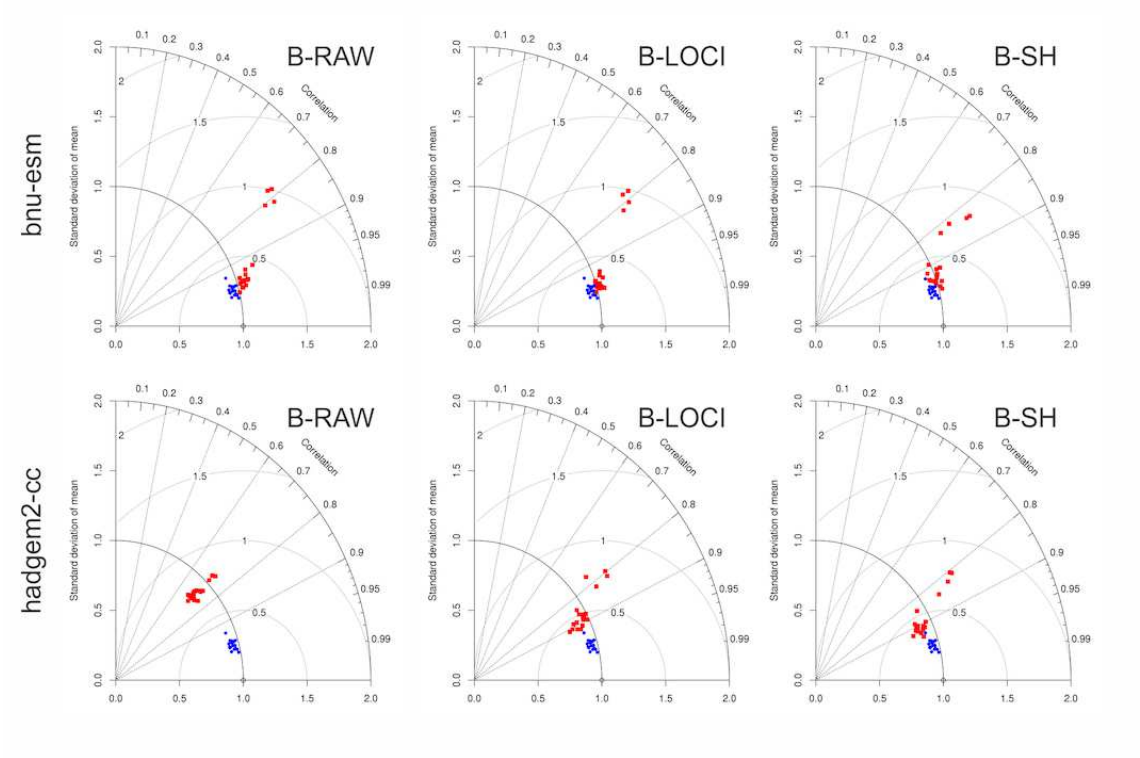

FIGURE 6.1: Taylor diagram showing the performance of the 19 parameter sets in relation to the spatial variation in mean yields for two different GCMs. Blue and red colours indicate control and raw or bias-corrected GCM output simulations (Table 6.1), respectively. Each dot represents a GLAM parameter ensemble member. Spatial standard deviations are normalised to observed, as is the $RMSE$.

The use of biased weather increased the differences in the skill across parameter sets distances among groups of coloured points in Figure 6.1 and 6.2. In particular, there was a group of parameter sets whose skill decreased significantly when used with biased weather. These four parameter sets depicted a very low LAI rate of development $[(\partial L/\partial t)_{max} = 0.01$ day$^{-1}]$, which in conjunction with C_{YG} and biased weather led to insufficient light absorption, biomass and yield accumulation (and hence unrealistically frequent low yields, see bottom row of Figure 6.3). In addition, the general lack of rainfall in the GCM simulations led to more frequent terminal drought stress, thus further shortening the cropping cycle and increasing crop failures (i.e. yields close to zero). For these parameter sets, not only the $RMSE$ is high and the correlation coefficients were low, but the ratio of standard deviations was high, indicating that interannual yield variability was largely overestimated. These four parameter sets were a clear indication of the risks of biasing crop model simulations and increasing uncertainties if insufficiently accurate crop model inputs are used.

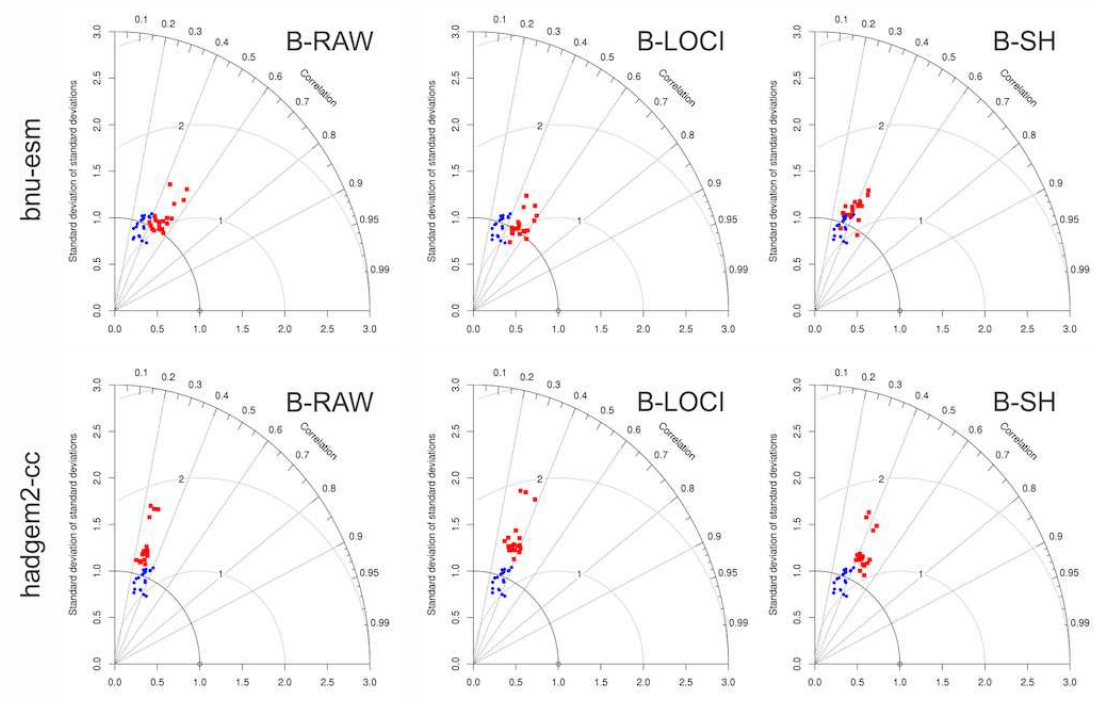

FIGURE 6.2: Taylor diagram showing the performance of the 19 parameter sets in relation to the spatial variation in mean yields for two different GCMs. Blue and red colours indicate control and raw or bias-corrected GCM output simulations (Table 6.1), respectively. Each dot represents a GLAM parameter ensemble member. Spatial standard deviations are normalised to observed, as is the $RMSE$.

Uncertainties in the crop yield response, as represented in the shading of the PDFs of Figure 6.3, increased in the majority of GCM-driven simulations as a result of the interaction between biased weather and the crop model structure and parameters. In some cases, the lack of rainfall triggered crop failure (see HadGEM2-CC simulations in Figure 6.3) and hence the probability of very low (or zero) yields increased significantly. In other cases, biases in temperature interacted with thermal time requirements (which are sometimes different across parameter sets) and increased the uncertainty in the response. Notably, models with high skill at reproducing climate fields in the historical period (see Figures 4.10-4.11, Chapter 4) were also observed to reproduce crop yields with considerable fidelity, particularly when precipitation was better simulated by the GCMs, crop simulation skill improved significantly. This occurred because water stress is the dominant driver of Indian groundnut crop yields (see Figure 5.1, Chapter 5). In this regard, some of the GCMs, namely, BNU-ESM, NCAR-CCSM4, CCCMA-CanESM2, INM-CM4, and MPI-ESM-LR (-MR), produced simulations that were in considerable agreement with the

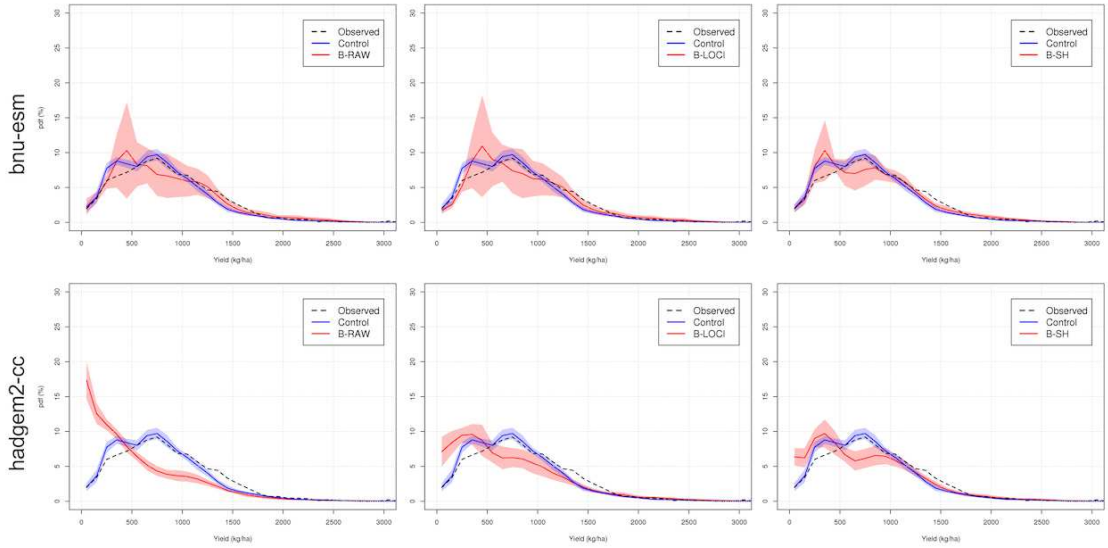

FIGURE 6.3: Probability density functions of baseline simulated and observed crop yields. Red continuous line represents the mean PDF of simulations driven raw or bias-corrected GCM output, blue line the those of the control simulation, and dashed black line is the PDF of yield observations. Shading correspond to 1 standard deviation around the mean PDF, computed using all ensemble members for each GCM simulation.

control and the observations, indicating that in some cases the GCM biases do not necessarily preclude a consistent crop simulation. GCM output bias correction, particularly the SH method, reduced uncertainty in the crop yield response and reduced the likelihood of failed seasons and/or very low simulated yields, thus increasing the overall skill of the crop simulation. However, no bias correction methodology was perfect, even for the 'best' GCMs (Figure 6.3, also see Chapter 4 and Ehret et al. 2012).

6.4.1.2 Effect on baseline simulations

Lack of model skill caused significant differences between simulations across different input types for all quantities of interest. Figure 6.4 shows the variation in simulated baseline mean yield and yield variability across the different input types. For mean yield the main differences arise when using uncorrected GCM output (B-RAW). However, the fact that most of these errors were significantly reduced in the B-LOCI simulations implies that most of the errors were related to biased rainfall (also see Sect. 6.4.1.1) and that C_{YG} cannot fully correct such biases (also see Watson and Challinor 2013). Yield variability seemed to be much more sensitive to errors in input weather, as it was overestimated by

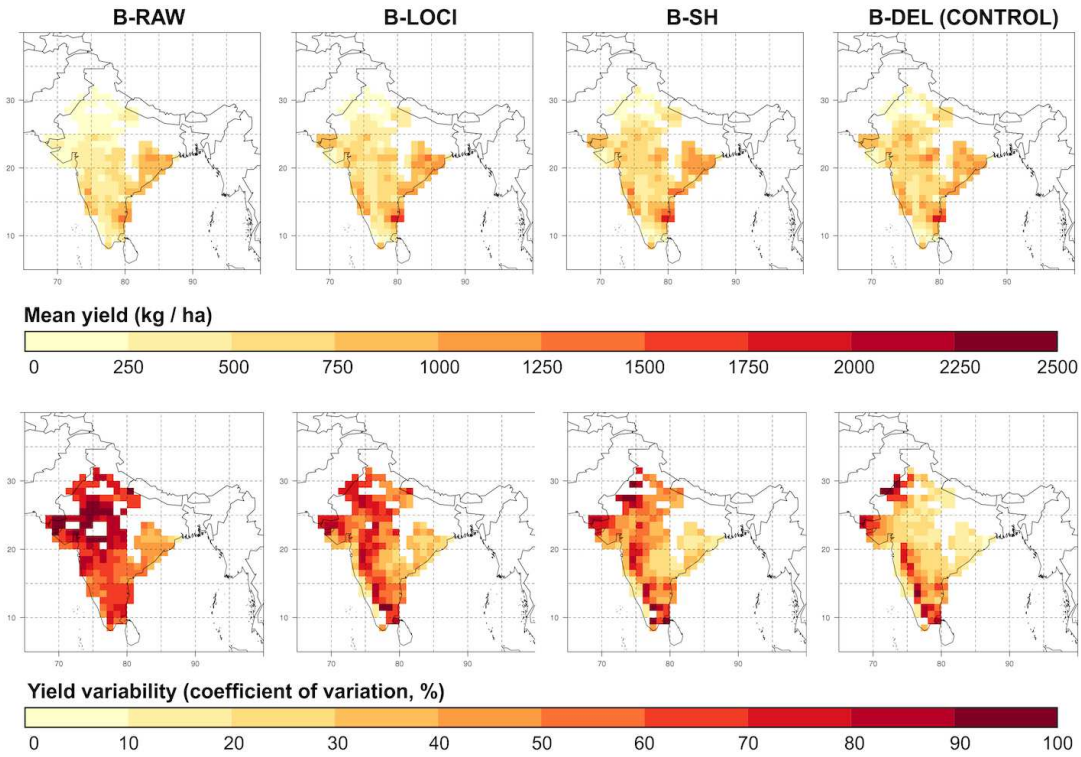

FIGURE 6.4: Mean and variability of crop yield in the baseline simulations for three different GCM-based inputs and the control simulations (driven by observed weather). All maps correspond to the Khariff (rainfed) season. Values shown are averages of all GCMs (if any) and all parameter ensemble members. See Table 6.1 for typology of the simulations.

all input types across central and some parts of western India. As with mean yield, the B-RAW simulations were the least similar to the control simulations. The importance of correcting precipitation bias is noted since the B-LOCI variability significantly improved the simulation, although it was still not perfect. Further, correcting temperatures (B-SH) produced yield variability estimates that were much more similar to the control simulation.

Figure 6.5 shows simulated mean duration and its associated temporal variability. The differences across the different input types were most notable between those where no correction to temperature was applied (B-RAW and B-LOCI) and those with correction of temperature bias (B-SH). Mean duration was overestimated in eastern India in the B-RAW and B-LOCI simulations, underestimated in the south-western coast. The fact that different duration in the B-LOCI simulations led to relatively consistent mean yield simulation highlighted the action of C_{YG} as a bias-correction factor. Duration variability

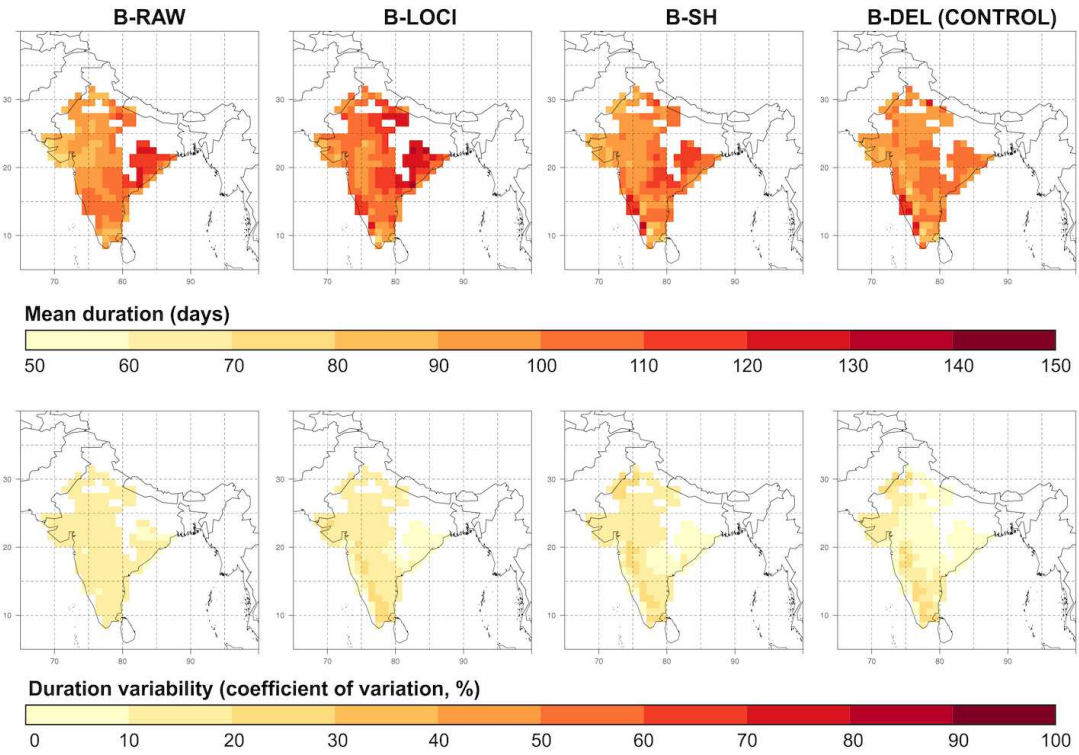

FIGURE 6.5: Mean and variability of crop duration in the baseline simulations for three different GCM-based inputs and the control simulations (driven by observed weather). Additional details as in Figure 6.4.

was less affected than crop yield variability, with high similarity across all input types except B-RAW, in which duration variability was underestimated in the south.

For the Rabi season, warm biases in temperatures increased crop duration and tended to cause overestimation of crop yields; however, as indicated earlier, the yield response varied on a GCM basis, owing to the varying quality in the GCM output (see Chapter 4 for an analysis of GCM skill).

6.4.1.3 Effect on projections of climate change impacts

As for baseline predictions, differences across projections of climate change impacts arose from the use of different weather input types. Figure 6.6 shows the projected change in mean crop yield (top row) and yield variability (coefficient of variation, bottom row). In general, for mean yields, P-RAW simulations showed larger relative changes across the most of India. In western India, for instance, average changes were between 30 and 60

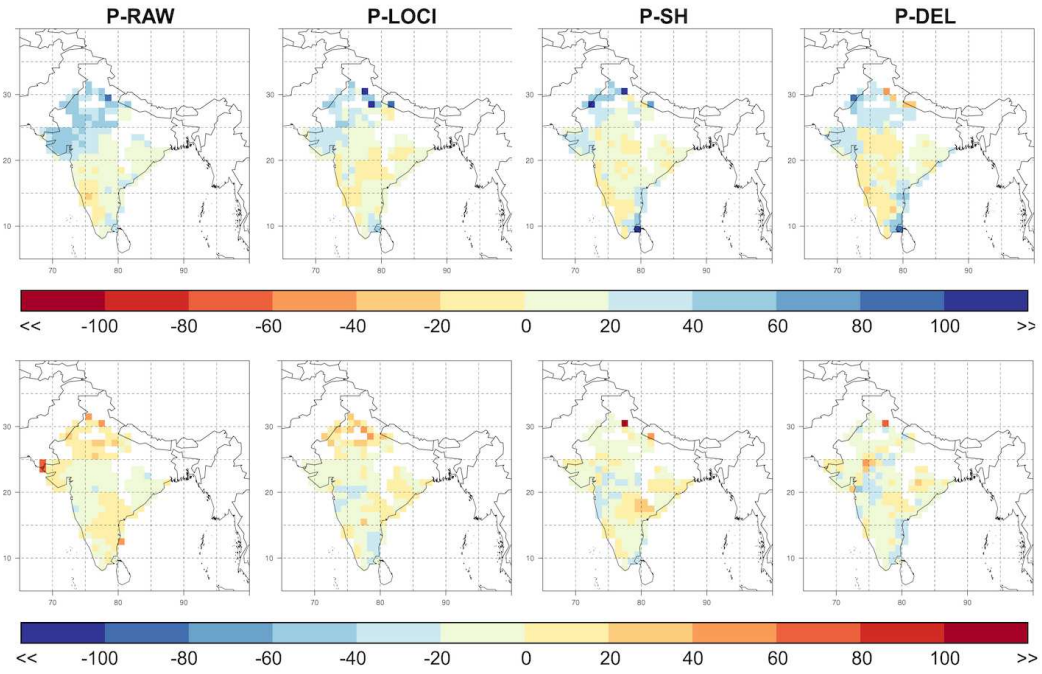

FIGURE 6.6: Projected changes in mean and variability of crop yield by 2030s for all weather input types. All maps correspond to the Khariff (rainfed) season. Values shown are ensemble averages for a given weather input. See Table 6.1 for typology of the simulations.

% for P-RAW, whereas those projected using all bias correction methods were below 40 %. Despite differences in rates of change, the direction of the change remained unchanged across most of India. This suggested that the choice of whether to bias correct the GCM simulated output is a significant source of uncertainty, but that it does not strongly affect the direction of the change (also see Sect. 6.4.4). For instance, yield variability increased by 20-80 % in Gujarat (mean) for the P-RAW simulations and by 10-15 % for the P-DEL simulations.

Differences were greater if the extremes of each set of simulations were considered, with P-RAW showing the largest relative changes. Crop yield changes were very high in the upper end of the simulations for the RAW output, which was associated with very low crop yields that were inconsistent with the control simulations in the baseline (Sect. 6.4.1.1). Inherently biased GCM input, hence, did not affect the direction of change but did so for the extent of the change.

As with mean yields, very high percentage changes in variability were associated with very low variability, which was generally a result of very low baseline crop yields (Figure 6.4), in turn caused by the very low "drizzle-type" rainfall typical of a poorly simulated monsoon season (Jourdain et al., 2013; Sperber et al., 2012). In addition, projections of changes in yield variability showed less consistent patterns. Relative changes in yield variability in northern India were similar between P-RAW and P-LOCI, but these differed from P-SH and P-DEL. Projections were similar between P-SH and P-DEL, particularly in western and southern India. In addition, the significant disagreement across northern and central India between projections in which temperature was corrected (P-SH, P-DEL) and those where not (P-RAW and P-LOCI) suggested that temperature bias played an important role in the changes in interannual yield variability in these regions. The impacts of biased weather on mean and variability of crop duration were less significant than those of mean yields, with inconsistent directions of change in the centre of the country, where durations were projected, on average, to decrease by P-DEL, but changes in a different direction were projected by the rest of the input types.

6.4.2 Climate change impacts on groundnut

6.4.2.1 Impacts on crop duration

Figures 6.7 shows the projected changes in mean crop duration for the Khariff season. A robust response was observed in the north-west (Gujarat and Rajasthan) across GCMs, ensemble members, and the different GCM bias correction methods. In these areas, durations are projected to increase between 5 and 20 %, on average. In the central-south zone (states of Maharashtra, Andhra Pradesh and Karnataka) the majority of simulations depict decreases in mean crop duration in at least 60 % of the areas. In this latter case, there is, however, some uncertainty in the response owing to the different GCMs and other model inputs (i.e.CO_2 response, parameter sets and planting dates), with the upper 25 % of the probability distribution indicating increases in mean duration between 0 and 5 %. In the Rabi season, significant agreement was observed across simulations, with central and northern India projected to experience duration reductions between 5 and 20 %, and southern and western India projected to experience increases between 5 and 10 %.

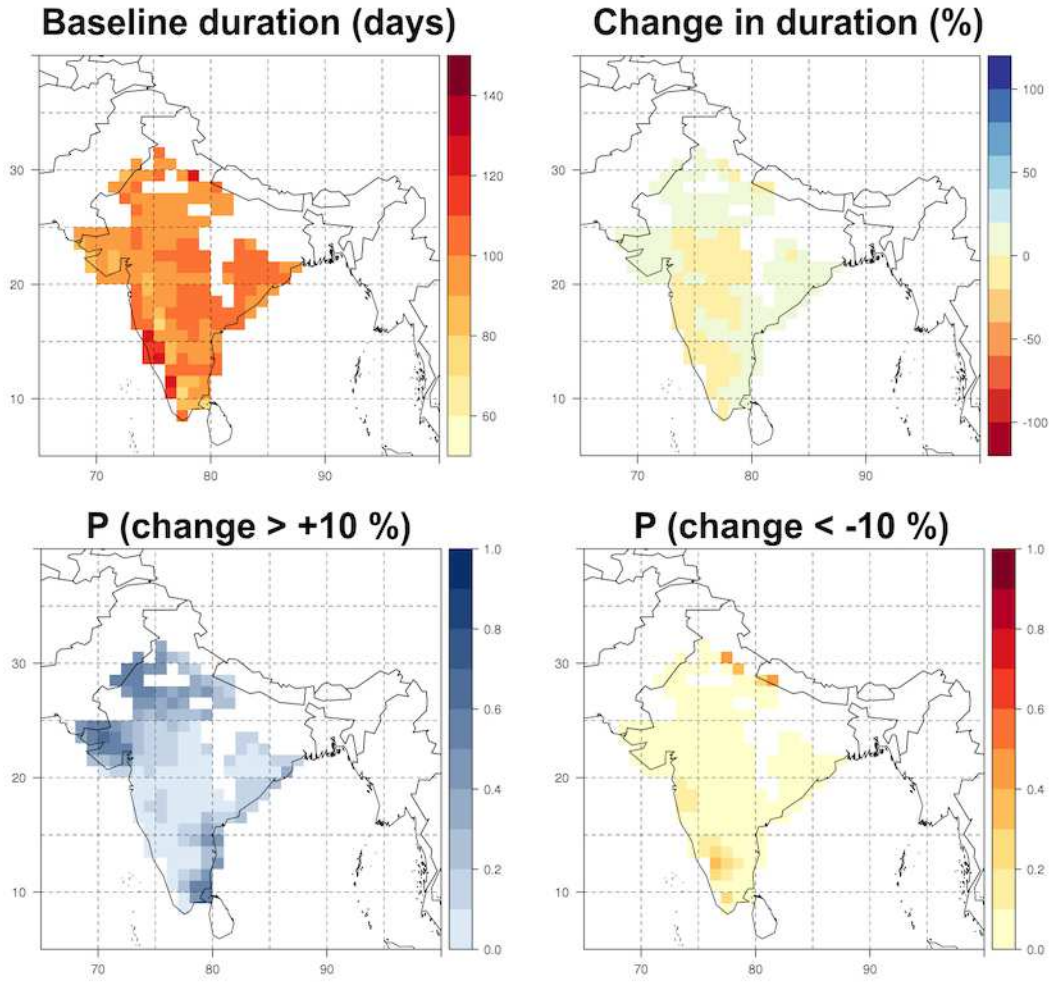

FIGURE 6.7: Impacts of projected 2030s climate on mean crop duration. Shown are the baseline averages, the projected changes in duration (departure from the baseline), the probability of increases of more than 10 %, and probabilities of decreases of more than 10 %. Values shown correspond to the P-DEL ensemble.

Despite uncertainties in the actual values of changes, probabilities derived from the large ensemble used here indicate that robust estimates of impacts can be drawn. Probabilities of changes beyond +10 % and -10 % are shown in Figure 6.7. Probabilities of significant reductions in cropping season length are very high (60-80 %) towards the south-west of India (west of Karnataka and Maharashtra). A high probability (80-90 %) of significant (>10 %) increases in cropping season length was projected in the north and west of India (Gujarat, Rajasthan, Haryana and parts of Uttar Pradesh). To a lesser extent (probabilities between 60-80 %) the east of the country (east of Andhra Pradesh, Tamil Nadu and Orissa) also depicted increases in cropping season length. In general, probabilities of larger

relative changes (i.e. beyond 20 %) for either increases or decreases in cropping season length were very low, probably as an effect of the moderate changes in climate projected to 2030s.

6.4.2.2 Impacts on crop yields

Changes in yield mean for the Khariff crop are shown in Figure 6.8. There were significant yield increases projected across the major growing areas in the west of India (Gujarat). By contrast, in eastern India, negative changes in mean crop yield were found. Crop yield decreases beyond 10 % across the south-western coast of India were found highly likely (probability above 70 %). Yield losses below 20 % were found highly unlikely (maximum 20 %). Yield gains above 5 % were found highly likely (probability $>$ 90 %) across most of western and northern India. There was significant uncertainty as per the direction of the change in central India, although the probability of a negative impact (between 55-60 %) was generally larger than that of a positive impact. Conversely, in eastern India, probabilities of yield gains were slightly higher than those of negative impacts but again there was high uncertainty in the direction of the change. These results broadly agree with those of Challinor et al. (2009a) and Challinor and Wheeler (2008b), who projected yield losses in Central India, and yield gains in north-west and western India. Mean Rabi crop yield was projected to be impacted to a lesser extent in the majority of India, although increases between 15-30 % in southern India (Andhra Pradesh) (also with significant increases in variability) and losses of up to 25 % (with 20-30 % increase in variability) in some simulations (central India) were projected.

At the sub-national and national level (as opposed to the grid cell level analysed above), both impacts and uncertainties varied both with scale and with the areas analysed. Figure 6.9 and Figure 6.10 show probability density functions of projected changes in mean yield and yield variability (respectively) constructed with all members of the large ensemble used here for the five growing zones and the whole of India. The figures show a PDF for each weather input type, including P-RAW for comparison. The extent and direction of impacts varied between the zones and was also different to the whole-India impact distribution. The north-west and west of India show a higher likelihood of yield gains (with decreases in variability). In particular, there was a peak at around 10-20 % and 20-30 % yield gain for the north-western region and western region, respectively.

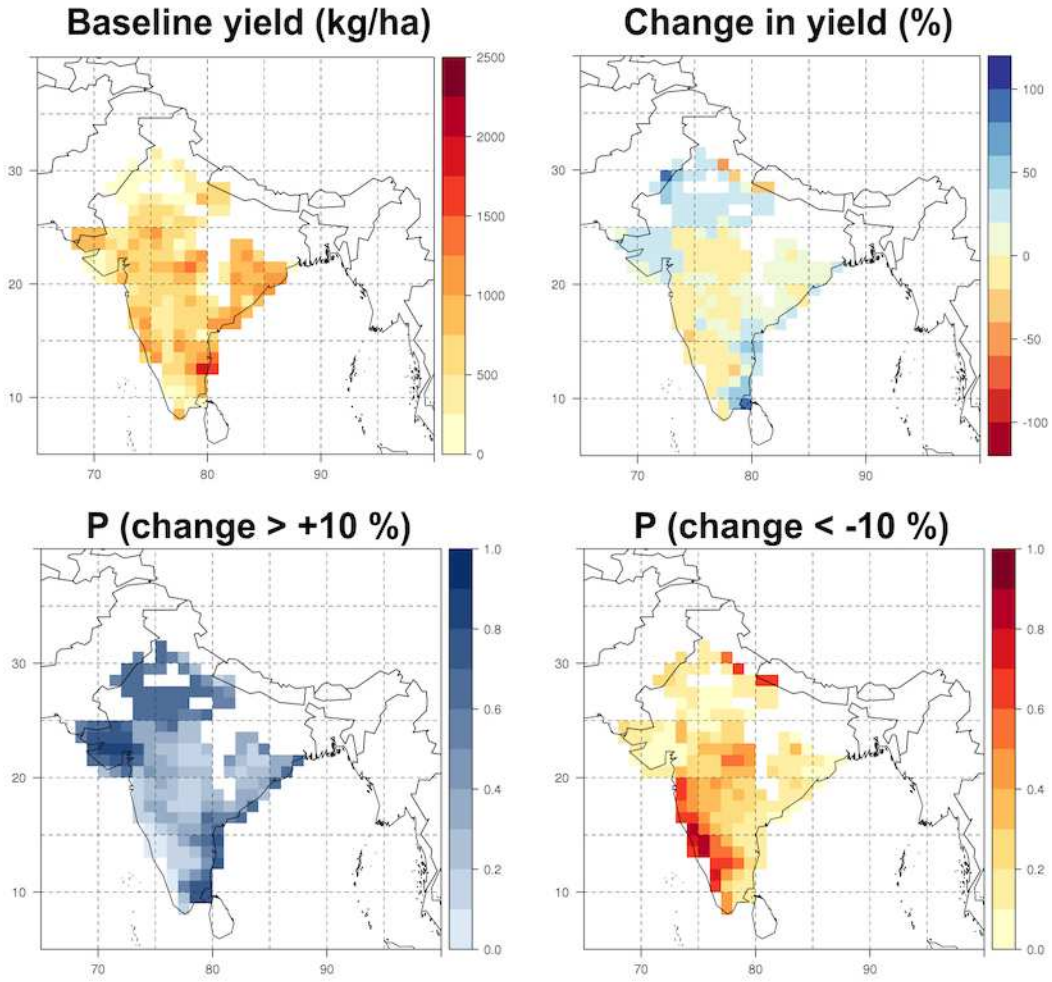

FIGURE 6.8: Impacts of projected 2030s climate on mean crop yield. Shown are the baseline averages, the projected changes in duration (departure from the baseline), the probability of increases of more than 10 %, and probabilities of decreases of more than 10 %. Values shown correspond to the P-DEL ensemble. See Figure 6.6 for mean changes of other weather input types.

High likelihood of positive impacts were also observed (although to a lesser extent) in the south-eastern zone. Negative effects were observed mostly in central India, with the most likely scenario presenting yield losses of 10-20 %. In southern India, the uncertainty arising from the use of different weather input types precludes identifying a clear signal. India as a whole does show an overall trend of increasing crop yields and mixed impacts in terms of variability though with higher likelihood of variability decreasing. The P-DEL projections show the most optimistic scenarios, with the least decreases and/or the most significant yield gains owing to neglecting changes in climate variability. On the whole, however, productivity of groundnut grain is not severely impacted across the largest producing

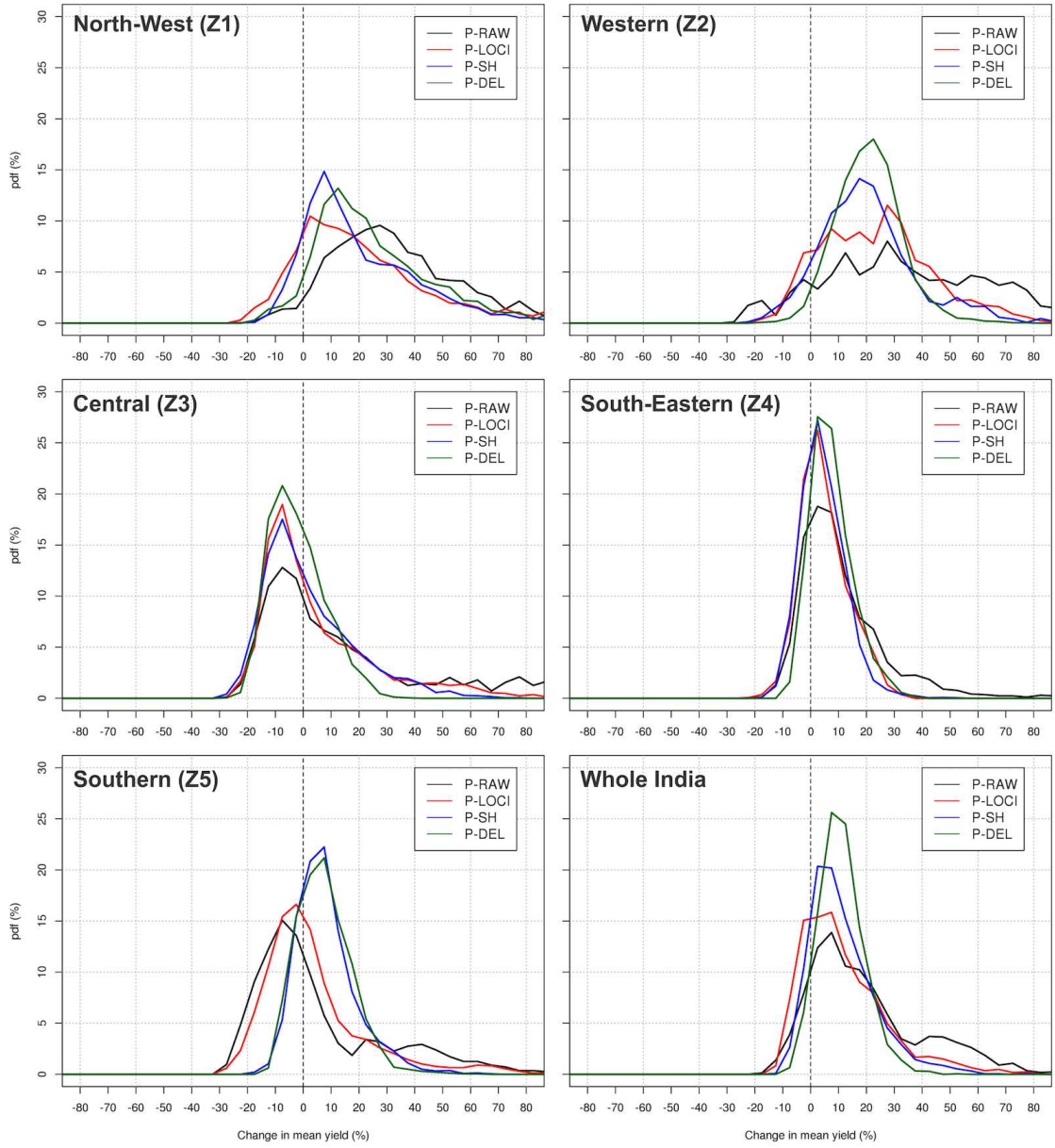

FIGURE 6.9: Probability density functions of changes in mean regional and national yield mean. Subnational-level changes in yield follow the groundnut growing zones defined in Figure 3.2. Lines indicate different input types (see Table 6.1).

areas of India, exception being made for central and (parts of) southern India. The Rabi crop depicted rather minor impacts, with high probability of yield gains in south-eastern and western India, and yield losses over central, eastern, and south-western India.

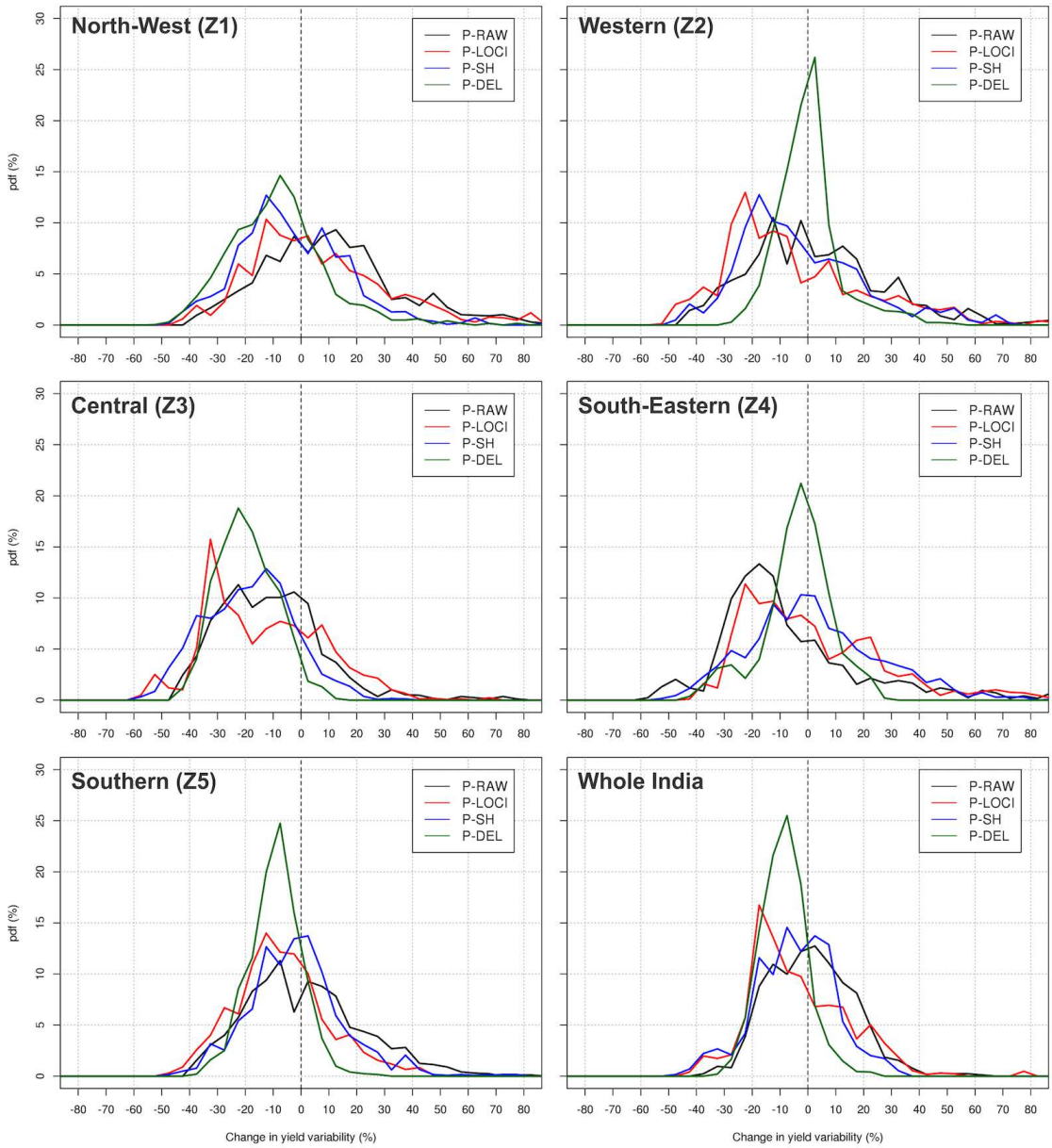

FIGURE 6.10: Probability density functions of changes in mean regional and national yield variability. Additional details as in Figure 6.9.

6.4.3 Key processes under climate change

Determining the processes behind a given projected impact is perhaps as important as determining the direction and/or the extent of the change. Consistency in processes across crop model simulations can be an indicator of robustness (Challinor et al., 2013) and can help in the design of adaptation strategies (Lobell et al., 2013). Investigating processes can also help identifying key uncertainties (Challinor and Wheeler, 2008b). The purpose of this section is to describe the main processes related to the projected changes in crop yields that were described in Sect. 6.4.2.2 so as to be able to identify the main physiological aspects of the crop that require attention from an adaptation perspective.

In spite of uncertainty in the extent of yield changes and in some cases also in the direction of the yield responses, significant similarity arose in terms of the driving processes of yield increases across weather input types and regions. For yield gains, in general, the main process that seemed to cause most yield gains was the reduced terminal drought due to an overall increase in seasonal rainfall. Indirectly, the lesser effect of terminal drought increased cropping season length, hence countering some of the negative effects of increased temperature on crop development. Such increases in crop duration allowed greater radiation absorption, total water uptake and hence more biomass accumulation. This finding was consistent across all growing zones, highlighting the importance of water availability for the groundnut cropping systems analysed, as well as the need for water-use-efficient genotypes that allow coping with drought stress and/or capitalise on potential increases in available water. In most of the simulations with yield gains, however, a decrease in the mean total percentage of pods due to heat stress (HIT) was also observed (i.e. more heat stress). These changes were small and were compensated by increases in seasonal rainfall and crop duration, but suggested that with higher degrees of warming high temperature stress may become an important constraint to crop yields (Challinor et al., 2007), particularly because these increases in heat stress occurred at various degrees of warming (Figure 6.11).

Processes driving yield losses varied across the different zones. In the north-western, western and south-eastern growing areas, projections of yield loss were, at least to some extent, related to decreases in crop duration (50 and 30 % of simulations with yield loss showed decreases in duration). In these cases, changes projected precipitation increases

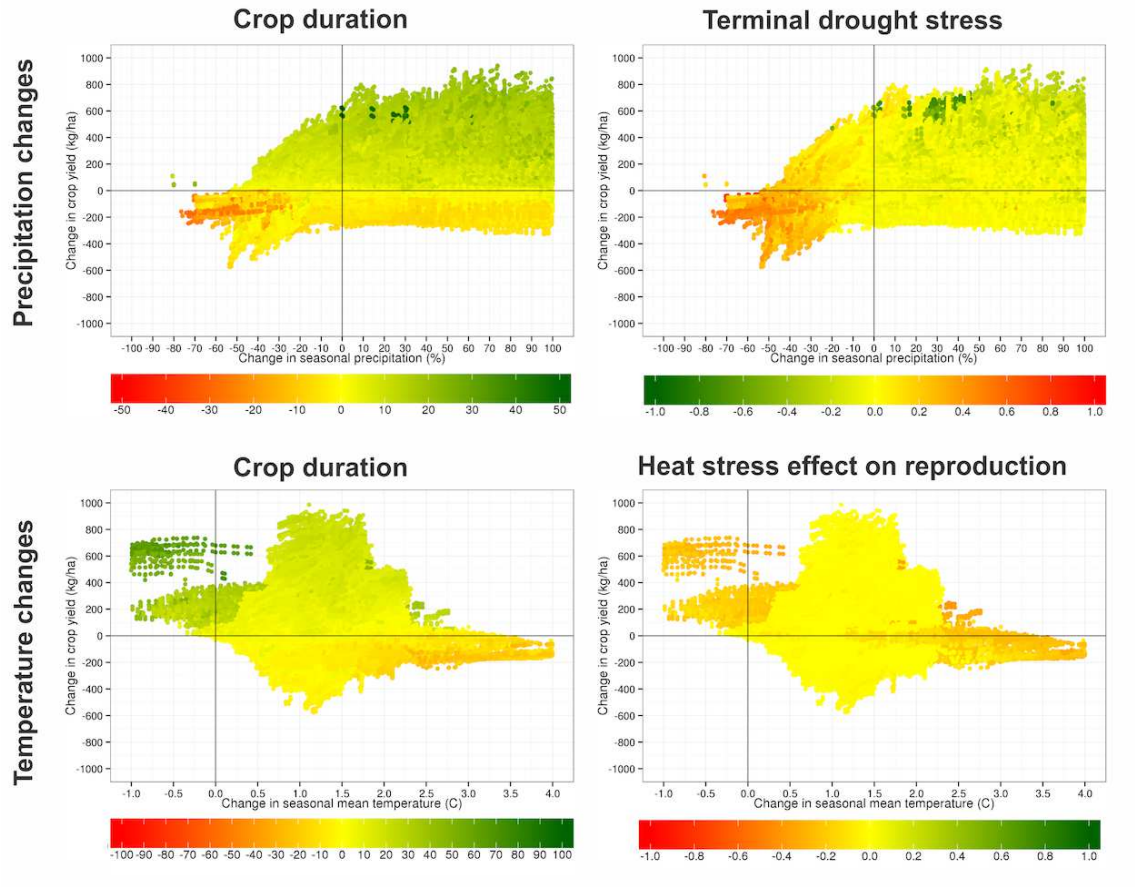

FIGURE 6.11: Variation in crop yield response with respect to precipitation (top row) and temperature changes and a third variable (varying depending upon the panel). Results shown are for 'P-DEL' rainfed simulations in the western zone (Z2).

by the GCMs were not sufficiently large so as to counter the hastened crop development that arose from higher temperatures. However, some of these losses were enhanced by heat stress (average 70 % simulations across GCMs) and an increased effect of terminal drought (65 %). As reductions in cropping cycle duration also impacted total potential water uptake and total absorbed radiation, it was difficult to separate their individual effects without carrying out separate fixed-duration simulations (see e.g. Challinor and Wheeler 2008b and Figures 6.11 and 6.12). In general, however, a greater proportion of simulations showed decreases in absorbed radiation (75 %) as compared to those showing decreases in crop duration (< 50 %) and this suggests that decreases in solar radiation during the rainy season would have independently enhanced yield losses. Decreased solar radiation may be a result of increased cloudiness in the climate model owing to increased precipitation during the monsoon season (Haywood et al., 2011; Menon et al., 2002).

In the central region (Z3) and the southern region, decreases in cropping cycle duration were more severe (occurring in some 70 % of simulations), even though there was a general trend for an increase in seasonal rainfall (in ∼65 % of simulations) and little effect from heat stress (<5 % of simulations). Crop duration decreases arose because mean temperature was in the future scenarios closer to the optimal development temperature (also see (Challinor et al., 2009a)), but these were enhanced and to some extent (∼50 % simulations) also by terminal drought (Figure 6.12). The yield responses in the Rabi crop were primarily constrained by crop duration, although reduced solar radiation played an important role, particularly in central and south-western India.

Remarkably, in spite of the lack of agreement observed in yield changes for certain growing regions, agreement in terms of the importance of certain processes across the different types of simulations was found in most cases. It was also observed that similarity in driving processes (e.g. between Z1, Z2, Z4 and between Z3, Z5, see Figures 6.11 and 6.12 for added detail on Z2 and Z3 as representative examples) was related to the direction of the changes (Z1, Z2, and Z4 generally showing yield gains, and Z3 and Z5 with yield loss being predominant, see Figure 6.11).

6.4.4 Sources of uncertainty

As stated earlier (see Sect. 6.3.2.4). The objective of the analysis was to determine the relative importance of the different sources of uncertainty so as to be able to identify the specific points in the 'uncertainty cascade' that are the most relevant to the study of groundnut yields under future scenarios. Since uncertainty was decomposed separately for simulations that used raw GCM output and those that were bias corrected, and separately for the baseline (Figure 6.13) and the 2030s (Figure 6.14), this allowed the robust determination of the main sources of uncertainty and their spatio-temporal variation. The sources investigated here were: parametric uncertainty (from the GLAM parameter ensemble), GCM structure (from the ensemble of GCMs), CO_2 response (from the CO_2 response parameterisations of Table 3.6), and sowing dates (arising from the variation in start of planting window).

Very similar results were found for the Khariff and Rabi crops and thus only the Khariff crop is described. Climate was the largest source of uncertainty, either via the large (>70

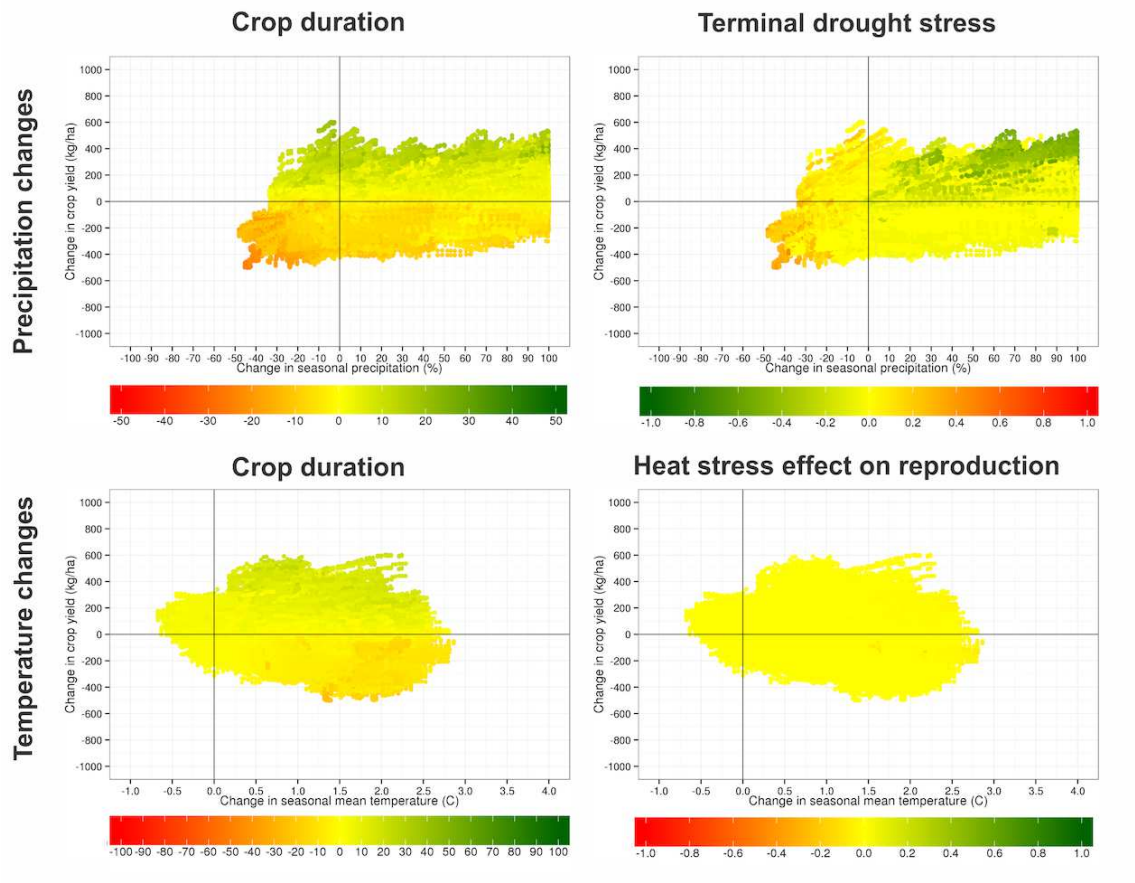

FIGURE 6.12: Variation in crop yield response with respect to precipitation (top row) and temperature changes and a third variable (varying depending upon the panel). Results shown are for 'P-DEL' rainfed simulations in the central zone (Z3).

%) relative contribution of GCM structure to total uncertainty in the P-RAW simulations, or via the combination of bias correction methods and the GCM structure. Climate uncertainty was followed in importance by parametric uncertainty (20-30 % relative contribution), and then by CO_2 response (< 10 %) and sowing dates (< 5 %). In the case of CO_2 response, in particular, the sampling of the uncertainty space was limited to only 4 combinations of parameters (Table 3.6) so as to reduce computational needs, but previous studies have considered a more complete sampling of this source of uncertainty (Challinor and Wheeler, 2008b).

In addition to the above, four main points arose from decomposing uncertainty:

- Firstly, total yield uncertainty was higher when raw GCM output was entered into the crop model. The main reason for this is the obvious biases in monsoon rainfall in many GCMs that triggered the occurrence of terminal drought in many years,

particularly in the dry areas of north-western India. The wide array of GCM simulations used in the present study differed significantly in their biases with respect to observed climate, particularly for rainfall (see Chapter 4). By bias correcting the GCM output, biases were reduced, but GCMs were brought closer to a single common point (i.e. the observations), which reduced the GCM structural uncertainty and thus the resulting total yield uncertainty. The use of a limited number of bias correction methods as opposed to the wide array of GCMs, thus, produced a reduction on the total uncertainty.

- Secondly, the P-RAW simulations consistently showed a very high contribution of GCM structure. The relative contributions from the different sources were different in the P-RAW simulations as compared to the bias-corrected simulations. In particular, the relative contribution of GCM structure in the P-RAW simulations (top row in Figure 6.13 and 6.14) was roughly 25 % larger in the P-RAW as compared to the bias corrected simulations. Uncertainty arising from the structure of GCMs was above 70 % in most of the study area (baseline), but it did not exceed 50 % in the bias corrected baseline simulations. This difference was very similar for the future simulations, though the contribution of GCM structure to total uncertainty was lower, owing to the introduction of two additional uncertainty sources: CO_2 response and sowing dates. The geographic patterns were, however, very similar between the P-RAW and the bias corrected simulations. Despite the differences in the relative contribution of GCM structure, the relative importance of the rest of the uncertainty sources was similar.

- Thirdly, the spread across members of the ensemble was lower in the P-RAW as compared to the bias-corrected simulations. Much more agreement (and less significant percentage changes) were observed in the DEL simulations (one of the most frequently used methods in the impacts literature, see White et al. 2011b). However, DEL does not account for changes in intra-seasonal and interannual variability, and could thus likely underestimate the impacts of extreme events, which are projected to increase towards the future (Orlowsky and Seneviratne, 2012; Sillmann et al., 2013). By contrast, the use of raw GCM output allows including all relevant climate system features and their evolution toward the future; however, inherent biases in GCMs

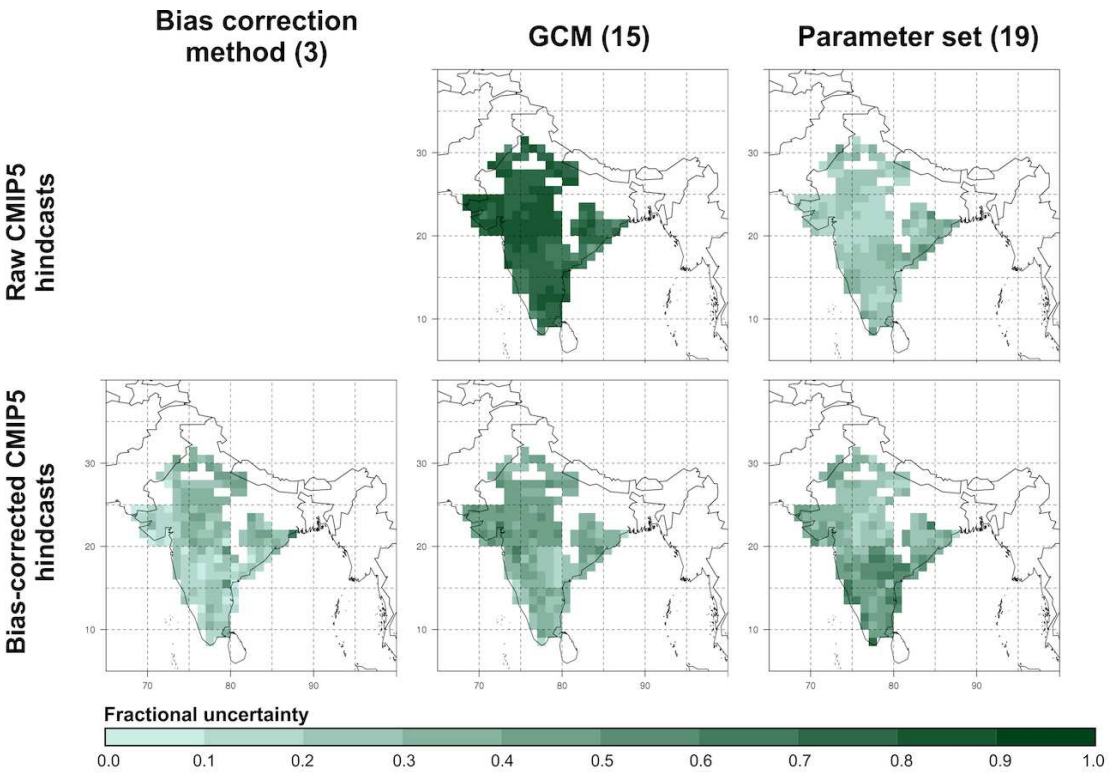

FIGURE 6.13: Fractional uncertainty in mean yield from different sources in the baseline. Uncertainty was decomposed separately for simulations where GCM bias correction was not performed (top) or was performed (bottom).

(particularly the too-much-drizzle-type problem that is frequently mentioned the literature) leads to above-normal crop failures and unrealistic crop responses in both the baseline and the projection periods (also see Sect. 6.5.2, and Ramirez-Villegas et al. 2013a). This was also evidenced in the fact that the Rabi crops GCM-related uncertainty was generally lower.

- Finally, the contribution of the uncertainty in the decision of whether to bias-correct the climate simulations, which is shown in Figure 5.19, was large, and importantly, in some cases larger than the total of uncertainty from all other sources. This was observed particularly in western India for the calibrated GCM output, where the uncertainty in the decision was generally 20-25 % greater than the total uncertainty from all other sources. Because the total uncertainty arising from the GCMs in the P-RAW simulations was very large, the uncertainty in the decision was comparatively lower (25-30 % lower) in the same area. Uncertainty in the decision, however,

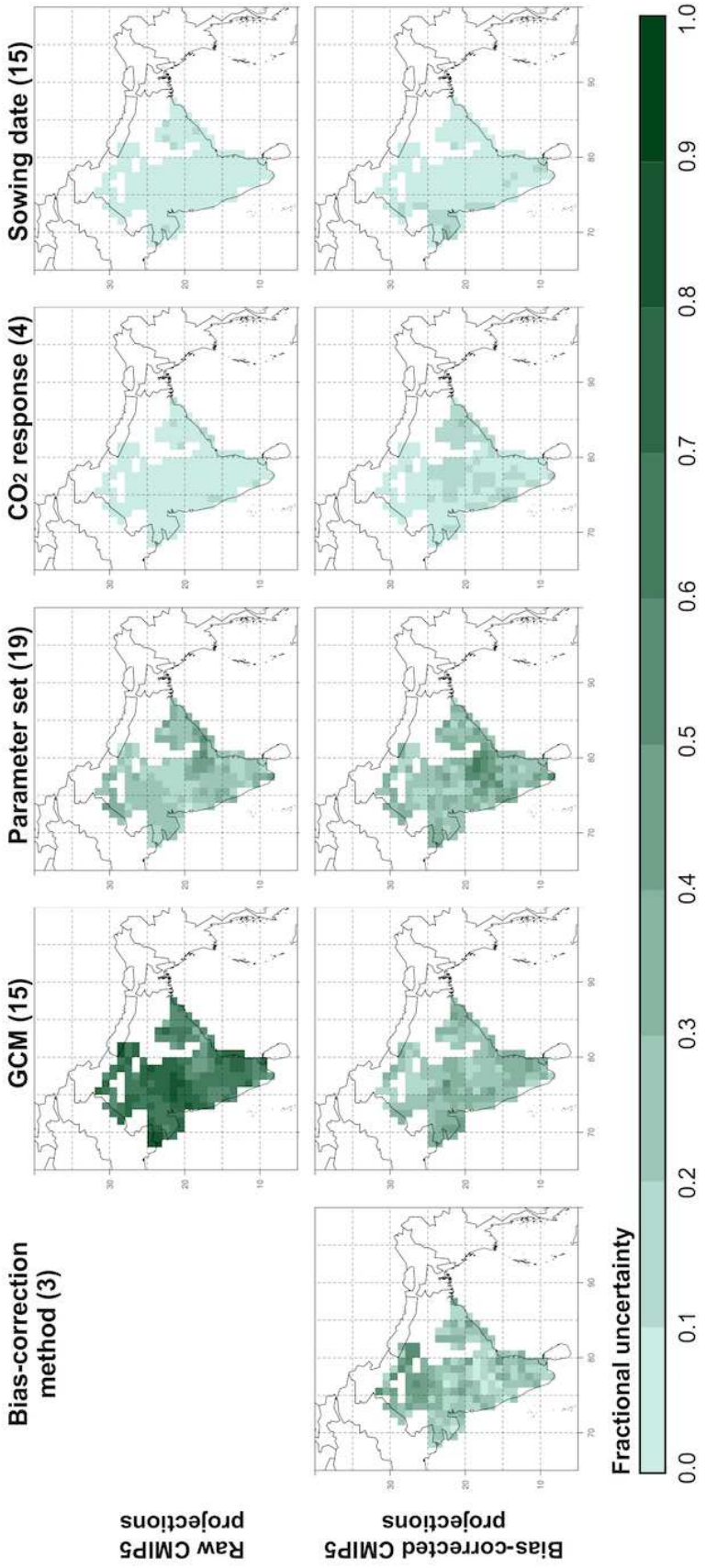

FIGURE 6.14: Fractional uncertainty in mean yield from different sources in the 2030s. Uncertainty was decomposed separately for simulations where GCM bias correction was not performed (top) or was performed (bottom). Note the increase in importance in parameter uncertainty when bias-corrected GCM projections are used.

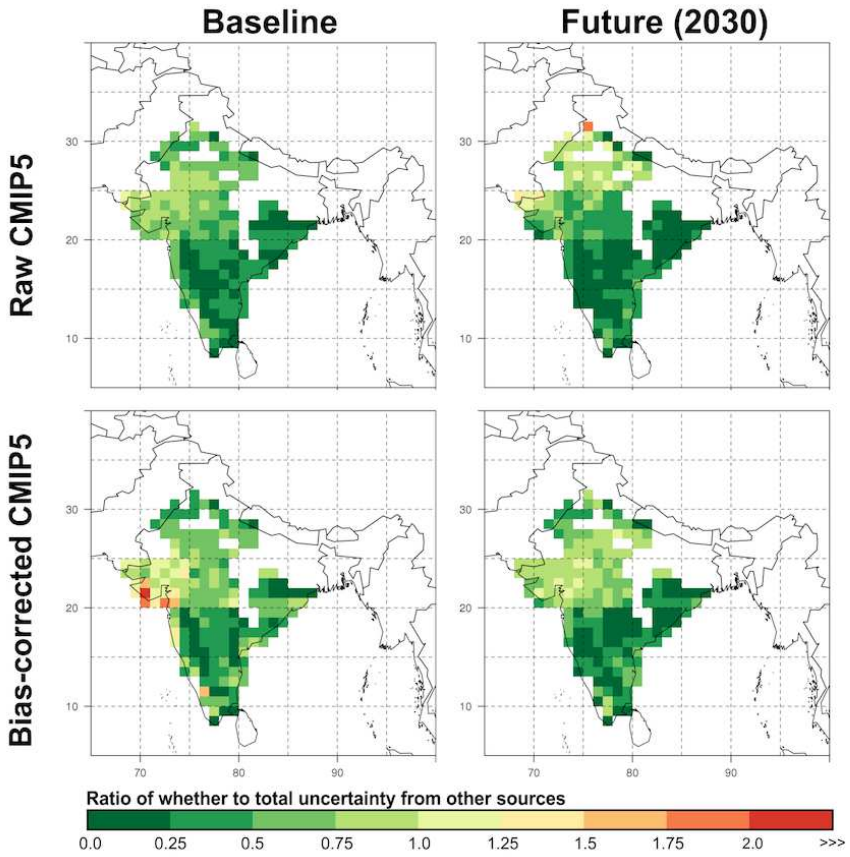

FIGURE 6.15: Uncertainty in the decision of whether to bias-correct the GCM simulations, shown as a fraction of the total uncertainty in each set of simulations. Values above 1 indicate areas where uncertainty in the decision is greater than that arising from all other sources together.

increased in importance in time in the P-RAW simulations and decreased in importance in the bias-corrected GCM simulations (Figure 5.19) but there was spatial variation in this response.

6.5 Discussion

6.5.1 National and sub-national level implications of crop yield changes

In relation with other crops (e.g. rice, wheat, maize) (Fraser et al., 2013; Knox et al., 2012; Parry et al., 2005), the impacts of climate change on groundnut crop yields have been far less investigated. Currently, most of the Indian groundnut production happens in low-input systems under rainfed conditions, and this makes the system highly sensitive

to climate variations (Mehrotra, 2011). However, this also indicates that significant yield gains could occur at present if input use is increased and optimised to close yield gaps (Bhatia et al., 2009). The impacts of climate change on groundnut productivity have been projected to vary according to the geographic location within India (Sect. 6.4.2), which at first highlights the need for spatially-disaggregated information and conclusions. Previous estimates of future groundnut productivity (at the national level) by the same period studied here have highlighted uncertain impacts closely centred around "0 %" (Lobell et al., 2008), which may reflect the large spatial variation of crop yield response reported here.

Under the future climate scenarios explored here, the effects of climate change are moderately negative or in many cases even positive. This was particularly the case for the largest producing state –Gujarat. In Gujarat, and also in the north-west of India, increased water availability enhanced biomass accumulation, but also increased crop duration as it reduced terminal drought. Temperature had a minor role given the relatively low levels of warming observed by 2030s (Knutti and Sedlacek, 2012). In these areas, crop yield changes were consistent with the studies of Challinor et al. (2007), Challinor and Wheeler (2008b), Challinor et al. (2009c) and Singh et al. (2012), which have projected crop yield gains towards the west and north-west of India and crop yield losses towards the south-east (Figure 6.8 and 6.9). In the first three studies, yield gains were reported as a result of increased crop duration due to the exceedance of optimal temperatures for development –though for instance in Challinor and Wheeler (2008b) the findings were not consistent across the three crop models used. Differences in the processes may arise between this study and others partly because these studies focused on climate scenarios of greater warming (i.e. by 2100), and partly because the terminal drought stress mechanism (a key one in this chapter) was not included in two of the mentioned studies. In the study of Singh et al. (2012), however, processes were not explicitly investigated, but the reported increases in seasonal precipitation, the little impact of temperature change in crop duration, and the fact that yield gains were reported even without accounting for CO_2 stimulation, suggest that reduced water stress and increased biomass production were the causes for the yield gains.

Disagreement with respect to the abovementioned studies, however, arose in eastern and south-eastern India, where the present study projected a higher likelihood of crop yield

gains, while the other two studies projected yield loss. The reason behind these differences may be in the fact that yield changes may change in direction with larges increases in temperature. For instance, Thornton et al. (2009) reported that in some 20 % of bean producing regions of East Africa experience yield increases in the near term (ca. 2020) just before crop yields decline significantly towards the mid- and end- of the 21st century. The results presented herein and those of Singh et al. (2012) (by 2050s) and Challinor et al. (2007) (by 2100) would imply that similar trends are to be expected in some of the areas (e.g. southern Gujarat, and eastern India) although any remarkable differences could also be caused by choice of climate simulations, emissions scenario, crop model and model parameters.

Despite relative increases in crop yields in some areas, actual crop productivity under future climate is still expected to remain low in relation with other producing countries, unless improved management and input optimisation is further pursued across major producing areas. In addition, in spite of a significant reduction in drought stress across western and north-western India, drought impact will likely still be a major player by the 2030s, suggesting that further breeding of drought tolerant genotypes may be warranted toward the future. Furthermore, the fact that interannual variability was projected to increase in many areas is particularly worrisome, since the low inputs of majority of groundnut systems across India and the large yield gaps may indicate very low coping capacities at local levels Bhatia et al. (2009); Licker et al. (2010). To this aim, genotype characterisation, targeting and improvement activities carried out by both national (e.g. Directorate of Groundnut Research) (Ajay et al., 2012; Nautiyal et al., 2012) and international (e.g. the International Crops Research Institute for the Semi-Arid Tropics, ICRISAT) (Upadhyaya, 2005) research organisations are of high relevance to maintain and improve groundnut production in both quantity and stability.

6.5.2 Sources of uncertainty in crop yield simulation

Crop modelling studies have typically focused on reporting total uncertainties (e.g. Osborne et al. 2013 and Sultan et al. 2013), with few studies also analysing individual uncertainty sources (Koehler et al., 2013; Vermeulen et al., 2013). A thorough understanding of uncertainties and their main sources is a critical piece of information for both research and policy purposes. Assessing and reporting associated uncertainties with a given impact

can, at the very least, help focusing the spatio-temporal scale of future attempts to adaptation and vulnerability reduction (Vermeulen et al., 2013). Here it was shown that robust impacts estimates can also be obtained by using large crop-climate prediction ensembles. Attention must be paid to the design of the ensemble and to the key uncertainties that need to be reduced, or whose impact was the largest and thus need to be further investigated.

Various important points arose from the analyses and results presented here. Firstly, the assessment of uncertainty sources revealed that the largest source of uncertainty was the structure of the GCMs, with 1.2-1.7 times more relative importance than the second most important source –crop model parameters. GCM uncertainty did not only affect the direction and extent of impact, but it also affected the driving process of the impact. This became evident since the use of raw GCM data reduced the model skill in the baseline, caused an unrealistically large and widespread impact of drought stress (Figure 6.3), and unrealistically increased the effect of heat stress in certain areas (e.g. southern India). However, it is worth noting that there were some climate simulations for which realistic simulations were achieved. Thus, although the risks posed to impact prediction by climate uncertainties seem rather high, they depend on the quality of the underlining GCM simulation (Baigorria et al., 2008; Randall et al., 2007). On this last point, for instance, (Challinor et al., 2005a) reported skilful crop simulations when climate model output was used directly into GLAM, but (Koehler et al., 2013). Further, Hawkins et al. (2013a) concluded that correcting the means can be as important as correcting the daily variability of the GCM simulations. Furthermore, while there are obvious benefits in bias correcting GCM output for impact assessment, there is a vast diversity of bias correction methods (Ehret et al., 2012). Importantly, some cases qualitative conclusions were contingent on the choice of method (see Figure 6.6). This has also been shown in existing literature for other crops and/or regions (Iizumi et al., 2012a; Koehler et al., 2013). This suggests that there is no general prescription regarding the treatment of climate model information for impact assessment and probably highlights the need of developing an appropriate understanding the realism of a given GCM simulation is for a given region, and how the bias can be corrected. Such understanding may entail many of the aspects analysed in Chapter 4 of this thesis, but may also require a sufficient understanding of the regional circulation patterns (Jourdain et al., 2013). In this chapter, for instance, the unrealistic simulation of the monsoon in the HadGEM2- models led to crop simulations that were inconsistent with the control simulations. In fact, the varying quality of the monsoon simulation was

vastly different across the GCMs generated a broad range of responses in both the baseline and projection periods. Equally important to assessing the needs and usefulness of bias correction on a study-specific basis, an assessment of the uncertainty in the choice of bias correction method is important for impact studies.

Secondly, even though the response of crops to CO_2 has been regarded as one of the largest sources of 'unknown unknowns' in the crop modelling literature (Challinor and Wheeler, 2008b; Leakey et al., 2009; Long et al., 2006), this study reports that it is a relatively minor source of uncertainty. There may be two reasons for this: (1) the projections assessed here focus on near-term (i.e. 2030s) climate change and a relatively moderate RCP scenario (also see Ruane et al. 2013); and (2) the parameterisation of CO_2 response in GLAM is prescribed using one specific method, and it is likely that using different approaches (e.g. radiation-use efficiency as in some CERES models, Jones et al. 1986; Nain et al. 2004), or the increase in gross canopy photosynthesis of the CROPGRO models (Alagarswamy et al., 2006; Boote et al., 1998) in conjunction with the one used here may lead to a larger uncertainty contribution (Tubiello and Ewert, 2002).

Thirdly, despite uncertainties it was possible to identify both robust signals in crop yield and duration changes under the future climate scenarios considered. Projections of increases in crop yields were highly likely across north-western and western India. There was a more uncertain signal elsewhere, with a higher likelihood of negative impacts in central and south-western India, and a slightly higher likelihood of yield gains than of yield losses in south-eastern and southern India. Hence, the use of an ensemble of crop-climate simulations led to a clearer understanding of impacts by both drawing probability distributions (Sect. 6.4.2) and disentangling the key processes behind the projected changes (Sect. 6.4.3). Similarly, it was possible to identify key uncertainties that need to be reduced and potential shortcomings in the framework. The most critical uncertainty source to be reduced is that of arising from climate modelling. However, it was also found that certain crop model parameters contribute to uncertainty in the response and thus that could be better constrained. In particular, the rate of change in LAI ($(\partial L/\partial t)_{max}$) was found to produce unrealistically low crop yields in some simulations, particularly when biased GCM weather was used into the crop model (Sect. 6.4.1).

The simulations of this study were internally consistent and realistic. However, additional uncertainties may arise from empirical components in GLAM –also typically present in

other crop models (Jones and Thornton, 2003; Lizaso et al., 2011; Ritchie et al., 2009). Clear examples of such components in GLAM are the responses to high temperature stress developed using regressions from field experiments (see Sect. 3.5.1.8 and Challinor et al. 2005b), the simple parameterisation of rate of growth of leaf area index (i.e. a linear growth rate), and the simplistic simulation of assimilate partitioning in the plant (Boote et al., 2013; Challinor et al., 2005d). Empirical components could lead to lack of transferability and the need of re-calibration, and thus become a limitation for climate change impacts projections. In this work, GLAM was cross-calibrated for two different time periods and the simulations found consistent (see Sect. 5.4.2.3). However, future studies using GLAM should aim at testing the model in environmental conditions under which the model was not developed (e.g. under extreme temperatures or extreme drought) as well as more systematically testing its transferability both in space and time.

6.5.3 Adaptation of groundnut systems to climate change

The vast diversity in growing conditions and management across India implies that adapting groundnut systems has no single 'silver-bullet' solution, but rather that a set of measures may be required to either abate negative effects or capitalise significant opportunities. The most promising strategy for climate adaptation is the development of improved germplasm. Targeting crop improvement activities on the basis of crop model simulations requires deeper analyses (see Chapter 8 and Singh et al. 2012). Additionally, as stressed earlier (see Sect. 6.4.2 and 6.4.3), the many interacting factors in a crop yield simulation under future climates are difficult to isolate and thus further complicate preliminary assessments of potential crop improvement scenarios. The simulations and processes of importance suggest some that the most important avenue for crop improvement is the increase of drought-tolerance traits in existing germplasm; however, a more profound investigation of genotypic adaptation is presented in Chapter 8.

Chapter 7

GLAM and EcoCrop: a joint assessment of future groundnut cultivation

"... y mi sombra,
por los rayos de la luna proyectada,
iba sola,
iba sola,
iba sola por la estepa solitaria..."
J. A. Silva

7.1 Summary

Suitability and productivity have both been used to predict and project crop responses to the environment. Using models, modellers have assessed either, but rarely both together. This is partly because the availability of information often constrains the choice of modelling strategy (e.g. Schroth et al. 2009). This chapter uses the niche-based model EcoCrop to project changes in crop suitability and produce a joint assessment of crop suitability and crop productivity (Objective 4-B, Sect. 1.6). The niche-based model EcoCrop was first used to (1) simulate present-day climatic suitability, and (2) project future (i.e. 2030s,

RCP4.5) climate change impacts on groundnut suitability. Present-day and future suitability simulations were compared with present-day and future GLAM simulations. The skill of EcoCrop was measured using the area under the receiving operating characteristic curve (AUC_I) –a measure of discrimination accuracy, the true negative rate (TNR) and the false negative rate (FNR). Baseline suitability predictions were first regressed against simulated GLAM yield and production (i.e. yield $*$ area harvested). The residuals of any significant regressions were then regressed against sub-seasonal GLAM prognostic variables (e.g. number of water-stress days, number of heat-stress days). Future projections of suitability were then produced to quantify the climate change impacts on groundnut suitability. The agreement between suitability and yield projections was finally assessed and further compared with literature on climate change impacts on groundnut productivity.

The skill of EcoCrop in the baseline period was high, with AUC_I (area under the receiving operating characteristic curve) between 0.67 to 0.74, true negative rates (TNR) in all cases above 90 %, and false negative rates (FNR) values between 1 and 10 %. Simulated present-day suitability was found to not be related to crop yield, but it was found to be significantly ($p < 0.05$) related to crop production (i.e. yield $*$ area harvested). Multiple regressions of residuals of suitability vs. production relationships indicated that within-season water stress was a key driver behind these differences, and that the amount of heat units and total effective solar radiation played a secondary, yet important, role in GLAM production simulations. Future projections of EcoCrop indicated that on average, suitability losses were in the range -34 to +20 %. Crop suitability was projected to decrease in the majority of areas, mostly as a result of increased temperature. However, in a number of cases (10-15 % simulations) the change in precipitation niche was also a cause of suitability loss. These projections were in little agreement with those of GLAM (Chapter 6), except for central India –where both models and previous literature suggested negative impacts – though driven by different factors. Furthermore, there was limited or no spatial agreement between crop yield and gains or losses in suitable areas.

Much of this disagreement can be attributed to: (1) the different response to increases in precipitation in EcoCrop, which projected range loss –as opposed to the increase in total biomass and yield projected by GLAM, particularly at elevated CO_2 concentrations; and (2) the apparent higher sensitivity of crop suitability estimates to temperature increases

that triggers range loss –whereas in GLAM exceedance of optimal temperatures increases crop duration and tends to increase crop yield (as long as critical temperatures for flowering are not exceeded). The results herein presented imply that uncertainties arising from the use of various impacts estimates (suitability vs. yield) are large. Model outputs of a single crop model should be interpreted carefully and at the very least compared with existing estimates of climate impacts in the search for robustness.

7.2 Introduction

Understanding patterns and mechanisms of plant responses to environmental changes is central for climate change impacts and adaptation. Two measures have been used to project responses of crop plants under future climate scenarios: crop suitability (e.g. probability of occurrence) and abundance (e.g. population density, biomass, yield) (Estes et al., 2013a; VanDerWal et al., 2009a) (see Sect. 3.2 for definitions). Models exist to predict both quantities. Species suitability –mostly studied by ecologists (but see Estes et al. 2013a,b), is typically modelled using a type of empirical model called 'species distributions models', or simply 'niche-based models' (see Sect. 2.3.2.2 for a description of these models). Suitability (or success of a population) can also be modelled using mechanistic models (e.g. Keenan et al. 2011), although these are very data intensive and hence less widely used (Estes et al., 2013a). Abundance (i.e. crop yield) can be modelled either via empirical or process-based models. Empirical models are achieved through statistical regressions of historical crop yields (e.g. Lobell and Burke 2010, Sect. 2.3.2.1). Conversely, process-based models are physiologically-based models that explicitly account for non-linearities in the plant-soil-environment interaction through detailed equations that describe soil-root water and often also nutrient dynamics, assimilate production, respiration and evapo-transpiration, light interception, and reproductive development (Boote et al., 2011; Challinor et al., 2009b) (see Sect. 2.3.2.3 and 2.3.2.4 for a more complete description of process-based models).

Significant structural differences exist between suitability and process-based models (Challinor et al., 2009b; Keenan et al., 2011), which stresses the need for both types of models outputs to be used in appropriate contexts. Even though research has been conducted earlier with regards to the agreement between empirical and process-based models, very little

research has been done that combines both approaches (Estes et al., 2013a; Morin and Thuiller, 2009; Serra-Diaz et al., 2013). However, the combination of both approaches is contingent on an appropriate understanding of the relationship between abundance (crop yield) and suitability, which can be contradictory: Pearce and Ferrier (2001) concluded that the positive relationship between probability of occurrence and abundance was artificially caused by the difference between occupied and unoccupied sites (extremes of suitability), and Nielsen et al. (2005) demonstrated that the environmental drivers of suitability are not the same as those of abundance. However, VanDerWal et al. (2009b) showed that suitability can be a good predictor of the upper level of abundance in a significant number of species in eastern Australia.

This chapter addresses Objective 4-B (Sect. 1.6). To that aim, observations of crop presence were used to parameterise the EcoCrop model. Baseline suitability predictions were first regressed against GLAM predicted yield and total production. The residuals of these regressions were then regressed against sub-seasonal groundnut-specific meteorological indicators. Future (i.e. RCP4.5, 2030s) simulations of crop suitability were performed and compared with yield impact estimates of GLAM (fully presented in Chapter 6). Finally, an analysis of possible niche expansion and/or contraction was performed in order to highlight areas where there could be potential for groundnut production in the future, or where groundnut production is expected to become unsuitable. The underlining hypotheses here are: (1) that suitability and a number of sub-seasonal climatic indicators can be used to predict crop yield and/or total crop production, (2) that such relationship leads to coherent projection of climate change impacts across both models, and (3) that given the coherent projection of impacts, the possible range expansion projected by EcoCrop can be used to define areas where the crop can be grown in the future.

7.3 Methodology

The approach followed in this chapter has four different steps:

- the parameterization and evaluation of the EcoCrop model for Indian groundnut using present-day climate and crop occurrence data;

- the comparison of EcoCrop present-day suitability and GLAM simulated potential production and the establishment of a relationship between the two biophysical measures; and
- the analysis of similarity between the projected climate change impacts by the two ensembles of model simulations: EcoCrop and GLAM.

7.3.1 EcoCrop calibration

The process herein termed model calibration is the process of determining ecological parameters for the crop to be modelled, based on crop presence data (Sect. 3.4.2.2) and 20^{th} century spatially explicit climatology data (CL_WC-QA, Sect. 3.4.1, Table 3.1). The aim of determining the ecological parameters is to explore the data using some basic statistical concepts and understand the ecological ranges of the crop. For this purpose, 80 % of the presence points were used to develop a set of ecological parameter sets, and the remaining 20 % of the points were used for selecting those that represented the crop's suitability most realistically.

For each of the data points in the EcoCrop calibration dataset (described in Sect. 3.4.2.2), the corresponding monthly temperature (maximum, minimum and mean) and precipitation data were extracted from CL_WC-QA (Table 3.1). Data were extracted only for those months that defined the crop growing season (as prescribed by the E-LGP dataset, Sect. 3.4.2.3). Using the monthly data, for each point, the mean, maximum and minimum of each of the temperature variables (i.e. maximum, mean, and minimum temperatures) were calculated. For precipitation, only the total across all months was computed over the prescribed growing season. This resulted in a set of 10 variables (9 for temperature and 1 for precipitation, each being a vector of $n = 1,464$ of occurrence points) that describe the growing season conditions under which the crop is typically grown. The maximum, mean and minimum values of T_{MIN}, T_{MAX}, and T_{MEAN} were then combined into one single vector. These data were then used to calculate different parameter sets as explained below.

In order to determine the crop ecological parameters, a probability density function (PDF) was first drawn using both the temperature and precipitation vectors (see Figure 7.1 for an example) and used as the base to derive a set of potential parameter sets. A 'reference

point' was chosen for each PDF as the point of highest likelihood of presence of the crop (i.e., the point at which the centre of the optimal conditions is expected, continuous vertical red line in Figure 7.1). Five temperature and four precipitation thresholds were extracted and assigned as the different ecological parameters to be used for running the EcoCrop model (Figure 7.1). The position of these thresholds was calculated using the proportional area under the PDF curve to each side of the reference point. For T_{KILL}, the minimum absolute temperature was used (i.e. 100 % area to the left of the reference point). For the remainder of parameters, various proportional areas were used in order to reflect uncertainty on the choice of thresholds. This allowed constructing a perturbed parameter ensemble.

Thresholds were carefully chosen so that the range between T_{MIN-C} (R_{MIN-C}) and $T_{OPMIN-C}$ ($R_{OPMIN-C}$) did not overlap with the range between $T_{OPMAX-C}$ ($R_{OPMAX-C}$) and T_{MAX-C} (R_{MAX-C}). Ranges chosen followed typical EcoCrop ranges (e.g. Ramirez-Villegas et al. 2013b 40 % and 80 %) but were broader so as to account for possible parameter variability. For temperatures, thresholds were equidistant from the reference point since the temperature PDF derived from the occurrence point followed a normal distribution. For minimum and maximum absolute temperatures (T_{MIN-C} and T_{MAX-C}) six equally-distanced values between 90 % and 100 % (to the left and right of the reference point, respectively) were used, and for $T_{OPMIN-C}$ and $T_{OPMAX-C}$ five equally-distanced values between 40 % and 60 % were extracted.

In the case of precipitation, the PDF followed a gamma distribution. The parameter selection thus had to take into account the skewness of the PDF, with values closer to the reference point for R_{MIN-C} and $R_{OPMIN-C}$, and values closer to the tail for R_{MAX-C} and R_{OPMAX}. R_{MIN-C} was thus given values at six equally-spaced positions between 85 % and 100 %, while $R_{OPMIN-C}$ was given values between 40 % and 60 % to the left of the reference point. R_{MAX-C} was defined between 97.5 and 100 % and $R_{OPMAX-C}$ adopted values between 85 % and 95 % to the right of the reference point. This procedure resulted in 30 potential parameter sets that were assessed for skill (see Sect. 7.3.2 below).

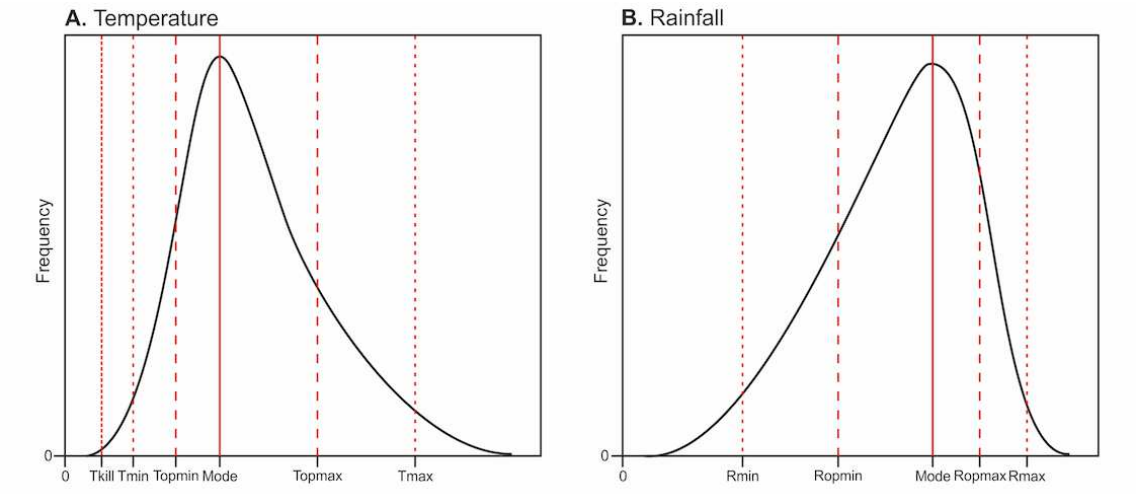

FIGURE 7.1: Example of parameter selection for the climate distribution of a particular crop for (A) temperature and (B) precipitation. Vertical red continuous line represents the highest frequency value of each distribution, long-dashed lines show the optimal parameter values, short-dashed lines show the marginal parameter values. Dotted line in (A) indicates T_{KILL}.

7.3.2 Parameter selection and model evaluation

A very first set of simulations was performed to evaluate the model with the independent district-level presence-absence data (described in Sect. 3.4.2.2). These simulations were conducted at 2.5 arc-minutes (CL_WC-QA) and 1 degree (combining CL_CRU-EC and CL_IMD-EC) resolutions (see Sect. 3.4.1, Table 3.1). The latter simulation is also referred to as control simulation –CTRL (Table 7.1). The skill of EcoCrop was assessed in order to develop a final parameter ensemble. The following measures of accuracy were computed:

- The omission rate (OR, Eqn. 7.1) was computed using the 20 % of testing points as the number of locations that fall in suitable areas (i.e. $SUIT > 0\%$) (n_{NZ}) to the total number of points (n).

$$OR = \frac{n_{NZ}}{n} \tag{7.1}$$

- The $RMSE$ equation (Eq. 3.46) was modified so that $O = 1$ for all locations (Eqn. 7.2).

$$RMSE = \sqrt{\frac{\sum_{i=1}^{n}(1 - P_i)^2}{n}} \tag{7.2}$$

where O_i is the predicted value and n is the number of points used for the calculation. EcoCrop yields an spatial prediction for a climatological mean and in consequence the $RMSE$ was calculated spatially –i.e. using all grid cells in the study area.

- The true positive rate (TPR, Eq. 7.3) as the number of pixels predicted as suitable by the model and marked as cropped in the evaluation data (NTP) to the total number of available pixels to assess (N_{TOTAL}). To calculate TPR, only suitable pixels (i.e. $SUIT$ >0 %) were used.

$$TPR = \frac{NTP}{N_{TOTAL}} \tag{7.3}$$

- The false negative rate (FNR, Eq. 7.4) as the number of pixels predicted by the model to not be suitable for the crop, but marked as cropped in the evaluation data (NFN) to the total number of available pixels to assess (with the same suitability threshold being used).

$$FNR = \frac{NFN}{N_{TOTAL}} \tag{7.4}$$

- The independent-evaluation area under the receiving operating characteristic (ROC) curve (AUC_I) was used as it is a threshold-independent measure of model accuracy (Peterson et al., 2008; Smith et al., 2013). AUC_I measures the ability of a model to discriminate between presences and absences by constructing a plot of the omission and the commission errors for a sequence of suitability thresholds (Peterson et al., 2008). Given that the absence of the crop is not purely driven by the environment, but is also dependent on other factors such as market access, commodity price, input availability, and culture (most of which are difficult to quantify in the models used here), the calculated AUC_I probably represents the lower bound of model performance. This also meant that neither the true negative nor false positive rates could be calculated.

A parameter was selected for the final ensemble of suitability simulations if it met the following two criteria:

1. The AUC_I in both high (2.5 arc-min) and low (1-degree) resolution simulations was above 0.7 (Warren et al., 2013).

2. Following Ramirez-Villegas et al. (2013b) the upper limits for OR and $RMSE$ were 0.1 and 0.5, respectively. A minimization of both OR and $RMSE$ values was not sought when assessing the preliminary suitability runs as it is not certain how suitable these environments are and therefore, in the comparison between the randomly selected known presences of the crop and the suitability surfaces it cannot be assumed that a presence point means the crop is 100 % suitable.

The TPR and FNR were not used since both measures were already contained in the AUC_I. Finally, a visual assessment of the suitability predictions was done by comparing these against the known distribution of the crop (Monfreda et al., 2008; Portmann et al., 2010; You et al., 2009).

7.3.3 Simulations of crop suitability

In addition to the BE-EVAL and BE-CTRL simulations (see above), the selected EcoCrop parameterisations were used to conduct two additional sets of simulations. The first set is referred to as the baseline simulations and used two sets of baseline climates: BE-RAW and BE-LOCI, both at a resolution of 1 degree (note that the BE-CTRL runs are also part of the baseline simulations). The second set of simulations used the future climate projections (P-RAW, P-LOCI, and P-DEL), all at a resolution of 1 degree. A summary of all simulations is given in Table 7.1.

7.3.4 GLAM simulated output

Since crop suitability is most likely to be related with the upper bound of crop productivity (see Sect. 7.2 and VanDerWal et al. 2009a), simulated GLAM yield and total production were taken to be the maximum possible in each pixel. Given that GLAM was optimised using the maximum yield per groundnut growing zone (see Sect. 5.3.2), simulations with $C_{YG} = 1$ would reflect the upper level of simulated yields (i.e. maximum potential farmer's yield) of each grid cell. $C_{YG} = 1$ simulations were hence used to assess the relationship between crop suitability, productivity and production.

GLAM's 28-year yield simulations were first averaged for each pixel and converted to total production by multiplying the crop yield times the observed mean harvested area. Crop

TABLE 7.1: Simulations performed in this chapter. All simulations, except BE-EVAL were performed at 1x1 degree resolution.

ID	Type	Description
BE-EVAL	Baseline	Simulation using CL_WC-QA at 2.5 arc-min for model evaluation
BE-CTRL	Baseline	Control simulation using observed climate data (baseline corresponding to the P-DEL simulations). Also used for model evaluation
BE-RAW	Baseline	Original GCM output (i.e. without bias correction)
BE-LOCI	Baseline	GCM output with Local Intensity Scaling on precipitation
P-RAW	Projection	Original GCM output (i.e. without bias correction)
P-LOCI	Projection	GCM output with Local Intensity Scaling on precipitation
P-DEL	Projection	GCM output with delta method applied to the means

yield (Y) and total production (T_P) values were then linearly scaled so that the minimum received a value of 0 and the maximum received a value of 1 (Eq. 7.5).

$$X_S = \frac{X_i - max(X)}{max(X) - min(X)} \tag{7.5}$$

where the subscript S indicates scaled value, i refers to each location within India, and X is either crop yield or total crop production. The maximum and minimum values were calculated using the time-averaged yield and production values of all grid cells.

7.3.5 Assessment of yield- and production-suitability relationships

As stated above, one of the objectives of this chapter was to compare estimates of crop suitability, productivity and total production. To that aim, four types of analyses were performed:

1. **Comparison of classes:** EcoCrop's scale was divided into 11 classes: values equal to zero and 10 equally-spaced classes (of 10 % range each class). A box plot with mean suitability and production values across classes was produced. Similarly, the scaled GLAM yield and production were divided into 11 equally-spaced classes. A box plot for each mean yield and production and suitability values was produced.

2. **Spatial similarity:** Similarity between simulations of both models was assessed by computing the relative rank score (RR) (Warren and Seifert, 2010). The RR measures ranges from zero to one and measures the probability that both models infer the same relative rank of any two randomly chosen locations, irrespective of the exact value of their normalised scores. RR was estimated by randomly sampling two points without replacement in geographic space (until all points were sampled) and then determining for each pair of points whether their ranking (i.e. point 1 has a larger value than point 2, or vice versa) was the same in both models. The number of successes was divided by the number of comparisons.

3. **Regressions:** GLAM simulated potential yield and total production were each regressed against suitability using three types of regressions: (a) linear, (b) log-linear, and (c) robust linear regression (Maronna et al., 2006). Only these three models were used since there was no evidence for a more complex fit (Vermeulen et al., 2013). Robust regression was used in order to assess the influence of outliers that may arise from errors in the structure of either EcoCrop or GLAM so as to be able to detect the yield-suitability signal more clearly (Serra-Diaz et al., 2013).

4. **Analysis of residuals:** Residuals of these three regressions were then used as dependent variables in a multiple regression against climatological means and standard deviations of 17 sub-seasonal agro-meteorological indicators (AMIs, Table 7.2) derived from GLAM's simulated daily output. These 17 variables were chosen as they provide a complete description of the main groundnut processes in GLAM (i.e. radiation absorption, crop development, water stress) in addition to intra-seasonal variability (temperature and precipitation coefficient of variation) and temperature and precipitation extremes (number of days above various thresholds). The time-means and standard deviations of each AMI were computed. This produced a total of 17 * 2 = 34 variables for the regressions.

   For all regressions, 100-fold leave-one-out cross-validation regressions were performed, and Akaike's Information Criterion (AIC) used to select the most parsimonious model in each fold. Interactions were not considered in the models and only quadratic terms were allowed (Lobell and Burke, 2010). This meant that a total of 34 * 2 = 68 potential predictors were initially used for the regressions. In order to avoid overfitting, the 100-fold cross-validated regressions were repeated only with those predictors whose

Table 7.2: Agro-meteorological indices used to explain the yield/production-suitability relationship.

Parameter	Name	Units
RD.0	Number of days with precipitation (precipitation > 0 mm)	days
RD.2	Number of days with more than 2 mm precipitation	days
RD.5	Number of days with more than 5 mm precipitation	days
RD.10	Number of days with moderate precipitation (precipitation > 10 mm)	days
RD.15	Number of days with moderate to high precipitation (precipitation > 15 mm)	days
RD.20	Number of days with high precipitation (precipitation > 20 mm)	days
HTS1	Number of days with maximum temperature above 34 °C	days
HTS2	Number of days with maximum temperature above 40 °C	days
TETR1	Number of days with maximum temperature above 35 °C	days
TETR2	Number of days with maximum temperature above 47 °C	days
RCOV	Coefficient of variation of growing season precipitation	mm
TCOV	Coefficient of variation of growing season temperature	C
ERATIO25	Number of days with ratio of actual to potential evapotranspiration below 0.25	days
ERATIO50	Number of days with ratio of actual to potential evapotranspiration below 0.50	days
ERATIO75	Number of days with ratio of actual to potential evapotranspiration below 0.75	days
EFF.GD	Total number of days in which days mean temperature is above 8 °C, minimum temperature is above 0 °C, and ratio of actual to potential ET is above 0.5	days
EFF.SRAD	Sum of solar radiation during days where mean temperature is above 8 °C, minimum temperature is above 0 °C, and ratio of actual to potential ET is above 0.5	W m^{-2}

either quadratic or linear form were present in at least 50 % of the initial regressions within the 100 initial regressions.

7.3.6 Patterns of agreement across future projections

Using the future projections of suitability, changes in suitability (ΔS) were calculated as the difference between projected future suitability and baseline suitability. Three comparisons were performed:

1. Spatially-explicit changes in climatic suitability as simulated by EcoCrop were compared across the 1-degree size grid cells of India with the changes in simulated yield.

Geographic patterns of agreement were used to identify areas where differences between suitability and productivity estimates differed, thus likely increasing impact uncertainties.

2. Following Ramirez-Villegas et al. (2013b), a comparison between future projections of EcoCrop, those of GLAM (Chapter 6) and those reported in previous studies was performed. To that aim, a compilation of existing studies assessing climate change impacts on groundnut crop yields in India was done in order to assess the agreement of previous estimates with those of EcoCrop. Estimates of future changes in crop yields from the studies of Lobell et al. (2008) (LO2008); Challinor et al. (2007) (CH2007); Challinor and Wheeler (2008b) (CW2008); Challinor et al. (2009a) (CH2009) and Singh et al. (2012) (S2012) were plotted for comparison with the simulations of this thesis. It must be noted, though, that it is difficult to quantitatively compare results from other studies mainly because they used (a) a different emissions scenario, (b) a different set of GCMs, (c) a different time period, or (d) a combination of (a), (b) and (c).

3. Using the future projections of suitability, the possible expansion / contraction of groundnut suitable areas was assessed using a threshold of suitability determined by examining the ROC curve constructed in Sect. 7.3.2. The threshold used here is often referred in the niche-modelling literature as the "max SSS", which is the maximum sum of sensitivity and specificity, or in other words the top-leftmost point of the ROC curve. This threshold was chosen due to its demonstrated performance in the niche-modelling literature (see Liu et al. 2013). Areas below such threshold both at present and in the future were considered as unsuitable, whereas areas above the threshold were considered as suitable. Since future harvested area cannot be estimated with GLAM and was hence assumed to remain constant by 2030s, the direction of yield changes is the same to that of changes in total production. Thus, only crop yield changes were analysed in areas that either become suitable or unsuitable by 2030s.

7.4 Results

7.4.1 Baseline suitability simulations

7.4.1.1 Skill of suitability simulations

Figure 7.2 shows the FPR, FNR and AUC_I values for low (1x1 degree) and high (2.5 arc-min) resolution baseline simulations. A total of 18 (60 %) of the ensemble members were highly accurate (i.e. $OR < 0.1$ and $RMSE$ between 0.25 and 0.5) and showed an $AUC_I < 0.7$. Omission rates were in the range 1 to 6 % for all ensemble members. There was some overlap in the upper bound of the $RMSE$ range for both sets of ensemble members, with $RMSE$ values between 0.21-0.38 for all ensemble members. AUC_I varied between 0.67 to 0.74, with slightly lower values for the low-resolution simulations. Values of TNR were in all cases above 90 %, while FNR values were between 1 and 10 %.

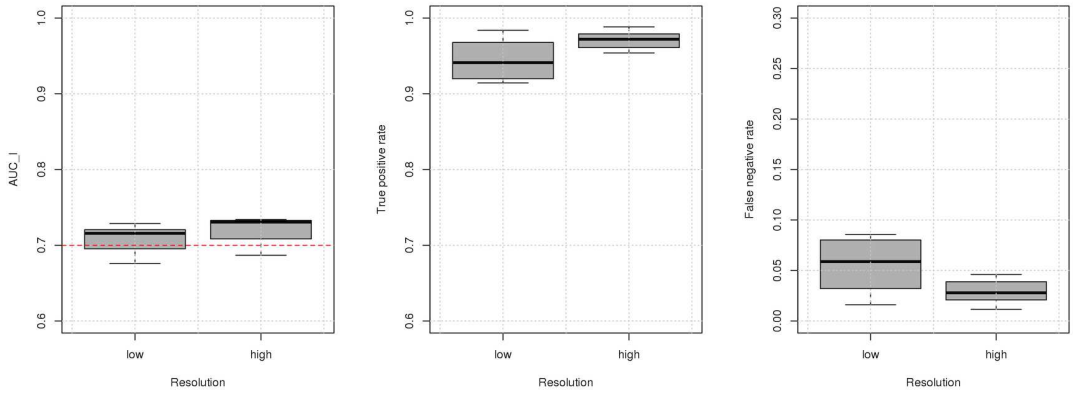

(a) AUC_I (b) TPR (c) FNR

FIGURE 7.2: Results of independent evaluation of EcoCrop: (a) AUC_I, (b) true positive rate, and (c) false negative rate.

The rather small differences between the two spatial resolutions at which simulations were conducted indicated that the up-scaling of input data had little impact on model skill. Some differences were observed between selected and discarded ensemble members at both resolutions (Figure 7.3), particularly in eastern India and some parts of central India, where groundnut is grown less intensely or is totally absent. The discarded ensemble members indicated very high climatic suitability.

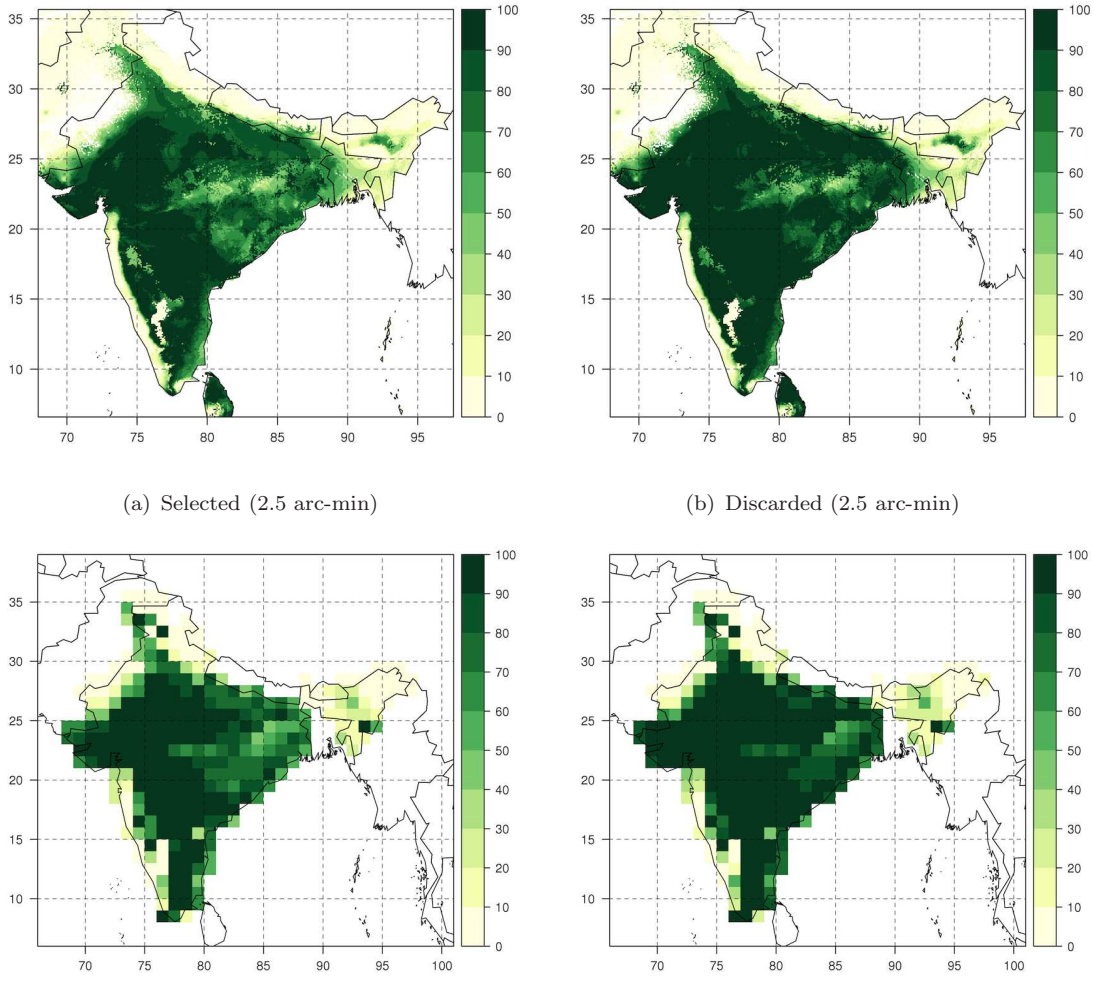

(a) Selected (2.5 arc-min)

(b) Discarded (2.5 arc-min)

(c) Selected (1x1 degree)

(d) Discarded (1x1 degree)

FIGURE 7.3: Mean crop suitability across selected and discarded EcoCrop ensemble members at 2.5 arc-minute (a, b) and 1x1 degree (c, d) resolutions.

Significant agreement was observed between EcoCrop's simulated suitability and the reported area harvested of the crop (Figure 7.4). The areas where the crop is most intensively grown are located in the states of Andhra Pradesh (southern) and Gujarat (western). These match the high suitability areas of the model predictions.

Values for model parameters are shown in Figure 7.5. These indicated that low temperature constraints may arise if minimum monthly temperatures go below 5 °C [-4 °C = 1], is not suited if mean temperatures are below 11.3 ± 3.3 °C, thrives optimally between 21.2 °C and 29 °C and is heat stressed if temperatures are above 34.7 ± 1.5 °C. Regarding precipitation, the crop is harmfully stressed if the total rainfall during the growing season

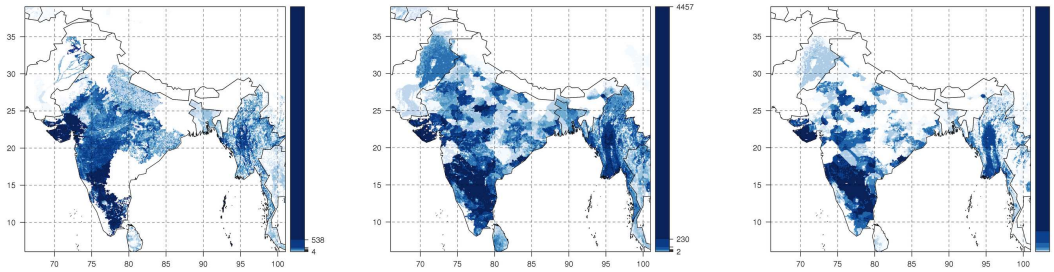

(a) SPAM (b) MIRCA2000 (c) Monfreda

FIGURE 7.4: Harvested area as reported by different spatial datasets: (a) spatial allocation model (SPAM) (You et al., 2009); (b) MIRCA2000 (Portmann et al., 2010); and (c) Monfreda et al. (2008).

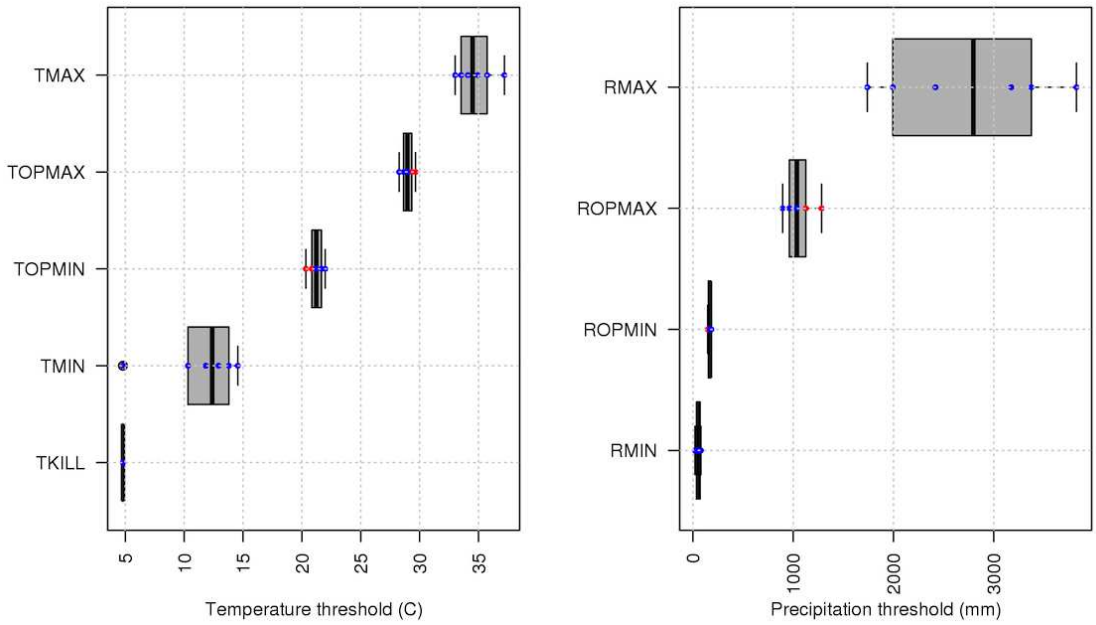

(a) Temperature (b) Precipitation

FIGURE 7.5: Values adopted by temperature (a) and precipitation (b) EcoCrop's model parameters. Blue dots represent selected parameter sets, and red dots represent parameter sets that were deemed not accurate enough according the $RMSE$, OR and AUC_I (Fig. 7.2).

is less than 53 ± 21 mm (drought) or above 2,754 ± 780 mm (excess water, or waterlogging). Groundnut develops best between 170 and 1,036 mm of rainfall during the growing season.

7.4.1.2 Modelled productivity- and production-suitability relationships

Boxplots of yield and production across suitability classes are shown in Figure 7.6. This exploration of spatially-explicit suitability and potential yield and production simulations indicated that, as expected, simulated normalised production increased across suitability classes. High normalised production was never found within low suitability areas (i.e. $<$ 15 %). Nevertheless, the same was not observed for crop yields, which tended to stay constant or to decrease at values of suitability above 30 %.

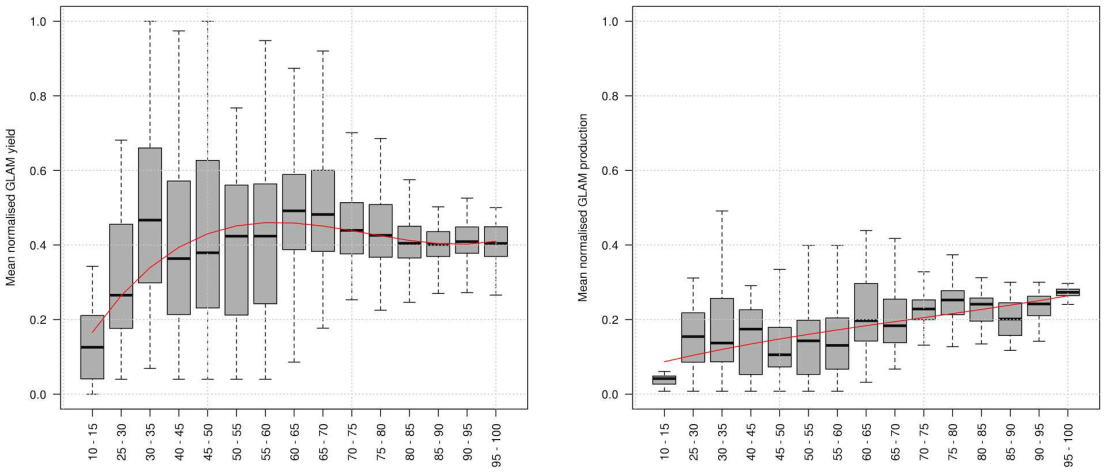

(a) Yield (b) Total production

FIGURE 7.6: Variation of (a) mean normalised GLAM yield, and (b) mean normalised GLAM production across equally-spaced suitability classes. Spread in the boxplots arises from combinations of individual EcoCrop and GLAM ensemble members. Black horizontal lines represent the median of each class, boxes enclose 25-75 % of the data and whiskers represent the 5-95 % percentiles. The red continuous line is a spline with 3 degrees of freedom fitted through the medians.

The variation of suitability across GLAM potential yield values indicated that high productivity values are as likely as low productivity values to be associated with low crop suitability (Figure 7.7). Conversely, at high suitability classes (i.e. $>$ 80 %), extremely low values of crop production were rarely found. There were a number of suitability classes that presented a mixture of high and low normalised production values, indicating that climatic suitability alone may not be the only predictor of crop production. Values of suitability in general showed decreasing variance for higher production classes. The fact that a large spread of values was found in various classes highlighted the importance of other factors driving the presence and actual production of the crop in the different areas.

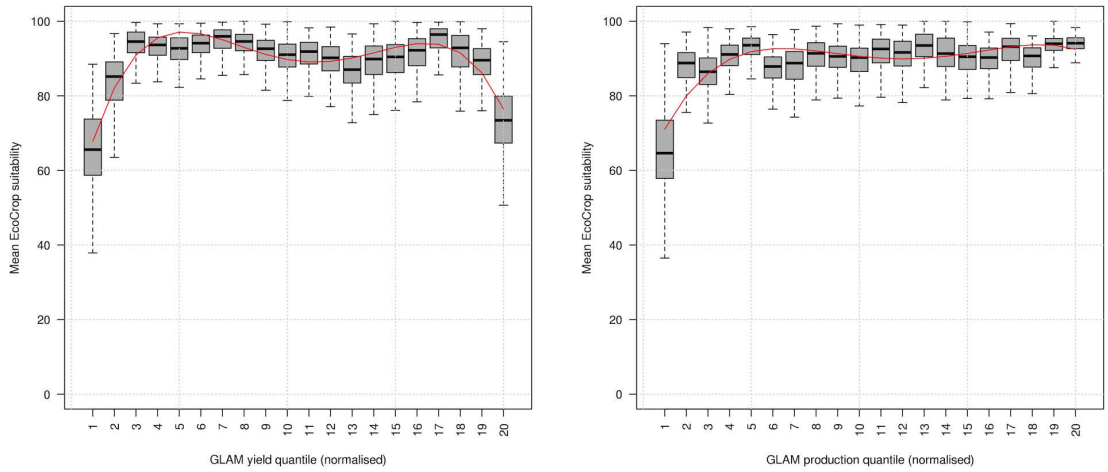

(a) Yield (b) Total production

FIGURE 7.7: Relationship between suitability and equally-spaced values of (a) mean normalised GLAM yield, and (b) mean normalised GLAM production. Additional details as in Figure 7.6.

As stated above, the next step in the comparison of both models was the spatial comparison of their predictions. The relative rank score –a measure of how similar is the ranking of sites for the measures in question, is shown in Figure 7.8. In general, greater similarity between suitability and total production was observed. The RR varied between 0.38 and 0.65 for total production (mean=0.54), whereas it varied between 0.25 and 0.6 for crop yield (mean=0.45). This result confirmed the fact that an stronger relationship was to be found between suitability and total production, and not yield. For total production, the two measures agreed, on average, in roughly 50 % of the cases when ranking locations, at least 20 % more than the measured spatial agreement between suitability and crop yield.

The final step when comparing suitability, yield and total production was to regress suitability against both total production and yield. Figure 7.9 shows a scattergram of predicted baseline suitability to productivity (Figure 7.9(a)) and also suitability to production (Figure 7.9(b)). The relationship between crop yield and suitability was unclear, with both low and high values of crop yield occurring along the whole range of suitability. Conversely, the relationship between total crop production and suitability occurred as expected. This is, in general, low values of suitability were never associated with high or even moderately high values of crop production. Similarly, the range of production values increased across the suitability scale, with the highest values of suitability (i.e. $>$ 90 %) showing a large spread of production values. This result indicated that low crop production occurs mainly

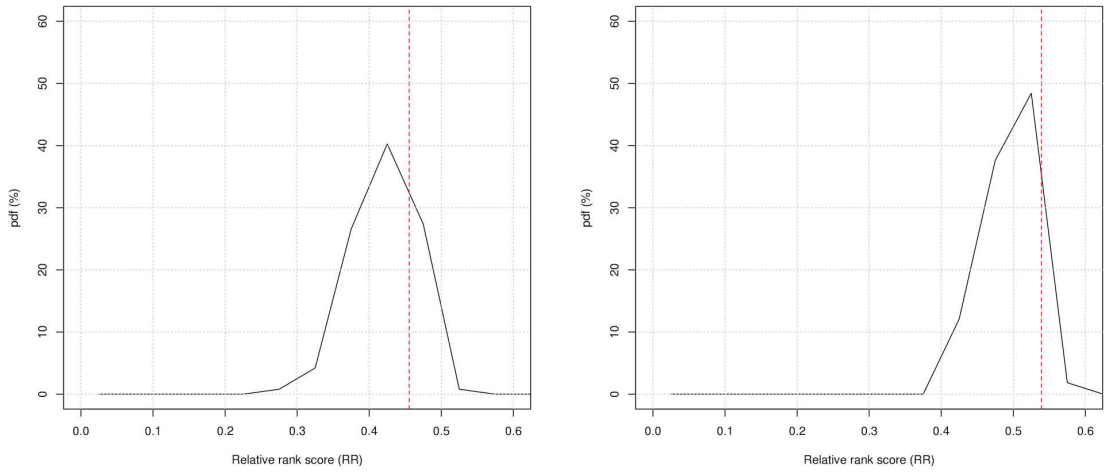

(a) Yield (b) Total production

FIGURE 7.8: Spatial similarity between EcoCrop and GLAM's simulations as measured by the relative rank score (RR) for (a) crop yield and (b) total crop production (yield * area harvested). PDFs are formed using paired comparisons of all ensemble members of EcoCrop and GLAM. Vertical lines show the comparison of the ensemble means of each model.

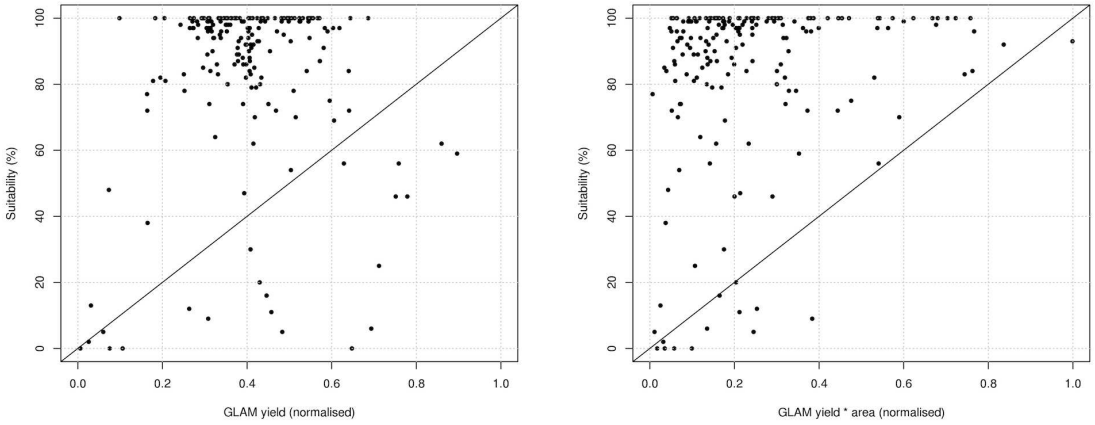

(a) Yield (b) Total production

FIGURE 7.9: Scatterplot of the ensemble mean suitability (x-axis) and GLAM simulated yield (a) or total production (b).

because of lack of climatic suitability to grow the crop, but that at high climatic suitability crop production can be either high or low –owing to a variety of reasons, including market preferences, pests and diseases, or crop management.

Regressions of suitability and production in all cases indicated that there is a strong and statistically significant relationship between the suitability of a crop as simulated by

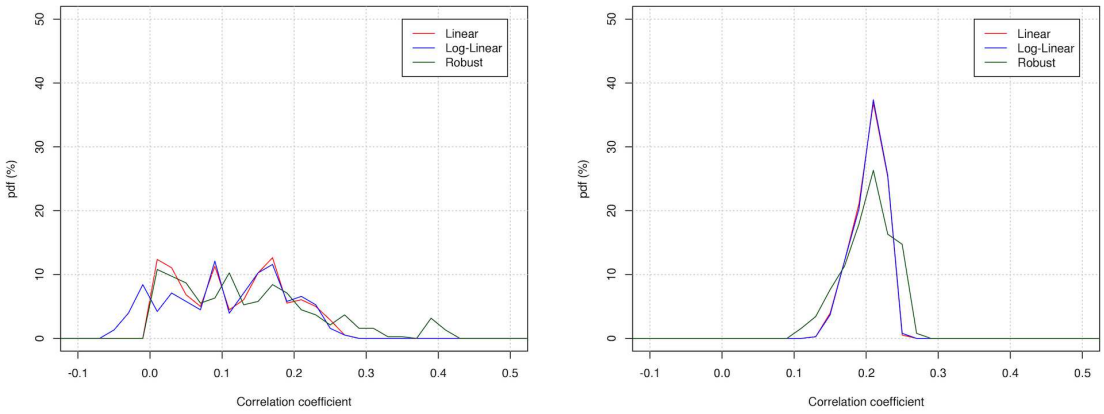

(a) Yield (b) Total production

FIGURE 7.10: PDFs of the leave-one-out cross-validation correlation coefficient of the regressions between (a) suitability and yield, and (b) suitability and production. Only for total production (b) all correlation coefficients were significant at the p<0.05 level. PDFs are formed by all combinations of GLAM and EcoCrop ensemble members, including the mean.

EcoCrop and the normalised production as simulated by GLAM (Figure 7.10). Pearson's product-moment correlation coefficient of these regressions as assessed by leave-one-out cross-validation varied between 0.1 and 0.3 for total production, but it was very low, negative and not statistically significant ($p < 0.05$) in many cases (see Figure 7.10(a)). For total production, even though the correlation coefficient was not very high, it was statistically significant in all cases ($p < 0.05$), whereas the same was not observed for crop yield. The relatively low (i.e. < 0.5) correlation coefficients in these regressions implies that a significant portion of the variance in the normalised GLAM production could not be explained by EcoCrop's climatic suitability. This suggested that additional factors needed to be taken into account in order to assess total production variations.

The slope of the production vs. suitability regression was in all cases positive and varied from 0.05 to 0.25 [in units of normalised production divided by fraction suitability], with higher values for the simple linear regressions. Importantly, the result is consistent across all combinations of ensemble members, the ensemble means, and the three regression methods. The same was not observed for crop yields, in which case the slope of the three types of regressions was negative in more than 50 % of the cases, particularly for the linear regressions. Since the relationship between suitability and yield was unclear and non-existent in many cases, all following analyses were only performed for total production.

7.4.1.3 Unexplained suitability-production variance and sub-seasonal weather variations

Regressing the residuals of the suitability-production regressions resulted in the identification of key sub-seasonal variability descriptors that allowed a robust prediction of crop production on the basis of suitability. Out of the total 68 potential predictors, the mean and standard deviation of the heat-stress AMIs (i.e. $TETR1$, $TETR2$, $HTS1$ and $HTS2$) and their quadratic forms had very low variance and were thus statistically insignificant in all regressions. This reduced the total number of predictors to 52. Figure 7.11 shows the PDF of the correlation coefficient for multiple regressions between suitability-production residuals and the 17 AMIs of Table 7.2. The continuous lines show the bootstrapped correlation coefficient for the initial regressions containing the remaining 52 potential predictors (step-wise selected using AIC), with colours indicating the three different sets of residuals (from linear, log-linear and robust regressions). The dashed lines show the bootstrapped correlation coefficient for the final regressions, in which only those AMIs that were present in at least 50 % of the initial 100 cross-validated folds were used.

Agro-meteorological indices (AMIs) explained a large amount of the variance in the residuals of the suitability-production relationships described above. Using all possible terms in the multiple regression (continuous lines in Figure 7.11), around 40-80 % of the variance in the residuals was explained. However, using all AMIs and their quadratic transformations (i.e. a total of 52 possible predictors) also produced large variation in the correlation coefficient across the bootstrapped trials. Out of the 52 potential predictors in the initial regressions, 23 (44 %) were present in 50 % or more of the bootstrapped trials (linear residuals). A lower number of predictors showed a frequency above 50 % for log-linear (19 predictors, 36 %) and robust (20 predictors, 38.4 %) regressions. Among these predictors the time-mean coefficient of variation of total precipitation (RCOV, present in 90-94 % of the bootstraps) was the most important one, followed by the time-mean number of days with extreme water stress (ERATIO25, 86-91 %). The temporal standard deviation coefficient of the temperature coefficient of variation (TCOV) was present in 76-90 % of the bootstraps, while the temporal variability in effective solar radiation (EFF.SRAD, 72-86 %), the time-mean effective number of growing days (EFF.GD, 69-86 %), and the square of ERATIO25 (80-82 %) were also highly important for the three types of regressions. Conversely, the number of rainy days (RD.0), the number of days with precipitation above

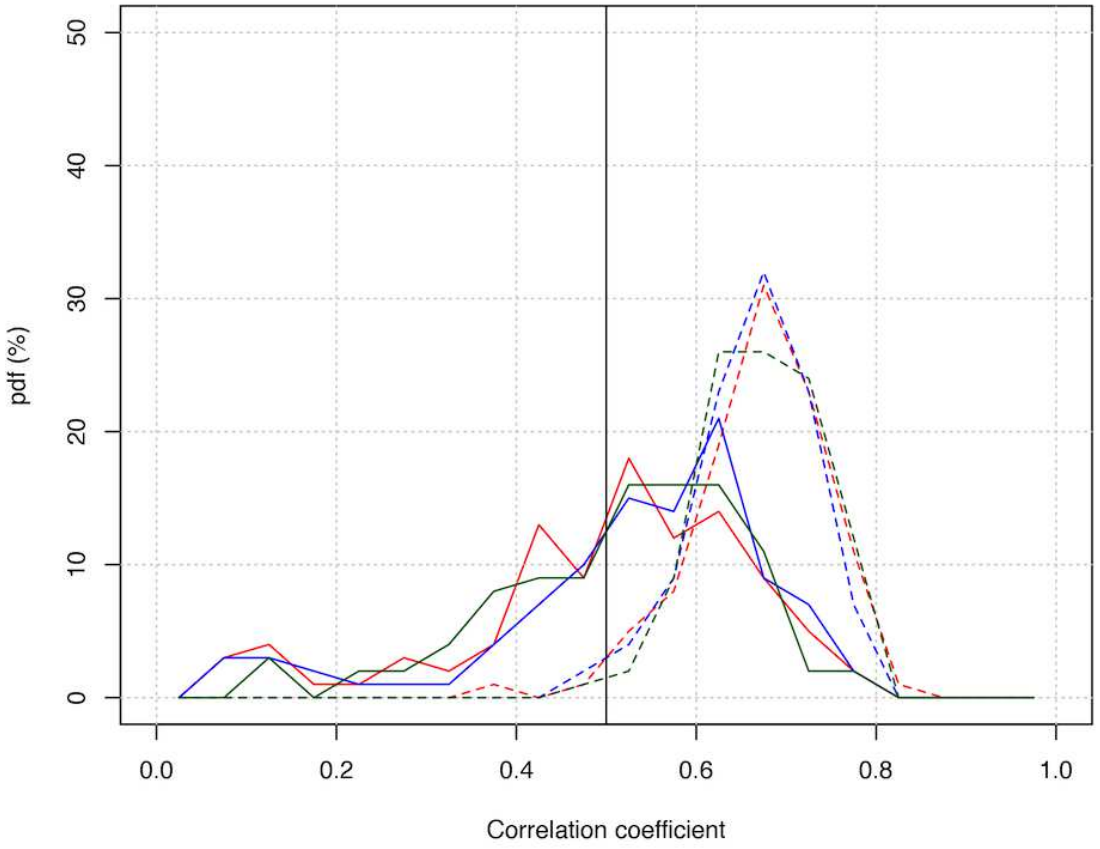

FIGURE 7.11: Results of multiple regressions between residuals of linear (red), log-linear (blue) and robust (green) regressions and the agro-meteorological indices (AMIs) listed in Table 7.2. PDFs are the result of 100 bootstrapped samples. Continuous lines correspond to the first iteration (i.e. where all AMIs were used) and dashed lines correspond to the second iterations (i.e. where only AMIs occurring in > 50 % of the bootstraps of the first iteration were used).

2 mm (RD.2) and 20 mm (RD.20), as well as their squared transformations were present in less than 30 % of the bootstraps. The results were consistent across the three types of residuals (i.e. linear, log-linear and robust).

Permutation importance was calculated for the final set of multiple regressions. Permutation importance is often used to measure variable importance in an statistical model (Altmann et al., 2010). To calculate permutation importance, each of the predictors in the models was separately randomised. A model prediction was made each time and the result then compared with the original prediction (i.e. the one with true values for predictors) using the Pearson product-moment correlation. Permutation importance was calculated as 1 minus the correlation coefficient. Figure 7.12 shows the permutation importance for

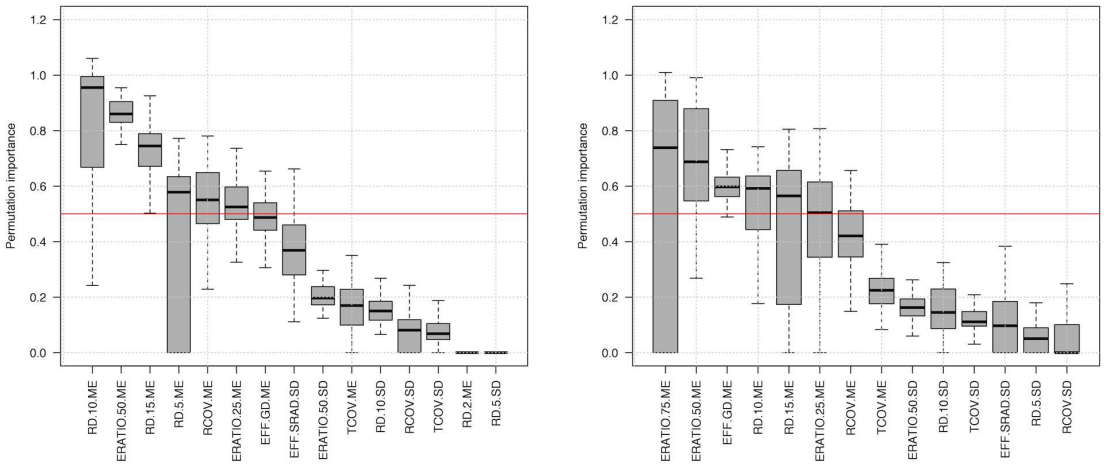

(a) Linear (b) Robust

FIGURE 7.12: Permutation importances of predictors in multiple regressions between residuals of linear (a) and robust (b) suitability-production regressions and AMIs. Names of predictors are given in Table 7.2. The labels "ME" and "SD" at the end of the name of the predictor indicate time-means or standard deviations, respectively.

all selected variables in the second iteration of the multiple regressions. Results indicated that the most influential variables in the models were the time-means of the number of days with precipitation above 10 mm (RD.10), 5 mm (RD.5) and 15 mm (RD.15), the number of days with $^{Ea}/_{Ep}$ ratio below 0.5 (ERATIO.50), the coefficient of variation in seasonal precipitation (RCOV), the number of days with $^{Ea}/_{Ep}$ ratio above 0.25 (ERATIO.25). The least important variables were generally related to interannual variations of the same predictors (Figure 7.12). These results were consistent across the different regression residuals (i.e. linear, log-linear and robust).

Predictors were also found to have consistent coefficients across the bootstraps, the two iterations and the three different regression residuals. Such coefficients were also sensibly related to the residual values. For instance, the intra-seasonal precipitation variability (RCOV) always had a positive coefficient (ranging between 0.1 and 1.53), indicating that large positive residuals (which occur when the normalised production is larger than predicted by the suitability-production regression) are typically associated with more variable precipitation (i.e. less uniform) during the growing season. This is probably due to the occurrence of larger-than-normal precipitation (i.e. $>$ 10 to 20 mm day^{-1} events) that provide soil moisture for relatively long periods of time. This is confirmed by the fact that the time-mean number of days with precipitation above 15 mm also showed positive

coefficients. Similarly, the number of days with extreme water stress (ERATIO.25) showed negative coefficients (-0.01 to -0.05), indicating its association with the negative residuals that occur when actual production is below the prediction of the suitability-production regression.

7.4.2 Impacts of climate change on crop suitability

Figure 7.13 shows the projected impacts of 2030s climate conditions on crop suitability as a function of the different bias correction methods (Table 7.1). Average projected changes in suitability were in the range -34 to 16 % (P-DEL), -19 to 13 % (P-RAW) and -26 to 20 % (P-LOCI). Crop suitability was projected to decrease in the majority of areas, with the most significant decreases occurring in the north-western and the western regions. The western region has the largest area harvested across the country. These results were consistent across the three bias correction methods, though the extent of the change was greater for P-DEL simulations. In the west of the eastern part of India, where groundnut is currently less intensely grown (as compared to the west and south of India), changes in suitability were positive. Central India depicted a relatively uncertain outcome, though with a greater proportion of simulations indicating negative impacts.

Even though significant variation was observed across ensemble members owing to the different parameter sets and GCMs used, robust signals were found in certain areas of India. Probabilities of exceeding 10 % change in suitability are shown in Figure 7.14. The probability of exceeding -10 % change in suitability was 80 % or more in the western part of India and in some areas of the south-eastern coasts, particularly for P-DEL simulations. Similarly, moderate (30-50 %) probabilities of increases in suitability were found in central India, with significant differences across bias correction methods.

Figure 7.15 shows the importance of temperature and precipitation for future suitability projections. The top row shows the proportion of model simulations (with respect to the total number of simulations that showed negative changes in suitability) in which changes in temperature-related suitability (T_{SUIT}) were larger than changes in precipitation-related suitability (R_{SUIT}). The bottom row shows the proportion of simulations in which changes in R_{SUIT} were larger than changes in T_{SUIT}. In all cases, negative changes in crop suitability entailed changes in both T_{SUIT} and R_{SUIT}, indicating that crop suitability was

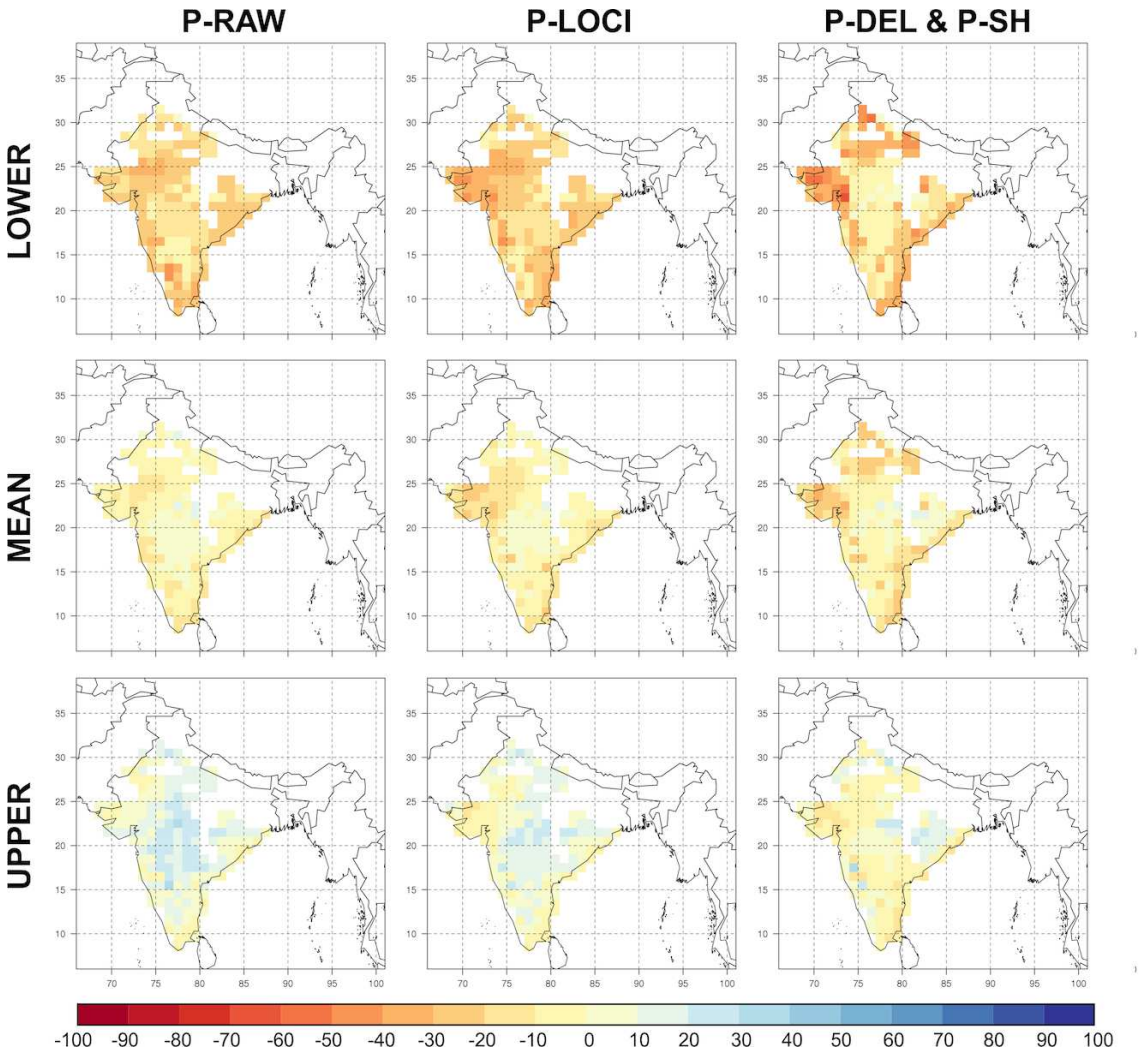

FIGURE 7.13: Impacts of climate change on groundnut suitability as predicted by the EcoCrop model. Each row shows a different statistical feature of the ensemble of 18 parameter sets and 32 GCM simulations. Lower: the lower quartile (bottom 25 %), mean: average of all simulations, and upper: the upper quartile (top 25 %). Each column refers to a method of bias-correcting the climate model output (see Table 7.1).

sensitive to changes in both variables. Across most of India, increases in growing season temperature were the most prominent cause of negative effects, with more than 70-100 % of the simulations showing more drastic drops in T_{SUIT} than drops in R_{SUIT} for most grid cells. However, precipitation was highly important for some areas in the very eastern, the centre and at the south-west coast.

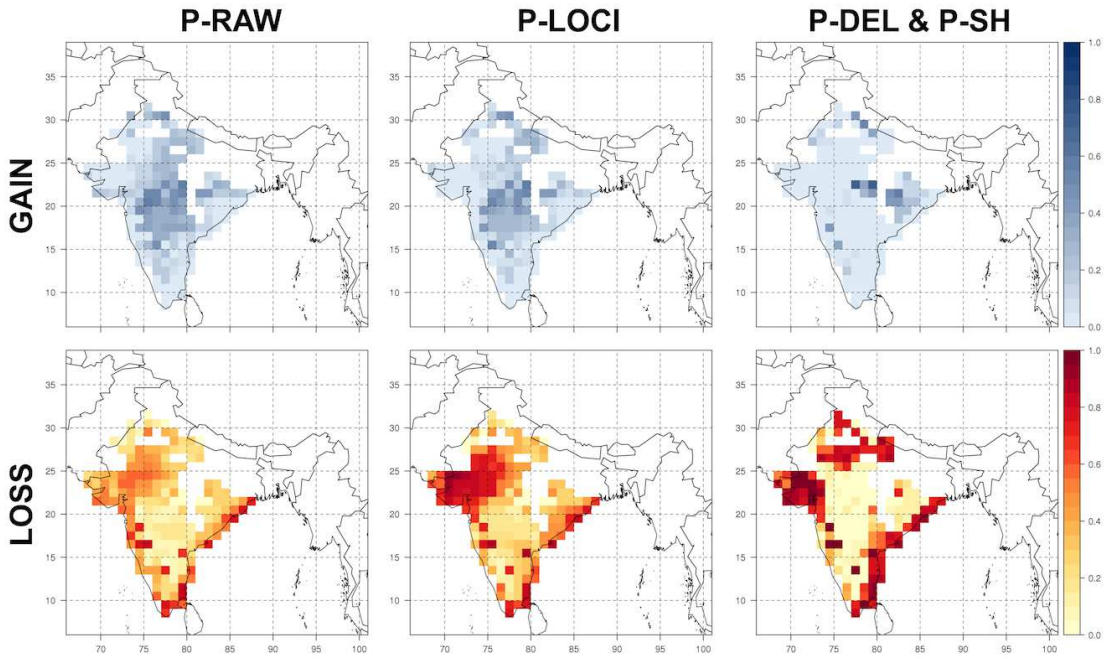

FIGURE 7.14: Probability of exceeding 10 % positive (top row) or negative (bottom row) change in crop suitability with respect to the baseline. Each column refers to a method of bias-correcting the climate model output (see Table 7.1).

7.4.3 Uncertainty in projections of crop suitability

As has been reported earlier in this thesis, climate uncertainty plays a very important role in crop simulation under future scenarios (see Chapter 6). As done in Chapter 5 for GLAMs yield simulations, uncertainty in future suitability was decomposed herein (Figure 7.16). Only model parameters and input climate data were investigated as sources of uncertainty since for EcoCrop these are the most relevant inputs to the model. For future projections of crop suitability, the contribution of climate uncertainty to total uncertainty was above 50 % for all bias correction methods. Fractional climate uncertainty was remarkably high for P-RAW and P-LOCI simulations (> 80 %), indicating that the noise that arises from climate model structure is very high even for climatological averages of both temperature and precipitation (also see Joshi et al. 2011 and Forster et al. 2013). The contribution of climate to total uncertainty decreased from left to right of Figure 7.16, as more variables were bias corrected in P-DEL with respect to P-LOCI, and in P-LOCI with respect to P-RAW.

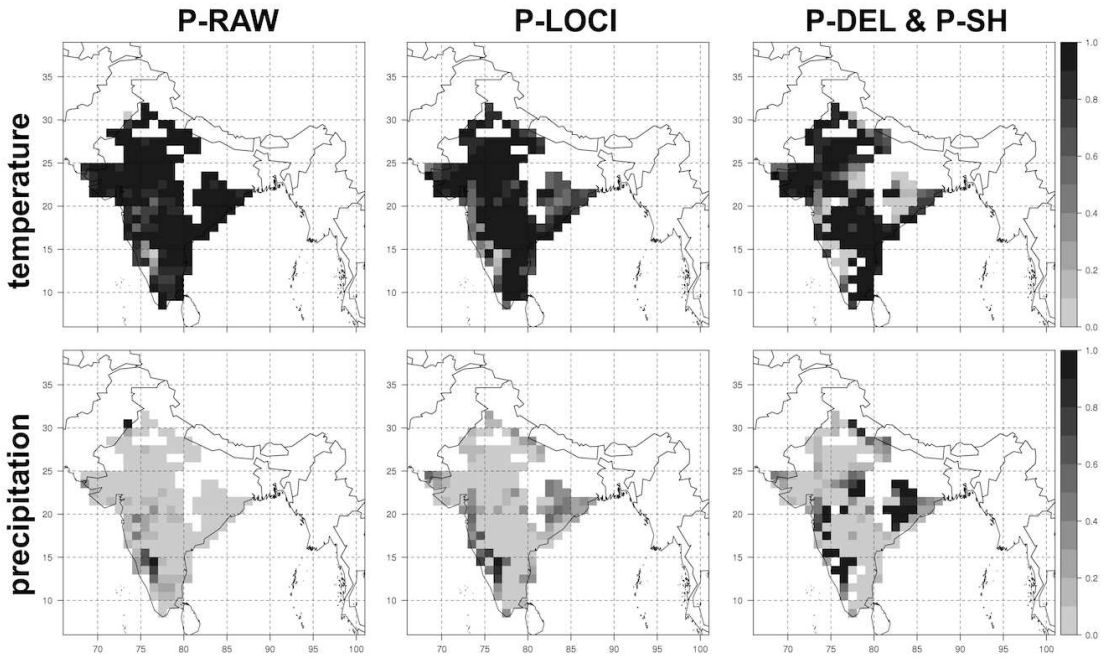

FIGURE 7.15: Importance of temperature and precipitation in EcoCrops projected future suitability. The top row shows the proportion of ensemble members that show larger decreases in temperature-related suitability (T_{SUIT}, Eq. 3.43) as compared to precipitation-related suitability (R_{SUIT}, Eq. 3.44) to the total number of ensemble members that show decreases in suitability. The bottom row shows the proportion of ensemble members that show larger decreases in precipitation-related suitability to the total number of ensemble members. Columns indicate different bias-correction methods (see Table 7.1).

7.4.4 Implications of suitability changes for major growing regions in India

At the sub-national and national level, average suitability changes depicted different degrees of agreement across the ensemble of model simulations (Figure 7.17). The north-west and west of India show in all cases a higher likelihood of negative changes, peaking at a decrease of 10 to 20 % in crop suitability. The central zone depicted an uncertain response, with slightly higher likelihood of negative changes. In this region, changes were much lower in extent than those in the west and north-west. In the southern and south-eastern zone, P-DEL simulations showed negative changes, whereas P-RAW and P-LOCI showed two peaks –one in the positive side and other in the negative side.

In most regions the differences stemming from the use of different bias correction methods did not alter significantly the direction of the change. The use of raw temperature or precipitation data changed the direction or the likelihood of either negative or positive

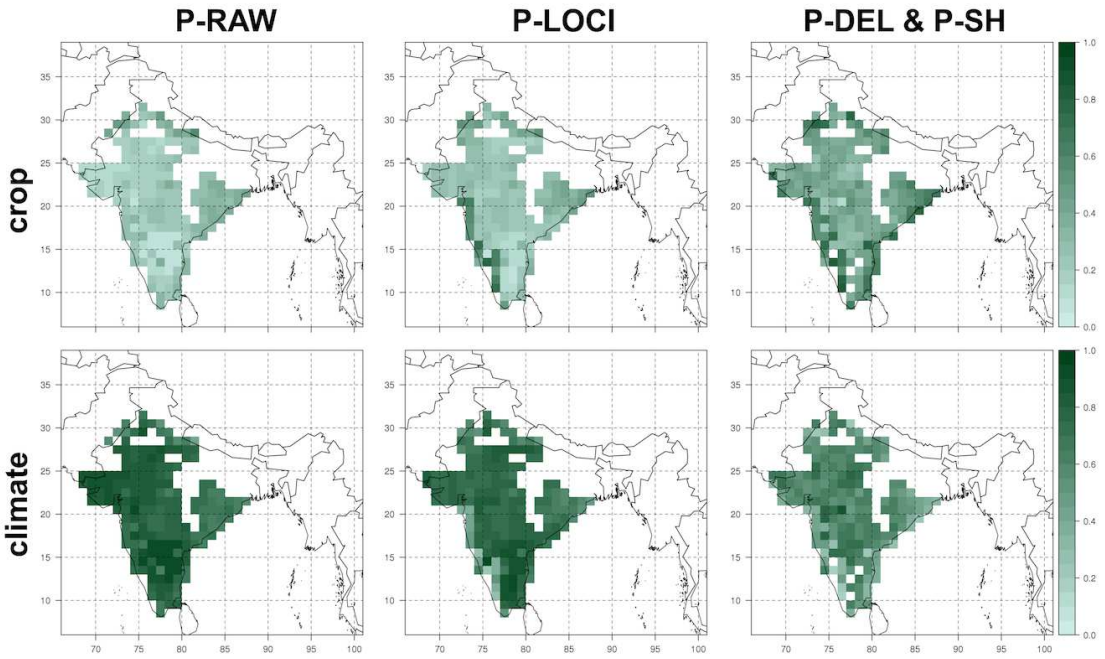

FIGURE 7.16: Contribution of crop model parameters (top row) and climate model structure (bottom row) to total uncertainty in suitability. Each column refers to a method of bias-correcting the climate model output (see Table 7.1).

climate change impacts. In the north-west, correcting precipitation increased the likelihood of negative impacts. For this region, further increases in the likelihood of negative effects were observed if both GCM temperature and precipitation data were corrected. The western region showed substantial similarities between P-DEL and P-LOCI, indicating that robustness was mostly contingent on precipitation responses. Conversely, the central and south-eastern zones depicted high similarity between the P-LOCI and P-RAW, whilst P-DEL showed a PDF shifted to the right (positive impacts) and thus a response that was much more contingent on the EcoCrop ensemble member used. In the southern region, P-LOCI and P-RAW showed a similar response –with a general trend for suitability loss, whereas P-DEL depicted more substantial suitability losses.

7.4.5 Agreement in impacts projections

A comparison was performed between the projected changes in crop suitability and the projected changes in crop yields presented in Chapter 6. Sub-national comparisons indicated very little agreement between the models in all areas except central India, where

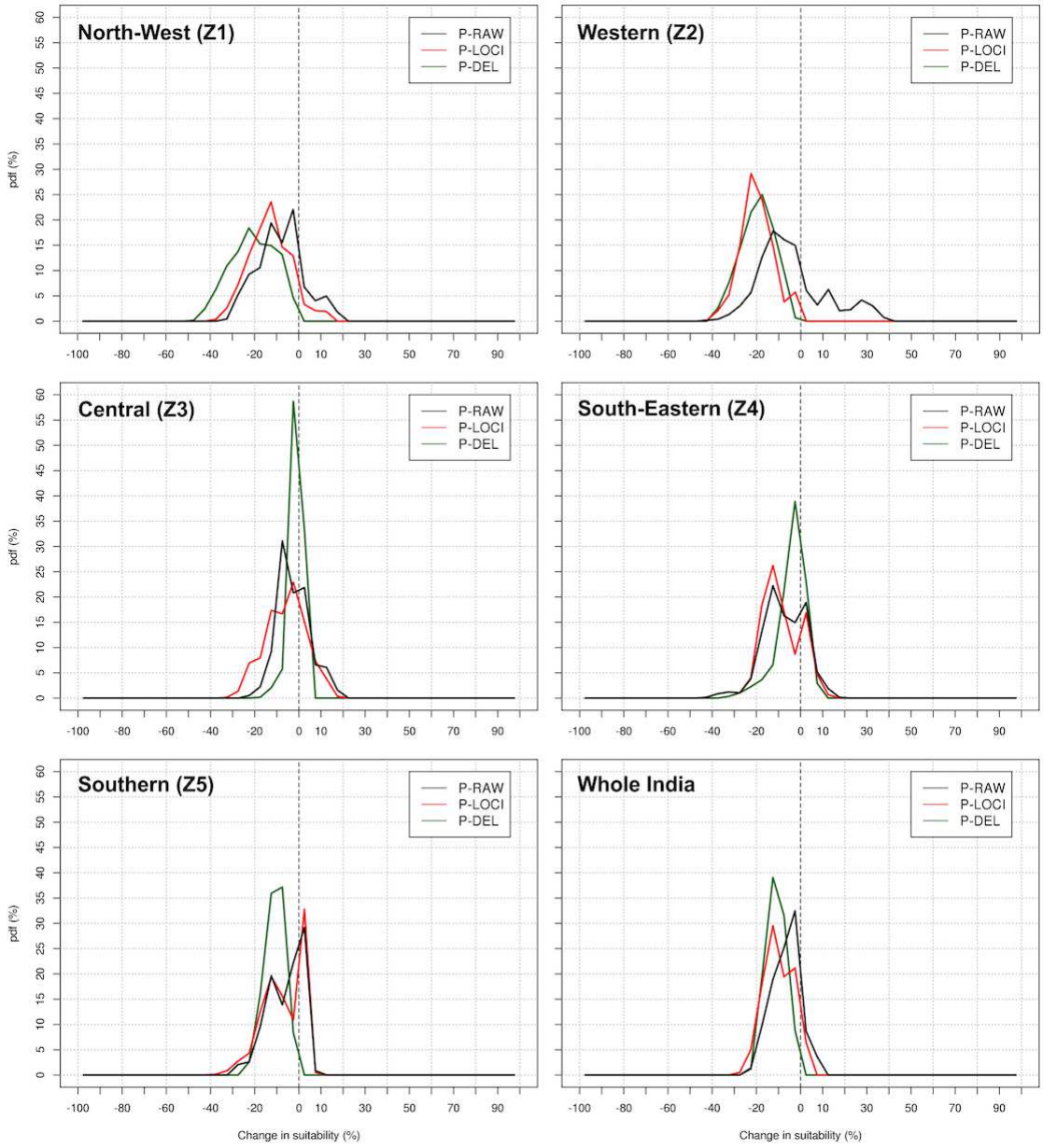

FIGURE 7.17: Probability density functions of changes in mean suitability across various regions of India and in the country as a whole. Sub-national-level changes were computed following the growing zones defined in Figure 3.2 (Chapter 3). Lines indicate different bias-correction methods (see Table 7.1).

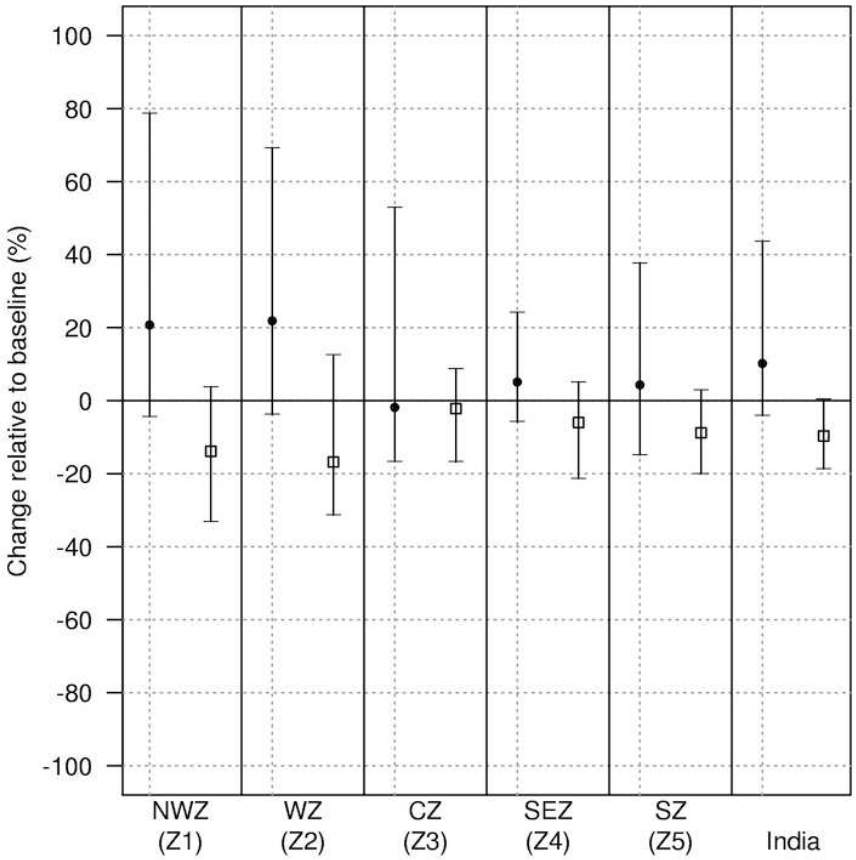

FIGURE 7.18: Projected changes in groundnut crop yield (filled circles) as simulated by GLAM and suitability (hollow squares) as simulated by EcoCrop. Each of the regions and the whole country of India are shown. Dots show the median and bars extend to 5-95 % of the data. The spread in GLAM results arises from the ensemble of runs described in Chapter 5, whereas the spread in EcoCrop results arises from multiple crop ecological parameter ensemble, GCM simulations and bias-correction methods. Naming of zones follows that of Figure 7.17: NWZ (North-western), WZ (Western), CZ (Central), SEZ (South-Eastern), and SZ (Southern).

the mean of both ensembles indicated negative impacts (Figure 7.18), though with large dispersion toward the positive side in the case of GLAM (also see Figure 6.9). In addition, there was significant spread in both model ensembles (particularly in GLAM's), and this caused some overlap in the projections of both ensembles for the south-eastern and the southern zone. Nevertheless, changes in the main producing areas of the west of India were in almost complete disagreement: while GLAM's ensemble projected a median change of +20 % (varying from -5 to 80 %), EcoCrop's ensemble projected a median change of -16 % (varying from 5 to -35 %).

With respect to previous estimates of climate change impacts on groundnut, at the country-level, agreement was significant only with Challinor et al. (2007) [CH2007], although in that case CO_2 fertilisation was not accounted for and projections are for the year 2100. In addition, even though the Lobell et al. (2008) [LO2008] study assessed an area larger than India using a statistical model, differences were not too large (see Figure 7.19). In central India (CZ), agreement between previous studies and the simulations presented in this chapter and in Chapter 6 was substantial. Thus, a negative impact signal is likely in central India. In the north-west and west of India, previous studies suggested impacts in the same direction as those of GLAM. In southern India, projected changes in the study of Singh et al. (2012) [SI2012] were in agreement with EcoCrop but in disagreement with those of GLAM. In a previous study, Ramirez-Villegas et al. (2013b) reported that agreement between EcoCrop and previous estimates of climate impacts varied depending upon the region of study.

7.4.6 Combining suitability and productivity simulations

EcoCrop can be used either to assess the change in the degree of climatic suitability, but also to assess changes in niche breadth (e.g. Warren and Seifert 2010, Ramirez-Villegas et al. 2013b). Even though projected changes in suitability were not found to completely agree to changes in yield or total production (see Sect. 7.4.5), reductions in niche extent may be indicative of areas where future productivity is very low and thus growing the crop is unfeasible. Increases in niche extent could indicate areas where productivity could be high enough so as to grow the crop profitably.

The comparison presented in this section aimed at identifying what are the changes in productivity associated with changes in niche breadth (also referred to as range size, or range extent). Figure 7.20 shows the yield change PDFs for the three bias-correction methods associated with EcoCrop simulations (different-lines Table 7.1). Colours indicate yield responses in areas that were considered unsuitable in the baseline but became suitable in the future (became suitable 'BS', blue lines), and in areas that were considered suitable in the baseline but became unsuitable in the future (became unsuitable 'BU', red lines). If both models are to be combined, it follows that BU sites should depict the largest yield losses, thus indicating that in such areas production is unfeasible. The analyses performed indicate that this is not the case (Figure 7.20). For the three bias-correction methods,

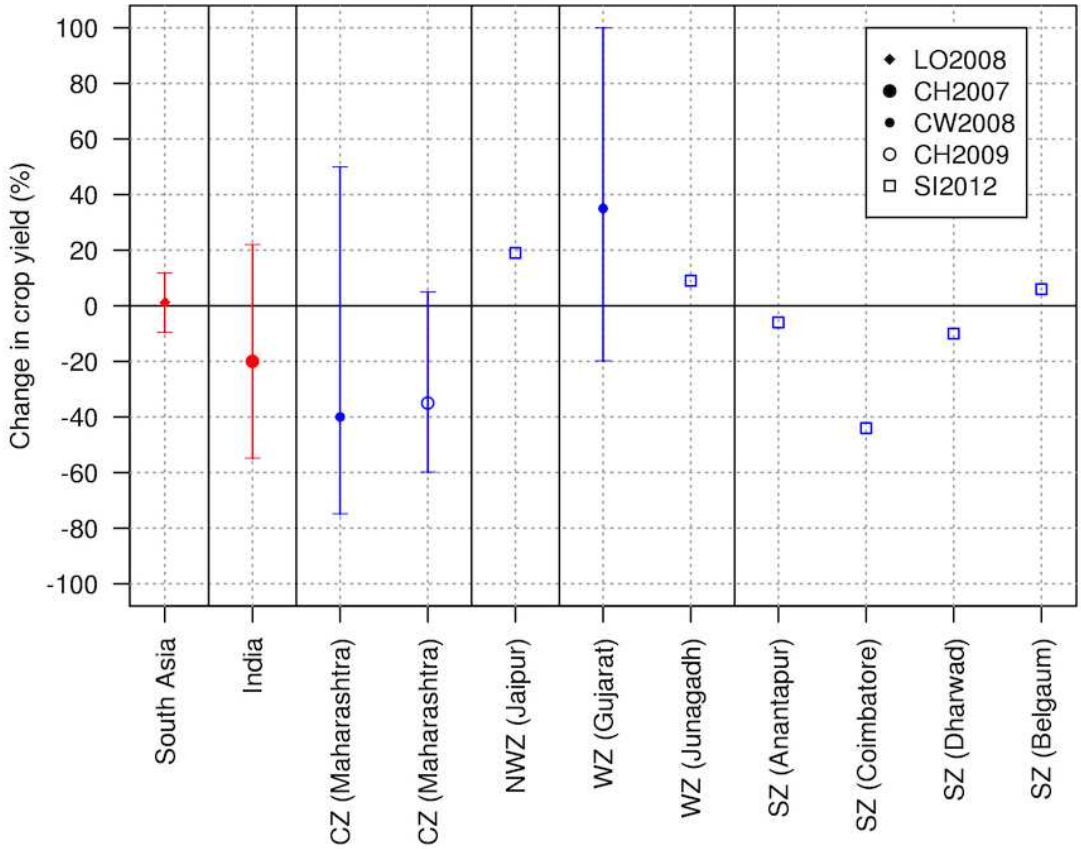

FIGURE 7.19: Projected changes in groundnut yields as reported in previous literature. LO2008: Lobell et al. (2008); CH2007: Challinor et al. (2007); CH2009: Challinor et al. (2009a); CW2008: Challinor and Wheeler (2008b); and SI2012: Singh et al. (2012). Dots indicate median prediction and bars extend to reported maximum or minimum (CH2007, CH2009) or 5-95 % percentiles of the data (LO2008, CW2008). Colours are indicative of whether (blue) or not (red) CO_2 fertilisation effects were taken into account in the studies. CH2007, CH2009 and CW02008 are projections for 2100, LO2008 for 2030, and SI2012 for 2050.

yield changes were more positive for BU sites as compared to BS sites. Differences between the PDFs of BU and BS sites were similar and relatively large for P-LOCI and P-DEL projections, but were relatively minor for P-RAW projections –suggesting that much of the difference can be attributed the differences in temperature responses in both GLAM and EcoCrop.

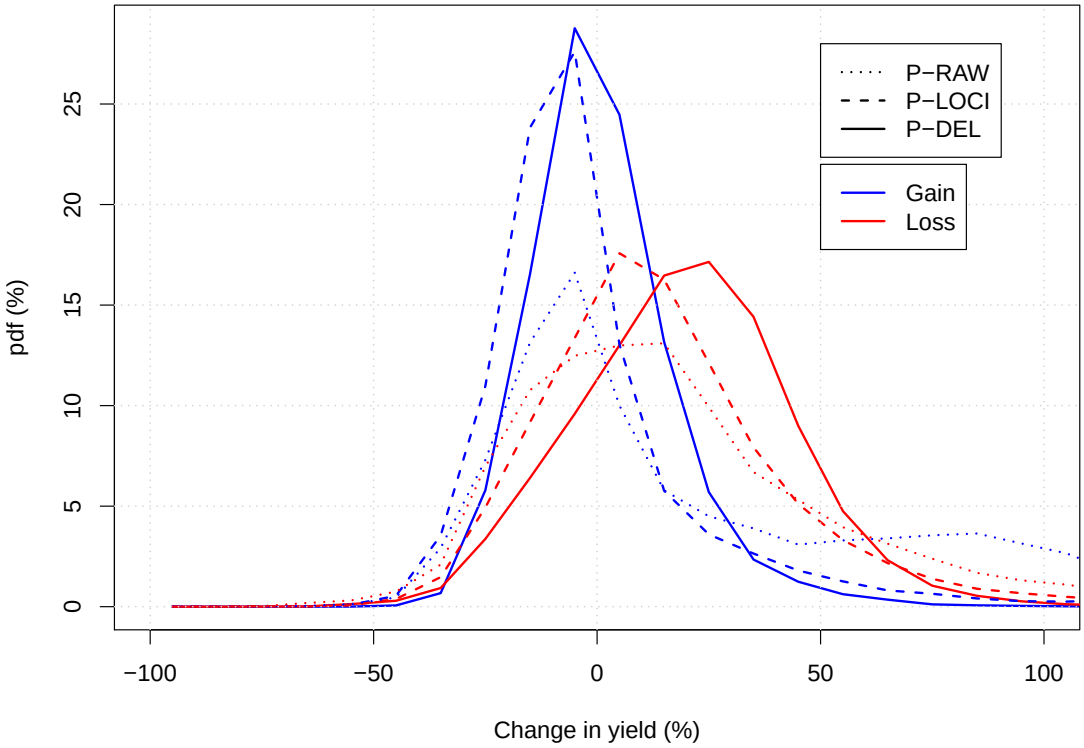

FIGURE 7.20: Projected changes in GLAM crop yield for areas where suitability gains (blue lines) or losses (red lines) are projected with EcoCrop.

7.5 Discussion

7.5.1 Relationships between suitability, productivity and production

The benefits of a simplistic approach, like EcoCrop, are considerable. EcoCrop reduces the parameterizations to a minimum while at the same time making sense of the biology of the crop species (Hijmans et al., 2001). EcoCrop describes the relationship between the crop's presence and the prevailing climate conditions in the locations where the crop is known to be present. Nevertheless, such relationship may not be necessarily related with the abundance of the crop (i.e. crop yield). This may be because potential ecological presence may be related to the occurrence of optimal growing conditions during a sufficiently long period of time (Elith and Leathwick, 2009; Soberon and Nakamura, 2009). Here, suitability was found to be related to total production, suggesting that EcoCrop predictions are related to extent of occurrence or, in other words, relative occurrence rates –not to crop yield. This result may arise in part because crop yield is a complex trait resulting from

many non-linear interactions between the plant and its surrounding environment (Bertin et al., 2010; Nigam et al., 2005). These findings are in agreement with those of Estes et al. (2013a), who demonstrated that a model of probability of presence across the whole ecological range of the crop bears little relationship with crop abundance.

The analyses conducted here also showed that suitability alone cannot be used as a surrogate of crop production (Sect. 7.4.1.3). Previous studies have highlighted the significant differences between suitability and abundance simulations and their respective models (Morin and Thuiller, 2009; Serra-Diaz et al., 2013; VanDerWal et al., 2009a) as well as the potential caveats in niche-based models for future climate change impact studies (Hijmans and Graham, 2006; Keenan et al., 2011). No studies, however, have assessed these differences directly and/or attempted to attribute these to sub-seasonal stresses. The findings of the present study suggest a significant role of these stresses in shaping the probability distribution of the crop production response by reducing the mean and increasing the variance (see Figure 7.9). Sub-seasonal stresses are not included in EcoCrop (Ramirez-Villegas et al., 2013b), and hence this may be the main cause for the reported differences between baseline suitability, productivity and production simulations. Water stress, in particular, and day-to-day precipitation and temperature variations played the most important role, whilst the amount of heat units available (a surrogate of crop development) as well as solar radiation played a secondary role (see Sect. 7.4.1.3).

The fact that water stress was the major driver behind the differences between the suitability and production model simulations highlights one of the main limitations of EcoCrop and of other niche-based models (see e.g. Serra-Diaz et al. 2013): the lack of soil water dynamics mechanisms (see Sect. 7.5.2). It is likely that incorporating additional complexity into EcoCrop would improve the agreement between its suitability simulations and the production simulations of GLAM, but such additional complexity would be at the expense of input data requirements –something that will inevitably bring along additional uncertainties into the niche-based modelling process (Adam et al., 2011; Watson and Challinor, 2013).

7.5.2 Combining projections of process- and niche-based models

As reported above, the relationship between crop yield and suitability was non-existent. In addition, despite a statistically significant and strong relationship between suitability and total production, the lack of agreement between impacts projections of both models suggests that it is difficult to combine both models' projections. This may be attributed to various reasons. Foremost, decreases in crop suitability may not necessarily imply decreases in productivity (see Sect. 7.4.5). In addition, apart from a disagreement in the direction of the change, the projections of both models disagreed in the reasons behind the change (i.e. responses to temperature and water availability) (see Figure 7.15).

In ecological studies, evidence for a relationship between abundance and suitability is scarce and contradictory (Nielsen et al., 2005; Pearce and Ferrier, 2001). Limited evidence also exists regarding the agreement between both niche and process-based model projections (Morin and Thuiller, 2009; Serra-Diaz et al., 2013). This lack of agreement suggests that if anything, uncertainties in projections of climate change impacts remain large. For Indian groundnut, suitability and productivity projections showed disagreement across most of India, except in the central zone, where even though the median change was found to agree in direction, there was large spread in both GLAM and EcoCrop model ensembles. In the present study, the difference in the response of EcoCrop to temperature and precipitation with respect to GLAM, constituted the main difference between both model projections.

Increases in precipitation amounts generally increase available soil water, water uptake, actual evapotranspiration, carbon exchange rates and biomass (Boote and Sinclair, 2006). However, increases in heavy precipitation events can cause waterlogging and decrease crop productivity (Kahlown and Azam, 2002). Since waterlogging is not parameterised in GLAM (Challinor et al., 2004), the second main factor to which differences in future projections can be attributed is the response to increased water availability. Such response to increased water availability is of particular importance herein because projections of June-July-August precipitation for India depict a higher likelihood of increases by 2030s (Figure 7.21).

The difficulty in representing responses to increased precipitation has been hypothesised as the main factor leading to differences between suitability and abundance (Serra-Diaz

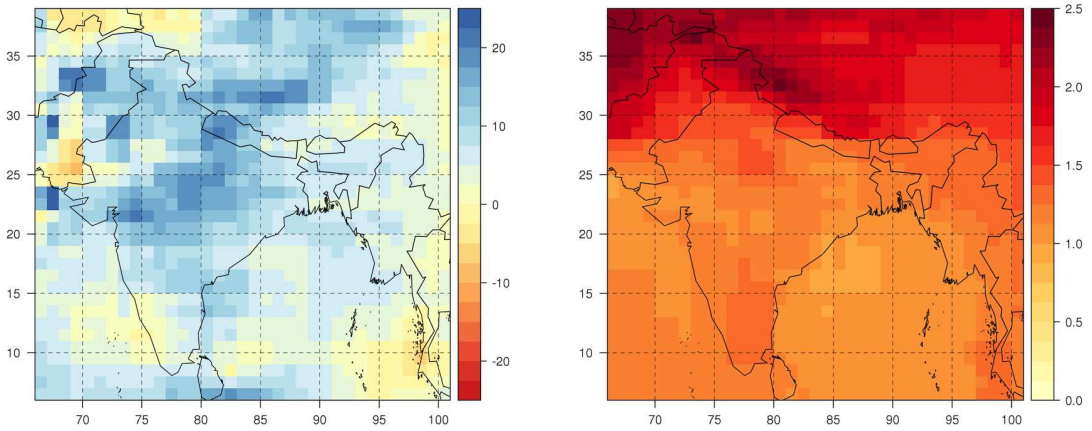

(a) Precipitation

(b) Temperature

FIGURE 7.21: Changes in June-July-August (JJA) total precipitation (a) and mean temperature (b) as projected by the CMIP5 ensemble by 2030s (RCP4.5). Values shown correspond to the mean of the GCM ensemble. Models included in the calculation are listed in Table 3.4, (Chapter 3).

et al., 2013). Because currently grown varieties and crops are adapted to the existing ecological niche and because EcoCrop is parameterised under the assumption that climate is the major driver of the distribution of the crop at present (see Sect. 7.3.1), areas at or above the optimum rainfall are likely to experience unrealistic suitability losses. This is because even very limited increases in rainfall cause a niche shift (in EcoCrop), whereas such increases in a process-based model like GLAM would typically enhance biomass accumulation and yield –particularly with CO_2 stimulation. In western India in particular, there was substantial disagreement between EcoCrop and GLAM projections (Figure 7.18), and also between EcoCrop and previous estimates of climate impacts on groundnut yields (Figure 7.19). It is likely that the lack of an appropriate water balance mechanism in EcoCrop, in conjunction with increased water-use efficiency due to CO_2 stimulation, is the cause of these differences.

An additional factor that may account for some of the differences between suitability and productivity may be the mechanisms through which temperatures have an impact in the two measures. In GLAM, mean temperatures act by changing crop duration –which in turn affects totals of precipitation, solar radiation, biomass and yield (Challinor and Wheeler, 2008b) or by increasing evapotranspiration and thus enhancing water stress (at constant or decreasing precipitation levels). Extreme temperatures in GLAM cause direct yield

loss through effects on reproductive units (Challinor et al., 2005b). In the simulations presented in Chapter 6, temperature increases do not increase water stress since precipitation and water-use efficiency increase (Sect. 6.4.3, Chapter 6, and Figure 7.21); crop duration increases as the optimal temperature for crop development (typically around 28 °C) is exceeded; and there is little impact of heat stress on reproductive units (see Sect. 6.4.3, Chapter 6). In EcoCrop, as optimal temperatures are exceeded and duration stays constant at the monthly scale, suitability decreases linearly until the maximum temperature (T_{MAX}, 34-40 °C in this study) is exceeded and the crop is deemed unsuitable for that particular site. In EcoCrop, therefore, not only optimal temperatures can be exceeded with relatively low levels of change in seasonal temperatures, but also increasing mean temperatures tend to have a much more marked negative effect if optimal temperatures are exceeded (also see Vermeulen et al. 2013). In particular, in the simulations presented here mean temperatures are the most important driver of crop suitability changes (see Sect. 7.4.2). In southern India, differences occurred between GLAM, previous estimates and EcoCrop simulations. This may be in part because heat stress is projected to impact crop yields at longer lead times in process-based crop models (see Singh et al. 2012, which focuses in the 2050s and Challinor et al. (2007), which focuses in 2100).

Additional factors may also cause differences between suitability, productivity and production simulations, and these include errors in the structure of the models (see Chapter 5), responses to aggregation errors (Angulo et al., 2013b), the difference in temporal scales at which the two models operate (Vermeulen et al., 2013), and possible problems in model evaluation (DelSole and Yang, 2011). The latter is of particular importance because it has the potential to affect parameter values and/or the acceptance of parameter sets. Model evaluation for both GLAM and EcoCrop was in this work carried out by directly comparing observed and simulated quantities (see Sect. 3.6). However, a more robust model evaluation procedure could have been achieved by performing field significance tests. Methods for testing single- and multi-variable field significance have been proposed mostly in climate science, and these focus on testing how consistent si a trend or pattern in relation to what is expected just by pure chance (DelSole and Yang, 2011; Livezey and Chen, 1983; Wilks, 2006). While the results of performing more robust model evaluation tests have not been investigated in this work and it is hence difficult to determine their actual impact on both model optimisation and skill, the uncertainty bounds in historical simulations of both yield and suitability generally captured observations (see e.g. Figure 5.14, and Figure 7.2)

and can thus be considered believable (Beven, 2002; Beven and Binley, 1992). Given the scarcity of these tests in the crop modelling literature, a further investigation of the robustness of the model evaluation metrics provided by this study using field significance tests may be warranted.

Combining both models is thus a challenging task. One possible way to achieve the combination of both models is to use their information in a complementary way, as done in Sect. 7.4.6. Such analysis, however, revealed that where projections of suitability indicate a possible expansion of the crop ecological niche, productivity was projected to decrease, and *vice versa* (see Sect. 7.20). Niche models are useful tools for analysing the distributional range of a species and can be used at regional scales to produce estimates of presence and absence areas and their changes within certain environmental boundaries (e.g. Araujo et al. 2005; Fischer et al. 2005; Jarvis et al. 2012). However, niche-based models are not capable to appropriately capture the complex non-linearities involved in the response of the crop to climate and hence cannot be used to model productivity. In particular, for regionalised analyses of relativelly widely-adapted crops, there is a risk that the responses to changes in environmental factors are exaggerated in the niche models (see e.g. Läderach et al. 2013 for an example) –though in other cases the responses are realistic (e.g. Schroth et al. 2009). Thus, the use of niche models in agricultural impact studies should be exercised with caution and in all cases interpreted carefully and where possible, their impacts estimates compared with those of previous studies.

7.5.3 Known caveats and potential for model improvement

EcoCrop offers multiple advantages. First, model parameters and model inputs can easily be altered to investigate a broader range of crops and/or regions (e.g. Jarvis et al. 2012). This allows assessing relevant topics related to food security, transformational change and the development of national or regional policies for climate change adaptation (e.g. Peterson et al. 2012). However, niche-based models may have a number of limitations that require further research and work if such models are to be used more widely for agriculture under climate change:

1. For EcoCrop, perhaps the most important aspect meriting improvement is the relationship between model parameters and the agronomic or physiological characteristics of the crop. Although the simplistic approach in EcoCrop tries to simulate the non-linear effects of temperature and precipitation-related stresses, it fails to capture many relevant plant-soil-atmosphere interactions, and thus may over-estimate potential changes in productivity. Therefore, suitability indices and their likely changes in future climate scenarios need to be interpreted carefully as the ability of a certain environment to allow the growth of a certain species in a broad sense. As such, suitability models may be more useful at regional scales for predicting changes in distributional ranges rather than at smaller scales to predict changes in abundance (see Ramirez-Villegas et al. 2013b and Hannah et al. 2013).

2. The model does not account for drought, waterlogging, excessive heat or cold during key physiological periods (i.e. fruit filling, flowering), leading to a climatic suitability over-estimation. Moreover, the application of the model relies upon monthly data, whilst stressful conditions may occur in shorter periods.

3. For perennial crops (many of which are also difficult to model in a process-based manner), it is harder to calibrate and/or parameterise the modelling approach, since the rainfall and temperatures during the growing season are equal to the annual rainfall and temperature, which results in neglecting within-year seasonality. A good option to overcome this issue would be the development of a function to involve the concept of degree days (Neild et al., 1983), though at the expense of data input and calibration requirements.

Given the flexibility of EcoCrop, it can be continuously improved, and some additional processes can be incorporated. Continuous improvements to the model to allow better simulating responses to increased precipitation, assessing soil suitability and parameterising a larger number of crops and regions so as to assess climate change impacts on food security are topics meriting future research.

Chapter 8

Developing a genotypic adaptation strategy using GLAM

" 'We also have our diplomatic secrets,
said he', and picking up his hat he
turned to the door"
Sir A. C. Doyle

8.1 Summary

Crop improvement strategies have been major factors in increasing food production during the so-called green revolution (Chapman, 2002). Under climate change, cultivar substitution as well as the development of 'climate-ready' cultivars will likely be one of the most important adaptation strategies (Burke et al., 2009; Foley et al., 2011). In view of the climate change impacts estimates presented earlier in this thesis (see Chapter 6), a genotypic adaptation strategy for Indian groundnut was developed (Objective 5, Sect. 1.6). To that aim, GLAM was used to estimate the changes in mean yields, and importantly, also in inter-annual yield variability. Traits explored included crop growth (maximum photosynthetic rate, maximum rate of transpiration and biomass partitioning to seeds), crop phenology (duration of each crop stage) and tolerance to high temperature stress. Each trait was mapped onto as many as possible GLAM parameters, resulting in a total of 13 GLAM

parameters to be perturbed. Those corresponding to crop growth were: transpiration efficiency (E_T) and maximum normalised transpiration efficiency ($E_{TN,max}$) as surrogates of maximum photosynthetic rates; the maximum rate of tranpiration (TT_{max}); and the harvest index ($^{\partial H_I}/_{\partial t}$) as a surrogate of partitioning to seeds. Phenology parameters included the four thermal durations (t_{TT0} to t_{TT3}). Adaptation to temperature extremes focused on two processes. Firstly, high temperature stress during flowering (Sect. 3.5.1.8), for which the critical temperature for damage to flowers (T_{crit}^{min}), the limit temperature for damage to flowers (T_{lim}^{min}), and the steepness of the response to daily increases in day temperature (T_{ia}) were perturbed. Secondly, reduced photosynthetic rates at high temperatures, for which the critical temperature for reduction in transpiration efficiency was chosen (T_{ter1}).

The results indicate that adaptation is possible through genotypic improvement. On average, the most effective single trait for boosting mean yields was increased partitioning to seeds (i.e. harvest index, $^{\partial H_I}/_{\partial t}$, 30–80 % increase), followed by increases in the rate of transpiration (TT_{max}, 40–70 %). In dry areas (e.g. Gujarat and Andhra Pradesh), however, increasing the transpiration rate increased water stress and was thus not beneficial. Increased partitioning to seeds was beneficial throughout the whole country, but it increased yield variability by up to 60 % as a result of earlier triggering of terminal drought. By contrast, improved photosynthetic rates increased mean yield and decreased yield variability. Duration traits were less effective (with a maximum mean yield gain of 25 %) as gains from enhanced durations were limited by the duration of the monsoon period. The grain-filling duration showed the greatest effectiveness in increasing mean yield, but the increase in vegetative and flowering period being the most effective trait at improving yield variability. Due to the lack of heat stress by 2030s, the response of yield means and variability to heat stress tolerance traits was negligible. According to the results, a first breeding cycle of 2030-ready crops should keep the current focus on water-use efficiency and better partitioning over the whole of India, and avoid focusing on heat stress. However, towards the end of the 21st, previous studies have highlighted the need for heat-tolerant germplasm (Challinor et al., 2007; Singh et al., 2012). It is important to note that the traits included in physiological models cover only a part of the crop breeding picture, since plasticity and stability may also beimportant characteristics –but are ones that can only be achieved through the combined effect of many genes. Thus, future studies should focus on the mapping of genetic characteristics and the use of quantitative trait

loci (QTL) or genetic models for assessing the genetic background of existing germplasm, along with the feasibility of achieving crosses that hold the proposed characteristics.

8.2 Introduction

Global food production has increased significantly given the increasing need to feed a globally growing population that has just recently passed the 7 billion people (World-Bank, 2012). Crop improvement strategies have been major players in such increases, by boosting crop yields and thus increasing the overall production intensity (i.e. efficiency in use of resources, particularly land) in the global food system (Chapman, 2002; Foley et al., 2011). Genotypic adaptation, defined as the development and/or targeting of crop cultivars better suited to novel climate conditions, is also one of the most important adaptation strategies to projected climate change (Burke et al., 2009; Challinor et al., 2009a). This type of adaptation involves the incorporation of desirable traits aimed at tolerating stresses to achieve higher and more stable yields, and more broadly the design of crop "ideotypes" (i.e. varieties with ideal genetic characteristics) (Cock et al., 1979; Donald, 1968; Suriharn et al., 2011). Ideotypes have been hypothesised for a number of crops, including rice (Peng et al., 2008), wheat (Berry et al., 2007; Semenov and Halford, 2009), maize (Mock and Pearce, 1975), cassava (Cock et al., 1979), and groundnut (Suriharn et al., 2011). For Indian groundnut, specifically, Singh et al. 2012 modelled an ideal 2050 climate ready genotype with increased photosynthetic rates, greater partitioning to seed, increased in the duration of the seed filling stage, greater specific leaf area and heat stress tolerance (also see Challinor et al. 2007).

Chapter 6 of this thesis concluded with a thorough identification of impacts across India and elucidated some potential avenues for adapting Indian groundnut systems to future climate change (i.e. RCP4.5, 2030s). While impacts on the main production areas of western and north-western India were primarily positive owing to increases in total seasonal rainfall, the likelihood of negative impacts was significantly larger in the southern state of Andhra Pradesh, as well as over central India (Maharashtra and Madhya Pradesh), where ca. 25 % of groundnut production by weight is concentrated (Challinor et al., 2003; Mehrotra, 2011). The results of Chapter 6 stressed the need for a more profound investigation of the effects of genotypic adaptation, not only to abate any negative climate

change impacts, but also to capitalise on the abovementioned potential gains. In particular, enhancing plant mechanisms for countering drought stress was suggested (e.g. increased grain filling period, higher partitioning, and higher transpiration efficiency).

The analyses performed in this chapter aim at combining previously assessed impacts of climate change (Chapter 6) with a framework designed at quantifying the benefit of early breeding of specific traits in groundnut. The analyses build up on previous work by Challinor et al. (2007), Singh et al. (2012) and Challinor et al. (2009a) by investigating traits other than temperature-related and hence providing a better account of genotypic adaptation gains and their associated uncertainties. By focusing on the 2030s period the analyses presented here are also more likely to be of use to the breeding community in early breeding cycles during the 21^{st} century. In this chapter, specifically,

1. Important genotypic properties were identified in the literature and mapped onto the GLAM parameter space. Since GLAM parameters are defined regionally, it may be difficult to link hypothesised and real-world genotypes, thus limiting the conclusions reached to the scale at which the model is used. Nonetheless, the mapping of crop traits onto the GLAM parameter space ensured that the traits analysed were fully represented in the simulations. Further links to genomics have proven difficult even in more complex process-based crop models (Boote et al., 2003; Semenov and Halford, 2009).

2. The identified GLAM parameters were perturbed from the values specified in Chapters 3 and 5 to reflect hypothetical crop improvement scenarios. Parameters were perturbed both individually and in combination.

3. Mean and interannual variability of crop yields in these simulations were compared with those reported in Chapter 6 so as to assess the potential benefit from crop improvement.

An ensemble of crop model simulations (similar to the one in Chapter 6) was used to achieve the three objectives. The effectiveness of the potential genotypic adaptation options in abating negative or capitalising positive impacts was assessed by quantifying yield gains. The results are discussed in light of previous work on groundnut breeding and more broadly in the context of agricultural adaptation.

8.3 Methodology

8.3.1 Crop model

GLAM was used to capture the response of groundnut to changes in climates at the regional scale as well as to understand how the response of the crop changes under hypothetical crop improvement scenarios. GLAM was deemed a suitable model for the purposes of this chapter because it is a physiological process-based model (Challinor and Wheeler, 2008b; Challinor et al., 2004) and as such allows to analyse the benefits from phisiology-oriented improvements in crop characteristics (see e.g. Bertin et al. 2010; Challinor et al. 2007; Semenov and Halford 2009). Because the crop model can skilfully reproduce observed crop-climate relationships (see Sect. 5.3.5), it follows that perturbing model parameters within realistic (observed) ranges will reflect a realistic response of the crop to prevailing climate conditions (e.g. Boote et al. 2003; Challinor et al. 2007; Semenov and Halford 2009). As used here, this is a direct estimate of the potential impact of genotypic adaptation, as it reflects the effect of varying the genotypic characteristics (expressed through physiological responses) of the crop.

8.3.2 Identification of traits and mapping onto GLAM parameter space

Literature on groundnut breeding and genetics is generally abundant (see e.g. Upadhyaya 2005, Rao and Nigam 2003, and Nautiyal et al. 2012), but perhaps the earliest complete description of a groundnut ideotype was done by Nigam (2009). According to that study, an ideotype of groundnut should present the following characteristics: "*(1) rapid emergence, (2) early growth vigour (roots and shoots), (3) early flowering, (4) insensitivity to photoperiod, (5) high radiation-use-efficiency (narrow leaves), (6) high transpiration efficiency (thick leaves), (7) high harvest index and minimum thermal time to physiological maturity*". Further, Nautiyal et al. (2012) report the partitioning to pods as the most important trait for achieving high yields, besides the total number of pods, the length of the pod-filling phase and the maximum photosynthetic rate. The same study suggests that a crop ideotype should show reduced SLA, plant height, petiole length, leaflets length and width, together with increased number of branches and reproductive sink size.

Table 8.1 shows the main studies that have assessed the genotypic improvement of groundnut using crop models. The different studies highlight the importance of four types of genotypic properties: (a) tolerance to high temperature events, (b) development rates –particularly that of the grain filling phase, (c) increasing the total biomass through increases in the photosynthetic rate and/or improvements in leaf thickness or size, and (d) increasing the fraction of assimilate that is partitioned to the seeds.

GLAM parameters corresponding to each of the genotypic properties are shown in Table 8.2. As surrogates of the maximum rate of photosynthesis, the transpiration efficiency (E_T), maximum normalised transpiration efficiency ($E_{TN,max}$) and maximum transpiration rate (TT_{max}) were used. The rate of change in the harvest index ($^{\partial H_I}/_{\partial t}$) was used as a surrogate of the fraction of assimilate partitioned to seeds. SLA is a model product in GLAM, and hence only the initial-condition control SLA_{max} was used to reflect improvements in leaf thickness. The four thermal durations ($t_{TT0...3}$) were also considered. Finally, four extreme temperature thresholds were studied: three relating to heat stress during flowering (T_{crit}^{min}, T_{lim}^{min}, and T_{ia}, see Sect. 3.5.1.8) and the last one relating to reduced transpiration efficiency at high temperatures (T_{ter1}, see Sect. 3.5.1.10). The root traits studied by Singh et al. (2012) were not considered since the response of the crop was negligible or detrimental. Due to the reduced complexity of GLAM and the lack of parameters related to individual seed and pod growth, nitrogen content, and individual leaf size, these traits were not analysed.

The upper-bound for each of the target parameters was derived from existing literature, except for phenology traits, as for these literature was not specific enough (see Table 8.2). Ranges used were broad enough so as to include potential from available germplasm in other parts of the world (Upadhyaya, 2005). Using ranges for as many parameters as possible was preferred instead of using a 'conservative improvement percentage' for all parameters (e.g. Singh et al. 2012), since it provides a more realistic estimate of genotypic adaptation limits (see e.g. Challinor et al. 2009a).

8.3.3 Crop improvement scenarios

Crop improvement scenarios were generated by perturbing model parameters within the updated range shown in Table 8.2 as follows:

TABLE 8.1: Summary of studies of genotypic adaptation and ideotype design.

Study	Region	Genotypic property	Crop response
Challinor et al. (2009a)	India	Total thermal requirement	Increases in thermal time requirement are needed between 20-30 % to counter yield loss by 2100
Challinor et al. (2007)	India	Tolerance to high temperatures	Increased heat stress tolerance reduces yield loss by 50-80 % by 2100
		Change in optimal temperature for development	No beneficial effect observed with increases in T_{opt} from 28 °C to 36 °C
Suriharn et al. (2011)	Thailand	Thermal requirement during vegetative phase	Yield gain when vegetative duration was decreased
		Thermal requirement during pod filling phase	Yield gain when pod filling duration was increased
		Thermal requirement from flowering to max. LAI	Increases are critical for achieving high LAI
		Maximum leaf size	Minimal effect due side-effect of increasing light competition
		Specific leaf area	Increases in yield, but countered increases in max. photosynthetic rate ($P_{N,max}$)
		Maximum rate of photosynthesis	Increases of 7 % in $P_{N,max}$increased yield by up to 150 %.
		Partitioning to seed	Increases of up to 10 % increased yields by 200 %
Singh et al. (2012)	India	Thermal requirement from emergence to flowering	Increases produced little gain or loss in yield
		Thermal requirement during pod-filling phase	Increase of 10 % produced yield gains of 2.5-8 %
		Maximum leaf size	Little or no yield gain
		Specific leaf area	Gains restricted to low temperature areas, where VPD is low
		Maximum rate of photosynthesis	Gains between 4-5 % at all locations
		Seed filling duration	Gains between 3-5 % at all locations
		Nitrogen mobilisation rate	Small yield gains between 1-2.5 % at all locations
		Pod adding duration	Moderate (2-5 %) yield gain restricted to warm sites
		Fraction assimilate partitioned to seed	Increased yield by up to 5 % at all locations
		Fraction assimilate partitioned to roots	Detrimental to yield
		Root biomass distribution across profile	Little gain or yield loss
		Velocity of extraction front	Little to no yield gain
		Temperature tolerance for pod-set, partitioning to pods and individual seed growth	Large yield gains (8-13 %) in warm areas

TABLE 8.2: List of physiological traits, their corresponding GLAM parameters, and their updated maximum values for crop improvement scenarios (see Table 5.2 for calibration range of each parameter).

Genotypic property	Parameter	Max. value	Reference(s)
Maximum photosynthetic rate	E_T	5.8 Pa	Brown and Byrd (1996) Rao and Nigam (2003) Jyostna Devi et al. (2009, 2010)
	$E_{TN,max}$	7 g kg^{-1}	Brown and Byrd (1996) Bhatnagar-Mathur et al. (2007) Jyostna Devi et al. (2009)
	TT_{max}	0.7 cm day^{-1}	Hammer et al. (1995) Rao and Nigam (2003)
Partitioning to seeds	$\partial H_I/\partial t$	0.015 day^{-1}	Hammer et al. (1995)
Leaf thickness and size	SLA_{max}	315 g cm^{-2}	Phakamas et al. (2008) Banterng et al. (2003) Sheshshayee et al. (2006)
Crop development rate	t_{TT0}	-20 %	N/A
	t_{TT0}	+20 %	N/A
	t_{TT1}	+20 %	N/A
	t_{TT2}	+20 %	N/A
	t_{TT3}	+20 %	N/A
Temperature tolerance	T_{crit}^{min}	38 °C	Vara Prasad et al. (2003) Challinor et al. (2005b)
	T_{lim}^{min}	38 °C	Challinor et al. (2005b)
	T_{ia}	44 °C	Challinor et al. (2005b)
	T_{ter1}	64 °C	Challinor et al. (2005b)

1. **Crop growth**: the transpiration efficiency (E_T), the normalised transpiration efficiency ($E_{TN,max}$), the maximum transpiration rate (TT_{max}), and the specific leaf area (SLA_{max}) were increased by 25 %, 50 % and 100 % of the range between the optimal parameter value, i.e., those defined in Chapter 5, including the CO_2 response perturbations described in Chapter 6, and the updated upper bound of the range (shown in Table 8.2).

2. **Phenology**: the thermal duration from planting to start of flowering (t_{TT0}) and from flowering to start of pod-filling (t_{TT1}) were increased by 5 %, 10 % and 20 %. The thermal duration from planting to start of flowering (t_{TT0}) was decreased by 5 %, 10 % and 20 %. The thermal duration between start of pod-filling and LAI max (t_{TT2}) and the thermal duration between LAI max and maturity (t_{TT3}) were increased by the same percentages as t_{TT0} and t_{TT1}.

3. **Temperature extremes**: as with crop growth parameters, these changes were done at 25 %, 50 % and 100 % of the range between the maximum reported value

(Table 8.2) and the optimal values used in Chapters 5 and 6.

Each parameter was first tested in isolation (i.e. 14 parameter * 3 perturbations = 42 individual perturbations) and then in combination with all other parameters. The combined parameter scenarios were constructed so that upper and lower bounds of each type of trait (i.e. crop growth, phenology and temperature extremes) were combined with each other. Since within the phenology traits the perturbation of t_{TT0} had to be done in two directions this meant that each of the groups of parameters had to be tested once with increased t_{TT0} and once with decreased t_{TT0} (i.e. 2 directions$^{3 \text{ groups}} * 2$ bounds = 16). The total number of perturbations was thus 42 (individual) + 16 (combined) = 58. These were then applied to the permutation of 19 baseline parameter sets and 4 CO_2 response parameterisations (Chapter 6). This totalled 19 * 4 * 58 = 4,408 hypothetical crop improvement scenarios (i.e. parameter sets) to be tested in any given grid cell. Examples of single and combined scenarios are shown in Table 8.3 and Table 8.4 (respectively) for a parameter set of Western India.

TABLE 8.3: Hypothetical crop improvement scenarios using single-parameter (S) perturbations for a given parameter set of Western India. Each row represents three scenarios, specified in the last three columns in the right.

Group	Perturbation	Parameter	Low	Mid	Top
Crop growth	S1 to S3	E_T	4.8	5.1	5.8
	S4 to S6	$E_{TN,max}$	5.4	6	7
	S7 to S9	$^{\partial H_I}/_{\partial t}$	0.0081	0.0104	0.0150
	S10 to S12	TT_{max}	0.56	0.54	0.7
	S13 to S15	SLA_{max}	295	302	315
Phenology	S16 to S18	t_{TT0}	390	351	332
	S19 to S21	t_{TT0}	410	429	468
	S22 to S24	t_{TT1}	334	350	382
	S25 to S27	t_{TT2}	212	221	240
	S28 to S30	t_{TT3}	529	553	600
T. extremes	S31 to S33	T_{crit}^{min}	35	36	38
	S34 to S36	T_{lim}	41	42	44
	S37 to S39	T_{ia}	61	62	64
	S40 to S42	T_{ter1}	36.3	37.5	40.0

8.3.4 Crop model simulations

As in Chapter 6, crop simulations were conducted using the future climate scenarios described in Sect. 3.4.1.5. Four sets of model simulations were conducted: I-RAW, I-LOCI,

TABLE 8.4: Hypothetical crop improvement scenarios using combined-parameter (C) perturbations for an example parameter set of Western India. Scenarios from C1-8 are related to decreases in t_{TT0}, while scenarios C9-16 are related to increases in t_{TT0}.

Pert.	Phenology				Crop growth					T. extremes			
	t_{TT0}	t_{TT1}	t_{TT2}	t_{TT3}	E_T	$E_{TN,max}$	$\partial H_I/\partial t$	TT_{max}	SLA_{max}	T_{crit}^{min}	T_{lim}	T_{ia}	T_{ter1}
C1	370	334	212	529	4.8	5.4	0.0081	0.5	295	35.0	41.0	61.0	36.3
C2	370	334	212	529	5.8	7.0	0.0150	0.7	315	35.0	41.0	61.0	36.3
C3	312	382	240	600	4.8	5.4	0.0081	0.5	295	35.0	41.0	61.0	36.3
C4	312	382	240	600	5.8	7.0	0.0150	0.7	315	35.0	41.0	61.0	36.3
C5	370	334	212	529	4.8	5.4	0.0081	0.5	295	38.0	44.0	64.0	40.0
C6	370	334	212	529	5.8	7.0	0.0150	0.7	315	38.0	44.0	64.0	40.0
C7	312	382	240	600	4.8	5.4	0.0081	0.5	295	38.0	44.0	64.0	40.0
C8	312	382	240	600	5.8	7.0	0.0150	0.7	315	38.0	44.0	64.0	40.0
C9	410	334	212	529	4.8	5.4	0.0081	0.5	295	35.0	41.0	61.0	36.3
C10	410	334	212	529	5.8	7.0	0.0150	0.7	315	35.0	41.0	61.0	36.3
C11	468	382	240	600	4.8	5.4	0.0081	0.5	295	35.0	41.0	61.0	36.3
C12	468	382	240	600	5.8	7.0	0.0150	0.7	315	35.0	41.0	61.0	36.3
C13	410	334	212	529	4.8	5.4	0.0081	0.5	295	38.0	44.0	64.0	40.0
C14	410	334	212	529	5.8	7.0	0.0150	0.7	315	38.0	44.0	64.0	40.0
C15	468	382	240	600	4.8	5.4	0.0081	0.5	295	38.0	44.0	64.0	40.0
C16	468	382	240	600	5.8	7.0	0.0150	0.7	315	38.0	44.0	64.0	40.0

I-SH and I-DEL. Each set consisted of 13 GCM simulations, 19 parameter ensemble members, 4 CO_2 parameterisations (see Sect. 3.5.1.13, Chapter 6), the 58 crop improvement scenarios (Sect. 8.3.3) and 195 grid cells. No offset in sowing date was attempted since the changes in sowing date were found in Chapter 6 to be a relatively insignificant uncertainty source. Thus, a total of 11,174,280 simulations (57,304 simulations per grid cell) were conducted for each set. Simulations were conducted exclusively for the future (i.e. RCP4.5, 2030s). Yield gap parameter (C_{YG}) values for each grid cell were taken from the respective baseline simulation and in the case of DEL-bias-corrected crop simulations from the control simulations.

Model output was verified for consistency using maximum values reported in the literature for three key variables: (a) crop yield, (b) crop duration, and (c) end of season harvest index. Simulations with time-mean yields larger than 6,300 kg ha^{-1}(Balota et al., 2012; Caliskan et al., 2008), mean duration greater than 150 days (Nigam, 2009; Singh et al., 2012), or harvest index greater than 0.66 (Nigam et al., 2001) were considered unrealistic and hence rejected.

8.3.5 Data analysis

The numerical analyses focused on mean crop yields ($\bar{Y}$) and their variability (coefficient of variation, CV). Changes in crop yields and variability were first quantified as per cent deviation from the corresponding Chapter 6's future yield projection (Eq. 8.1).

$$\Delta X = \frac{X_I - X_F}{X_F} * 100 \tag{8.1}$$

where X represents the mean crop yield or its coefficient of variation, and the symbol Δ is used to indicate a change. The change is expressed as percentage of the difference between the improvement scenario (X_I) and scenario with no improvement (X_F) (i.e. the future scenario of Chapter 6), with respect to X_F. These calculations were done per grid cell, for each GCM, GCM bias correction method, parameter ensemble member, CO_2 response parameterisation, and crop improvement scenario. For mean yields exclusively, simulations where ΔX was negative were rejected since the primary objective of the simulations was to

assess yield gains –rather than yield losses. Using these values, maps and box plots of the potential improvement from each trait and each group of traits were finally constructed.

The impacts of parameter perturbations were analysed by grouping parameters into three groups, according to the main abiotic stress being abated. Three groups were discerned:

- Drought management: drought escape through reduced thermal time requirement during vegetative phase (t_{TT0}), increased water-use efficiency through increases in transpiration efficiency (T_E, $E_{TN,max}$), harvest index ($^{\partial H_I}/_{\partial t}$), maximum transpiration rate (TT_{max}) and specific leaf area (SLA_{max}).
- Increased duration to enhance LAI growth and biomass accumulation through increases in all thermal time requirements (t_{TT0} to t_{TT3}).
- Reduced effect of temperature extremes through increased tolerance to high temperature during flowering (T_{crit}^{min}, T_{lim}, T_{ia}), and improved photosynthesis response to temperature (T_{ter1}).

These groups are hereafter used to present and discuss the results.

8.4 Results

8.4.1 Gains from drought escape and improved water-use efficiency

Figure 8.1 shows the potential mean yield gains from improving drought-related traits for I-DEL simulations. In this and the following sections, plots and descriptions focus on the I-DEL simulations because these were representative of the remainder sets of simulations (I-RAW, I-LOCI and I-SH). Improving the partitioning to seeds ($^{\partial H_I}/_{\partial t}$) was by far the most effective trait, with mean yield gains above 80 % in central and eastern India. Improving photosynthetic rates ($E_{TN,max}$, $E_{TN,max}$) proved to be less effective than improving partitioning; however, significant gains in southern areas were achieved from improving this trait. Gains from improved assimilate production ranged between 10 and 40 % for most of India, though most of the benefits were concentrated in the very south and the north-west of the country. The impact of enhanced maximum transpiration rate

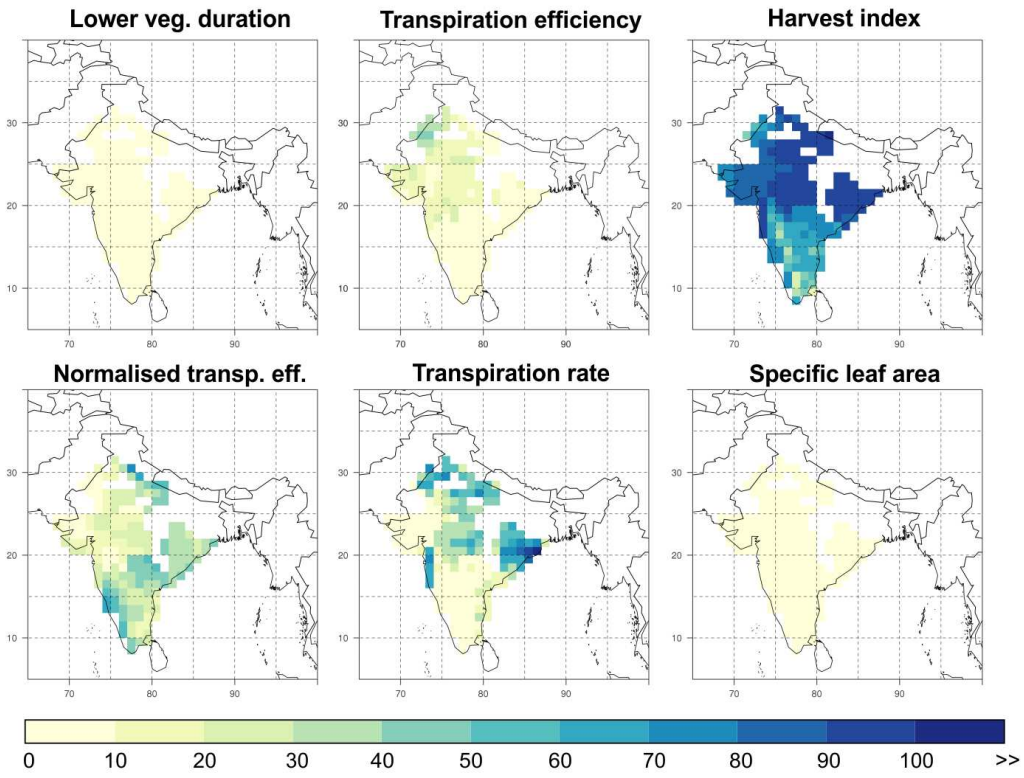

FIGURE 8.1: Mean crop yield increase as a result of crop improvement related to drought scape and water use efficiency. Shown are the ensemble mean results of I-DEL simulations middle crop improvement range (see Table 8.2) for each of the model parameters. Only values of $\Delta\bar{Y} > 0$ were plotted.

was often larger, but located in different areas as compared to photosynthetic rates, suggesting geographic complementarity between the two responses. Improving leaf thickness (to the extent that GLAM allows via SLA_{max}) did not show any significant benefit. The least effective trait was the duration of the vegetative stage: decreasing t_{TT0} had little impact on yields or was detrimental to crop productivity.

Yield variability changes are shown in Figure 8.2. Changes in yield variability were much more geographically variable than those of mean yields, indicating that greater yield means may not necessarily improve temporal yield stability. Overall, improving the maximum photosynthetic rate ($E_{TN,max}$, $E_{TN,max}$) produced the greatest improvement in yield stability –although these were concentrated in the east, some parts of the west and the south. This was because higher maximum transpiration efficiency enhances biomass accumulation in wet years with low maximum temperatures (when VPD is low). Because the east is one of the wettest areas in the country –and hence the likelihood of wet years is higher

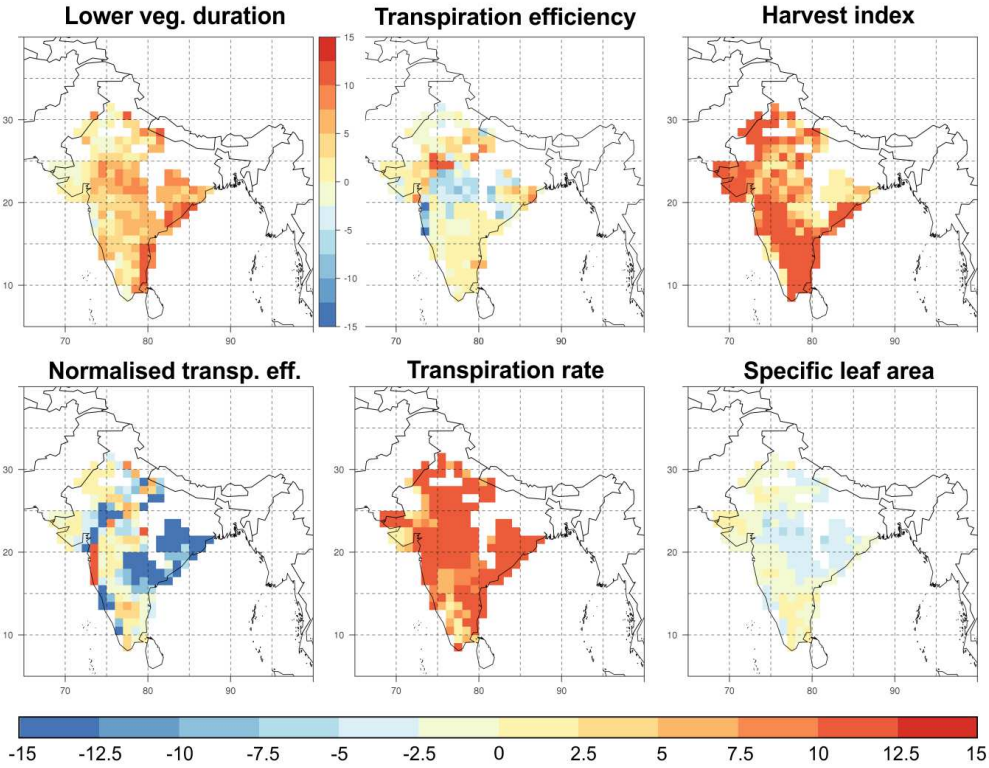

FIGURE 8.2: Crop yield variability changes as a result of crop improvement related to drought scape and water use efficiency. Additional details as in Figure 8.1.

(Figure 3.3), achieving a greater $E_{TN,max}$ produces a more temporally uniform response. Improving partitioning to seeds ($^{\partial H_I}/_{\partial t}$) and the maximum transpiration rate (TT_{max}) were found detrimental to crop yield stability. Reductions in vegetative stage duration were detrimental to temporal yield stability in the majority of India, except in the very west.

8.4.2 Gains from increased crop duration

Crop yield gains from increased durations were most effective when the duration from maximum LAI to maturity (t_{TT3}) was increased (Figure 8.3). The greatest yield gains from this trait were observed in eastern India, where yield gains were in the range 12 – 15 %. Gains from t_{TT3} were lower in western and southern India (< 8 %). The effectiveness of t_{TT3} was followed by the duration from the start of pod-filling to LAI max (t_{TT2}), indicating that substantial yield gains would be achieved if both were increased simultaneously (i.e. overall increasing the grain filling period). For t_{TT2}, the most significant yield gains

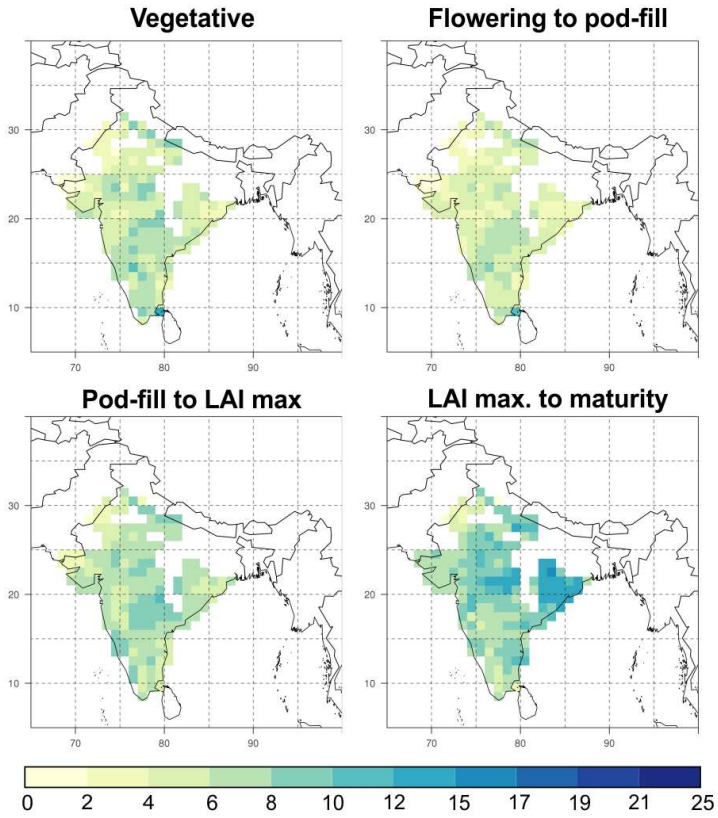

FIGURE 8.3: Mean crop yield changes as a result of increased crop duration. Additional details as in Figure 8.1.

were found in central-southern India (8 – 10 %). A longer vegetative period (t_{TT0}) was less effective, with yield gains in the range generally below 10 % (compared to 8 – 15 % for t_{TT2} and t_{TT3}). The least effective trait was the duration of the flowering stage (t_{TT1}), with yield gains generally below 6 %.

In contrast with the geographically inconsistent changes in yield variability produced by the drought management traits, increased duration traits showed more consistent result (Figure 8.4). In particular, improvements in yield stability were found in most of India for t_{TT0} and t_{TT1}. Yield CV increased by up to 15 % in the east –where monsoon precipitation is higher (Figure 3.3). For these two traits, CV decreased between -5 and -15 %. Increases in the duration of the grain filling period ($t_{TT2} + t_{TT3}$) both caused less stable yields. This result may be caused because a longer grain filling period can increase the crop's exposure to periods of intense drought towards the end of the growing period. This is confirmed by the fact that western India, the most drought-prone area of the country, showed decreased yield stability for all traits.

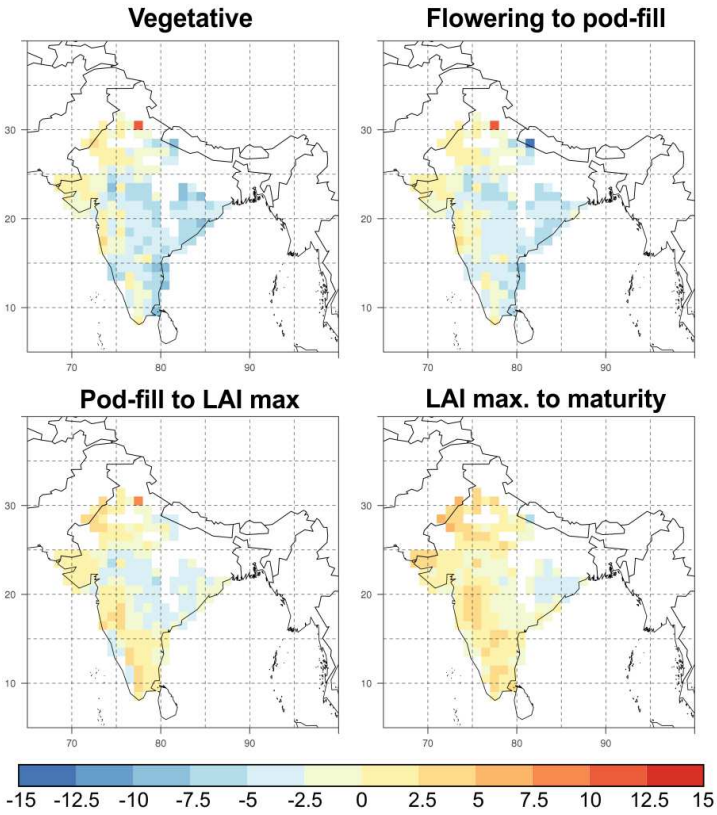

FIGURE 8.4: Crop yield variability changes as a result of increased crop duration. Additional details as in Figure 8.1.

8.4.3 Importance of heat stress tolerance

As expected from the little effect of heat stress on crop yields reported in Chapter 6, the yield gains from improved heat stress were negligible across the whole country (yield gain < 1 %). Figures are intentionally not shown because they bear little information (but see Figure 8.6). As discussed in Sect. 6.5.3, the lack of effect of temperature extremes on crop productivity may highlight the fact that the first breeding cycle (to target cultivar release by 2030) should not focus on improved heat tolerance. This conclusion holds valid for both heat stress during the flowering period (Challinor et al., 2007; Vara Prasad et al., 2003) and for the effect of heat stress on photosynthesis (Challinor et al., 2009a). Previous studies focusing on longer lead times have, however, found that heat stress is an important trait beyond 2050, particularly in southern India (Challinor et al., 2007; Singh et al., 2012).

8.4.4 Gains from breeding multiple traits

Combined traits yield gains are shown in Figure 8.5. In general, combining traits boosted crop yields across the whole study area. Since the effect of heat stress traits was very limited, all these gains can be attributed to increased thermal durations in addition to greater water-use efficiency. In many areas, crop yield gains exceeded 100 % relative to the future climate scenario projected productivity. The fact that these increases were so large can be attributed in part to the strong effect of WUE traits and their geographical complementarity (see Figure 8.1). In the combined scenarios, yield gains were generally lower (about 50 % below) in the dry areas of the west and the south, indicating that drought may preclude from fully capitalising breeding gains. However, these are the areas where most of the groundnut production is currently located (Challinor et al., 2003). Additionally, simulations in which improvement included reduced t_{TT0} all showed lower values than those where t_{TT0} was increased (Figure 8.5). This suggested that the duration of the vegetative phase needs to be sufficiently long in order to allow the crop to establish at the beginning of the cropping season.

Interannual yield variability, as with individual traits, showed a relatively inconsistent response both across the geographic space and across the two types of modifications (top-right panel for decreased t_{TT0}, bottom-right panel for increased t_{TT0}, Figure 8.5). Importantly, however, yields were much more stable across most of the territory if the vegetative time was slightly reduced, with reductions in CV beyond 15 % in many areas of eastern-southern India, as well as in the north. These areas also showed CV reductions in the range 5 – 10 %. In the rest of the study area, however, CV increases above 15 % were observed. These increases in yield variability may be strongly related with the fact that important traits such as $\partial H_I/\partial t$ and the TT_{max} both increased yield variability often above 15 % (Sect. 8.4.1)

The breeding of multiple traits may, however, prove difficult in practice, particularly if quality traits are also to be bred, or need to be preserved, in the genotypes. These results, nevertheless, stress that in many of the areas where negative productivity impacts are expected (e.g. central India, and to some extent also the south, see Sect. 6.4.2.2), countering of such negative impacts is possible through breeding appropriate drought

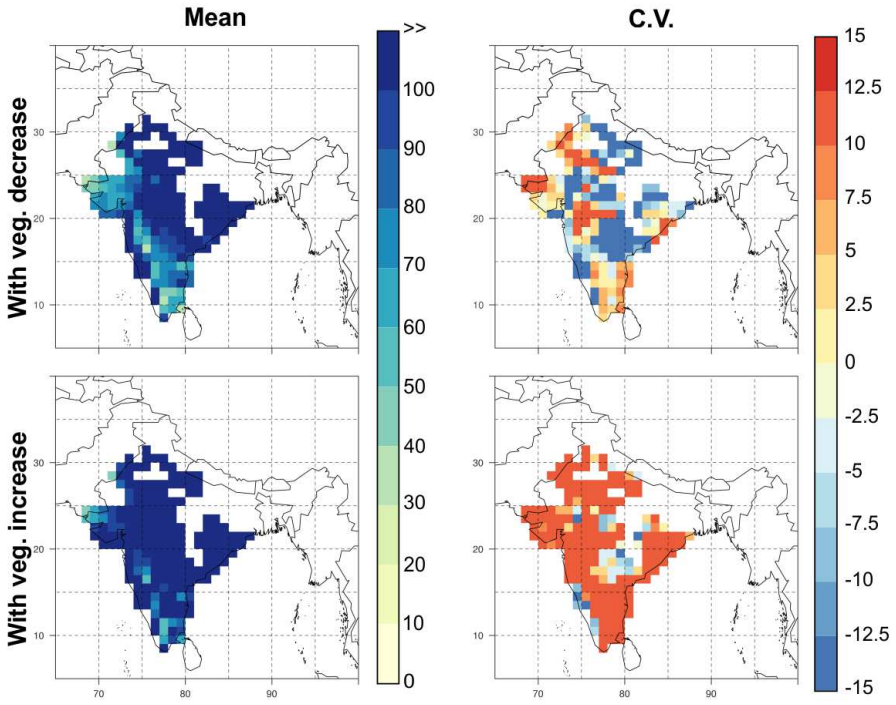

FIGURE 8.5: Crop yield mean and variability changes as a result of combined-trait improvement scenarios. Only results from I-DEL simulations are shown given their similarity with respect to other sets of simulations. The top (bottom) row shows the C1 (C9) simulations.

tolerance mechanisms and/or slightly lengthening the growing cycle –particularly the grain filling period (also see Singh et al. 2012).

8.4.5 Compared trait effectiveness

The relative effectiveness of the different traits and trait groups varied significantly for both yield means and yield variability (Figure 8.6). Improving the partitioning to seeds ($\partial H_I/\partial t$) had a greater impact than all other individual traits, as it boosted mean yields above 50 % in more than 50 % of the grid cells (Figure 8.6(a)). This suggests that partitioning to seeds should be a high priority trait in any breeding effort now so as to develop resilient germplasm that can be tested sufficiently early so as to be prepared for 2030 climates. In fact, there were greater mean yield gains from virtually all drought-related traits as compared with longer duration traits (Figure 8.7). As mentioned above (see Sect. 8.4.3), traits related to temperature extremes showed little or no effect and hence may not be a high priority for adaptation in the early 21^{st} century.

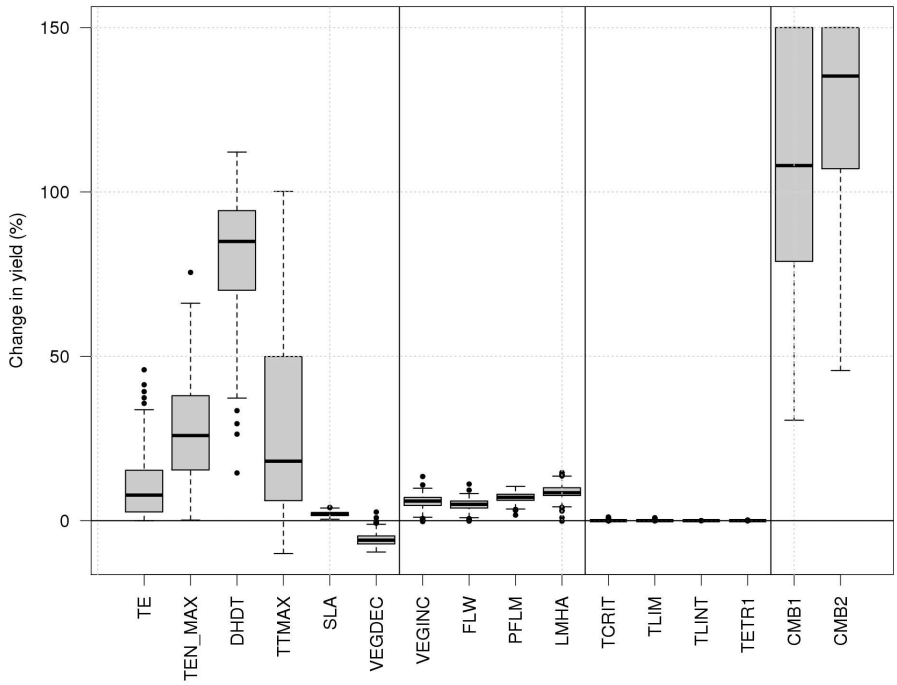

(a) $\bar{Y}$

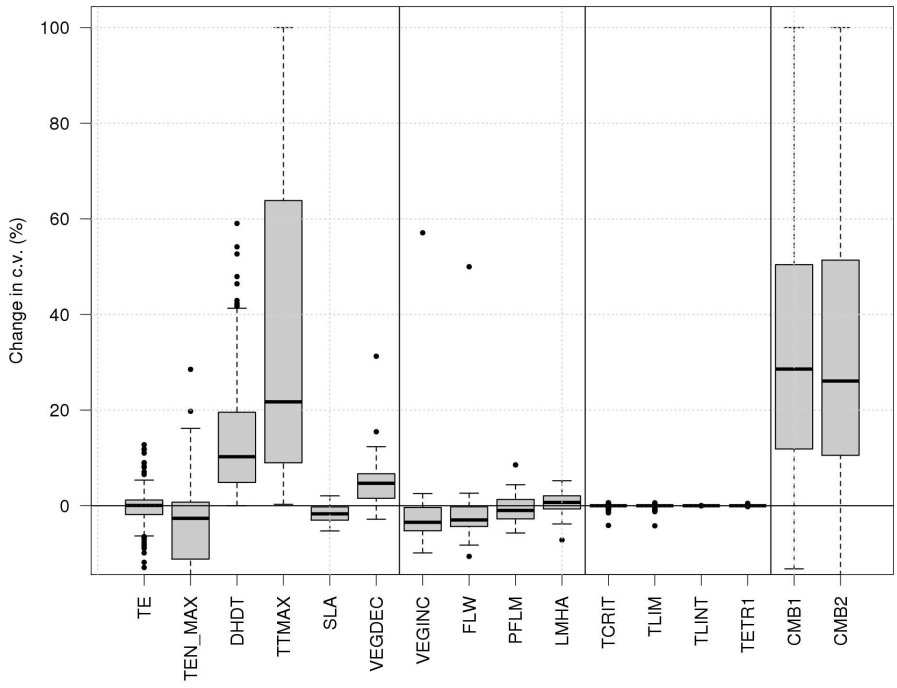

(b) CV

FIGURE 8.6: Comparative mean yield ($\bar{Y}$) and yield variability (CV) changes from different traits. The spread shows the spatial variation in the response of each quantity (means across simulations for each grid cell). Names of traits are as follows: TE (T_E), TEN_MAX ($E_{TN,max}$), DHDT ($\partial H_I/\partial t$), TTMAX (TT_{max}), SLA (SLA_{max}), VEGDEC (t_{TT0} decreased), VEGINC (t_{TT0} increased), FLW (t_{TT1}), PFLM (t_{TT2}), LMHA (t_{TT3}), TCRIT (T_{crit}^{lim}), TLIM (T_{lim}), TLINT (T_{ia}), TETR1 (T_{ter1}), CMB1 (C1), CMB2 (C9). Thick horizontal line is the median, boxes mark the 25 and 75 % of the data and whiskers extend to 5 and 95 % of the data.

For yield variability (Figure 8.6(a)), it is important to note that more stability was only achieved through traits that only improved WUE or the total assimilate production (i.e. increases in photosynthetic rates: T_E, $E_{TN,max}$), through traits that improved the effective LAI (SLA_{max}, increased t_{TT0}), and also through increases in the length of the flowering period (t_{TT1}). Combined traits showed little benefit to yield stability, indicating that capitalising yield gains in 'good' years through certain traits may come at the expense of a less resilient response in 'bad' years. On average, however, it was observed that drought-related traits were less effective in improving yield stability if bred together than those related to duration, though none was perfect (Figure 8.7). This highlights the need to understand and manage year-to-year yield responses through crop management (e.g. shifts in sowing dates, supplementary irrigation).

8.5 Discussion

8.5.1 Importance of traits and underlining processes

Gains in mean crop yields were observed across virtually all the different simulated traits across the study area, except for the reduction in the vegetative stage duration (t_{TT0}). This result seems robust and was in agreement with previous studies where yield gains were reported either by enhancing crop duration or by improving crop growth and phenology traits (see Challinor et al. 2009a; Singh et al. 2012). It must be noted, however, that the mean yield gains reported here were much more spatially consistent than those of Singh et al. (2012). Such differences may be attributed to the fact that Singh et al. (2012) used very conservative (10 %) percentage changes in the model parameters, they assessed only a handful of sites, a different period (2050), and they used a different crop model (CROPGRO, Hoogenboom et al. 1992). Here, the most effective set of traits for improving mean yields were those related to improved WUE (Figure 8.7(a)), and in particular a better partitioning to the seeds (herein measured using the harvest index change rate, $^{\partial H_I}/_{\partial t}$, Figure 8.6(a)). In this regard, for instance, Singh et al. (2012) reported that increased partitioning to seed presented a more spatially consistent and stronger response than an increase in the photosynthetic rate –as was found here. Better assimilate allocated to the seeds has been pointed out as one of the most important traits for achieving greater yields

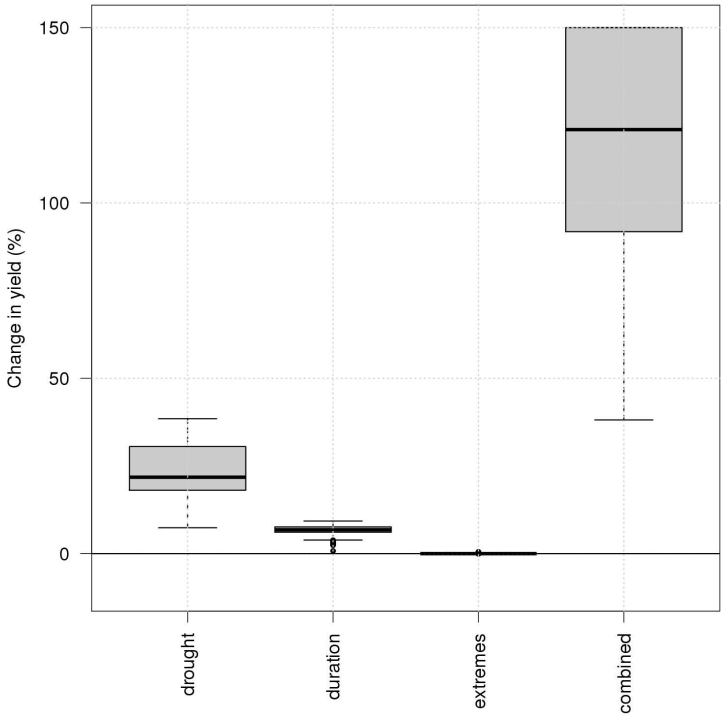

(a) $\bar{Y}$

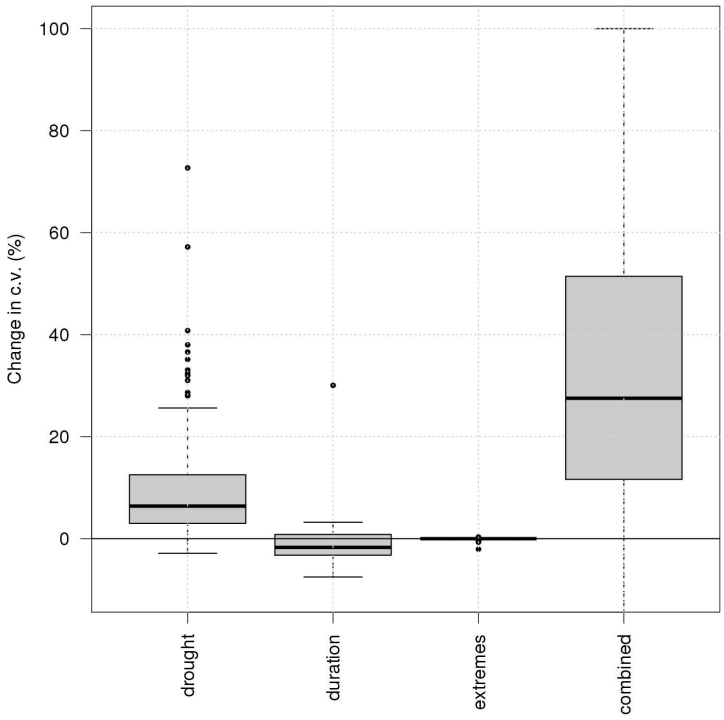

(b) CV

FIGURE 8.7: Comparative mean yield ($\bar{Y}$) and yield variability (CV) changes from different trait groups. The spread shows the spatial variation in the response of each quantity (means across simulations for each grid cell). Combined traits only display C1 and C9, for convenience. Thick horizontal line is the median, boxes mark the 25 and 75 % of the data and whiskers extend to 5 and 95 % of the data.

(Nigam, 2009; Nigam and Aruna, 2008; Upadhyaya, 2005). H_I is also a trait that shows large variation within the groundnut genepool (Rao and Nigam, 2003).

GLAM is based in the principle that $Y = T * E_T * H_I$ (where T is total transpiration) (see Sect. 3.5.1), which has been largely used in groundnut breeding (Nigam, 2009; Nigam and Aruna, 2008). The results presented here indicate that, as stressed by other authors (see Nigam 2009), gains from improvements in the transpiration rate are limited to areas where available soil moisture is sufficient during the the growing season. This was clearly evidenced since the dry areas of Gujarat (western India) and of the south (primarily Andhra Pradesh) showed little yield gains from improving this trait (Figure 8.1). In these environments, however, yield gains could be achieved through greater photosynthetic rates (higher E_T or $E_{TN,max}$, also see Nigam 2009). From these, it was apparent that $E_{TN,max}$ (as used in GLAM) had a greater impact, which may have been caused by the lower air moisture (i.e. high vapour pressure deficit) in many areas that enhances the response of total transpiration and total assimilate production, particularly in the south (Challinor and Wheeler, 2008b; Challinor et al., 2007).

Another important aspect of crop production, which is rarely assessed in climate change studies (e.g. Easterling et al. 2007; Singh et al. 2012) is the temporal stability of yield. Farming communities require stable harvests so as to be able to maintain and, where possible, increase the flow of produce to national and international markets (Wheeler and von Braun, 2013). Food security is also highly dependent on spatio-temporally stable crop yields (Vermeulen et al., 2013; Wheeler and von Braun, 2013). Changes in temporal variability of crop yields cause instability in the food system and the producers income. Because such changes can increase vulnerability locally and regionally, adaptation to climatic extremes is needed. In this study, the most effective traits in increasing mean yields also caused increased vulnerability to extremes (i.e. larger yield CV). These included the harvest index (most effective individual trait for mean yields), the maximum transpiration rate, and the increases in duration of grain filling (t_{TT2} + t_{TT3}). Mechanisms for these results can be inferred in some cases. In the case of the harvest index, for instance, decreases were concentrated in dry areas. This suggested that while in wet years increased harvest index allowed attaining higher yields, in very dry years a higher $\partial H_I/\partial t$ may trigger terminal drought earlier than normal (see Challinor et al. 2009a). Similarly, a longer reproductive period may expose the crops to terminal drought in very dry years.

TT_{max} caused the greatest yield stability reduction, probably via increased water stress in dry years (Nigam, 2009). These results suggest that yield means and yield stability may be achieved through different traits. There is no 'silver-bullet' trait for all regions, but it is likely that the combination of traits would be beneficial for many regions at once (Figure 8.5, also see Nigam 2009). The difficulty, however, is incorporating such multiple traits in practice through conventional breeding.

In general, in rainfed areas where crop duration is heavily restricted by the length of the rainy season, as in the states of Gujarat and Andhra Pradesh (where the majority of groundnut is grown) achieving a sufficiently dense canopy in a relatively short vegetative period is paramount for achieving stable yields (Nautiyal et al., 2012; Nigam, 2009; Rao and Nigam, 2003). Here, decreases in t_{TT0} alone were detrimental to crop yield stability (Figure 8.4), probably through reductions in LAI. However, when decreased t_{TT0} was coupled with WUE traits, stability was gained in many areas (Figure 8.5, right). In areas where soil moisture is not a limitation, the growing season can be increased so as to capitalise on available water.

Additional constraints other than biophysical are also present in groundnut cropping systems, indicating that an integral approach to crop adaptation is needed. These include pests and diseases (Singh et al., 1997) and sub-optimal crop management (Bhatia et al., 2009). The preservation of a genetic pool with sufficiently diverse genetic backgrounds (including wild species, Upadhyaya 2005) will provide the means for overcoming current biotic and abiotic constraints, capitalising on the potential benefits from and abating the negative impacts of climate change.

8.5.2 Crop breeding under uncertainty

Decisions on how and where to adapt a given cropping system cannot be delayed until outcomes are predicted with absolute certainty. In terms of breeding, this study demonstrated that despite uncertainty, GLAM can be used to make decisions related to the germplasm that can be used under future conditions (Vermeulen et al., 2013; Weaver et al., 2013). The methodology employed here can also be used with other crop models, thereby exploiting the modelling tools for defining key breeding traits under climate change (also see Singh et al. 2012; Suriharn et al. 2011). There was substantial uncertainty in the actual yield

changes both with and without adaptation (also see Chapter 6), with percentage changes varying substantially (see for instance the width of the PDFs of Figure 6.9). This, however, did not preclude a consistent and coherent simulation of adaptation. Robustness in the direction of yield changes and, importantly, in the processes behind such changes provide important insight and are critical to assessing the extent to which a decision can be made (see Chapter 6). The main challenge is thus to carefully interpret the model outcomes so as to provide information that is of use for breeders. This study demonstrated that adaptation to climate change in Indian groundnut cultivation is possible through improvements in the genotypic properties of currently grown cultivars. There was very high certainty that adaptation to climate change in groundnut cultivation is possible through increases in maximum photosynthetic rates, total asssimilate partitioned to seeds, and, only in areas with sufficient soil moisture, also through increases in the maximum transpiration rate. It can also be said with high certainty that heat stress is not a major concern in the next 20-30 years for breeders, though varietal substitutions may be required at local levels in cases (Challinor et al., 2005b, 2007; Craufurd et al., 2003).

An overarching issue when breeding climate-ready crops is to identify the correct sources of genetic variation. The most used sources of genetic variation are currently grown cultivars, and particularly hardy landraces (Nigam, 2009; Singh et al., 1997). The literature review used to set out the extended ranges for perturbing GLAM parameters indicated that currently grown cultivars can be of use for breeding groundnut under a climate of change. However, special attention must be paid to wild species both in terms of abiotic and biotic traits. Substantial genetic and environmental variability is reported in wild *Arachis* populations towards north-eastern Brazil, where drought is prevalent (Ferguson et al., 2005; Jarvis et al., 2003). In particular, populations *A. dardani* and *A. triseminata* have been found in areas where annual rainfall is below 550 mm and 750 mm, respectively (Ferguson et al., 2005). Other wild species have been reported to have desirable agronomic traits in conjunction with pest and/or disease resistance (e.g. *A. batizocoi*, *A. cardenansii*, and *A. duranensis*) (Nigam, 2009; Singh et al., 1997). The results of this study suggest that the current focus of groundnut breeding is well on target, but that particular attention has to be paid to the risks of increasing yield variability under future climate.

A last important aspect is the selection and adoption of appropriate cultivars in the field. Two complementary strategies may be followed: (a) the use of simple measures to measure

complex traits, and (b) farmer-based trial networks (e.g. Jarvis et al. 2011a). In practice, the selection of genotypes with high E_T or $E_{TN,max}$ can be achieved through selecting for greater SLA (i.e. thicker leaves) (Nigam, 2009; Nigam and Aruna, 2008; Rao and Nigam, 2003) or using the leaf chlorophyll concentration (Sheshshayee et al., 2006). Selecting for higher harvest index is easier, as it is a easily measurable at harvest. Ultimately, the adoption of novel germplasm by the farmers will depend on the demonstrated benefits of the new cultivars as well as on the degree of involvement of such farmers in the selection process (Mehrotra, 2011; Talawar, 2004). Thus, in order to improve farming conditions and facilitate the adoption of novel climate-ready germplasm the implementation of farmer-based experimental networks may prove effective (Nigam, 2009; van Etten, 2011).

Chapter 9

Conclusions

An assessment of the impacts of and adaptation to climate change for Indian groundnut cultivation was performed. Models of climate and crops were used to simulate the spatio-temporal variability of groundnut yields and suitability in present-day climates, and then to produce future projections, and an extensive set of simulations of genotypic adaptation. Many aspects make the presented work a unique contribution to the climate change impacts and modelling literature. Foremost, the results presented constitute the first ensemble of such size used for informing climate impacts and adaptation. The thorough consideration of both climate and crop sources of uncertainty made the construction of robust projections of climate change impacts possible, and this allowed identifying key processes under future climate change. The agreement in driving processes across the simulations presented ascertained various genotypic adaptation strategies. The further comparison of a niche model (EcoCrop) and GLAM presented in Chapter 7 was critical for contextualising all presented modelling results as well as to set out future challenges in crop-climate prediction.

9.1 Main findings and conclusions

The analyses presented in this thesis have led to the following main conclusions.

1. Agricultural impact studies are heavily reliant on high spatio-temporal resolution climate data. Typical is to find studies that use crop models that require high spatial resolution daily data for simulating agricultural productivity. However, existing data do not meet such requirements, or if they do, these are not accessible. Analyses of weather station networks and climate model simulations were performed in Chapter 4. The main problems in the climate data were associated with lack of accuracy in regions where landscape complexity forces large variations in meteorological fields in short intervals of time or space. Particularly in the context of projection-based climate change impacts and adaptation approaches, large errors in both observed and simulated climate can severely bias impacts estimates. The results suggest that a careful treatment of climate model bias and the creation of ensembles are critical needs for projection-based approaches, as this allows analysing more than one aspect of crop-climate simulation, and account for possible errors in model formulation, observational data, knowledge on responses to environmental factors, and initial conditions.

2. Crop model parametric uncertainty was investigated in Chapter 5. The belief that parameters in physiologically-oriented process-based crop models are *"mathematical constructs that reflect real world genotypes"* has prevented crop modellers –at least to some extent, from quantifying parametric uncertainty. This parameter uncertainty is relevant to climate change impacts since insufficiently constrained parameter values can lead to bias in the sampling of the crop's response probability distribution. The findings imply that none of GLAM parameters could be sufficiently constrained by the available observational data (i.e. crop yield), and, importantly, the majority of them did not necessarily follow a normal distribution. This indicated, firstly, that realistic yield simulations are not associated with a single 'perfect' combination of parameters, and secondly, that assumptions on the parameter probability distributions should be exercised with care. The result is consistent with previous work from Iizumi et al. (2011) and Tao et al. (2009). Further simulations (Chapter 6) showed that parametric uncertainty constitutes a relevant source of uncertainty, sometimes more important than the parameterised response to increased CO_2 concentrations, and in some cases comparable to climate model structure uncertainty.

3. The nature of coupled or uncoupled crop-climate simulations makes them highly

uncertain. Easterling et al. (2007) reported large spread in impacts estimates even at large scales, at which projected quantities are generally more robust (see Figure 1.5). The ensemble of simulations constructed here proved that coherent crop yield projections can be obtained despite uncertainty in actual yield values. This was attributed to the positive changes in precipitation projected by the majority of GCMs, which enhanced assimilate production in the simulated crop, reduced the impact of terminal drought (hence increasing crop duration) and generally indicated positive impacts from climate change for groundnut. Uncertainties in the projected yield values across the GLAM ensemble were large in cases, but did not preclude robust statements being made in four out of five regions of India. A shift from a 'predictive' impacts science to a more 'process-oriented' science, where both quantities predicted and underlining processes are reported is warranted.

4. Chapter 7 investigated the agreement between and attempted to combine GLAM and EcoCrop. The author of this thesis has published research using EcoCrop (see e.g. Jarvis et al. 2012; Ramirez-Villegas et al. 2013b), with the model outputs generally agreeing with previously published results (e.g. Fig. 7 in Ramirez-Villegas et al. 2013b). In Chapters 5 and 6, GLAM was used to simulate present and future climate responses of groundnut –thus providing the author (and the reader) a deep understanding of the model, its constitution and predicted responses to current and future climate. Using both models for groundnut, this work reports substantial differences between present-day suitability and productivity, and their projected changes. These differences can be attributed to various factors, but perhaps the most important one is the fact that simulating suitability (with EcoCrop) does not involve accounting for any sub-seasonal weather variation. If anything, this highlights the importance of comparing impacts estimates with those of previous studies regardless of the nature of the model used. This also implies a challenge in reconciling both measures (suitability and productivity) –clearly a subject of future study.

5. Existing work on genotypic adaptation has focused on assessing the impact of various genotypic properties using highly detailed and data-demanding field-scale crop models, but at the expense of quantifying uncertainties or mapping of probabilities and/or probability distributions (see e.g. Semenov and Halford 2009; Singh et al.

2012; Suriharn et al. 2011). Chapter 8 demonstrated that the development of adaptation strategies for groundnut was not contingent on the climate scenarios or crop model parameter set chosen. Adaptation through improving the genotypic properties of existing cultivars is possible in groundnut. The results implied that current breeding strategies seem to be well on track at least until 2030s, but reconsiderations could be done towards the end of the 21^{st} century so as to prioritise heat stress.

9.2 Implications of this research

As pointed out in Chapter 4 and in existing literature (see Challinor et al. 2009b and Ramirez-Villegas et al. 2013a), the thoughtful creation of robust crop model ensembles is a necessary step when aiming at improving agricultural decision making. In that sense, the present work is a substantial way forward. In short, it provides a thorough investigation of climate change impacts for groundnut as well as of the associated uncertainties. The study sets out a methodology for assessing impacts and developing genotypic adaptation strategies at the regional scale, and opens the possibility of deepening the analyses at more local scales.

In terms of using climate models for impacts research, this study is the first in identifying (together with Ramirez-Villegas et al. 2013a) the impacts of CMIP5 model bias on agricultural impacts assessment. Climate model output should be treated with caution, and such treatment is dependent on the scale of the impact analysis intended (Masson and Knutti, 2011). The analyses presented in Chapter 6 imply that the decision of whether to bias-correct a climate model output or not, and the choice of bias-correction and/or downscaling method are significant sources of uncertainty, often larger than the structure of climate models. In general, future impacts studies should provide a better account of these uncertainties in order to avoid generating 'over-confidence' in their projections.

Impacts-based approaches are one of two main action pathways for adapting agriculture to climate change (Challinor et al., 2013; Mearns, 2010). This work has demonstrated that impacts-based (also referred to as top-down or projection-based) approaches can provide information that is useful for adaptation. For the case of groundnut cultivation, robustness in GLAM projections was achieved in virtually all India. This proved that projection-based

approaches are not necessarily limited by modelling uncertainties. Future studies on crop-climate impacts should attempt at assessing robustness in a similar way as done here, as this would enhance the impacts evidence base and would hence facilitate climate change adaptation (see e.g. Koehler et al. 2013 for an example). Lack of robustness represents a challenge to scientists and policy makers, but it is important to identify areas and periods where lack of robustness hinders projections of climate impacts (e.g. Koehler et al. 2013). In those cases, a better understanding of local processes so as to adopt a more bottom-up approach (i.e. capacity based, as in Vermeulen et al. 2013) to adaptation may be warranted.

Perhaps the main intended users of genotypic adaptation information (as that provided in Chapter 8) are crop breeders. However, physiological crop models are limited to providing physiology-level conclusions. This information is often of limited use for breeders because it does not provide sufficient detail on the genetic background of the material that could be used for crop improvement, particularly for large-area models whose parameters are difficult to assimilate as real world genotypes. It is thus important that the challenges of combining physiological- and genetic-level information are overcome, without excessive increases in model complexity and uncertainty.

9.3 Future work

The work presented in this thesis has opened a number of potential areas of future work. First of all, work on uncertainty quantification remains incipient in many aspects of crop modelling. Existing studies limit the quantification of modelling uncertainty to either using multiple GCMs with a single crop model (e.g. Lobell et al. 2008; Ruane et al. 2013; Thornton et al. 2009), to the use of crop model parameter ensembles with a single bias-corrected set of GCM simulations (e.g. Tao et al. 2009), or to the use of multiple crop models with a single bias-corrected set of GCM simulations (e.g. Asseng et al. 2013; Palosuo et al. 2011; Rotter et al. 2011). This study quantifies all sources of uncertainty to the extent that available computational capacity allows. Nevertheless, it falls short in quantifying structural uncertainty in crop models. This is clearly a point for future work.

This thesis has provided an assessment of climate model errors (Chapter 4) and of their effect on GLAM simulations (Sect. 6.4.1). Watson and Challinor (2013) provided an

overview of GLAM responses to errors in meteorological data at different scales for a location in India. In line with the two studies, the identification of GCM characteristics (e.g. components included, skill in reproducing modes of variability and teleconnection) that lead to coherent crop simulations could be a topic for future studies.

With regards of niche-based models, EcoCrop was used to simulate groundnut suitability. Nevertheless, other types of niche models exist, including species distributions models (SDMs, as described in Sect. 2.3.2.2). SDMs are to an extent similar to EcoCrop, but have a different structure and tend to be more flexible. Recent work on comparing SDMs and process-based models for forest species has revealed that relationships are difficult to find and highly non-linear (e.g. Keenan et al. 2011; Morin and Thuiller 2009; Serra-Diaz et al. 2013). The combination and comparison of suitability and productivity measures could potentially be expanded to SDMs.

A final topic of interest relating to this thesis is the scaling down of genotypic adaptation. In this regard, using field-scale crop models that allow a better mapping of traits on the model parameter space as well as investigating the possible coupling of physiological information and quantitative trait loci data are topics that warrant future research.

Appendix A

Material used in Chapter 3

List of publications revised from which the meta-analysis of climate data usage was done.

1. Adam M, Van Bussel LGJ, Leffelaar PA, Van Keulen H, Ewert F (2011) Effects of modelling detail on simulated potential crop yields under a wide range of climatic conditions. Ecological Modelling 222: 131-143.
2. Aggarwal PK, Mall RK (2002) Climate Change and Rice Yields in Diverse Agro-Environments of India. II. Effect of Uncertainties in Scenarios and Crop Models on Impact Assessment. Climatic Change 52: 331-343.
3. Aggarwal PK, Banerjee B, Daryaei MG, Bhatia A, Bala A, et al. (2006) InfoCrop: A dynamic simulation model for the assessment of crop yields, losses due to pests, and environmental impact of agro-ecosystems in tropical environments. II. Performance of the model. Agricultural Systems 89: 47-67.
4. Alagarswamy G, Boote KJ, Allen LH, Jones JW (2006) Evaluating the CROPGRO-soybean model ability to simulate photosynthesis response to carbon dioxide levels. Madison, WI, ETATS-UNIS: American Society of Agronomy. 9 p.
5. Alcamo J, Dronin N, Endejan M, Golubev G, Kirilenko A (2007) A new assessment of climate change impacts on food production shortfalls and water availability in Russia. Global Environmental Change 17: 429-444.
6. Alcamo J, Dll P, Henrichs T, Kaspar F, Lehner B, et al. (2003) Global estimates of water withdrawals and availability under current and future business-as-usual conditions. Hydrological Sciences Journal 48: 339-348.
7. Alexandrov V, Eitzinger J, Cajic V, Oberforster M (2002) Potential impact of climate change on selected agricultural crops in north-eastern Austria. Global Change Biology 8: 372-389.
8. Alig RJ, Adams DM, McCarl BA (2002) Projecting impacts of global climate change on the US forest and agriculture sectors and carbon budgets. Forest Ecology and Management 169: 3-14.

9. Andrade-Piedra JL, Hijmans RJ, Juárez HS, Forbes GA, Shtienberg D, et al. (2005) Simulation of Potato Late Blight in the Andes. II: Validation of the LATEBLIGHT Model. Phytopathology 95: 1200-1208.

10. Andrasson J, Bergstrom S, Carlsson B, Graham LP, Lindstrm G (2004) Hydrological Change Climate Change Impact Simulations for Sweden. AMBIO: A Journal of the Human Environment 33: 228-234.

11. Apipattanavis S, Bert F, Podestá G, Rajagopalan B (2010) Linking weather generators and crop models for assessment of climate forecast outcomes. Agricultural and Forest Meteorology 150: 166-174.

12. Asada H, Matsumoto J (2009) Effects of rainfall variation on rice production in the Ganges-Brahmaputra Basin. Climate Research 38: 249-260.

13. Asseng S, Jamieson PD, Kimball B, Pinter P, Sayre K, et al. (2004) Simulated wheat growth affected by rising temperature, increased water deficit and elevated atmospheric CO_2. Field Crops Research 85: 85-102.

14. Audsley E, Pearn KR, Simota C, Cojocaru G, Koutsidou E, et al. (2006) What can scenario modelling tell us about future European scale agricultural land use, and what not? Environmental Science & Policy 9: 148-162.

15. Baigorria GA, Jones JW, O'Brien JJ (2008) Potential predictability of crop yield using an ensemble climate forecast by a regional circulation model. Agricultural and Forest Meteorology 148: 1353-1361.

16. Bakker MM, Govers G, Ewert F, Rounsevell M, Jones R (2005) Variability in regional wheat yields as a function of climate, soil and economic variables: Assessing the risk of confounding. Agriculture, Ecosystems & Environment 110: 195-209.

17. Baron C, Sultan B, Balme M, Sarr B, Traore S, et al. (2005) From GCM grid cell to agricultural plot: scale issues affecting modelling of climate impact. Philosophical Transactions of the Royal Society B: Biological Sciences 360: 2095-2108.

18. Barrios S, Ouattara B, Strobl E (2008) The impact of climatic change on agricultural production: Is it different for Africa? Food Policy 33: 287-298.

19. Battisti DS, Naylor RL (2009) Historical Warnings of Future Food Insecurity with Unprecedented Seasonal Heat. Science 323: 240-244.

20. Betts RA, Falloon PD, Goldewijk KK, Ramankutty N (2007) Biogeophysical effects of land use on climate: Model simulations of radiative forcing and large-scale temperature change. Agricultural and Forest Meteorology 142: 216-233.

21. Blenkinsop S, Fowler HJ (2007) Changes in drought frequency, severity and duration for the British Isles projected by the PRUDENCE regional climate models. Journal of Hydrology 342: 50-71.

22. Boomiraj K, Chakrabarti B, Aggarwal PK, Choudhary R, Chander S (2010) Assessing the vulnerability of Indian mustard to climate change. Agriculture, Ecosystems & Environment 138: 265-273.

23. Boote KJ, Jones JW, Batchelor WD, Nafziger ED, Myers O (2003) Genetic coefficients in the CROPGRO-Soybean model: Links to field performance and genomics. Agronomy Journal 95: 32-51.

24. Boote KJ, Kropff MJ, Bindraban PS (2001) Physiology and modelling of traits in crop plants: implications for genetic improvement. Agricultural Systems 70: 395-420.

25. Brooks RJ, Semenov MA, Jamieson PD (2001) Simplifying Sirius: sensitivity analysis and development of a meta-model for wheat yield prediction. European Journal of Agronomy 14: 43-60.

26. Brown RA, Rosenberg NJ (1999) Climate Change Impacts on the Potential Productivity of Corn and Winter Wheat in Their Primary United States Growing Regions. Climatic Change 41: 73-107.

27. Buytaert W, Vuille M, Dewulf A, Urrutia R, Karmalkar A, et al. (2010) Uncertainties in climate change projections and regional downscaling: implications for water resources management. Hydrol Earth Syst Sci Discuss 7: 1821-1848.

28. Buytaert W, Clleri R, Timbe L (2009) Predicting climate change impacts on water resources in the tropical Andes: Effects of GCM uncertainty. Geophys Res Lett 36: L07406.

29. Calanca P, Vuichard N, Campbell C, Viovy N, Cozic A, et al. (2007) Simulating the fluxes of CO2 and N2O in European grasslands with the Pasture Simulation Model (PaSim). Agriculture, Ecosystems & Environment 121: 164-174.

30. Carberry PS, Ranganathan R, Reddy LJ, Chauhan YS, Robertson MJ (2001) Predicting growth and development of pigeonpea: flowering response to photoperiod. Field Crops Research 69: 151-162.

31. Carbone GJ, Mearns LO, Mavromatis T, Sadler EJ, Stooksbury D (2003) Evaluating CROPGRO-Soybean Performance for Use in Climate Impact Studies. Agron J 95: 537-544.

32. Cesaraccio C, Dettori M, Ducel P, Spano D, Motroni A, et al. (2008) Using Long-Term Data and Crop Modelling to Assess Climate Change Impacts on Durum Wheat Production in the Mediterranean. Italian Journal of Agronomy 3: 733-734.

33. Challinor AJ, Wheeler TR (2008) Use of a crop model ensemble to quantify CO2 stimulation of water-stressed and well-watered crops. Agricultural and Forest Meteorology 148: 1062-1077.

34. Challinor AJ, Wheeler TR, Craufurd PQ, Slingo JM, Grimes DIF (2004) Design and optimisation of a large-area process-based model for annual crops. Agricultural and Forest Meteorology 124: 99-120.

35. Challinor AJ, Wheeler TR, Slingo JM, Craufurd PQ, Grimes DIF (2005) Simulation of Crop Yields Using ERA-40: Limits to Skill and Nonstationarity in WeatherYield Relationships. Journal of Applied Meteorology 44: 516-531.

36. Challinor AJ, Slingo JM, Wheeler TR, DoblasReyes FJ (2005) Probabilistic simulations of crop yield over western India using the DEMETER seasonal hindcast ensembles. Tellus A 57: 498-512.

37. Challinor AJ, Wheeler TR, Craufurd PQ, Slingo JM (2005) Simulation of the impact of high temperature stress on annual crop yields. Agricultural and Forest Meteorology 135: 180-189.

38. Challinor AJ, Wheeler TR, Slingo JM, Hemming D (2005) Quantification of physical and biological uncertainty in the simulation of the yield of a tropical crop using present-day and doubled CO2 climates. Philosophical Transactions of the Royal Society B: Biological Sciences 360: 2085-2094.

39. Challinor AJ, Wheeler TR, Craufurd PQ, Ferro CAT, Stephenson DB (2007) Adaptation of crops to climate change through genotypic responses to mean and extreme temperatures. Agriculture, Ecosystems & Environment 119: 190-204.

40. Challinor AJ, Wheeler TR, Hemming D, Upadhyaya HD (2009) Ensemble yield simulations: crop and climate uncertainties, sensitivity to temperature and genotypic adaptation to climate change. Climate Research 38: 117-127.

41. Challinor AJ, Simelton ES, Fraser EDG, Hemming D, Collins M (2010) Increased crop failure due to climate change: assessing adaptation options using models and socio-economic data for wheat in China. Environmental Research Letters 5: 034012.

42. Chander S, Ahuja LR, Peairs FB, Aggarwal PK, Kalra N (2006) Modeling the effect of Russian wheat aphid, Diuraphis noxia (Mordvilko) and weeds in winter wheat as guide to management. Agricultural Systems 88: 494-513.

43. Chang H, Knight C, Staneva M, Kostov D (2002) Water resource impacts of climate change in southwestern Bulgaria. GeoJournal 57: 159-168.

44. Chavas DR, Izaurralde RC, Thomson AM, Gao X (2009) Long-term climate change impacts on agricultural productivity in eastern China. Agricultural and Forest Meteorology 149: 1118-1128.

45. Chipanshi AC, Chanda R, Totolo O (2003) Vulnerability Assessment of the Maize and Sorghum Crops to Climate Change in Botswana. Climatic Change 61: 339-360.

46. Choudhury BJ (2000) A sensitivity analysis of the radiation use efficiency for gross photosynthesis and net carbon accumulation by wheat. Agricultural and Forest Meteorology 101: 217-234.

47. Choudhury BJ (2001) Modeling radiation- and carbon-use efficiencies of maize, sorghum, and rice. Agricultural and Forest Meteorology 106: 317-330.

48. Christidis N, Stott PA, Brown S, Karoly DJ, Caesar J (2007) Human Contribution to the Lengthening of the Growing Season during 195099. Journal of Climate 20: 5441-5454.

49. Chung SO, Rodrguez-Díaz JA, Weatherhead EK, Knox JW (2011) Climate change impacts on water for irrigating paddy rice in South Korea. Irrigation and Drainage 60: 263-273.

50. Cooper PJM, Dimes J, Rao KPC, Shapiro B, Shiferaw B, et al. (2008) Coping better with current climatic variability in the rain-fed farming systems of sub-Saharan Africa: An essential first step in adapting to future climate change? Agriculture, Ecosystems & Environment 126: 24-35.

51. Corre-Hellou G, Faure M, Launay M, Brisson N, Crozat Y (2009) Adaptation of the STICS intercrop model to simulate crop growth and N accumulation in pea-barley intercrops. Field Crops Research 113: 72-81.

52. Craufurd PQ, Qi A (2001) Photothermal adaptation of sorghum (Sorghum bicolour) in Nigeria. Agricultural and Forest Meteorology 108: 199-211.

53. De Silva CS, Weatherhead EK, Knox JW, Rodriguez-Diaz JA (2007) Predicting the impacts of climate change–A case study of paddy irrigation water requirements in Sri Lanka. Agricultural Water Management 93: 19-29.

54. Deressa TT, Hassan RM (2009) Economic Impact of Climate Change on Crop Production in Ethiopia: Evidence from Cross-section Measures. Journal of African Economies.

55. Dixit PN, Cooper PJM, Dimes J, Rao KP (2011) Adding Value to Field-Based Agronomic Research Through Climate Risk Assessment: A Case Study of Maize Production in Kitale, Kenya. Experimental Agriculture 47: 317-338.

56. Easterling WE, Chhetri N, Niu X (2003) Improving the Realism of Modeling Agronomic Adaptation to Climate Change: Simulating Technological Substitution. Climatic Change 60: 149-173.

57. Eitzinger J, Stastn M, Zalud Z, Dubrovsk M (2003) A simulation study of the effect of soil water balance and water stress on winter wheat production under different climate change scenarios. Agricultural Water Management 61: 195-217.

58. Estrella N, Sparks TH, Menzel A (2007) Trends and temperature response in the phenology of crops in Germany. Global Change Biology 13: 1737-1747.

59. Etchevers P, Golaz C, Habets F, Noilhan J (2002) Impact of a climate change on the Rhone river catchment hydrology. J Geophys Res 107: 4293.

60. Evans N, Baierl A, Semenov MA, Gladders P, Fitt BDL (2008) Range and severity of a plant disease increased by global warming. Journal of The Royal Society Interface 5: 525-531.

61. Everingham YL, Smyth CW, Inman-Bamber NG (2009) Ensemble data mining approaches to forecast regional sugarcane crop production. Agricultural and Forest Meteorology 149: 689-696.

62. Ewert F, Porter JR (2000) Ozone effects on wheat in relation to CO2: modelling short-term and long-term responses of leaf photosynthesis and leaf duration. Global Change Biology 6: 735-750.

63. Ewert F, Rodriguez D, Jamieson P, Semenov MA, Mitchell RAC, et al. (2002) Effects of elevated CO2 and drought on wheat: testing crop simulation models for different experimental and climatic conditions. Agriculture, Ecosystems & Environment 93: 249-266.

64. Ewert F, Rounsevell MDA, Reginster I, Metzger MJ, Leemans R (2005) Future scenarios of European agricultural land use: I. Estimating changes in crop productivity. Agriculture, Ecosystems & Environment 107: 101-116.

65. Ewert F, van Oijen M, Porter JR (1999) Simulation of growth and development processes of spring wheat in response to CO2 and ozone for different sites and years in Europe using mechanistic crop simulation models. European Journal of Agronomy 10: 231-247.

66. Falloon P, Betts R (2010) Climate impacts on European agriculture and water management in the context of adaptation and mitigation–The importance of an integrated approach. Science of The Total Environment 408: 5667-5687.

67. Falloon P, Smith P, Bradley RI, Milne R, Tomlinson R, et al. (2006) RothCUK a dynamic modelling system for estimating changes in soil C from mineral soils at 1-km resolution in the UK. Soil Use and Management 22: 274-288.

68. Falloon PD, Betts RA (2006) The impact of climate change on global river flow in HadGEM1 simulations. Atmospheric Science Letters 7: 62-68.

69. Farrow A, Musoni D, Cook S, Buruchara R (2011) Assessing the risk of root rots in common beans in East Africa using simulated, estimated and observed daily rainfall data. Experimental Agriculture 47: 357-373.

70. Felkner J, Tazhibayeva K, Townsend R (2009) Impact of Climate Change on Rice Production in Thailand. American Economic Review 99: 205-210.

71. Fischer G, Shah M, N. Tubiello F, van Velhuizen H (2005) Socio-economic and climate change impacts on agriculture: an integrated assessment, 19902080. Philosophical Transactions of the Royal Society B: Biological Sciences 360: 2067-2083.

72. Fischer G, Tubiello FN, van Velthuizen H, Wiberg DA (2007) Climate change impacts on irrigation water requirements: Effects of mitigation, 1990-2080. Technological Forecasting and Social Change 74: 1083-1107.

73. Fleischer A, Lichtman I, Mendelsohn R (2008) Climate change, irrigation, and Israeli agriculture: Will warming be harmful? Ecological Economics 65: 508-515.

74. Folliard A, Traor PCS, Vaksmann M, Kouressy M (2004) Modeling of sorghum response to photoperiod: a threshold-hyperbolic approach. Field Crops Research 89: 59-70.

75. Fraisse CW, Cabrera VE, Breuer NE, Baez J, Quispe J, et al. (2008) El NioSouthern Oscillation influences on soybean yields in eastern Paraguay. International Journal of Climatology 28: 1399-1407.

76. Guerea A, Ruiz-Ramos M, Díaz-Ambrona CH, Conde JR, Mnguez MI (2001) Assessment of Climate Change and Agriculture in Spain Using Climate Models. Agron J 93: 237-249.

77. Hadria R, Duchemin B, Lahrouni A, Khabba S, Erraki S, et al. (2006) Monitoring of irrigated wheat in a semiarid climate using crop modelling and remote sensing data: Impact of satellite revisit time frequency. International Journal of Remote Sensing 27: 1093-1117.

78. Haim D, Shechter M, Berliner P (2008) Assessing the impact of climate change on representative field crops in Israeli agriculture: a case study of wheat and cotton. Climatic Change 86: 425-440.

79. Hansen JW, Indeje M (2004) Linking dynamic seasonal climate forecasts with crop simulation for maize yield prediction in semi-arid Kenya. Agricultural and Forest Meteorology 125: 143-157.

80. Hansen JW, Potgieter A, Tippett MK (2004) Using a general circulation model to forecast regional wheat yields in northeast Australia. Agricultural and Forest Meteorology 127: 77-92.

81. Hansen JW, Mishra A, Rao KPC, Indeje M, Ngugi RK (2009) Potential value of GCM-based seasonal rainfall forecasts for maize management in semi-arid Kenya. Agricultural Systems 101: 80-90.

82. Hay LE, Clark MP, Wilby RL, Gutowski WJ, Leavesley GH, et al. (2002) Use of Regional Climate Model Output for Hydrologic Simulations. Journal of Hydrometeorology 3: 571-590.

83. Hebbar KB, Venugopalan MV, Seshasai MVR, Rao KV, Patil BC, et al. (2008) Predicting cotton production using Infocrop-cotton simulation model, remote sensing and spatial agro-climatic data. Current Science 95: 1570-1579.

84. Hijmans R (2003) The effect of climate change on global potato production. American Journal of Potato Research 80: 271-279.

85. Hijmans RJ, Forbes GA, Walker TS (2000) Estimating the global severity of potato late blight with GIS-linked disease forecast models. Plant Pathology 49: 697-705.

86. Holden NM, Brereton AJ, Fealy R, Sweeney J (2003) Possible change in Irish climate and its impact on barley and potato yields. Agricultural and Forest Meteorology 116: 181-196.

87. Ibez I, Primack RB, Miller-Rushing AJ, Ellwood E, Higuchi H, et al. (2010) Forecasting phenology under global warming. Philosophical Transactions of the Royal Society B: Biological Sciences 365: 3247-3260.

88. Iglesias A, Rosenzweig C, Pereira D (2000) Agricultural impacts of climate change in Spain: developing tools for a spatial analysis. Global Environmental Change 10: 69-80.

89. Jagtap SS, Jones JW (2002) Adaptation and evaluation of the CROPGRO-soybean model to predict regional yield and production. Agriculture, Ecosystems & Environment 93: 73-85.

90. Jamieson PD, Brooking IR, Porter JR, Wilson DR (1995) Prediction of leaf appearance in wheat: a question of temperature. Field Crops Research 41: 35-44.

91. Jamieson PD, Porter JR, Goudriaan J, Ritchie JT, van Keulen H, et al. (1998) A comparison of the models AFRCWHEAT2, CERES-Wheat, Sirius, SUCROS2 and SWHEAT with measurements from wheat grown under drought. Field Crops Research 55: 23-44.

92. Jamieson PD, Berntsen J, Ewert F, Kimball BA, Olesen JE, et al. (2000) Modelling CO2 effects on wheat with varying nitrogen supplies. Agriculture, Ecosystems & Environment 82: 27-37.

93. Jimnez D, Cock J, Jarvis A, Garcia J, Satizbal HF, et al. (2010) Interpretation of commercial production information: A case study of lulo (Solanum quitoense), an under-researched Andean fruit. Agricultural Systems In Press, Corrected Proof.

94. Jochec KG, Mjelde JW, Lee AC, Conner JR (2001) Use of Seasonal Climate Forecasts in Rangeland-Based Livestock Operations in West Texas. Journal of Applied Meteorology 40: 1629-1639.

95. Jones PG, Thornton PK (2003) The potential impacts of climate change on maize production in Africa and Latin America in 2055. Global Environmental Change 13: 51-59.

96. Jones PG, Thornton PK (2009) Croppers to livestock keepers: livelihood transitions to 2050 in Africa due to climate change. Environmental Science & Policy 12: 427-437.

97. Jones PD, Lister DH, Jaggard KW, Pidgeon JD (2003) Future Climate Impact on the Productivity of Sugar Beet (*Beta vulgaris* L.) in Europe. Climatic Change 58: 93-108.

98. Juen I, Kaser G, Georges C (2007) Modelling observed and future runoff from a glacierized tropical catchment (Cordillera Blanca, Per). Global and Planetary Change 59: 37-48.

99. Kenny GJ, Warrick RA, Campbell BD, Sims GC, Camilleri M, et al. (2000) Investigating Climate Change Impacts and Thresholds: An Application of the CLIMPACTS Integrated Assessment Model for New Zealand Agriculture. Climatic Change 46: 91-113.

100. Ko J, Piccinni G, Steglich E (2009) Using EPIC model to manage irrigated cotton and maize. Agricultural Water Management 96: 1323-1331.

101. Kouressy M, Dingkuhn M, Vaksmann M, Heinemann AB (2008) Adaptation to diverse semi-arid environments of sorghum genotypes having different plant type and sensitivity to photoperiod. Agricultural and Forest Meteorology 148: 357-371.

102. Krishnan P, Swain DK, Chandra Bhaskar B, Nayak SK, Dash RN (2007) Impact of elevated CO2 and temperature on rice yield and methods of adaptation as evaluated by crop simulation studies. Agriculture, Ecosystems & Environment 122: 233-242.

103. Kucharik CJ, Serbin SP (2008) Impacts of recent climate change on Wisconsin corn and soybean yield trends. Environmental Research Letters 3: 034003.

104. Krishna Kumar K, Rupa Kumar K, Ashrit RG, Deshpande NR, Hansen JW (2004) Climate impacts on Indian agriculture. International Journal of Climatology 24: 1375-1393.

105. Lehner B, Dll P, Alcamo J, Henrichs T, Kaspar F (2006) Estimating the Impact of Global Change on Flood and Drought Risks in Europe: A Continental, Integrated Analysis. Climatic Change 75: 273-299.

106. Li Y, Ye W, Wang M, Yan X (2009) Climate change and drought: a risk assessment of crop-yield impacts. Climate Research 39: 31-46.

107. Liu J, Fritz S, van Wesenbeeck CFA, Fuchs M, You L, et al. (2008) A spatially explicit assessment of current and future hotspots of hunger in Sub-Saharan Africa in the context of global change. Global and Planetary Change 64: 222-235.

108. Liu J, Williams JR, Zehnder AJB, Yang H (2007) GEPIC - modelling wheat yield and crop water productivity with high resolution on a global scale. Agricultural Systems 94: 478-493.

109. Lobell DB, Asner GP (2003) Climate and Management Contributions to Recent Trends in U.S. Agricultural Yields. Science 299: 1032.

110. Lobell DB, Burke MB (2010) On the use of statistical models to predict crop yield responses to climate change. Agricultural and Forest Meteorology 150: 1443-1452.

111. Lobell DB, Burke MB (2008) Why are agricultural impacts of climate change so uncertain? The importance of temperature relative to precipitation. Environmental Research Letters 3: 034007.

112. Lobell DB, Field CB (2007) Global scale climatecrop yield relationships and the impacts of recent warming. Environmental Research Letters 2: 014002.

113. Lobell DB, Banziger M, Magorokosho C, Vivek B (2011) Nonlinear heat effects on African maize as evidenced by historical yield trials. Nature Clim Change 1: 42-45.

114. Lobell DB, Burke MB, Tebaldi C, Mastrandrea MD, Falcon WP, et al. (2008) Prioritizing Climate Change Adaptation Needs for Food Security in 2030. Science 319: 607-610.

115. Lobell DB, Field CB, Cahill KN, Bonfils C (2006) Impacts of future climate change on California perennial crop yields: Model projections with climate and crop uncertainties. Agricultural and Forest Meteorology 141: 208-218.

116. Ludwig B, Bergstermann A, Priesack E, Flessa H (2011) Modelling of crop yields and N2O emissions from silty arable soils with differing tillage in two long-term experiments. Soil and Tillage Research 112: 114-121.

117. Ludwig F, Milroy S, Asseng S (2009) Impacts of recent climate change on wheat production systems in Western Australia. Climatic Change 92: 495-517.

118. Mall RK, Aggarwal PK (2002) Climate Change and Rice Yields in Diverse Agro-Environments of India. I. Evaluation of Impact Assessment Models. Climatic Change 52: 315-330.

119. Maurer EP, Adam JC, Wood AW (2009) Climate model based consensus on the hydrologic impacts of climate change to the Rio Lempa basin of Central America. Hydrol Earth Syst Sci 13: 183-194.

120. Meinke H, Hammer GL, van Keulen H, Rabbinge R, Keating BA (1997) Improving wheat simulation capabilities in Australia from a cropping systems perspective: water and nitrogen effects on spring wheat in a semi-arid environment. In: Ittersum MKv, Geijn SCvd, editors. Developments in Crop Science: Elsevier. pp. 99-112.

121. Menzel L, Brger G (2002) Climate change scenarios and runoff response in the Mulde catchment (Southern Elbe, Germany). Journal of Hydrology 267: 53-64.

122. Meza FJ, Silva D, Vigil H (2008) Climate change impacts on irrigated maize in Mediterranean climates: Evaluation of double cropping as an emerging adaptation alternative. Agricultural Systems 98: 21-30.

123. Mishra A, Hansen JW, Dingkuhn M, Baron C, Traor SB, et al. (2008) Sorghum yield prediction from seasonal rainfall forecasts in Burkina Faso. Agricultural and Forest Meteorology 148: 1798-1814.

124. Mo X, Liu S, Lin Z, Guo R (2009) Regional crop yield, water consumption and water use efficiency and their responses to climate change in the North China Plain. Agriculture, Ecosystems & Environment 134: 67-78.

125. Moriondo M, Giannakopoulos C, Bindi M (2011) Climate change impact assessment: the role of climate extremes in crop yield simulation. Climatic Change 104: 679-701.

126. Mozny M, Tolasz R, Nekovar J, Sparks T, Trnka M, et al. (2009) The impact of climate change on the yield and quality of Saaz hops in the Czech Republic. Agricultural and Forest Meteorology 149: 913-919.

127. Mulligan M, Fisher M, Sharma B, Xu ZX, Ringler C, et al. (2011) The nature and impact of climate change in the Challenge Program on Water and Food (CPWF) basins. Water International 36: 96-124.

128. Nain AS, Dadhwal VK, Singh TP (2004) Use of CERES-Wheat model for wheat yield forecast in central Indo-Gangetic Plains of India. The Journal of Agricultural Science 142: 59-70.

129. Neild RE, Logan J, Cardenas A (1983) Growing season and phenological response of sorghum as determined from simple climatic data. Agricultural Meteorology 30: 35-48.

130. Nisar Ahamed TR, Gopal Rao K, Murthy JSR (2000) GIS-based fuzzy membership model for crop-land suitability analysis. Agricultural Systems 63: 75-95.

131. Niu X, Easterling W, Hays CJ, Jacobs A, Mearns L (2009) Reliability and input-data induced uncertainty of the EPIC model to estimate climate change impact on sorghum yields in the U.S. Great Plains. Agriculture, Ecosystems & Environment 129: 268-276.

132. Olesen J, Carter T, Daz-Ambrona C, Fronzek S, Heidmann T, et al. (2007) Uncertainties in projected impacts of climate change on European agriculture and terrestrial ecosystems based on scenarios from regional climate models. Climatic Change 81: 123-143.

133. Olmstead AL, Rhode PW (2011) Adapting North American wheat production to climatic challenges, 18392009. Proceedings of the National Academy of Sciences 108: 480-485.

134. Ortiz R, Sayre KD, Govaerts B, Gupta R, Subbarao GV, et al. (2008) Climate change: Can wheat beat the heat? Agriculture, Ecosystems & Environment 126: 46-58.

135. Osborne TM, Lawrence DM, Challinor AJ, Slingo JM, Wheeler TR (2007) Development and assessment of a coupled cropclimate model. Global Change Biology 13: 169-183.

136. Paeth H, Capo-Chichi A, Endlicher W (2008) Climate change and food security in tropical West Africa -A dynamic-statistical modelling approach. Erkunde 62: 101-115.

137. Parry M, Rosenzweig C, Iglesias A, Fischer G, Livermore M (1999) Climate change and world food security: a new assessment. Global Environmental Change 9: S51-S67.

138. Parry M, Rosenzweig C, Livermore M (2005) Climate change, global food supply and risk of hunger. Philosophical Transactions of the Royal Society B: Biological Sciences 360: 2125-2138.

139. Parry ML, Rosenzweig C, Iglesias A, Livermore M, Fischer G (2004) Effects of climate change on global food production under SRES emissions and socio-economic scenarios. Global Environmental Change 14: 53-67.

140. Parsons D, Nicholson CF, Blake RW, Ketterings QM, Ramrez-Aviles L, et al. (2011) Development and evaluation of an integrated simulation model for assessing smallholder crop-livestock production in Yucatn, Mexico. Agricultural Systems 104: 1-12.

141. Piao S, Ciais P, Huang Y, Shen Z, Peng S, et al. (2010) The impacts of climate change on water resources and agriculture in China. Nature 467: 43-51.

142. Potgieter AB, Hammer GL, Doherty A, de Voil P (2005) A simple regional-scale model for forecasting sorghum yield across North-Eastern Australia. Agricultural and Forest Meteorology 132: 143-153.

143. Priya S, Shibasaki R (2001) National spatial crop yield simulation using GIS-based crop production model. Ecological Modelling 136: 113-129.

144. Purkey D, Joyce B, Vicuna S, Hanemann M, Dale L, et al. (2008) Robust analysis of future climate change impacts on water for agriculture and other sectors: a case study in the Sacramento Valley. Climatic Change 87: 109-122.

145. Quiroga S, Iglesias A (2009) A comparison of the climate risks of cereal, citrus, grapevine and olive production in Spain. Agricultural Systems 101: 91-100.

146. Reidsma P, Ewert F, Boogaard H, Diepen Kv (2009) Regional crop modelling in Europe: The impact of climatic conditions and farm characteristics on maize yields. Agricultural Systems 100: 51-60.

147. Reji G, Chander S, Aggarwal PK (2008) Simulating rice stem borer, Scirpophaga incertulas Wlk., damage for developing decision support tools. Crop Protection 27: 1194-1199.

148. Rinaldi M (2001) Application of EPIC model for irrigation scheduling of sunflower in Southern Italy. Agricultural Water Management 49: 185-196.

149. Rodriguez D, Ewert F, Goudriaan J, Manderscheid R, Burkart S, et al. (2001) Modelling the response of wheat canopy assimilation to atmospheric CO2 concentrations. New Phytologist 150: 337-346.

150. Rounsevell MDA, Ewert F, Reginster I, Leemans R, Carter TR (2005) Future scenarios of European agricultural land use: II. Projecting changes in cropland and grassland. Agriculture, Ecosystems & Environment 107: 117-135.

151. Salinari F, GiosuÉ S, Tubiello F-N, Rettori A, Rossi V, et al. (2006) Downy mildew (Plasmopara viticola) epidemics on grapevine under climate change. Global Change Biology 12: 1299-1307.

152. Schlenker W, Lobell DB (2010) Robust negative impacts of climate change on African agriculture. Environmental Research Letters 5: 014010.

153. Schlenker W, Roberts MJ (2009) Nonlinear temperature effects indicate severe damages to U.S. crop yields under climate change. Proceedings of the National Academy of Sciences.

154. Scholze M, Knorr W, Arnell NW, Prentice IC (2006) A climate-change risk analysis for world ecosystems. Proceedings of the National Academy of Sciences 103: 13116-13120.

155. Schroth G, Laderach P, Dempewolf J, Philpott S, Haggar J, et al. (2009) Towards a climate change adaptation strategy for coffee communities and ecosystems in the Sierra Madre de Chiapas, Mexico. Mitigation and Adaptation Strategies for Global Change 14: 605-625.

156. Semenov MA (2009) Impacts of climate change on wheat in England and Wales. Journal of The Royal Society Interface 6: 343-350.

157. Semenov MA, Halford NG (2009) Identifying target traits and molecular mechanisms for wheat breeding under a changing climate. Journal of Experimental Botany 60: 2791-2804.

158. Seo S, Mendelsohn R (2008) A Ricardian Analysis of the impact of climate change on Latin American farms. Chilean Journal of Agricultural Research 68: 69-79.

159. Seo S, Mendelsohn R, Dinar A, Hassan R, Kurukulasuriya P (2009) A Ricardian Analysis of the Distribution of Climate Change Impacts on Agriculture across Agro-Ecological Zones in Africa. Environmental and Resource Economics 43: 313-332.

160. Sheffield J, Wood EF (2008) Global Trends and Variability in Soil Moisture and Drought Characteristics, 19502000, from Observation-Driven Simulations of the Terrestrial Hydrologic Cycle. Journal of Climate 21: 432-458.

161. Shin DW, Baigorria GA, Lim YK, Cocke S, LaRow TE, et al. (2009) Assessing Maize and Peanut Yield Simulations with Various Seasonal Climate Data in the Southeastern United States. Journal of Applied Meteorology and Climatology 49: 592-603.

162. Singels A, van den Berg M, Smit MA, Jones MR, van Antwerpen R (2010) Modelling water uptake, growth and sucrose accumulation of sugarcane subjected to water stress. Field Crops Research 117: 59-69.

163. Smith JO, Smith P, Wattenbach M, Zaehle S, Hiederer R, et al. (2005) Projected changes in mineral soil carbon of European croplands and grasslands, 19902080. Global Change Biology 11: 2141-2152.

164. Soltani A, Meinke H, de Voil P (2004) Assessing linear interpolation to generate daily radiation and temperature data for use in crop simulations. European Journal of Agronomy 21: 133-148.

165. Southworth J, Pfeifer RA, Habeck M, Randolph JC, Doering OC, et al. (2002) Sensitivity of winter wheat yields in the Midwestern United States to future changes in climate, climate variability, and CO2 fertilization. Climate Research 22: 73-86.

166. Spitters CJT, Schapendonk AHCM (1990) Evaluation of breeding strategies for drought tolerance in potato by means of crop growth simulation. Plant and Soil 123: 193-203.

167. Srivastava A, Naresh Kumar S, Aggarwal PK (2010) Assessment on vulnerability of sorghum to climate change in India. Agriculture, Ecosystems & Environment 138: 160-169.

168. Stern RD, Cooper PJM (2011) Assessing Climate Risk and Climate Change Using Rainfall Data: A Case Study from Zambia. Experimental Agriculture 47: 241-266.

169. Sun L, Li H, Ward MN, Moncunill DF (2007) Climate Variability and Corn Yields in Semiarid Cear, Brazil. Journal of Applied Meteorology and Climatology 46: 226-240.

170. Supit I, van Diepen CA, de Wit AJW, Kabat P, Baruth B, et al. (2010) Recent changes in the climatic yield potential of various crops in Europe. Agricultural Systems 103: 683-694.

171. Tan G, Shibasaki R (2003) Global estimation of crop productivity and the impacts of global warming by GIS and EPIC integration. Ecological Modelling 168: 357-370.

172. Tao F, Zhang Z, Liu J, Yokozawa M (2009) Modelling the impacts of weather and climate variability on crop productivity over a large area: A new super-ensemble-based probabilistic projection. Agricultural and Forest Meteorology 149: 1266-1278.

173. Tebaldi C, Lobell DB (2008) Towards probabilistic projections of climate change impacts on global crop yields. Geophys Res Lett 35: L08705.

174. Thornton PK, Jones PG, Ericksen PJ, Challinor AJ (2011) Agriculture and food systems in sub-Saharan Africa in a 4C+ world. Philosophical Transactions of the Royal Society A: Mathematical, Physical and Engineering Sciences 369: 117-136.

175. Thornton PK, Herrero M (2010) Potential for reduced methane and carbon dioxide emissions from livestock and pasture management in the tropics. Proceedings of the National Academy of Sciences.

176. Thornton PK, Jones PG, Alagarswamy G, Andresen J (2009) Spatial variation of crop yield response to climate change in East Africa. Global Environmental Change 19: 54-65.

177. Thornton PK, Fawcett RH, Galvin KA, Boone RB, Hudson JW, et al. (2004) Evaluating management options that use climate forecasts: modelling livestock production systems in the semi-arid zone of South Africa. Climate Research 26: 33-42.

178. Thornton PK, Bowen WT, Ravelo AC, Wilkens PW, Farmer G, et al. (1997) Estimating millet production for famine early warning: an application of crop simulation modelling using satellite and ground-based data in Burkina Faso. Agricultural and Forest Meteorology 83: 95-112.

179. Travasso MI, Magrin GO, Grondona MO, Rodriguez GR (2009) The use of SST and SOI anomalies as indicators of crop yield variability. International Journal of Climatology 29: 23-29.

180. Trnka M, Dubrovsk M, Semerdov D, alud Z (2004) Projections of uncertainties in climate change scenarios into expected winter wheat yields. Theoretical and Applied Climatology 77: 229-249.

181. Tubiello FN, Fischer G (2007) Reducing climate change impacts on agriculture: Global and regional effects of mitigation, 2000-2080. Technological Forecasting and Social Change 74: 1030-1056.

182. Tubiello FN, Rosenzweig C, Goldberg RA, Jagtap S, Jones JW (2002) Effects of climate change on US crop production: simulation results using two different GCM scenarios. Part I: Wheat, potato, maize, and citrus. Climate Research 20: 259-270.

183. Tubiello FN, Donatelli M, Rosenzweig C, Stockle CO (2000) Effects of climate change and elevated CO2 on cropping systems: model predictions at two Italian locations. European Journal of Agronomy 13: 179-189.

184. van Delden A, Kropff MJ, Haverkort AJ (2001) Modeling temperature- and radiation-driven leaf area expansion in the contrasting crops potato and wheat. Field Crops Research 72: 119-141.

185. van Ittersum MK, Howden SM, Asseng S (2003) Sensitivity of productivity and deep drainage of wheat cropping systems in a Mediterranean environment to changes in CO2, temperature and precipitation. Agriculture, Ecosystems & Environment 97: 255-273.

186. Walker NJ, Schulze RE (2008) Climate change impacts on agro-ecosystem sustainability across three climate regions in the maize belt of South Africa. Agriculture, Ecosystems & Environment 124: 114-124.

187. Wang S, Davidson A (2007) Impact of climate variations on surface albedo of a temperate grassland. Agricultural and Forest Meteorology 142: 133-142.

188. Wang J, Mendelsohn R, Dinar A, Huang J, Rozelle S, et al. (2009) The impact of climate change on China's agriculture. Agricultural Economics 40: 323-337.

189. Willocquet L, Aubertot JN, Lebard S, Robert C, Lannou C, et al. (2008) Simulating multiple pest damage in varying winter wheat production situations. Field Crops Research 107: 12-28.

190. Wolf J, Van Oijen M (2003) Model simulation of effects of changes in climate and atmospheric CO2 and O3 on tuber yield potential of potato (cv. Bintje) in the European Union. Agriculture, Ecosystems & Environment 94: 141-157.

191. Wu W, Shibasaki R, Yang P, Tan G, Matsumura K-i, et al. (2007) Global-scale modelling of future changes in sown areas of major crops. Ecological Modelling 208: 378-390.

192. Xiong W, Holman I, Conway D, Lin E, Li Y (2008) A crop model cross calibration for use in regional climate impacts studies. Ecological Modelling 213: 365-380.

193. Xiong W, Matthews R, Holman I, Lin E, Xu Y (2007) Modelling Chinas potential maize production at regional scale under climate change. Climatic Change 85: 433-451.

194. Wei X, Declan C, Erda L, Yinlong X, Hui J, et al. (2009) Future cereal production in China: The interaction of climate change, water availability and socio-economic scenarios. Global Environmental Change 19: 34-44.

195. Yan W, Wallace DH (1998) Simulation and Prediction of Plant Phenology for Five Crops Based on PhotoperiodTemperature Interaction. Annals of Botany 81: 705-716.

196. Yang HS, Dobermann A, Lindquist JL, Walters DT, Arkebauer TJ, et al. (2004) Hybrid-maize–a maize simulation model that combines two crop modeling approaches. Field Crops Research 87: 131-154.

197. Yano T, Aydin M, Haraguchi T (2007) Impact of Climate Change on Irrigation Demand and Crop Growth in a Mediterranean Environment of Turkey. Sensors 7: 2297-2315.

198. Yao F, Xu Y, Lin E, Yokozawa M, Zhang J (2007) Assessing the impacts of climate change on rice yields in the main rice areas of China. Climatic Change 80: 395-409.

199. Yin X, Kropff MJ, Nakagawa H, Horie T, Goudriaan J (1997) A model for photothermal responses of flowering in rice II. Model evaluation. Field Crops Research 51: 201-211.

200. You L, Rosegrant MW, Wood S, Sun D (2009) Impact of growing season temperature on wheat productivity in China. Agricultural and Forest Meteorology 149: 1009-1014.

201. Yun JI (2003) Predicting regional rice production in South Korea using spatial data and crop-growth modeling. Agricultural Systems 77: 23-38.

202. Žalud Z, Dubrovský M (2002) Modelling climate change impacts on maize growth and development in the Czech Republic. Theoretical and Applied Climatology 72: 85-102.

203. Zhang XC, Nearing MA (2005) Impact of climate change on soil erosion, runoff, and wheat productivity in central Oklahoma. CATENA 61: 185-195.

204. Zhang T, Zhu J, Yang X (2008) Non-stationary thermal time accumulation reduces the predictability of climate change effects on agriculture. Agricultural and Forest Meteorology 148: 1412-1418.

205. Zierl B, Bugmann H (2005) Global change impacts on hydrological processes in Alpine catchments. Water Resour Res 41: W02028.

Appendix B

Preliminary optimisation experiments

Introduction

Various optimisation strategies are possible in GLAM. Optimisation can be performed using one single grid cell where crop-climate relationships are strong (Challinor et al., 2004), using various grid cells simultaneously by randomly sampling the parameter space (Nicklin, 2013), by manually tuning the model so that it performs well on a variety of circumstances (Li, 2008), or by iteratively optimising all parameters using GLAM's built-in hypercube optimisation (Challinor, 2009).

The final objective of the parameter sets developed in Chapter 5 was the assessment of genotypic adaptation options (Chapter 8). Work on genotypic adaptation focuses on altering values of crop model parameters that represent useful breeding traits (see Chapter 8, Singh et al. 2012 and Suriharn et al. 2011 for more details) to then find combinations of these that abate any negative impacts of climate change or capitalise positive ones. For this reason, it is important that the optimal values of crop model parameters are not influenced by the C_{YG}. This means that the value of C_{YG}, which can be spatially variable, has to be constant during the optimisation process. Apart from this, the selection of an appropriate optimisation strategy is important because it can have an effect on model skill

(Angulo et al., 2013a). Three fundamental decisions needed to be made before performing any further analyses:

1. which grid cell(s) are to be used for optimisation?;
2. what are the initial values of the C_{YG} for the grid cells of (1) above, which need to be constant during the optimisation of all other model parameters in order to reduce the dependence of optimal parameters on the chosen C_{YG} values?;
3. which of the parameters of Table 5.2 need to to be optimised, so that only uncertainty-relevant parameters are further studied?

Materials and methods

Crop model and input data

The model used was GLAM, as fully described in Sect. 3.5.1 of Chapter 3. GLAM inputs (i.e. weather, soils, planting dates, and crop yields) were all as in Sect. 5.3.2 of Chapter 5.

Configuration of simulations

Four different sets of simulations (i.e. experiments) were carried out in order to assess each of the three abovementioned decisions. The experiments varied in terms of the number of grid cells used for the optimisation and the initial value of the C_{YG}. All experiments were performed for each zone separately (see Figure 3.2). The experiments were as follows:

1. In the first experiment (PE1), a total of 10 grid cells were selected for each zone so that they spanned a range of mean crop yields (i.e. a range of responses) so to capture spatio-temporal variability of crop yields. A C_{YG} value was pre-calculated for each optimisation grid cell using the ratio between the mean crop yield of each grid cell (Y_i) and the maximum mean crop yield amongst the 50 optimisation grid cells (10 grid cells * 5 zones) (Eq. B.1).

$$C_{YG} = \frac{Y_i}{max(Y_i, Y_{i+1}, \ldots, Y_{50})} \tag{B.1}$$

2. The second experiment (PE2) used the same 10 grid cells as in PE1. C_{YG} values were calculated in a similar way as in PE1, but using the maximum of the 10 grid cells of each growing zone, instead of the whole set of 50 optimisation grid cells used in PE1 (Eq. B.2).

$$C_{YG} = \frac{Y_i}{max(Y_i, Y_{i+1}, \ldots, Y_{10})} \tag{B.2}$$

3. The third experiment (PE3) used the same grid cells as in PE1 and PE2, but this time a value of C_{YG} =1 in all optimisation grid cells was adopted during the optimisation procedure.

4. For the last experiment (PE4), a single optimisation grid cell was used for each zone. Each grid cell was carefully selected so that it showed the highest crop yield in the whole growing zone. This was done based on the rationale that these grid cells are those where farmers achieve maximum possible region-specific yields. The use of a constant C_{YG}=1 seemed obvious in this case.

The following steps were then followed:

1. The order in which parameters were optimised, which due to the compensatory nature of parameters is known to have an effect on the final parameter values, was pre-defined. This order was chosen at random, and follows that of Table B.1 from top to bottom row. The order was kept the same across the four experiments.

2. A total of 15 iterations to be performed were chosen. This was done because the optimisation of a parameter can cause the optimal values of other parameters to vary. This ensured that the optimum values of the parameters were stable; that is, the local minimum error (see Eq. 3.46) was reached.

3. The 23 target model parameters (excluding C_{YG}, Table 5.2) were optimised sequentially (following the order defined in (1) above). Optimisation was done by iteratively testing different values of each parameter within the ranges of values reported in Table 5.2, and assessing the model simulated yield against observed yields using the $RMSE$ (Eq. 3.46).

For each model parameter and zone, the variation in the $RMSE$ ($RMSE_V$) was then calculated to measure the effect of the parameter on the model output (Eq. B.3)

$$RMSE_V = \frac{RMSE_{max} - RMSE_{min}}{RMSE_{min}} * 100 \tag{B.3}$$

where $RMSE_{max}$ and $RMSE_{min}$ are the maximum $RMSE$ values that the parameter produced within the range suggested in Table 5.2. $RMSE_V$ was used as a standardised measure across parameters because minimum $RMSE$ values for each model parameter were different. The $RMSE_V$ measured how much relative increase in $RMSE$ causes a given parameter over the local minima that can be reached for that same parameter. Using $RMSE_{max}$ as the standardising value produced the same qualitative results. Ranges of parameters were all taken from the study of Challinor et al. (2004), unless otherwise stated (e.g. Chapter 3, Sect. 3.5.1.12).

4. Once the 23 model parameters were optimised, the planting date was determined for each grid cell. For each grid cell, the start of a planting window was varied across reported ranges in the Sacks et al. (2010) dataset (Chapter 4, Sect. 3.4.2.3) so that the $RMSE$ (Eq. 3.46) was minimised for that grid cell. This procedure ensured that the choice of the planting date did not affect model skill, while ensuring the planting windows were in agreement with observations (Sacks et al., 2010). In each model simulation (i.e. in each year and location), the actual sowing date was defined as the simulated first day with a soil moisture availability of at least 50 % (Challinor et al., 2004).

5. C_{YG} values were determined for each grid cell by iteratively running the model with C_{YG} set between 0.01 and 1.0 (in steps of 0.01). The value that minimised the $RMSE$ as the optimal value.

In all cases, the Rabi (irrigated winter) season was simulated separately for each gridcell where irrigated area was reported by planting the crop between the 15^{th} of November and 15^{th} of January, defined per growing zone according to Talawar (2004). An irrigated-fraction weighted-average of the Rabi and Kharif runs was done and this was the value used to calculate $RMSE$ during the optimisation and calibration procedures. This was done because the crop yield data was reported as the average of both seasons per year (i.e. total production by total area).

Assessment of model skill

Skill of the model in each of the four experiments (PE1 through PE4) was measured using four simple measurements: (1) the spatial correlation coefficient of mean yields; (2) the spatial correlation coefficient of yield standard deviations; (3) the mean (and standard deviation) of the $RMSE$ values; and (4) the mean and standard deviation of $PRMSE$ values. The spatial variation of the correlation coefficient and the maximum farmers yield were mapped out.

Results

Table B.1 shows the overall skill of the model in the four experiments. Experiment PE3 (where 10 grid cells were used with a C_{YG}=1) showed the lowest skill, with a correlation coefficient of 0.89 and 0.39 for yield mean and standard deviations, respectively. Mean values of $RMSE$ ($PRMSE$) across grid cells in this experiment were 287 kg ha^{-1} (56 %), while standard deviations were 212 kg ha^{-1} (89.1 %). Although experiment PE1 (where 10 grid cells were used with pre-calculated C_{YG}) showed better skill, with correlation coefficients of 0.92 and 0.42 for yield mean and standard deviations, respectively), values of $RMSE$ and $PRMSE$ and their respective standard deviations were large (see Table B.1).

Table B.1: Overall skill of the different optimisation experiments.

ID	$R(\bar{Y})$	$R(\sigma)$	$RMSE(\pm s.d.)$ (kg ha^{-1})	$PRMSE(\pm s.d.)(\%)$
PE1	0.92	0.43	271.5 ± 191.8	57.6 ± 107.6
PE2	0.98	0.47	289.8 ± 173.4	47.2 ± 25.9
PE3	0.89	0.39	287.0 ± 212.0	56.0 ± 89.1
PE4	0.96	0.45	281.8 ± 177.3	45.6 ± 26.1

Notes: $R(\bar{Y})$ and $R(\sigma)$ refer to the spatial correlation coefficients of mean (Y) and standard deviation (σ), respectively. $PRMSE$ refers to the $RMSE$ standardised by mean yields.

Experiments PE2 and PE4 showed the best performance overall, with PE2 depicting the highest correlation coefficients, the lowest $RMSE$, as well as a relatively low $PRMSE$ (Table B.1). This result indicated that these two optimisation strategies were promissory. Nevertheless, the spatial variation of the correlation coefficient was remarkably different between the two experiments (Figure B.1). A large number of grid cells showed negative

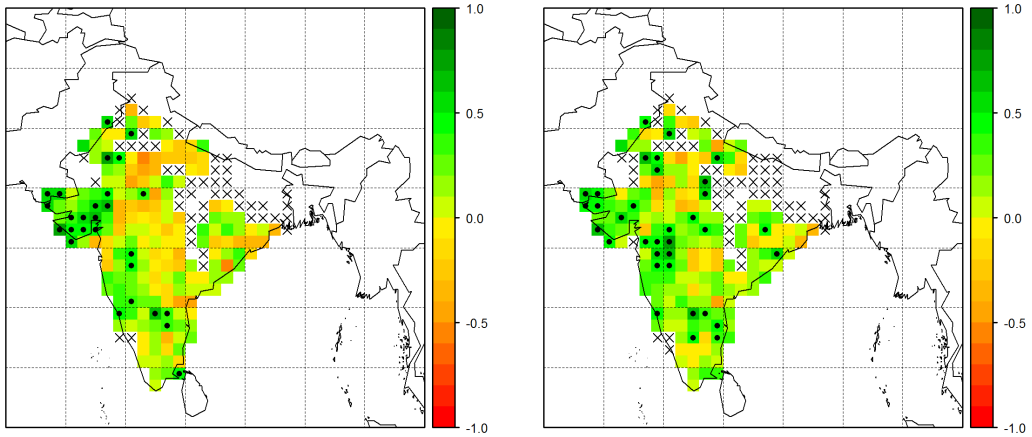

(a) PE2 (b) PE4

FIGURE B.1: Spatial variation in the correlation coefficient for experiment PE2 and PE4.

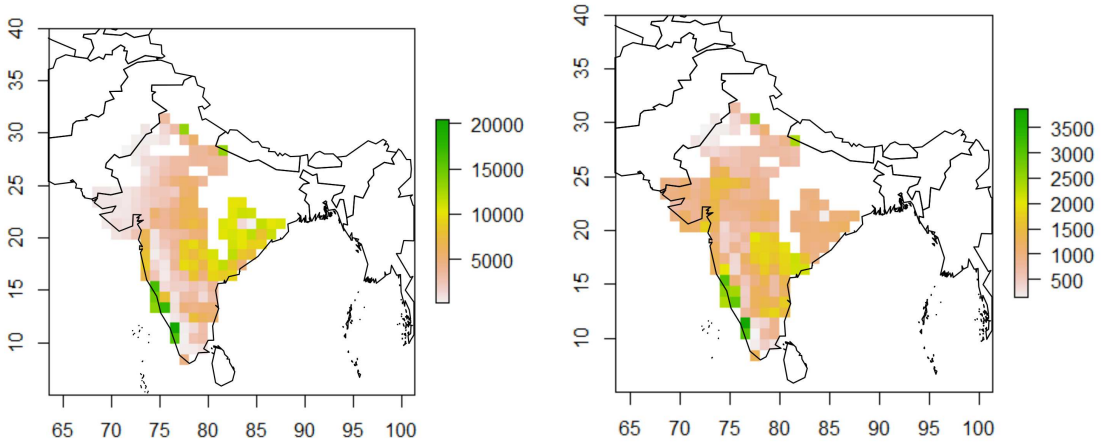

(a) PE2 (b) PE4

FIGURE B.2: Spatial variation of mean crop yields for simulations where C_{YG}=1 for experiments PE2 and PE4.

correlation coefficients throughout the analysis domain in PE2 (Figure B.1). In addition, in PE2 (Figure B.2), simulations of maximum farmers yields (i.e. C_{YG}=1) showed mean yield values of up to 20,000 kg ha^{-1} in the north of India and the west coast. This was deemed unrealistic (Singh et al., 2012; Suriharn et al., 2011).

Variation in $RMSE$, as measured by the $RMSE_V$ indicated that 19 out of the 23 parameters produced variations that were large enough as to be considered in the analyses further developed in Chapter 4 (Table B.2). Values of these parameters were assigned as described in Chapter 5 (Sect. 5.3.2).

TABLE B.2: Optimal values and sensitivity of GLAM to variation in parameters for experiment PE4.

Parameter	Adopted value	Z1		Z2		Z3		Z4		Z5	
		Value	$RMSE_V$	Value	$RMSE_V$	Value	$RMSE_V$	Value	$RMSE_V$	Value	$RMSE_V$
DLDTMX	OP	0.09	278.9	0.1	104.9	0.09	337.4	0.1	130.6	0.08	93.2
EXTC	OP	0.8	230.1	0.8	65.4	0.78	263.5	0.5	60.7	0.8	55.2
SHF_CTE	OP	0.31	10.9	0.5	0.5	0.22	21.6	0.51	10.2	0.3	8.1
ALBEDO	OP	0.12	20	0.28	0.9	0.12	33.7	0.28	9	0.28	15.3
DLDLAI	OP	4.4	0.4	5	0.3	5	9.8	5	7.3	1.85	3.8
VPD_CTE	OP	0.44	11.5	0.42	72.8	0.7	34.5	0.42	51.7	0.42	93.6
CRIT_LAI_T	0.7	1.2	1.3	0.9	0	0.84	0.8	0.9	0	0.74	1.5
EFV	OP	2	28.4	2	16.1	1	19.9	2	18.5	1	10.8
SWF_THRESH	0.7	0.5	0.9	0.5	0.3	0.5	2.1	0.5	2.3	0.62	1.6
UPDIFC	0.3	0.3	0.8	0.3	0.1	0.3	9	0.3	0.8	0.3	2.1
RLVEF	0.42	0.42	1	0.41	0.1	0.42	8.3	0.2	0.2	0.42	2.2
VPD_REF	OP	0.6	16.8	1.4	0.8	0.6	30.4	1.05	4.9	0.8	9.3
P_TRANS_MAX	OP	0.4	203.1	0.4	62.4	0.39	197.2	0.37	38.9	0.39	58.4
TE	OP	4.2	98.5	3.7	92.6	4.5	305	4.5	99	3.6	105.1
TEN_MAX	OP	2.3	429.4	5	72	4.4	289.5	4.8	110.2	4.9	93.7
DHDT	OP	0.0042	552.7	0.0052	129.4	0.0042	630.6	0.0042	227.5	0.0058	102.2
TB	OP	8	211.8	8	96.2	8	434	8	122.5	10	31.9
TO	OP	28	77.6	28	34.7	30	14.3	28	13.5	28	48.7
TM	OP	49	20.9	40	7.2	45.5	0.3	48.5	2.4	40	18.7
GCPLFL	OP	360	14.1	390	3.3	359	16.6	362	4.7	358	11.3
GCFLPF	OP	327	16	311	1.1	318	11.5	310	4.2	321	6.7
GCPFLM	OP	216	33.5	200	15.2	210	66.3	206	16.1	224	14.8
GCLMHA	OP	510	197.8	500	78.8	500	309.9	500	81	510	87.7

Notes: In **bold** are those parameters whose effect was considered negligible across all growing zones, and thus were not used in any further optimisation. Final values adopted are those of Challinor et al. (2004), unless otherwise stated. Names of parameters as in Table 5.2.

Discussion

The use of various grid cells when optimising GLAM poses the problem of selecting an appropriate value for C_{YG}. Setting a spatially constant C_{YG} and optimising over more than one grid cell (i.e. PE3) resulted in parameter sets that could not appropriately simulate crop yields in grid cells where mean crop yields were high. This happened because optimal values for all model parameters were determined under the assumption that all grid cells had exactly the same influence of non-climatic processes (i.e. those accounted for by the C_{YG}). On the other hand, the use of pre-calculated spatially-variable C_{YG} values (PE1 and PE2), produced simulations with better skill. However, C_{YG} is used to account for non-climatic drivers of crop yields, while the fraction calculated by means of Eq. B.1 and Eq. B.2 involves both climatic and non-climatic processes. This means that a C_{YG} calculated in such a way would constrain the model output beyond non-climatic processes, which is unrealistic. Since the optimisation procedure aims at reducing the $RMSE$ and no constraints on parameter combinations other than the SLA (see Chapter 3, Sect. 3.5.1.12) were imposed during the optimisation procedure, this produced parameter sets that tended to simulate more biomass and yield than required under non-C_{YG} constrained conditions (Figure B.2). Maximum groundnut crop yields between 6,000 and 6,300 kg ha^{-1} have been reported under well-watered experiments (Balota et al., 2012; Caliskan et al., 2008), as well as in field-scale groundnut simulations (Singh et al., 2012; Suriharn et al., 2011). Experiments PE1 and PE2 showed values 150 % larger than these, and hence were not be considered for any further analyses.

Experiment PE4 showed performance similar to pre-calibrating the C_{YG} using data and also kept simulated farmers' and potential (i.e. C_{YG} =1) yields within realistic ranges. This approach was also conceptually more sensible, since the use of C_{YG}=1 in a location where crop yields are the maximum possible can be referred to as non-limited farmers yield. This simulation is in Chapter 5 and hereafter referred to as the "first successful simulation (SR-1)".

Conclusions

Four preliminary optimisation experiments were performed in order to define the most appropriate optimisation strategy. The use of more than one grid cell was considered unsuitable for the purposes of the work described in Chapter 5 and further used in Chapter 6 and 8, as these involved the need of selecting a value for C_{YG}, which proved difficult to determine. Performance of experiments where more than one grid cell was used for optimisation (i.e. PE1, PE2 and PE3) was limited or parameter sets produced simulations with unrealistically high yield values.

For these reasons, one single grid cell per zone was selected for all further optimisation of GLAM (see Chapter 5, Sect. 5.3.2). This single optimisation grid cell was chosen so that it had the largest possible mean 1966-1993 crop yield. This experiment (PE4) also suggested that only 19 out of the 23 initial set of parameters needed to be optimised. Although selecting one single best grid cell was not the most obvious choice because using a single grid cell could lead to developing parameter sets that were too local, such approach proved to overcome the difficulty in pre-selecting a value for the C_{YG}. The use of one single grid cell with maximum yields also maintained a realistic yield simulation.

References

Adam, M.; Van Bussel, L. G. J.; Leffelaar, P. A.; Van Keulen, H., and Ewert, F. Effects of modelling detail on simulated potential crop yields under a wide range of climatic conditions. *Ecological Modelling*, 222(1):131–143, 2011.

Adiku, S. G. K.; Braddock, R. D., and Rose, C. W. Simulating root growth dynamics. *Environmental Software*, 11(1-3):99–103, 1996.

Adler, R. F.; Huffman, G. J.; Chang, A.; Ferraro, R.; Xie, P.-P.; Janowiak, J.; Rudolf, B.; Schneider, U.; Curtis, S.; Bolvin, D.; Gruber, A.; Susskind, J.; Arkin, P., and Nelkin, E. The version-2 global precipitation climatology project (gpcp) monthly precipitation analysis (1979present). *Journal of Hydrometeorology*, 4(6):1147–1167, 2003.

Affholder, F.; Tittonell, P.; Corbeels, M.; Roux, S.; Motisi, N.; Tixier, P., and Wery, J. Ad hoc modeling in agronomy: What have we learned in the last 15 years? *Agron. J.*, 104(3):735–748, 2012.

Affholder, F.; Scopel, E.; Neto, J. M., and Capillon, A. Diagnosis of the productivity gap using a crop model. methodology and case study of small-scale maize production in central brazil. *Agronomie*, 23(4):305–325, 2003.

Aggarwal, P. K. Global climate change and indian agriculture: impacts, adaptation and mitigation. *Indian Journal of Agricultural Sciences*, 78(10):911–919, 2008.

Aggarwal, P. K.; Joshi, P. K.; Ingram, J. S. I., and Gupta, R. K. Adapting food systems of the indo-gangetic plains to global environmental change: key information needs to improve policy formulation. *Environmental Science & Policy*, 7(6):487–498, 2004.

Ainsworth, E. A. and Long, S. P. What have we learned from 15 years of free-air co2 enrichment (face)? a meta-analytic review of the responses of photosynthesis, canopy properties and plant production to rising co2. *New Phytologist*, 165(2):351–372, 2005.

Ajay, B. C.; Gowda, M. V. C.; Rathnakumar, A. L.; Kusuma, V. P.; Abdul Fiyaz, R.; Holajjer, P.; Ramya, K. T.; Govindaraj, G., and Prashanth Babu, H. Improving Genetic Attributes of Confectionary Traits in Peanut (Arachis hypogaea L.) Using Multivariate Analytical Tools. *Journal of Agricultural Science*, 4(3):247–258, 2012.

Alagarswamy, G.; Boote, K. J.; Allen, L. H., and Jones, J. W. *Evaluating the CROPGRO-soybean model ability to simulate photosynthesis response to carbon dioxide levels*, volume 98. American Society of Agronomy, Madison, WI, ETATS-UNIS, 2006.

Allen, L.; Boote, K. J.; Vara Prasad, P.; Thomas, J., and Vu, J. Hazards of temperature on food availability in changing environments (hot-face): Global warming could cause failure of seed yields of major food crops. 2005.

Allen, R.; Pereira, L.; Raes, D., and Smith, M. Crop evapotranspiration. guidelines for computing crop water requirements. Technical report, FAO, 1998.

Altmann, A.; Toloi, L.; Sander, O., and Lengauer, T. Permutation importance: a corrected feature importance measure. *Bioinformatics*, 26(10):1340–1347, 2010. doi: 10.1093/bioinformatics/btq134. URL `http://bioinformatics.oxfordjournals.org/content/26/10/1340.abstract`.

Alvarez-Villa, O. D.; Velez, J. I., and Poveda, G. Improved long-term mean annual rainfall fields for colombia. *International Journal of Climatology*, pages n/a–n/a, 2010.

Amthor, J. S. Effects of atmospheric co2 concentration on wheat yield: review of results from experiments using various approaches to control co2 concentration. *Field Crops Research*, 73(1):1–34, 2001.

Angulo, C.; Roetter, R.; Lock, R.; Enders, A.; Fronzek, S., and Ewert, F. Implication of crop model calibration strategies for assessing regional impacts of climate change in europe. *Agricultural and Forest Meteorology*, 170:32–46, 2013a.

Angulo, C.; Rötter, R.; Trnka, M.; Pirttioja, N.; Gaiser, T.; Hlavinka, P., and Ewert, F. Characteristic fingerprints of crop model responses to weather input data at different spatial resolutions. *European Journal of Agronomy*, 49(0):104–114, 2013b. doi:

http://dx.doi.org/10.1016/j.eja.2013.04.003. URL `http://www.sciencedirect.com/science/article/pii/S1161030113000506`.

Anyia, A. O. and Herzog, H. Water-use efficiency, leaf area and leaf gas exchange of cowpeas under mid-season drought. *European Journal of Agronomy*, 20(4):327–339, 2004.

Araujo, M. B.; Pearson, R. G.; Thuiller, W., and Erhard, M. Validation of speciesclimate impact models under climate change. *Global Change Biology*, 11(9):1504–1513, 2005.

Asseng, S.; Jamieson, P. D.; Kimball, B.; Pinter, P.; Sayre, K.; Bowden, J. W., and Howden, S. M. Simulated wheat growth affected by rising temperature, increased water deficit and elevated atmospheric co2. *Field Crops Research*, 85(2-3):85–102, 2004.

Asseng, S.; Ewert, F.; Rosenzweig, C.; Jones, J. W.; Hatfield, J. L.; Ruane, A. C.; Boote, K. J.; Thorburn, P. J.; Rotter, R. P.; Cammarano, D.; Brisson, N.; Basso, B.; Martre, P.; Aggarwal, P. K.; Angulo, C.; Bertuzzi, P.; Biernath, C.; Challinor, A. J.; Doltra, J.; Gayler, S.; Goldberg, R.; Grant, R.; Heng, L.; Hooker, J.; Hunt, L. A.; Ingwersen, J.; Izaurralde, R. C.; Kersebaum, K. C.; Muller, C.; Naresh Kumar, S.; Nendel, C.; O/'Leary, G.; Olesen, J. E.; Osborne, T. M.; Palosuo, T.; Priesack, E.; Ripoche, D.; Semenov, M. A.; Shcherbak, I.; Steduto, P.; Stockle, C.; Stratonovitch, P.; Streck, T.; Supit, I.; Tao, F.; Travasso, M.; Waha, K.; Wallach, D.; White, J. W.; Williams, J. R., and Wolf, J. Uncertainty in simulating wheat yields under climate change. *Nature Clim. Change*, advance on, 2013. doi: 10.1038/nclimate1916. URL `http://dx.doi.org/10.1038/nclimate1916`.

Austin, M. P. Spatial prediction of species distribution: an interface between ecological theory and statistical modelling. *Ecological Modelling*, 157(2-3):101–118, 2002.

Azam-Ali, S. N. Environmental and physiological control of transpiration by groundnut crops. *Agricultural and Forest Meteorology*, 33(23):129–140, 1984.

Bachelet, D. and Gay, C. A. The impacts of climate change on rice yield: a comparison of four model performances. *Ecological Modelling*, 65(12):71–93, 1993.

Baenziger, P. S.; McMaster, G. S.; Wilhelm, W. W.; Weiss, A., and Hays, C. J. Putting genes into genetic coefficients. *Field Crops Research*, 90(1):133–143, 2004.

Baigorria, G.; Jones, J.; Shin, D. W.; Mishra, A., and Brien, J. Assessing uncertainties in crop model simulations using daily bias-corrected regional circulation model outputs. *Climate Research*, 34(3):211–222, 2007.

Baigorria, G. A.; Jones, J. W., and O'Brien, J. J. Potential predictability of crop yield using an ensemble climate forecast by a regional circulation model. *Agricultural and Forest Meteorology*, 148(8-9):1353–1361, 2008.

Baigorria, G. A.; Chelliah, M.; Mo, K. C.; Romero, C. C.; Jones, J. W.; O'Brien, J. J., and Higgins, R. W. Forecasting cotton yield in the southeastern united states using coupled global circulation models. *Agron. J.*, 102(1):187–196, 2010.

Baker, J. T.; Allen, L. H.; Boote, K. J.; Jones, P., and Jones, J. W. Response of soybean to air temperature and carbon dioxide concentration. *Crop Sci.*, 29(1):98–105, 1989.

Bakker, M. M.; Govers, G.; Ewert, F.; Rounsevell, M., and Jones, R. Variability in regional wheat yields as a function of climate, soil and economic variables: Assessing the risk of confounding. *Agriculture, Ecosystems & Environment*, 110(3-4):195–209, 2005.

Balota, M.; Isleib, T. G., and Tallury, S. Variability for drought related traits of virginia-type peanut cultivars and advanced breeding lines. *Crop Sci.*, 52(6):2702–2713, 2012.

Banterng, P.; Patanothai, A.; Pannangpetch, K.; Jogloy, S., and Hoogenboom, G. Seasonal variation in the dynamic growth and development traits of peanut lines. *The Journal of Agricultural Science*, 141(01):51–62, 2003.

Baron, C.; Sultan, B.; Balme, M.; Sarr, B.; Traore, S.; Lebel, T.; Janicot, S., and Dingkuhn, M. From gcm grid cell to agricultural plot: scale issues affecting modelling of climate impact. *Philosophical Transactions of the Royal Society B: Biological Sciences*, 360(1463):2095–2108, 2005.

Basu, M. and Nautiyal, P. C. Improving water use efficiency and drought tolerance in groundnut by trait based breeding programmes in india. In Fischer, T.; Turner, N.; Angus, J.; McIntyre, L.; Robertson, M.; Borrell, A., and Lloyd, D., editors, *4th International Crop Science Congress*. The Regional Institute, 2004.

Batjes, N. H. Harmonized soil profile data for applications at global and continental scales: updates to the wise database. *Soil Use and Management*, 25(2):124–127, 2009.

Beaver, J. S.; Rosas, J. C.; Myers, J.; Acosta, J.; Kelly, J. D.; Nchimbi-Msolla, S.; Misangu, R.; Bokosi, J.; Temple, S.; Arnaud-Santana, E., and Coyne, D. P. Contributions of the bean/cowpea crsp to cultivar and germplasm development in common bean. *Field Crops Research*, 82(2-3):87–102, 2003.

Benayas, J. M. R.; Newton, A. C.; Diaz, A., and Bullock, J. M. Enhancement of biodiversity and ecosystem services by ecological restoration: A meta-analysis. *Science*, 325 (5944):1121–1124, 2009.

Berg, A.; Sultan, B., and Noblet-Ducoudr, de N. What are the dominant features of rainfall leading to realistic large-scale crop yield simulations in west africa? *Geophys. Res. Lett.*, 37(5):L05405, 2010.

Berry, P.; Ramirez-Villegas, J.; Bramley, H.; Mgonja, M., and Mohanty, S. *Chapter 5: Regional impacts of climate change on agriculture and the role of adaptation*, pages 263–306. CAB International, Wallingford, UK, 2013.

Berry, P.; Sylvester-Bradley, R., and Berry, S. Ideotype design for lodging-resistant wheat. *Euphytica*, 154(1-2):165–179, 2007.

Bertin, N.; Martre, P.; Gnard, M.; Quilot, B., and Salon, C. Under what circumstances can process-based simulation models link genotype to phenotype for complex traits? case-study of fruit and grain quality traits. *Journal of Experimental Botany*, 61(4): 955–967, 2010.

Beven, K. Towards a coherent philosophy for modelling the environment. *Proceedings of the Royal Society of London. Series A: Mathematical, Physical and Engineering Sciences*, 458(2026):2465–2484, 2002. doi: 10.1098/rspa.2002.0986. URL `http://rspa.royalsocietypublishing.org/content/458/2026/2465.abstract`.

Beven, K. A manifesto for the equifinality thesis. *Journal of Hydrology*, 320(12):18–36, 2006. doi: http://dx.doi.org/10.1016/j.jhydrol.2005.07.007. URL `http://www.sciencedirect.com/science/article/pii/S002216940500332X`.

Beven, K. and Binley, A. The future of distributed models: model calibration and uncertainty prediction. *Hydological Processes*, 6:279–298, 1992.

Bhatia, V. S.; Singh, P.; Wani, S. P.; Kesava Rao, A. V. R., and Srinivas, K. Yield gap analysis of soybean, groundnut, pigeonpea and chickpea in india using simulation

modeling. global theme on agroecosystems report no. 31. Technical report, International Crops Research Institute for the Semi-Arid Tropics (ICRISAT), 2006.

Bhatia, V. S.; Singh, P.; Kesava Rao, A. V. R.; Srinivas, K., and Wani, S. P. Analysis of water non-limiting and water limiting yields and yield gaps of groundnut in india using cropgro-peanut model. *Journal of Agronomy and Crop Science*, 195(6):455–463, 2009.

Bhatnagar-Mathur, P.; Devi, M. J.; Reddy, D. S.; Lavanya, M.; Vadez, V.; Serraj, R.; Yamaguchi-Shinozaki, K., and Sharma, K. Stress-inducible expression of at dreb1a in transgenic peanut (arachis hypogaea l.) increases transpiration efficiency under water-limiting conditions. *Plant Cell Reports*, 26(12):2071–2082, 2007.

Bhattacharya, N. C.; Biswas, P. K.; Battacharya, S.; Sionit, N., and strain, B. R. Growth and yield response of sweet potato to atmospheric co2 enrichment1. *Crop Sci.*, 25(6): 975–981, 1985.

Boateng, I. An assessment of the physical impacts of sea-level rise and coastal adaptation: a case study of the eastern coast of ghana. *Climatic Change*, 114(2):273–293, 2012.

Bolton, D. The computation of equivalent potential temperature. *Monthly Weather Review*, 108:1046–1053, 1980.

Boontang, S.; Girdthai, T.; Jogloy, S.; Akkasaeng, C.; Vorasoot, N.; Patanothai, A., and Tantisuwichwong, N. Responses of released cultivars of peanut to terminal drought for traits related to drought tolerance. *Asian Journal of Plant Sciences*, 9:423–431, 2010.

Boote, K. J. Using a crop growth model to hypothesize genetic traits to improve peanut yield under water-limited environments. In Fischer, T.; Turner, N.; Angus, J.; McIntyre, L.; Robertson, M.; Borrell, A., and Lloyd, D., editors, *4th International Crop Science Congress*. The Regional Institute, 2004.

Boote, K. J.; Jones, J. W., and Pickering, N. B. Potential uses and limitations of crop models. *Agronomy Journal*, 88(5):704–716, 1996. ISI Document Delivery No.: VJ227 Times Cited: 147 Cited Reference Count: 80 Amer soc agronomy Madison.

Boote, K. J.; Jones, J. W., and Hoogenboom, G. *Simulation of crop growth: CROPGRO model*, pages 651–692. Marcel Dekker Inc, New York, Gainesville, Florida, 1998.

Boote, K. J.; Kropff, M. J., and Bindraban, P. S. Physiology and modelling of traits in crop plants: implications for genetic improvement. *Agricultural Systems*, 70(2-3): 395–420, 2001.

Boote, K. J.; Jones, J. W.; Batchelor, W. D.; Nafziger, E. D., and Myers, O. Genetic coefficients in the cropgro-soybean model: Links to field performance and genomics. *Agronomy Journal*, 95:32–51, 2003.

Boote, K. J.; Allen, L.; Vara Prasad, P.; Baker, J.; Gesch, R.; Snyder, A.; Pan, D., and Thomas, J. Elevated temperature and co2 impacts on pollination, reproductive growth, and yield of several globally important crops. *Japanese Journal of Meteorology*, 60(5): 469–474, 2005.

Boote, K. J.; Allen, L. H.; Vara Prasad, P. V., and Jones, J. W. Chapter 6: Testing Effects of Climate Change in Crop Models. In Hillel, D. and Rosenzweig, C., editors, *Handbook of Climate Change and Agroecosystems. Impacts, Adaptation and Mitigation*. Imperial College Press, London, UK, 2011.

Boote, K. J.; Jones, J. W.; White, J. W.; Asseng, S., and Lizaso, J. I. Putting Mechanisms into Crop Production Models. *Plant, Cell & Environment*, 36:16581672, 2013. doi: 10.1111/pce.12119. URL `http://dx.doi.org/10.1111/pce.12119`.

Boote, K. and Sinclair, T. Crop physiology. *Crop science*, 46(5):2270–2277, 2006.

Booth, B. B. B.; Dunstone, N. J.; Halloran, P. R.; Andrews, T., and Bellouin, N. Aerosols implicated as a prime driver of twentieth-century north atlantic climate variability. *Nature*, 484(7393):228–232, 2012. 10.1038/nature10946.

Brisson, N.; Gary, C.; Justes, E.; Roche, R.; Mary, B.; Ripoche, D.; Zimmer, D.; Sierra, J.; Bertuzzi, P.; Burger, P.; Bussire, F.; Cabidoche, Y. M.; Cellier, P.; Debaeke, P.; Gaudillre, J. P.; Hnault, C.; Maraux, F.; Seguin, B., and Sinoquet, H. An overview of the crop model stics. *European Journal of Agronomy*, 18(34):309–332, 2003.

Brown, R. and Byrd, G. Transpiration efficiency, specific leaf weight, and mineral concentration in peanut and pearl millet. *Crop Science*, 36:475–480, 1996.

Bunce, J. A. Stomatal conductance, photosynthesis and respiration of temperate deciduous tree seedlings grown outdoors at an elevated concentration of carbon dioxide. *Plant, Cell & Environment*, 15(5):541–549, 1992.

Burke, M. B.; Lobell, D. B., and Guarino, L. Shifts in african crop climates by 2050, and the implications for crop improvement and genetic resources conservation. *Global Environmental Change*, 19(3):317–325, 2009.

Busby, J. Bioclima bioclimate analysis and prediction system. *Plant Protection Quarterly*, 6:8–9, 1991.

Caliskan, S.; Caliskan, M. E.; Arslan, M., and Arioglu, H. Effects of sowing date and growth duration on growth and yield of groundnut in a mediterranean-type environment in turkey. *Field Crops Research*, 105(12):131–140, 2008.

Carney, S. and Shackley, S. The greenhouse gas regional inventory project (grip): Designing and employing a regional greenhouse gas measurement tool for stakeholder use. *Energy Policy*, 37(11):4293–4302, 2009.

Challinor, A. J. General large-area model for annual crops (glam) documentation for release 2. Technical report, Institute for Climate and Atmospheric Science, School of Earth and Environment, University of Leeds, 2009.

Challinor, A. J. and Wheeler, T. R. Use of a crop model ensemble to quantify co2 stimulation of water-stressed and well-watered crops. *Agricultural and Forest Meteorology*, 148(6-7):1062–1077, 2008a.

Challinor, A. J. and Wheeler, T. R. Crop yield reduction in the tropics under climate change: Processes and uncertainties. *Agricultural and Forest Meteorology*, 148(3):343–356, 2008b.

Challinor, A. J.; Slingo, J. M.; Wheeler, T. R.; Craufurd, P. Q., and Grimes, D. I. F. Toward a combined seasonal weather and crop productivity forecasting system: Determination of the working spatial scale. *Journal of Applied Meteorology*, 42(2):175–192, 2003.

Challinor, A. J.; Wheeler, T. R.; Craufurd, P. Q.; Slingo, J. M., and Grimes, D. I. F. Design and optimisation of a large-area process-based model for annual crops. *Agricultural and Forest Meteorology*, 124(1-2):99–120, 2004.

Challinor, A. J.; Slingo, J. M.; Wheeler, T. R., and DoblasReyes, F. J. Probabilistic simulations of crop yield over western india using the demeter seasonal hindcast ensembles. *Tellus A*, 57(3):498–512, 2005a.

Challinor, A. J.; Wheeler, T. R.; Craufurd, P. Q., and Slingo, J. M. Simulation of the impact of high temperature stress on annual crop yields. *Agricultural and Forest Meteorology*, 135(1-4):180–189, 2005b.

Challinor, A. J.; Wheeler, T. R.; Slingo, J. M.; Craufurd, P. Q., and Grimes, D. I. F. Simulation of crop yields using era-40: Limits to skill and nonstationarity in weatheryield relationships. *Journal of Applied Meteorology*, 44(4):516–531, 2005c.

Challinor, A. J.; Wheeler, T. R.; Osborne, T. M., and Slingo, J. M. *Assessing the vulnerability of crop productivity to climate change thresholds using an integrated crop-climate model.* Avoiding Dangerous Climate Change. Cambridge University Press, Cambridge, UK, 2006.

Challinor, A. J.; Wheeler, T. R.; Craufurd, P. Q.; Ferro, C. A. T., and Stephenson, D. B. Adaptation of crops to climate change through genotypic responses to mean and extreme temperatures. *Agriculture, Ecosystems & Environment*, 119(1-2):190–204, 2007.

Challinor, A. J.; Wheeler, T. R.; Hemming, D., and Upadhyaya, H. Ensemble yield simulations: crop and climate uncertainties, sensitivity to temperature and genotypic adaptation to climate change. *Climate Research*, 38(2):117–127, 2009a.

Challinor, A. J.; Stafford, M. S., and Thornton, P. Use of agro-climate ensembles for quantifying uncertainty and informing adaptation. *Agricultural and Forest Meteorology*, 170:2–7, 2013.

Challinor, A.; Wheeler, T.; Slingo, J., and Hemming, D. Quantification of physical and biological uncertainty in the simulation of the yield of a tropical crop using present-day and doubled co2 climates. *Philosophical Transactions of the Royal Society B: Biological Sciences*, 360(1463):2085–2094, 2005d.

Challinor, A. Towards a science of adaptation that prioritises the poor. *IDS Bulletin*, 39 (4):81–86, 2008.

Challinor, A. J.; Ewert, F.; Arnold, S.; Simelton, E., and Fraser, E. Crops and climate change: progress, trends, and challenges in simulating impacts and informing adaptation. *Journal of Experimental Botany*, 60(10):2775–2789, 2009b.

Challinor, A. J.; Simelton, E. S.; Fraser, E. D. G.; Hemming, D., and Collins, M. Increased crop failure due to climate change: assessing adaptation options using models and socio-economic data for wheat in china. *Environmental Research Letters*, 5(3):034012, 2010.

Challinor, A. J.; Osborne, T.; Shaffrey, L.; Weller, H.; Morse, A.; Wheeler, T., and Vidale, P. L. Methods and resources for climate impacts research. *Bulletin of the American Meteorological Society*, 90(6):836–848, 2009c.

Challinor, A.; Martre, P.; Asseng, S.; Thornton, P., and Ewert, F. Making the most of climate impacts ensembles. *Nature Climate Change*, 4(2):77–80, 2014.

Chapman, G. *"The Green Revolution"*, pages 155–159. Arnold, 2002.

Chapman, S. C.; Ludlow, M. M.; Blamey, F. P. C., and Fischer, K. S. Effect of drought during early reproductive development on growth of cultivars of groundnut (arachis hypogaea l.). i. utilization of radiation and water during drought. *Field Crops Research*, 32(34):193–210, 1993.

Chen, J. J. and Sung, J. M. Gas Exchange Rate and Yield Responses of Virginia-type Peanut to Carbon Dioxide Enrichment. *Crop Sci.*, 30(5):1085–1089, 1990. doi: 10.2135/cropsci1990.0011183X003000050025x. URL `https://www.agronomy.org/publications/cs/abstracts/30/5/1085`.

Choudhury, B. J.; Idso, S. B., and Reginato, R. J. Analysis of an empirical model for soil heat flux under a growing wheat crop for estimating evaporation by an infrared-temperature based energy balance equation. *Agricultural and Forest Meteorology*, 39(4): 283–297, 1987.

Clifford, S. C.; Stronach, I. M.; Black, C. R.; Singleton-Jones, P. R.; Azam-Ali, S. N., and Crout, N. M. J. Effects of elevated CO2, drought and temperature on the water relations and gas exchange of groundnut (Arachis hypogaea) stands grown in controlled environment glasshouses. *Physiologia Plantarum*, 110(1):78–88, 2000. doi: 10.1034/j.1399-3054.2000.110111.x. URL `http://dx.doi.org/10.1034/j.1399-3054.2000.110111.x`.

Cock, J. H.; Franklin, D.; Sandoval, G., and Juri, P. The ideal cassava plant for maximum yield. *Crop Sci.*, 19(2):271–279, 1979.

Collins, W. D.; Bitz, C. M.; Blackmon, M. L.; Bonan, G. B.; Bretherton, C. S.; Carton, J. A.; Chang, P.; Doney, S. C.; Hack, J. J.; Henderson, T. B.; Kiehl, J. T.; Large, W. G.; McKenna, D. S.; Santer, B. D., and Smith, R. D. The community climate system model version 3 (ccsm3). *Journal of Climate*, 19(11):2122–2143, 2006.

Cooper, P. J. M.; Keatinge, J. D. H., and Hughes, G. Crop evapotranspiration -a technique for calculation of its components by field measurements. *Field Crops Research*, 7(299-312), 1983.

Cooper, P.; Stern, R.; Noguer, M., and Gathenya, M. Supporting evidence-based research in sub-saharan africa for the adaptation of rainfed agriculture to climate change: Laying the foundations stones of success. In press, 2012.

Crafts-Brandner, S. J. and Salvucci, M. E. Rubisco activase constrains the photosynthetic potential of leaves at high temperature and co2. *Proceedings of the National Academy of Sciences*, 97(24):13430–13435, 2000.

Craufurd, P. Q.; Wheeler, T. R.; Ellis, R. H.; Summerfield, R. J., and Vara Prasad, P. V. Escape and tolerance to high temperature at flowering in groundnut (arachis hypogaea l.). *The Journal of Agricultural Science*, 135(04):371–378, 2000.

Craufurd, P. Q.; Vara Prasad, P. V., and Summerfield, R. J. Dry matter production and rate of change of harvest index at high temperature in peanut. *Crop Sci.*, 42(1):146–151, 2002.

Craufurd, P. Q.; Prasad, P. V. V.; Kakani, V. G.; Wheeler, T. R., and Nigam, S. N. Heat tolerance in groundnut. *Field Crops Research*, 80(1):63–77, 2003.

Craufurd, P. Q.; Vadez, V.; Jagadish, S. V. K.; Vara Prasad, P. V., and Zaman-Allah, M. Crop science experiments designed to inform crop modeling. *Agricultural and Forest Meteorology*, 170:8–18, 2013.

Dalirie, M.; Sharifi, R., and Farzaneh, S. Evaluation of yield, dry matter accumulation and leaf area index in wheat genotypes as affected by terminal drought stress. *Notulae Botanicae Horti Agrobotanici Cluj-Napoca*, 38(1):182–186, 2010.

Dardanelli, J. L.; Bachmeier, O. A.; Sereno, R., and Gil, R. Rooting depth and soil water extraction patterns of different crops in a silty loam haplustoll. *Field Crops Research*, 54(1):29–38, 1997.

Deckmyn, G. and Impens, I. Uv-b increases the harvest index of bean (phaseolus vulgaris l.). *Plant, Cell & Environment*, 18(12):1426–1433, 1995.

DeGaetano, A. T. Attributes of several methods for detecting discontinuities in mean temperature series. *Journal of Climate*, 19(5):838–853, 2006.

DelSole, T. and Yang, X. Field significance of regression patterns. *Journal of Climate*, 24 (19), 2011.

Delworth, T. L.; Broccoli, A. J.; Rosati, A.; Stouffer, R. J.; Balaji, V.; Beesley, J. A.; Cooke, W. F.; Dixon, K. W.; Dunne, J.; Dunne, K. A.; Durachta, J. W.; Findell, K. L.; Ginoux, P.; Gnanadesikan, A.; Gordon, C. T.; Griffies, S. M.; Gudgel, R.; Harrison, M. J.; Held, I. M.; Hemler, R. S.; Horowitz, L. W.; Klein, S. A.; Knutson, T. R.; Kushner, P. J.; Langenhorst, A. R.; Lee, H.-C.; Lin, S.-J.; Lu, J.; Malyshev, S. L.; Milly, P. C. D.; Ramaswamy, V.; Russell, J.; Schwarzkopf, M. D.; Shevliakova, E.; Sirutis, J. J.; Spelman, M. J.; Stern, W. F.; Winton, M.; Wittenberg, A. T.; Wyman, B.; Zeng, F., and Zhang, R. Gfdl's cm2 global coupled climate models. part i: Formulation and simulation characteristics. *Journal of Climate*, 19(5):643–674, 2006.

Deque, M.; Dreveton, C.; Braun, A., and Cariolle, D. The arpege/ifs atmosphere model: a contribution to the french community climate modelling. *Climate Dynamics*, 10(4): 249–266, 1994.

Dessai, S.; Hulme, M.; Lempert, R., and Pielke, R. J. *Climate prediction: a limit to adaptation?* Adapting to climate change: thresholds, values, governance. Cambridge University Press, Cambridge, 2009.

Diansky, N. and Zalensky, V. Simulation of present-day climate with a coupled atmosphere-ocean general circulation model. *Izvestiya, Atmospheric and Ocean Physiscs*, 38(6): 732–747, 2002.

Dixit, P. N.; Cooper, P. J. M.; Dimes, J., and Rao, K. P. Adding value to field-based agronomic research through climate risk assessment: A case study of maize production in kitale, kenya. *Experimental Agriculture*, 47(Special Issue 02):317–338, 2011.

Donald, C. M. The breeding of crop ideotypes. *Euphytica*, 17(3):385–403, 1968.

Dornbos, D. L.; Mullen, R. E., and Shibles, R. E. Drought stress effects during seed fill on soybean seed germination and vigor. *Crop Sci.*, 29(2):476–480, 1989.

Douglass, D. H.; Christy, J. R.; Pearson, B. D., and Singer, S. F. A comparison of tropical temperature trends with model predictions. *International Journal of Climatology*, 28 (13):1693–1701, 2008.

Drake, J. M.; Randin, C., and Guisan, A. Modelling ecological niches with support vector machines. *Journal of Applied Ecology*, 43(3):424–432, 2006.

Dusen, E. V.; Gauchan, D., and Smale, M. On-farm conservation of rice biodiversity in nepal: A simultaneous estimation approach. *Journal of Agricultural Economics*, 58(2): 242–259, 2007.

Earl, H. J. and Davis, R. F. Effect of drought stress on leaf and whole canopy radiation use efficiency and yield of maize. *Agron. J.*, 95(3):688–696, 2003.

Easterling, W.; Aggarwal, P.; Batima, P.; Brander, K.; Erda, L.; Howden, S.; Kirilenko, A.; Morton, J.; Soussana, J.-F.; Schmidhuber, J., and Tubiello, F. *Food, fibre and forest products*, pages 273–313. Cambridge University Press, Cambridge, UK, 2007.

Easterling, W. E.; Chhetri, N., and Niu, X. Improving the realism of modeling agronomic adaptation to climate change: Simulating technological substitution. *Climatic Change*, 60(1):149–173, 2003.

Eccel, E.; Rea, R.; Caffarra, A., and Crisci, A. Risk of spring frost to apple production under future climate scenarios: the role of phenological acclimation. *International Journal of Biometeorology*, 53(3):273–286, 2009.

Ehret, U.; Zehe, E.; Wulfmeyer, V.; Warrach-Sagi, K., and Liebert, J. Should we apply bias correction to global and regional climate model data? *Hydrology and Earth System Sciences Discussions*, 9:5355–5387, 2012.

El-Sharkawy, M. How can calibrated research-based models be improved for use as a tool in identifying genes controlling crop tolerance to environmental stresses in the era of genomicsfrom an experimentalist's perspective. *Photosynthetica*, 43(2):161–176, 2005.

El-Sharkawy, M. Stress-tolerant cassava: The role of integrative ecophysiology-breeding research in crop improvement. *Open Journal of Soil Science*, 2:162–186, 2012.

El-Sharkawy, M. and Cock, J. Response of cassava to water stress. *Plant and Soil*, 100 (1):345–360, 1987.

El-Sharkawy, M.; Cock, J., and Hernandez, A. Stomatal response to air humidity and its relation to stomatal density in a wide range of warm climate species. *Photosynthesis Research*, 7(2):137–149, 1985.

El-Sharkawy, M. A.; Cock, J. H., and Held, A. A. Photosynthetic responses of cassava cultivars (manihot esculenta crantz) from different habitats to temperature. *Photosynthesis Research*, 5(3):243–250, 1984.

El-Sharkawy, M. A.; De Tafur, S. M., and Cadavid, L. F. Potential photosynthesis of cassava as affected by growth conditions. *Crop Sci.*, 32(6):1336–1342, 1992.

Elith, J.; Leathwick, J. R., and Hastie, T. A working guide to boosted regression trees. *Journal of Animal Ecology*, 77(4):802–813, 2008.

Elith, J. and Leathwick, J. R. Species distribution models: Ecological explanation and prediction across space and time. *Annual Review of Ecology, Evolution, and Systematics*, 40(1):677–697, 2009.

Elith, J.; Graham, C.; Anderson, R.; Dudk, M.; Ferrier, S.; Guisan, A.; Hijmans, R.; Huettmann, F.; Leathwick, J.; Lehmann, A.; Li, J.; Lohmann, L.; Loiselle, B.; Manion, G.; Moritz, C.; Nakamura, M.; Nakazawa, Y.; Overton, J.; Peterson, A.; Phillips, S.; Richardson, K.; Scachetti-Pereira, R.; Schapire, R.; Sobern, J.; Williams, S.; Wisz, M., and Zimmermann, N. Novel methods improve prediction of species distributions from occurrence data. *Ecography*, 29(2):129–151, 2006.

Ellis, E. C.; Klein Goldewijk, K.; Siebert, S.; Lightman, D., and Ramankutty, N. Anthropogenic transformation of the biomes, 1700 to 2000. *Global Ecology and Biogeography*, 19(5):589–606, 2010.

Eltahir, E. A. B. and Gong, C. Dynamics of wet and dry years in west africa. *Journal of Climate*, 9(5):1030–1042, 1996.

Ericksen, P.; Thornton, P. K.; Notenbaert, A.; Cramer, L.; Jones, P., and Herrero, M. Mapping hotspots of climate change and food insecurity in the global tropics. CCAFS Report no. 5. Technical report, Copenhagen, Denmark, 2011.

Estes, L. D.; Bradley, B. A.; Beukes, H.; Hole, D. G.; Lau, M.; Oppenheimer, M. G.; Schulze, R.; Tadross, M. A., and Turner, W. R. Comparing mechanistic and empirical model projections of crop suitability and productivity: implications for ecological forecasting. *Global Ecology and Biogeography*, 22(8):1007–1018, 2013a. doi: 10.1111/geb.12034. URL `http://dx.doi.org/10.1111/geb.12034`.

Estes, L. D.; Beukes, H.; Bradley, B. A.; Debats, S. R.; Oppenheimer, M.; Ruane, A. C.; Schulze, R., and Tadross, M. Projected climate impacts to south african maize and wheat production in 2055: A comparison of empirical and mechanistic modeling approaches. *Global Change Biology*, pages n/a–n/a, 2013b. ISSN 1365-2486. doi: 10.1111/gcb.12325. URL `http://dx.doi.org/10.1111/gcb.12325`.

Ewert, F. and Porter, J. R. Ozone effects on wheat in relation to co2: modelling short-term and long-term responses of leaf photosynthesis and leaf duration. *Global Change Biology*, 6(7):735–750, 2000.

FAO, . The ecocrop database, 2000.

FAO, . Faoclim 2.0 a world-wide agroclimatic database, 2001.

FAO, . Giews workstation, 2007.

FAO, . *The State of Food and Agriculture*. FAO, Rome, Italy, 2009.

FAO, . Faostat, 2012.

FAO/UNESCO, . Fao/unesco soil map of the world 1:5,000,000, ten volumes. Technical report, FAO/UNESCO, 1974.

Ferguson, M. E.; Jarvis, A.; Stalker, H. T.; Williams, D. E.; Guarino, L.; Valls, J. F.; Pittman, R. N.; Simpson, C. E., and Bramel, P. J. Biogeography of wild arachis (leguminosae): distribution and environmental characterisation. *Biodiversity & Conservation*, 14(7):1777–1798, 2005.

Ferreyra, R. A.; Pachepsky, L. B.; Collino, D., and Acock, B. Modeling peanut leaf gas exchange for the calibration of crop models for different cultivars. *Ecological Modelling*, 131(23):285–298, 2000.

Fischer, G.; Velthuizen, van H.; Shah, M., and Nachtergaele, F. *Global Agro-ecological Assessment for Agriculture in the 21st Century: Methodology and Results*. IASA, FAO, Vienna, Austria, 2002.

Fischer, G.; Shah, M.; N. Tubiello, F., and Velhuizen, van H. Socio-economic and climate change impacts on agriculture: an integrated assessment, 19902080. *Philosophical Transactions of the Royal Society B: Biological Sciences*, 360(1463):2067–2083, 2005.

Foley, J. A.; Ramankutty, N.; Brauman, K. A.; Cassidy, E. S.; Gerber, J. S.; Johnston, M.; Mueller, N. D.; O/'Connell, C.; Ray, D. K.; West, P. C.; Balzer, C.; Bennett, E. M.; Carpenter, S. R.; Hill, J.; Monfreda, C.; Polasky, S.; Rockstrom, J.; Sheehan, J.; Siebert, S.; Tilman, D., and Zaks, D. P. M. Solutions for a cultivated planet. *Nature*, 478(7369): 337–342, 2011. 10.1038/nature10452.

Forster, P. M.; Andrews, T.; Good, P.; Gregory, J. M.; Jackson, L. S., and Zelinka, M. Evaluating adjusted forcing and model spread for historical and future scenarios in the cmip5 generation of climate models. *Journal of Geophysical Research: Atmospheres*, 2013.

Foster, G. and Rahmstorf, S. Global temperature evolution 19792010. *Environmental Research Letters*, 6(4):044022, 2011.

Frahm, M.; Rosas, J.; Mayek, P.; rez, N.; Salinas, pez E.; Acosta-Gallegos, J., and Kelly, J. Breeding beans for resistance to terminal drought in the lowland tropics. *Euphytica*, 136(2):223–232, 2004.

Fraser, E. D. G.; Simelton, E.; Termansen, M.; Gosling, S. N., and South, A. vulnerability hotspots: Integrating socio-economic and hydrological models to identify where cereal production may decline in the future due to climate change induced drought. *Agricultural and Forest Meteorology*, 170:195–205, 2013.

Fredeen, A. L.; Raab, T. K.; Rao, I. M., and Terry, N. Effects of phosphorus nutrition on photosynthesis in <i>glycine max</i> (l.) merr. *Planta*, 181(3):399–405, 1990.

Freer, J.; Beven, K., and Ambroise, B. Bayesian estimation of uncertainty in runoff prediction and the value of data: An application of the glue approach. *Water Resources*

Research, 32(7):2161–2173, July 1996. ISSN 00431397. doi: 10.1029/95WR03723. URL `http://doi.wiley.com/10.1029/95WR03723`.

Friedlingstein, P.; Houghton, R. A.; Marland, G.; Hackler, J.; Boden, T. A.; Conway, T. J.; Canadell, J. G.; Raupach, M. R.; Ciais, P., and Le Quere, C. Update on co2 emissions. *Nature Geoscience*, 3(12):811–812, 2010. 10.1038/ngeo1022.

Fuhrer, J. Agroecosystem responses to combinations of elevated co2, ozone, and global climate change. *Agriculture, Ecosystems & Environment*, 97(1-3):1–20, 2003.

Furevik, T.; Bentsen, M.; Drange, H.; Kindem, I. K. T.; Kvamst, N. G., and Sorteberg, A. Description and evaluation of the bergen climate model: Arpege coupled with micom. *Climate Dynamics*, 21(1):27–51, 2003.

Gaidashova, S. V.; Van Asten, P. J. A.; Jefwa, J. M.; Delvaux, B., and Declerck, S. Arbuscular mycorrhizal fungi in the east african highland banana cropping systems as related to edapho-climatic conditions and management practices: case study of rwanda. *Fungal Ecology*, 3(3):225–233, 2010.

Gallee, H.; Moufouma-Okia, W.; Bechtold, P.; Brasseur, O.; Dupays, I.; Marbaix, P.; Messager, C.; Ramel, R., and Lebel, T. A high-resolution simulation of a west african rainy season using a regional climate model. *J. Geophys. Res.*, 109(D5):D05108, 2004.

Garrett, K. A.; Dobson, A. D. M.; Kroschel, J.; Natarajan, B.; Orlandini, S.; Tonnang, H. E. Z., and Valdivia, C. The effects of climate variability and the color of weather time series on agricultural diseases and pests, and on decisions for their management. *Agricultural and Forest Meteorology*, 170:216–227, 2013.

Giorgi, F. Simulation of regional climate using a limited area model nested in a general circulation model. *Journal of Climate*, 3(9):941–963, 1990.

Giorgi, F.; Jones, C., and Asrar, G. R. Addressing climate information needs at the regional level: the cordex framework. *World Meteorological Organization Bulletin*, 58 (3):175–183, 2009.

Gleckler, P. J.; Taylor, K. E., and Doutriaux, C. Performance metrics for climate models. *J. Geophys. Res.*, 113(D6):D06104, 2008.

Gleckler, P. J.; Santer, B. D.; Domingues, C. M.; Pierce, D. W.; Barnett, T. P.; Church, J. A.; Taylor, K. E.; AchutaRao, K. M.; Boyer, T. P.; Ishii, M., and Caldwell, P. M. Human-induced global ocean warming on multidecadal timescales. *Nature Clim. Change*, 2(7):524–529, 2012. 10.1038/nclimate1553.

Glenn, M.; Kim, S.; Ramirez-Villegas, J., and Laderach, P. Response of perennial horticultural crops to climate change. *Horticultural Reviews*, 41:197–200, 2013. ISSN 978-1-1187-0737-1.

Gollin, D.; Parente, S. L., and Rogerson, R. The food problem and the evolution of international income levels. *Journal of Monetary Economics*, 54(4):1230–1255, 2007.

Gordon, C.; Cooper, C.; Senior, C. A.; Banks, H.; Gregory, J. M.; Johns, T. C.; Mitchell, J. F. B., and Wood, R. A. The simulation of sst, sea ice extents and ocean heat transports in a version of the hadley centre coupled model without flux adjustments. *Climate Dynamics*, 16(2):147–168, 2000.

Gordon, H. B.; Rotstayn, L. D.; McGregor, J. L.; Dix, M. R.; Kowalczyk, E. A.; O'Farrell, S. P.; Waterman, L. J.; Hirst, A. C.; Wilson, S. G.; Collier, M. A.; Watterson, I. G., and Elliott, T. The csiro mk3 climate system model. Technical report, Aspendale: CSIRO Atmospheric Research, 2002.

Gouache, D.; Bensadoun, A.; Brun, F.; Pag, C.; Makowski, D., and Wallach, D. Modelling climate change impact on septoria tritici blotch (stb) in france: Accounting for climate model and disease model uncertainty. *Agricultural and Forest Meteorology*, 170:242–253, 2013.

Gourdji, S. M.; Mathews, K. L.; Reynolds, M.; Crossa, J., and Lobell, D. B. An assessment of wheat yield sensitivity and breeding gains in hot environments. *Proceedings of the Royal Society B: Biological Sciences*, 280(1752), 2013.

Groetzner, A.; Sausen, R., and Claussen, M. The impact of sub-grid scale sea-ice inhomogeneities on the performance of the atmospheric general circulation model echam3. *Climate Dynamics*, 12(7):477–496, 1996.

Gualdi, S.; Scoccimarro, E., and Navarra, A. Changes in tropical cyclone activity due to global warming: Results from a high-resolution coupled general circulation model. *Journal of Climate*, 21(20):5204–5228, 2008.

Guarino, L. and Lobell, D. B. A walk on the wild side. *Nature Clim. Change*, 1(8):374–375, 2011. 10.1038/nclimate1272.

Guisan, A.; Edwards Jr, T. C., and Hastie, T. Generalized linear and generalized additive models in studies of species distributions: setting the scene. *Ecological Modelling*, 157(23):89–100, 2002. doi: http://dx.doi.org/10.1016/S0304-3800(02)00204-1. URL `http://www.sciencedirect.com/science/article/pii/S0304380002002041`.

Habash, D. Z.; Kehel, Z., and Nachit, M. Genomic approaches for designing durum wheat ready for climate change with a focus on drought. *Journal of Experimental Botany*, 60 (10):2805–2815, 2009.

Hajjar, R. and Hodgkin, T. The use of wild relatives in crop improvement: a survey of developments over the last 20 years. *Euphytica*, 156(1):1–13, 2007.

Hammer, G. L.; Sinclair, T. R.; Boote, K. J.; Wright, G. C.; Meinke, H., and Bell, M. J. A peanut simulation model: I. model development and testing. *Agron. J.*, 87(6):1085–1093, 1995.

Hannah, L.; Roehrdanz, P. R.; Ikegami, M.; Shepard, A. V.; Shaw, M. R.; Tabor, G.; Zhi, L.; Marquet, P. A., and Hijmans, R. J. Climate change, wine, and conservation. *Proceedings of the National Academy of Sciences*, 110(17):6907–6912, 2013. doi: 10.1073/pnas.1210127110. URL `http://www.pnas.org/content/110/17/6907.abstract`.

Hansen, J.; Johnson, D.; Lacis, A.; Lebedeff, S.; Lee, P.; Rind, D., and Russell, G. Climate impact of increasing atmospheric carbon dioxide. *Science*, 213(4511):957–966, 1981.

Hansen, J.; Sato, M., and Ruedy, R. Radiative forcing and climate response. *J. Geophys. Res.*, 102(D6):6831–6864, 1997.

Hansen, J.; Sato, M.; Ruedy, R.; Kharecha, P.; Lacis, A.; Miller, R.; Nazarenko, L.; Lo, K.; Schmidt, G.; Russell, G.; Aleinov, I.; Bauer, S.; Baum, E.; Cairns, B.; Canuto, V.; Chandler, M.; Cheng, Y.; Cohen, A.; Del Genio, A.; Faluvegi, G.; Fleming, E.; Friend, A.; Hall, T.; Jackman, C.; Jonas, J.; Kelley, M.; Kiang, N.; Koch, D.; Labow, G.; Lerner, J.; Menon, S.; Novakov, T.; Oinas, V.; Perlwitz, J.; Perlwitz, J.; Rind, D.; Romanou, A.; Schmunk, R.; Shindell, D.; Stone, P.; Sun, S.; Streets, D.; Tausnev, N.;

Thresher, D.; Unger, N.; Yao, M., and Zhang, S. Climate simulations for 18802003 with giss modele. *Climate Dynamics*, 29(7):661–696, 2007.

Hansen, J. W. and Jones, J. W. Scaling-up crop models for climate variability applications. *Agricultural Systems*, 65(1):43–72, 2000.

Hansen, J. W.; Mishra, A.; Rao, K. P. C.; Indeje, M., and Ngugi, R. K. Potential value of gcm-based seasonal rainfall forecasts for maize management in semi-arid kenya. *Agricultural Systems*, 101(1-2):80–90, 2009.

Harper, C. R. and Zilberman, D. Pest externalities from agricultural inputs. *American Journal of Agricultural Economics*, 71(3):692–702, 1989.

Hasumi, H. and Emori, S. K-1 coupled gcm (miroc) description. Technical report, CCSR, NIES and FRCGC, 2004.

Hawkins, E. and Sutton, R. The potential to narrow uncertainty in regional climate predictions. *Bulletin of the American Meteorological Society*, 90(8):1095–1107, 2009.

Hawkins, E.; Fricker, T. E.; Challinor, A. J.; Ferro, C. A. T.; Kit Ho, C., and Osborne, T. M. Increasing influence of heat stress on french maize yields from the 1960s to the 2030s. *Global Change Biology*, 2013a.

Hawkins, E.; Osborne, T. M.; Ho, C. K., and Challinor, A. J. Calibration and bias correction of climate projections for crop modelling: an idealised case study over europe. *Agricultural and Forest Meteorology*, 170:19–31, 2013b.

Haywood, J. M.; Bellouin, N.; Jones, A.; Boucher, O.; Wild, M., and Shine, K. P. The roles of aerosol, water vapor and cloud in future global dimming/brightening. *J. Geophys. Res.*, 116(D20):D20203, 2011.

Hew, C.-S.; Krotkov, G., and Canvin, D. T. Effects of temperature on photosynthesis and co2 evolution in light and darkness by green leaves. *Plant Physiology*, 44(5):671–677, 1969.

Hewitson, B. C. and Crane, R. G. Consensus between gcm climate change projections with empirical downscaling: precipitation downscaling over south africa. *International Journal of Climatology*, 26(10):1315–1337, 2006.

Hijmans, R. J. Cross-validation of species distribution models: removing spatial sorting bias and calibration with a null model. *Ecology*, 93(3):679–688, 2012.

Hijmans, R. J. and Graham, C. H. The ability of climate envelope models to predict the effect of climate change on species distributions. *Global Change Biology*, 12(12): 2272–2281, 2006.

Hijmans, R. J.; Guarino, L.; Cruz, M., and Rojas, E. Computer tools for spatial analysis of plant genetic resources data: 1. diva-gis. *Plant Genetic Resources Newsletter*, 127: 15–19, 2001.

Hijmans, R. J.; Cameron, S. E.; Parra, J. L.; Jones, P. G., and Jarvis, A. Very high resolution interpolated climate surfaces for global land areas. *International Journal of Climatology*, 25(15):1965–1978, 2005.

Hollaway, M. J.; Arnold, S. R.; Challinor, A. J., and Emberson, L. D. Intercontinental trans-boundary contributions to ozone-induced crop yield losses in the northern hemisphere. *Biogeosciences Discuss.*, 8(4):8645–8691, 2011. BGD.

Hoogenboom, G.; Jones, J. W.; Wilkens, P. W.; Batchelor, W. D.; Bowen, W. T.; Hunt, L. A.; Pickering, N. B.; Singh, U.; Godwin, D. C.; Baer, B.; Boote, K. J.; Ritchie, J. T., and White, J. W. *Crop Models*. Decision Support System for Agrotechnology Transfer, Version 3.0 (DSSAT V3.0), vol. 22. International Benchmark Sites Network for Agrotechnology Transfer (IBSNAT) Project. University of Hawaii, Department of Agronomy and Soil Science, Honolulu, Hawaii, 1994.

Hoogenboom, G. and White, J. W. Improving physiological assumptions of simulation models by using gene-based approaches. *Agron. J.*, 95(1):82–89, 2003.

Hoogenboom, G.; Jones, J. W., and Boote, K. J. Modeling growth, development, and yield of grain legumes using soygro, pnutgro, and beangro: A review. *Transactions of the ASABE*, 36(5):2043–2056., 1992.

Howden, S. M.; Crimp, S., and Nelson, R. N. Australian agriculture in a climate of change. In Jubb, I.; Holper, P., and Cai, W., editors, *Managing Climate Change: Papers from GREENHOUSE 2009 Conference*, pages 101–112. CSIRO Publishing, Melbourne, Australia, 2010.

Howden, S. M.; Soussana, J.-F.; Tubiello, F. N.; Chhetri, N.; Dunlop, M., and Meinke, H. Adapting agriculture to climate change. *Proceedings of the National Academy of Sciences*, 104(50):19691–19696, 2007.

Hudson, D. and Jones, R. Regional climate model simulations of present-day and future climates of southern africa. Technical report, MetOffice, Hadley Centre, UK, 2002.

Huffman, G. J.; Adler, R. F.; Bolvin, D. T., and Gu, G. Improving the global precipitation record: Gpcp version 2.1. *Geophys. Res. Lett.*, 36(17):L17808, 2009.

Hulme, M.; Doherty, R.; Ngara, T.; New, M., and Lister, D. African climate change: 1900-2100. *Climate Research*, 17(2):145–168, 2001.

Hunt, L. A. and Pararajasingham, S. Cropsim-wheat: A model describing the growth and development of wheat. *Canadian Journal of Plant Science*, 75:619–632, 1995.

Huntingford, C.; Hugo Lambert, F.; Gash, J. H.; Taylor, C. M., and Challinor, A. J. Aspects of climate change prediction relevant to crop productivity. *Philosophical Transactions of the Royal Society B: Biological Sciences*, 360(1463):1999–2009, 2005.

Hutchinson, J. J.; Campbell, C. A., and Desjardins, R. L. Some perspectives on carbon sequestration in agriculture. *Agricultural and Forest Meteorology*, 142(24):288–302, 2007.

Hutchinson, M. F. Interpolating mean rainfall using thin plate smoothing splines. *International Journal of Geographical Information Systems*, 9(4):385 – 403, 1995.

Iizumi, T.; Uno, F., and Nishimori, M. Climate downscaling as a source of uncertainty in projecting local climate change impacts. *Journal of the Meteorological Society of Japan*, 90(B):83–90, 2012a.

Iizumi, T.; Nishimori, M., and Yokozawa, M. Diagnostics of climate model biases in summer temperature and warm-season insolation for the simulation of regional paddy rice yield in japan. *Journal of Applied Meteorology and Climatology*, 49(4):574–591, 2009a.

Iizumi, T.; Yokozawa, M., and Nishimori, M. Parameter estimation and uncertainty analysis of a large-scale crop model for paddy rice: Application of a bayesian approach. *Agricultural and Forest Meteorology*, 149(2):333–348, 2009b.

Iizumi, T.; Yokozawa, M., and Nishimori, M. Probabilistic evaluation of climate change impacts on paddy rice productivity in japan. *Climatic Change*, 107(3):391–415, 2011.

Iizumi, T.; Semenov, M. A.; Nishimori, M.; Ishigooka, Y., and Kuwagata, T. Elpis-jp: a dataset of local-scale daily climate change scenarios for japan. *Philosophical Transactions of the Royal Society A: Mathematical, Physical and Engineering Sciences*, 370 (1962):1121–1139, 2012b.

IMD-AGRIMET, . Crop weather calendar of different states of the country, 2008.

Ines, A. V. M.; Hansen, J. W., and Robertson, A. W. Enhancing the utility of daily gcm rainfall for crop yield prediction. *International Journal of Climatology*, 31(14): 2168–2182, 2011.

Ines, A. V. and Hansen, J. W. Bias correction of daily gcm rainfall for crop simulation studies. *Agricultural and forest meteorology*, 138(1):44–53, 2006.

IPCC, . *Special Report on Emission Scenarios. Summary for policymakers*. IPCC, Geneva, Switzerland, 2000.

IPCC, . *IPCC Third Assessment Report: Climate Change 2001 (TAR)*. IPCC, Geneva, Switzerland, 2001.

IPCC, . *IPCC Fourth Assessment Report: Climate Change 2007 (AR4)*. IPCC, Geneva, Switzerland, 2007.

Jackson, S. T. and Overpeck, J. T. Responses of plant populations and communities to environmental changes of the late quaternary. *Paleobiology*, 26(sp4):194–220, 2000.

Jagtap, S. S. and Jones, J. W. Adaptation and evaluation of the cropgro-soybean model to predict regional yield and production. *Agriculture, Ecosystems & Environment*, 93 (1-3):73–85, 2002.

Jamieson, P. D.; Porter, J. R.; Goudriaan, J.; Ritchie, J. T.; Keulen, van H., and Stol, W. A comparison of the models afrcwheat2, ceres-wheat, sirius, sucros2 and swheat with measurements from wheat grown under drought. *Field Crops Research*, 55(1-2):23–44, 1998.

Jansky, S. H.; Simon, R., and Spooner, D. M. A test of taxonomic predictivity: Resistance to the colorado potato beetle in wild relatives of cultivated potato. *Journal of Economic Entomology*, 102(1):422–431, 2009.

Jarvis, A.; Ferguson, M. E.; Williams, D. E.; Guarino, L.; Jones, P. G.; Stalker, H. T.; Valls, J. F. M.; Pittman, R. N.; Simpson, C. E., and Bramel, P. Biogeography of wild arachis: Assessing conservation status and setting future priorities. *Crop Science*, 43 (3):1100–1108, 2003.

Jarvis, A.; Reuter, H. I.; Nelson, A., and Guevara, E. Hole-filled seamless srtm data v4, 2008.

Jarvis, A.; Ramirez, J.; Anderson, B.; Leibing, C., and Aggarwal, P. *Scenarios of Climate Change Within the Context of Agriculture*. CAB International, 2010.

Jarvis, A.; Lau, C.; Cook, S.; Wollenberg, E.; Hansen, J.; Bonilla, O., and Challinor, A. An integrated adaptation and mitigation framework for developing agricultural research: Synergies and trade-offs. *Experimental Agriculture*, 47(Special Issue 02):185–203, 2011a.

Jarvis, A.; Ramirez-Villegas, J.; Bonilla-Findji, O., and Zapata, E. *Chapter 3.1: Impacts of Climate Change on Crop Production in Latin America*. Crop Adaptation to Climate Change. Wiley & Sons, 2011b.

Jarvis, A.; Ramirez-Villegas, J.; Herrera Campo, B., and Navarro-Racines, C. Is cassava the answer to african climate change adaptation? *Tropical Plant Biology*, 5(1):9–29, 2012.

Jimenez-Valverde, A.; Lobo, J. M., and Hortal, J. Not as good as they seem: the importance of concepts in species distribution modelling. *Diversity and Distributions*, 14(6): 885–890, 2008.

Johns, T. C.; Durman, C. F.; Banks, H. T.; Roberts, M. J.; McLaren, A. J.; Ridley, J. K.; Senior, C. A.; Williams, K. D.; Jones, A.; Rickard, G. J.; Cusack, S.; Ingram, W. J.; Crucifix, M.; Sexton, D. M. H.; Joshi, M. M.; Dong, B. W.; Spencer, H.; Hill, R. S. R.; Gregory, J. M.; Keen, A. B.; Pardaens, A. K.; Lowe, J. A.; Bodas-Salcedo, A.; Stark, S., and Searl, Y. The new hadley centre climate model (hadgem1): Evaluation of coupled simulations. *Journal of Climate*, 19(7):1327–1353, 2006.

Jones, C.; Kiniry, J., and Dyke, P. *CERES-Maize: a simulation model of maize growth and development*. Texas A&M University Press, 1986.

Jones, J. W.; Hoogenboom, G.; Porter, C. H.; Boote, K. J.; Batchelor, W. D.; Hunt, L. A.; Wilkens, P. W.; Singh, U.; Gijsman, A. J., and Ritchie, J. T. The dssat cropping system model. *European Journal of Agronomy*, 18(3-4):235–265, 2003.

Jones, P. G. *Chapter 8: Current Availability and Deficiencies in Data Relevant to Agro-ecological Studies in the Geographic Area Covered by the IARCs*. Agricultural Envrionments: Characterisation, Classification and Mapping. CAB International, UK, 1987.

Jones, P. G. and Thornton, P. K. Fitting a third-order markov rainfall model to interpolated climate surfaces. *Agricultural and Forest Meteorology*, 97(3):213–231, 1999.

Jones, P. G. and Thornton, P. K. Marksim: Software to generate daily weather data for latin america and africa. *Agron. J.*, 92(3):445–453, 2000.

Jones, P. G. and Thornton, P. K. The potential impacts of climate change on maize production in africa and latin america in 2055. *Global Environmental Change*, 13(1): 51–59, 2003.

Jones, P. G. and Thornton, P. K. Croppers to livestock keepers: livelihood transitions to 2050 in africa due to climate change. *Environmental Science & Policy*, 12(4):427–437, 2009.

Jones, P. and Thornton, P. Generating downscaled weather data from a suite of climate models for agricultural modelling applications. *Agricultural Systems*, 114(2013):1–5, 2013.

Jones, P.; Thornton, P. K., and Heinke, J. Generating characteristic daily weather data using downscaled climate model data from the ipcc's fourth assessment. Technical report, ILRI, 2009.

Joshi, M.; Hawkins, E.; Sutton, R.; Lowe, J., and Frame, D. Projections of when temperature change will exceed 2c above pre-industrial levels. *Nature Clim. Change*, 1(8): 407–412, 2011. 10.1038/nclimate1261.

Jourdain, N.; Gupta, A.; Taschetto, A.; Ummenhofer, C.; Moise, A., and Ashok, K. The indo-australian monsoon and its relationship to enso and iod in reanalysis data and the

cmip3/cmip5 simulations. *Climate Dynamics*, pages 1–30, 2013. ISSN 0930-7575. doi: 10.1007/s00382-013-1676-1. URL `http://dx.doi.org/10.1007/s00382-013-1676-1`.

Jun, M.; Knutti, R., and Nychka, D. W. Spatial analysis to quantify numerical model bias and dependence. *Journal of the American Statistical Association*, 103(483):934–947, 2008.

Jungclaus, J. H.; Keenlyside, N.; Botzet, M.; Haak, H.; Luo, J. J.; Latif, M.; Marotzke, J.; Mikolajewicz, U., and Roeckner, E. Ocean circulation and tropical variability in the coupled model echam5/mpi-om. *Journal of Climate*, 19(16):3952–3972, 2006.

Jury, W. and Tanner, C. Advection modification of the priestley and taylor evapotranspiration formula. *Agronomy Journal*, 67(6):840–842, 1975.

Jyostna Devi, M.; Sinclair, T. R.; Vadez, V., and Krishnamurthy, L. Peanut genotypic variation in transpiration efficiency and decreased transpiration during progressive soil drying. *Field Crops Research*, 114(2):280–285, 2009.

Jyostna Devi, M.; Sinclair, T. R., and Vadez, V. Genotypic variation in peanut for transpiration response to vapor pressure deficit. *Crop Sci.*, 50(1):191–196, 2010.

Kahlown, M. A. and Azam, M. Individual and combined effect of waterlogging and salinity on crop yields in the indus basin. *Irrigation and Drainage*, 51(4):329–338, 2002.

Kakani, V. *Quantifying the effects of high temperature and water stress in Groundnut*. PhD thesis, 2001.

Keating, B. A.; Carberry, P. S.; Hammer, G. L.; Probert, M. E.; Robertson, M. J.; Holzworth, D.; Huth, N. I.; Hargreaves, J. N. G.; Meinke, H.; Hochman, Z.; McLean, G.; Verburg, K.; Snow, V.; Dimes, J. P.; Silburn, M.; Wang, E.; Brown, S.; Bristow, K. L.; Asseng, S.; Chapman, S.; McCown, R. L.; Freebairn, D. M., and Smith, C. J. An overview of apsim, a model designed for farming systems simulation. *European Journal of Agronomy*, 18(34):267–288, 2003.

Keatinge, J. D. H.; Ledesma, D. R.; Keatinge, F. J. D., and Hughes, J. D. Projecting annual air temperature changes to 2025 and beyond: implications for vegetable production worldwide. *The Journal of Agricultural Science*, FirstView:1–20, 2012.

Keenan, T.; Maria Serra, J.; Lloret, F.; Ninyerola, M., and Sabate, S. Predicting the future of forests in the Mediterranean under climate change, with niche- and process-based models: CO2 matters! *Global Change Biology*, 17(1):565–579, 2011. doi: 10.1111/j.1365-2486.2010.02254.x. URL `http://dx.doi.org/10.1111/j.1365-2486.2010.02254.x`.

Kemanian, A. R.; Stckle, C. O., and Huggins, D. R. Variability of barley radiation-use efficiency. *Crop Sci.*, 44(5):1662–1672, 2004.

Kennedy, M. C. and O'Hagan, A. Bayesian calibration of computer models. *Journal of the Royal Statistical Society: Series B (Statistical Methodology)*, 63(3):425–464, 2001.

Khan, M. S.; Coulibaly, P., and Dibike, Y. Uncertainty analysis of statistical downscaling methods. *Journal of Hydrology*, 319(14):357–382, 2006.

Kimball, B. A.; Kobayashi, K., and Bindi, M. *Responses of agricultural crops to free-air CO2 enrichment*, volume Volume 77, pages 293–368. Academic Press, 2002.

Kiniry, J. R.; Simpson, C. E.; Schubert, A. M., and Reed, J. D. Peanut leaf area index, light interception, radiation use efficiency, and harvest index at three sites in texas. *Field Crops Research*, 91(23):297–306, 2005.

Klink, C. A. and Machado, R. B. Conservation of the brazilian cerrado. *Conservation Biology*, 19(3):707–713, 2005.

Knox, J.; Hess, T.; Daccache, A., and Wheeler, T. Climate change impacts on crop productivity in africa and south asia. *Environmental Research Letters*, 7(3):034032, 2012.

Knutti, R. and Sedlacek, J. Robustness and uncertainties in the new cmip5 climate model projections. *Nature Clim. Change*, 3:369–373, 2012. 10.1038/nclimate1716.

Kobza, J. and Edwards, G. E. Influences of leaf temperature on photosynthetic carbon metabolism in wheat. *Plant Physiology*, 83(1):69–74, 1987.

Koehler, A.-K.; Challinor, A. J.; Hawkins, E., and Asseng, S. Influences of increasing temperature on indian wheat: quantifying limits to predictability. *Environmental Research Letters*, 8(3):034016, 2013.

Krishna Kumar, K.; Rupa Kumar, K.; Ashrit, R. G.; Deshpande, N. R., and Hansen, J. W. Climate impacts on indian agriculture. *International Journal of Climatology*, 24 (11):1375–1393, 2004.

Krishnamurthy, L.; Vadez, V.; Devi, M. J.; Serraj, R.; Nigam, S. N.; Sheshshayee, M. S.; Chandra, S., and Aruna, R. Variation in transpiration efficiency and its related traits in a groundnut (arachis hypogaea l.) mapping population. *Field Crops Research*, 103 (3):189–197, 2007.

Kristjanson, P.; Neufeldt, H.; Gassner, A.; Mango, J.; Kyazze, F.; Desta, S.; Sayula, G.; Thiede, B.; Frch, W.; Thornton, P., and Coe, R. Are food insecure smallholder households making changes in their farming practices? evidence from east africa. *Food Security*, pages 1–17, 2012.

Kroschel, J.; Sporleder, M.; Tonnang, H. E. Z.; Juarez, H.; Carhuapoma, P.; Gonzales, J. C., and Simon, R. Predicting climate-change-caused changes in global temperature on potato tuber moth phthorimaea operculella (zeller) distribution and abundance using phenology modeling and gis mapping. *Agricultural and Forest Meteorology*, 170:228–241, 2013.

Kumar, D. and Tieszen, L. L. Photosynthesis in coffea arabica. i. effects of light and temperature. *Experimental Agriculture*, 16(01):13–19, 1980.

Läderach, P.; Martinez-Valle, A.; Schroth, G., and Castro, N. Predicting the future climatic suitability for cocoa farming of the worlds leading producer countries, ghana and côte divoire. *Climatic Change*, pages 1–14, 2013.

Laderach, P.; Lundy, M.; Jarvis, A.; Ramirez, J.; Portilla, E. P.; Schepp, K., and Eitzinger, A. *Predicted Impact of Climate Change on Coffee Supply Chains*, pages 703–723. Climate Change Management. Springer Berlin Heidelberg, 2011.

Lal, C.; Hariprasanna, K.; Rathnakumar, A. L.; Gor, H. K., and Chikani, B. M. Gene action for surrogate traits of water-use efficiency and harvest index in peanut (arachis hypogaea). *Annals of Applied Biology*, 148(2):165–172, 2006.

Lane, A. and Jarvis, A. Changes in climate will modify the geography of crop suitability: Agricultural biodiversity can help with adaptation. *Journal of the Semi-Arid Tropics*, 4(1):1–12, 2007.

Leakey, A. D. B.; Ainsworth, E. A.; Bernacchi, C. J.; Rogers, A.; Long, S. P., and Ort, D. R. Elevated co2 effects on plant carbon, nitrogen, and water relations: six important lessons from face. *Journal of Experimental Botany*, 60(10):2859–2876, 2009.

Lebel, T.; Delclaux, F.; Le Barb, L., and Polcher, J. From gcm scales to hydrological scales: rainfall variabiliy in west africa. *Stochastic Environmental Research and Risk Assessment*, 14:275–295, 2000.

Li, S. *Investigating the impacts of climate change on wheat in China*. PhD thesis, 2008.

Li, S.; Wheeler, T.; Challinor, A.; Lin, E.; Ju, H., and Xu, Y. The observed relationships between wheat and climate in china. *Agricultural and Forest Meteorology*, 150(11): 1412–1419, 2010.

Licker, R.; Johnston, M.; Foley, J. A.; Barford, C.; Kucharik, C. J.; Monfreda, C., and Ramankutty, N. Mind the gap: how do climate and agricultural management explain the yield gap of croplands around the world? *Global Ecology and Biogeography*, 19(6): 769–782, 2010.

Liu, C.; Allan, R. P., and Huffman, G. J. Co-variation of temperature and precipitation in cmip5 models and satellite observations. *Geophysical Research Letters*, in press, 2012.

Liu, C.; White, M., and Newell, G. Selecting thresholds for the prediction of species occurrence with presence-only data. *Journal of Biogeography*, 40(4):778–789, 2013. doi: 10.1111/jbi.12058. URL `http://dx.doi.org/10.1111/jbi.12058`.

Livezey, R. E. and Chen, W. Statistical field significance and its determination by monte carlo techniques. *Monthly Weather Review*, 111(1):46–59, 1983.

Lizaso, J.; Boote, K. J.; Jones, J.; Porter, C.; Echarte, L.; Westgate, M., and Sonohat, G. Csm-ixim: A new maize simulation model for dssat version 4.5. *Agronomy Journal*, 103 (3):766–779, 2011.

Lobell, D. B.; Cassman, K. G., and Field, C. B. Crop yield gaps: Their importance, magnitudes, and causes. *Annual Review of Environment and Resources*, 34:179–204, 2009.

Lobell, D. B. and Burke, M. B. On the use of statistical models to predict crop yield responses to climate change. *Agricultural and Forest Meteorology*, 150(11):1443–1452, 2010.

Lobell, D. B.; Burke, M. B.; Tebaldi, C.; Mastrandrea, M. D.; Falcon, W. P., and Naylor, R. L. Prioritizing climate change adaptation needs for food security in 2030. *Science*, 319(5863):607–610, 2008.

Lobell, D. B.; Banziger, M.; Magorokosho, C., and Vivek, B. Nonlinear heat effects on african maize as evidenced by historical yield trials. *Nature Clim. Change*, 1(1):42–45, 2011a. 10.1038/nclimate1043.

Lobell, D. B.; Schlenker, W., and Costa-Roberts, J. Climate trends and global crop production since 1980. *Science*, 333(6042):616–620, 2011b.

Lobell, D. B.; Sibley, A., and Ivan Ortiz-Monasterio, J. Extreme heat effects on wheat senescence in india. *Nature Clim. Change*, 2:186–189, 2012. 10.1038/nclimate1356.

Lobell, D. B.; Hammer, G. L.; McLean, G.; Messina, C.; Roberts, M. J., and Schlenker, W. The critical role of extreme heat for maize production in the United States. *Nature Clim. Change*, advance on, 2013. doi: 10.1038/nclimate1832. URL `http://dx.doi.org/10.1038/nclimate1832`.

Loiselle, B. A.; Jrgensen, P. M.; Consiglio, T.; Jimnez, I.; Blake, J. G.; Lohmann, L. G., and Montiel, O. M. Predicting species distributions from herbarium collections: does climate bias in collection sampling influence model outcomes? *Journal of Biogeography*, 35(1):105–116, 2008.

Long, S. P.; East, T. M., and Baker, N. R. Chilling damage to photosynthesis in young zea mays. *Journal of Experimental Botany*, 34(2):177–188, 1983.

Long, S. P.; Ainsworth, E. A.; Leakey, A. D. B.; Nsberger, J., and Ort, D. R. Food for thought: Lower-than-expected crop yield stimulation with rising co2 concentrations. *Science*, 312(5782):1918–1921, 2006.

Longstreth, D. J. and Nobel, P. S. Nutrient influences on leaf photosynthesis. *Plant Physiology*, 65(3):541–543, 1980.

Ma, L.; Zhang, T.; Frauenfeld, O. W.; Ye, B.; Yang, D., and Qin, D. Evaluation of precipitation from the era-40, ncep-1, and ncep-2 reanalyses and cmap-1, cmap-2, and gpcp-2 with ground-based measurements in china. *J. Geophys. Res.*, 114(D9):D09105, 2009.

Mall, R. K. and Aggarwal, P. K. Climate change and rice yields in diverse agro-environments of india. i. evaluation of impact assessment models. *Climatic Change*, 52(3):315–330, 2002.

Maronna, R. A.; Martin, R. D., and Yohai, V. J. *Robust statistics*. J. Wiley, 2006. ISBN 0470010924.

Marti, O.; Braconnot, P.; Bellier, J.; Benshila, R.; Bony, S.; Brockmann, P.; Cadule, P.; Caubel, A.; Denvil, S.; Dufresne, J.-L.; Fairhead, L.; Filiberti, M.-A.; Foujols, M.-A.; Fichefet, T.; Friedlingstein, P.; Gosse, H.; Grandpeix, J.-Y.; Hourdin, F.; Krinner, G.; Levy, C.; Madec, G.; Musat, I.; Noblet, N. d.; Polcher, J., and Talandier, C. The new ipsl climate system model: Ipsl-cm4. Technical report, Institute Pierre Simon Laplace, 2005.

Masson, D. and Knutti, R. Spatial-scale dependence of climate model performance in the cmip3 ensemble. *Journal of Climate*, 24(11):2680–2692, 2011.

Matthews, R. B. and Hunt, L. A. Gumcas: a model describing the growth of cassava (manihot esculenta l. crantz). *Field Crops Research*, 36(1):69–84, 1994.

Matthews, R. B.; Harris, D.; Rao, R. C. N.; Williams, J. H., and Wadia, K. D. R. The physiological basis for yield differences between four genotypes of groundnut (arachis hypogaea) in response to drought. i. dry matter production and water use. *Experimental Agriculture*, 24(02):191–202, 1988.

Mearns, L. The drama of uncertainty. *Climatic Change*, 100(1):77–85, 2010.

Medek, D. E.; Ball, M. C., and Schortemeyer, M. Relative contributions of leaf area ratio and net assimilation rate to change in growth rate depend on growth temperature: comparative analysis of subantarctic and alpine grasses. *New Phytologist*, 175(2):290–300, 2007.

Meehl, G.; Stocker, T.; Collins, W.; Friedlingstein, P.; Gaye, A.; Gregory, J.; Kitoh, A.; Knutti, R.; Murphy, J.; Noda, A.; Raper, S.; Watterson, I.; Weaver, A., and Zhao, Z.-C.

Global Climate Projections. In: Climate Change 2007: The Physical Science Basis. Contribution of Working Group I to the Fourth Assessment Report of the Intergovernmental Panel on Climate Change. Cambridge University Press, Cambridge, United Kingdom and New York, NY, USA., 2007a.

Meehl, G. A.; Washington, W. M.; Collins, W. D.; Arblaster, J. M.; Hu, A.; Buja, L. E.; Strand, W. G., and Teng, H. How much more global warming and sea level rise? *Science*, 307(5716):1769–1772, 2005.

Meehl, G. A.; Covey, C.; Taylor, K. E.; Delworth, T.; Stouffer, R. J.; Latif, M.; McAvaney, B., and Mitchell, J. F. B. The wcrp cmip3 multimodel dataset: A new era in climate change research. *Bulletin of the American Meteorological Society*, 88(9):1383–1394, 2007b.

Meehl, G. A.; Goddard, L.; Murphy, J.; Stouffer, R. J.; Boer, G.; Danabasoglu, G.; Dixon, K.; Giorgetta, M. A.; Greene, A. M.; Hawkins, E.; Hegerl, G.; Karoly, D.; Keenlyside, N.; Kimoto, M.; Kirtman, B.; Navarra, A.; Pulwarty, R.; Smith, D.; Stammer, D., and Stockdale, T. Decadal prediction. *Bulletin of the American Meteorological Society*, 90 (10):1467–1485, 2009.

Mehrotra, N. Groundnut. Technical report, Department of Economic Analysis and Research, National Bank for Agriculture and Rural Development, 2011.

Meinke, H.; Hammer, G. L.; Keulen, van H.; Rabbinge, R., and Keating, B. A. *Improving wheat simulation capabilities in Australia from a cropping systems perspective: water and nitrogen effects on spring wheat in a semi-arid environment*, volume Volume 25, pages 99–112. Elsevier, 1997.

Meinshausen, M.; Smith, S. J.; Calvin, K.; Daniel, J. S.; Kainuma, M. L. T.; Lamarque, J. F.; Matsumoto, K.; Montzka, S. A.; Raper, S. C. B.; Riahi, K.; Thomson, A.; Velders, G. J. M., and Vuuren, D. P. P. The RCP greenhouse gas concentrations and their extensions from 1765 to 2300. *Climatic Change*, 109(1-2):213–241, 2011. doi: 10.1007/s10584-011-0156-z. URL `http://dx.doi.org/10.1007/s10584-011-0156-z`.

Menon, S.; Hansen, J.; Nazarenko, L., and Luo, Y. Climate Effects of Black Carbon Aerosols in China and India. *Science*, 297(5590):2250–2253, 2002. doi: 10.1126/science.1075159. URL `http://www.sciencemag.org/content/297/5590/2250.abstract`.

Merow, C.; Smith, M. J., and Silander, J. A. A practical guide to MaxEnt for modeling species distributions: what it does, and why inputs and settings matter. *Ecography*, pages no–no, 2013. doi: 10.1111/j.1600-0587.2013.07872.x. URL `http://dx.doi.org/10.1111/j.1600-0587.2013.07872.x`.

Mitchell, T.; Carter, T. R.; Jones, P.; Hulme, M., and New, M. A comprehensive set of high-resolution grids of monthly climate for europe and the globe: the observed record (1901-2000) and 16 scenarios (2001-2100). Technical report, Tyndall Centre for Climate Change Research, 2004.

Mitchell, T. D. and Jones, P. D. An improved method of constructing a database of monthly climate observations and associated high-resolution grids. *International Journal of Climatology*, 25(6):693–712, 2005.

Mock, J. and Pearce, R. An ideotype of maize. *Euphytica*, 24(3):613–623, 1975.

Mohamed, H. *Varietal differences in the temperature responses of germination and crop establishment*. PhD thesis, 1984.

Monfreda, C.; Ramankutty, N., and Foley, J. A. Farming the planet: 2. geographic distribution of crop areas, yields, physiological types, and net primary production in the year 2000. *Global Biogeochem. Cycles*, 22(1):GB1022, 2008.

Monteith, J. and Unsworth, M. *Principles of Environmental Physics*. Edward Arnold, London, UK, 2nd edition, 1990.

Morin, X. and Thuiller, W. Comparing niche- and process-based models to reduce prediction uncertainty in species range shifts under climate change. *Ecology*, 90(5):1301–1313, 2009. doi: 10.1890/08-0134.1. URL `http://dx.doi.org/10.1890/08-0134.1`.

Moser, S. C. and Ekstrom, J. A. A framework to diagnose barriers to climate change adaptation. *Proceedings of the National Academy of Sciences*, 107(51):22026–22031, 2010.

Moss, R. H.; Edmonds, J. A.; Hibbard, K. A.; Manning, M. R.; Rose, S. K.; Vuuren, van D. P.; Carter, T. R.; Emori, S.; Kainuma, M.; Kram, T.; Meehl, G. A.; Mitchell, J. F. B.; Nakicenovic, N.; Riahi, K.; Smith, S. J.; Stouffer, R. J.; Thomson, A. M.; Weyant, J. P., and Wilbanks, T. J. The next generation of scenarios for climate change research and assessment. *Nature*, 463(7282):747–756, 2010. 10.1038/nature08823.

Mueller, N. D.; Gerber, J. S.; Johnston, M.; Ray, D. K.; Ramankutty, N., and Foley, J. A. Closing yield gaps through nutrient and water management. *Nature*, advance online publication, 2012. 10.1038/nature11420.

Muller, C. Agriculture: Harvesting from uncertainties. *Nature Clim. Change*, 1(5):253–254, 2011. 10.1038/nclimate1179.

Murphy, J.; Booth, B.; Collins, M.; Harris, G.; Sexton, D., and Webb, M. A methodology for probabilistic predictions of regional climate change from perturbed physics ensembles. *Philosophical Transactions of the Royal Society A: Mathematical, Physical and Engineering Sciences*, 365(1857):1993–2028, 2007.

Nain, A. S.; Dadhwal, V. K., and Singh, T. P. Use of ceres-wheat model for wheat yield forecast in central indo-gangetic plains of india. *The Journal of Agricultural Science*, 142(01):59–70, 2004.

Nakicenovic, N.; Alcamo, J.; Davis, G.; Vries, de B.; Fenham, J.; Gaffin, S. R.; Gregory, K.; Grubler, A.; Jung, T. Y.; Kram, T.; La Rovere, E. L.; Michaelis, L.; Mori, S.; Morita, T.; Pepper, W.; Pitcher, H.; Price, L.; Riahi, K.; Roehrl, A.; Rogner, H. H.; Sankovski, A.; Schlesinger, M.; Shukla, P.; Smith, S.; Swart, R.; Rooijen, van S.; Victor, N., and Dadi, Z. *Special Report on Emissions Scenarios*. Cambridge University Press, Cambridge, UK and New York, NY, USA, 2000.

Nautiyal, P. C.; Ravindra, V.; Rathnakumar, A. L.; Ajay, B. C., and Zala, P. V. Genetic variations in photosynthetic rate, pod yield and yield components in spanish groundnut cultivars during three cropping seasons. *Field Crops Research*, 125(0):83–91, 2012.

Neild, R. E.; Logan, J., and Cardenas, A. Growing season and phenological response of sorghum as determined from simple climatic data. *Agricultural Meteorology*, 30(1): 35–48, 1983.

New, M.; Hulme, M., and Jones, P. Representing twentieth-century spacetime climate variability. part i: Development of a 196190 mean monthly terrestrial climatology. *Journal of Climate*, 12(3):829–856, 1999.

New, M.; Hulme, M., and Jones, P. Representing twentieth-century spacetime climate variability. part ii: Development of 190196 monthly grids of terrestrial surface climate. *Journal of Climate*, 13(13):2217–2238, 2000.

New, M.; Lister, D.; Hulme, M., and Makin, I. A high-resolution data set of surface climate over global land areas. *Climate Research*, 21(1):1–25, 2002.

Nicklin, K. *Integrated crop-climate modelling for seasonal prediction of yield in the Sahel*. PhD thesis, 2013.

Nielsen, S. E.; Johnson, C. J.; Heard, D. C., and Boyce, M. S. Can models of presence-absence be used to scale abundance ? Two case studies considering extremes in life history. 2(October 2004):197–208, 2005.

Nigam, S. N. Crop improvement strategies in groundnut. *Journal of Agricultural Science*, pages 1–12, 2009.

Nigam, S. N.; Rao, R. C. N.; Wynne, J. C.; Williams, J. H.; Fitzner, M., and Nagabhushanam, G. V. S. Effect and interaction of temperature and photoperiod on growth and partitioning in three groundnut (arachis hypogaea l.) genotypes1. *Annals of Applied Biology*, 125(3):541–552, 1994.

Nigam, S. N.; Upadhyaya, H. D.; Chandra, S.; Rao, R. C. N.; Wright, G. C., and Reddy, A. G. S. Gene effects for specific leaf area and harvest index in three crosses of groundnut (arachis hypogaea). *Annals of Applied Biology*, 139(3):301–306, 2001.

Nigam, S. N.; Chandra, S.; Sridevi, K. R.; Bhukta, M.; Reddy, A. G. S.; Rachaputi, N. R.; Wright, G. C.; Reddy, P. V.; Deshmukh, M. P.; Mathur, R. K.; Basu, M. S.; Vasundhara, S.; Varman, P. V., and Nagda, A. K. Efficiency of physiological trait-based and empirical selection approaches for drought tolerance in groundnut. *Annals of Applied Biology*, 146(4):433–439, 2005.

Nigam, S. and Aruna, R. Stability of soil plant analytical development (spad) chlorophyll meter reading (scmr) and specific leaf area (sla) and their association across varying soil moisture stress conditions in groundnut (arachis hypogaea l.). *Euphytica*, 160(1): 111–117, 2008.

Nikulin, G.; Jones, C.; Giorgi, F.; Asrar, G.; Büchner, M.; Cerezo-Mota, R.; Christensen, O. B.; Déqué, M.; Fernandez, J.; Hänsler, A., and others, . Precipitation climatology in an ensemble of cordex-africa regional climate simulations. *Journal of Climate*, 25(18): 6057–6078, 2012.

Oldeman, L. *An Agroclimatic Characterization of Madagascar*. International Soil Reference and Information Centre, Wageningen, Netherlands, 1988.

Ong, C. K. Agroclimatological factors affecting phenology of groundnut. In *Proceedings of the International Simposium on Agrometeorology of Groundnut*, pages 115–125, 1986.

Orlowsky, B. and Seneviratne, S. Global changes in extreme events: regional and seasonal dimension. *Climatic Change*, 110(3):669–696, 2012.

Ortiz, R.; Sayre, K. D.; Govaerts, B.; Gupta, R.; Subbarao, G. V.; Ban, T.; Hodson, D.; Dixon, J. M.; Ivn Ortiz-Monasterio, J., and Reynolds, M. Climate change: Can wheat beat the heat? *Agriculture, Ecosystems & Environment*, 126(1-2):46–58, 2008.

Osborne, T.; Rose, G., and Wheeler, T. Variation in the global-scale impacts of climate change on crop productivity due to climate model uncertainty and adaptation. *Agricultural and Forest Meteorology*, 170:183–194, 2013.

Osborne, T. M.; Lawrence, D. M.; Challinor, A. J.; Slingo, J. M., and Wheeler, T. R. Development and assessment of a coupled cropclimate model. *Global Change Biology*, 13(1):169–183, 2007.

Palosuo, T.; Kersebaum, K. C.; Angulo, C.; Hlavinka, P.; Moriondo, M.; Olesen, J. E.; Patil, R. H.; Ruget, F.; Rumbaur, C.; Takáč, J., and others, . Simulation of winter wheat yield and its variability in different climates of europe: a comparison of eight crop growth models. *European Journal of Agronomy*, 35(3):103–114, 2011.

Pandey, A.; Tomer, A.; Bhandari, D., and Pareek, S. Towards collection of wild relatives of crop plants in india. *Genetic Resources and Crop Evolution*, 55(2):187–202, 2008.

Park, S. E.; Marshall, N. A.; Jakku, E.; Dowd, A. M.; Howden, S. M.; Mendham, E., and Fleming, A. Informing adaptation responses to climate change through theories of transformation. *Global Environmental Change*, 22(1):115–126, 2012.

Parry, M. L.; Rosenzweig, C.; Iglesias, A.; Livermore, M., and Fischer, G. Effects of climate change on global food production under sres emissions and socio-economic scenarios. *Global Environmental Change*, 14(1):53–67, 2004.

Parry, M.; Rosenzweig, C.; Iglesias, A.; Fischer, G., and Livermore, M. Climate change and world food security: a new assessment. *Global Environmental Change*, 9(Supplement 1):S51–S67, 1999.

Parry, M.; Rosenzweig, C., and Livermore, M. Climate change, global food supply and risk of hunger. *Philosophical Transactions of the Royal Society B: Biological Sciences*, 360(1463):2125–2138, 2005.

Parry, M.; Canziani, O.; Palutikof, J.; Linden, van der P., and Hanson, C. E. *Climate Change 2007: Impacts, Adaptation and Vulnerability. Contribution of Working Group II to the Fourth Assessment Report of the Intergovernmental Panel on Climate Change, 2007*. Cambridge University Press, Cambridge, United Kingdom and New York, NY, USA, 2007.

Passioura, J. Roots and drought resistance. *Agric. Water Manag.*, 7:265–280, 1983.

Pathak, H.; Ladha, J. K.; Aggarwal, P. K.; Peng, S.; Das, S.; Singh, Y.; Singh, B.; Kamra, S. K.; Mishra, B.; Sastri, A. S. R. A. S.; Aggarwal, H. P.; Das, D. K., and Gupta, R. K. Trends of climatic potential and on-farm yields of rice and wheat in the indo-gangetic plains. *Field Crops Research*, 80(3):223–234, 2003.

Patil, B. L. and Fauquet, C. M. Cassava mosaic geminiviruses: actual knowledge and perspectives. *Molecular Plant Pathology*, 10(5):685–701, 2009.

PCMDI, . Ipcc model output, 26 September 2009 2007. URL `http://www.pcmdi.llnl.gov/ipcc/about_ipcc.php`.

Pearce, J. and Ferrier, S. The practical value of modelling relative abundance of species for regional conservation planning : a case study. *Biological Conservation*, 98:33–43, 2001.

Peng, S.; Khush, G. S.; Virk, P.; Tang, Q., and Zou, Y. Progress in ideotype breeding to increase rice yield potential. *Field Crops Research*, 108(1):32–38, 2008.

Peterson, A. T.; Papes, M., and Sobern, J. Rethinking receiver operating characteristic analysis applications in ecological niche modeling. *Ecological Modelling*, 213(1):63–72, 2008.

Peterson, C.; Nowak, A.; Jarvis, A.; Navarrete, C.; Figueroa, A.; Riaño, N., and Vargas, J. Analysing vulnerability: a multi-dimensional approach from Colombia's Upper River Basin. Technical report, 2012.

Peterson, T. C. and Vose, R. S. An overview of the global historical climatology network temperature database. *Bulletin of the American Meteorological Society*, 78(12):2837–2849, 1997.

Peterson, T. A.; Pape, M., and Eaton, M. Transferability and model evaluation in ecological niche modeling: a comparison of garp and maxent. *Ecography*, 30(4):550–560, 2007.

Phakamas, N.; Patanothai, A.; Pannangpetch, K.; Jogloy, S., and Hoogenboom, G. Seasonal responses and genotype-by-season interactions for the growth dynamic and development traits of peanut. *The Journal of Agricultural Science*, 146(03):311–323, 2008.

Phillips, S. J.; Anderson, R. P., and Schapire, R. E. Maximum entropy modeling of species geographic distributions. *Ecological Modelling*, 190(3-4):231–259, 2006.

Piani, C. and Haerter, J. O. Two dimensional bias correction of temperature and precipitation copulas in climate models. *Geophys. Res. Lett.*, 39(20):L20401, 2012.

Pielke, S. R. A.; Adegoke, J. O.; Chase, T. N.; Marshall, C. H.; Matsui, T., and Niyogi, D. A new paradigm for assessing the role of agriculture in the climate system and in climate change. *Agricultural and Forest Meteorology*, 142(2-4):234–254, 2007.

Pierce, D. W.; Barnett, T. P.; Santer, B. D., and Gleckler, P. J. Selecting global climate models for regional climate change studies. *Proceedings of the National Academy of Sciences*, 106(21):8441–8446, 2009.

Pincus, R.; Batstone, C. P.; Hofmann, R. J. P.; Taylor, K. E., and Glecker, P. J. Evaluating the present-day simulation of clouds, precipitation, and radiation in climate models. *Journal of Geophysical Research: Atmospheres*, 113(D14):n/a–n/a, 2008.

Pongratz, J.; Lobell, D. B.; Cao, L., and Caldeira, K. Crop yields in a geoengineered climate. *Nature Clim. Change*, 2(2):101–105, 2012. 10.1038/nclimate1373.

Portmann, F. T.; Siebert, S., and Dll, P. Mirca2000 –global monthly irrigated and rainfed crop areas around the year 2000: A new high-resolution data set for agricultural and hydrological modeling. *Global Biogeochem. Cycles*, 24(1):GB1011, 2010.

Pretty, J.; Sutherland, W. J.; Ashby, J.; Auburn, J.; Baulcombe, D.; Bell, M.; Bentley, J.; Bickersteth, S.; Brown, K.; Burke, J.; Campbell, H.; Chen, K.; Crowley, E.; Crute, I.; Dobbelaere, D.; Edwards-Jones, G.; Funes-Monzote, F.; Godfray, H. C. J.; Griffon, M.; Gypmantisiri, P.; Haddad, L.; Halavatau, S.; Herren, H.; Holderness, M.; Izac, A.-M.; Jones, M.; Koohafkan, P.; Lal, R.; Lang, T.; McNeely, J.; Mueller, A.; Nisbett, N.; Noble, A.; Pingali, P.; Pinto, Y.; Rabbinge, R.; Ravindranath, N. H.; Rola, A.; Roling, N.; Sage, C.; Settle, W.; Sha, J. M.; Shiming, L.; Simons, T.; Smith, P.; Strzepeck, K.; Swaine, H.; Terry, E.; Tomich, T. P.; Toulmin, C.; Trigo, E.; Twomlow, S.; Vis, J. K.; Wilson, J., and Pilgrim, S. The top 100 questions of importance to the future of global agriculture. *International Journal of Agricultural Sustainability*, 8(4):219–236, 2010.

Priestley, C. H. B. and Taylor, R. J. On the assessment of surface heat flux and evaporation using large-scale parameters. *Monthly Weather Review*, 100(2):81–92, 1972.

Puangbut, D.; Jogloy, S.; Vorasoot, N.; Akkasaeng, C.; Kesmala, T.; Rachaputi, R. C. N.; Wright, G. C., and Patanothai, A. Association of root dry weight and transpiration efficiency of peanut genotypes under early season drought. *Agricultural Water Management*, 96(10):1460–1466, 2009.

Quilambo, O. A. *Functioning of peanut (Arachis hypogaea L.) under nutrient deficiency and drought stress in relation to symbiotic associations.* PhD thesis, 2000.

Rajeevan, M. and Bhate, J. A high resolution daily gridded rainfall data set (1971-2005) for mesoscale meteorological studies. Technical report, National Climate Centre, India Meteorological Department, 2008.

Rajeevan, M.; Bhate, J.; Kale, J. D., and Lal, B. Development of a high resolution daily gridded rainfall data for the indian region. Technical report, National Climate Centre, India Meteorological Department, Government of India, 2005.

Rajeevan, M.; Bhate, J.; Kale, J. D., and Lal, B. High resolution daily gridded rainfall data for the india region: Analysis of break and active monsoon spells. *Current Science*, 91(3):296–306, 2006.

Ramankutty, N.; Evan, A. T.; Monfreda, C., and Foley, J. A. Farming the planet: 1. geographic distribution of global agricultural lands in the year 2000. *Global Biogeochem. Cycles*, 22(1):GB1003, 2008.

Ramirez-Villegas, J.; Challinor, A. J.; Thornton, P. K., and Jarvis, A. Implications of regional improvement in global climate models for agricultural impact research. *Environmental Research Letters*, 8(2):024018, 2013a. URL `http://stacks.iop.org/1748-9326/8/i=2/a=024018`.

Ramirez-Villegas, J. and Challinor, A. Assessing relevant climate data for agricultural applications. *Agricultural and Forest Meteorology*, 161:26–45, 2012.

Ramirez-Villegas, J. and Khoury, C. K. Reconciling approaches to climate change adaptation for colombian agriculture. *Climatic Change*, 119(3-4):575–583, 2013. ISSN 0165-0009. doi: 10.1007/s10584-013-0792-6. URL `http://dx.doi.org/10.1007/s10584-013-0792-6`.

Ramirez-Villegas, J.; Jarvis, A., and Laderach, P. Empirical approaches for assessing impacts of climate change on agriculture: The ecocrop model and a case study with grain sorghum. *Agricultural and Forest Meteorology*, 170:67–78, 2013b.

Randall, D.; Wood, R.; Bony, S.; Colman, R.; Fichefet, T.; Fyfe, J.; Kattsov, V.; Pitman, A.; Shukla, J.; Srinivasan, J.; Stouffer, R.; Sumi, A., and Taylor, K. *Chapter 8: Climate Models and Their Evaluation*, pages 273–313. Cambridge University Press, Cambridge, UK, 2007.

Ranger, N.; Millner, A.; Dietz, S. FankhauserS.; Lopez, A., and Ruta, G. Adaptation in the uk: a decision making process. Technical report, Grantham Research Institute/CCCEP Policy Brief, London School of Economics and Political Science, 2010.

Rao, R. C. N. and Wright, G. C. Stability of the relationship between specific leaf area and carbon isotope discrimination across environments in peanut. *Crop Sci.*, 34(1):98–103, 1994.

Rao, R. C. N.; Williams, J. H., and Singh, M. Genotypic sensitivity to drought and yield potential of peanut. *Agron. J.*, 81(6):887–893, 1989.

Rao, R. and Nigam, S. *Genetic Options for Drought Management in Groundnut*, pages 123–141. Science Publishers, Inc, 2003.

Ratnakumar, P. and Vadez, V. Groundnut (arachis hypogaea) genotypes tolerant to intermittent drought maintain a high harvest index and have small leaf canopy under stress. *Functional Plant Biology*, 38(12):1016–1023, 2011.

Ratnakumar, P.; Vadez, V.; Nigam, S. N., and Krishnamurthy, L. Assessment of transpiration efficiency in peanut (arachis hypogaea l.) under drought using a lysimetric system. *Plant Biology*, 11:124–130, 2009.

Rattalino Edreira, J. I.; Budakli Carpici, E.; Sammarro, D., and Otegui, M. E. Heat stress effects around flowering on kernel set of temperate and tropical maize hybrids. *Field Crops Research*, 123(2):62–73, 2011.

Reay, D. S.; Davidson, E. A.; Smith, K. A.; Smith, P.; Melillo, J. M.; Dentener, F., and Crutzen, P. J. Global agriculture and nitrous oxide emissions. *Nature Clim. Change*, 2 (6):410–416, 2012. 10.1038/nclimate1458.

Reichler, T. and Kim, J. How well do coupled models simulate today's climate? *Bulletin of the American Meteorological Society*, 89(3):303–311, 2008.

Reifen, C. and Toumi, R. Climate projections: Past performance no guarantee of future skill? *Geophys. Res. Lett.*, 36(13):L13704, 2009.

Reynolds, M. P.; Hellin, J.; Govaerts, B.; Kosina, P.; Sonder, K.; Hobbs, P., and Braun, H. Global crop improvement networks to bridge technology gaps. *Journal of Experimental Botany*, 63(1):1–12, 2011.

Rickards, L. and Howden, S. M. Transformational adaptation: agriculture and climate change. *Crop and Pasture Science*, 63(3):240–250, 2012.

Ritchie, J. T.; Porter, C. H.; Judge, J.; Jones, J. W., and Suleiman, A. A. Extension of an existing model for soil water evaporation and redistribution under high water content conditions. *Soil Science Society of America Journal*, 73(3):792–801, 2009.

Rivington, M. and Koo, J. Report on the meta-analysis of crop modelling for climate change and food security survey. Technical report, CGIAR Research Program on Climate Change, Agriculture and Food Security, 2011.

Rohde, R.; Muller, R. A.; Jacobsen, R.; Muller, E.; Perlmutter, S.; Rosenfeld, A.; Wurtele, J.; Groom, D., and Wickham, C. New estimate of the average earth surface land temperature spanning 1753 to 2011. *Geoinfor. Geostat.: An Overview*, 1, 2013.

Rosati, A. and Dejong, T. M. Estimating photosynthetic radiation use efficiency using incident light and photosynthesis of individual leaves. *Annals of Botany*, 91(7):869–877, 2003.

Rosenthal, D. M.; Slattery, R. A.; Miller, R. E.; Grennan, A. K.; Cavagnaro, T. R.; Fauquet, C. M.; Gleadow, R. M., and Ort, D. R. Cassava about-face: Greater than expected yield stimulation of cassava (manihot esculenta) by future co2 levels. *Global Change Biology*, 18(8):2661–2675, 2012.

Rosenzweig, C.; Jones, J. W.; Hatfield, J. L.; Ruane, A. C.; Boote, K. J.; Thorburn, P.; Antle, J. M.; Nelson, G. C.; Porter, C.; Janssen, S.; Asseng, S.; Basso, B.; Ewert, F.; Wallach, D.; Baigorria, G., and Winter, J. M. The agricultural model intercomparison and improvement project (agmip): Protocols and pilot studies. *Agricultural and Forest Meteorology*, 170:166–182, 2013.

Rotter, R. P.; Carter, T. R.; Olesen, J. E., and Porter, J. R. Crop-climate models need an overhaul. *Nature Clim. Change*, 1(4):175–177, 2011. 10.1038/nclimate1152.

Rötter, R. P.; Palosuo, T.; Kersebaum, K. C.; Angulo, C.; Bindi, M.; Ewert, F.; Ferrise, R.; Hlavinka, P.; Moriondo, M.; Nendel, C., and others, . Simulation of spring barley yield in different climatic zones of northern and central europe: a comparison of nine crop models. *Field Crops Research*, 133:23–36, 2012.

Roudier, P.; Sultan, B.; Quirion, P., and Berg, A. The impact of future climate change on west african crop yields: What does the recent literature say? *Global Environmental Change*, 21(3):1073–1083, 2011.

Ruane, A. C.; Cecil, L. D.; Horton, R. M.; Gordn, R.; McCollum, R.; Brown, D.; Killough, B.; Goldberg, R.; Greeley, A. P., and Rosenzweig, C. Climate change impact uncertainties for maize in panama: Farm information, climate projections, and yield sensitivities. *Agricultural and Forest Meteorology*, 170:132–145, 2013.

Rufino, M.; Thornton, P.; Nganga, S.; Mutie, I.; Jones, P., and Herrero, M. Households responses to climate in east africa: impacts on food security and poverty in crop-livestock systems. In press, 2012.

Russell, G.; Miller, J., and Rind, D. A coupled atmosphere-ocean model for transient climate change studies. *Atmosphere-Ocean*, 33(4):683–730, 1995.

Sacks, W. J.; Deryng, D.; Foley, J. A., and Ramankutty, N. Crop planting dates: an analysis of global patterns. *Global Ecology and Biogeography*, 19(5):607–620, 2010.

Sage, R. F. and Kubien, D. S. The temperature response of c3 and c4 photosynthesis. *Plant, Cell & Environment*, 30(9):1086–1106, 2007.

Salas-Mlia, D.; Chauvin, F.; Dqu, M.; Douville, H.; Gueremy, J.; Marquet, P.; Planton, S.; Royer, J., and Tyteca, S. Description and validation of the cnrm-cm3 global coupled model. Technical report, CNRM, 2005.

Saman, M.; Sepehri, A.; Ahmadvand, G., and Sabaghpour, S. Effect of terminal drought on yield and yield components of five chickpea genotypes. *Iranian Journal of Field Crop Science*, 41, 2010.

Scherrer, S. C. Present-day interannual variability of surface climate in cmip3 models and its relation to future warming. *International Journal of Climatology*, 31(10):1518–1529, 2011.

Schlenker, W. and Lobell, D. B. Robust negative impacts of climate change on african agriculture. *Environmental Research Letters*, 5(1):014010, 2010.

Schlenker, W. and Roberts, M. J. Nonlinear temperature effects indicate severe damages to u.s. crop yields under climate change. *Proceedings of the National Academy of Sciences*, 2009.

Schmidli, J.; Frei, C., and Vidale, P. L. Downscaling from gcm precipitation: a benchmark for dynamical and statistical downscaling methods. *International Journal of Climatology*, 26(5):679–689, 2006.

Schmidt, G. A.; Ruedy, R.; Hansen, J. E.; Aleinov, I.; Bell, N.; Bauer, M.; Bauer, S.; Cairns, B.; Canuto, V.; Cheng, Y.; Del Genio, A.; Faluvegi, G.; Friend, A. D.; Hall, T. M.; Hu, Y.; Kelley, M.; Kiang, N. Y.; Koch, D.; Lacis, A. A.; Lerner, J.; Lo, K. K.;

Miller, R. L.; Nazarenko, L.; Oinas, V.; Perlwitz, J.; Perlwitz, J.; Rind, D.; Romanou, A.; Russell, G. L.; Sato, M.; Shindell, D. T.; Stone, P. H.; Sun, S.; Tausnev, N.; Thresher, D., and Yao, M.-S. Present-day atmospheric simulations using giss modele: Comparison to in situ, satellite, and reanalysis data. *Journal of Climate*, 19(2):153–192, 2006.

Schneider, U.; Becker, A.; Meyer-Christoffer, A.; Ziese, M., and Rudolf, B. Global precipitation analysis products of the gpcc. Technical report, Global Preciptation Climatology Centre (GPCC), 2010.

Schroth, G.; Laderach, P.; Dempewolf, J.; Philpott, S.; Haggar, J.; Eakin, H.; Castillejos, T.; Garcia Moreno, J.; Soto Pinto, L.; Hernandez, R.; Eitzinger, A., and Ramirez-Villegas, J. Towards a climate change adaptation strategy for coffee communities and ecosystems in the sierra madre de chiapas, mexico. *Mitigation and Adaptation Strategies for Global Change*, 14(7):605–625, 2009. in SciEArchive.

Scinocca, J. F.; McFarlane, N. A.; Lazare, M.; Li, J., and Plummer, D. The cccma third generation agcm and its extension into the middle atmosphere. *Atmos. Chem. Phys. Discuss.*, 8(2):7883–7930, 2008. ACPD.

Seeni, S. and Gnanam, A. Carbon Assimilation in Photoheterotrophic Cells of Peanut (Arachis hypogaea L.) Grown in Still Nutrient Medium. *Plant Physiology*, 70(3):823–826, 1982. doi: 10.1104/pp.70.3.823. URL `http://www.plantphysiol.org/content/70/3/823.abstract`.

Semenov, M.; Donatelli, M.; Stratonovitch, P.; Chatzidaki, E., and Baruth, B. Elpis: a dataset of local-scale daily climate scenarios for europe. *Climate research (Open Access for articles 4 years old and older)*, 44(1):3, 2010.

Semenov, M. A. and Halford, N. G. Identifying target traits and molecular mechanisms for wheat breeding under a changing climate. *Journal of Experimental Botany*, 60(10): 2791–2804, 2009.

Serra-Diaz, J. M.; Keenan, T. F.; Ninyerola, M.; Sabaté, S.; Gracia, C., and Lloret, F. Geographical patterns of congruence and incongruence between correlative species distribution models and a process-based ecophysiological growth model. *Journal of Biogeography*, pages n/a–n/a, 2013. doi: 10.1111/jbi.12142. URL `http://dx.doi.org/10.1111/jbi.12142`.

Sheffield, J.; Goteti, G., and Wood, E. F. Development of a 50-year high-resolution global dataset of meteorological forcings for land surface modeling. *Journal of Climate*, 19(13): 3088–3111, 2006.

Shepard, D. A two-dimensional interpolation function for irregularly spaced data. In *Proceedings 1968 ACM National Conference*, pages 517–524, 1968.

Sheshshayee, M. S.; Bindumadhava, H.; Rachaputi, N. R.; Prasad, T. G.; Udayakumar, M.; Wright, G. C., and Nigam, S. N. Leaf chlorophyll concentration relates to transpiration efficiency in peanut. *Annals of Applied Biology*, 148(1):7–15, 2006.

Sillmann, J.; Kharin, V. V.; Zhang, X.; Zwiers, F. W., and Bronaugh, D. Climate extremes indices in the CMIP5 multimodel ensemble: Part 1. Model evaluation in the present climate. *Journal of Geophysical Research: Atmospheres*, 118(4):1716–1733, 2013. doi: 10.1002/jgrd.50203. URL `http://dx.doi.org/10.1002/jgrd.50203`.

Simmonds, L. P. and Azam-Ali, S. N. Population, growth and water use of groundnut maintained on stored water. iv. the influence of population on water supply and demand. *Experimental Agriculture*, 25(01):87–98, 1989.

Sinclair, T. R. and Horie, T. Leaf nitrogen, photosynthesis, and crop radiation use efficiency: A review. *Crop Sci.*, 29(1):90–98, 1989.

Sinclair, T. R. and Seligman, N. G. Crop modeling: From infancy to maturity. *Agron. J.*, 88(5):698–704, 1996.

Singh, A.; Mehan, V., and Nigam, S. Sources of resista.nce diseases: an update and appraisal. information bulletin no. 50. Technical report, International Crops Research Institute for the Semi-Arid Tropics, 1997.

Singh, A.; Hariprassana, K., and Solanki, R. Screening and selection of groundnut genotypes for tolerance of soil salinity. *Australian Journal of Crop Science*, 1(3):66–77, 2008.

Singh, P.; Boote, K. J.; Kumar, U.; Srinivas, K.; Nigam, S. N., and Jones, J. W. Evaluation of genetic traits for improving productivity and adaptation of groundnut to climate change in india. *Journal of Agronomy and Crop Science*, 198(5):399–413, 2012.

Skinner, L. A long view on climate sensitivity. *Science*, 337(6097):917–919, 2012.

Smith, A. B.; Santos, M. J.; Koo, M. S.; Rowe, K. M. C.; Rowe, K. C.; Patton, J. L.; Perrine, J. D.; Beissinger, S. R., and Moritz, C. Evaluation of species distribution models by resampling of sites surveyed a century ago by Joseph Grinnell. *Ecography*, pages no–no, 2013. doi: 10.1111/j.1600-0587.2013.00107.x. URL `http://dx.doi.org/10.1111/j.1600-0587.2013.00107.x`.

Smith, L. A. and Stern, N. Uncertainty in science and its role in climate policy. *Philosophical Transactions of the Royal Society A: Mathematical, Physical and Engineering Sciences*, 369(1956):4818–4841, 2011.

Smith, M. S.; Horrocks, L.; Harvey, A., and Hamilton, C. Rethinking adaptation for a 4c world. *Philosophical Transactions of the Royal Society A: Mathematical, Physical and Engineering Sciences*, 369(1934):196–216, 2011.

Soberon, J. and Nakamura, M. Niches and distributional areas: Concepts, methods, and assumptions. *Proceedings of the National Academy of Sciences*, 106(Supplement 2): 19644–19650, 2009.

Solomon, S.; Qin, D.; Manning, M.; Chen, Z.; Marquis, M.; Averyt, K.; Tignor, M., and Miller, H. *Climate Change 2007: The Physical Science Basis. Contribution of Working Group I to the Fourth Assessment Report of the Intergovernmental Panel on Climate Change, 2007*. Cambridge University Press, Cambridge, United Kingdom and New York, NY, USA, 2007.

Songsri, P.; Jogloy, S.; Holbrook, C. C.; Kesmala, T.; Vorasoot, N.; Akkasaeng, C., and Patanothai, A. Association of root, specific leaf area and spad chlorophyll meter reading to water use efficiency of peanut under different available soil water. *Agricultural Water Management*, 96(5):790–798, 2009.

Sperber, K. R.; Annamalai, H.; Kang, I. S.; Kitoh, A.; Moise, A.; Turner, A.; Wang, B., and Zhou, T. The Asian summer monsoon: an intercomparison of CMIP5 vs. CMIP3 simulations of the late 20th century. *Climate Dynamics*, pages 1–34, 2012. doi: 10.1007/s00382-012-1607-6. URL `http://dx.doi.org/10.1007/s00382-012-1607-6`.

Sponchiado, B. N.; White, J. W.; Castillo, J. A., and Jones, P. G. Root growth of four common bean cultivars in relation to drought tolerance in environments with contrasting soil types. *Experimental Agriculture*, 25(02):249–257, 1989.

Stainforth, D. A.; Aina, T.; Christensen, C.; Collins, M.; Faull, N.; Frame, D. J.; Kettleborough, J. A.; Knight, S.; Martin, A.; Murphy, J. M.; Piani, C.; Sexton, D.; Smith, L. A.; Spicer, R. A.; Thorpe, A. J., and Allen, M. R. Uncertainty in predictions of the climate response to rising levels of greenhouse gases. *Nature*, 433(7024):403–406, 2005. 10.1038/nature03301.

Stamp, P. and Visser, R. The twenty-first century, the century of plant breeding. *Euphytica*, pages 1–7, 2012.

Stanciel, K.; Mortley, D. G.; Hileman, D. R.; Loretan, P. A.; Bonsi, C. K., and Hill, W. A. Growth, Pod, and Seed Yield, and Gas Exchange of Hydroponically Grown Peanut in Response to CO2 Enrichment. *HortScience*, 35(1):49–52, 2000. URL `http://hortsci.ashspublications.org/content/35/1/49.abstract`.

Steduto, P.; Hsiao, T. C.; Raes, D., and Fereres, E. Aquacropthe fao crop model to simulate yield response to water: I. concepts and underlying principles. *Agron. J.*, 101 (3):426–437, 2009.

Steiner, J.; Howell, T., and Schneider, A. Lysimetric evaluation of daily potential evapotranspiration models for grain sorghum. *Agronomy Journal*, 83:240–247, 1991.

Stephens, C. R.; Heau, J. G.; Gonzlez, C.; Ibarra-Cerdea, C. N.; Snchez-Cordero, V., and Gonzlez-Salazar, C. Using biotic interaction networks for prediction in biodiversity and emerging diseases. *PLoS ONE*, 4(5):e5725, 2009.

Subash, N. and Ram Mohan, H. S. Evaluation of the impact of climatic trends and variability in ricewheat system productivity using cropping system model dssat over the indo-gangetic plains of india. *Agricultural and Forest Meteorology*, 164(0):71–81, 2012.

Suleiman, A. A. *Assessing and modeling the spatial variability of soil water redistribution and wheat yield along a sloping landscape*. PhD thesis, 1999.

Suleiman, A. A. and Ritchie, J. T. Estimating saturated hydraulic conductivity from soil porosity. *Transactions of the ASAE*, 44(2):235–239, 2001.

Suleiman, A. A. and Ritchie, J. T. Modeling soil water redistribution during second-stage evaporation. *Soil Sci. Soc. Am. J.*, 67(2):377–386, 2003.

Sultan, B.; Roudier, P.; Quirion, P.; Alhassane, A.; Muller, B.; Dingkuhn, M.; Ciais, P.; Guimberteau, M.; Traore, S., and Baron, C. Assessing climate change impacts on sorghum and millet yields in the Sudanian and Sahelian savannas of West Africa. *Environmental Research Letters*, 8(1):14040, 2013. URL `http://stacks.iop.org/1748-9326/8/i=1/a=014040`.

Sun, L.; Semazzi, F. H. M.; Giorgi, F., and Ogallo, L. Application of the ncar regional climate model to eastern africa 2. simulation of interannual variability of short rains. *J. Geophys. Res.*, 104(D6):6549–6562, 1999.

Suriharn, B.; Patanothai, A.; Boote, K. J., and Hoogenboom, G. Designing a peanut ideotype for a target environment using the csm-cropgro-peanut model. *Crop Sci.*, 51 (5):1887–1902, 2011.

Tabor, K. and Williams, J. W. Globally downscaled climate projections for assessing the conservation impacts of climate change. *Ecological Applications*, 20(2):554–565, 2010.

Talawar, S. Peanut in india: History, production and utilization. Technical report, University of Georgia, 2004.

Tanner, C. and Sinclair, T. R. *Efficient water use in crop production: Research or research?* Limitations to Efficient Water Use in Crop Production. ASA, CSSA, and SSA, Madison, Wisconsin, USA, 1983.

Tao, F.; Yokozawa, M., and Zhang, Z. Modelling the impacts of weather and climate variability on crop productivity over a large area: A new process-based model development, optimization, and uncertainties analysis. *Agricultural and Forest Meteorology*, 149(5): 831–850, 2009.

Taylor, K. E.; Stouffer, R. J., and Meehl, G. A. An overview of cmip5 and the experiment design. *Bulletin of the American Meteorological Society*, pages 1–39, 2012.

Taylor, K. E. Summarizing multiple aspects of model performance in a single diagram. *J. Geophys. Res.*, 106(D7):7183–7192, 2001.

Tebaldi, C. and Lobell, D. B. Towards probabilistic projections of climate change impacts on global crop yields. *Geophys. Res. Lett.*, 35(8):L08705, 2008.

Teixeira, E. I.; Fischer, G.; Velthuizen, van H.; Walter, C., and Ewert, F. Global hotspots of heat stress on agricultural crops due to climate change. *Agricultural and Forest Meteorology*, (170):206–215, 2013.

Terribile, L.; Diniz-Filho, J., and De Marco Jr., P. How many studies are necessary to compare niche-based models for geographic distributions? inductive reasoning may fail at the end. *Brazilian Journal of Biology*, 70:263–269, 2010.

Tesfaye, K.; Walker, S., and Tsubo, M. Radiation interception and radiation use efficiency of three grain legumes under water deficit conditions in a semi-arid environment. *European Journal of Agronomy*, 25(1):60–70, 2006.

Themessl, J. M.; Gobiet, A., and Leuprecht, A. Empirical-statistical downscaling and error correction of daily precipitation from regional climate models. *International Journal of Climatology*, 31(10):1530–1544, 2011.

Themessl, M.; Gobiet, A., and Heinrich, G. Empirical-statistical downscaling and error correction of regional climate models and its impact on the climate change signal. *Climatic Change*, 112(2):449–468, 2012.

Thornton, P. K. and Herrero, M. Potential for reduced methane and carbon dioxide emissions from livestock and pasture management in the tropics. *Proceedings of the National Academy of Sciences*, 2010.

Thornton, P. K.; Jones, P. G.; Alagarswamy, G., and Andresen, J. Spatial variation of crop yield response to climate change in east africa. *Global Environmental Change*, 19 (1):54–65, 2009.

Thornton, P. K.; Jones, P. G.; Ericksen, P. J., and Challinor, A. J. Agriculture and food systems in sub-saharan africa in a 4c+ world. *Philosophical Transactions of the Royal Society A: Mathematical, Physical and Engineering Sciences*, 369(1934):117–136, 2011.

Thuzar, M.; Puteh, A.; Abdullah, N.; Lassim, M., and Jusoff, K. The effects of temperature stress on the quality and yield of soya bean [(glycine max l.) merrill.]. *Journal of Agricultural Science*, 2(1):172–179, 2010.

Tilman, D.; Cassman, K. G.; Matson, P. A.; Naylor, R., and Polasky, S. Agricultural sustainability and intensive production practices. *Nature*, 418(6898):671–677, 2002. 10.1038/nature01014.

Tompkins, E. L.; Adger, W. N.; Boyd, E.; Nicholson-Cole, S.; Weatherhead, K., and Arnell, N. Observed adaptation to climate change: Uk evidence of transition to a well-adapting society. *Global Environmental Change*, 20(4):627–635, 2010.

Trnka, M.; Olesen, J. E.; Kersebaum, K. C.; SkjelvG, A. O.; Eitzinger, J.; Seguin, B.; Peltonen-Sainio, P.; RTter, R.; Iglesias, A. N. A.; Orlandini, S.; Dubrovsk, M.; Hlavinka, P.; Balek, J.; Eckersten, H.; Cloppet, E.; Calanca, P.; Gobin, A.; VuEti, V.; Nejedlik, P.; Kumar, S.; Lalic, B.; Mestre, A.; Rossi, F.; Kozyra, J.; Alexandrov, V.; SemerDov, D., and Alud, Z. Agroclimatic conditions in europe under climate change. *Global Change Biology*, 17(7):2298–2318, 2011.

Tubiello, F. N. and Ewert, F. Simulating the effects of elevated co2 on crops: approaches and applications for climate change. *European Journal of Agronomy*, 18(12):57–74, 2002.

UN, . World population prospects: The 2010 revision (available from: http://esa.un.org/unpd/wpp/index.htm). Technical report, 2010.

UNFCCC, . Conference of parties: Report of the conference of the parties on its seventeenth session, held in durban from 28 november to 11 december 2011, available at http://unfccc.int/resource/docs/2011/cop17/eng/09a02.pdf. Technical report, United Nations Framework Convention on Climate Change, 2012.

Upadhyaya, H. D. Variability for drought resistance related traits in the mini core collection of peanut. *Crop Sci.*, 45(4):1432–1440, 2005.

Uppala, S. M.; Kllberg, P. W.; Simmons, A. J.; Andrae, U.; Bechtold, V. D. C.; Fiorino, M.; Gibson, J. K.; Haseler, J.; Hernandez, A.; Kelly, G. A.; Li, X.; Onogi, K.; Saarinen, S.; Sokka, N.; Allan, R. P.; Andersson, E.; Arpe, K.; Balmaseda, M. A.; Beljaars, A. C. M.; Berg, L. V. D.; Bidlot, J.; Bormann, N.; Caires, S.; Chevallier, F.; Dethof, A.; Dragosavac, M.; Fisher, M.; Fuentes, M.; Hagemann, S.; Hlm, E.; Hoskins, B. J.; Isaksen, L.; Janssen, P. A. E. M.; Jenne, R.; McNally, A. P.; Mahfouf, J. F.; Morcrette, J. J.; Rayner, N. A.; Saunders, R. W.; Simon, P.; Sterl, A.; Trenberth, K. E.; Untch, A.; Vasiljevic, D.; Viterbo, P., and Woollen, J. The era-40 re-analysis. *Quarterly Journal of the Royal Meteorological Society*, 131(612):2961–3012, 2005.

USDA, . Major world crop areas and climatic profiles, 2006.

USDA-FAS, . Index of agricultural crop calendars for australia, bangladesh, india, pakistan, 2003.

USDA-FAS, . Crop explorer, 2008.

USDA-NASS, . Usual planting and harvesting dates for u.s. field crops. agricultural handbook no. 628, 1997.

USDA-SCS, . *National Engineering Handbook, Section 4, Part I, Watershed Planning*. Soil Conservation Service, US Department of Agriculture, Washington, DC, USA, 1964.

Asten, van P. J. A.; Fermont, A. M., and Taulya, G. Drought is a major yield loss factor for rainfed east african highland banana. *Agricultural Water Management*, 98(4):541–552, 2011.

Bussel, van L. G. J.; Ewert, F., and Leffelaar, P. A. Effects of data aggregation on simulations of crop phenology. *Agriculture, Ecosystems & Environment*, 142(12): 75–84, 2011.

Velde, van der M.; Tubiello, F.; Vrieling, A., and Bouraoui, F. Impacts of extreme weather on wheat and maize in france: evaluating regional crop simulations against observed data. *Climatic Change*, 113(3):751–765, 2012.

Etten, van J. Crowdsourcing crop improvement in sub-saharan africa: A proposal for a scalable and inclusive approach to food security. *IDS bulletin*, 42(4):102–110, 2011.

Wart, van J.; Bussel, van L. G. J.; Wolf, J.; Licker, R.; Grassini, P.; Nelson, A.; Boogaard, H.; Gerber, J.; Mueller, N. D.; Claessens, L.; Ittersum, van M. K., and Cassman, K. G. Use of agro-climatic zones to upscale simulated crop yield potential. *Field Crops Research*, In press, 2013.

VanDerWal, J.; Shoo, L. P.; Johnson, C. N., and Williams, S. E. Abundance and the environmental niche: environmental suitability estimated from niche models predicts the upper limit of local abundance. *The American naturalist*, 174(2):282–91, August 2009a. ISSN 1537-5323. doi: 10.1086/600087. URL `http://www.ncbi.nlm.nih.gov/pubmed/19519279`.

VanDerWal, J.; Shoo, L. P., and Williams, S. E. New approaches to understanding late quaternary climate fluctuations and refugial dynamics in australian wet tropical rain forests. *Journal of Biogeography*, 36(2):291–301, 2009b.

Vara Prasad, P. V.; Boote, K. J.; Allen, L. H., and Thomas, J. M. G. Effects of elevated temperature and carbon dioxide on seed-set and yield of kidney bean (phaseolus vulgaris l.). *Global Change Biology*, 8(8):710–721, 2002.

Vara Prasad, P. V.; Boote, K. J.; Hartwell Allen, L., and Thomas, J. M. G. Super-optimal temperatures are detrimental to peanut (arachis hypogaea l.) reproductive processes and yield at both ambient and elevated carbon dioxide. *Global Change Biology*, 9(12): 1775–1787, 2003.

Vara Prasad, P. V.; Boote, K. J., and Allen Jr, L. H. Adverse high temperature effects on pollen viability, seed-set, seed yield and harvest index of grain-sorghum [sorghum bicolor (l.) moench] are more severe at elevated carbon dioxide due to higher tissue temperatures. *Agricultural and Forest Meteorology*, 139(34):237–251, 2006.

Vara Prasad, P. V.; Craufurd, P. Q.; Summerfield, R. J., and Wheeler, T. R. Effects of short episodes of heat stress on flower production and fruitset of groundnut (arachis hypogaea l.). *Journal of Experimental Botany*, 51(345):777–784, 2000.

Vara Prasad, P.; Craufurd, P., and Summerfield, R. Sensitivity of peanut to timing of heat stress during reproductive development. *Crop Sci.*, 39(5):1352–1357, 1999.

Velde, M. v. d.; See, L.; Fritz, S.; Verheijen, F. G. A.; Khabarov, N., and Obersteiner, M. Generating crop calendars with web search data. *Environmental Research Letters*, 7(2): 024022, 2012.

Venkatarao, M. *Physiological Investigations on groundnut [Arachis hypogaea L.] in a teak based Agroforestry System*. PhD thesis, 2005.

Ver Hoef, J. M. Who invented the delta method? *The American Statistician*, 66(2): 124–127, 2012.

Vermeulen, S. J.; Challinor, A. J.; Thornton, P. K.; Campbell, B. M.; Eriyagama, N.; Vervoort, J. M.; Kinyangi, J.; Jarvis, A.; Laderach, P.; Ramirez-Villegas, J.; Nicklin, K. J.; Hawkins, E., and Smith, D. R. Addressing uncertainty in adaptation planning for

agriculture. *Proceedings of the National Academy of Sciences*, 110(21):8357–8362, 2013. doi: 10.1073/pnas.1219441110.

Viglizzo, E. F.; Frank, F. C.; CarreO, L. V.; JobbGy, E. G.; Pereyra, H.; Clatt, J.; PincN, D., and Ricard, M. F. Ecological and environmental footprint of 50 years of agricultural expansion in argentina. *Global Change Biology*, 17(2):959–973, 2011.

Walker, W.; Harremoes, P.; Rotmans, J.; Sluijs, J. v. d.; Asselt, M. v.; Janssen, P., and Krauss, M. K. v. Defining uncertainty: A conceptual basis for uncertainty management in model-based decision support. *Integrated Assessment*, 4(1):5–17, 2003.

Walsh, J. E.; Chapman, W. L.; Romanovsky, V.; Christensen, J. H., and Stendel, M. Global climate model performance over alaska and greenland. *Journal of Climate*, 21 (23):6156–6174, 2008.

Warren, D. L. and Seifert, S. N. Ecological niche modeling in Maxent: the importance of model complexity and the performance of model selection criteria. *Ecological Applications*, 21(2):335–342, 2010. doi: 10.1890/10-1171.1. URL `http://dx.doi.org/10.1890/10-1171.1`.

Warren, R.; VanDerWal, J.; Price, J.; Welbergen, J.; Atkinson, I.; Ramirez-Villegas, J.; Osborn, T.; Jarvis, A.; Shoo, L.; Williams, S., and others, . Quantifying the benefit of early climate change mitigation in avoiding biodiversity loss. *Nature Climate Change*, 3:678–682, 2013.

Washington, W. M.; Weatherly, J. W.; Meehl, G. A.; Semtner Jr, A. J.; Bettge, T. W.; Craig, A. P.; Strand Jr, W. G.; Arblaster, J.; Wayland, V. B.; James, R., and Zhang, Y. Parallel climate model (pcm) control and transient simulations. *Climate Dynamics*, 16(10):755–774, 2000.

Watson, J. and Challinor, A. The relative importance of rainfall, temperature and yield data for a regional-scale crop model. *Agricultural and Forest Meteorology*, 170:47–57, 2013.

Weaver, C. P.; Lempert, R. J.; Brown, C.; Hall, J. A.; Revell, D., and Sarewitz, D. Improving the contribution of climate model information to decision making: the value and demands of robust decision frameworks. *Wiley Interdisciplinary Reviews: Climate*

Change, 4(1):39–60, 2013. ISSN 1757-7799. doi: 10.1002/wcc.202. URL `http://dx.doi.org/10.1002/wcc.202`.

Webster, M.; Sokolov, A.; Reilly, J.; Forest, C.; Paltsev, S.; Schlosser, A.; Wang, C.; Kicklighter, D.; Sarofim, M.; Melillo, J.; Prinn, R., and Jacoby, H. Analysis of climate policy targets under uncertainty. *Climatic Change*, 112(3):569–583, 2012.

Weedon, G. P.; Gomes, S.; Viterbo, P.; Shuttleworth, W. J.; Blyth, E.; sterle, H.; Adam, J. C.; Bellouin, N.; Boucher, O., and Best, M. Creation of the watch forcing data and its use to assess global and regional reference crop evaporation over land during the twentieth century. *Journal of Hydrometeorology*, 12(5):823–848, 2011.

West, P. C.; Gibbs, H. K.; Monfreda, C.; Wagner, J.; Barford, C. C.; Carpenter, S. R., and Foley, J. A. Trading carbon for food: Global comparison of carbon stocks vs. crop yields on agricultural land. *Proceedings of the National Academy of Sciences*, 2010.

Wheeler, T. and Braun, von J. Climate change impacts on global food security. *Science*, 341(6145):508–513, 2013.

Whisler, F. D.; Acock, B.; Baker, D. N.; Fye, R. E.; Hodges, H. F.; Lambert, J. R.; Lemmon, H. E.; McKinion, J. M., and Reddy, V. R. *Crop Simulation Models in Agronomic Systems*, volume Volume 40, pages 141–208. Academic Press, 1986.

White, J. W. *Modeling and crop improvement*, volume 7 of *Understanding Options for Agricultural Production*. Kluwer Academic Publishers, Dordrecht, The Netherlands, 1998.

White, J. W. Comments on a report of regression-based evidence for impact of recent climate change on winter wheat yields. *Agriculture, Ecosystems & Environment*, 129(4):547–548, 2009.

White, J. W.; Kornegay, J., and Cajiao, C. Inheritance of temperature sensitivity of the photoperiod response in common bean (phaseolus vulgaris l.). *Euphytica*, 91(1):5–8, 1996.

White, J. W.; Hoogenboom, G.; Kimball, B. A., and Wall, G. W. Methodologies for simulating impacts of climate change on crop production. *Field Crops Research*, 124(3): 357–368, 2011a.

White, J. W.; Hoogenboom, G.; Wilkens, P. W.; Stackhouse, P. W., and Hoel, J. M. Evaluation of satellite-based, modeled-derived daily solar radiation data for the continental united states. *Agron. J.*, 103(4):1242–1251, 2011b.

Whitmore, A. P. and Whalley, W. R. Physical effects of soil drying on roots and crop growth. *Journal of Experimental Botany*, 60(10):2845–2857, 2009.

Wiens, J. A.; Stralberg, D.; Jongsomjit, D.; Howell, C. A., and Snyder, M. A. Niches, models, and climate change: Assessing the assumptions and uncertainties. *Proceedings of the National Academy of Sciences*, 106(Supplement 2):19729–19736, 2009. doi: 10.1073/pnas.0901639106. URL `http://www.pnas.org/content/106/suppl.2/19729.abstract`.

Wilby, R. L.; Troni, J.; Biot, Y.; Tedd, L.; Hewitson, B. C.; Smith, D. M., and Sutton, R. T. A review of climate risk information for adaptation and development planning. *International Journal of Climatology*, 29(9):1193–1215, 2009.

Wilks, D. On field significance and the false discovery rate. *Journal of Applied Meteorology & Climatology*, 45(9), 2006.

Williams, J.; Jones, C.; Kiniry, J., and Spanel, D. The epic crop growth model. *Transactions of the ASAE*, 32(2):497–511, 1989.

Willmott, C.; Rowe, C., and Philpot, W. Small-scale climate maps: A sensitivity analysis of some common assumptions associated with grid-point interpolation and contouring. *American Cartographer*, 12:5–16, 1985.

Willmott, C. J. Some comments on the evaluation of model performance. *Bulletin of the American Meteorological Society*, 63(11):1309–1313, 1982.

Willocquet, L.; Aubertot, J. N.; Lebard, S.; Robert, C.; Lannou, C., and Savary, S. Simulating multiple pest damage in varying winter wheat production situations. *Field Crops Research*, 107(1):12–28, 2008.

Wolf, J. and Van Oijen, M. Model simulation of effects of changes in climate and atmospheric co2 and o3 on tuber yield potential of potato (cv. bintje) in the european union. *Agriculture, Ecosystems & Environment*, 94(2):141–157, 2003.

World-Bank, . World development indicators, online database, 2012.

Wright, G. and Nageswara Rao, R. *The Groundnut Crop: A Scientific Basis for Improvement*. Chapman and Hall, London, 1994.

WWRP, . Recommendations for the verification and intercomparison of qpfs and pqpfs from operational nwp models. Technical report, WMO/TD - No. 1485, World Meteorological Organization, available at: www.wmo.int, 2009.

Xiong, W.; Holman, I.; Conway, D.; Lin, E., and Li, Y. A crop model cross calibration for use in regional climate impacts studies. *Ecological Modelling*, 213(3-4):365–380, 2008.

Yongqiang, Y.; Xuehong, Z., and Yufu, G. Global coupled ocean-atmosphere general circulation models in lasg/iap. *Advances in Atmospheric Sciences*, 21(3):444–455, 2004.

You, L.; Wood, S., and Wood-Sichra, U. Generating plausible crop distribution maps for sub-saharan africa using a spatially disaggregated data fusion and optimization approach. *Agricultural Systems*, 99(2-3):126–140, 2009.

Yukimoto, S.; Noda, A.; Kitoh, A.; Sugi, M.; Kitamura, Y.; Hosaka, M.; Shibata, K.; Maeda, S., and Uchiyama, T. The new meteorological research institute coupled gcm (mri-cgcm2) model climate and variability. *Papers in Meteorology and Geophysics*, 51 (2):47–88, 2001.

Zhang, T.; Simelton, E.; Huang, Y., and Shi, Y. A bayesian assessment of the current irrigation water supplies capacity under projected droughts for the 2030s in china. *Agricultural and Forest Meteorology*, in press, 2012.

Ziervogel, G. and Ericksen, P. J. Adapting to climate change to sustain food security. *Wiley Interdisciplinary Reviews: Climate Change*, 1(4):525–540, 2010.